Dynamique de la diversité microbienne dans la grotte de Lascaux

Zélia Bontemps

THESE de DOCTORAT DE
L'UNIVERSITE CLAUDE BERNARD LYON 1

École Doctorale N°341
Évolution Écosystème Microbiologie et Modélisation

Discipline : Microbiologie

Soutenue publiquement le 13/12/2022, par :
Zélia BONTEMPS

Dynamique de la diversité microbienne dans la grotte de Lascaux

---

Devant le jury composé de :

DI MARTINO, Patrick, Professeur, Université Cergy-Pontoise	Rapporteur
UROZ, Stéphane, Directeur de recherche, Université de Lorraine	Rapporteur
GERARD, Emmanuelle, Ingénieure de recherche, Université Paris cité	Examinatrice
RODRIGUEZ-NAVA, Veronica, Professeure, Université Lyon 1	Présidente
MOËNNE-LOCCOZ, Yvan, Professeur, Université Lyon 1	Directeur de thèse
HUGONI, Mylène, Maitresse de conférences, Université Lyon 1	Co-directrice de thèse

Université Claude Bernard – LYON 1

Président de l'Université	M. Frédéric FLEURY
Président du Conseil Académique	M. Hamda BEN HADID
Vice-Président du Conseil d'Administration	M. Didier REVEL
Vice-Présidente de la Commission Formation et de la Vie Universitaire	Mme Céline BROCHIER
Vice-Président de la Commission Recherche	M. Petru MIRONESCU
Directeur Général des Services	M. Pierre ROLLAND

COMPOSANTES SANTE

Faculté de Médecine Lyon-Est – Claude Bernard	Doyen : M. Gilles RODE
Faculté de Médecine et Maïeutique Lyon Sud Charles Mérieux	Doyen : M. Philippe PAPAREL
UFR d'Odontologie	Doyen : M. Jean-Christophe MAURIN
Institut des Sciences Pharmaceutiques et Biologiques	Directeur : M. Claude DUSSART
Institut des Sciences et Techniques de la Réadaptation	Directeur : M. Jacques LUAUTE
Département de Formation et Centre de Recherche en Biologie Humaine	Directrice : Mme Laetitia BIGNON

COMPOSANTES SECTEUR SCIENCES & TECHNOLOGIE

UFR Biosciences	Directrice : Kathrin GIESELER
Département Génie Electrique et des Procédés	Ad. prov. : Mme Rosaria FERRIGNO
Département Informatique	Directeur : M. Behzad SHARIAT
Département Mécanique	Directeur : M. Marc BUFFAT
UFR-Facultés des Sciences	Directeur : M. Bruno ANDRIOLETTI
UFR STAPS	Directeur : M. Guillaume BODET
Observatoire de Lyon	Directrice : Mme Isabelle DANIEL
Ecole Polytechnique Universitaire de Lyon	Directrice : M. Emmanuel PERRIN
Ecole Supérieure de Chimie, Physique, Electronique	Directeur : M. Gérard PIGNAULT
Institut Universitaire de Technologie de Lyon 1	Directeur : M. Michel MASSENZIO
Institut de Science Financière et d'Assurances	Directeur : M. Nicolas LEBOISNE
Institut National Supérieur du Professorat et de l'Education	Directeur : M. Pierre CHAREYRON

La vérité scientifique sera toujours plus belle que les créations de notre imagination et que les illusions de notre ignorance.

Claude Bernard 1813-1878

Remerciements

Je remercie M. Patrick Di Martino et M. Stéphane Uroz d'avoir accepté d'évaluer ces travaux de thèse ainsi que Mme Emmanuelle Gérard et Mme Veronica Rodriguez-Navaet Mme Muriel Mauriac de s'être jointes à eux pour constituer mon jury.

Je tiens également à remercier Vincent Grossi, mon tuteur ainsi que les membres de mon comité de suivi Didier Debroas, Thomas Pommiers et Delphine Ropers pour leur écoute et leurs conseils.

Je souhaite remercier mon directeur de thèse Yvan Moënne-Loccoz pour m'avoir fait confiance et laissé des libertés d'initiative tout au long de ces trois années de travail en commun. Tu t'es impliqué dans l'orientation de mes travaux et tu as été de bon conseil pour mon avenir. Tu n'y étais pas obligé et je t'en suis reconnaissante. Merci pour ton honnêteté, tes discussions scientifiques et tes nombreuses blagues (les Jeannettes n'oublieront plus jamais le 1er avril !) qui ont contribué au déroulement de ma thèse dans d'excellentes conditions. Tu as eu un réel impact positif sur mon parcours professionnel et personnel. Merci.

Merci à ma co-directrice de thèse Mylène Hugoni d'avoir cru en moi avant même le début de cette thèse. Merci pour toutes ces discussions scientifiques et non scientifiques qui m'ont accompagnée tout au long de ces années. Merci également à Maxime qui a toujours pris du temps pour répondre à mes questions.

Je voudrais remercier tous les membres de l'équipe 3 et M2E de m'avoir si bien accueillie, écoutée et conseillée au fil du temps.

Je tiens à remercier tous les membres du projet Lascaux, en particulier Christophe Douady et Thomas Tully ainsi que l'équipe présente sur place, Sandrine Géraud, Diane Henry-Lormelle, Jean-Christophe Portais, Thierry Baritaud.

Une thèse c'est aussi un challenge administratif. Je tiens à remercier toute l'équipe administrative du LEM pour son accueil, son aide et sa bonne humeur. Mention spéciale pour DelPon, toi qui aimes tellement ce beau surnom il sera inscrit dans un document officiel eheh ! Merci Betty pour ton implication dans le projet, d'avoir partagé la galère des marchés et pour ton écoute.

Un grand merci à iBio où j'ai partagé un certain nombre de cafés scientifiques (et non scientifiques). Merci DanisSSSSSS pour ta disponibilité, ton écoute, tes conseils en bioinfo (bashlover), tes blagues et tes alliances contre Cécile Gruet la méchante. Merci à Daniel pour toutes tes blagues (enfin c'est toi qui devrais me remercier d'être un si bon public) mais aussi pour la science. Promis un jour je viendrai au bureau avec une tarte au concombre et ce sera un mercredy !

Merci Jeanne (JJDD) pour ton aide et ton soutien tout au long de cette thèse. Les cafés et ton écoute en fin de thèse ont été très précieux pour moi. J'espère que tu vas lire ces remerciements sur une moto direction le Dam's !

La vie de labo c'est super important alors je tiens à remercier tous les membres du 3ème étage du Mendel (Claire, Juliana, Guilhem, Florence WD et Laurent), Corinne, Jonathan (et sa fabuleuse Verveine), Abi, Pascale, Petar, Sonia, Patricia, Franck et Ludo. Merci aussi à Madame Edwige, Delphine, Marie-André et Laurent avec qui j'ai passé de super moments au Lwoff. Vous avez toujours été présents quand j'en avais besoin. Merci également à Monsieur Van qui m'a appris beaucoup de choses inoubliables (TVV75 !).

La vie de labo c'est aussi et surtout les doctorants et post-doctorants avec qui j'ai passé mes trois années de thèse et mon master, Mélanie, Mathilde, Aline, Anaëlle, Tim, Marine, Théo, Mathis, Pénélope, Maxime, Simon, Amandine, Béa, William, Sam, Colin, Florian et Lucas. Merci à vous tous pour les bons moments partagés.

Merci à Margot et Antonio de m'avoir si bien accueillie au Pasteur. Merci pour les très bons moments partagés.

Merci Tristan pour ta bonne humeur, tes conseils et ton initiation à la chasse aux trésors des orobanches (enfin je ne sais pas si je dois te dire merci pour ça ?). J'espère qu'on verra ce magnifique concert de rock un jour au LEM, vive la flûte de pan !

Merci à Pauline et Adrian de m'avoir supportée au bureau dans cette dernière année de thèse, on a bien rigolé. J'espère qu'on continuera à fêter les demi-thèses, les lundis 7 mars, que le riz va (enfin) pousser (avec la bonne concentration d'AK) et qu'on ira ensemble à la stor korvmassa.

Je ne peux pas parler de bureau sans parler de Flavien, après 7 bureaux partagés ensemble (tu ne veux pas me lâcher...) c'est la fin d'une aventure pleine de rebondissements. Merci pour toutes ces discussions scientifiques (ou pas), ces moments où nous avons refait le monde, ton écoute, tes danses (que je garde précieusement pour ton film de thèse), tes coups de flips, tes vidéos et toutes tes blagues nulles ! Et là ... j'oublie un truc fondamental : Les memes ! J'espère que tu vas m'en envoyer des kilos pendant encore un long moment. Bonne continuation Fla et courage pour la fin (tu vas y arriver car tu as eu 19 en IMS, que tu as un beau camion et que vendredi c'est le jour du poisson).

Merci Cocotte pour ta bonne humeur permanente, tes blagues et tes guets-apens inoubliables. J'espère que tu aimes l'écriture 'atypique' de ces remerciements ! A bientôt pour un nouveau guet-apens (mais cette fois on prendra les gâteaux du même nom).

Merci à Irena (IrIna), grande fan de Beyonce avec qui j'ai passé de super moments (surtout en buvant de la 'slivovica' accompagnée d'une gratinée), maintenant c'est à nous de venir te voir en Serbie pour faire la fête !

Un remerciement aussi aux membres de l'asso DocE2M2, pour les évènements et colloques que j'ai eu la chance d'organiser avec une belle équipe, et les blind tests (victorieux) du lundi

soir.

Je remercie ensuite mes amis, à commencer par Antoine, mon super coloc de choc grâce à qui la vie canadienne a été marquée par des souvenirs inoubliables, merci pour tous ces moments partagés, au baro et ailleurs.

Merci à mes amies Nancéennes, on n'oublie pas ses racines, celles qui me soutiennent depuis les premières années de fac, Marion, Vanille et Justine. Merci d'être venues jusqu'à Lyon pour me changer les idées.

Merci à toutes les personnes avec qui j'ai pu partager quelques notes de musique (Nicolas, Oliver, Magalie, Maryline, Eloïse, et tous ceux que j'oublie). Avec une mention particulière pour le chef, Stéphane Garaffi, sans qui je ne serai probablement pas devenue la personne que je suis aujourd'hui.

Un grand merci à Justine et Aurélien pour leur soutien durant ces dernières années et pour tous les moments partagés à Commercy, Nancy, Lyon, Lloret del Mare, etc. !! Ces moments resteront inoubliables. La thèse ne nous a pas permis de nous voir autant que je l'aurais souhaité mais on se rattrapera après j'en suis sûr.

Bien évidemment un grand merci au μbio-gang (2) ceux qui ont égayé ces années lyonnaises, qui ont toujours été là pour me soutenir, merci pour tous ces supers moments passés ensemble et que ça dure encore longtemps. Mathieu et Laura, avec qui j'irai peut-être un jour à Lorient en buvant de la peche melbouche devant la Comedia del arte où l'acteur principal se nommerai Mr Bourgeois ?. Merci à Thomas qui est toujours là, prêt à nous emmener avec Josi et qui nous écoute toujours d'une oreille bienveillante. Merci à Vincent (qui était le plus riche de tous, oui je parle au passé), membre de notre mythique frontière avec qui j'ai passé (et je passerai toujours) de solides moments inoubliables (tu feras ça bien hein, qu'on ne soit pas em***dé).

Morgano isotopique, la plus belle plage du monde qui n'aime pas les gens... Merci pour ces 5 années passées ensemble à rigoler, travailler (un peu) et discuter longuement de tout et de rien. Merci pour tous les moments partagés en tant que fan de fromage (les meules en chambre froide, y'a pas de saison pour le reblochon (et la pêche)). Les excuses de la sncf sur la ligne Saint Etienne – Lyon vont me manquer, mais tu me raconteras tout ça sur la plage en Suède avec toute ta petite famille (Merci également à Mathias : Comment est votre blanquette ?).

Merci à Cécile Gruet (CCGG) à qui je dédie un paragraphe, même si je ne suis pas sûre qu'elle le mérite... Il faudrait écrire un livre pour pouvoir te remercier dignement mais je vais essayer en quelques lignes. Comment ne pas parler des brins d'herbe, de la recherche de l'ARN perdu, des 271 pages de thèse apprises par coeur et de ton second métier ('choisisseuse' de couleur officielle) mais ce que je retiens c'est nos rires, nos heures de travail manuel (ton troisième métier), le recap' télé d'après la deuxième pub, nos moments de joie, de stress (vive le magnésium en barre), les châteaux de sable (toujours là après 3 ans), Bourges il est 8h, les manteaux sans doublure et bien évidement notre divorce (+ bébé Chantale). Merci pour ta bonne humeur permanente et ton écoute. Les cafés du matin n'auront plus la même saveur à présent, oui Cécile Gruet tu vas me manquer !

Merci à ma famille qui a toujours été là pour me soutenir durant toutes ces années. Merci à mes tantes, oncles, cousins et cousines qui ont toujours pris des nouvelles même s'ils ne comprennent pas tout ce que je fais.

Merci à mes frères Adrien et Dr. Jean Baptiste Bontemps (il faut bien que ce titre serve un jour (et oui ma thèse avance, la preuve...)) ainsi qu'à mes belles sœurs Adeline et Géraldine pour leur soutient et tous les moments que l'on partage. Merci à mes neveux Nylo et Elio qui m'apportent du bonheur et avec qui je ne m'ennuie jamais !

Merci à Estelle et Etienne qui ont joué un grand rôle dans mes études. Merci de m'avoir accueillie il y a maintenant 9 ans à Toronto et de m'avoir initiée au monde de la recherche. Sans vous il n'y aurai pas eu cette thèse. A bientôt en Suède.

Merci à ma belle-famille, Christian, Christine, Marion, Sébastien, Soline et Hugo pour votre soutien, leur générosité et la confiance qu'ils m'ont témoignée durant ces années.

Merci à mes parents pour leur soutien dans tout ce que j'ai entrepris dans ma vie, pour leur disponibilité et tout ce qu'ils font pour nous.

Un très grand merci à Victor qui m'a toujours soutenue et encouragée. Merci de m'avoir supportée dans les périodes les plus difficiles et d'avoir pris soin de moi.

A mes grands-parents,
Qui après une visite à Lascaux ont ramené un souvenir de la boutique.

Résumé

Les grottes paléolithiques attirent un million de touristes par an, faisant d'elles des milieux fortement anthropisés. L'anthropisation de la grotte de Lascaux, célèbre pour son art pariétale, à entrainé un déséquilibre du microbiote de la grotte et une prolifération anormale de certains microorganismes. Aujourd'hui deux types d'altérations microbiennes (taches noires et zones sombres) sur les parois de la grotte sont des menaces pour sa conservation.

L'objectif général de cette thèse était de mieux comprendre les dynamiques des communautés microbiennes des trois domaines du vivant, au niveau des altérations (taches noires et zones sombres) présentes sur les parois de la grotte de Lascaux. Il s'agissait notamment d'identifier les communautés microbiennes de la grotte à différentes échelles spatio-temporelles et de comprendre les dynamiques de la diversité microbienne lors de la formation, l'évolution et la dissémination des altérations en utilisant le séquençage à haut débit d'acides nucléiques par des approches ciblées (métabarcoding MiSeq) et non ciblées (métagénomique shotgun). Ces recherches visaient à tester quatre hypothèses : (i) la formation et l'évolution des zones sombres seraient liées à des successions microbiennes rapides car les zones altérées et zones saines sont visuellement très différentes, sans zone de transition apparente, (ii) au moins une partie des changements de la communauté microbienne liés à la formation de zone sombre implique des taxons cosmopolites à l'échelle de la grotte, mais aussi des taxons endémiques conformément aux spécificités du microbiote des différentes pièces ou surfaces, (iii) les dynamiques de régression et de repousse de certaines taches noires seraient liées à des successions microbiennes particulières, et (iv) les taches noires étant attribuées à l'activité des champignons pigmentés, la synthèse de pigments concernerait des taxons spécialistes des conditions environnementales particulières correspondant aux altèrations.

Nos recherches ont montré, premièrement, que la formation des zones sombres implique un changement brutal de la communauté microbienne impliquant une seule zone de transition en bordure de zone altérée. Deuxièmement, les zones sombres présentent un mélange de taxons cosmopolites des altérations et de taxons endémiques à chaque endroit de Lascaux, suggérant que la propagation de ces altérations pourrait se poursuivre en fonction de la zone de distribution des taxons cosmopolites. Troisièmement, le nettoyage mécanique des taches noires a mis en évidence des taxons spécifiques liés à la recolonisation des zones altérées sur les parois, tandis que l'atténuation des taches noires (uniquement dans le Cabinet des Félins) est probablement liée à la sélection déterministe de taxons de la biosphère rare. Quatrièmement, le potentiel génétique analysé pour les deux types d'altérations a mis en évidence (i) un lien possible entre la dégradation du chlorure de benzalkonium (biocide utilisé à Lascaux) et la biosynthèse de pigments, et (ii) la présence de voies métaboliques de synthèse de mélanines et de caroténoïdes dans les communautés des deux types d'altérations, chez les bactéries et les microeucaryotes.

Ce projet a caractérisé l'impact de la perturbation anthropique sur la diversité, la structure, la composition et le potentiel génétique des communautés microbiennes de la grotte de Lascaux. Il a permis de mieux comprendre les dynamiques microbiennes associées à la formation, l'évolution et la dissémination des altérations apportant de nouvelles connaissances pour mieux guider les stratégies de conservation de ce site paléolithique emblématique.

Mots-clés : Grotte de Lascaux, Perturbation, Altérations des parois, Successions microbiennes, Potentiel fonctionnel, Mélanines, MAGs

Summary

Paleolithic caves attract a million tourists per year, making them highly anthropized environments. The anthropization of Lascaux Cave, famous for its parietal art, has led to an imbalance in the microbiota of the cave and abnormal proliferation of certain microorganisms. Today two types of microbial alterations (black stains and dark zones) on cave walls are threats to its conservation.

The general objective of this thesis was to better understand the dynamics of the microbial communities of the three domains of life at the level of the alterations (black stains and dark zones) present on the walls of Lascaux Cave. The aim was to identify the microbial communities of the cave at different spatio-temporal scales and to understand the dynamics of microbial diversity during the formation, evolution and dissemination of the alterations using high-throughput nucleic acid sequencing targeted (MiSeq metabarcoding) and non-targeted (shotgun metagenomics) approaches. This research aimed at testing four hypotheses : (i) the formation and evolution of dark zones would be related to rapid microbial successions because altered and unaltered zones are visually very different, with no apparent transition zone, (ii) at least part of the changes in the microbial community related to dark zone formation involve cosmopolitan taxa (at cave level), but also endemic taxa in accordance with the specificities of the microbiota of the different rooms or surfaces, (iii) the dynamics of regression or regrowth of certain black stains would be linked to particular microbial successions, and (iv) the alterations being attributed to the activity of pigmented fungi, the synthesis of pigments would concern taxa specializing in particular environmental conditions corresponding to the alterations.

Our research has shown firstly that the formation of the dark zones involves a brutal change in the microbial community, with a single transition zone at the edge of the altered zone. Secondly, the dark zones show a set-up of cosmopolitan taxa from the alterations and endemic taxa to each location in Lascaux Cave, suggesting that the spread of these alterations could continue depending on the area of distribution of cosmopolitan taxa. Thirdly, the mechanical cleaning of black stains revealed specific taxa during the recolonization of the wall surfaces, while the attenuation of black stains (only in the Chamber of Felines) is probably related to the deterministic selection of the rare biosphere taxa. Fourthly, the genetic potential analyzed for both types of alterations revealed (i) a possible link between the degradation of benzalkonium chloride (biocide used at Lascaux) and pigment biosynthesis, and (ii) the presence of metabolic pathways for melanin and carotenoid synthesis in communities of both types of alterations, in bacteria and microeukaryotes.

This project characterized the impact of anthropogenic disturbance on the diversity, structure, composition and genetic potential of microbial communities in Lascaux Cave. It allows us to better understand the microbial dynamics associated with the formation, evolution and dissemination of alterations, providing new knowledge to better guide the conservation strategies of this iconic Paleolithic site.

Keywords : Lascaux Cave, Disturbance, Cave alterations, Microbial successions, Functional potential, Melanins, MAGs.

Abréviations

A
ADN : Acide DésoxyriboNucléique
AIC : Akaike Information Criterion
ANOSIM : ANalysis Of SIMilarities
ANOVA : ANalysis Of VAriance
ARN : Acide RiboNucléique
ART : Always Rare Taxa
ASV : Amplicon Single Variant
AT : ATtenuated stain
B
BAC : BenzAlkonium Chloride
BGC : Biosynthetic Gene Clusters
BDMA : BenzylDiMethylAmine
BIC : Bayesian Information Criterion
BLASTn : Basic Local Alignment Search Tool nucleotide
βMNTD : Beta Mean Nearest Taxon Distance
βNTI : Beta Nearest Taxon Index
BP : Before Present
BS : Black Stain
C
COG : Clusters of Orthologous Groups
CRT : Conditionally Rare Taxa
CStain : Cleaned Stain
D
DEM : Dynamic Equilibrium Models
DGGE : Denaturing Gradient Gel Electrophoresis
DRAC : Direction Régionale des Affaires Culturelles
DT : Dominant Taxa
DUN : Distal UNmarked surface
DZ : Dark Zone
E
EC : Enzyme Commission numbers
EBI : European Bioinformatics Institute
F
FLASh : Fast Length Adjustment of Short reads
FROGS : Find, Rapidly, OTUs with Galaxy Solution
I
IDH : Intermediate Disturbance Hypothesis
IDZ : Intermediate Dark Zone
IPH : Intermediate Productivity Hypothesis
iTOL : interative Tree Of Life
ITS : Internal Transcribed Spacer
K
KEGG : Kyoto Encyclopedia of Genes and Genomes
M
MAFFT : Multiple Alignment using Fast Fourier Transform
MAG : Metagenome Assembled Genomes
MT : Moderate Taxa
N
NCBI : National Center for Biotechnology Information
NCM : Neutral Community Model
NDZ : New Dark Zone
NMDS : Non-Metric multi-Dimentional Scaling
O
ODZ : Old Dark Zone
OTU : Operational Taxonomic Unit
P
PAST : PAleontological STatistics
PCR : Polymerase Chain Reaction
qPCR : quantitative Polymerase Chain Reaction
PERMANOVA : PERMutational ANalysis Of VAriance
PFAM : Protein FAMilies database
PUN : Proximal UNmarked surface
PVMF : PolyVinyl ForMal
R
RCbray : Raup Crick Bray Curtis
RDP : Ribosomal Database Project
S
SEM : Scanning Electron Microscopy
SSerr : Sum of Squares error
SSMS : Shallow Shotgun Metagenome Sequencing
SStotal : Sum of Squares
StARS : Stability Approach to Regularization Selection
T
TN : Tache Noire
TOC : Total Organic Carbon
U
UNESCO : United Nations Educational, Scientific and Cultural Organisation
UV : Ultra Violet
Z
ZS : Zone Sombre

Table des matières

Table des figures

Liste des tableaux

Introduction générale

La Terre s'est formée il y a 4,5 milliards d'années et les microorganismes, premières formes de vie cellulaires, sont apparus au cours des millions d'années qui ont suivi [Bell *et al.*, 2015]. Dès lors, ces organismes se sont diversifiés et ont évolué rapidement, grâce aux transferts horizontaux de gènes ou à des mutations, permettant l'occupation de chaque habitat disponible sur Terre [Prescott *et al.*, 2018]. Les microorganismes sont des contributeurs clés aux cycles biogéochimiques et représentent un compartiment de la biosphère qu'il est nécessaire de prendre en compte pour étudier les changements globaux [Madsen, 2011]. De nombreux processus écosystémiques sont pilotés par les assemblages microbiens et leurs interactions entre eux et avec leur environnement dans divers habitats (sol, corps humain, etc.) [Konopka, 2009].

Les écosystèmes peuvent être stables bien que confrontés à des variations naturelles des conditions environnementales (cycles quotidiens de lumière et température, variations saisonnières, etc.). Un écosystème sera stable tant que ces variations n'auront pas d'impact significatif sur la diversité ou la fonction des communautés microbiennes vivantes. Cette stabilité peut signifier que les variations environnementales sont modestes, mais elle peut également être due à l'asynchronisme des réponses des espèces aux fluctuations environnementales [Loreau et De Mazancourt, 2013, Abreu *et al.*, 2019]. Les écosystèmes peuvent également faire face à un ou des événements imposant une variabilité plus forte qu'habituellement. Ces évènements peuvent être naturels (gel, sécheresse, etc.) ou non (déforestation, activités touristiques, etc.), provoquant de façon provisoire une détérioration des composants de l'habitat ou de la biocénose, ce qui correspond en écologie à une perturbation [Rykiel J, 1985, Glasby et Underwood, 1996]. Dans ce contexte, comprendre la relation de cause à effet entre une perturbation et les changements de diversité est l'un des enjeux majeurs en écologie microbienne pour prédire comment une perturbation affecte les communautés microbiennes et leur fonctionnement [Shade *et al.*, 2012]. Cette relation entre perturbation et diversité microbienne fait écho au dilemme de la poule et de l'œuf : dans quel sens cette relation fonctionne-t-elle ?

La perturbation affecte la diversité microbienne. Une perturbation dans un écosystème peut être difficile à définir, car sa définition dépend de l'échelle et du contexte étudiés. Les perturbations se produisent à diverses échelles spatiales, et temporelles [Paine *et al.*, 1998], à différentes fréquences, intensités et périodicités [Shade *et al.*, 2012]. Cependant, les recherches ont montré que les conséquences d'une perturbation (quelle que soit son type) sont souvent similaires, entrainant la suppression de certains organismes, par mort ou déplacement, et modifiant directement ou indirectement la communauté [Sousa, 1984, Grime, 1977, White *et al.*, 1985, Allison, 2004, Plante, 2017, Shade *et al.*, 2012]. Dans ce contexte, il existe un nombre considérable d'études examinant les effets de perturbations sur la diversité des espèces microbiennes, dont une grande partie se positionne par rapport à trois concepts majeurs. Le premier concept repose sur l'hypothèse de perturbation intermédiaire (Intermediate Disturbance Hypothesis, IDH). L'IDH propose (i) que la diversité est maximale pour des perturbations moyennes, (ii) la richesse spécifique reste basse quand les perturbations sont fréquentes et/ou importantes, car le temps de colonisation est bref et seules les espèces à cycle court peuvent se maintenir avec succès, et (iii) la diversité est faible en l'absence de perturbation car la compétition interspécifique fixe une limite au nombre d'espèces capables de coexister [Barbault, 1997, Connell, 1997] (Figure 1). Cependant, l'IDH ne s'applique pas aux espèces mobiles en raison d'une exclusion compétitive

réduite, en particulier dans les habitats complexes. En effet, leur mobilité leur permet de disposer d'un espace de niche plus développé lors d'une faible perturbation [Bruno *et al.*, 2003]. Le deuxième concept correspond à l'hypothèse de productivité intermédiaire (Intermediate Productivity Hypothesis, IPH). L'IPH est proposé comme une modélisation de la diversité des espèces considérées le long d'un gradient de productivité, correspondant à la capacité de croissance microbienne [Al-Mufti *et al.*, 1977]. L'IPH prédit que (i) la diversité est maximale pour un taux de productivité moyen, (ii) la richesse spécifique reste basse quand la productivité est importante, et (iii) la diversité est faible en l'absence de productivité [Grime, 1977] (Figure 1). Cependant, Fox (2012) et Alder et al. (2011) ont fourni une critique détaillée de ces hypothèses. En effet, l'IDH et l'IPH sont prises en compte séparément alors que l'interaction entre les deux est le processus clé qui sous-tend le modèle d'équilibre dynamique (DEM) [Huston, 2014].

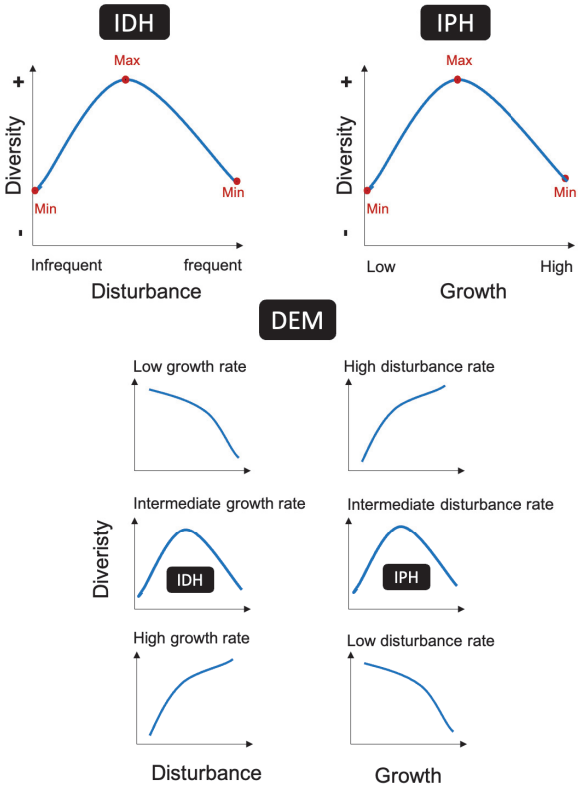

Figure 1. Représentation graphique simplifiée des hypothèses écologiques concernant les effets d'une perturbation sur la diversité des communautés microbiennes.Représentation graphique simplifiée des hypothèses écologiques concernant les effets d'une perturbation sur la diversité des communautés microbiennes.(i) IDH : l'hypothèse de perturbation, qui postule que la diversité devrait être la plus élevée aux niveaux intermédiaires de perturbation et la plus faible aux l'extrémité du gradient de perturbation. (ii) IPH : hypothèse de productivité intermédiaire, qui postule que la diversité devrait être la plus élevée aux niveaux intermédiaires de productivité et la plus faible aux extrémités du gradient de taux de croissance (growth). (iii) DEM : modèle d'équilibre dynamique, qui postule que la diversité est liée aux gradients de perturbation et de productivité, indiquant que l'IDH et l'IPH sont des cas particuliers du DEM. Modifié de Connell (1978) et de Huston (2004).

Le DEM prédit la modulation de la diversité des espèces en prenant en compte le taux d'exclusion concurrentielle (déterminé par la productivité) et le taux de perturbation (Figure 1). La perturbationest généralement acceptée comme étant le processus le plus important qui favorise l'invasion des espèces, impactant ainsi les espèces adaptées aux conditions initiales de

l'habitat, dites espèces endémiques (c'est-à-dire des espèces susceptibles d'être métaboliquement actives en fonction des conditions environnementales imposées) [Cox *et al.*, 2019, Huston, 2014, MacDougall et Turkington, 2005]. Le DEM permet d'aborder spécifiquement (i) la probabilité d'établissement d'un individu envahisseur, et (ii) la probabilité qu'un taxon envahisseur établi ait un effet significatif (dominant) sur la communauté envahie [Huston, 2014, Kilroy, 2007]. Basé sur ces approches, plusieurs études ont montré qu'un faible niveau de perturbation permet le maintien des taxons généralistes de l'habitat (taxons à répartition cosmopolite, métaboliquement actifs selon leur niveau de tolérance aux conditions environnementales) [Cox *et al.*, 2019, Kilroy *et al.*, 2007] alors qu'un niveau de perturbation plus important a un impact négatif sur ces taxons et favorise la colonisation de l'environnement par des taxons endémiques. Les espèces à distribution cosmopolite sont de meilleurs colonisateurs et ont une dispersion plus élevée que les espèces endémiques (souvent à aire de répartition restreinte) [Kilroy *et al.*, 2007].

La diversité module les effets de la perturbation. En écologie microbienne, trois types de réponses à une perturbation sont mises en évidence : (i) la résistance, définie comme le degré auquel une communauté est insensible à une perturbation, (ii) la résilience, qui est la vitesse à laquelle une communauté revient à un état antérieur à la perturbation, et (iii) un état stable alternatif, à savoir la mise en place d'une nouvelle communauté, se produisant si la résistance et la résilience sont faibles ou si la perturbation est de haute intensité [Pimm, 1984, Allison et Martiny, 2008, Beisner *et al.*, 2003, Jentsch *et al.*, 2011, Zaneveld *et al.*, 2017]. La diversité, à différentes échelles (de la souche à la communauté) va contribuer à ces différents types de réponses.

Le rôle individuel des microorganismes dans la réponse aux perturbations est généralement important lors de modifications environnementales légères et/ou temporaires. En effet, les communautés résistantes et résilientes dans ces conditions seront composées de microorganismes capables de plasticité phénotypique, de tolérance aux stress ou de dormance [Maurice *et al.*, 2013, Allison et Martiny, 2008].

Une population sera capable de moduler la réponse à la perturbation grâce aux trois processus suivants : (i) L'adaptation et l'évolution d'une population peut conduire à des mutations et des transferts horizontaux en grand nombre, facilitant la réponse de type résistance et résilience à des perturbations répétées, à forte intensité ou longues [Bennett et Lenski, 1993]. (ii) La capacité concurrentielle d'une population (taux de croissance élevé et capacité d'utilisation des ressources disponibles) permet de réagir aux perturbations, participant à la résilience microbienne lors des perturbations longues [Stevenson et Schmidt, 2004]. Enfin, (iii) l'expression stochastique des gènes et les capacités de dispersion rapide des populations peuvent jouer un rôle important dans le rétablissement des communautés après une perturbation [Avery, 2006, Shade *et al.*, 2012].

Grâce à la diversité, le renouvellement et les interactions d'une communauté microbienne peuvent moduler les réponses à une perturbation. La diversité et la résilience sont liées, selon l'hypothèse d'assurance [Yachi et Loreau, 1999], qui considère que les communautés génétiquement plus diversifiées sont plus susceptibles de contenir des taxons avec des traits de réponse complémentaires et une capacité de croissance rapide après l'arrivée d'une perturbation, pouvant favoriser la résilience. Le renouvellement de la communauté, défini par le remplacement et la substitution des membres de la communauté le long d'un gradient environnemental ou

temporel [Wilson et Shmida, 1984], est dirigé par la croissance des populations et détermine la rapidité avec laquelle une communauté atteint la résilience après perturbation. Les interactions entre membres de la communauté (e.g. compétition, mutualisme) sont importantes pour déterminer la réponse de la communauté à une perturbation, cependant les mécanismes sous-jacents de ces interactions sont souvent inconnus et difficiles à explorer au sein des écosystèmes [Little *et al.*, 2012, Shade *et al.*, 2012].

L'apparition de taxons envahisseurs est généralement importante après une perturbation de forte intensité et/ou longue. Ces taxons permettent la recolonisation de l'écosystème en impliquant un nouveau fonctionnement écologique, permettant de survivre en présence de fortes modifications des conditions environnementales, et conduisant à la mise en place d'un état alternatif stable. Cependant, le retour de la communauté à la composition ou à la fonction initiale peut être difficile une fois cet équilibre alternatif mis en place [Botton *et al.*, 2006].

Les perturbations et la diversité interagissent-elles l'une avec l'autre ? La perturbation peut favoriser la coexistence d'espèces moins communes en empêchant l'exclusion compétitive, ainsi les taxons rares (dont l'abondance relative est typiquement inférieure à 0,01% et qui sont souvent qualifiés de biosphère rare, [Sogin *et al.*, 2006]) pourraient fortement influencer la réponse des communautés microbiennes aux perturbations [Shade *et al.*, 2012, Sousa, 1984, Lyons *et al.*, 2005]. De plus, la relation perturbation-diversité peut être considérée comme cyclique, en effet la perturbation modifie la diversité, ce qui modifie la réponse de la communauté aux perturbations futures, et ainsi de suite [Huston, 2014]. Les mécanismes contrôlant la rareté des microorganismes et les processus favorisant le développement de la biosphère rare sont très peu décrits. La prise en compte des interactions et des facteurs d'assemblage des communautés (stochastiques et déterministes) permettrait une meilleure compréhension de la relation de cause à effet entre l'impact d'une perturbation et la diversité des communautés microbiennes.

Ce contexte représente cependant une image simplifiée de la situation, car la plupart des connaissances décrites ci-dessus provient soit d'expériences simplifiées ne possédant pas le réalisme des écosystèmes naturels, soit d'écosystèmes complexes présentant un grand nombre d'entités qui interagissent de manière non linéaire, ce qui limite la portée des investigations. La complexité d'un écosystème peut également être due à son hétérogénéité spatiale et temporelle. La spatialité doit être prise en compte à différentes échelles (centimétrique, régionale...), car les microorganismes étant par définition microscopiques, une variation de distance peut avoir une influence significative sur les communautés microbiennes. La temporalité est aussi essentielle car les changements microbiens se produisent en quelques secondes (expression des gènes, activités enzymatiques) ou quelques heures seulement (croissance) [Prieur, 2015]. L'hypothèse de l'hétérogénéité de l'habitat [MacArthur et MacArthur, 1961] propose qu'une forte hétérogénéité de l'écosystème puisse conduire à une augmentation de la diversité des espèces au sein de celui-ci, mettant en évidence le lien entre la diversification de la composition taxonomique en fonction des attributs de l'habitat (défini comme l'ensemble des ressources et des conditions présentes au sein d'une aire et qui permettent à une espèce d'occuper l'espace [Hall *et al.*, 1997]).

Hétérogénéité spatio-temporelle, statut écologique des taxons, et réponse aux perturbations. L'hétérogénéité spatio-temporelle des habitats a des implications en termes de diversité microbienne, mais elle conduit également à prendre davantage en compte les particu-

larités écologiques des taxons, notamment lorsque l'on s'intéresse à la réponse à des perturbations [Zhou et Ning, 2017, Philippot *et al.*, 2021]. L'un des traits importants est le caractère endémique ou cosmopolite des taxons, à l'échelle d'un habitat donné [Kilroy *et al.*, 2007]. Une forte hétérogénéité de l'écosystème peut conduire à de nombreux sous-habitats, impliquant une diversité élevée en raison de la présence de taxons endémiques susceptibles d'être actifs dans des conditions environnementales spécifiques. En revanche, la diversité peut être faible dans les systèmes où les habitats sont fragmentés et de faible étendue en raison du manque de spécialisation des espèces et de la concurrence intense entre taxons cosmopolites [Cramer et Willig, 2002]. Un autre trait important est le caractère généraliste ou spécialiste des taxons [Devictor *et al.*, 2008]. L'hétérogénéité de l'écosystème conduit donc à celle des communautés microbiennes, commençant à l'échelle de l'individu par des mutations spontanées ou induites générant des sous-populations qui elles-mêmes peuvent présenter une hétérogénéité phénotypique et métabolique. Ces sous-populations se spécialisent généralement pour occuper des niches métaboliques particulières, ce qui pourrait augmenter le taux de résilience de la communauté. Cependant, d'autres populations sont généralistes et occupent différents habitats, ce qui pourrait leur permettre de résister mieux aux fluctuations et perturbations de l'écosystème [McKinney et Lockwood, 1999, Warren *et al.*, 2001]. Enfin, un trait considéré comme majeur dans les travaux récents en écologie microbienne est le caractère dominant ou rare des taxons [Jiao et Lu, 2020, Santillan *et al.*, 2020], car les taxons rares peuvent avoir une importance significative dans le fonctionnement des écosystèmes et dans la réponse à une perturbation [Jiao et Lu, 2020]. La connaissance et la prise en compte de l'hétérogénéité au sein de l'écosystème, ainsi que du statut écologique des taxons microbiens, sont nécessaires pour définir la structure des communautés microbiennes installées et expliquer leur fonctionnement, notamment lorsque ce milieu a subi une perturbation.

Dans ce contexte, **l'hypothèse générale de ces travaux de thèse est que les perturbations, en lien avec l'hétérogénéité de l'écosystème, aboutissent à des modifications de l'assemblage communautaire, impactant notamment la répartition des taxons (endémiques vs cosmopolites) et leurs abondances (dominants vs rares) dans la communauté microbienne**.

Pour tester cette hypothèse, les écosystèmes karstiques sont des modèles de choix fournissant un ensemble unique de variables environnementales stables, en termes de lumière (absence), d'humidité relative (99%-100%), de concentrations de CO_2 (généralement 2-4%), de température ($\pm$ 0,5°C), éléments nutritifs (oligotrophie) [Canaveras *et al.*, 2001, Barton et Jurado, 2007, Bastian et Alabouvette, 2009, Cuezva *et al.*, 2009, Engel, 2010, Pašić *et al.*, 2009, Banerjee et Joshi, 2013,De Leo *et al.*, 2012]. Étudier les conséquences d'une perturbation dans un écosystème stable, permet donc d'avoir le réalisme naturel de l'environnement mais de s'affranchir des effets induits par la variation des variables environnementales. Certains écosystèmes karstiques ont subi une perturbation anthropique résultant des processus de découvertes, des aménagements et des visites touristiques. Par exemple la grotte de Lascaux a fait face à une perturbation non naturelle (anthropique) correspondant aux effets de l'aménagement du site permettant l'activité touristique, aux visites touristiques elles-mêmes et leurs conséquences (apparition d'altérations sur les parois et application de produits chimiques et antibiotiques pour les traiter). De plus, cet écosystème fait l'objet d'un suivi climatique, hydrogéologique et microbiologique depuis plus

d'une décennie. Cette grotte présente une hétérogénéité spatiale ainsi que des altérations visuelles sur les parois, nous permettant d'étudier avec réalisme les conséquences d'une perturbation anthropique sur les communautés microbiennes des trois domaines du vivant.

La grotte de Lascaux

La grotte de Lascaux (France), classée au patrimoine mondial de l'UNESCO en 1979, est une grotte calcaire de Dordogne célèbre pour ses peinture et gravures rupestres [Bastian *et al.*, 2010]. Pour permettre les visites touristiques aá partir de 1948 (qui seront interdites aá partir de 1963), de nombreux aménagements (installation d'escaliers, systèmes de renouvellement de l'air, etc.) ont eéteé effectués [Bastian *et al.*, 2010]. Ces aménagements de grande envergure et les nombreux visiteurs (2000/jour) ont perturbé l'équilibre de la grotte et le déséquilibre observé a été accentué lors des applications de biocides et d'antibiotiques sur les parois [Alonso *et al.*, 2018, Martin-Sanchez *et al.*, 2015]. Cette perturbation a engendreé des modifications visuelles de la surface d'une partie des parois de la grotte, attribuées à une prolifération anormale de microorganismes [Martin-Sanchez *et al.*, 2015]. Ces modifications visuelles ont été considérées comme des dysbioses de la cavité, et ont été qualifiées de crises microbiologiques et/ou de maladies. Une première crise microbienne, communément appelée 'maladie verte' apparue en 1955 étant notamment la conséquence de la lumière utilisée dans la grotte. Elle consiste en un biofilm vert présent sur les parois, du´ aá l'algue verte *Brateacoccus minor* ; cette maladie a eéteé éliminée par application de produits chimiques et antibiotiques [Lefèvre, 1974]. En 2001, un duvet blanc correspondant au champignon *Fusarium solani* se forme sur les parois ; cette prolifération microbienne a eéteé également éliminée par application de traitements chimiques, antibiotiques et par nettoyage manuel [Allemand et Bahn, 2005]. Enfin, la 'maladie noire' consistant en l'apparition de taches noires (attribuées aá des champignons pigmentes ; [Bastian *et al.*, 2010]) est apparue fin 2001, initialement dans une salle de la grotte appelée le Passage (Figure 2A, 2C), et s'est ensuite largement développée dans les autres salles de la grotte (Nef, Salle des Taureaux, Abside, etc.), aá partir de 2006. Elle a conduit aá un nettoyage mécanique et l'application de traitements chimiques jusqu'en 2008 [Bastian *et al.*, 2010]. Les taches noires se développent peu actuellement, et il a été observé (i) dans le Cabinet des Feélins que certaines taches avaient subi un processus d'atténuation, alors que (ii) dans l'Absidiole, des taches nettoyées mécaniquement en 2015 par les restauratrices se sont reformées dans les mois qui suivent (Figure 2C). A partir de 2008, d'autres altérations appelées zones sombres ont eéteé observées, notamment dans l'Abside (Figure 2B, 2C). Les zones sombres sont des alteérations preésentant un aspect de surface humide et grisâtre de la surface rocheuse. Ainsi, la grotte de Lascaux a subi des perturbations d'origine anthropique dues aux différents aménagements, aux visites touristiques et aux traitements chimiques. A ce jour, les taches noires et zones sombres évoluent toujours dans la grotte et sont donc des enjeux d'actualité au cœur des politiques de conservation.

Dès lors, des études scientifiques ont eéteé menées dans un premier temps par l'INRA de Dijon (coord. C. Alabouvette) puis par le Laboratoire Écologie Microbienne de Lyon (coord. Y. Moënne-Loccoz) afin de caractériser l'écologie microbienne de la grotte de Lascaux aá l'échelle écosystémique. Le premier projet, basé sur des méthodes de clonage/séquençage Sanger a permis l'identification de deux espèces fongiques dans les taches noires, *Ochroconis lascauxensis*

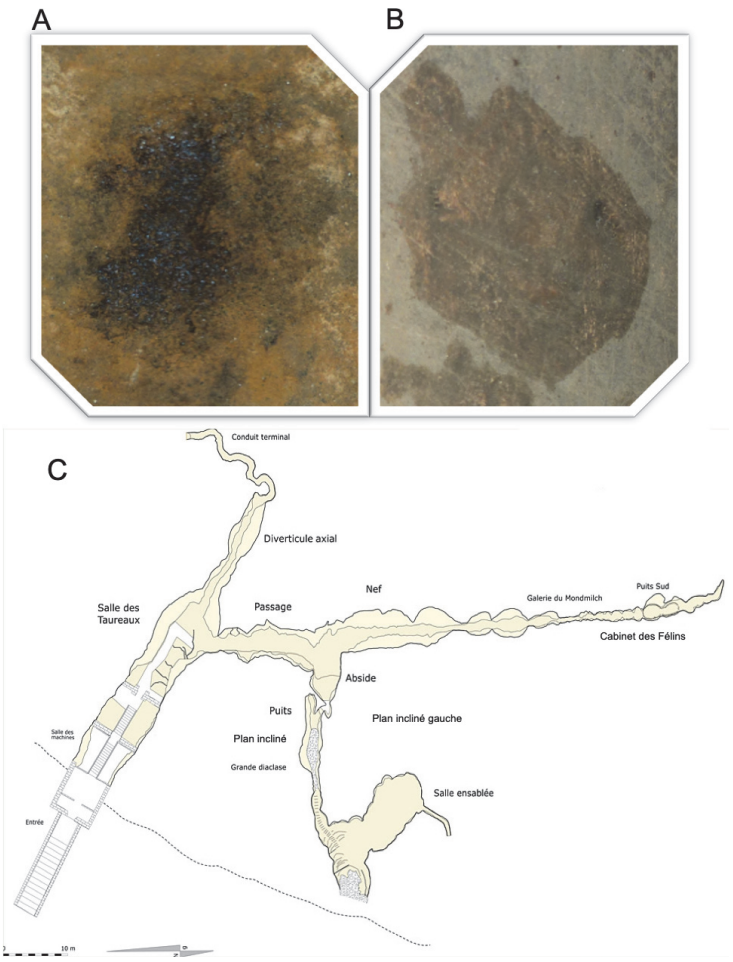

Figure 2. Photographie des altérations de type tache noire (A) et zone sombre (B). Carte de la grotte de Lascaux (d'après N. Aujoulat) (C).

(majoritaire) et *Ochroconis anomala* [Bastian *et al.*, 2010], et a montré in vitro le rôle des arthropodes (collemboles) dans la dissémination des champignons noirs qui sont présents dans les taches noires [Bastian *et al.*, 2009b], dont la production de mélanine est stimulée en présence des produits chimiques utilisés [Bastian *et al.*, 2009a]. Le second projet, basé sur des techniques de séquençage à haut débit ciblé (métabarcoding) a permis de compléter la description microbiologique de la grotte. Il a notamment été mis en évidence (i) une forte prédominance des bactéries *Pseudomonas* sur paroi non altérée (mais pas dans les taches noires ou zones sombres) et (ii) une prédominance des champignons pigmentés dans les taches noires ou zones sombres (mais pas sur les parois non altérées) (thèse de Lise Alonso 2018). L'étude des communautés microbiennes, aá savoir Archées, Bactéries et Microeucaryotes présents dans la grotte de Lascaux, a montré des structures de communautés différentes (i) dans certaines salles entre les surfaces actuellement altérées (i.e. taches noires et zones sombres) et les surfaces non-alteéreées, (ii) d'une salle aá l'autre (i.e. Passage, Salle des Taureaux, etc.) ou (iii) d'un substrat géologique aá l'autre [Alonso, 2018]. Par contraste, les communautés microbiennes présentent très peu de variabilité saisonnière (i.e. hiver versus eéteé) et interannuelle.

Ces précédents projets ont permis d'établir un état des lieux microbien de la grotte et de proposer des hypothèses quant aá la formation des altérations. Cependant, ils n'ont pas traiteé

des processus de formation et d'évolution des altérations, qui restent encore non caractérisés aá ce jour. En particulier, on ne sait pas comment se produit le développement des altérations d'un point de vue microbiologique. Bien que l'état sanitaire de la grotte se soit globalement stabiliseé ces dernières années, certaines altérations continuent de se développer. Afin de combler le manque de connaissances sur les processus de formation, d'évolution et de régression (éventuelle) des altérations, un troisième projet d'écologie microbienne a été mis en place en 2019. Ce projet basé sur des approches de séquençage à haut débit (métabarcoding et métagénomique), va permettre d'investiguer les processus régissant la mise en place de ces altérations, par un suivi temporel et à différentes échelles dans la grotte, permettant l'étude des conséquences d'une perturbation sur la diversité microbienne des trois domaines du vivant. Ce projet est coordonné par Yvan Moënne-Loccoz (UMR CNRS 5557 Ecologie Microbienne, Université Claude Bernard Lyon 1).

Objectifs du projet 'Écologie microbienne de la grotte de Lascaux'

Le projet 'Écologie microbienne de la grotte de Lascaux' (2019-2023) est basé sur plusieurs observations clés : les zones altérées et zones saines étant visuellement très différentes en termes de couleur et d'aspect de surface, sans zone de transition apparente, on peut donc penser que la formation de ces altérations implique une succession microbienne rapide pendant laquelle se produit l'apparition des champignons pigmentés (ou leur disparition en cas d'atténuation des altérations). Les observations réalisées suggèrent aussi que les collemboles *Folsomia candida* jouent un rôle cléé facilitant la dissémination des champignons pigmentés hors des parties altérées, car ils sont présents sur les altérations (taches noires et zones sombres) et pourraient déclencher les successions microbiennes impliquées dans la mise en place des altérations sur les parois saines. Ces observations ont permis de définir plusieurs objectifs dans ce projet, (i) caractériser les communautés microbiennes des zones visuellement contaminées des parois en fonction du temps et à plusieurs échelles spatiales de la grotte, en ciblant plus particulièrement la formation des zones sombres et les phénomènes de recolonisation/régression des taches noires dans l'Abside et le Cabinet des Félins ; (ii) caractériser la pigmentation microbienne des parois, en étudiant le métagénome des altérations afin de rechercher les gènes associés à la pigmentation/dépigmentation, analyser la composition en mélanines des zones sombres et évaluer in vitro les méthodes (physiques et chimiques non agressives) pour la dépigmentation des mélanines microbiennes ou champignons pigmentés, réalisé avec le Centre d'Étude des Substances Naturelles (CESN) de l'UMR Écologie Microbienne ; (iii) étudier le rôle des collemboles dans la dissémination des microorganismes responsables d'altérations en utilisant des méthodes moléculaires. Ce dernier objectif est réalisé en collaboration avec l'équipe de C. Douady du Laboratoire d'Écologie des Hydrosystèmes Naturels et Anthropisés (LEHNA) et T. Tully de l'Institut d'Ecologie et des Sciences de l'Environnement de Paris (IESS).

Afin d'étudier la communauté microbienne de façon globale, la technique de séquençage à haut débit des acides nucléiques a été utilisée, avec une approche de métabarcode ciblant les trois domaines de la vie, via l'ARNr 16S des bactéries, l'ARNr 16S des archées, l'ARNr 18S des micro-eucaryotes et l'Internal Transcribed Spacer 2 (ITS2) pour identifier la communauté fongique. C'est dans ce contexte qu'a été réalisée cette thèse, qui répond en partie aux deux premiers objectifs du projet.

Objectifs et démarche de la thèse

L'objectif principal de cette thèse était de comprendre les dynamiques de la diversité microbienne lors de la formation et l'évolution des altérations (taches noires et zones sombres) déclenchées par l'ensemble des perturbations anthropiques survenues dans la grotte de Lascaux, en utilisant les nouvelles technologies de séquençage à haut-débit. Cet objectif vise notamment à explorer les successions microbiennes impliquées dans l'évolution (formation ou atténuation) des altérations, à plusieurs échelles spatio-temporelles, et à identifier les interactions et processus microbiens sous-jacents.

Pour atteindre cet objectif général, quatre hypothèses de travail ont été définies et testées, en lien avec des sous objectifs particuliers, comme suit. **Premièrement**, la formation et l'évolution des zones sombres seraient liées à des successions microbiennes rapides car les zones altérées et zones saines sont visuellement très différentes, sans zone de transition apparente. Si cette hypothèse est valide, on s'attend à ce que l'abondance des champignons pigmentés (*Ochroconis*, *Exophiala*, etc.) soit faible sur les surfaces non altérées tandis que leur abondance augmenterait très fortement, rapidement et de façon très nette dans les parties altérées. Le sous objectif associé à cette hypothèse est de caractériser à micro-échelle spatiotemporelle la dynamique des trois domaines du vivant lors de l'évolution des zones sombres.

Deuxièmement, au moins une partie des changements de la communauté microbienne liés à la formation de zone sombre implique des taxons cosmopolites, car ces zones sombres se développent dans différents habitats microbiens au sein de Lascaux, mais aussi des taxons endémiques conformément aux spécificités du microbiote des différentes pièces ou surfaces. Si cette hypothèse est valide, on s'attend à ce que la structure et la composition microbienne des zones sombres soient différentes en fonction des propriétés des salles et des surfaces géologiques. Le sous objectif associé à cette hypothèse, est de caractériser la dynamique de la diversité microbienne au niveau des zones sombres, à l'échelle spatiale de l'ensemble de la grotte.

Troisièmement, les dynamiques de régression (atténuation) de certaines taches noires dans le Cabinet des Félins et de repousse des taches noires dans l'Absidiole seraient liées à des successions microbiennes particulières, impliquant des taxons rares de la communauté car ils peuvent présenter des comportements/fonctions particulier(e)s dans ces dynamiques, et peut-être même des successions opposées car des phénomènes de régression et de recolonisation sont observés. Visuellement, les phénomènes de régression sont associés à une transition de teintes noire à grise tandis que les phénomènes de recolonisation sont associés à une transition de teinte 'calcaire' beige à noire. Si cette hypothèse est confirmée, alors les successions microbiennes impliquées lors des modifications des taches noires supporteront des processus microbiens opposés, avec certains taxons impliqués qui sont peut-être les mêmes au cours des deux types de dynamiques étudiées, lors des étapes intermédiaires. Le sous objectif associé à cette hypothèse est d'identifier, d'une part, des populations microbiennes potentiellement en lien avec la dépigmentation des parois et, d'autre part, celles qui correspondent aux premiers stades de recolonisation des surfaces lors de la reformation de ces altérations.

Quatrièmement, les taches noires étant attribuées à l'activité des champignons pigmentés et ces champignons colonisant les deux types d'altérations, nous pouvons penser que les mêmes types de fonctions fongiques de pigmentation seraient impliquées dans les deux cas et qu'elles

concerneraient des taxons spécialistes des conditions environnementales particulières correspondant aux altérations. Si cette hypothèse est correcte, cela impliquerait que les gènes contribuant à la synthèse de mélanines et autres pigments noirs seraient davantage présents dans la communauté microbienne des zones altérées. Le sous objectif associé à cette hypothèse de caractériser le métagénome de plusieurs taches noires et zones sombres en comparaison avec la paroi non altérée, et d'analyser les gènes de pigmentation microbienne.

Structure de la thèse

Le manuscrit de thèse est structuré en cinq parties. **La première partie** regroupe deux synthèses bibliographiques. La première traite du microbiote des grottes datant du paléolithique ayant subi une perturbation de type anthropisation impliquant une activité touristique, prenant en compte les caractéristiques endémiques du microbiote des grottes et la comparaison entre grottes anthropisées et non anthropisées. La deuxième synthèse s'intéresse aux enjeux des nouvelles techniques de séquençage dans la compréhension des écosystèmes karstiques, comprenant l'évolution des techniques d'études (de la culture jusqu'aux méthodes -omiques) ainsi que l'utilisation d'approches intégratives dans ces écosystèmes.

La deuxième partie teste (i) si la formation et l'évolution des zones sombres sont liées à des successions microbiennes rapides ; pour ce faire, un échantillonnage à micro-échelle spatio-temporelle a été réalisé en avril 2019, décembre 2019 et avril 2021 sur le plan incliné gauche de l'Abside, comparant cinq situations évolutives (surfaces non marquées distantes et proches de la zone sombre, zone sombre nouvelle, zone sombre intermédiaire et zone sombre vieille) ; (ii) si les changements de la communauté microbienne liés à la formation de zones sombres sont spécifiques à la pièce/surface ; pour ce faire, une étude comparative de neufs zones sombres et des surfaces non altérées voisines a été réalisé à partir d'échantillons prélevés en septembre 2020 dans l'ensemble de la grotte, permettant la prise en compte de différents types de substrats minéraux (calcaire natif, banquette maçonnée et blocs de calcaire Santonien). Dans les deux cas, la structure et la composition des communautés microbiennes ont été analysées par séquençage à haut débit ciblant les marqueurs taxonomiques (ARNr 16S bactéries, ARNr 16S archées, ARNr 18S micro-eucaryotes et ITS2 fongique) ainsi que l'abondance des bactéries, micro-eucaryotes et champignons par PCR quantitative. De plus, la construction de réseaux de co-occurrence et la quantification des processus d'assemblage des communautés ont été effectuées pour comprendre l'évolution des zones sombres à micro-échelle spatio-temporelle.

La troisième partie teste si les dynamiques de régression (atténuation) de certaines taches noires dans les Félins et de repousse des taches noires dans l'Absidiole sont liées à des successions microbiennes particulières a été réalisée en étudiant les populations microbiennes des trois domaines du vivant impliquées dans ces dynamique (régression et recolonisation) ont été identifiées par séquençage à haut débit (ciblant l'ARNr 16S bactéries, ARNr 16S archées, ARNr 18S micro-eucaryotes et ITS2 fongique). Le phénomène d'atténuation naturelle des taches noires mis en évidence dans l'entrée du Cabinet des Félins et échantillonné en 2017 a fait l'objet de l'étude des processus d'assemblage des communautés microbiennes en réponse à une perturbation pour les trois domaines du vivant et plusieurs catégories de taxons (abondants, modérés, rares, etc.) conduisant à l'identification de scenari écologiques. Tandis que l'occurrence de dy-

namique contraire concernant la recolonisation de taches noires a été étudié dans l'Abside suite à un nettoyage mécanique réalisé en septembre 2020 et analysée à partir de plusieurs dates d'échantillonnage, permettant d'investiguer la structure et la composition des communautés microbiennes de cette dynamique.

La quatrième partie teste si une activité des champignons pigmentés est identifiée dans les deux types d'altérations (taches noires et zones sombres). Cette partie a été réalisée par approche métagénomique, permet l'étude des processus de pigmentation/dépigmentation des parois et également du potentiel métabolique des communautés microbiennes présentes. Cette approche concerne des zones altérées récentes, (i) des taches noires et leurs témoins échantillonnées dans la Nef et (ii) des zones sombre et leur témoin échantillonnées dans l'Abside en décembre 2020 et avril 2021 et sur les banquettes maçonnées du Passage en avril 2021. Dans un premier temps l'abondance relative et le potentiel métabolique ont été étudiés ; dans un second temps les génomes ont été reconstruits (MAG, Metagenome Assembled Genomes) et annotés pour chaque condition.

La cinquième partie est consacrée à la discussion générale de l'ensemble des travaux réalisés et aux perspectives de ces recherches.

CHAPITRE 1

Synthèse bibliographique

Avant propos

Cette thèse qui traite de la dynamique de la diversité microbienne dans les environnements karstiques a été démarrée par un état de l'art concernant les communautés microbiennes hébergées dans ce type d'environnement. Ces aspects ont été passés en revue au travers d'une synthèse bibliographique

Les micro-organismes colonisent abondamment les grottes et, dans les grottes ouvertes au tourisme, ils peuvent provoquer des altérations sur les surfaces murales [Engel, 2010, Martin-Sanchez *et al.*, 2015]. C'est une préoccupation majeure dans les grottes présentant de l'art pariétal, qui est généralement fragile et peut être irrémédiablement endommagé par des altérations microbiennes. Récemment, le développement des technologies de séquençage à haut débit a permis plusieurs descriptions de la diversité microbienne des grottes permettant d'étudier l'impact de l'anthropisation liée au tourisme sur les microorganismes des grottes paléolithiques, et le développement des altérations microbiennes sur les parois de ces grottes pour les trois domaines du vivant (Bactéries, Archées, microeucaryotes). Cette revue met en évidence que les phyla microbiens prévalents dans les grottes vierges sont similaires à ceux mis en évidence dans les microbiotes de l'eau, du sol, des plantes et des métazoaires, mais les spécificités aux niveaux taxonomiques inférieurs restent à clarifier. Le tourisme peut provoquer différents types d'altérations (modifications du microbiote) des grottes paléolithiques, mais des études à plus grande échelle sont nécessaires car ces modifications peuvent différer d'une grotte à l'autre. De nombreux micro-organismes potentiellement impliqués dans ces altérations ont été identifiés, mais les analyses de diversité n'incluent pas systématiquement une comparaison avec des zones voisines non altérées comme témoins, ce qui rend ces associations incertaines.

Cette revue a été rédigée en utilisant une partie de la synthèse bibliographique effectuée précédemment par Lise Alonso durant sa thèse (premier projet d'écologie microbienne de la grotte de Lascaux), qui concernait les processus de colonisation des microorganismes dans les grottes. Mon rôle dans ce travail a été de mettre à jour les connaissances disponibles, d'ajouter des nouvelles connaissances bibliographiques (microorganismes présents dans les grottes, effet de l'anthropisation sur le microbiote des grottes et la composition des altérations microbiennes sur les parois des grottes), et d'effectuer des comparaisons de microbiote provenant de plusieurs écosystèmes. Pour cela j'ai effectué des recherches bibliographiques, compilé les résultats de plusieurs études et réalisé des figures pour illustrer mes propos.

Cette synthèse bibliographique 'Microbial ecology of Paleolithic caves' **(Article 1)** a été publiée dans le journal 'Science of the Total Environment' en décembre 2021.

Article 1. Microbial ecology of Paleolithic Cave

ZELIA BONTEMPS[1], LISE ALONSO[1], THOMAS POMMIER[1], MYLENE HUGONI[1,2] AND YVAN MOENNE-LOCCOZ[1]

[1]Univ Lyon, Université Claude Bernard Lyon 1, CNRS, INRAE, VetAgro Sup, UMR Ecologie Microbienne, F-69622 Villeurbanne, France
[2]Institut Universitaire de France (IUF)

Current address for Lise Alonso : INRS, 1 rue du Morvan, CS 60027, F-54519 Vandoeuvre-lès-Nancy, France

Corresponding author
Yvan Moënne-Loccoz
Univ Lyon, Université Claude Bernard Lyon 1, CNRS, INRAE, VetAgro Sup, UMR5557 Ecologie Microbienne, 43 bd du 11 novembre 1918, F-69622 Villeurbanne, France
yvan.moenne-loccoz@univ-lyon1.fr

Article history
Received 16 August 2021
Received in revised form 19 October 2021
Accepted 3 November 2021
Available online http ://dx.doi.org/10.1016/j.scitotenv.2021.151492
Editor : Ewa Korzeniewska

Highlights

- High-throughput sequencing is shedding new light on the cave microbiota
- At the phylum level, microbial composition of caves and other ecosystems is similar
- It is needed to explore the cave microbiota at a finer taxonomic level
- Tourism may cause significant shifts in the microbiota of Paleolithic caves
- Tourism-related microbial alterations require further research attention

Abstract

Microorganisms colonize caves extensively, and in caves open for tourism they may cause alterations on wall surfaces. This is a major concern in caves displaying Paleolithic art, which is usually fragile and may be irremediably damaged by microbial alterations. Therefore, many caves were closed for preservation purposes, e.g. Lascaux (France), Altamira (Spain), while others were never opened to the public to avoid microbial contamination, e.g. Chauvet Cave (France), etc. The recent development of high-throughput sequencing technologies allowed several descriptions of cave microbial diversity and prompted the writing of this review, which focuses on the cave microbiome for the three domains of life (Bacteria, Archaea, microeukaryotes), the impact of tourism-related anthropization on microorganisms in Paleolithic caves, and the development of microbial alterations on the walls of these caves. This review shows that the microbial phyla prevalent in pristine caves are similar to those evidenced in water, soil, plant and metazoan microbiomes, but specificities at lower taxonomic levels remain to be clarified. Most of the data relates to Bacteria and Fungi, while other microeukaryotes and Archaea are poorly documented. Tourism may cause shifts in the microbiota of Paleolithic caves, but larger-scale investigation are required as these shifts may differ from one cave to the next. Finally, different types of alterations can occur in caves, especially in Paleolithic caves. Many microorganisms potentially involved have been identified, but diversity analyses of these alterations have not always included a comparison with neighboring unaltered zones as controls, making such associations uncertain. It is expected that omics technologies will also allow a better understanding of the functional diversities of the cave microbiome. This will be needed to decipher microbiome dynamics in response to touristic frequentation, to guide cave management, and to identify the most appropriate reclamation approaches to mitigate microbial alterations in tourist Paleolithic caves.

Graphical abstract

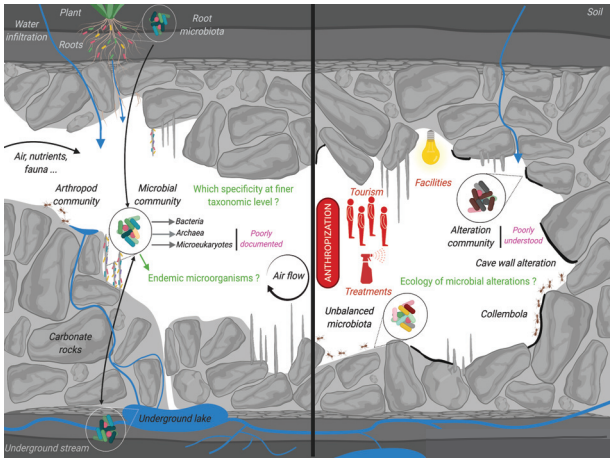

Key words

Tourist caves ; anthropization ; microbial colonization ; microbiome ; Paleolithic art ; rock surface alteration.

1. INTRODUCTION

Karsts correspond to particular landscapes formed on carbonate rocks (limestone, dolomite, marble, etc.) or evaporites (gypsum, etc.) and that are characterized by the development of an extensive underground drainage network (Bakalowicz, 1999 ; Engel and Northup, 2008). Water infiltration through carbonate rocks is instrumental in CO_2-mediated chemical dissolution of limestone and dolomite, and it may result in the formation of karstic caves (Cuezva et al., 2012). On one hand, karstic caves are characterized by the corrosion and/or erosion processes at the origin of the karstification phenomenon. On the other hand, they are also typified by the subsequent carbonate precipitation taking place depending on the behavior of underground water, and leading to the formation of speleothems such as stalactites and stalagmites (Perrette et al., 2000).

Karstic caves display particular environmental conditions, characterized by darkness, high level of relative humidity (near saturation), stable temperatures (Bastian and Alabouvette, 2009, Cuezva et al., 2009 ; Pasić et al., 2010) and elevated CO_2 concentrations (Banerjee and Joshi, 2013). Levels of minerals are high (Barton and Jurado, 2007 ; Bastian et al., 2010) but caves are oligotrophic regarding organic matter (Cañveras et al., 2001 ; Cuezva et al., 2009 ; Jurado et al., 2010), with typically less than 2 mg of total organic carbon per liter (Barton and Jurado, 2007). Most organic carbon in caves originates from the surface and makes its way into the endokarst via water percolation through plant root channels and cracks in the epikarst (i.e. the overlying rock), air flows transporting minute organic particles and gaseous organics, or animal dejections e.g. bat guano (Saiz-Jimenez and Hermosin, 1999 ; Barton and Jurado, 2007 ; Cuezva et al., 2009 ; Pasić et al., 2010 ; Vanderwolf et al., 2013). Caves may also represent heterogeneous systems because of the nature and surface properties of the various internal rock layers, the architecture and connectivity of the cave (Cañveras et al., 2001 ; Nehme, 2013), as well as airflow and climatic exchanges with the outside atmosphere (Russell, 1998 ; Banerjee and Joshi, 2013). Outside conditions impact most on the entrance zone of caves (Banerjee and Joshi, 2013), and thus climatic fluctuations within caves depend on the distance to the entrance, as well as epikarst thickness (Cuezva et al., 2009).

Despite the particular, apparently unfriendly environmental conditions prevailing in caves (Schabereiter-Gurtner et al., 2002 ; Cuezva et al., 2009), these underground ecosystems appear to host a broad range of microorganisms (Engel and Northup, 2008 ; Saiz-Jimenez, 2012) and current high-throughput sequencing methods have started to document the extent of microbial diversity in caves (Pfendler et al., 2018 ; Alonso et al., 2019 ; Thompson et al., 2019). Bacteria, Archaea and microeukaryotes typically coexist within microbial communities in all ecosystems, and caves are no exception to this. This microbial world can play significant roles in caves, starting from the modulation of geochemical processes responsible for cave formation (Jurado et al., 2010). Indeed, microorganisms are involved in the karstification process through chemical weathering (by releasing organic acids), biological physical weathering (by fungal growth-mediated breaking down and mechanical dislodging of loose limestone particles) and enzymatic weathering (by the production of carbonic anhydrase enzymes) (Lian et al., 2011 ; Hou et al., 2013). In addition, microbial activity might contribute to the formation of various mineral constituents in caves, including moonmilk, saltpeter, mineral precipitates, etc. (Northup, 1997 ; Cañveras et

al., 2001 ; Brannen-Donnelly and Engel, 2015). Finally, microorganisms play a key role in the production and turnover of organic matter (Barton and Northup, 2007 ; Jurado et al., 2010 ; García Antón et al., 2013). Microbial activities may be of particular importance in certain Paleolithic caves, where excessive tourism has enhanced organic C inputs facilitating thus microbial proliferation, which might threaten artwork quality (Cañveras et al., 2001 ; Bastian et al., 2010 ; Martin-Sanchez et al., 2012a). This review deals with the microbial ecology of karstic caves, with a focus on tourist Paleolithic caves for which conservation issues represent a challenge. The processes of microbial colonization in caves are described, along with the resulting microbial diversity expected in caves. The impact of tourism on the microbiota of Paleolithic caves is then reviewed, including its consequences in terms of microbial proliferation and alteration of cave surfaces and Paleolithic art.

2. PROCESSES OF MICROBIAL COLONIZATION IN CAVES

2.1 Microbial entry into caves and adhesion to cave surfaces

Caves represent underground and enclosed environments, but they are connected with the surrounding environment present outside the cave (Garcia-Antón et al., 2013 ; Hershey and Barton, 2018 ; Morse et al., 2021). Thus, microorganisms may enter in caves and karst ecosystems following passive dissemination by infiltrating water (Dupont et al., 2007 ; Davis et al., 2020) or air currents (Engel and Northup, 2008 ; Cuezva et al., 2009 ; Vanderwolf et al., 2013). Concerning air dissemination, Fungi are probably largely transported as spores, whereas Bacteria are more likely to enter caves as cells adhering to dust particles (Dupont et al., 2007 ; Chen et al., 2009 ; Garcia-Antón et al., 2013). Biotic vectors may also be involved, especially incoming humans or animals such as arthropods (Barton and Jurado, 2007 ; Dupont et al., 2007) and bats (Vanderwolf et al., 2013). In the case of tourist caves, humans might constitute the most important factor favoring microbial arrival. Arthropods can differently promote the dispersion of Bacteria (Scheu and Simmerling, 2004), Archaea (Moissl-Eichinger and Huber, 2011) and Fungi (Thimm et al., 1998) by carrying these microorganisms on their bodies or hosting them in their gut (Thimm et al., 1998). Therefore, most microorganisms present in caves were considered, at least in earlier studies, to have been transported there, which means they have often been regarded as not representing a cave-specific microbiota (Keswick et al., 1982 ; Palmer et al., 1991 ; Cunningham et al., 1993 ; Northup et al., 1994 ; Rusterholtz and Mallory, 1994 ; Gorbushina, 2007 ; Herzog Velikonja et al., 2014). For instance, in Lascaux Cave, this allochthonous status has been proposed for the facultative entomophilous *Geosmithia* species (Bastian et al., 2009b). However, evidence also points to the occurrence of microorganisms as intrinsic cave inhabitants (Schabereiter-Gurtner et al., 2004). The Schneider-Racoviță classification of underground species as trogloxenes, troglophiles or troglobionts (troglobitic) according to their preferred habitat and origin(s) (Mammola, 2019) is little implemented yet for microorganisms (Snider et al., 2009 ; Zhang et al., 2018), but this concept deserves attention as it might prove useful as well to characterize the status of microbial species. The main process(es) leading to the entry of allochtonous microorganisms into caves varies according to cave specifics. In Altamira Cave, gaseous phase exchanges with the outside atmosphere matter most (Cuezva et al., 2009 ; Saiz-Jimenez et al.,

2011 ; Garcia-Antón et al, 2013), whereas in Lascaux Cave the arthropods are thought to play a larger role (Bastian et al., 2009b ; Bastian et al., 2010).

Once entered in the cave, microorganisms might colonize and proliferate on the surfaces available. The establishment of microorganisms on cave walls requires adhesion to the wall surface (Cuezva et al., 2009). The most studied adhesion mechanism in Bacteria and Fungi is the secretion of extracellular polysaccharides (Gorbushina, 2007 ; Zucconi et al., 2012), leading to biofilm formation and facilitating adhesion for additional microorganisms like Cyanobacteria and other Bacteria, Fungi and microalgae (Riding, 2000). In the case of Fungi, hyphae can also penetrate directly into microporous wall surfaces (Sterflinger, 1998 ; Kumar and Kumar, 1999 ; Gorbushina, 2007), thereby promoting colonization of these rock materials (Stupar et al., 2014). Microclimatic conditions may modulate adhesion conditions, as condensation on walls forms clouds of water microparticles (named hydroaerosols) that support adhesion for microorganisms carried by air particles (Cuezva et al., 2009 ; Garcia-Antón et al., 2013). In turn, microbial adhesion to rock surfaces may facilitate biotransformations of minerals that provide nutriments or energy (Riding, 2000), as well as microbial growth (Cuezva et al., 2009).

2.2 Microbial growth and establishment in caves

Once microorganisms interact with cave surfaces, the particular microclimate and resource availability on rock surfaces will determine the possibilities of microbial growth and colonization (Gorbushina, 2007 ; Cuezva et al., 2009). Although the majority of cave microorganisms do not function as autotrophs (Laiz et al., 1999 ; Simon et al., 2019 ; Bastian et al., 2009a), photosynthesis takes place in tourist caves where artificial lights are operated, and consequently chemoautotrophy may play an important role by providing organic matter (Cañveras et al., 2001 ; Barton and Jurado, 2007 ; Barton and Northup, 2007). Overall, oligotrophic conditions on rock surfaces lead to low growth rates (Portillo and Gonzalez, 2010), where the availability of organic carbon is often limiting (Stomeo et al., 2009). In such cases, inputs of organic matter into the cave (through infiltrating water, air-borne particles, human inputs, incoming fauna or flooding by subterranean streams in certain cases ; Cañveras et al., 2001 ; Morse et al., 2021) will play an important role (Jurado et al., 2010 ; Garcia-Antón et al., 2013). Experimental analysis of sterilized rock tablets placed in Altamira Cave showed that bacterial and fungal colonization, based on visible growth and scanning electron microscopy, needed several months (Jurado et al., 2009). In certain cases where nutrients are not limiting, cave conditions promote microbial proliferation and may lead to the formation of stains, as reported in Lascaux Cave (Bastian et al., 2010), or visible colonies as described in Altamira Cave (Schabereiter-Gurtner et al., 2002 ; Portillo et al., 2008). Rather than forming single microcolonies, Fungi, algae and Bacteria are likely to coexist (Gorbushina, 2007), often in mixed biofilms (Schabereiter-Gurtner et al., 2002 ; Portillo et al., 2008).

Microbial interactions taking place in caves remain largely undocumented. Cave oligotrophy probably leads to strong competition for substrates among microorganisms (Bhullar et al., 2012). This competition is probably assisted by the release of antimicrobial secondary metabolites, and both microorganisms with antimicrobials production ability (Ghosh et al., 2017) and antibiotic resistance traits (Bhullar et al., 2012) can be isolated from caves. Yet, species coexistence within

cave microbial communities raises the possibility that even positive interactions, such as cooperation and mutualism, are also taking place (Barton and Jurado, 2007). Due to the presence of light, lichens may often be found near the entrance of certain caves (Roldán and Hernández-Mariné, 2009). Bacterial chemoautotrophs have been suggested to interact with heterotrophic microorganisms in various caves (Cunnigham et al., 1993 ; Vanderwolf et al., 2013). Indeed, it is likely that a large number of microorganisms rely on organic substrates (carbon and energy sources) provided by other microbial community members (Barton and Jurado, 2007 ; Barton, 2006), as in other types of environments.

Once established in caves, microorganisms may be remobilized and spread further, but probably across shorter distances than during initial arrival of external microorganisms into these underground ecosystems. Wind currents within Altamira Cave are thought to favor formation of Bacteria-containing aerosols from condensed water present on rock surfaces in the cavity, thereby enhancing bacterial spread (Garcia-Antón et al., 2013). In Lascaux, arthropods such as collembola are likely to disseminate cave Bacteria and Fungi, specifically those associated with black stains (Bastian et al., 2010). Therefore, certain areas within caves might also serve as microbial reservoirs, both for indigenous and allochthonous microorganisms, with the possibility of subsequent recolonization processes from one cave area to the other (Engel, 2010 ; De Mandal et al., 2016).

3. MICROORGANISMS TYPICALLY PRESENT IN CAVES

The structure of cave microbial communities is rather stable in time (Tomczyk-Żak and Zielenkiewicz, 2016 ; Alonso et al., 2018) but it can vary according to (i) local conditions, such as the type (Jones and Macalady, 2016) and heterogeneity (Cuezva et al., 2009) of mineral or organic surfaces, and (ii) many specific physicochemical factors including pH, nutrient availability, etc. (Engel, 2010 ; De Leo et al., 2012). Caves are thought to be colonized by highly-specialized microorganisms (Schabereiter-Gurtner et al., 2002 ; Bastian and Alabouvette, 2009 ; De Leo et al., 2012), and both culture-dependent and culture-independent methods have evidenced that Bacteria and Fungi inhabiting karstic caves are very diverse (Schabereiter-Gurtner et al., 2002 ; Barton and Northup, 2007 ; Jurado et al., 2010 ; Alonso et al., 2019). Culture-independent methods especially with the advent of high-throughput sequencing are now providing an exhaustive view of microbial richness and diversity, and also facilitate the inventory of Archaea and non-fungal microeukaryotes, so far neglected in most investigations (Table 1, Fig. 1).

3.1 Bacteria in caves

Data obtained across a broad range of caves, especially using culture-independent methods, indicate that the bacterial community is largely dominated by Proteobacteria and Actinobacteria (Table 2) (Cañveras et al., 2001 ; Cuezva et al., 2009 ; Saiz-Jimenez, 2012 ; Diaz-Herraiz et al., 2014 ; Dhami et al., 2018 ; Zhu et al., 2019). The high abundance of Proteobacteria may be partly due to their ability to degrade a wide range of organic compounds, whereas Actinobacteria members are involved in biomineralization processes (De Leo et al., 2012 ; Tomczyk-Żak

and Zielenkiewicz, 2016). Other phyla identified through high-throughput sequencing methods include Acidobacteria, Firmicutes and Nitrospirae, which are also abundant in caves, as well as Gemmatimonadetes, Planctomycetes, Verrucomicrobia and Cyanobacteria whose members are not recovered by conventional laboratory cultivation methods (Table 1). These phyla were shown to be abundant in many caves from Australia, China, Spain and the USA (Barton and Jurado, 2007 ; Bastian and Alabouvette, 2009 ; Adetutu et al., 2012 ; Ortiz et al., 2014 ; Yun et al., 2016). The 11 main phyla gather the vast majority of bacterial sequences, whereas 8.3% of the sequences shown in Fig. 1a correspond to the rarest phyla, so far hardly documented. Fluctuations in the relative abundance of phyla in the eight cave conditions shown in Appendix S1 (Table S1) are quite substantial, especially when comparing with the stalactites (which represent specific physico-chemical properties ; Ortiz et al., 2014 ; Zepeda Mendoza et al., 2016) of Cave Herrenberg and the floor of Cave Buraco da Sopradeira, located in a semi-arid region (e.g. with a difference of 14% for Proteobacteria) (Marques et al., 2019). Indeed, different bacterial communities can be evidenced when comparing different caves (Saiz-Jimenez, 2012 ; Alonso et al., 2019 ; Zhu et al., 2019) or different conditions within a cave (Schabereiter-Gurtner et al., 2002 ; Cuezva et al., 2009 ; Yun et al., 2016 ; Dhami et al., 2018 ; Alonso et al., 2018).

Table 1. Mean, minimal and maximal relative abundance (%) of phyla retrieved in the microbiome of non-anthropized caves with culture-dependent approaches. Minimal and max- imal abundances of phyla, number of caves and number of countries are calculated without considering the null values. Hyphens are used when no data is available. Archaea are not included as they are not readily amenable to cultivation. Non-fungal microeukaryotes (Amoebozoa, Stramenopiles, Alveolata, Chlorophyta) have hardly been investi- gated and are not shown.

Phyla	Relative abundance (%)			Number of caves *(where evidenced)*	References
	Min	Max	Mean		
BACTERIA					
Proteobacteria	2.4	41.1	22.4	7	Adetutu et al. 2012; Barton 2015; Griffin et al. 2014; Herzog Velikonja et al. 2013; Northup et al. 2003; Schabereiter-Gurtner et al. 2004
Actinobacteria	11.6	95.1	35.7	6	Adetutu et al. 2012; Barton 2015; Griffin et al. 2014; Northup et al. 2003; Schabereiter-Gurtner et al. 2004
Chloroflexi	1.2	1.2	0.2	1	Schabereiter-Gurtner et al. 2004
Acidobacteria	16.5	16.5	7.9	2	Herzog Velikonja et al. 2013; Schabereiter-Gurtner et al. 2004
Bacteroidetes	4.9	6.3	4.5	6	Barton 2015; Griffin et al. 2014; Herzog Velikonja et al. 2013; Nováková et al. 2005; Schabereiter-Gurtner et al. 2004
Firmicutes	5.0	37.9	10.2	4	Adetutu et al. 2012; Barton 2015; Northup et al. 2003
Gemmatimonadetes	-	-	-	-	-
Planctomycetes	-	-	-	-	-
Nitrospirae	15.5	15.5	1.9	1	Northup et al. 2003
Verrucomicrobia	-	-	-	-	-
Cyanobacteria	-	-	-	-	-
Other taxa	1.2	93.7	14.4	3	Adetutu et al. 2012; Nováková et al. 2005; Schabereiter-Gurtner et al. 2004
Unidentified taxa	0.1	0.1	0	1	Schabereiter-Gurtner et al. 2004
FUNGI					
Ascomycota	5.5	96.1	94.9	5	Adetutu et al. 2011; Belyagoubi et al. 2018; Jacobs et al. 2017; Nováková et al. 2005; Vaughan et al. 2011
Basidiomycota	1.9	7.6	2.5	3	Adetutu et al. 2011; Jacobs et al. 2017; Nováková et al. 2005; Vaughan et al. 2012
Zygomycota	2.6	2.6	1.8	3	Belyagoubi et al. 2018; Jacobs et al. 2017; Nováková et al. 2005; Vaughan et al. 2011
Chytridiomycota	-	-	-	-	-
Mucoromycota	2.7	2.7	0.5	1	Nováková et al. 2005
OTHER SITUATIONS					
Other micro-eukaryotes	0.2	5.0	1.1	3	Adetutu et al. 2011; Belyagoubi et al. 2018; Vaughan et al. 2011
Unidentified micro-eukaryotic taxa	-	-	-	-	-

The comparison of caves (little or not anthropized) with soil, aquatic, soil, plant and metazoan ecosystems evidences similarities in terms of the main bacterial phyla present (Fig. 1a), which denotes the ecological success and adaptability of these phyla across contrasted environments (Prescott et al., 2018). However, one can also wonder to which extent microorganisms from these types of ecosystems might be connected to cave microbiomes. In this context, the above finding may also be an indication of the occurrence of metapopulations and microbial dissemination into caves, involving soil above caves, water infiltration into caves (for example via

rhizosphere channels through the epikarst), and microbial carriage by arthropods or mammals (cited above). Thus, the composition of the bacterial community of karstic caves in limestone, dolomite or marble rock layers (Bakalowicz, 1999 ; Rusznyák et al., 2012 ; Alonso et al., 2019 ; Marques et al., 2019 ; Wiseschart et al., 2019) may be close to that of calcareous soils (Fig. 1a). Even though caves are inhabited by metazoa, the composition of cave communities is more distant from those of metazoan ecosystems, as caves display a higher abundance of Gemmatimonadetes, Nitrospirae, Acidobacteria, Chloroflexi and Planctomycetes, and a lower abundance of Bacteroidetes (Fig. 1a). This is compatible with the proposed status of Bacteroidetes as bio-indicators of anthropization, whereas the Nitrospirae phylum is associated with limited anthropization (Castro et al., 2002 ; Herrmann et al., 2015 ; Alonso et al., 2019).

3.2 Archaea in caves

The archaeal community (which is not readily recovered by laboratory cultivation) of non-anthropized caves is mainly composed of Thaumarchaeota and Euryarchaeota on the basis of culture-independent data (Table 1, Table 2) (Ortiz et al., 2014 ; Carmichael et al., 2015 ; Alonso et al., 2019). The Thaumarchaeota phylum represents more than 70% of the archaeal sequences in non-anthropized caves (Table 2, Fig. 1b) and literature reported its involvement in CO_2 fixation and ammonia oxidation (Ortiz et al., 2014). The Crenarchaeota phylum is also retrieved in caves, representing about 10% of the archaeal sequences. These Archaea are mostly documented as thermophilic (Bonch-Osmolovskaya et al., 2018) and historically included the mesophilic Crenarchaeota (Schleper et al., 2005 ; Tomczyk-Żak and Zielenkiewicz, 2016), now recognized as the Thaumarchaeota phylum. The role and activity of the archaeal microorganisms in natural ecosystems is still mysterious, especially in caves (De Mandal et al., 2016 ; Hershey and Barton, 2018 ; Alonso et al., 2019). Some differences in archaeal communities can be evidenced when comparing different caves. The Crenarchaeaota were absent from some caves in France (Allas, Mouflon, Pilier, Reille ; Alonso et al., 2019), Thailand (Manao-Pee ; Wiseschart et al., 2019) and China (Heshang ; Yun et al., 2016), but represented the most abundant phylum in Lechuguilla cave (New Mexico) (Northup et al., 2003). This finding is probably due to taxonomic shortcomings in earlier, pioneering work carried out at a time where the Thaumarchaeota were still included within the Crenarchaeota.

Archaeal community composition in caves is distinct from that of the metazoan microbiome shown in Fig. 1b. Indeed, Euryarchaeota are particularly abundant in metazoa (about 30% of sequences) while representing $< 10\%$ of archaeal sequences in caves. This may be related to the anaerobic conditions prevailing in gut systems, where methane production by Euryarchaeota may take place (Liu and Whitman, 2008). The archaeal community composition of non-anthropized caves resembles that of plants (Fig. 1b), which raises the possibility that some Archaea could originate from the rhizosphere of plants growing above caves, after entry into the caves by water infiltration through the porosity adjacent to the root (microbial dissemination in caves is described above).

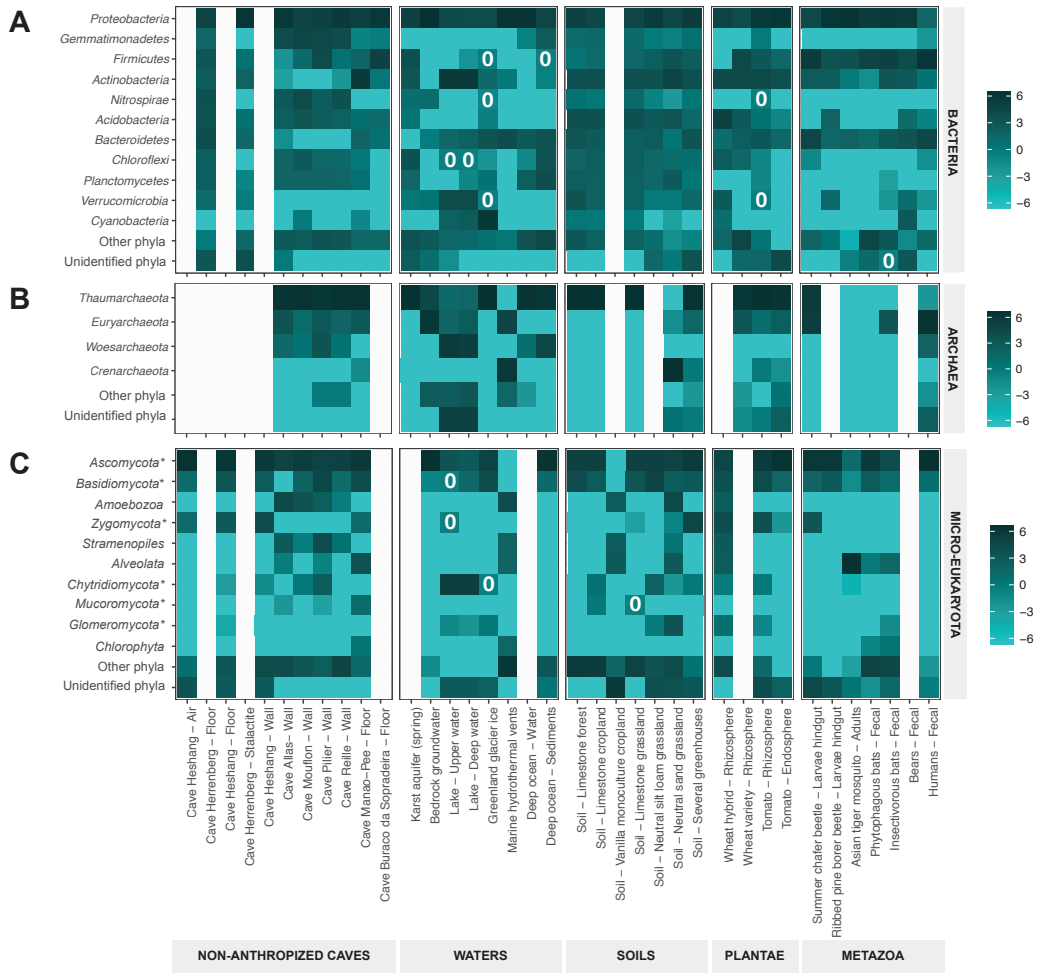

Figure 1. Heatmap of major phyla affiliated with (A) Bacteria, (B) Archaea and (C) microeukaryotes in the microbiome of non-anthropized caves and water, soil, plantae and metazoan microbiomes, based on data from selected publications. Criteria considered for selection of these publications included (i) the combined analysis of different domains of life (ideally bacteria, archaea as well as micro-eukaryotes), (ii) the use of separate primer sets for bacteria and archaea, and (iii) the same types of sequencing technologies to facilitate comparisons. Sequences were retrieved in the Results sections or Supplementary data of research articles, or in sequence databases (e.g. RDP classifier, Greengenes, 119 SILVA, 123 SILVA, 123.1 SILVA, UNITE 7.0, etc.). These sequences were affiliated according to the best hit obtained by BLASTn against Nucleotid collection (nr/nt) and the relative abundance of phyla was calculated. Heatmaps were generated using R (v.4.0.2) software with ggplot2 package (Wickham, 2016). The color intensity in each cell denotes the relative abundance the corresponding phylum, after [log2(x + 0.01)] transformation : phyla of average abundance are shown in medium turquoise blue, whereas dominant phyla are in dark blue/grey and poorly abundant phyla in light turquoise blue. A 0 value is shown for visual clarity when relative abundance of sequences is 0%. White cells are used when data is not available. The asterisks indicate micro-eukaryotic phyla corresponding to fungi. See Appendix S1 : Table S1 for further information on the experimental conditions that are included in the comparison. (For interpretation of the references to color in this figure legend, the reader is referred to the web version of this article.)

3.3 Fungi and other microeukaryotes in caves

The microeukaryotic community in non-anthropized caves is predominantly composed by the fungal phylum Ascomycota (about half the available sequences) (Zepeda Mendoza et al., 2016 ; Man et al, 2018 ; Alonso et al., 2019 ; Wiseschart et al., 2019), a highly diverse phylum involved in the decay of organic substrates and in intimate relations with animals, plants and other Fungi (Northup et al., 2003). Within Ascomycota, *Fusarium spp.* were the only species documented by both cultivation and molecular methods in Doña Trinidad Cave (Stomeo et al., 2009). The next prevalent phylum is the Basidiomycota (10%), which is less adapted to oligotrophic conditions compared to Ascomycota (Vanderwolf et al., 2013) (Table 1, Table 2, Fig. 1c). Different fungal communities can be found in different caves (Alonso et al., 2019 ; Zhang et al., 2019), or when comparing different conditions and substrates within a cave (Man et al., 2018 ; Zhang et al., 2019). For example, the fungal phylum Zygomycota represented about 16% of all microeukaryotes in weathered rocks at Heshang Cave (China) (Man et al., 2018) vs only 2% on the floor of Manao-Pee Cave (Thailand) (Wiseschart et al., 2019). However, non-fungal taxa present in the cave microeukaryotic community have rarely been considered, and their ecological importance remains largely undocumented. To date, there have been few studies of protists in non-anthropized caves (Zepeda Mendoza et al., 2016). Alonso et al. (2019) described protist taxa in a larger investigation of the microeukaryotic community in four pristine caves in France (Allas, Mouflon, Pilier and Reille), where fungal taxa were more abundant than protists.

The microeukaryotic community of non-anthropized caves is largely similar to those in the other ecosystems compared (Fig. 1c). The Ascomycota are prevalent in caves, but they are also prevalent in soils worldwide (Schoch et al., 2009). The non-fungal groups Amoebozoa and Alveolata are often found in soil and water, respectively (Antranikian et al., 2017 ; Sauvadet et al., 2010 ; Xiong et al., 2018), a feature shared by karst environments which are also hydrogeological systems, with a well-developed underground drainage network (Bakalowicz, 1999 ; Engel, 2010).

3.4 Endemic features of the cave microbiome

Overall, the main microbial phyla prevalent in pristine caves are similar to those evidenced in other ecosystems, especially water and soil. However, the situation is not as clear when considering lower taxonomic levels (Saiz-Jimenez, 2012), and many microorganisms typical of caves are thought to be limited to underground environments (Engel, 2019). For instance, evidence was found for a new cave-adapted methane-oxidizing bacterial species from the genus Methylomonas (Kumaresan et al., 2018). Regarding fungi, many species have only been reported in caves (Zhang et al., 2018), such as the *Ochroconis* species *O. anellii, O. anomala* and *O. lascauxensis* (Martin-Sanchez et al., 2012b ; Giraldo et al., 2014 ; Samerpitak et al., 2015), the *Mortierella* species *M. rhinolophicola, M. multispora* and *M. yunnanensis,* and *Neocosmospora pallidimors* (Karunarathna et al., 2020). However, the absence of these species outside caves remains to be clarified. The bat pathogen *Pseudogymnoascus destructans* is believed to have evolved from a cave-endemic *Pseudogymnoascus* species (Hershey and Barton, 2018). Additional endemic taxa might be identified with a more detailed appraisal of the rare cave biosphere (Hershey and Barton, 2018). At intra-species levels, the descriptions of cave-adapted genotypes (or strains)

Table 2. Mean, minimal and maximal relative abundance (%) of phyla found in the microbiome of non-anthropized caves with culture-independent method. Minimal and maximal abundances of phyla, number of caves and number of countries are calculated without considering the null values. Hyphens are used when no data is available.

Phyla	Relative abundance (%)			Number of caves *(where evidenced)*	References
	Min	Max	Mean		
BACTERIA					
Proteobacteria	2.8	94.5	43.3	27	Alonso et al. 2019; Barron et al. 2010; Carmichael et al. 2013; D'Auria et al. 2018; De Mandal et al. 2017; De Mandal et al. 2016; Epure et al. 2014; Lü et al. 2018; Marques et al. 2019; Zepeda Mendoza et al. 2016; Ortiz et al. 2014; Pašić et al. 2009; Porter et al. 2009; Rusznyák et al. 2012; Wiseschart et al. 2019; Yun et al. 2016
Actinobacteria	0.6	90.1	18.1	18	Barron et al. 2010; D'Auria et al. 2018; De Mandal et al. 2017; De Mandal et al. 2016; Marques et al. 2019; Zepeda Mendoza et al. 2016; Ortiz et al. 2014; Pašić et al. 2009; Rusznyák et al. 2012; Wiseschart et al. 2019
Chloroflexi	0.7	24.0	5.1	19	Alonso et al. 2019; Barron et al. 2010; Carmichael et al. 2013; D'Auria et al. 2018; De Mandal et al. 2016; Epure et al. 2014; Lü et al. 2018; Marques et al. 2019; Zepeda Mendoza et al. 2016; Ortiz et al. 2014; Pašić et al. 2009
Acidobacteria	0.7	23.0	4.7	23	Alonso et al. 2019; Barron et al. 2010; Carmichael et al. 2013; D'Auria et al. 2018; De Mandal et al. 2017; De Mandal et al. 2016; Epure et al. 2014; Lü et al. 2018; Marques et al. 2019; Zepeda Mendoza et al. 2016; Pašić et al. 2009; Porter et al. 2009; Ortiz et al. 2014; Rusznyák et al. 2012; Yun et al. 2016
Bacteroidetes	0.9	26.0	4.6	15	Alonso et al. 2019; Barron et al. 2010; Carmichael et al. 2013; D'Auria et al. 2018; De Mandal et al. 2017; De Mandal et al. 2016; Lü et al. 2018; Marques et al. 2019; Zepeda Mendoza et al. 2016; Pašić et al. 2009; Rusznyák et al. 2012; Wiseschart et al. 2019; Yun et al. 2016
Firmicutes	0.9	34.0	4.3	17	Alonso et al. 2019; Barron et al. 2010; D'Auria et al. 2018; De Mandal et al. 2017; Epure et al. 2014; Lü et al. 2018; Marques et al. 2019; Zepeda Mendoza et al. 2016; Ortiz et al. 2014; Rusznyák et al. 2012; Wiseschart et al. 2019; Yun et al. 2016
Gemmatimonadetes	0.6	24.5	3.9	15	Alonso et al. 2019; Barron et al. 2010; D'Auria et al. 2018; De Mandal et al. 2017; Epure et al. 2014; Lü et al. 2018; Marques et al. 2019; Pašić et al. 2009; Porter et al. 2009; Rusznyák et al. 2012; Wiseschart et al. 2019; Yun et al. 2016
Planctomycetes	0.6	23.0	3.5	18	Alonso et al. 2019; Barron et al. 2010; Carmichael et al. 2013; De Mandal et al. 2016; Zepeda Mendoza et al. 2016; Ortiz et al. 2014; Pašić et al. 2009; Porter et al. 2009; Rusznyák et al. 2012; Wiseschart et al. 2019; Yun et al. 2016
Nitrospirae	0.9	17.8	3.3	13	Alonso et al. 2019; De Mandal et al. 2017;Epure et al. 2014; Lü et al. 2018; Ortiz et al. 2014; Pašić et al. 2009; Rusznyák et al. 2012
Verrucomicrobia	0.5	7.0	0.6	7	Carmichael et al. 2013; Lü et al. 2018; Pašić et al. 2009; Rusznyák et al. 2012; Yun et al. 2016
Cyanobacteria	0.5	2.0	0.2	5	Alonso et al. 2019; Lü et al. 2018; Zepeda Mendoza et al. 2016; Ortiz et al. 2014
Other taxa	0.7	32.7	5.3	22	Alonso et al. 2019; Barron et al. 2010; Carmichael et al. 2013; D'Auria et al. 2018; De Mandal et al. 2017; De Mandal et al. 2016; Epure et al. 2014; Lü et al. 2018; Marques et al. 2019; Zepeda Mendoza et al. 2016; Ortiz et al. 2014; Porter et al. 2009; Rusznyák et al. 2012; Wiseschart et al. 2019
Unidentified taxa	0.5	46.0	3.3	11	Alonso et al. 2019; Barron et al. 2010; De Mandal et al. 2016; Zepeda Mendoza et al. 2016; Rusznyák et al. 2012
ARCHAEA					
Thaumarchaeota	40.0	97.0	71.2	8	Alonso et al. 2019; Carmichael et al. 2013; Ortiz et al. 2014; Wiseschart et al. 2019; Yun et al. 2016
Euryarchaeota	2.4	60.0	13.3	9	Alonso et al. 2019; Carmichael et al. 2013; Northup et al. 2003; Vaughan et al. 2011; Wiseschart et al. 2019; Yun et al. 2016
Crenarchaeota	6.0	91.0	10.8	2	Northup et al. 2003; Ortiz et al. 2014
Woesearchaeota	1.63	11.6	2.8	4	Alonso et al. 2019
Other taxa	0.5	1.3	0.3	3	Alonso et al. 2019; Ortiz et al. 2014; Yun et al. 2016
Unidentified taxa	18.0	18.0	2.0	1	Alonso et al. 2019; Ortiz et al. 2014
FUNGI					
Ascomycota	32.2	100	54.1	12	Alonso et al. 2019; Epure et al. 2014; Man et al. 2018; Zepeda Mendoza et al. 2016; Rusznyák et al. 2012; Wiseschart et al. 2019; Zorn 2014
Basidiomycota	2.6	45.1	10.1	11	Alonso et al. 2019; Man et al. 2018; Zepeda Mendoza et al. 2016; Rusznyák et al. 2012; Wiseschart et al. 2019; Zorn 2014
Zygomycota	2.4	16.2	2.9	6	Alonso et al. 2019; Man et al. 2018; Rusznyák et al. 2012; Zorn 2014
Chytridiomycota	1.2	6.4	0.6	2	Alonso et al. 2019
Mucoromycota	0.1	2.4	0.2	3	Alonso et al. 2019; Wiseschart et al. 2019
NON-FUNGAL MICROEUKARYOTIC PHYLA					
Amoebozoa	0.6	22.9	3.2	5	Alonso et al. 2019; Ortiz et al. 2014
Stramenopiles	0.9	17.7	3.2	6	Alonso et al. 2019; Zepeda Mendoza et al. 2016; Ortiz et al. 2014
Alveolata	0.7	12.5	2.3	5	Alonso et al. 2019; Zepeda Mendoza et al. 2016; Ortiz et al. 2014; Wiseschart et al. 2019
Chlorophyta	1.4	13.0	1.7	3	Zepeda Mendoza et al. 2016; Ortiz et al. 2014; Wiseschart et al. 2019
OTHER SITUATIONS					
Other taxa	2.1	48.0	12.1	11	Alonso et al. 2019; Man et al. 2018; Zepeda Mendoza et al. 2016; Rusznyák et al. 2012; Wiseschart et al. 2019; Zorn 2014
Unidentified taxa	5.0	21.0	6.2	7	Man et al. 2018; Zepeda Mendoza et al. 2016; Zorn 2014

in fluorescent *Pseudomonas* (Hershey and Barton, 2018 ; Turrini et al., 2020) and *Streptomyces lavendulae* or related species (Gosse et al., 2019) point towards endemic distributions. UV resistance is thought to be counter-selected in troglobitic bacteria (Snider et al., 2009).

Even though microorganisms from other environments can be transferred into caves, where they may represent environmental contaminants rather than endemic cave inhabitants (Vanderwolf et al., 2013 ; Davis et al., 2020 ; Morse et al., 2021), they are confronted to strong Darwinian selection once in caves (Hershey and Barton, 2018). Therefore, microbial communities in cave may display taxa common to those from other environments, but present at very different population levels. Thus, higher abundances in caves have been highlighted for e.g. the bacterial phyla Acidobacteria, Deltaproteobacteria and Nitrospira, and the Betaproteobacteria families Oxalobacteraceae, Methylophilaceae, and Comamonadaceae (Schabereiter-Gurtner et al., 2002 ; Ivanova et al., 2013), as well as the fungal class of Sordariomycetes (50-60% of sequences in caves vs $< 10\%$ in soils or metazoa ; Alonso et al., 2018 ; Ziganshina et al., 2018 ; Zheng et al., 2019) or the fungal genus *Alternaria* well present underground (Man et al., 2018). On this basis, data point mostly to the occurrence of specialized microbial communities endemic to caves (Ivanova et al., 2013 ; Hershey and Barton, 2018 ; Engel, 2019 ; Davis et al., 2020 ; Morse et al., 2021) rather than cave-endemic microbial taxa per se, but further microbial diversity descriptions are needed for a more robust appraisal.

4. TOURIST PALEOLITHIC CAVES AND EFFECTS OF CONTEMPORARY ANTHROPIZATION ON MICROORGANISMS

4.1 Tourist Paleolithic caves

Paleolithic caves represent a very particular kind of underground systems. They are caves harboring archaeological artwork, which is thought to date from the end of the Middle Paleolithic (the Middle Paleolithic lasted from 300,000-200,000 to 50,000-30,000 years Before Present (BP)) and especially the Upper Paleolithic (50,000-30,000 to 12,000-10,000 years BP) (Mohen and Taborin, 2009). In these caves, parietal artwork includes engravings, drawings, paintings and sometimes carvings, which are present on the walls and ceiling of the cavities.

Caves that were subsequently used for artwork started to form long (millions years) before humans started their exploration. Cave formation took place during the Cretaceous (145-66 million years BP) or the Neogene (2.3-2.6 million years BP), as illustrated in Fig. 2 for the Large Cave (Grande Grotte) of Arcy-sur-Cure (France), Chauvet Cave (France) and Cave of Altamira (Spain). Perhaps the time of formation of these caves, their geologic history and ancient biological events (e.g. their mode of frequentation by animals in the distant past) are important factors that would need to be considered to understand their legacy for the ecology of current microorganisms and microbial adaptation to pristine cave conditions.

During the second half of the Lower Paleolithic (the Lower Paleolithic lasted from around 3 million years to 300,000 years BP), prehistoric men occupied caves, mainly at their entrance (Cauche, 2009) as they provided a protected environment. In certain caves, human occupation extended over 200,000 years, as in the caves of Arcy-sur-Cure (Fig. 2) (Baffier and Girard, 1997). Hundreds of caves have been decorated. Human traces left in these caves (e.g. bones, objects and parietal art) can be analyzed using various techniques (14C dating, thermoluminescence,

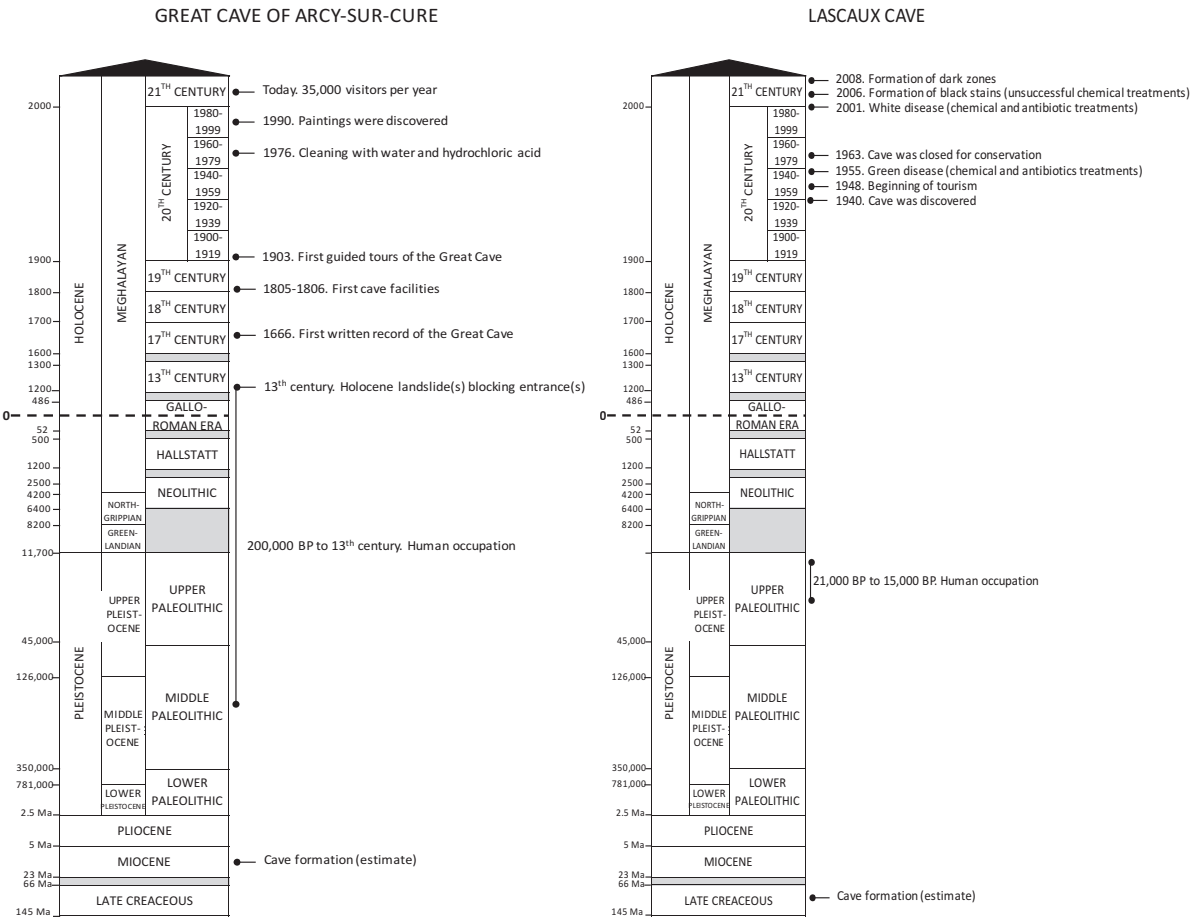

Figure 2. Timeline of selected prominent Paleolithic caves open for tourism (Arcy-sur-Cure, France), formerly open (Altamira in Spain and Lascaux in France), or never open for tourist visits (Chauvet, France). Key geological processes, human occupations and modern events are indicated.

optically stimulated luminescence, uranium-thorium radiometry, etc.) (Sauvet, 2015), allowing to date the artwork of the caves of El Castillo (Spain), Altamira (Spain), Chauvet (France), Tito Bustillo (Spain), Lascaux (France) and Magura (Bulgaria) at about 41,000, 36,000-13,000, 33,000, 20,000, 18,000 and 10,000 years BP, respectively (Glory, 1964 ; Hoyos et al., 1998 ; Valladas et al., 2005 ; Pike et al., 2012 ; Biot, 2013 ; Ivanova et al., 2013). Landslides blocking the entrance terminated human presence in certain caves. Chauvet Cave was frequented by humans during the Aurignacian (43,000 – 29,000 years BP) until a first landslide, and then during the Gravettian (33,000 – 21,000 years BP) till a second landslide dated 13,000 years BP caused the closure of the cave, which was rediscovered in 1994 (Le Guillou, 2005).

The history of human presence after the Paleolithic is poorly documented. During antiquity, the Romans and the Greeks used certain caves for thermalism, made pilgrimages and practiced religious and funeral activities in caves (Verde, 2000). In the Middle Ages, the caves served as refuges during wars or epidemics (Cigna et al., 2013). The earliest descriptions of caves date back to Roman times and later the Renaissance (Biot, 2006 ; Cigna, 1993 ; Cigna et al., 2013 ; Cigna, 2016). The first tourist visits to a cave, i.e. for the sake of pleasure and recreation, might have taken place 3100 years BP in Turkey (Cigna et al., 2013). Tourism as we know it nowadays, i.e. with the commercial provision of services, started in Vilenica Cave (Slovenia) at

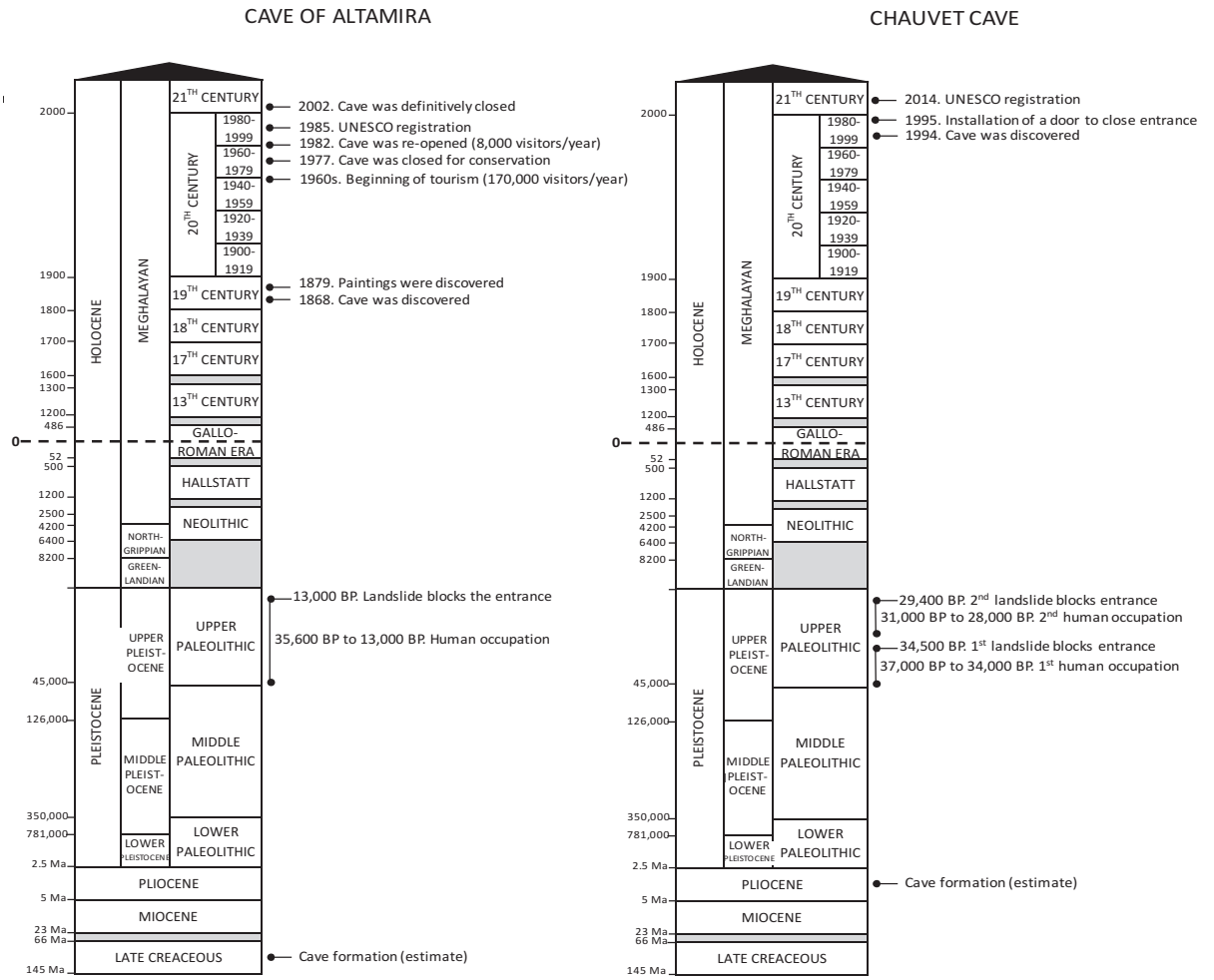

Figure 2. (Suite) Timeline of selected prominent Paleolithic caves open for tourism (Arcy-sur-Cure, France), formerly open (Altamira in Spain and Lascaux in France), or never open for tourist visits (Chauvet, France). Key geological processes, human occupations and modern events are indicated.

the beginning of the 17th century (Cigna et al., 2013). Thus, natural caves have been opened to tourists for 400 years (Pfendler et al., 2018). A show cave (also called tourist cave or public cave) is a cave that has been made accessible to the public for guided visits (Cigna et al., 2013 ; Cigna, 2016 ; Cigna and Burri, 2000). In France, 80 underground cavities have been developed as show caves for touristic purposes from 1919 to 2005 (Biot, 2006, 2013). Nowadays, more than 800 caves worldwide are open to the public (Fig. 3) and 250 million tourists visit them each year (Cigna, 2016 ; Pfendler et al., 2018). Caves attract tourist attention for concretions (stalactites and stalagmites), underground lakes and/or prehistoric artwork. The majority of decorated caves dating from the Paleolithic are found in western Europe (especially France and Spain) (Fig. 3). Some of them are now classified as United Nations Educational, Scientific and Cultural Organisation (UNESCO) World Heritage Sites, such as Lascaux (in 1979), Altamira (1985) and Chauvet (2014).

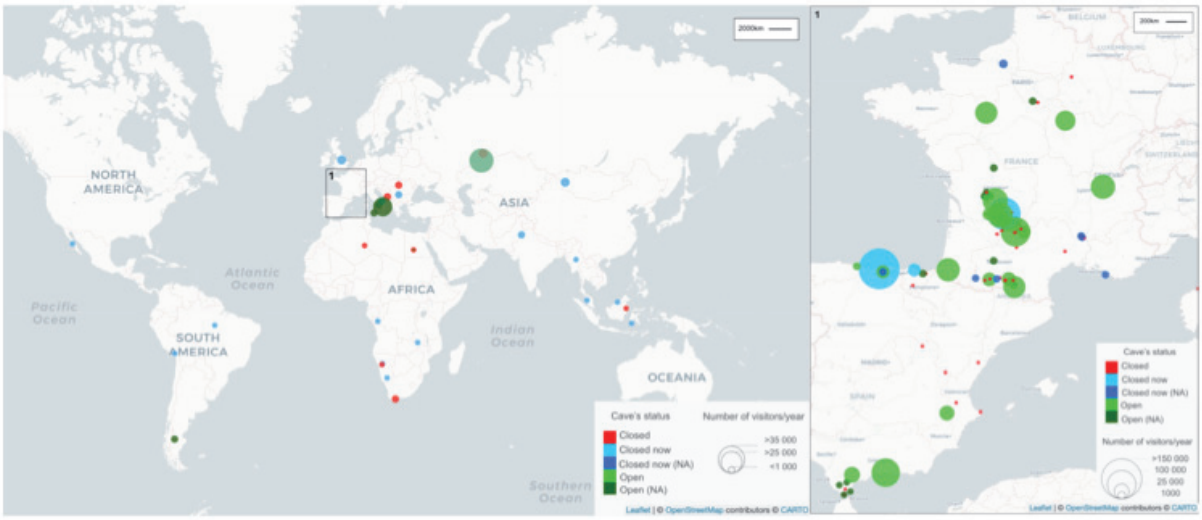

Figure 3. Geographic location of 125 selected Paleolithic caves, with (i) their touristic status i.e. never open ('Closed' / red circles), now closed after having been open for visits ('Closed now' / blue circles or 'Closed now (NA)' / dark blue circles), open for tourism ('Open' / green circles or 'Open (NA)' / dark green circles), (ii) the number of visitors per year (including for previously-open caves before they became closed ; 'NA' means that data is not available and the corresponding circles were arbitrarily set to minimum size). More information on these caves is given in Appendix S2 : Table S2. (For interpretation of the references to color in this figure legend, the reader is referred to the web version of this article.)

4.2 Anthropization of Paleolithic caves related to tourism

The opening of Paleolithic caves for tourism can modify strongly environmental conditions prevailing in these underground systems. The resulting alterations that were observed can be problematic for preservation of artwork, and this forced many caves to close for preservation purposes (Fig. 3). This is in particular the case of the emblematic caves of Lascaux (more than 100 000 visitors per year in the early 1960s, closed in 1963) and Altamira (more than 170,000 visitors per year in the 1960s, closed in 2002) (Fig. 2 and 3). Many Paleolithic caves are closed to the public, yet 45% of them are still open for visits (Fig. 3, Appendix S2 : Table S2) (Ministère de la Culture et de la Communication, 2020).

In certain cases, cave disturbance started even earlier than the implementation of tourism, i.e. with the initial opening of caves so far largely disconnected from the outside environment, sometimes following geologic events such as landslides, etc. This can immediately cause major changes in the cave, especially of climatic conditions (Bastian et al., 2010). In tourist caves, some of the facilities to accommodate visitors were developed as early as in the 1630s for Vilenica Cave (Slovenia) (Cigna et al., 2013) and the 1800s for the Large Cave of Arcy-sur-Cure (France) (Baffier and Girard, 1997 ; Cigna et al., 2013). The soil surfaces of King Salomons Cave (in Tasmania) and Lascaux Cave (in South-West France) were also excavated to facilitate access (Russell and MacLean, 2008). Often, stairs and artificial light were installed (Dupont et al., 2007), and sometimes also concrete pathways (Russell and MacLean, 2008), which can significantly impact environmental conditions within caves. In Lascaux Cave, machinery was installed in 1958 to limit water evaporation and condensation (Brunet et al., 1987 ; Bastian et al., 2010), and equipment for climatic regulation of the cave was replaced and modified in 1966 and in the early 2000 (Dupont et al., 2007), prior to its phasing out in 2015. The visitors themselves can cause strong changes in cave microclimate, with an increase in temperature, CO_2 concentrations

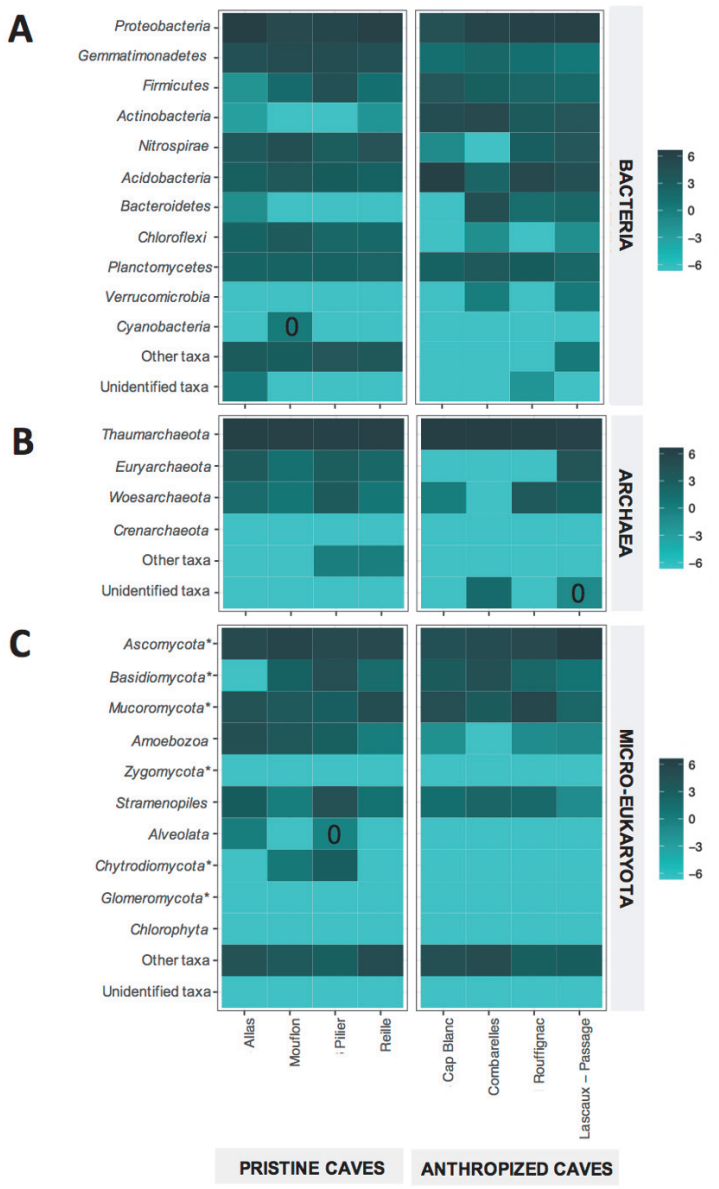

Figure 4. Microbiome of Paleolithic caves open (or previously open) for tourism vs pristine caves, based on selected data in Alonso et al. (2019). Heatmaps are shown for major phyla affiliated with (A) Bacteria, (B) Archaea and (C) microeukaryotes. These sequences were affiliated according to the best hit obtained by BLASTn and the abundance of phyla was calculated. Heatmaps were generated using R (v.4.0.2) software with ggplot2 package (Wickham, 2016). The color intensity in each cell denotes the relative abundance the corresponding phylum, after [log2(x + 0.01)] transformation : phyla of average abundance are shown in medium turquoise blue, whereas dominant phyla are in dark blue/grey and poorly-abundant phyla in light turquoise blue. A 0 value is shown for visual clarity when relative abundance of sequences is 0%. White cells are used when data is not available. The asterisks indicate micro-eukaryotic phyla corresponding to fungi. See Appendix S3 : Table S3 for further information on the experimental conditions that are included in the comparison. (For interpretation of the references to color in this figure legend, the reader is referred to the web version of this article.)

(which can affect the chemical equilibrium of calcite) and water vapor levels (Cañveras et al., 2001 ; Russel et al., 2008 ; Bastian et al., 2009b ; Diaz-Herraiz et al., 2014). In Tito Bustillo and Altamira caves, water vapor exhaled by visitors resulted in condensed aerosols on cave surfaces (Cañveras et al., 2001 ; Espino del Castillo et al., 2018). Therefore, these visitors can also bring organic matter and dust from the outside on their shoes, or drop strands of hair and flakes of

skin (Cañveras et al., 2001). A tourist that became sick during his visit to Castañar de Ibor Cave (Spain) raised organic carbon content of the cave sediment from 0.10% to 0.28% where he vomited (Jurado et al., 2010). Changes in temperature (often increases) were evidenced in several frequented Paleolithic caves, e.g. ±0.20°C in Tito Bustillo Cave, ±0.25°C in Altamira Cave (Cañveras et al. 2001) and +1.50°C in Lascaux Cave (Dupont et al., 2007) compared with original temperatures. As a result, ecological perturbation undergone by these show caves materialized by multiple changes in environmental features, which was likely to impact the structure and functioning of microbial communities.

The introduction of allochthonous nutrients in tourist caves may favor the growth of heterotrophic Bacteria, the development of new microbial populations, and/or the inhibition of indigenous populations (Groth et al., 1999 ; Bastian et al., 2009a ; Bastian and Alabouvette, 2009 ; Espino del Castillo et al., 2018 ; Wasti and Seelan, 2019). The microbial diversity of anthropized and non-anthropized Paleolithic caves has been investigated for the three domains of life using new generation sequencing techniques (Alonso et al., 2019). This work showed a unique microbiota for the most anthropized cave (Lascaux Cave), as well as a higher proportion of Bacteroidetes (6.0% vs 0.1%) and the absence of Euryarchaeota and Woesearchaeota in anthropized caves compared with pristine caves (Fig. 4). Indeed, Bacteroidetes have been proposed as bioindicators of human disturbance in tourist caves (Mulec et al., 2017 ; Espino del Castillo et al., 2018). Certain visited caves may even represent a reservoir of pathogens (reviewed by Saiz-Jimenez, 2012) e.g. *Staphylococcus* and *Escherichia coli* (Espino del Castillo et al., 2018 ; Dhawi, 2020), likely linked to human inputs. Specific microbiota modifications due to anthropization may be expected at community level, with changes in species richness or community structure (Ikner et al., 2007 ; Ager et al., 2010 ; Alonso et al., 2019). In South-West France, cave anthropization resulted in lower species richness and altered structure of prokaryotic communities on the wall of the caves (Alonso et al., 2019) (Fig. 4). Impacts were stronger on the prokaryotic communities rather than on eukaryotic communities, irrespective of cave physicochemical propeties (Ikner et al., 2007 ; Alonso et al., 2019). However, fungal diversity might also be impacted, with higher tourism level correlating with lower fungal species richness (Joshi and Chettri, 2019 ; Wasti and Seelan, 2019). Tourism impact on microorganisms might be indirect, e.g. mediated by anthropization effects on cave fauna. In the Grotta di Catellana (Italy), indigenous species of beetles initially observed near the tourist trails were restricted to more remote parts of the cave after a few years of exploitation, while the section visited became dominated by mice feeding on visitors waste (Cigna, 1993). Non-native vertebrates or invertebrates in caves might act as reservoirs of entomopathogenic microorganisms, such as *Mucor circinelloides* found in rodent droppings (Jurado et al., 2010) or *Chrysosporium, Gliocladium* and *Verticillium* isolated from the corpses of crickets (Bastian et al., 2009b).

Overall, the assessment of anthropization effects has focused so far on Bacteria and Fungi, and therefore these effects remain incompletely documented. In addition, a wider range of geological and climatic settings should be considered in these assessments, including caves that have undergone different levels or types of anthropization, to establish the genericity of findings.

5. MICROBIAL ALTERATION OF ROCK SURFACES IN TOURIST PALEOLITHIC CAVES

5.1 Microbial alteration processes in Paleolithic caves

Cave biota imbalance following anthropization may cause microbial alteration of rock surfaces (Table 3), which can entail (i) excessive growth of microorganisms (resulting in colored stains), (ii) chemical reactions carried out by microorganisms or facilitated by microbial constituents, and/or (iii) mechanical alteration, often due to the rupture of rock substrates by Fungi (Cañveras et al., 2001 ; Barton and Jurado, 2007 ; Cuezva et al., 2012 ; Stupar et al., 2014 ; Pfendler et al., 2018).

Table 3. Selected cases of microbial alterations documented in Paleolithic caves.

Alteration	Colour	Cave	Microbial process proposed	Reference
Biofilm	Green	Many caves worldwide	Growth of algae and other microorganisms	Lefévre 1974, Baquenado Estévez et al. 2019
Calcite veil	Translucent	Caves of Arcy-sur-Cure[1]	Precipitation of calcium carbonate which involved bacteria (*Pseudomonas, Bacillus and Myxococcus*)	Chalmin et al. 2007
	Opaque	Caves of Arcy-sur-Cure, Lascaux Cave[1]	Precipitation of calcium carbonate which involved bacteria (*Pseudomonas, Bacillus and Myxococcus*)	Chalmin et al. 2007, Martin-Sanchez et al. 2015
Efflorescence	White	Sorcerer's Cave[1]	Gypsum precipitation	Lepinay et al. 2018
Stains	White	Cave of Altamira[2], Lascaux Cave	Growth of white fungi and of bacteria (*Proteobacteria*, *Acidobacteria*)	Bastian et al. 2010, Portillo et al. 2008, 2009
	Black	Lascaux Cave, Cave of Bats[2]	Growth of black fungi	Bastian et al. 2010, Urzi et al. 2010, De Leo et al. 2012
	Yellow	Cave of Altamira, Pajsarjeva Jama Cave[3]	Growth of bacteria (*Xanthomonodales)*	Portillo et al. 2008, Pašić et al. 2009
	Grey	Cave of Altamira, Pajsarjeva Jama Cave	Growth of bacteria (*Thauera)*	Portillo et al. 2008, Pašić et al. 2010
	Red	Cave of Bats	Unknown	Urzi et al. 2009
Microbial structure	Blue-black	Driny Cave[4]	Growth of *Penicillium glandicola*	Ogórek et al. 2016

Caves are located in France[1], Spain[2], Slovenia[3], Slovakia[4]

Excessive growth of Archaea, Bacteria and microeukaryotes is one of the main factor responsible for the degradations observed in caves (Cañveras et al., 2001 ; Wang et al., 2010 ; Mihajlovski et al., 2019). This is well documented for 'lampenflora', an invasive and opportunistic community due to the artificial lighting implemented in caves, which forms green stains in the vicinity of light systems (Saiz-Jimenez, 2012). Lampenflora consist mainly of Cyanobacteria and Chrysophyta (Stramenopiles), as well as Plantae members especially algae (Chlorophyta) (Bastian et al., 2010 ; Baquedano Estévez et al., 2019). Lampenflora are common in tourist Paleolithic caves, and in Lascaux in the 1960s they were termed the green disease considering their significant development (Lefèvre, 1974 ; Bastian and Alabouvette, 2009 ; Bastian et al., 2010 ; Baquedano Estévez et al., 2019). At later times in Lascaux Cave, other cases of microbial outgrowth occurred on cave surfaces and resulted in the formation of problematic stains (Mauriac, 2014). Early 2001, spectacular development of the white fungus *Fusarium solani* took place, first in the entrance zone and later in most rooms of the cave (Bastian et al., 2009b ; Bastian et al., 2010). The resulting white stains corresponded to the fungal mycelium itself. Towards the end of 2001 and especially a few years later, black stains also appeared, in relation to the development

of black Fungi (Bastian et al., 2009b ; Bastian et al., 2010 ; Alonso et al., 2018). This time, the stains corresponded to the presence of back pigments (melanins) synthesized by the fungi (De la Rosa et al., 2017) rather than the mycelia themselves. Several black Fungi were identified from stains, including *Ochroconis lascauxensis* (Sympoventuriaceae family), *Acremonium nepalense* (Hypocreaceae family) and *Exophiala castellanii* (Herpotrichiellaceae family) (Martin-Sanchez et al., 2012b ; Alonso et al., 2018). Microbial diversity was not markedly different inside vs outside black stains, and black Fungi were also present outside of stains, highlighting the potential for new black stain formation (Alonso et al., 2018). Black Fungi from the Hypocreaceae (i.e. *Acremonium* species) and Teratosphaeriaceae families have been evidenced in comparable settings corresponding respectively to tumulus walls in Japan (Kiyuna et al., 2011) and a cave with medieval wall paintings (Zucconi et al., 2012), whereas *Streptomyces* isolates from ancient Egyptian paintings could produce black pigments (Abdel-Haliem et al., 2013). Surface alteration resulting from microbial outgrowth has also been documented in Altamira Cave, where yellow and gray stains that formed on walls displayed microbial specificities (Saiz-Jimenez, 2012). For example, Xanthomonadales (Gammaproteobacteria) were only found in yellow stains, whereas the prevalence of *Thauera* (Betaproteobacteria) was higher in grey stains than in yellow stains (Cañveras et al., 2001 ; Portillo et al., 2008). In the Sorcerer's cave (Vézère Valley, France), natural crystallization of gypsum salt following capillarity transport covered prehistoric artwork (Lepinay et al., 2018). However, these saline efflorescences promoted the proliferation of halotolerant and/or halophilic microorganisms, with the formation of microbial pigments that led to surface coloration (Lepinay et al., 2018 ; Mihajlovski et al., 2019).

In addition, cave wall alteration may also entail chemical reactions catalyzed by microorganisms such as Bacteria (especially from the Actinobacteria), which result in biotransformations of mineral surfaces in caves (Diaz-Herraiz et al., 2014 ; Tomczyk-Żak and Zielenkiewicz, 2016). This possibility is particularly documented for calcium carbonate, with microbial dissolution of limestone as well as precipitation leading to the formation of a calcite veil, but it may also concern other mineral constituents. The dissolution of rocks by Bacteria and Fungi occurs through the release of organic and mineral acids (Northup and Lavoie, 2001), e.g. sulfuric acid produced from bacterial oxidation of iron, sulfur, or manganese as documented in Lechuguilla and Spider caves in New Mexico. This dissolution could also be done by secretion of extracellular enzymes, but this has not yet been demonstrated to date (Sand, 1997 ; Northup and Lavoie, 2001). Limestone dissolution can also implicate (micro)organisms already acting by causing stain formation, as documented for lampenflora, in relation to the production of carbonic acid during respiration (Baquedano Estévez et al., 2019). Precipitation processes can be passive, when a specific cellular activity solely directs the spontaneous nucleation, growth, morphology and final location of a mineral, or active when bacterial enzymes are involved or the metabolic activity of microorganisms changes the pH or modulates redox transformations in the microenvironment (Northup and Lavoie, 2001 ; Barton and Jurado, 2007 ; Lepinay et al., 2018). In the large cave of Arcy-sur-Cure, two types of biogenic calcites (translucent and opaque) were obstructing artwork on cave walls, which involved bacteria thought to belong to *Pseudomonas fluorescens*, *Bacillus megaterium* or *Myxococcus xanthus* (Chalmin et al., 2007). Whether microorganisms were also involved in the formation of the white calcite veil (termed white disease) that prompted closure

of Lascaux Cave is not clear.

Finally, cave wall alteration by microorganisms can also involve active mechanical processes as certain microorganisms, during their growth, induce a physical pressure capable of breaking up mineral particles (Lian et al., 2011). This is particularly the case of Fungi, whose mycelium penetrates, envelops and cracks surface particles (Sterflinger, 1998 ; Kumar and Kumar, 1999).

Different types of cave alterations have been investigated, but the comparison with neighboring, unaltered rock surface is often lacking (Fig. 5). In addition, when culture-dependent approaches were used, Archaea could not be recovered. In comparison with unaltered surfaces, black stains in Lascaux did not display differences in the composition of bacterial and fungal phyla, but differences were found at the genus level. In particular, the fungal genera *Ochroconis* and *Exophiala* showed a higher abundance in stains (respectively 26% and 37%, vs 1.1% and 0.2% of sequences outside the stains) and the bacterial genus *Pseudomonas* a lower abundance (0.01-0.11%, vs 34-63% of sequences outside stains) (Alonso, 2018). Overall, considerable information is available on microbial alteration that may take place in tourist Paleolithic caves. However, the role of microorganisms is not always well documented, and especially information is scarce on the contribution of Archaea and non-fungal microeukaryotes, which might play a key role in these alterations. High-throughput sequencing methods now available have started to be implemented to assess microbial alterations, and this should help identify putative microbial actors. A more thorough description of microbial communities will also be important if the aim is to understand microbial functioning leading to surface alterations.

5.2 Attempts to tackle microbial alterations in Paleolithic caves

Since microbial growth and functioning on cave walls may have a deleterious impact on rock art paintings and engravings (Jurado et al., 2010 ; Wang et al., 2010), various corrective actions have been tested to curb microbial spread (Tiano, 2016). First, the most common corrective action is the application of antimicrobial chemicals, such as biocides (e.g. formaldehyde, hydrogen peroxide, quicklime, benzalkonium chloride, fungicides) or antibiotics (e.g. streptomycin, penicillin, polymyxin) (Dupont et al., 2007 ; Bastian et al., 2009a ; Jurado et al., 2010), and often different chemicals are used together. In certain cases, treatments may be applied repeatedly (Dupont et al., 2007) or by alternating the types of products (Langsrud et al., 2003 ; Bastian et al., 2009a). The use of antimicrobials in caves has become increasingly controversial (Diaz-Herraiz et al., 2014), as they may be used as growth substrates by certain microorganisms or might promote the development of resistance mechanisms (Martin-Sanchez et al., 2012a), thereby favouring microbial proliferation (Stomeo et al., 2009), as developed below. Moreover, some of these chemicals may be dangerous for humans, representing a health concern for staff and visitors. Finally, certain biocides can have harmful effects on the mineral surfaces themselves, by causing discoloration, oxidation/reduction of minerals, salt formation, exfoliation, etc. (Tiano, 2016). Second, climatic conditions can be regulated to provide indirect microbial control, especially with the physical modification of passageways or the installation of air-conditioning systems (Dupont et al., 2007). Third, mechanical cleaning with swabs or sponges is effective to remove microbial biomass, in particular with profuse fungal development (Jurado et al., 2010). Fourth, microbial populations may be challenged with physical methods, such as UV light (Borderie et al., 2014 ;

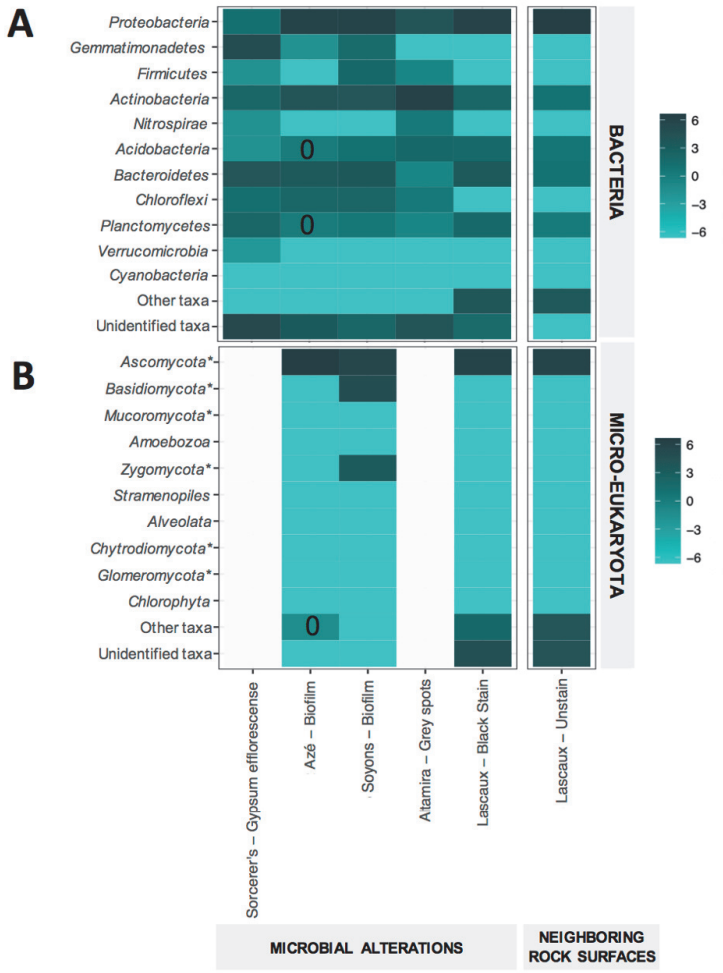

Figure 5. Microbiome changes related to the occurrence of cave wall alterations in Paleolithic caves. Heatmaps are shown for major phyla affiliated with (A) Bacteria and (B) microeukaryotes. Sequences were retrieved in the Results section or Supplementary data of research articles (see Table S4), or in sequence databases (RDP classifier, 119 SILVA and 123 SILVA, 128 SILVA, UNITE v6, etc.). These sequences were affiliated according to the best hit obtained by BLASTn and the abundance of phyla was calculated. Heatmaps were generated using R (v.4.0.2) software with ggplot2 package (Wickham, 2016). The color intensity in each cell denotes the relative abundance the corresponding phylum, after [log2(x + 0.01)] transformation : phyla of average abundance are shown in medium turquoise blue, whereas dominant phyla are in dark blue/grey and poorly-abundant phyla in light turquoise blue. A 0 value is shown for visual clarity when relative abundance of sequences is 0%. White cells are used when data is not available. The asterisks indicate micro-eukaryotic phyla corresponding to fungi. See Appendix S4 : Table S4 for further information on the experimental conditions that are included in the comparison. (For interpretation of the references to color in this figure legend, the reader is referred to the web version of this article.)

Tiano, 2016).

Chemical treatments and antibiotics, frequently used to curb microbial outgrowth in caves, may not ensure efficient control in the longer term, as some microorganisms have or develop means of resistance to these treatments (Bastian et al., 2010). Therefore, the repeated use of biocides to control certain microbial populations might, in fine, favor the development of other microbial populations and hence trigger additional and/or new alterations (Stomeo et al., 2009). In Lascaux Cave, this is likely to have facilitated the development of the white fungus *Fusarium solani* and later of black melanized Fungi (Martin-Sanchez et al., 2012a). The

thick, melanized cell wall of these Fungi (along with Extracellular Polymeric Substance (EPS) production) confers tolerance to antimicrobial treatments (Zucconi et al., 2012). The application of quaternary ammonium compounds against algal-cyanobacterial biofilm on early Christian wall paintings in St Paul Cave (Ephesus, Turkey) favored melanized Fungi (Sterflinger and Piñar, 2013).

Resistance to the biocide benzalkonium chloride, which has been largely used in Lascaux Cave (Mauriac, 2014), is found in Gram-negative Bacteria due to cell wall properties (Nagai et al., 1996) and biofilm formation (Bastian et al., 2009a). Furthermore, some can use as carbon sources the biodegradation products of benzalkonium chloride, i.e. benzyldimethylamine, benzylamine, benzaldehyde and benzoic acid (Patrauchan and Oriel, 2003). Martin-Sanchez et al. (2012a) and Bastian et al. (2009a) highlighted diversified bacterial and fungal communities after biocide treatments in Lascaux, using cloning-sequencing methods. Biocide treatments are thought to have favored particular Bacteria, such as *Ralstonia* (biodegradation of xenobiotic compounds) rarely present in pristine caves (Bastian et al., 2009a ; Alonso et al., 2018). Similarly, treatment with hydrochloric acid in the large cave of Arcy-sur-Cure stimulated microbial formation of calcite on artwork (Chalmin et al., 2007).

Microbial alterations in caves may be intensified by the activities of arthropods that feed on microorganisms. These arthropods act as vectors for microorganisms, such as entomopathogenic Fungi (e.g. *Acremonium, Beauvaria, Geomyces*, etc.) (Greif and Currah, 2007). The best described case is that of springtails (Collembola, Isotomidae) affiliated to *Folsomia candida*, which are opportunistic troglophiles found in caves around the world (Faddeeva-Vakhrusheva et al., 2017). They are mainly mycophagous, but they also feed on Bacteria, algae and nematodes (Bastian et al., 2009b ; Bastian et al., 2010). Within Lascaux cave, these springtails are highly prevalent in black stains, suggesting a relation with black Fungi (Bastian et al., 2010 ; Alonso 2018). Isotopic analysis indicated that *Folsomia candida* can consume melanized Fungi isolated from black stains (unpublished data), whereas conidia from black Fungi are disseminated by the springtail and develop in springtail feces (Bastian et al., 2010).

Therefore, it appears that many corrective actions implemented in tourist Paleolithic caves had limited success, and in some cases they were even instrumental in triggering a stronger microbial imbalance and the development of additional alteration forms, as seen with the use of chemical biocides in Lascaux (Bastian and Alabouvette, 2009 ; Saiz-Jimenez, 2012 ; Martin-Sanchez et al., 2015). More sustainable approaches, minimizing disturbance and stress on the cave microbiome, are needed to optimize conservation of cave heritage (Saiz-Jimenez et al., 2011 ; Mauriac, 2014).

6. CONCLUSIONS

The use of new generation sequencing technologies has started to shed new light on the cave microbiome, showing that the main microbial phyla prevalent in other ecosystems also predominate in caves, i.e. Proteobacteria for Bacteria, Thaumarchaeota for Archaea, and Ascomycota for Fungi. The importance of microbial dissemination as a key driver accounting for microbial presence in underground systems is long recognized, but biodiversity data also raise the possi-

bility that certain cave microorganisms are part of metapopulations established in aboveground environments (e.g. rhizosphere, water, metazoan microbiota, etc.). Despite common cave features and climatic stability, cave microbiota appears to fluctuate significantly across caves or different locations within a given cave, but the underlying factors are poorly documented. The development of sequencing technologies should help address this issue, as well as enable a wider exploration of the place of Archaea and protists, neglected so far, in caves.

Data available to date do not indicate that Paleolithic caves would exhibit a distinct microbial community in comparison with other types of caves, but existing information remains very limited. In contrast, it emerges that cave anthropization related to touristic operations can be a major factor modulating microbial diversity, in caves that are Paleolithic or not. The comparison of anthropized and pristine caves points to the identification of potential bioindicator taxa, such as the Bacteroidetes (most abundant in disturbed settings) and Nitrospirae (well adapted to pristine ecological conditions).

Paleolithic caves are fragile environments, with outstanding conservation issues regarding the preservation of ancient artwork. In several cases, excessive frequentation of tourist Paleolithic caves resulted in microbial imbalance, with the proliferation of particular organisms associated with alterations on rock wall surface. These alterations typically occur as disconnected stains developing on walls, sometimes in the vicinity or directly on artwork. Various types of microorganisms have been evidenced on stains, such as the Cyanobacteria *Scytonema julianum* in lampenflora (Tito Bustillo), the Gammaproteobacteria Xanthomonadales in yellow stains (Altamira), as well as the Ascomycota Fungi *Fusarium solani* in white stains and pigmented Ascomycota Fungi in black stains (both instances in Lascaux). Microbiome analyses indicated that these black pigmented Fungi were also present outside stains, but they were at levels insufficient to cause visual alteration or perhaps they were not physiologically active. Chemical treatments sometimes used to curb microbial outgrowth in tourist Paleolithic caves can cause further microbiome imbalance and lead to new alterations (e.g. black stains) implicating resistant microorganisms. Indeed, Lascaux Cave displayed an unusual microbiome when compared with other anthropized Paleolithic caves from the same region. However, little has been done so far to document microbiome changes related to cave wall alterations.

Microorganisms play significant roles in cave dynamics, including in tourist Paleolithic caves, but functional knowledge is much less developed than the level of taxonomic information. It is therefore of prime importance to better understand the functioning of the cave microbiome (Saiz-Jimenez, 2012), and metagenomic/metatranscriptomic approaches should help fill this gap by identifying key genes and the expression of microbial functions. In the case of tourist Paleolithic caves, this could be particularly useful to decipher the formation of microbial alterations and underpin the development of sustainable cave management strategies compatible with the constraints of Paleolithic art conservation.

CREDIT AUTHORSHIP CONTRIBUTION STATEMENT

Zélia Bontemps : Writing – Original draft preparation, Resources, Visualization **Lise Alonso :**

Writing – Original draft preparation, Visualization **Thomas Pommier :** Conceptualization, Validation **Mylène Hugoni :** Visualization, Validation **Yvan Moënne-Loccoz :** Funding acquisition, Project administration, Conceptualization, Writing – Review & Editing.

DECLARATION OF COMPETING INTEREST

The authors declare that they have no known competing financial interest or personal relationships that could have appeared to influence the work reported in this paper.

ACKNOWLEDGEMENTS

Funding was provided by DRAC Nouvelle Aquitaine (Bordeaux, France). We thank S. Géraud, J.C. Portais, A. Rieu and M. Mauriac (DRAC Nouvelle Aquitaine), and Lascaux Scientific Board for helpful discussions.

REFERENCES

Abdel-Haliem, M.E.F., Sakr, A.A., Ali, M.F., Ghaly, M.F., Sohlenkamp, C. 2013. Characterization of Streptomyces isolates causing colour changes of mural paintings in ancient Egyptian tombs. Microbiol. Res. 168, 428-437.

Adetutu, E.M., Thorpe, K., Bourne, S., Cao, X., Shahsavari, E., Kirby, G., Ball, A.S., 2011. Phylogenetic diversity of fungal communities in areas accessible and not accessible to tourists in Naracoorte Caves. Mycologia 103, 959–968.

Adetutu, E., Thorpe, K., Shahsavari, E., Bourne S., Cao, X., Fard, R.M.N., Kirby, G., and Ball, A. 2012. Bacterial community survey of sediments at Naracoorte Caves, Australia. Int. J Speleol. 41,137-147.

Ager, D., Evans, S., Li, H., Lilley, A.K., Van Der Gast, C.J., 2010. Anthropogenic disturbance affects the structure of bacterial communities. Environ. Microbiol. 12, 670–678.

Alonso, L., 2018. Hétérogénéité spatio-temporelle du microbiote de la grotte de Lascaux (These de doctorat). Lyon.

Alonso, L., Creuzé-des-Châtelliers, C., Trabac, T., Dubost, A., Moënne-Loccoz, Y., Pommier, T., 2018. Rock substrate rather than black stain alterations drives microbial community structure in the passage of Lascaux Cave. Microbiome 6, 216.

Alonso, L., Pommier T., Kaufmann, B., Dubost, A., Chapulliot, D., Doré, J., Douady, C.J, and Moënne-Loccoz, Y. 2019. Anthropization level of Lascaux Cave microbiome shown by regional-scale comparisons of pristine and anthropized caves. Mol. Ecol. 28, 3383–3394.

Antranikian, G., Suleiman, M., Schäfers, C., Adams, M.W.W., Bartolucci, S., Blamey, J.M., Birkeland, N.-K., Bonch-Osmolovskaya, E., da Costa, M.S., Cowan, D., Danson, M., Forterre, P., Kelly, R., Ishino, Y., Littlechild, J., Moracci, M., Noll, K., Oshima, T., Robb, F., Rossi, M., Santos, H., Schönheit, P., Sterner, R., Thauer, R., Thomm, M., Wiegel, J., Stetter, K.O., 2017. Diversity of bacteria and archaea from two shallow marine hydrothermal vents from Vulcano Island. Extrem. Life Extreme Cond. 21, 733–742.

Baffier, D., Girard, M., 1997. The karst of Arcy-sur-Cure (Yonne) and its palaeolithic human occupations. Quaternaire 8, 245–255.

Bakalowicz, M., 1999. Connaissance et gestion des ressources en eaux souterraines dans les régions karstiques. 7-8, 122-126.

Banerjee, S., and Joshi, S.R. 2013. Insights into cave architecture and the role of bacterial biofilm. Proceedings of the National Academy of Sciences, India, Section B : Biol Sci. 83, 277–290.

Baquedano Estévez, C., Merino, L.M., Román, A. de la L., Valsero, J.D., 2019. The lampenflora in show caves and its treatment : an emerging ecological problem. Int. J. Speleol. 48, 4.

Barron, S.K., Murdock, C.A., Blair, B.G., Meade, M.E., Barger, W., 2010. Analysis of bacterial diversity in soils from blowing spring cave. J. Ala. Acad. Sci. 81, 1–10.

Barton, H.A., 2015. Starving artists : bacterial oligotrophic heterotrophy in caves. Life Extreme Environ. Microb. Life Cave Syst. 79–104. Barton, H.A., 2006. Introduction to cave microbiology : a review for the non-specialist. J. Cave Karst Stud. 68, 43–54.

Barton, H.A., Jurado, V., 2007. What's Up Down There ? Microbial Diversity in Caves Microorganisms in caves survive under nutrient-poor conditions and are metabolically versatile and unexpectedly diverse. 2, 132-138.

Barton, H.A., and Northup, D.E. 2007. Geomicrobiology in cave environments : past, current and future perspectives. J. Cave Karst Stud. 69, 163–178.

Bastian, F., Alabouvette, C., 2009. Lights and shadows on the conservation of a rock art cave : The case of Lascaux Cave. Int. J. Speleol. 38, 55-60.

Bastian, F., Alabouvette, C., Jurado, V., Saiz-Jimenez, C., 2009a. Impact of biocide treatments on the bacterial communities of the Lascaux Cave. Naturwissenschaften 96, 863–868.

Bastian, F., Alabouvette, C., Saiz-Jimenez, C., 2009b. The impact of arthropods on fungal community structure in Lascaux Cave. J. Appl. Microbiol. 106, 1456–1462.

Bastian, F., Jurado, V., Nováková, A., Alabouvette, C., Saiz-Jimenez, C., 2010. The microbiology of Lascaux Cave. Microbiol. Read. Engl. 156, 644–652.

Belyagoubi, L., Belyagoubi-Benhammou, N., Jurado, V., Dupont, J., Lacoste, S., Djebbah, F., Ounadjela, F., Benaissa, S., Habi, S., Abdelouahid, D., Saiz-Jimenez, C., 2018. Antimicrobial activities of culturable microorganisms isolated from Chaabe Cave, Algeria. Int. J. Speleol. 47, 189–199.

Bhullar, K., Waglechner, N., Pawlowski A., Koteva, K., Banks, E.D., Johnston, M.D., Barton, H.A. and Wright, G.D. 2012. Antibiotic resistance is prevalent in an isolated cave microbiome. PLoS ONE 7, e34953.

Biot, V., 2013. Les grottes ornées, des géosites culturels à la ressource territoriale. Collect. EDYTEM Cah. Géographie 15, 119–126.

Biot, V., 2006. Le tourisme souterrain en France. Karstologia Mémoires. Bomberg, M., Claesson Liljedahl, L., Lamminmäki, T., Kontula, A., 2019. Highly Diverse Aquatic Microbial Communities Separated by Permafrost in Greenland Show Distinct Features According to Environmental Niches. Front. Microbiol. 10, 1583.

Bonch-Osmolovskaya, E., A. Elcheninov, K. Zayulina, and I. Kublanov. 2018. New thermophilic prokaryotes with hydrolytic activities. Microbiol. Aust. 39, 122–125.

Borbón-García, A., Reyes, A., Vives-Flórez, M., Caballero, S., 2017. Captivity Shapes the Gut Microbiota of Andean Bears : Insights into Health Surveillance. Front. Microbiol. 8, 1316.

Borderie, F., Tête, N., Cailhol, D., Alaoui-Sehmer, L., Bousta, F., Rieffel, D., Aleya, L., and Alaoui-Sossé, B. 2014. Factors driving epilithic algal colonization in show caves and new insights into combating biofilm development with UV-C treatments. Sci. Total Environ. 484, 43–52.

Brannen-Donnelly, K., and Engel, A.S. 2015. Bacterial diversity differences along an epigenic cave stream reveal evidence of community dynamics, succession, and stability. Front. Microbiol 6 :729.

Brunet, J., Vidal, P., Vouvé, J., 1987. The conservation of rock art. Studies and documents on the cultural heritage.

Cañveras, C.S.-J., S. Sanchez-Moral, V. Sloer, 2001. Microorganisms and Microbially Induced Fabrics in Cave Walls. Geomicrobiol. J. 18, 223–240. Carmichael, S.K., Zorn, B.T., Santelli, C.M., Roble, L.A., Carmichael, M.J., and Bräuer, S.L. 2015. Nutrient input influences fungal community composition and size and can stimulate manganese (II) oxidation in caves. Environ. Microbiol. Rep. 7, 592–605.

Castro, H., Reddy, K.R., Ogram, A., 2002. Composition and Function of Sulfate-Reducing Prokaryotes in Eutrophic and Pristine Areas of the Florida Everglades. Appl. Environ. Microbiol. 68, 6129–6137.

Cauche, D., 2009. Les stratégies de débitage dans les industries lithiques archaïques des premiers habitants de l'Europe. L'Anthropologie, Les premiers habitants de l'Europe 113, 178–190.

Chalmin, E., d'Orlyé, F., Zinger, L., Charlet, L., Geremia, R.A., Orial, G., Menu, M., Baffier, D., Reiche, I., 2007. Biotic versus abiotic calcite formation on prehistoric cave paintings : the Arcy-sur-Cure 'Grande Grotte' (Yonne, France) case. Geol. Soc. Lond. Spec. Publ. 279, 185–197.

Chen, Y., Wu, L., Boden, R., Hillebrand, A., Kumaresan, D., Moussard, H., Baciu, M., Lu, Y., and Colin Murrell, J. 2009. Life without light : microbial diversity and evidence of sulfur- and ammonium-based chemolithotrophy in Movile Cave. ISME J. 3,1093–1104.

Cigna, A., 2016. Tourism and show caves. Geomorphol. Suppl. Issues 60, 217–233.

Cigna, A., 1993. Environmental management of tourist caves. Environ. Geol. 21, 173–180.

Cigna, A., Burri, E., 2000. Development, management and economy of show caves. Int. J. Speleol. 29, 1.

Cigna, A., Forti, P., Moreira, J.C., Carvalho, C.N. de, 2013. Caves : the most important geotouristic feature in the world. Tour. Karst Areas 6, 9–26.

Cuezva, S., Sanchez-Moral, S., Saiz-Jimenez, C., and Cañaveras, J.C. 2009. Microbial communities and associated mineral fabrics in Altamira Cave, Spain. International J. Speleol. 38, 83-92.

Cuezva, S., Fernandez-Cortes, A., Porca, E., Pašić, L., Jurado, V., Hernandez-Marine, M., Serrano-Ortiz, P., Hermosin, B., Cañaveras, J.C., Sanchez-Moral, S., 2012. The biogeochemical role of actinobacteria in Altamira cave, Spain. FEMS Microbiol. Ecol. 81, 281–290.

Cunnigham, K.I., DuChene, H.R., and Spirakis, C.S. 1993. Elemental sulfur in caves of the Guadalupe Mountains, New Mexico. New Mexico Geological Society Guidebook 44th Field Conference, Carlsbad region, New Mexico and west Texas, pp 129–136.

Davis, M.C., Messina, M.A., Nicolosi, G., Petralia, S., Baker, M.D., Mayne, C.K.S., Dinon, C.M., Moss, C.J, Onac, B.P, and Garey, J.R. 2020. Surface runoff alters cave microbial community structure and function. PLoS ONE 15, e0232742.

D'Auria, G., Rojas, R., Bautista, J., Méndez, R., Gamboa, J., Goméz-Cruz, R., 2018. Metagenomics of Bacterial Diversity in Villa Luz Caves with Sulfur Water Springs. Genes 9, 55.

De la Rosa, J.M., Martin-Sanchez, P.M, Sanchez-Cortes, S., Hermosin, B., Knicker, H., and Saiz-Jimenez, C. 2017. Structure of melanins from the fungi Ochroconis lascauxensis and Ochroconis anomala contaminating rock art in the Lascaux Cave. Sci. Rep. 7, 13441.

De Leo, F., Iero, A., Zammit, G., and Urzi, C.E. 2012. Chemoorganotrophic bacteria isolated from biodeteriorated surfaces in cave and catacombs. Int. J. Speleol. 41,125–136.

De Mandal, S., Chatterjee, R., Kumar, N.S., 2017. Dominant bacterial phyla in caves and their predicted functional roles in C and N cycle. BMC Microbiol. 17, 90.

De Mandal, S., Zothansanga, null, Panda, A.K., Bisht, S.S., Senthil Kumar, N., 2016. MiSeq HV4 16S rRNA gene analysis of bacterial community composition among the cave sediments of Indo-Burma biodiversity hotspot. Environ. Sci. Pollut. Res. Int. 23, 12216–12226.

Dhami, N.K., Mukherjee, A., Watkin, E.L.J., 2018. Microbial Diversity and Mineralogical-Mechanical Properties of Calcitic Cave Speleothems in Natural and in Vitro Biomineralization Conditions. Front. Microbiol. 9, 40.

Dhawi, F., 2020. Bacterial screening of historic site of Qarah caves, biosphere analysis. Agric. Biol. Res. 36, 1–4.

Diaz-Herraiz, M., Jurado, V., Cuezva, S., Laiz, L., Pallecchi, P., Tiano, P., Sanchez-Moral, S., and Saiz-Jimenez, C. 2014. Deterioration of an Etruscan tomb by bacteria from the order Rhizobiales. Sci. Rep. 4, 3610.

Dupont, J., Jacquet, C., Dennetière, B., Lacoste, S., Bousta, F., Orial, G., Cruaud, C., Couloux, A., and Roquebert, M.-F. 2007. Invasion of the French Paleolithic painted cave of

Lascaux by members of the Fusarium solani species complex. Mycologia 99, 526–533.

Engel, A.S., 2010. Microbial Diversity of Cave Ecosystems. Geomicrobiology : Molecular and Environmental Perspective. Springer Netherlands, Dordrecht, 1, 219–238.

Engel, A.S. 2019. Microbes. Chapter 83. in W. B. White, D. C. Culver, and T. Pipan, editors. Encyclopedia of Caves. Academic Press, London pp 691-698.

Engel, A. S., and Northup, D.E. 2008. Caves and karst as model systems for advancing the microbial sciences. Frontiers of Karst Research 13, 37-48.

Epure, L., Meleg, I.N., Munteanu, C.-M., Roban, R.D., Moldovan, O.T., 2014. Bacterial and Fungal Diversity of Quaternary Cave Sediment Deposits.

Geomicrobiol. J. 31, 116–127.

Espino del Castillo, A., Beraldi-Campesi, H., Amador-Lemus, P., Beltrán, H.I., Borgne, S.L., 2018. Bacterial diversity associated with mineral substrates and hot springs from caves and tunnels of the Naica Underground System (Chihuahua, Mexico). Int. J. Speleol. 47, 213–227.

Faddeeva-Vakhrusheva, A., Kraaijeveld, K., Derks, M.F.L., Anvar, S.Y., Agamennone, V., Suring, W., Kampfraath, A.A., Ellers, J., Le Ngoc, G., van Gestel, C.A.M., Mariën, J., Smit, S., van Straalen, N.M., Roelofs, D., 2017. Coping with living in the soil : the genome of the parthenogenetic springtail Folsomia candida. BMC Genomics 18, 493.

Garcia-Anton, E., Fernandez-Cortes, A., Alvarez-Gallego, M., Sanchez-Moral, S., Cuezva, S., Sanz-Rubio, E., Jurado, V., Porca, E., and Saiz-Jimenez, C. 2013. Entry and dispersion of microorganisms inside Altamira Cave : new evidences from aerobiological and atmospheric gases surveys. M. A. Rogeiro-Candelera, M. Lazzari, and E. Cano, editors. Science and Technology for the Conservation of Cultural Heritage. pp 55-58.

Ghosh, S., Kuisiene, N., and Cheeptham, N. 2017. The cave microbiome as a source for drug discovery : Reality or pipe dream ? Biochem. Pharmacol. 134, 18–34.

Giraldo, A., Sutton, D.A., Samerpitak, K., De Hoog, G.S., Wiederhold, N.P, Guarro, J., and Gené, J. 2014. Occurrence of Ochroconis and Verruconis species in clinical specimens from the United States. J. Clin. Microbiol. 52, 4189–4201.

Glory, A. 1964. Datation des peintures de Lascaux par le Radio-Carbone. Bulletin de la Société préhistorique française. 61,114–117.

Gorbushina, A.A. 2007. Life on the rocks. Env. Microbiol. 9, 1613-1631. Gosse, J.T., Ghosh, S., Sproule, A., Overy, D., Cheeptham, N., and Boddy, C.N. 2019. Whole genome sequencing and metabolomic study of cave Streptomyces isolates ICC1 and ICC4. Front. Microbiol. 10, 1020.

Greif, M.D., Currah, R.S., 2007. Development and dehiscence of the cephalothecoid peridium in Aporothielavia leptoderma shows it belongs in Chaetomidium. Mycol. Res. 111, 70–77.

Griffin, D.W., Gray, M.A., Lyles, M.B., Northup, D.E., 2014. The Transport of Nonindigenous Microorganisms Into Caves by Human Visitation : A Case Study at Carlsbad Caverns National Park. Geomicrobiol. J. 31, 175–185. Groth, I., Vettermann, R., Schuetze, B., Schumann, P., Saiz-Jimenez, C., 1999. Actinomycetes in Karstic caves of northern Spain (Altamira and Tito Bustillo). J. Microbiol. Methods. 36, 115–122.

Herrmann, M., Rusznyák, A., Akob, D.M., Schulze, I., Opitz, S., Totsche, K.U., Küsel, K., 2015. Large Fractions of CO_2-Fixing Microorganisms in Pristine Limestone Aquifers Appear To Be Involved in the Oxidation of Reduced Sulfur and Nitrogen Compounds. Appl. Environ. Microbiol. 81, 2384–2394.

Hershey, O.S., Kallmeyer, J., Wallace, A., Barton, M.D., Barton, H.A., 2018. High Microbial Diversity Despite Extremely Low Biomass in a Deep Karst Aquifer. Front. Microbiol. 9, 2823.

Herzog Velikonja, B.H., Tkavc, R., and Pasić, L. 2014. Diversity of cultivable bacteria involved in the formation of macroscopic microbial colonies (Cave silver) on the walls of a cave in Slovenia. Int. J. Speleol. 43, 45–56.

Hou, W., Dou, C., Lian, B., and Dong, H. 2013. The interaction of fungus with calcite and the effects on aqueous Geochemistry in karst systems. Carbonates Evaporites 28, 413–418.

Hoyos, M., Soler, V., Cañaveras, J.C., Sánchez-Moral, S., Sanz-Rubio, E., 1998. Microclimatic characterization of a karstic cave : human impact on microenvironmental parameters of a prehistoric rock art cave (Candamo Cave, northern Spain). Environ. Geol. 33, 231–242.

Ikner, L.A., Toomey, R.S., Nolan, G., Neilson, J.W., Pryor, B.M., Maier, R.M., 2007. Culturable microbial diversity and the impact of tourism in Kartchner Caverns, Arizona. Microb. Ecol. 53, 30–42.

Ivanova, V., Tomova, I., Kamburov, A., Tomova, A., Vasileva-Tonkova, E., Kambourova, M., 2013. High Phylogenetic Diversity of Bacteria in the Area of Prehistoric Paintings in Magura Cave, Bulgaria. Journl Cave Karst Stud. 75, 218–228.

Jacobs, A., Msimang, D., Venter, E., 2017. First survey of the fungi from the Bakwena Cave in South Africa suggests low human disturbance. J. Cave Karst Stud. 79, 89–94.

Jones, B., 2010. Microbes in caves : agents of calcite corrosion and precipitation. Geol. Soc. Lond. Spec. Publ. 336, 7–30.

Joshi, S.R., Chettri, U., 2019. Fungi in Hypogean Environment : Bioprospection Perspective, in : Satyanarayana, T., Deshmukh, S.K., Deshpande, M.V. (Eds.), Advancing Frontiers in Mycology & Mycotechnology : Basic and Applied Aspects of Fungi. Springer, Singapore, pp 539–561.

Jurado, V., Fernandez-Cortes, A., Cuezva, S., Laiz, L., Cañaveras, J.C., Sanchez-Moral, S., and Saiz-Jimenez, C. 2009. The fungal colonisation of rock-art caves : experimental evidence. Naturwissenschaften 96, 1027–1034.

Jurado, V., Porca, E., Cuezva, S., Fernandez-Cortes, A., Sanchez-Moral, S., and Saiz-Jimenez, C. 2010. Fungal outbreak in a show cave. Sci. Total Environ. 408, 3632–3638.

Karunarathna, S.C., Dong, Y., Karasaki, S., Tibpromma, S., Hyde, K.D, Lumyong, S., Xu, J., Sheng, J., and Mortimer, P.E. 2020. Discovery of novel fungal species and pathogens on bat carcasses in a cave in Yunnan Province, China. Emerg. Microbes Infect. 9, 1554-1566.

Keswick, B.H., Wang, D.-S., Gerba, C.P., 1982. The Use of Microorganisms as Ground-Water Tracers : A Review. Groundwater 20, 142–149.

Kiyuna, T., An, K.D, Kigawa, R., Sano, C., Miura, S., and Sugiyama, J. 2011. Molecular assessment of fungi in "black spots" that deface murals in the Takamatsuzuka and Kitora Tumuli in Japan : Acremonium sect. Gliomastix including Acremonium tumulicola sp. nov. and Acremonium felinum comb. nov. Mycoscience 52, 1-17.

Koskinen, K., Pausan, M.R., Perras, A.K., Beck, M., Bang, C., Mora, M., Schilhabel, A., Schmitz, R., Moissl-Eichinger, C., 2017. First Insights into the Diverse Human Archaeome : Specific Detection of Archaea in the Gastrointestinal Tract, Lung, and Nose and on Skin. mBio 8, e00824-17.

Kumar, R., and Kumar, A.V. 1999. Biodeterioration of Stone in Tropical Environments : An Overview. The Getty Conservation Institute, Los Angeles.

Kumaresan, D., Stephenson, J., Doxey, A.C, Bandukwala, H., Brooks, E., Hillebrand-Voicules -cu, A., Whiteley, A.S., and Murrell, J.C. 2018. Aerobic proteobacterial methylotrophs in Movile Cave : genomic and metagenomic analyses. Microbiome 6, 1-10.

Laiz, L., Groth, I., Gonzalez, I., and Saiz-Jimenez, C. 1999. Microbiological study of the dripping waters in Altamira cave (Santillana del Mar, Spain). J. Microbiol Methods 36, 129–138.

Langsrud, S., Sidhu, M.S., Heir, E., and Holck, A.L. 2003. Bacterial disinfectant resistance—a challenge for the food industry. Int. Biodeterior. Biodegrad. 51, 283–290.

Le Guillou, Y., 2005. Circulations humaines et occupation de l'espace souterrain à la grotte Chauvet-Pont-d'Arc. Bull. Société Préhistorique Fr. 102, 117–134.

Lee, S.A., Kim, Y., Kim, J.M., Chu, B., Joa, J.-H., Sang, M.K., Song, J., Weon, H.-Y., 2019. A preliminary examination of bacterial, archaeal, and fungal communities inhabiting different rhizocompartments of tomato plants under real-world environments. Sci. Rep. 9, 9300.

Lefèvre, M., 1974. La 'Maladie Verte' De Lascaux. Stud. Conserv. 19, 126–156.

Lepinay, C., Mihajlovski, A., Touron, S., Seyer, D., Bousta, F., Di Martino, P., 2018. Bac-

terial diversity associated with saline efflorescences damaging the walls of a French decorated prehistoric cave registered as a World Cultural Heritage Site. Int. Biodeterior. Biodegrad. 130, 55–64.

Li, J., Li, L., Jiang, H., Yuan, L., Zhang, L., Ma, J.-E., Zhang, X., Cheng, M., Chen, J., 2018. Fecal Bacteriome and Mycobiome in Bats with Diverse Diets in South China. Curr. Microbiol. 75, 1352–1361.

Lian, B., Yuan, D., Liu, Z., 2011. Effect of microbes on karstification in karst ecosystems. Chin. Sci. Bull. 56, 3743–3747.

Liu, Y., and Whitman, W.B. 2008. Metabolic, phylogenetic, and ecological diversity of the methanogenic archaea. Ann. N. Y. Acad. Sci. 1125, 171–189.

Lü, X., He, Q., Wang, Zhao, R., Zhang, H., 2018. Impact of Tourism on Bacterial Communities of Karst Underground River : A Case Study from Two Caves in Fengdu, Chongqing. Huan Jing Ke Xue Huanjing Kexue 39, 2389–2399.

Mammola, S., 2019. Finding answers in the dark : caves as models in ecology fifty years after Poulson and White. Ecography 42, 1331–1351.

Man, B., Wang, H., Yun, Y., Xiang, X., Wang, R., Duan, Y., and Cheng, X. 2018. Diversity of fungal communities in Heshang Cave of Central China revealed by mycobiome-sequencing. Front. Microbiol. 9, 1400.

Maron, P.-A., Sarr, A., Kaisermann, A., Lévêque, J., Mathieu, O., Guigue, J., Karimi, B., Bernard, L., Dequiedt, S., Terrat, S., Chabbi, A., Ranjard, L., 2018. High Microbial Diversity Promotes Soil Ecosystem Functioning. Appl. Environ. Microbiol. 84, e02738-17.

Marques, E.L.S., Dias, J.C.T., Gross, E., Silva, A.B. de C. e, de Moura, S.R., Rezende, R.P., 2019. Purple Sulfur Bacteria Dominate Microbial Community in Brazilian Limestone Cave. Microorganisms 7, 29.

Martin-Sanchez, P.M., Miller, A.Z., and Saiz-Jimenez, C. 2015. Lascaux Cave : an example of fragile ecological balance in subterranean environments. A.S. Engel, editor. Microbial Life in Cave Systems. De Gruyter pp 279-301

Martin-Sanchez, Pedro Maria, Nováková, A., Bastian, F., Alabouvette, C., Saiz-Jimenez, C., 2012a. Two new species of the genus Ochroconis, O. lascauxensis and O. anomala isolated from black stains in Lascaux Cave, France. Fungal Biol. 116, 574–589.

Martin-Sanchez, Pedro M., Nováková, A., Bastian, F., Alabouvette, C., Saiz-Jimenez, C., 2012b. Use of Biocides for the Control of Fungal Outbreaks in Subterranean Environments : The Case of the Lascaux Cave in France. Environ. Sci. Technol. 46, 3762–3770.

Mauriac, M. 2014. Lascaux : preserving a 20 000-year old legacy of Paleolithic art. Medicographia 36, 238-252.

Mihajlovski, A., Lepinay, C., Mirval, A.-L., Touron, S., Bousta, F., Di Martino, P., 2019. Characterization of the archaeal and fungal diversity associated with gypsum efflorescences on the walls of the decorated Sorcerer's prehistoric cave. Ann. Microbiol. 69, 1071–1078. Ministère de la Culture et de la Communication, 2020. Art rupestre et grottes ornées [WWW Document]. URL https ://www.culture.gouv.fr/Sites-thematiques/Archeologie/Centre-national-de-prehistoire-Art-rupestre-Grottes-ornees/Art-rupestre-Grottes-ornees (accessed 5.19.20).

Mohen, J., Taborin, Y., 2019. Les sociétés de la préhistoire, Hachette éducation. ed. Hachette.

Moissl-Eichinger, C., and Huber, H. 2011. Archaeal symbionts and parasites. Curr. Opin. Microbiol. 14, 364–370.

Morse, K.V., Richardson, D.R, Brown, T.R, Vangundy, R.D, and Cahoon, A.B. 2021. Longitudinal metabarcode analysis of karst bacterioplankton microbiomes provide evidence of epikarst to cave transport and community succession. PeerJ 9, e10757.

Mulec, J., Oarga-Mulec, A., Šturm, S., Tomazin, R., Matos, T., 2017. Spacio-Temporal Distribution and Tourist Impact on Airborne Bacteria in a Cave (Škocjan Caves, Slovenia). Diversity 9, 28.

Nagai, K., Ohta, S., Zenda, H., Matsumoto, H., and Makinom M. 1996. Biochemical charac-

terization of a Pseudomonas fluorescens strain isolated from a benzalkonium chloride solution. Biol Pharm Bull. 19, 873–875.

Nehme, C. 2013. The use of passive seismological imaging in speleogenetic studies ; an example from Kanaan Cave, Lebanon. Int. J. Speleol. 42, 97–108.

Northup, D.E., Carr, D.L., Crocker, M.T., Cunningham, K.I., Hawkins, L.K., Leonard, P., Welbourn, W.C., 1994. Biological investigations in Lechuguilla Cave. NSS Bull. 56, 54–63.

Northup, D.E. 1997. Balancing conservation of unusual cave microbial communities with exploration and research in Lechuguilla Cave, Carlsbad Caverns. National Park, New Mexico. Final Report to the Anne D. Morrow and Charles A. Lindbergh Foundation and the National Park Service.

Northup, D.E., Barns, S.M, Yu, L.E., Spilde, M.N, Schelble, R.T., Dano, K.E., Crossey, L.J., Connolly, C.A., Boston, P.J, Natvig, D.O., and Dahm, C.N. 2003. Diverse microbial communities inhabiting ferromanganese deposits in Lechuguilla and Spider Caves. Environ. Microbiol. 5, 1071–1086.

Northup, D., and Lavoie, K. 2001. Geomicrobiology of caves : a review. Geomicrobiol. J. 18, 199–222.

Novakova, A., Elhottová, D., Kristufek, V., Lukesova, A., Hill, P., Kovac, L., Mock, A., Luptacik, P., 2005. Feeding sources of invertebrates in Ardovská Cave and Domica Cave systems preliminary results. pp. 107–112. Nunoura, T., Nishizawa, M., Hirai, M., Shimamura, S., Harnvoravongchai, P., Koide, O., Morono, Y., Fukui, T., Inagaki, F., Miyazaki, J., Takaki, Y., Takai, K., 2018. Microbial Diversity in Sediments from the Bottom of the Challenger Deep, the Mariana Trench. Microbes Environ. 33, 186–194. Ogórek, R., Višňovská, Z., and Tančinová, D. 2016. Mycobiota of underground habitats : case study of Harmanecká Cave in Slovakia. Microb Ecol 71, 87–99. Ortiz, M., Legatzki, A., Neilson, J.W., Fryslie, B., Nelson, W.M., Wing, R.A., Soderlund, C.A., Pryor, B.M., Maier, R.M., 2014. Making a living while starving in the dark : metagenomic insights into the energy dynamics of a carbonate cave. ISME J. 8, 478–491.

Palmer, A.N., 1991. Origin and morphology of limestone caves. GSA Bull. 103, 1–21.

Patrauchan, M.A., Oriel, P.J., 2003b. Degradation of benzyldimethylalkylammonium chloride by Aeromonas hydrophila sp. K. J. Appl. Microbiol. 94, 266–272.

Perrette, Y., Delannoy, J.-J., Bolvin, H., Cordonnier, M., Destombes, J.-L., Zhilinskaya, E.A., Aboukais, A., 2000. Comparative study of a stalagmite sample by stratigraphy, laser induced fluorescence spectroscopy, EPR spectrometry and reflectance imaging. Chem. Geol. 162, 221–243.

Pfendler, S., Karimi, B., Maron, P.-A., Ciadamidaro, L., Valot, B., Bousta, F., Alaoui-Sosse, L., Alaoui-Sosse, B., Aleya, L., 2018. Biofilm biodiversity in French and Swiss show caves using the metabarcoding approach : First data. Sci. Total Environ. 615, 1207–1217.

Pike, A.W.G., Hoffmann, D.L., García-Diez, M., Pettitt, P.B., Alcolea, J., Balbín, R.D., González-Sainz, C., Heras, C. de las, Lasheras, J.A., Montes, R., Zilhão, J., 2012. U-Series Dating of Paleolithic Art in 11 Caves in Spain. Science 336, 1409–1413.

Porter, M., Engel, A., C, K., K, K., 2009. Porter ML, Engel AS, Kane TC, Kinkle BK.. Productivity-diversity relationships from chemolithoautotrophically based sulfidic karst systems. Int J Speleol 28 : 27-40. Int. J. Speleol. 38, 27–40.

Portillo, M.C., and Gonzalez, J.M. 2010. Differential effects of distinct bacterial biofilms in a cave environment. Curr. Microbiol. 60, 435–438.

Portillo, M.C., Gonzalez, J.M., Saiz-Jimenez, C., 2008. Metabolically active microbial communities of yellow and grey colonizations on the walls of Altamira Cave, Spain. J. Appl. Microbiol. 104, 681–691.

Prescott, L.-M., Willey, J.M., Sherwood, L.M., and Woolwerton, C.J. 2018. Microbiology (5th edn). De Boeck, Louvain-la-Neuve.

Prudence, S.M.M., Worsley, S., Balis, L., Murrell, J.C., Lehtovirta-Morley, L., Hutchings, M.L., 2019. Root-associated archaea : investigating the niche occupied by ammonia oxidising

archaea within the wheat root microbiome. Access Microbiol. 1, 253.

Purkamo, L., Kietäväinen, R., Miettinen, H., Sohlberg, E., Kukkonen, I., Itävaara, M., Bomberg, M., 2018. Diversity and functionality of archaeal, bacterial and fungal communities in deep Archaean bedrock groundwater. FEMS Microbiol. Ecol. 94, 116.

Roldán, M., and Hernández-Mariné, M. 2009. Exploring the secrets of the three-dimensional architecture of phototrophic biofilms in caves. Int. J. Speleol. 38, 41–53.

Riding, R. 2000. Microbial carbonates : the geological record of calcified bacterial–algal mats and biofilms. Sedimentology 47, 179-214.

Russell, A.D. 1998. Mechanisms of bacterial resistance to antibiotics and biocides. Prog Med Chem 35, 133–197.

Russell, M.J., and MacLean, V.L. 2008. Management issues in a Tasmanian tourist cave : potential microclimatic impacts of cave modifications. J. Environ. Manag. 87,474–483.

Rusterholtz, K.J., Mallory, L.M., 1994. Density, activity, and diversity of bacteria indigenous to a karstic aquifer. Microb. Ecol. 28, 79–99.

Rusznyák, A., Akob, D.M., Nietzsche, S., Eusterhues, K., Totsche, K.U., Neu, T.R., Frosch, T., Popp, J., Keiner, R., Geletneky, J., Katzschmann, L., Schulze, E.-D., Küsel, K., 2012. Calcite Biomineralization by Bacterial Isolates from the Recently Discovered Pristine Karstic Herrenberg Cave. Appl. Environ. Microbiol. 78, 1157–1167.

Saiz-Jimenez, C., 2012. Microbiological and environmental issues in show caves. World J. Microbiol. Biotechnol. 28, 2453–2464.

Saiz-Jimenez, C., Cuezva, S., Jurado, V., Fernandez-Cortes, A., Porca, E., Benavente, D., Cañaveras, J.C., and Sanchez-Moral, S. 2011. Paleolithic art in peril : policy and science collide at Altamira Cave. Science 334, 42-43. Saiz-Jimenez, C., and Hermosin, B. 1999. Thermally assisted hydrolysis and methylation of dissolved organic matter in dripping waters from the Altamira Cave. J. Anal. Appl. Pyrolysis 49, 337–347.

Samerpitak, K., Van Den Ende, A.H.G., Menken, S.B.J., and De Hoog, G.S. 2015. Three new species of the genus Ochroconis. Mycopathologia 180, 7–17.

Sand, W. 1997. Microbial mechanisms of deterioration of inorganic substrates—A general mechanistic overview. Int. Biodeter. Biodegrad. 40, 183–19

Sauvadet, A.-L., Gobet, A., Guillou, L., 2010. Comparative analysis between protist communities from the deep-sea pelagic ecosystem and specific deep hydrothermal habitats. Environ. Microbiol. 12, 2946–2964.

Schabereiter-Gurtner, C., Saiz-Jimenez, C., Piñar, G., Lubitz, W., and Rölleke, S. 2002. Altamira cave Paleolithic paintings harbor partly unknown bacterial communities. FEMS Microbiol Lett. 211, 7–11.

Schabereiter-Gurtner, C., Saiz-Jimenez, C., Piñar, G., Lubitz, W., and Rölleke, S. 2004. Phylogenetic diversity of bacteria associated with Paleolithic paintings and surrounding rock walls in two Spanish caves (Llonín and La Garma). FEMS Microbiol Ecol. 47, 235–247.

Scheu, S., and Simmerling, F. 2004. Growth and reproduction of fungal feeding Collembola as affected by fungal species, melanin and mixed diets. Oecologia 139, 347–353.

Schleper, C., Jurgens, G., Jonuscheit, M., 2005. Genomic studies of uncultivated archaea. Nat. Rev. Microbiol. 3, 479–488.

Schoch, C.L., Sung, G.-H., López-Giráldez, F., Townsend, J.P., Miadlikowska, J., Hofstetter, V., Robbertse, B., Matheny, P.B., Kauff, F., Wang, Z., Gueidan, C., Andrie, R.M., Trippe, K., Ciufetti, L.M., Wynns, A., Fraker, E., Hodkinson, B.P., Bonito, G., Groenewald, J.Z., Arzanlou, M., Sybren de Hoog, G., Crous, P.W., Hewitt, D., Pfister, D.H., Peterson, K., Gryzenhout, M., Wingfield, M.J., Aptroot, A., Suh, S.-O., Blackwell, M., Hillis, D.M., Griffith, G.W., Castlebury, L.A., Rossman, A.Y., Lumbsch, H.T., Lücking, R., Büdel, B., Rauhut, A., Diederich, P., Ertz, D., Geiser, D.M., Hosaka, K., Inderbitzin, P., Kohlmeyer, J., Volkmann-Kohlmeyer, B., Mostert, L., O'Donnell, K., Sipman, H., Rogers, J.D., Shoemaker, R.A., Sugiyama, J., Summerbell, R.C., Untereiner, W., Johnston, P.R., Stenroos, S., Zuccaro, A., Dyer, P.S., Crittenden, P.D., Cole,

M.S., Hansen, K., Trappe, J.M., Yahr, R., Lutzoni, F., Spatafora, J.W., 2009. The Ascomycota Tree of Life : A Phylum-wide Phylogeny Clarifies the Origin and Evolution of Fundamental Reproductive and Ecological Traits. Syst. Biol. 58, 224–239. Simon, K.S., 2019. Chapter 26 - Cave ecosystems, in : White, W.B., Culver, D.C., Pipan, T. (Eds.), Encyclopedia of Caves (Third Edition). Academic Press, pp. 223–226.

Snider, J.R., Goin, C., Miller, R.V., Boston, P.J., and Northup, D.E. 2009. Ultraviolet radiation sensitivity in cave bacteria : evidence of adaptation to the subsurface ? International J Speleol 38, 11-22.

Sterflinger, K. 1998. Temperature and NaCl- tolerance of rock-inhabiting meristematic fungi. Antonie van Leeuwenhoek 74, 271–281.

Sterflinger, K., and Piñar, G. 2013. Microbial deterioration of cultural heritage and works of art—tilting at windmills ? App Microbiol Biotech. 97, 9637-9646.

Stomeo, F., Portillo, M.C., Gonzalez, J.M., 2009. Assessment of bacterial and fungal growth on natural substrates : consequences for preserving caves with prehistoric paintings. Curr. Microbiol. 59, 321–325.

Stupar, M., Grbić, M.L., Džamić, A., Unković, N., Ristić, M., Jelikić, A., Vukojević, J., 2014. Antifungal activity of selected essential oils and biocide benzalkonium chloride against the fungi isolated from cultural heritage objects. South Afr. J. Bot. 93, 118–124.

Suhr, M.J., Banjara, N., Hallen-Adams, H.E., 2016. Sequence-based methods for detecting and evaluating the human gut mycobiome. Lett. Appl. Microbiol. 62, 209–215.

Thimm, T., Hoffmann, A., Borkott, H., Munch, J.C., and Tebbe, C.C. 1998. The gut of the soil microarthropod Folsomia candida (Collembola) is a frequently changeable but selective habitat and a vector for microorganisms. Appl Environ Microbiol 64, 2660–2669.

Thompson, B., Richardson, D., Vangundy, R.D., and Cahoon, A.B. 2019. Metabarcoding comparison of prokaryotic microbiomes from Appalachian karst caves to surface soils in southwest Virginia, USA. J Cave Karst Stud. 81, 244–253.

Thongsripong, P., Chandler, J.A., Green, A.B., Kittayapong, P., Wilcox, B.A., Kapan, D.D., Bennett, S.N., 2018. Mosquito vector-associated microbiota : Metabarcoding bacteria and eukaryotic symbionts across habitat types in Thailand endemic for dengue and other arthropod-borne diseases. Ecol. Evol. 8, 1352–1368.

Tiano, P. 2016. Biodeterioration of stone monuments a worldwide issue. Open Conf Proc J. 7, 29–38.

Tkacz, A., Pini, F., Turner, T.R., Bestion, E., Simmonds, J., Howell, P., Greenland, A., Cheema, J., Emms, D.M., Uauy, C., Poole, P.S., 2020. Agricultural Selection of Wheat Has Been Shaped by Plant-Microbe Interactions. Front. Microbiol. 11, 132. https ://doi.org/10.3389/fmicb.2020.00132

Tomczyk-Żak, K., Zielenkiewicz, U., 2016. Microbial Diversity in Caves. Geomicrobiol. J. 33, 20–38.

Turrini, P., Tescari, M., Visaggio, D., Pirolo, M., Lugli, G.A., Ventura, M., Frangipani, E., and Visca, P. 2020. The microbial community of a biofilm lining the wall of a pristine cave in Western New Guinea. Microbiol. Res 241, 126584.

Urich, T., Lanzén, A., Qi, J., Huson, D.H., Schleper, C., Schuster, S.C., 2008. Simultaneous Assessment of Soil Microbial Community Structure and Function through Analysis of the Meta-Transcriptome. PloS One 3, e2527.

Urzì, C., De Leo, F., Bruno, L., and Albertano, P. 2010. Microbial diversity in Paleolithic caves : a study case on the phototrophic biofilms of the Cave of Bats (Zuheros, Spain). Microb. Ecol. 60, 116–129.

Valladas, H., Tisnérat-Laborde, N., Cacher, H., Kaltnecker, E., Arnold, M., Oberlin, C., Evin, J., 2005. Bilan des datations carbone 14 effectuées sur des charbons de bois de la grotte Chauvet - Persée. Bull. Société Préhistorique Fr. 102, 109–113.

Vanderwolf, K.J., Malloch, D., McAlpine, D.F., and Forbes, G.J. 2013. A world review of

fungi, yeasts, and slime molds in caves. Int. J. Speleol. 42, 77-96.

Vaughan, M., Maier, R., Pryor, B., 2011. Fungal communities on speleothem surfaces in Kartchner Caverns, Arizona, USA. Int. J. Speleol. 40, 65–77. Verde, G., 2000. Il termalesimo di Sciacca dalla preistoria al XX secolo. Agrigento 280.

Wang, W., Ma, Xu, Ma, Y., Mao, L., Wu, F., Ma, Xiaojun, An, L., Feng, H., 2010. Seasonal dynamics of airborne fungi in different caves of the Mogao Grottoes, Dunhuang, China. Int. Biodeterior. Biodegrad. 64, 461–466.

Wasti, I.G., Seelan, J.S.S., 2019. The fungal diversity of madai cave, Sabah, Malaysia., in : Langkawi International Multidisciplinary Academic Conference (Limac 2019). p. 264.

Wickham, H. 2016. ggplot2 : Elegant Graphics for Data Analysis. Second edition. Springer International Publishing, Heidelberg.

Wiseschart, A., Mhuantong, W., Tangphatsornruang, S., Chantasingh, D., Pootanakit, K., 2019. Shotgun metagenomic sequencing from Manao-Pee cave, Thailand, reveals insight into the microbial community structure and its metabolic potential. BMC Microbiol. 19, 144.

Xiong, W., Jousset, A., Guo, S., Karlsson, I., Zhao, Q., Wu, H., Kowalchuk, G.A., Shen, Q., Li, R., Geisen, S., 2018. Soil protist communities form a dynamic hub in the soil microbiome. ISME J. 12, 634–638.

Xu, W., Gong, L., Pang, K.-L., Luo, Z.-H., 2018. Fungal diversity in deep-sea sediments of a hydrothermal vent system in the Southwest Indian Ridge. Deep Sea Res. Part Oceanogr. Res. 131, 16–26.

Yu, X., Wu, X., Qiu, L., Wang, D., Gan, M., Chen, X., Wei, H., Xu, F., 2015. Analysis of the intestinal microbial community structure of healthy and long-living elderly residents in Gaotian Village of Liuyang City. Appl. Microbiol. Biotechnol. 99, 9085–9095.

Yun, Y., Xiang, X., Wang, H., Man, B., Gong, L., Liu, Q., Dong, Q., and Wang, R. 2016. Five-year monitoring of bacterial communities in dripping water from the Heshang Cave in Central China : implication for paleoclimate reconstruction and ecological functions. Geomicrobiol. J. 33,1–11.

Zepeda Mendoza, M.L., Lundberg, J., Ivarsson, M., Campos, P., Nylander, J.A.A, Sallstedt, T., and Dalen, L. 2016. Metagenomic analysis from the interior of a speleothem in Tjuv-Ante's cave, northern Sweden. PLoS ONE 11, e0151577.

Zhang, Z.-F., Cai, L., 2019. Substrate and spatial variables are major determinants of fungal community in karst caves in Southwest China. J. Biogeogr. 46, 1504–1518.

Zhang, Z.F., Zhao, P., and Cai, L.. 2018. Origin of cave fungi. Front. Microbiol. 9,1407.

Zheng, Q., Hu, Y., Zhang, S., Noll, L., Böckle, T., Dietrich, M., Herbold, C.W., Eichorst, S.A., Woebken, D., Richter, A., Wanek, W., 2019. Soil multifunctionality is affected by the soil environment and by microbial community composition and diversity. Soil Biol. Biochem. 136, 107521

Zhu, H.-Z., Zhang, Z.-F., Zhou, N., Jiang, C.-Y., Wang, B.-J., Cai, L., Liu, S.-J., 2019. Diversity, Distribution and Co-occurrence Patterns of Bacterial Communities in a Karst Cave System. Front. Microbiol. 10, 1726. Ziganshina, E.E., Mohammed, W.S., Shagimardanova, E.I., Vankov, P.Y., Gogoleva, N.E., Ziganshin, A.M., 2018. Fungal, Bacterial, and Archaeal Diversity in the Digestive Tract of Several Beetle Larvae (Coleoptera). BioMed Res. Int. 2018.

Zorn, B., 2014. Illumina sequencing of fungal assemblages reveals compositional shifts as a result of nutrient loading within cave sediments. Zucconi, L., Gagliardi, M., Isola, D., Onofri, S., Andaloro, M.C., Pelosi, C., Pogliani, P., Selbmann, L., 2012. Biodeterioration agents dwelling in or on the wall paintings of the Holy Saviour's cave (Vallerano, Italy). Int. Biodeterior. Biodegrad. 70, 40–46.

Supplementary data

Appendix S1: Table S1. Detailed information on selected literature related to the bacterial, archaeal and micro-eukaryotic communities in the Cave, Water, Soil, Plantae and Metazoa ecosystems.

	Sample ID for Figure 3	Region/Province, Country	GPS coordinates (WGS 84)	Properties	Targeted microbiota	Primer pair	Sequence length (bp)	Sequencing approach	Reference
CAVE	Cave Heshang - Air	Qingjiang Valley, China	30°27'N, 110°25'E	Pristine karst cave in Cambrian dolomite, ~ 250 m long	Micro-eukaryota (ITS1)	ITS5-1737F/ITS2-2043R	~ 300	Illumina HiSeq	Man et al., 2018
	Cave Herrenberg - Stalactite	Thuringe, Germany	50°25'41.6''N, 11°01'007.5''E	Pristine karst cave in Middle Triassic limestone (discovered during the excavation of a railway tunnel)	Bacteria (16S rRNA genes)	fd1/rp2	~ 1500	Cloning and sequencing	Rusznyák et al., 2012
	Cave Heshang - Wall	Qingjiang Valley, China	30°27'N, 110°25'E	Pristine karst cave in Cambrian dolomite, ~ 250 m long	Micro-eukaryota (ITS1)	ITS5-1737F/ITS2-2043R	~ 300	Illumina HiSeq	Man et al., 2018
					Archaea (16S rRNA genes)	515F/915R	~ 420		
	Cave Allas - Wall	Vézère Valley, Dordogne, France	44°53'12''N, 1°10'03''E	Pristine karstic cave in limestone, 130 m long (discovered early 1900s)	Bacteria (16S rRNA genes)	341F/805R	~ 550	Illumina MiSeq	Alonso et al., 2019
					Micro-eukaryota (18S rRNA genes)	18S_0067a_deg/NSR399	~ 350		
					Micro-eukaryota (ITS)	ITS3_KYO2/ITS4	300-400		
					Archaea (16S rRNA genes)	515F/915R	~ 420		
	Cave Mouflon - Wall	Vézère Valley, Dordogne, France	45°07'09.5''N, 1°07'11.2''E	Pristine karstic cave in limestone, 2000 m long (discovered early 1900s)	Bacteria (16S rRNA genes)	341F/805R	~ 550	Illumina MiSeq	Alonso et al., 2019
					Micro-eukaryota (18S rRNA genes)	18S_0067a_deg/NSR399	~ 350		
					Micro-eukaryota (ITS)	ITS3_KYO2/ITS4	300-400		
					Archaea (16S rRNA genes)	515F/915R	~ 420		
	Cave Pilier - Wall	Vézère Valley, Dordogne, France	44°55'N, 1°01'E	Pristine karstic in limestone, 280 m long (discovered in 2008)	Bacteria (16S rRNA genes)	341F/805R	~ 550	Illumina MiSeq	Alonso et al., 2019
					Micro-eukaryota (18S rRNA genes)	18S_0067a_deg/NSR399	~ 350		
					Micro-eukaryota (ITS)	ITS3_KYO2/ITS4	300-400		
					Archaea (16S rRNA genes)	515F/915R	~ 420		
	Cave Reille - Wall	Vézère Valley, Dordogne, France	44°55'N, 1°01'E	Pristine karstic cave in limestone, 150 m long (discovered early 1900s)	Bacteria (16S rRNA genes)	341F/805R	~ 550	Illumina MiSeq	Alonso et al., 2019
					Micro-eukaryota (18S rRNA genes)	18S_0067a_deg/NSR399	~ 350		
					Micro-eukaryota (ITS)	ITS3_KYO2/ITS4	300-400		
	Cave Manao-Pee - Floor	Wang Khamen karst system, Kanchanaburi, Thailand	14°22'51.192N, 98°54'39.489''E	Pristine cave in limestone, with diversity of calcite speleothems (flowstones, dripstones)	Archaea, Bacteria (16S rRNA genes)	Not applicable (metagenomics)	*~1541 (Full genes)*	Ion Proton sequencing	Wisecshart et al., 2019
					Micro-eukaryota (18S rRNA genes)	Not applicable (metagenomics)	*~1869 (Full genes)*		
	Cave Buraco da Sopradeira - Floor	Bahia, Brazil	12°26,55''S, 44°57'56''W	Pristine iron-rich cave in Neoproterozoic metamorphic limestone	Bacteria (16S rRNA genes)	341F/806R	~ 550	Illumina MiSeq	Marques et al., 2019
	Cave Herrenberg - Floor	Thuringe, Germany	50°25'41.6''N, 11°01'007.5''E	Pristine karst cave in Middle Triassic limestone (discovered during the excavation of a railway tunnel)	Bacteria (16S rRNA genes)	fd1/rp2	~ 1500	Cloning and sequencing	Rusznyák et al., 2012
	Cave Heshang - Floor	Qingjiang Valley, China	30°27'N, 110°25'E	Pristine karst cave in Cambrian dolomite, ~ 250 m long	Micro-eukaryota (ITS1)	ITS5-1737F/ITS2-2043R	~ 300	Illumina HiSeq	Man et al., 2018
	Karst aquifer (spring)	Wind Cave, South Dakota	43°35'00''N, 103°26'00''O	Drilled as a source of drinking water, reaching a depth of ~208 m and drawing water of pH 7.7 from the Madison aquifer	Archaea and Bacteria (16S rRNA genes)	515F/806R	~ 250	454-pyrosequencing	Hershey et al., 2018
	Bedrock groundwater	Kainuu, Finland	64°13'5.330''N, 29°56'40.721''E	Groundwater of pH 6.6 from deep Archaean bedrock. The area mainly consists of Leucotonalite gneiss	Archaea (16S rRNA genes)	A109F/A915R and A344F/A744R	~ 800 and 400	454-pyrosequencing	Purkamo et al., 2018
					Bacteria (16S rRNA genes)	8F/P2	~ 500		
					Micro-eukaryota (ITS)	ITS1F/ITS4 or ITS2	~ 400 or ~ 800		

WATER	Talik lake - Upper water	Qeqqata, Greenland	3°1'24"N, 1°28'40"E	Water flows into the lake from the melting active layer of the permafrost. It is nitrogen deficient (nitrate concentrations below the detection limit of 0.2 mg/l) and pH is about 8.3	Archaea (16S rRNA genes)	S-D-Arch-0349-a-S-17/S-D-Arch-0787-a-A-20	~ 460			
					Bacteria (16S rRNA genes)	S-D-Bact-0341-b-S-17/S-D-Bact-0785-a-A-21	~ 440	Ion Torrent PGM	Bomberg et al., 2019	
					Micro-eukaryota (ITS)	ITS1/ITS2	400-500			
	Talik lake - Deep water	Qeqqata, Greenland	3°1'22"N, 1°28'40"E	Water flows into the lake from the melting active layer of the permafrost. It is nitrogen deficient (nitrate concentrations below the detection limit of 0.2 mg/l) and pH is about 8.3	Archaea (16S rRNA genes)	S-D-Arch-0349-a-S-17/S-D-Arch-0787-a-A-20	~ 460			
					Bacteria (16S rRNA genes)	S-D-Bact-0341-b-S-17/S-D-Bact-0785-a-A-21	~ 440	Ion Torrent PGM	Bomberg et al., 2019	
					Micro-eukaryota (ITS)	ITS1/ITS2	400-500			
	Greenland glacier ice	Qeqqata, Greenland	3°3'39"N, 1°29'46"E	Glacial ice with ph 6.3 sampled in Ilsunnguata Sermia glacier, which develops on glacial till and glaciofluvial deposits overlaid by eolian silt and fine sand	Archaea (16S rRNA genes)	S-D-Arch-0349-a-S-17/S-D-Arch-0787-a-A-20	~ 460			
					Bacteria (16S rRNA genes)	S-D-Bact-0341-b-S-17/S-D-Bact-0785-a-A-21	~ 440	Ion Torrent PGM	Bomberg et al., 2019	
					Micro-eukaryota (ITS)	ITS1/ITS2	400-500			
	Marine hydrothermal vents	Vulcano Island, Italy	38°24'59.5"N, 14°57'39.1"E	Submarine samples from the hot sea floor taken at a depth of 0.7 m in two hydrothermal vents, which were 2 m apart	Archaea (16S rRNA genes)	Arc334F/Arc915R	~ 570	Illumina MiSeq	Antranikian et al, 2017	
					Bacteria (16S rRNA genes)	314F/907R	~500			
	Marine hydrothermal vents	North Atlantic Ocean	37°18'N, 32°16'O	Pallial fluid collected at the hydrothermal stations Menez Gwen and Lucky Strike	Micro-eukaryota (18S rRNA genes)	Euk328f/Euk329r	Not indicated	Cloning and sequencing	Sauvadet et al., 2010	
	Deep ocean - Water	Challenger Deep, Occidental Pacific Ocean	11°22.25'N, 142°42.75'E	Water sampled from the sea surface to near the bottom of the trench in Challenger Deep, the deepest ocean on Earth	Archaea (16S rRNA genes)	Arch21F/Arch958R	~ 900	454-pyrosequencing	Nunoura et al., 2018	
					Bacteria (16S rRNA genes)	Bac27F/Bac927	~ 900			
	Deep ocean - Sediments	Southwest Indian Ocean	49°43'E 37°47'S, 49°48'E 37°50'S, 52°56'E 35°54'S, 52°59'E 35°56'S, 52°59'E 35°58'S, 47°31'E 38°47'S, 47°25'E 38°45'S	Seven deep-sea sediment samples that were rinsed with sterile seawater and then crushed	Micro-eukaryota (ITS)	ITS3_KYO2/ITS4	300-400	Illumina HiSeq	Xu et al., 2018	
SOIL	Soil - Limestone forest	Styria, Austria	47°29'N, 14°6'E	Sandy loam soil (5-15 cm depth) with pH 6.1 and 6.3% organic matter, dominated by spruce and ash	Archaea and Bacteria (16S rRNA genes)	515F/806R	~ 250	Illumina MiSeq	Zheng et al., 2019	
					Micro-eukaryota (ITS)	ITS1/ITS2	400-500			
	Soil - Limestone cropland	Styria, Austria	47°29'N, 14°6'E	Sandy soil (5-15 cm depth) with pH 8.1 and 8.1% of organic matter, cultivated with a mixture of vegetables	Archaea and Bacteria (16S rRNA genes)	515F/806R	~ 250	Illumina MiSeq	Zheng et al., 2019	
					Micro-eukaryota (ITS)	ITS1/ITS2	400-500			
	Soil - Vanilla monoculture cropland	Hainan, China	18°72'N-18°76'N, 110°19'E-110°22'E	Loam soil, with pH 4.9 and 3.2% of organic matter, grown 12 months with vanilla plants	Micro-eukaryota (18S rRNA genes)	1389F/1510R	~ 130	Illumina MiSeq	Xiong et al., 2018	
	Soil - Limestone grassland	Styria, Austria	47°30'N, 14°4'E	Sandy soil (5-15 cm depth) with pH 6.4 and 8.2% of organic matter, pasture grazed by cattle	Archaea and Bacteria (16S rRNA genes)	515F/806R	~ 250	Illumina MiSeq	Zheng et al., 2019	
					Micro-eukaryota (ITS)	ITS1/ITS2	400-500			
	Soil - Neutral silt loam grassland	Lusignan area, Vienne département, France	46°25'12.91"N, 0°07'29.3"E	Silt loam soil (0-10 cm depth) with pH 6.6 and 9.9% organic matter	Bacteria (16S rRNA genes)	F479/R888	~ 450	454-pyrosequencing	Maron et al., 2018	
					Micro-eukaryota (18S rRNA genes)	FR1/FF390	~ 350			
	Soil - Neutral sand grassland	Hesse, Germany	49°55'34" N 8°37'21.6" E	Sandy soil (0-10 cm), with pH of 7.1 and low nutrient contents (water-extractable organic carbon 7.6 mg/kg)	Archaea, Bacteria (16S and 23S rRNA genes)	Not applicable (metatranscriptomics)	~1541 and ~2904 (Full genes)	454-pyrosequencing	Urich et al., 2008	
					Micro-eukaryota (18S and 28S rRNA genes)	Not applicable (metatranscriptomics)	~1869 and ~5070 (Full genes)			
	[illegible]	[illegible]	33°17'45.78"N 126°12'32.06"E, 35°14'56.05"N	[illegible]	Archaea (16S rRNA genes)	515F/958R	~ 400			

	Soil - Several greenhouses	Ansa, Buyeo, Chuncheon, Haman, Jangseong and Jeyu, South Korea	126°50'41.80"E, 35°14'57.64"N 128°21'17.49"E, 36°17'30.19"N 126°55'58.12"E, 36°42'44.19"N 128°30'07.14"E, 37°20'28.48"N 126°51'27.43"E, 37°56'02.63"N, 127°46'12.40"E	Bulk soil of 23 tomato greenhouses. Soil pH from 4.8 to 7.8, organic matter content from 1.2% to 7.3%.	Bacteria (16S rRNA genes)	799F/1193R	~ 480	Illumina MiSeq	Lee et al., 2019
					Micro-eukaryota (ITS)	ITS3F/ITS4R	330		
PLANTAE	Wheat hybrid - Rhizosphere	Norfolk, England	52°37'39.35"N, 1°10'43"E	Synthetic wheat hybrid grown in naturally-grassed, unfertilized soil (luvisol), samples collected at the flowering stage	Bacteria (16S rRNA genes)	515F/806R	~ 250		
					Micro-eukaryota (18S rRNA genes)	1427F/1616R	~ 180	Illumina MiSeq	Tkacz et al. ,2020
					Micro-eukaryota (ITS)	ITS1F/ITS2	400-500		
	Wheat variety - Rhizosphere	Norfolk, England	52°37'39.35"N, 1°10'43"E	Wheat cultivar Paragon grown in crop soil (luvisol), samples collected at the heading stage	Archaea (16S rRNA genes)	A0349F/A0519R	~ 170	Illumina MiSeq	Prudence et al., 2019
					Bacteria (16S rRNA genes)	341/806	~ 460		
	Tomato - Rhizosphere	Ansa, Buyeo, Chuncheon, Haman, Jangseong and Jeyu, South Korea	33°17'45.78"N 126°12'32.06"E, 35°14'56.05"N 126°50'41.80"E, 35°14'57.64"N 128°21'17.49"E, 36°17'30.19"N 126°55'58.12"E, 36°42'44.19"N 128°30'07.14"E, 37°20'28.48"N 126°51'27.43"E, 37°56'02.63"N, 127°46'12.40"E	Tomato plants grown in 23 greenhouses, with soil pH from 4.8 to 7.8, organic matter content form 1.2% to 7.3%. Samples collected at the ripening stage	Archaea (16S rRNA genes)	515F/958R	~ 450		
					Micro-eukaryota (ITS)	ITS3F/ITS4R	462	Illumina MiSeq	Lee et al., 2019
	Tomato - Endosphere	Ansa, Buyeo, Chuncheon, Haman, Jangseong and Jeyu, South Korea	33°17'45.78"N 126°12'32.06"E, 35°14'56.05"N 126°50'41.80"E, 35°14'57.64"N 128°21'17.49"E, 36°17'30.19"N 126°55'58.12"E, 36°42'44.19"N 128°30'07.14"E, 37°20'28.48"N 126°51'27.43"E, 37°56'02.63"N, 127°46'12.40"E	Tomato plants grown in 23 greenhouses, with soil pH from 4.8 to 7.8, organic matter content form 1.2% to 7.3%. Samples collected at the ripening stage	Archaea (16S rRNA genes)	515F/958R	~ 450		
					Micro-eukaryota (ITS)	ITS3F/ITS4R	462	Illumina MiSeq	Lee et al., 2019
METAZOA	Summer chafer beetle - Larvae hindgut	Republic of Tatarstan, Russia	55°47'N , 49°10'E	Coleoptera found in aerial habitats such as grassland, park and gardens. Intestinal tract of second or third instar beetle larvae	Archaea (16S rRNA genes)	Arch349F/Arch806R	~ 520		
					Bacteria (16S rRNA genes)	Bakt341F/Bakt805R	~ 460	Illumina MiSeq	Ziganshina et al., 2018
					Micro-eukaryota (ITS)	ITS3 KYO2/ITS4	300-400		
	Ribbed pine borer beetle - Larvae hindgut	Republic of Tatarstan, Russia	55°47'N , 49°10'E	Species of forest beetle, landscape found above karst ecosystems. Intestinal tract of second or third instar beetle larvae	Bacteria (16S rRNA genes)	Bakt341F/Bakt805R	~ 460	Illumina MiSeq	Ziganshina et al., 2018
					Micro-eukaryota (ITS)	ITS3 KYO2/ITS4	300-400		
	Asian tiger mosquito - Adults	Nakhon Nayok, Thailand	14°12.362'N, 101°13.094"E	Invasive species, present on 4 continents in aquatic and aerial habitats. Whole bodies of adult females, not engorged with blood, were sampled	Archaea and Bacteria (16S rRNA genes)	U341F/U800R	~ 1000	454-pyrosequencing	Thongsripong et al., 2018
					Micro-eukaryota (18S rRNA genes)	Euk82F/Euk516R	~ 470		
	Phytophagous bats - Fecal	Guangdong and Yunnan, China	23°02'N 114°56'E, 24°53'N 113°11'E, 22°08'24"N 107°04'34"E, 21°58'N 100°28'E	Fresh feces from healthy adult cave bats (*Rousettus leschenaultii, Cynopterus sphinx*) caught in hoop nets when they flew out of the caves at night	Archaea and Bacteria (16S rRNA genes)	515F/806R	~ 250	Illumina HiSeq	Li et al., 2018
					Micro-eukaryota (18S rRNA genes)	1380F/1510R	~ 165		
	Insectivorous bats - Fecal	Guangdong, Guangxi and Yunnan, China	23°05'34"N 113° 21'18"E, 22°08'24"N 107°04'34"E	Fresh feces from healthy adult cave bats (*Myotis ricketti, Hipposideros larvatus, Tylonycteris pachypus, Pipistrellus abramus, Scotophilus heathi, Hipposideros armiger*) caught in hoop nets when they flew out of the caves at night	Archaea and Bacteria (16S rRNA genes)	515F/806R	~ 250	Illumina HiSeq	Li et al., 2018
					Micro-eukaryota (18S rRNA genes)	1380F/1510R	~ 165		
	Bears - Fecal	Cundinamarca, Colombia	4°54'46.394"N, 73°44'16.362"O	The Andean bears (*Tremarctos ornatus*) live in trees and do not hibernate. Feces were sampled	Bacteria (16S rRNA genes)	515F/806R	~ 250	Ion Torrent PGM	Borbón-García et al., 2017
	Humans - Fecal	Styria, Austria	47°4'N, 15°26'E	Feces from healthy adults	Archaea (16S rRNA genes)	344f and 915r, 349af/519ar and 519af/785ur	~ 560, ~ 170 and ~ 260	Illumina MiSeq	Koskinen et al., 2017
	Humans - Fecal	Hunan, China	28°08'30"N, 113°37'30"E	Feces from healthy people about 50 years old and without recent antibiotic treatments	Bacteria (16S rRNA genes)	515F/806R	~ 250	Illumina MiSeq	Yu et al., 2015
	Humans - Fecal	Midwestern United States	Not indicated	Feces from healthy vegetarian people about 23 years old	Micro-eukaryota (ITS)	Not indicated	Not indicated	454-pyrosequencing	Suhr et al., 2016

Appendix S2: Table S2. Detailed information on emblematic Paleolithic caves. NA and hyphens are used when data is not available and when the cave are closed, respectively.

Cave name	Latitude	Longitude	Number of visitors/year	Cave status	Closing date	UNESCO Classification	Country	Continent
Jabbaren Cave	26.4880835	8.3571492	-	Closed	-	UNESCO	Algeria	Africa
Cave of Beasts	24.8766665	28.7757345	-	Closed	-	Not classified	Egypt	Africa
Cave of Swimmers	24.8766665	28.7757345	< 1000	Open	-	Not classified	Egypt	Africa
Nsalu Cave	-12.8815165	30.5117653	NA	Open	-	Not classified	Malawi	Africa
Apollo 11 Cave	-26.8752094	17.7634818	NA	Open	-	Not classified	Namibia	Africa
Paula Cave	-21.4845308	15.8527818	NA	Open	-	Not classified	Namibia	Africa
Phillips Cave	-21.799728	15.6410286	-	Closed	-	Not classified	Namibia	Africa
Nkila-Ntari Cave	-4.1232157	13.8574995	NA	Open	-	Not classified	Republic of Congo	Africa
Bomblos Cave	-34.4131312	21.2202699	-	Closed	-	Not classified	South Africa	Africa
Padah-Lin Caves	21.162815	96.442291	NA	Open	-	Not classified	Birmania	Asia
Leang-Leang Caves	-4.9825494	119.6332922	NA	Open	-	UNESCO	Indonesia	Asia
Lubang Jeriji Saléh Cave	1.241473	117.329111	-	Closed	-	Not classified	Indonesia	Asia
Cave of Niah	3.8141112	113.7826843	NA	Open	-	Not classified	Malaysia	Asia
Tambun Cave	4.5832182	101.066906	NA	Open	-	Not classified	Malaysia	Asia
Khoit Tsenkher Cave	47.3486732	91.9548539	NA	Open	-	UNESCO	Mongolia	Asia
Tharia Cave	30.4278981	73.7483348	NA	Open	-	Not classified	Pakistan	Asia
Cave of Badanj	43.1010615	17.8956303	-	Closed	-	UNESCO	Bosnia and Herzegovina	Europe
Magoura Cave	43.718171	22.600288	NA	Open	-	UNESCO	Bulgaria	Europe
Bara-Bahau Cave	44.916061	0.933746	NA	Open	-	Not classified	France	Europe
Cantal Cave	44.5067942	1.662176	-	Closed	-	Not classified	France	Europe
Carriot Cave	44.4823833	1.6477817	-	Closed	-	Not classified	France	Europe
Cave of Arcy-sur-Cure	47.7664801	3.7501196	> 25 000	Open	-	Not classified	France	Europe
Cave of Baume d'Oullins	44.3458868	4.4590721	NA	Closed Now	1981	Not classified	France	Europe
Cave of Beideilhac	42.872938	1.567843	NA	Open	-	Not classified	France	Europe
Cave of Bernifal	44.9310707	1.0672089	NA	Open	-	UNESCO	France	Europe
Cave of Bigournal	44.4783789	1.5758931	-	Closed	-	Not classified	France	Europe
Cave of Cassegros	44.4415038	0.8599672	-	Closed	-	Not classified	France	Europe
Cave of Combe-Nègre	44.58529	1.133634	-	Closed	-	Not classified	France	Europe
Cave of Cougnac	44.7602305	1.3630467	25 000	Open	-	Not classified	France	Europe
Cave of Cussac	44.8297083	0.8479659	-	Closed	-	Not classified	France	Europe
Cave of Cuzoul des Brasconnies	44.579219	1.745926	-	Closed	-	Not classified	France	Europe
Cave of Foissac	44.5026281	2.006713	15 000	Open	-	Not classified	France	Europe
Cave of Fronsac	45.451417	0.453157	-	Closed	-	Not classified	France	Europe
Cave of Gabillou	45.038867	0.380087	-	Closed	-	Not classified	France	Europe
Cave of Gargas	43.055571	0.5362887	20 000	Open	-	Not classified	France	Europe
Cave of Gourdan	43.072356	0.5604588	-	Closed	-	Not classified	France	Europe
Cave of Gouy	49.360824	1.129739	NA	Closed Now	1996	Not classified	France	Europe
Cave of Grèze	44.9523778	1.089956	-	Closed	-	Not classified	France	Europe
Cave of La Balme	45.852456	5.338789	> 50 000	Open	-	Not classified	France	Europe
Cave of Larchand	48.2846954	2.5835803	-	Closed	-	Not classified	France	Europe

Cave of Laroque	43.917144	3.7333373	-	Closed	-	Not classified	France	Europe
Cave of Mas d'Azil	43.067768	1.355178	> 15 000	Open	-	Not classified	France	Europe
Cave of Points	44.3397865	4.487227	-	Closed	-	Not classified	France	Europe
Cave of Rocamadour	44.8051162	1.6253677	> 10 000	Open	-	Not classified	France	Europe
Cave of Roucadour	44.720677	1.815419	-	Closed	-	Not classified	France	Europe
Cave of Teyjat	45.585455	0.5750531	NA	Open	-	Not classified	France	Europe
Caves of Saulges	47.9915491	0.4044062	> 35 000	Open	-	Not classified	France	Europe
Chauvet Cave	44.3250667	4.541663	-	Closed	-	UNESCO	France	Europe
Christian Cave	44.3857029	4.4173762	-	Closed	-	Not classified	France	Europe
Cosquet Cave	43.2027482	5.449316	-	Closed	-	Not classified	France	Europe
Cow Cave	42.8206056	1.587798	> 1000	Open	-	Not classified	France	Europe
Ebbou Cave	44.3855805	4.4146286	NA	Closed Now	1964	Not classified	France	Europe
Enlène Cave	43.0325	1.20215	-	Closed	-	Not classified	France	Europe
Escabasses Cave	44.718015	1.798005	-	Closed	-	Not classified	France	Europe
Espélugues Cave	43.0940904	-0.0464975	NA	Closed Now	NA	Not classified	France	Europe
Figuier Cave	0.96675	33.82622	-	Closed	-	Not classified	France	Europe
Font de Gaume Cave	44.9353743	1.0283041	20 000	Open	-	UNESCO	France	Europe
Isturitz and Oxocelhaya Caves	43.3529497	-1.206027	> 50 000	Open	-	Not classified	France	Europe
Jovelle Cave	45.3602234	0.4299957	< 1000	Open	-	Not classified	France	Europe
La Marche Cave	46.406066	0.724796	NA	Open	-	Not classified	France	Europe
Labastide Cave	43.033007	0.3462473	-	Closed	-	Not classified	France	Europe
Lascaux Cave	45.0536353	1.1701008	100 000	Closed Now	1963	UNESCO	France	Europe
Les Combarelles Cave	44.9434213	1.0422972	10 000	Open	-	UNESCO	France	Europe
Marcenac Cave	44.5076416	1.6472787	-	Closed	-	Not classified	France	Europe
Marsoulas Cave	43.1047381	0.9861907	-	Closed	-	Not classified	France	Europe
Mayrière Cave	44.0402464	1.6832291	-	Closed	-	Not classified	France	Europe
Montespan Cave	43.0726916	0.8496536	NA	Closed Now	1985	Not classified	France	Europe
Moulin de Laguenay Cave	45.0952188	1.4704121	-	Closed	-	Not classified	France	Europe
Mouthe Cave	44.9247332	1.0207217	NA	Closed Now	NA	UNESCO	France	Europe
Niaux Cave	42.8198566	1.5938431	50 000	Open	-	Not classified	France	Europe
Pair-non-Pair Cave	45.0394981	0.5013461	> 10 000	Open	-	Not classified	France	Europe
Pape Cave	43.6294488	0.7186408	NA	Open	-	Not classified	France	Europe
Pech de l'Azé Cave	44.8549357	1.2760468	-	Closed	-	Not classified	France	Europe
Pech Merle Cave	44.5074288	1.6443131	> 50 000	Open	-	Not classified	France	Europe
Pergouset Cave	44.48603	1.614186	-	Closed	-	Not classified	France	Europe
Pestillas Cave	44.548361	1.063656	-	Closed	-	Not classified	France	Europe
Pigeonnier Cave	44.8112041	1.2297205	-	Closed	-	Not classified	France	Europe
Placard Cave	45.68861	0.420107	NA	Open	-	Not classified	France	Europe
Portel Cave	43.0313669	1.5404024	-	Closed	-	Not classified	France	Europe
Prinvaux Cave	48.3227801	2.3703552	NA	Open	-	Not classified	France	Europe
Roc-de-Sers	45.5744587	0.3289716	NA	Open	-	Not classified	France	Europe
Rouffignac Cave	45.0087737	0.987912	> 60 000	Open	-	UNESCO	France	Europe
Sainte-Eulalie Cave	44.593649	1.87575	-	Closed	-	Not classified	France	Europe

Saran IV Cave	48.998605	4.0100982	-	Closed	-	Not classified	France	Europe
Scritta Cave	42.7682213	9.3710518	-	Closed	-	Not classified	France	Europe
Sorcerer's Cave	44.9259783	0.9675154	25 000	Open	-	UNESCO	France	Europe
Trois-Frères Cave	43.0320293	1.2116808	-	Closed	-	Not classified	France	Europe
Tuc d'Audoubert Cave	43.0325	1.20215	-	Closed	-	Not classified	France	Europe
Villars Cave	45.4425621	0.785301	60 000	Open	-	Not classified	France	Europe
Visage Cave	45.684863	0.417574	-	Closed	-	Not classified	France	Europe
Felci Cave	40.5473327	14.2339896	5000	Open	-	Not classified	Italy	Europe
Genovese Cave	38.0018776	12.321893	6000	Open	-	Not classified	Italy	Europe
Paglicci Cave	41.6639475	15.5664152	NA	Open	-	Not classified	Italy	Europe
Romito Cave	39.9111228	15.9286478	40 000	Open	-	Not classified	Italy	Europe
Cave of Coliboaia	46.5308045	22.5974786	-	Closed	-	Not classified	Romania	Europe
Ignatievka Cave	54.898811	57.7818426	-	Closed	-	Not classified	Russia	Europe
Kapova Cave	53.0437475	57.0651917	> 35 000	Closed Now	2003	UNESCO	Russia	Europe
Araña Cave	39.1102652	-0.8644594	-	Closed	-	UNESCO	Spain	Europe
Cave of Altamira	43.3768445	-4.1197476	170 000	Closed Now	2002	UNESCO	Spain	Europe
Cave of Altxerri	43.2369112	-2.1489094	-	Closed	-	UNESCO	Spain	Europe
Cave of Bacinete	36.1999904	-5.5565763	-	Closed	-	UNESCO	Spain	Europe
Cave of Casares	40.9551147	-2.2931854	-	Closed	-	Not classified	Spain	Europe
Cave of El Castillo	38.768268	1.2581943	25 000	Open	-	UNESCO	Spain	Europe
Cave of Las Monedas	43.2910256	-3.9643047	15 000	Open	-	UNESCO	Spain	Europe
Cave of Moro	36.0080459	-5.6077646	-	Closed	-	Not classified	Spain	Europe
Cave of Zubialde	42.867886	-2.6996609	-	Closed	-	Not classified	Spain	Europe
Cocina Cave	40.094266	1.3201021	-	Closed	-	UNESCO	Spain	Europe
Ekain Cave	43.2361328	-2.2756492	NA	Closed Now	1975	UNESCO	Spain	Europe
Fosca Cave	38.8055502	0.1608379	-	Closed	-	Not classified	Spain	Europe
Laja Alta Cave	36.4346867	-5.4960515	NA	Open	-	Not classified	Spain	Europe
Las Chimenas Cave	43.2896135	-3.9644624	NA	Open	-	UNESCO	Spain	Europe
Las Palomas Cave	36.0080459	-5.6077646	NA	Open	-	Not classified	Spain	Europe
Los Caballos Cave	40.4154309	0.0671777	-	Closed	-	UNESCO	Spain	Europe
Nerja Cave	36.7618981	-3.8456045	100 000	Open	-	Not classified	Spain	Europe
Pasiega Cave	43.2896135	3.9644624	NA	Closed Now	NA	UNESCO	Spain	Europe
Pileta Cave	36.6912325	-5.2699924	30 000	Open	-	Not classified	Spain	Europe
Santimamiñe Cave	43.3465481	-2.6367509	> 10 000	Closed Now	NA	UNESCO	Spain	Europe
Tajo de la Figuras Caves	36.3427088	-5.8091329	NA	Open	-	Not classified	Spain	Europe
Tito Bustillos Cave	43.4606631	-5.0676633	5000	Open	-	UNESCO	Spain	Europe
Caves of Creswell Crags	53.2620418	-1.1991788	NA	Open	-	Not classified	United Kingdom	Europe
Gorham's Cave	36.1204578	-5.3420046	NA	Open	-	UNESCO	United Kingdom	Europe
Sierra de San Francisco	27.2030522	-113.3207274	NA	Open	-	UNESCO	Mexico	North America
Cave of Hands	-47.1636497	-70.7725881	> 1000	Open	-	UNESCO	Argentina	South America
Pedra Pintada Cave	-5.8049026	-54.0442521	NA	Open	-	Not classified	Brazil	South America
Toquepala Caves	-17.3034501	-70.7184549	NA	Open	-	Not classified	Peru	South America

Caves status: never open (‘Closed’), now closed after having been open for visits (‘Closed now’), open for tourism (‘Open’)

Appendix S3: Table S3. Detailed information of selected literature related to the bacterial, archaeal and micro-eukaryotic communities in the pristine and anthropized caves.

	Sample ID for Figure 4	Region/Province, Country	GPS coordinates (WGS 84)	Properties	Targeted microbiota	Primer pair	Sequence length (bp)	Sequencing approach	Reference
PRISTINE CAVES	Cave Alas- Wall	Vézère Valley, Dordogne, France	44°53'12"N, 1°10'03"E	Pristine karstic cave in limestone, 130 m long (discovered early 1900s)	Archaea (16S rRNA genes)	515F/915R	~420	Illumina MiSeq	Alonso et al., 2019
					Bacteria (16S rRNA genes)	341F/805R	~550		
					Micro-eukaryota (18S rRNA genes)	18S_0067a_deg/NSR399	~350		
					Micro-eukaryota (ITS)	ITS3_KYO2/ITS4	300-400		
	Cave Mouflon - Wall	Vézère Valley, Dordogne, France	45°07'09.5"N, 1°07'11.2"E	Pristine karstic cave in limestone, 280 m long (discovered early 1900s)	Archaea (16S rRNA genes)	515F/915R	~420	Illumina MiSeq	Alonso et al., 2019
					Bacteria (16S rRNA genes)	341F/805R	~550		
					Micro-eukaryota (18S rRNA genes)	18S_0067a_deg/NSR399	~350		
					Micro-eukaryota (ITS)	ITS3_KYO2/ITS4	300-400		
	Cave Pilier - Wall	Vézère Valley, Dordogne, France	44°55'N, 1°01'E	Pristine karstic cave in limestone, 150 m long (discovered in 2008)	Archaea (16S rRNA genes)	515F/915R	~420	Illumina MiSeq	Alonso et al., 2019
					Bacteria (16S rRNA genes)	341F/805R	~550		
					Micro-eukaryota (18S rRNA genes)	18S_0067a_deg/NSR399	~350		
					Micro-eukaryota (ITS)	ITS3_KYO2/ITS4	300-400		
	Cave Reille - Wall	Vézère Valley, Dordogne, France	44°55'N, 1°01'E	Pristine karstic cave in limestone, 2000 m long (discovered early 1900s)	Archaea (16S rRNA genes)	515F/915R	~420	Illumina MiSeq	Alonso et al., 2019
					Bacteria (16S rRNA genes)	341F/805R	~550		
					Micro-eukaryota (18S rRNA genes)	18S_0067a_deg/NSR399	~350		
					Micro-eukaryota (ITS)	ITS3_KYO2/ITS4	300-400		
ANTHROPIZED CAVES	Cap Blanc - Wall	Vézère Valley, Dordogne, France	44°56'44"N, 1°05'49"E	Anthropized rock shelter (converted into a cave set-up following the construction of a facade) in limestone, 13 m long (discovered in 1909, open since 1910)	Archaea (16S rRNA genes)	515F/915R	~420	Illumina MiSeq	Alonso et al., 2019
					Bacteria (16S rRNA genes)	341F/805R	~550		
					Micro-eukaryota (18S rRNA genes)	18S_0067a_deg/NSR399	~350		
					Micro-eukaryota (ITS)	ITS3_KYO2/ITS4	300-400		
	Combarelles - Wall	Vézère Valley, Dordogne, France	44°56'37"N, 1°02'32"E	Anthropized karstic cave in limestone, 300 m long (discovered in 1901, open since 1911)	Archaea (16S rRNA genes)	515F/915R	~420	Illumina MiSeq	Alonso et al., 2019
					Bacteria (16S rRNA genes)	341F/805R	~550		
					Micro-eukaryota (18S rRNA genes)	18S_0067a_deg/NSR399	~350		
					Micro-eukaryota (ITS)	ITS3_KYO2/ITS4	300-400		
	Rouffignac - Wall	Vézère Valley, Dordogne, France	45°00'31"N, 0°59'16"E	Anthropized karstic cave in limestone, 8000 m long (discovered in 1956, open since 1959)	Archaea (16S rRNA genes)	515F/915R	~420	Illumina MiSeq	Alonso et al., 2019
					Bacteria (16S rRNA genes)	341F/805R	~550		
					Micro-eukaryota (18S rRNA genes)	18S_0067a_deg/NSR399	~350		
					Micro-eukaryota (ITS)	ITS3_KYO2/ITS4	300-400		
	Lascaux Passage - Walkways	Vézère Valley, Dordogne, France	45°03'10"N, 1°10'12"E	Anthropized karstic cave in limestone, 17 m long (discovered in 1940, open since 1948)	Archaea (16S rRNA genes)	515F/915R	~420	Illumina MiSeq	Alonso et al., 2019
					Bacteria (16S rRNA genes)	341F/805R	~550		
					Micro-eukaryota (18S rRNA genes)	18S_0067a_deg/NSR399	~350		
					Micro-eukaryota (ITS)	ITS3_KYO2/ITS4	300-400		

Appendix S4: Table S4. Detailed information of selected literature related to the bacterial, archaeal and micro-eukaryotic communities in the microbial alteration and apart from alteration in caves.

	Sample ID for Figure 5	Region/Province, Country	GPS coordinates (WGS 84)	Properties	Targeted microbiota	Primer pair	Sequence length (bp)	Sequencing approach	Reference
MICROBIAL ALTERATIONS	Azé - Biofilm	Azé, Bourgogne-Franche-Comté, France	46°26'17"N, 4°45'42"E	Anthropized karstic cave in limestone, 300 m long with green biofilm (discovered in 1954)	Bacteria (16S rRNA genes)	799F/1115R	~300	Illumina MiSeq	Pfendler et al., 2018
					Micro-eukaryota (ITS)	ITS1F/ITS2R	400-500		
	Soyons - Biofilm	Rhône Valley, Ardèche, France	44°52'58"N, 4°50'51"E	Anthropized karstic cave in limestone, 60 m long with green biofilm treated with sodium hypochlorite (discovered at the end of the 19th century)	Bacteria (16S rRNA genes)	799F/1115R	~300	Illumina MiSeq	Pfendler et al., 2018
					Micro-eukaryota (ITS)	ITS1F/ITS2R	400-500		
	Altamira - Grey spots	Cantabria, Spain	43°22'57"N, 4°06'58"E	Anthropized karstic cave in limestone, 300 m long with grey and yellow stains on walls (discovered in 1879)	Bacteria (16S rRNA genes)	21F/1492R	~1400	Cloning and sequencing	Cuezva et al., 2012
	Sorcerer's - Gypsum efflorescense	Vézère Valley, Dordogne, France	44°55'34"N, 0°58'03"E	Anthropized karstic cave in limestone, 13 m long with gypsum efflorescences on walls (discovered in 1951)	Bacteria (16S rRNA genes)	27F/1492R	~1000	GS FLX pyrosequencing	Lepinay et al., 2017
					Bacteria (16S rRNA genes)	341F/805R	~550		
	Lascaux - Black stain	Vézère Valley, Dordogne, France	45°03'10"N, 1°10'12"E	Anthropized karstic cave in limestone, 150 m long with black stains on certains walls (discovered in 1940)	Micro-eukaryota (18S rRNA genes)	18S_0067a_deg/NSR399	~350	Illumina MiSeq	Alonso, 2018
					Micro-eukaryota (ITS)	ITS3_KYO2/ITS4	300-400		
NEIGHBORING ROCK SURFACES	Lascaux - Unstained	Vézère Valley, Dordogne, France	45°03'10"N, 1°10'12"E	Anthropized karstic cave in limestone, 150 m long (discovered in 1940)	Bacteria (16S rRNA genes)	341F/805R	~550	Illumina MiSeq	Alonso, 2018
					Micro-eukaryota (18S rRNA genes)	18S_0067a_deg/NSR399	~350		
					Micro-eukaryota (ITS)	ITS3_KYO2/ITS4	300-400		

CHAPITRE 2

Dynamiques microbiennes associées à la formation, à l'évolution et à la dissémination des zones sombres

Avant-propos

Dans les régions calcaires, la dissolution du calcaire peut conduire à la formation de grottes karstiques. Malgré un apport limité en nutriments, les communautés microbiennes établies dans les grottes sont plutôt abondantes et diversifiées [Tomczyk-Żak et Zielenkiewicz, 2016], et jouent des rôles importants dans ces environnements [Barton *et al.*, 2007]. Certaines grottes ont été aménagées par l'homme pour permettre l'activité touristique du site, provoquant ainsi une anthropisation de l'écosystème [Cigna, 2016]. L'anthropisation des grottes peut conduire à un déséquilibre du microbiote, pouvant provoquer une prolifération anormale d'un ou de plusieurs microorganismes sur les surfaces rocheuses. Cette prolifération anormale de microorganismes sur les parois peut induire (i) la biodétérioration des parois [He *et al.*, 2022], (ii) la Lampenflora (flore et microorganismes autotrophes qui se développent par l'utilisation des systèmes lumineux mis en place), principalement composée de Cyanobactéries et d'algues eucaryotes, qu'il s'agisse de Chrysophytes (brunes-jaunes) ou de Chlorophytes (vertes) [Lefèvre, 1974, Bastian *et al.*, 2010, Baquedano Estevez *et al.*, 2019], (iii) le développement d'un voile de calcite, impliquant éventuellement des genres bactériens tels que *Pseudomonas*, *Bacillus* et *Myxococcus* [Chalmin *et al.*, 2007] et (iv) des taches de différentes couleurs par exemple des taches blanches, noires, jaunes, grises et rouges attribuées à la prolifération de bactéries (ex. Xanthomonodales, *Thauera*, etc.) et/ou de champignons (ex. *Ochroconis*, *Exophiala*, *Acremonium*, *Fusarium*, etc.) [Portillo *et al.*, 2008, Portillo et Gonzalez, 2009, Urzì *et al.*, 2010, Bastian *et al.*, 2010]. Dans plusieurs grottes, des traitements antibiotiques (ex : streptomycine) et chimiques (ex : chlorure de benzalkonium) ont été appliqués sur les parois, accentuant quelquesfois le déséquilibre du microbiote des grottes [Bastian *et al.*, 2010, Martin-Sanchez *et al.*, 2015, Bontemps *et al.*, 2021]. A l'heure actuelle, deux grands types d'altérations sont retrouvées dans la grotte de Lascaux, (i) les taches noires qui sont plutôt stables ces dernières années et (ii) dans les salles les plus anthropisées comme l'Abside, des altérations appelées zones sombres qui se sont développées au cours des 14 dernières années. Ces zones sombres n'ont pas été traitées chimiquement et aucune zone de transition visuelle n'est observée entre la zone sombre et la paroi saine. Actuellement, aucune connaissance sur la formation, l'évolution et la dissémination des zones sombres n'est disponible. Une analyse microbienne préliminaire dans l'Abside a mis en évidence que les zones sombres sont caractérisées par des changements communautaires, notamment la sélection de champignons mélanisés *Ochroconis* et la contre-sélection de bactéries affiliées au genre *Pseudomonas* [Alonso, 2018]. On peut donc faire l'hypothèse que la formation et l'évolution des zones sombres seraient liées à des successions microbiennes rapides car les zones altérées et zones saines sont visuellement très différentes, sans zone de transition apparente. L'objectif associé est de caractériser à micro-échelle spatiotemporelle la dynamique des trois domaines du vivant lors de l'évolution des zones sombres **(Article 2)**. Jusqu'à récemment, ces modifications étaient considérées comme limitées à l'Abside. Cependant, une surveillance étroite dans plusieurs autres salles de la grotte (ex. Nef, Passage, Salle des Taureaux, etc.) a mis en évidence des changements visuels ressemblant à ceux des zones sombres de l'Abside. Suggérant qu'au moins une partie des changements de la communauté microbienne liés à la formation de zone sombre implique des taxons cosmopolites, car ces zones sombres se développent dans différents habitats microbiens au sein de Lascaux, mais aussi des taxons endémiques conformément aux spécificités du microbiote des dif-

férentes pièces ou surfaces. L'objectif associé à cette hypothèse est de caractériser la dynamique de la diversité microbienne au niveau des zones sombres, à l'échelle spatiale de l'ensemble de la grotte. **(Article 3)**.

La grotte de Lascaux étant un site paléolithique majeur, des dispositions particulières sont établies pour la préservation du site. Pour chaque campagne d'échantillonnage, la prise d'échantillons dans la grotte est répertoriée, documentée et validée en amont du prélèvement par le personnel de la DRAC Nouvelle-Aquitaine (M. Mauriac-Le-Hénon, S. Géraud, J.C Portais). Pour chaque prélèvement une photographie est réalisée et une base de données recense les prélèvements de l'ensemble des projets d'écologie microbienne de la grotte de Lascaux. Les prélèvements dans la grotte s'effectuent avec un équipement particulier incluant charlotte, masque, combinaison, gants et sur-chaussures. Afin de limiter la présence humaine dans la grotte seul un membre du projet d'écologie microbienne accompagné de la restauratrice Diane Henry-Lormelle entre dans la grotte avec un temps limité définit en accord avec la liste de prélèvement prévue. Après chaque entrée dans la grotte, un temps de pause est prévu afin que la température se stabilise impliquant à minima une journée de repos entre deux sessions d'échantillonnage. Six réplicats de prélèvement pour chaque condition étudiée ont été réalisés par la restauratrice à l'aide d'écouvillons stériles pour les échantillons de microbiologie et au 'mini-burin' pour les parois artificielles. Les échantillons ont ensuite été placés dans un conteneur d'azote liquide puis conservés à -80°C au laboratoire avant l'extraction des acides nucléiques. Pour chaque échantillon de microbiologie une extraction d'ADN a été réalisée à l'aide du kit FastDNA SPIN kit for Soil (MP Biomedical, France), les concentrations d'ADN ont été quantifiées en utilisant le kit Qubit DNAdb HS (Thermo Fisher Scientific, Etats-Unis). La diversité des communautés microbiennes a été étudiée par une approche de métabarcoding ciblant les marqueurs ribosomiques universels bactériens, archéens et eucaryotiques et la région ITS 2 (Internal Transcribed Spacer) fongique. Le séquençage a été réalisé avec la technologie Illumina MiSeq 2×300pb en vue de l'obtention de 70 000 séquences par échantillon (profondeur de séquençage estimée suffisante pour décrire la totalité de la richesse présente).

La première étude **(Article 2)** concernant l'identification des dynamiques microbiennes des zones sombres à une échelle micro-spatialisée a nécessité trois campagnes d'échantillonnage sur trois zones sombres du plan incliné gauche de l'Abside (avril 2019, décembre 2019 et avril 2021). Au total 198 échantillons ont été traités conformément au protocole décrit ci-dessus. Cinq conditions de surface ont été prélevées permettant d'observer en détail les dynamiques microbiennes associées au développement des zones sombres : (i) calcaire distant de la zone sombre, (ii) calcaire proche de la zone sombre, (iii) nouvelle zone sombre, (iv) zone sombre intermédiaire et (v) vieille zone sombre. Les résultats de cette étude montrent que trois groupes de surfaces (surfaces non marquées, nouvelle zone sombre, zone sombre intermédiaire et vieille) ont été mis en évidence pour les communautés bactériennes, micro-eucaryotiques et fongiques tandis que seulement deux groupes (surfaces non marquées et surfaces altérées) ont été observés chez les archées. Nous avons montré que le début de la formation des zones sombres coïncide avec le développement des genres bactériens *Labrys*, *Nonomuraea* et *Sphingomonas*, qui est concomitant

avec la prolifération des champignons *Ochroconis* et la contre-sélection des *Pseudomonas*. La modélisation des processus d'assemblage des communautés a mis en évidence que la dynamique des taxa rares dans les surfaces non marquées adjacentes aux zones sombres et dans les zones sombres nouvellement formées était régie en partie par des processus déterministes. Ces résultats suggèrent donc un changement brutal de la communauté lors de l'évolution des zones sombres sur les parois.

Mon rôle dans cette étude a été le suivant : j'ai participé à la mission d'échantillonnage en avril 2021 et à la réflexion sur les objectifs et démarches scientifiques. J'ai réalisé les étapes de biologie moléculaire avant séquençage (extraction ADN, contrôles qualité et PCR1). J'ai traité les données de séquençage brutes, j'ai ensuite analysé ces données permettant d'observer les processus microbiennes associés à la formation et à l'évolution des zones sombres dans l'Abside en utilisant notamment des statistiques multivariées, de la modélisation des processus d'assemblage des communautés et la réalisation de réseaux de co-occurrences. Des PCR quantitatives ont été réalisées par Alice Guillmot (stagiaire de Master 1 Microbiologie de Lyon) que j'ai eu l'occasion d'encadrer durant ma dernière année de doctorat.

La deuxième étude **(Article 3)** concerne la dissémination des zones sombres à l'échelle de la grotte. Cette étude a comparé neufs emplacements avec des caractéristiques différentes (substrat, salle, traitements chimiques et antibiotiques, etc.). Au total, 108 prélèvements ont été effectués en septembre 2020 et ont été traités conformément au protocole décrit ci-dessus. Les résultats de cette étude ont confirmé l'hétérogénéité du microbiote des surfaces non marquées ainsi qu'une différence significative entre les communautés microbiennes des surfaces non marquées et des zones sombres pour tous les emplacements. L'utilisation d'une matrice de décision a montré que les changements de microbiote liés à la formation des zones sombres pouvaient varier selon l'emplacement, mais que les zones sombres de différents emplacements présentaient des similitudes microbiennes. Également, nous avons mis en évidence que les zones sombres abritent des taxons bactériens et fongiques présents dans les deux conditions de surface et dans toutes les salles de la grotte (i.e. taxons cosmopolites de la grotte de Lascaux), ainsi que des taxons spécifiques aux zones sombres présents à tous les endroits (en particulier les bactéries). Cela suggère que le développement des altérations pourrait se poursuivre en fonction de la zone de distribution des taxons cosmopolites.

Mon rôle dans cette étude a été le suivant : j'ai participé aux missions d'échantillonnage, à la réflexion sur les objectifs scientifiques et au choix de la démarche expérimentale utilisée. J'ai réalisé les étapes de biologie moléculaire avant séquençage (extraction ADN, contrôles qualité et PCR1). J'ai traité les données de séquençage brutes, j'ai ensuite analysé ces données permettant d'observer les dynamiques microbiennes associées à la dissémination des zones sombres à l'aide de statistiques multivariées et à la mise en place d'une matrice décisionnelle. Les analyses de microscopie électronique ont été réalisées par Yvan Moënne-Loccoz en collaboration avec Claire Prigent-Combaret et les PCR quantitatives ont été réalisées par Alice Guillmot (stagiaire de Master 1 Microbiologie de Lyon).

L'ensemble de ce travail a permis la rédaction de deux publications 'Microscale dynamics

of dark zone alterations in anthropized karstic cave shows brutal microbial community switch' (soumission prévue fin 2022) et 'Dark-zone alterations expand throughout Paleolithic Lascaux Cave despite spatial heterogeneity of the cave microbiome' (soumission prévue fin 2022).

Article 2. Microscale dynamics of dark zone alterations in anthropized karstic cave shows brutal microbial community switch

ZELIA BONTEMPS[1], MYLENE HUGONI[1,2,3] AND YVAN MOENNE-LOCCOZ[1]

[1]Univ Lyon, Université Claude Bernard Lyon 1, CNRS, INRAE, VetAgro Sup, UMR Ecologie Microbienne, F-69622 Villeurbanne, France
[2]Univ Lyon, Université Claude Bernard Lyon 1, CNRS, INSA de Lyon, UMR Microbiologie Adaptation et Pathogénie, F-69622 Villeurbanne, France
[3]Institut Universitaire de France (IUF)

Current address for Mylène Hugoni : Univ Lyon, INSA Lyon, CNRS, UMR 5240 Microbiologie Adaptation et Pathogénie, F-69621 Villeurbanne, France

Corresponding author
Yvan MOENNE-LOCCOZ
Univ Lyon, Université Claude Bernard Lyon 1, CNRS, INRAE, VetAgro Sup, UMR5557 Ecologie Microbienne, 43 bd du 11 novembre 1918, F-69622 Villeurbanne, France
yvan.moenne-loccoz@univ-lyon1.fr

Highlights

- Dark zones are rock alterations of high concern for conservation of Paleolithic art
- Microbial dynamics during dark zone formation process were totally unknown so far
- We show that dark zone formation coincides with brutal microbial community switch
- Deterministic processes influenced dynamics of rare taxa in newly-formed dark zones
- Understanding alteration formation can help guide cave conservation strategies

Abstract

Strong anthropization of karstic caves may result in formation of various wall alterations including dark zones, whose microbial community differs from that of non-altered surfaces nearby. Dark zones grow quickly and without gradual visual changes, leading to the hypothesis of a simple process rather than complex microbial successions, but this is counter-intuitive as underground microbial changes are typically slow and dark zones are microbiologically very distinct from unmarked surfaces. We tested this hypothesis in Paleolithic Lascaux Cave, across two years of microscale sampling. Indeed, Illumina MiSeq metabarcoding evidenced only three community stages for bacteria, fungi and all microeukaryotes together (i.e. unmarked surfaces, newly-formed dark zones and intermediate/old dark zones) and just two stages for archaea (unmarked surfaces vs dark zones), indicating brutal community changes. The onset of dark zone formation coincided with the development of *Ochroconis* fungi, Bacteroidota and the bacterial genera *Labrys*, *Nonomuraea* and *Sphingomonas*, in parallel to *Pseudomonas* counter-selection. Modeling of community assembly processes highlighted that the dynamics of rare taxa in unmarked surfaces adjacent to dark zones and in newly-formed dark zones were governed in part by deterministic processes. This suggests that cooperative relationships between these taxa might be important to promote dark zone formation. Taken together, these findings indicate a brutal community switch as these new alterations form on Lascaux cave walls.

Graphical abstract

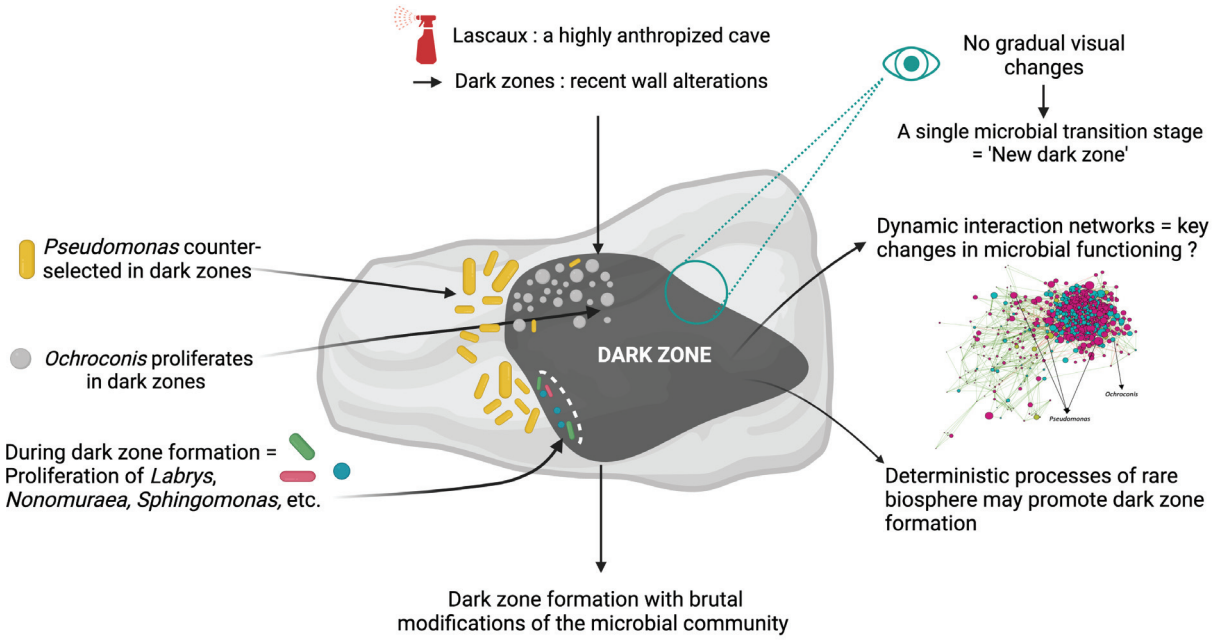

Key words

Lascaux Cave ; Cave alteration ; Community assembly processes ; Interaction networks ; Microbial succession.

Introduction

In calcareous regions, limestone dissolution may lead to the formation of karstic caves. Despite limited nutrient supply, the microbial community established in caves is rather abundant and diverse (Tomczyk-Żak and Zielenkiewicz, 2016), and microorganisms may play significant roles in these environments, including in the process of cave formation itself (Barton and Jurado, 2007).

Certain caves have attracted tourist attention because of particular geologic properties (speleothems) or ancient artistic features, such as paintings, engravings and/or carvings. Such Paleolithic art is documented in hundreds of caves worldwide. However, tourism-related anthropization can have a profound impact on the cave environment (with increases in temperature, CO_2 concentrations, water condensation on rock surfaces, organic carbon levels in cave sediment, etc.) (Bastian and Alabouvette, 2009 ; Cañveras, 2001 ; Diaz-Herraiz et al., 2014 ; Espino del Castillo et al., 2018 ; Jurado et al., 2010 ; Russell and MacLean, 2008). This impact may lead, in turn, to microbial community unbalance and excessive proliferation of particular microorganisms, materializing by the formation of stains on cave walls (De Leo et al., 2012 ; Pasić et al., 2010 ; Portillo et al., 2008). In certain caves, chemical methods have been used to curb microbial proliferation, with contrasted results (Bastian et al., 2009 ; Chalmin et al., 2007 ; Martin-Sanchez et al., 2012 ; Stupar et al., 2014). In Lascaux Cave (Périgord region, in south-western France), benzalkonium chloride (and other chemicals) were effective against white stains formed by the fungus *Fusarium solani* (early 2001) (Bastian et al., 2010), but were ineffective in the following years against black stains attributed to *Ochroconis lascauxensis* and other pigmented fungi (Martin-Sanchez et al., 2012). Chemical treatments are even thought to be a major factor promoting surface alterations in Lascaux (Bastian et al., 2009 ; Bontemps et al., 2021 ; Martin-Sanchez et al., 2012). In the most anthropized areas, other alterations distinct from black stains and termed dark zones (Fig. 1A) have formed and keep growing, but they were not treated chemically. Preliminary microbial analysis evidenced that dark zones are characterized by a particular microbial community, with higher levels of *Ochroconis* melanized fungi and much lower levels of *Pseudomonas* bacteria (Alonso et al., submitted). However, the population successions involved in dark zone formation are unknown, as well as the demographic processes underpinning these changes. Based on visual examination of dark zones, which did not reveal any gradual macroscopic change at the border of the altered zone, we hypothesized that dark zone enlargement implicates rather brutal microbiota changes, in parallel to the early development of melanized fungi. Microbial community collapse, i.e. strong counter-selection of a wide range of microbial taxa resulting in major changes in community functioning (Garris et al., 2018), might even take place. If it were the case, it would also imply that dark zone conditions lead to early counter-selection of *Pseudomonas* bacteria, as the latter might limit fungal expansion (Alonso et al. submitted).

The objective of this study was to decipher the process of dark zone development in karstic caves, using Lascaux as model of strongly-anthropized cave. First, we investigated microscale (centimetric) dynamics of dark zones across two years for the three domains of life, so as to characterize population successions during dark zone formation and assess the respective contributions of dominant and rare microbial taxa. Second, we aimed at quantifying the ecological processes governing microbial community assembly, i.e. (i) deterministic processes, in which

abiotic and biotic factors determine the occurrence and abundance of species associated with homogeneous or heterogeneous ecological selection, vs (ii) stochastic processes, related to probabilistic random changes that are not the consequence of environmental fitness (ecological drift, diversification and dispersal) (Hubbell, 2001 ; Leibold and McPeek, 2006 ; Zhou and Ning, 2017).

Materials and Methods

Sample collection

Lascaux Cave is located in the South-West of France (N 45°03'13.087" and E 1°10'12.362"). One major room inside Lascaux is the Apse (30 m^2), which contains more than a thousand Paleolithic figures, and where dark zones started to appear in 2008, on limestone wall surfaces termed the upper inclined planes. Samples were collected in April 2019, December 2019 and April 2021 from the upper inclined planes, in areas without Paleolithic art.

At each sampling time, three dark zones were considered, and up to five rock surface conditions were sampled for each of them, i.e. (i) distal unmarked surface, away from the dark zone (at the three dates), (ii) proximal unmarked surface, in the immediate vicinity of the dark zone (April 2019), (iii) new dark zone, located very close to the dark zone boundary and corresponding to the proximal unmarked status at the previous sampling (December 2019 and April 2021), (iv) intermediate dark zone, corresponding to the new dark zone status at the previous sampling (April 2021), and (v) old dark zone, located near the center of the dark zones (at the three dates) (Fig. 1B). Black stains might occasionally form in a few dark zones (Alonso et al., submitted), but they were not considered here because (i) the focus was on dark zone formation itself and (ii) black stains did not form during the course of the study. For each rock surface condition sampled, 6 replicates were taken per individual dark zone, using a swab that was rubbed against the surface. This gave 3 times x 3 dark zones x 6 replicates = 54 samples of distal unmarked surface, 2 x 3 x 6 = 36 samples of proximal unmarked surface, 2 x 3 x 6 = 36 samples new dark zone, 1 x 3 x 6 = 18 samples of intermediate dark zone, and 3 x 3 x 6 = 54 samples of old dark zone (198 samples in total). The swabs were broken at the edge of the tube and placed immediately in liquid nitrogen, before transfer to -80°C once in the laboratory.

DNA extraction and high-throughput sequencing

Total genomic DNA extraction was performed using the FastDNA SPIN Kit For Soil (MP Biomedicals, Illkirch, France), following manufacturer's instructions. The lysis solution was added to the tube containing the swab head. The elution step was achieved using 90 µl elution buffer for each sample. DNA concentration was assessed using the Qubit dsDNA HS Assay Kit (Invitrogen, Carlsbad, USA), following the manufacturer's instructions.

Four gene markers were analyzed in each individual sample. The V3-V4 region of the 16S rRNA genes was amplified for Bacteria and Archaea using the universal primers 341F/805R (Herlemann et al., 2011) and 515F/915R (Herfort et al., 2009), respectively. For Eukaryota, the V4 region of the 18S rRNA genes was amplified using the universal primers 0067a deg/NSR399 (Dollive et al., 2012) and the ITS2 region of Fungi using primers ITS3 KYO2/ITS4 (Toju et al., 2012) (Appendix S10 : Table S1). The PCR mix consisted in 5 µl of 5X Hot BioAmp Blend

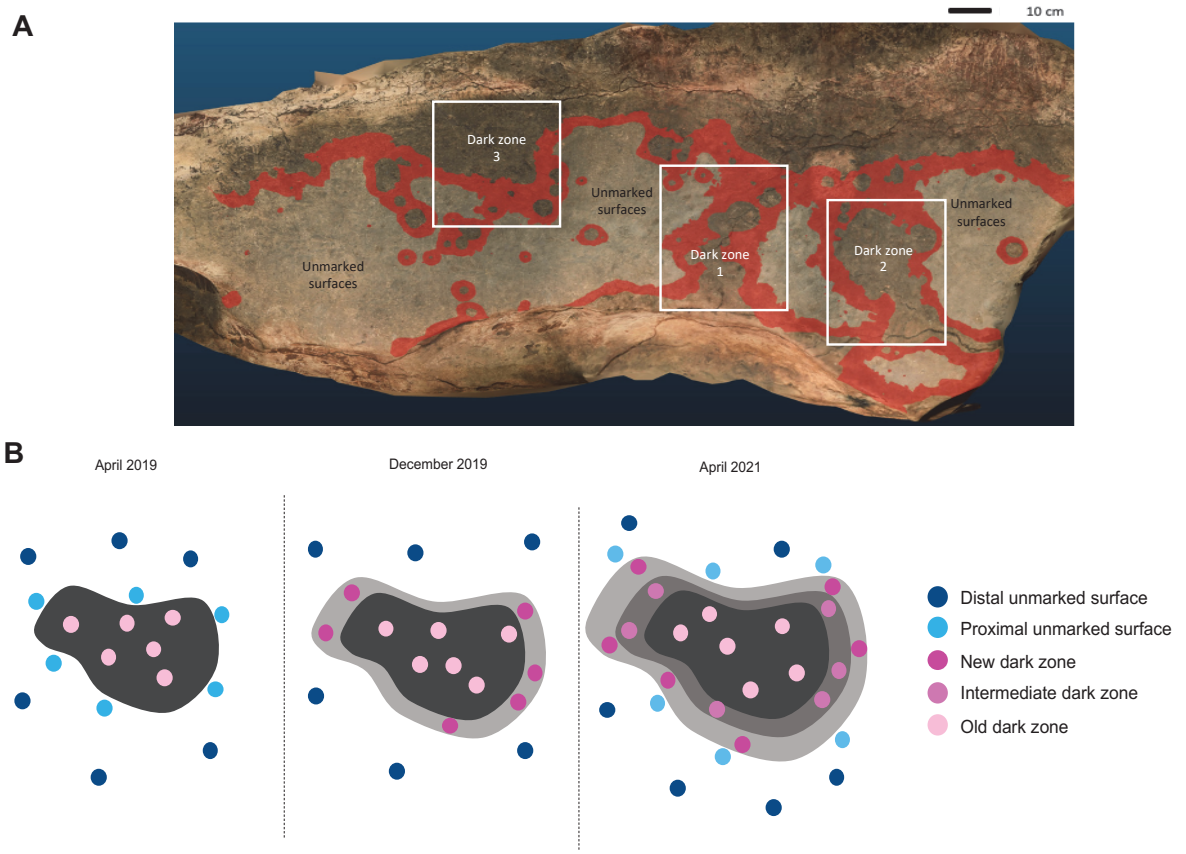

Fig 1. (A). Upper inclined planes in Lascaux's Apse, showing the three dark zones studied. The red area on photogrammetry represents the extension of dark zones during the course of the two-year study (source : S. Géraud, DRAC Nouvelle-Aquitaine). (B). Schematic layout of the 6 replicates in each rock surface condition, at the three samplings of a given dark zone. Unmarked surfaces and dark zone conditions are represented in shade of blue and pink, respectively.

Master Mix RTL (Biofidal, Vaulx-en-Velin, France), 0.1 μM of each primer, 0.1X of GC-rich-enhancer (Biofidal), 0.2 ng.μl-1 of Bovine Serum Albumin (Promega, Madison, USA) and 0.2-1.0 ng of template DNA. All amplifications were performed in triplicate, in a Bio-Rad T1000 thermal cycler (Bio-Rad, Hercules, USA). The PCR program for Bacteria was 3 min at 95°C, 28 cycles of 45 s at 95°C, 45 s at 50°C and 90 s at 72°C, followed by 7 min at 72°C. For Archaea, it consisted in 10 min at 94°C, 30 cycles of 1 min at 94°C, 1 min at 58°C and 90 s at 72°C, followed by 10 min at 72°C. For Eukaryota, it consisted in 10 min at 95°C, 30 cycles of 1 min at 94°C, 1 min at 55°C and 90 s at 72°C, followed by 10 min at 72°C. For Fungi, PCR was done with 10 min at 95°C, 28 cycles of 20 s at 94°C, 30 s at 47°C and 20 s at 72°C, followed by 7 min at 72°C. All primers were tagged with the Illumina adapter sequences (TCG TCG GCA GCG TCA GAT GTG TAT AAG AGA CAG and GTC TCG TGG GCT CGG AGA TGT GTA TAA GAG ACA G), allowing the construction of amplicon libraries by a two-step PCR. DNA extraction was carried out without any biological matrix and was considered a negative control to evaluate ambient contamination. PCR products were also verified, by electrophoresis on 1.5% agarose gel (100 V during 20 min) and UV visualization, which gave the correct length for each marker gene. High-throughput sequencing was achieved after pooling PCR triplicates. Illumina MiSeq with 2 x 300 bp, paired-end chemistry v3 was carried out by Biofidal.

Sequence processing

For each dataset, paired-end reads were demultiplexed in the different samples according to exact match adaptors (subsequently removed). The resulting reads were merged with a maximum of 10% mismatches in the overlap region using FLASh (Fast Length Adjustment of Short reads) (Magoč and Salzberg, 2011). Denoising procedures consisted in discarding reads without the expected length (200-500 bp) or with ambiguous bases (N). After sequence dereplication, the clusterization tool was run with SWARM (Mahé et al., 2014), which uses a local clustering threshold rather than a global clustering threshold and an aggregation distance of 3 for identification of operational taxonomic units (OTUs). Chimeric OTUs were removed using VSEARCH (Rognes et al., 2016) and low-abundance sequences were filtered at 0.005% of all sequences (Bokulich et al., 2013). Taxonomic affiliation of OTUs was performed with both RDP Classifier and BLASTn (Zhang and Madden, 1997) against the 138.1 SILVA database (Quast et al., 2013) for bacterial 16S rRNA genes, archaeal 16S rRNA genes and eukaryotic 18S rRNA genes and the 8.2 UNITE database for fungal ITS markers (Nilsson et al., 2019). This procedure was automated in the FROGS pipeline (Escudié et al., 2018). Contaminant OTUs identified from the negative control samples were removed. To compare samples, a normalization procedure was applied by randomly resampling down to 19,126, 1,248, 17,005 and 13,323 sequences per sample in the bacterial, archaeal, microeukaryotic and fungal datasets, respectively.

Alpha diversity indices including Chao-1 (which estimates OTUs richness) (Chao, 1987), Shannon H' (which takes into account both the numbers of individuals and of OTUs) (Shannon, 1948) and Simpson 1-D evenness index (which represents the probability that two individuals randomly selected from a sample belong to different taxa) (Simpson, 1949) were computed using the Paleontological Statistics (PAST) software (version 4.04) (Hammer et al., 2001) based on OTU table. The differences in diversity indices ($P < 0.05$) were assessed with Kruskal-Wallis tests and post-hoc Wilcoxon pairwise tests, or with ANOVA and post-hoc Tukey-HSD using 'vegan' package in R (version 4.0.3) (R Core Team, 2020). Microbial communities were primarily compared by non-metric multidimensional scaling (NMDS), which was done using 'phyloseq' package in R (McMurdie and Holmes, 2013). The stress value was calculated to measure the difference between the ranks on the ordination configuration and the ranks in the original similarity matrix for each replicate. Stress values below 0.1 are considered without risk and those not exceeding 0.2 are acceptable (Clarke, 1993). Non-parametric tests of analysis of similarities (ANOSIM) and pairwise multilevel comparison of Adonis were conducted using respectively the 'vegan' and 'pairwiseAdonis' packages in R (Arbizu, 2021 ; Oksanen et al., 2020) to test differences ($P < 0.05$) in overall microbial community composition. All analyses were based on the Bray-Curtis dissimilarity index and statistical analyses were performed using R software (version 4.0.3).

Construction of taxa association networks

Microbial association networks for each community were constructed using Sparse InversE Covariance Estimation for Ecological Association Inference (Kurtz et al., 2015), as implemented in the R package SpiecEasi (Kurtz et al., 2019). This approach allows the combination of independent composition matrices generated during separate sequencing runs and is thus well suited

for cross-domain studies (Tipton et al., 2018). We followed the overall methodology described in Escalas et al. (2021). The most parsimonious network structure was identified for each rock surface condition using Stability Approach to Regularization Selection (StARS) (Liu et al., 2010) and the Meinshausen and Buhlmann algorithm (Bühlmann et al., 2010).

Network attributes (Niquil et al., 2020) were analyzed using the R package igraph (Csárdi and Nepusz, 2006), as follows. Based on similar microbial community traits (see Results), data from all replicates and from all three sampling times were pooled for each of the five rock surface conditions. First, the global characteristics of each network were described using indices from the graph theory : number of nodes and edges, network density, average inter-nodes distance, centralized degree, betweenness and closeness, hub score (Delmas et al., 2018 ; Pellissier et al., 2018). Second, we identified modules, i.e. groups of taxa that tend to have many associations between them and fewer outside of the group, and that might constitute a functional group, using the algorithms spinglass, fast greedy, leading eigenvector and Louvain ; we then kept Louvain as it provided module numbers most comparable to the average from all four algorithms. Third, we assessed the size and taxonomic composition of modules from the five rock surface conditions. Fourth, we identified the proportion of positive and negative links in the five surface conditions, the links between them, and the nodes associated with *Ochroconis* or *Pseudomonas*.

Phylogenetic analysis

Phylogenetic distance was utilized to assess community assembly processes. Aligned sequences of representative OTUs were used in MAFFT for all marker genes (Kuraku et al., 2013), and gaps and poorly conserved regions were eliminated using Gblocks (Castresana, 2000 ; Talavera and Castresana, 2007). Finally, phylogeny was reconstructed using IQ-TREE-2 (Minh et al., 2020) (with default parameters), the best model being automatically chosen by the program based on Bayesian Information Criterion (BIC). Bootstraps (1000 replicates) were used to estimate node support. A minimum threshold of 6 OTUs was arbitrarily chosen for phylogenetic analyses.

Neutral model

The neutral community model (NCM) was used to estimate the importance of passive dispersal, by assessing the relationship between the frequency at which taxa occur in a set of local communities and their abundance across the wider meta-community. In this model, the migration rate (m) is used to evaluate the probability of a random loss of an OTU in a local community, to be replaced by an immigrant OTU from the meta-community (Hubbell, 2001). R^2 (overall fit to the neutral model) was obtained by comparing the sum of squares of the residuals (SSerr) with the total sum of squares (SStotal), with model fit = $1–SSerr/SStotal$ (i.e. generalized R^2). Calculation of 95% confidence intervals around all fittings statistics was done with 1000 bootstrap replicates and was conducted using the Wilson score interval, 'minpack.lm', 'Hmisc' and 'stats4' packages in R (Elzhov et al., 2016 ; Harrell and Dupont, 2018). The Akaike Information Criterion (AIC) and Bayesian Information Criterion (BIC) were calculated based on 1000 bootstrap replicates for the neutral, binomial and Poisson distribution models to determine the best model fit and whether the model was based on only the random sampling of the source meta-community. We separately used the datasets from each of the five rock surface conditions.

All computations were performed in R (version 4.0.3).

Definition of abundant and rare taxa

For a deeper analysis of community assembly processes, OTUs were classified into four established categories defined based on their relative abundance. Always-Rare Taxa (ART) have an abundance $< 0.01\%$ in all samples, Conditionally-Rare Taxa (CRT) an abundance $< 1\%$ in all samples and $< 0.01\%$ in some samples (maximum 33% of samples), Moderate Taxa (MT) an abundance $< 1\%$ and $> 0.01\%$ in all samples, and all other OTUs correspond to Dominant Taxa (DT), with an abundance $\geq 1\%$ of all sequences in all samples or that fluctuates strongly, i.e. $< 0.01\%$ in certain samples and $\geq 1\%$ in others.

Estimation of community assembly processes

A null model analysis was used to evaluate the assembly processes of all taxa, dominant taxa, moderate taxa, conditionally rare taxa and always rare taxa. The variations in phylogenetic diversity were measured using null model-based phylogenetic (βNTI) with R software (version 4.0.3), using scripts from Stegen et al. (Stegen et al., 2012) and 'picante' package (Kembel et al., 2010). βNTI is the difference between an observed value of the beta mean nearest taxon distance (βMNTD) and the mean of the null distribution of βMNTD normalized by its standard deviation (Stegen et al., 2012). It also estimates the phylogenetic turnover given stochastic and deterministic ecological processes (Dini-Andreote et al., 2015). βNTI values between -2 and 2 indicate dominance of stochastic processes, whereas βNTI values smaller than -2 or larger than 2 indicate that deterministic processes (i.e., homogeneous or heterogeneous selection) play a more important role (Zhou and Ning, 2017). The taxonomic β-diversity metric Bray-Curtis-based Raup-Crick (RCbray) was used to analyze pairwise comparisons that were not assigned to deterministic processes (i.e. $|\beta\text{NTI}| < 2$) and was calculated with 'iCAMP' package (Ning, 2021). $\text{RC}_bray < -0.95$ and $\text{RC}_bray > 0.95$ indicate relative dominant influence of homogenizing dispersal and dispersal limitation, respectively, and $|\text{RC}_bray| < 0.95$ indicates a crucial role of 'undominated' assembly, including weak selection, weak dispersal, diversification, and/or drift (Stegen et al., 2015).

Results

Microbial community structure in relation to dark zone growth

NMDS and ANOSIM analyses indicated that the effect of time on community structure was barely significant for bacteria ($P = 0.041$, $R^2 = 0.051$), archaea ($P = 0.048$, $R^2 = 0.049$), microeukaryotes ($P = 0.049$, $R^2 = 0.058$) and fungi ($P = 0.051$, $R^2 = 0.057$) for each of the five sample categories (i.e. Distal unmarked surface, Proximal unmarked surface, New dark zone, Intermediate dark zone, Old dark zone), meaning that microbial community was essentially stable for a given surface condition (Appendix S10 : Table S1). Therefore, Illumina MiSeq sequences from each rock surface condition were pooled.

For the bacterial community (Fig. 2A), the fungal community (Fig. 2D), and the microeukaryotic community at large (Fig. 2C), NMDS distinguished three significantly-different groups

of samples corresponding to (i) the two unmarked rock surfaces, (ii) the new dark zone, and (iii) the intermediate and old dark zone conditions. For the archaeal community, only two groups emerged from NMDS analysis, i.e. (i) the two unmarked rock surfaces and (ii) the three dark zone conditions (Fig. 2B).

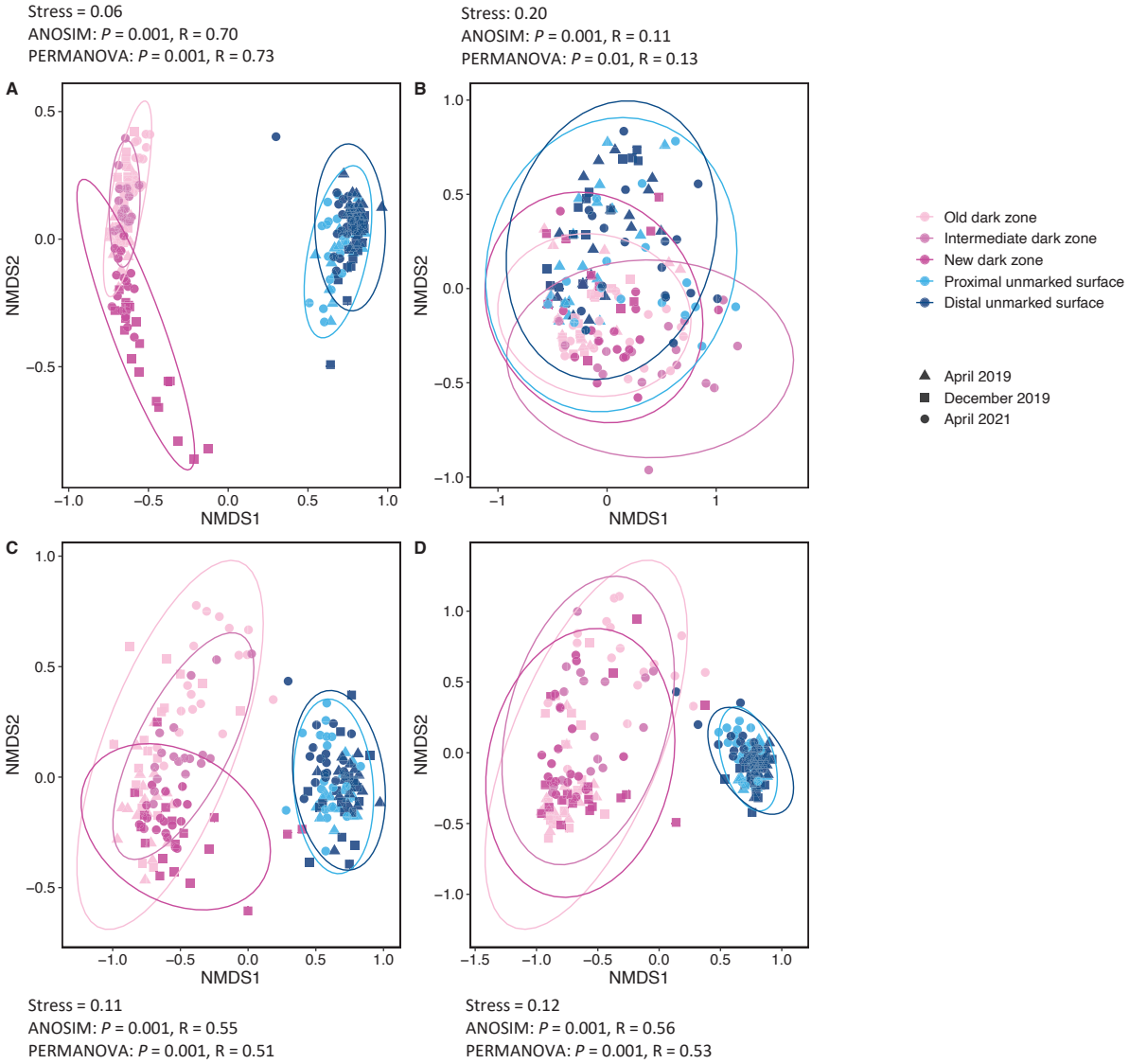

Fig 2. Non-metric multidimensional scaling (NMDS) analysis of microbial community structure in Lascaux's Apse according to rock surface condition and time. Ellipses (95% confidence intervals) indicate the different rock surface conditions for bacteria (16S rRNA genes) (A), archaea (16S rRNA genes) (B), microeukaryotes (18S rRNA genes) (C) and only fungi (ITS2) (D).

Microbial diversity level in relation to dark zone growth

Differences in Simpson 1-D ($P = 0.90$) and Shannon H' ($P = 0.90$) diversity indices for bacteria were not statistically significant (Wilcoxon test) between rock surface conditions, but Chao-1 index was higher for intermediate dark zone than unmarked surfaces and new/old dark zones

($P = 6.3 \times 10^{-8}$) (Appendix S1 : Figure S1).

For archaea, Simpson 1-D diversity index was higher for intermediate dark zone than the four other rock surface conditions ($P = 3.1 \times 10^{-4}$), whereas Shannon H' index was higher for both unmarked surfaces than for intermediate and old dark zones ($P = 2.0 \times 10^{-6}$), and differences in Chao-1 index were not significant (Appendix S1 : Figure S1). Simpson 1-D and Shannon H indices were lower for new/intermediate dark zones) than unmarked surfaces, when considering microeukaryotes ($P = 1.1 \times 10^{-5}$ and $P = 1.9 \times 10^{-5}$, respectively) or only fungi ($P = 1.5 \times 10^{-5}$ and $P = 1.9 \times 10^{-5}$, respectively). Higher values were recorded for old dark zones than new/intermediate dark zones, for microeukaryotes ($P = 5.3 \times 10^{-3}$ for Simpson 1-D and $P = 3.3 \times 10^{-3}$ for Shannon H') and fungi ($P = 8.0 \times 10^{-3}$ for Simpson 1-D and $P = 3.2 \times 10^{-5}$ for Shannon H'). Chao-1 index was statistically lower in dark zones than unmarked surfaces ($P = 1.6 \times 10^{-8}$ and $P = 6.9 \times 10^{-8}$ for all microeukaryotes or only fungi, respectively) (Appendix S1 : Figure S1).

Bacterial community composition in relation to dark zone growth

The normalized bacterial dataset consisted in 521 OTUs. Proteobacteria (64% of all bacterial sequences), Actinobacteriota (19.1%), Bacteroidota (7.4%) and Acidobacteriota (6.4%) predominated (Fig. 3).However, contrasted bacterial community composition was found depending on the surface condition sampled, as summarized below.

Proteobacteria amounted to 82.0% on unmarked surfaces, but only 61.1% on new dark zones and 43.1% on intermediate/old dark zones. At the genus level (Appendix S3 : Figure S3), *Pseudomonas* (Gammaproteobacteria) represented as much as 61.2% of bacterial sequences on unmarked surfaces versus as little as 7.6% on new dark zones and 0.1% on intermediate/old dark zones (Fig. 4A). *Stenotrophomonas* (Gammaproteobacteria) amounted to 5.8% on unmarked surfaces versus 3.1% on new dark zones and 0.3% on intermediate/old dark zones. *Dockdonella* (Gammaproteobacteria) accounted for 0.6% on unmarked surfaces, 4.1% on new dark zones and 1.6% on intermediate/old dark zones. *Labrys* (Alphaproteobacteria) corresponded to 2.8% of sequences on unmarked surfaces (more specifically, 0.9% on distal unmarked surface and 4.8% on proximal unmarked surface), 9.2% on new dark zones and 6.8% on intermediate/old dark zones. *Sphingomonas* (Alphaproteobacteria) represented only <0.05% of bacterial sequences on unmarked surfaces versus 4.7% on new dark zones and 4.0% on intermediate/old dark zones. *Reyranella* (Alphaproteobacteria) amounted to 3.0% of bacterial sequences on unmarked surfaces versus only 0.1% on new dark zones and <0.05% on intermediate/old dark zones.

Actinobacteriota accounted for 11.0% of bacterial sequences on unmarked surfaces and 14.9% on new dark zones, but as much as 32.8% on intermediate/old dark zones (Fig. 4A). At the genus level, *Nonomuraea*, *Pseudonocardia* and *Rhodococcus* amounted to 0.1%, 1.3% and 1.6% on unmarked surfaces, 4.5%, 1.0% and <0.05% on new dark zones and 12.1%, 2.2% and <0.05% of bacterial sequences on intermediate/old dark zones, respectively.

Bacteroidota represented as little as 0.3% on unmarked surfaces, versus as much as 19.9% on new dark zone and 10.3% on intermediate/old dark zones (Fig. 3). At genus level, *Chitinophaga* and *Pedobacter* amounted to only 0.3% and 0.1% of bacterial sequences on unmarked surfaces, versus 11.5% and 7.0% on new dark zone and 4.1% and 4.4% on intermediate/old dark zones,

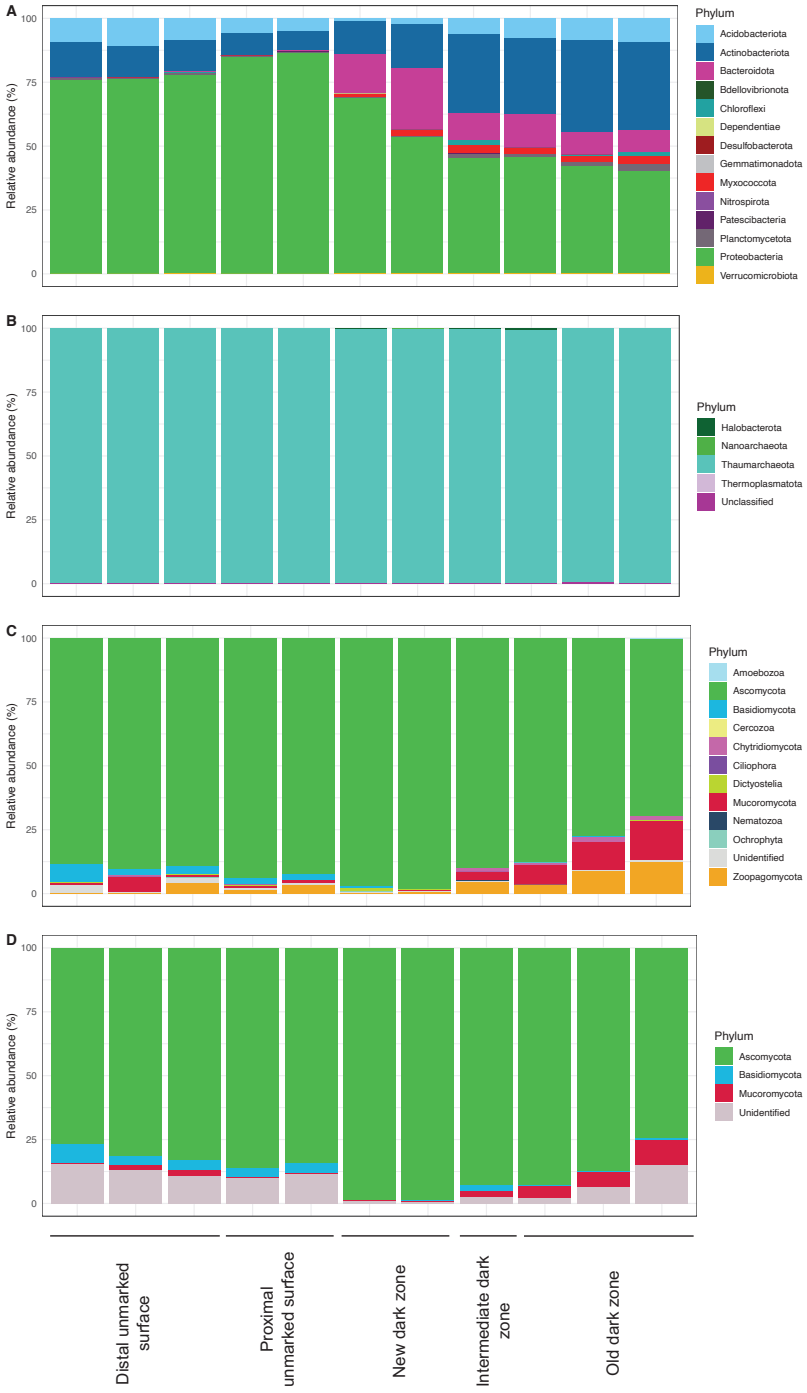

Fig 3. Relative abundance (% of sequences) of bacterial (16S rRNA genes) (A), archaeal (16S rRNA genes) (B), microeukaryotic (18S rRNA genes) (C) and fungal (ITS2) (D) phyla.

respectively (Fig. 4A).

Acidobacteriota amounted to 16.9% of bacterial sequences on unmarked surfaces, only 1.3% on new dark zone and 16.6% on intermediate/old dark zones (Fig. 3). At genus level, *Bryobacter* accounted for only 0.4% on unmarked surfaces, versus 1.7% on new dark zone and 7.6% on intermediate/old dark zones (Fig. 4A). An unidentified genus affiliated to the Vicinamibacteria class represented 0.3% on unmarked surfaces, versus 0.05% on new dark zone and 5.4% on intermediate/old dark zones (Appendix S2 : Figure S2).

Archaeal community composition in relation to dark zone growth

The normalized archaeal dataset consisted in 24 OTUs, with a very strong predominance (99.6%) of Thaumarchaeota (Fig. 3). At the lowest taxonomic level available (family), the Nitrososphaeraceae amounted to 99.9% of archaeal sequences on unmarked surfaces and 99.3% on dark zones, and the Haloferacaceae (affiliated to the Halobacterota phylum) less than 0.05% on unmarked surfaces versus 0.16% on dark zones (Appendix S2 : Figure S2 and Appendix S4 : Figure S4A).

Microeukaryotic community composition in relation to dark zone growth

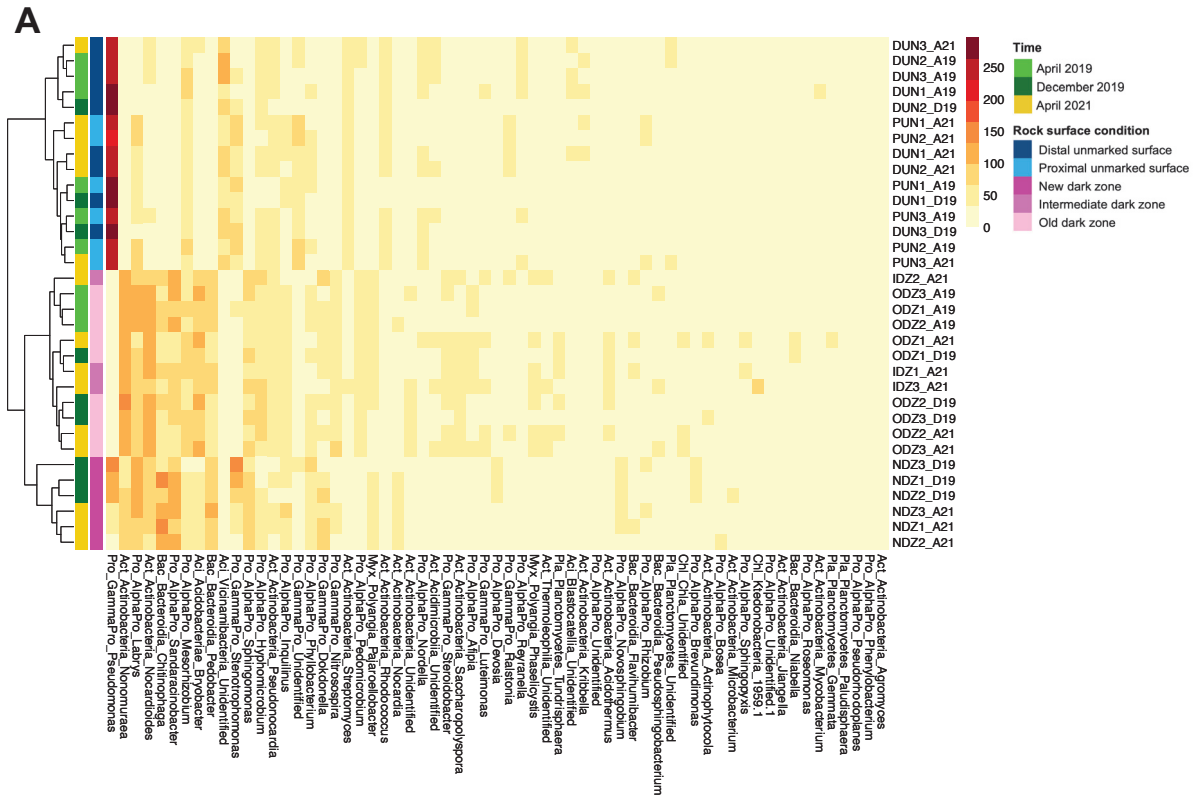

Fig 4A. Distribution of the most abundant bacterial (16S rRNA genes) genera according to rock surface condition and time. The heatmap was coupled to a hierarchical clustering analysis of the most abundant genera (i.e. consisting of > 0.05% of total normalized sequences) in each rock surface condition. Data was analyzed using a matrix that was square root-transformed to minimize the impact of highly dominant genera. ODZ : Old Dark Zone ; IDZ : Intermediate Dark Zone ; NDZ : New Dark Zone ; PUN : Proximal Unmarked Surface ; DUN : Distal Unmarked Surface ; A19 : April 2019 ; D19 : December 2019 ; A21 : April 2021 ; Act : *Actinobacterota* ; Pro : *Proteobacteria* ; Aci : *Acidobacteria* ; Bac : *Bacteroidota* ; Myx : *Myxococcota* ; Pla : *Planctomycetes* ; Chl : *Chloroflexi*

The normalized eukaryotic and fungal datasets consisted in 199 and 209 OTUs for 18S rRNA gene and ITS sequences, respectively. Most 18S rRNA sequences (99.6%) corresponded to fungi especially Ascomycota, which represented 89.3% of 18S rRNA sequences and 87.1% of ITS sequences (Fig. 3).

Ascomycota amounted to 86.6% of ITS sequences [and 90.9% of 18S rRNA sequences] on unmarked surfaces, 98.3% [97.7%] on new dark zone and 84.1% [81.1%] on intermediate/old dark zones (Fig. 3). At the genus level, *Ochroconis* represented only 3.4% of ITS sequences [and 5.6%

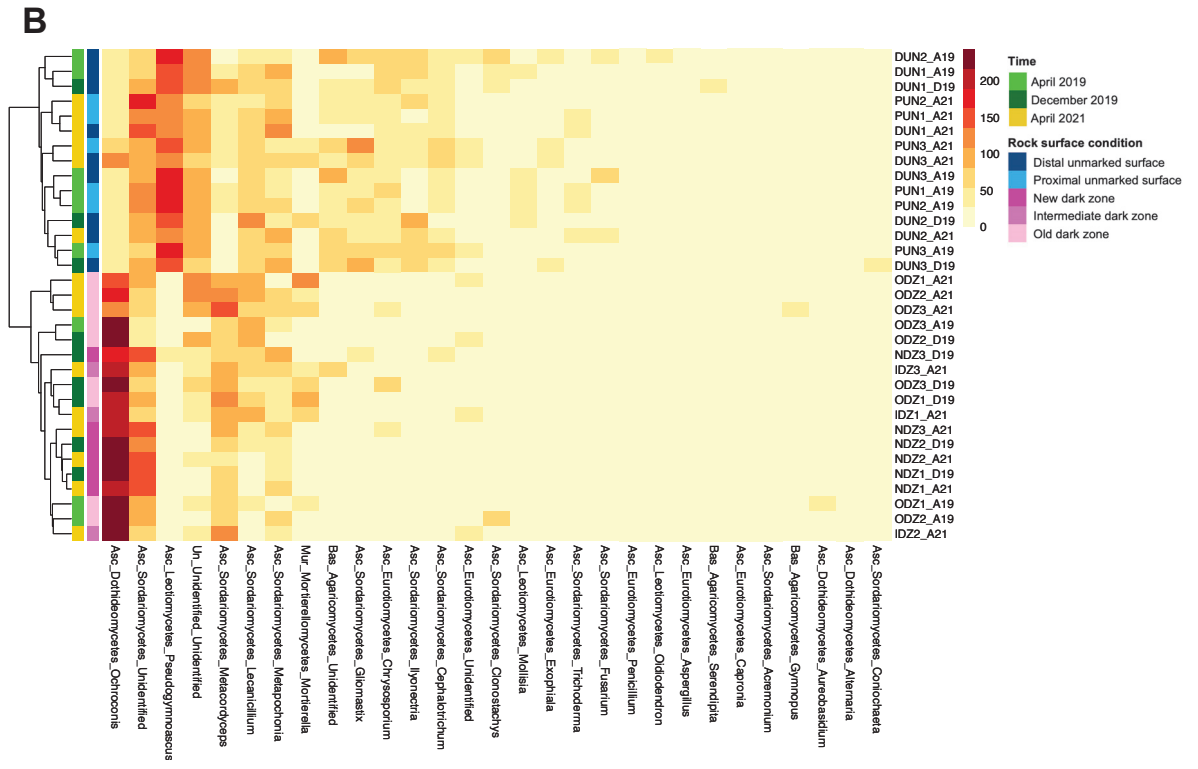

Fig 4B. Distribution of the most abundant fungal (ITS2) genera according to rock surface condition and time. The heatmap was coupled to a hierarchical clustering analysis of the most abundant genera (i.e. consisting of > 0.05% of total normalized sequences) in each rock surface condition. Data was analyzed using a matrix that was square root-transformed to minimize the impact of highly dominant genera. ODZ : Old Dark Zone ; IDZ : Intermediate Dark Zone ; NDZ : New Dark Zone ; PUN : Proximal Unmarked Surface ; DUN : Distal Unmarked Surface ; A19 : April 2019 ; D19 : December 2019 ; A21 : April 2021 ; Asc : *Ascomycota* ; Bas : *Basidiomycota* ; Mur : *Mucoromycota* ; Un : Unidentified.

of 18S rRNA sequences] on unmarked surfaces, versus 58.5% [51.6%] on new dark zone and 58.5% [52.3%] on intermediate/old dark zones (Fig. 4B and Appendix S4 : Figure S4B). In contrast, *Pseudogymonascus* amounted to 27.6% [28.7%] on unmarked surfaces, versus as little as 0.4% [0.5%] on new dark zone and 0.05% [0.5%] on intermediate/old dark zones (Appendix S3 : Figure S3A). *Gliomastix* and *Ilyonectria* represented respectively 4.1% and 3.3% [5.1% and 3.2%] on unmarked surfaces, versus 0.2% and 0.4% [0.7% and 0.3%] on new dark zone and <0.05% and <0.05% [<0.05% and <0.05%] on intermediate/old dark zones. *Exophiala* amounted to 0.9% [0%] on unmarked surfaces, 0.10% [0%] on new dark zone and 0.1% [0%] on intermediate/old dark zones.

Basidiomycota represent 3.4% of ITS sequences [and 4.5% of 18S rRNA sequences] on unmarked surfaces, versus 0.05% [0.06%] on new dark zones and 0.4% [0.9%] on intermediate/old dark zones (Fig. 3). An unidentified genus affiliated to the Agaricomycete class amounted to 3.8% [3.0%] on unmarked surfaces, versus <0.05% [0.3%] on new dark zone and 0.6% [0.02%] on intermediate/old dark zones (Fig. 4B and Appendix S2 : Figure S2 and Appendix S4 : Figure S4B).

Mucoromycota accounted for 0.9% of ITS sequences [and 1.9% of 18S rRNA sequences] on unmarked surfaces and 0.3% [0.5%] on new dark zone, versus 5.6% [9.2%] on intermediate/old dark zones (Fig. 3). The *Mortierella* genus amounted to 0.9% [0.8%] on unmarked surfaces and

0.3% [0.1%] on new dark zone, versus 4.6% [7.2%] on old/intermediate dark zones (Fig. 4B, Appendix S3 : Figure S3 and Appendix S4 : Figure S4B).

Association networks in relation to dark zone growth

Compared with the case of the two unmarked surfaces, the co-occurrence network of new dark zones displayed significantly smaller numbers of nodes (397 vs 656-685) and hub scores (119 vs 371-477), whereas intermediate values (495-575 nodes and 273-312 hub scores) were found for the intermediate and old dark zones (Table 1 and Appendix S5 : Figure S5). In contrast, the numbers of edges, network diameters, network densities and inter-node distances were at similar levels for the different rock surfaces conditions.

The Louvain algorithm identified 10 (new dark zone) to 13 modules (intermediate dark zone) (Appendix S11 : Table S2). In all rock surface conditions, the genera *Pseudomonas* and *Ochroconis* were found together in several modules, but occurred separately in other modules. *Pseudomonas* was present in 5 modules for old dark zones versus 7-9 modules elsewhere, and the number of *Pseudomonas* OTUs in each module was greater for the unmarked surfaces and the new dark zone than for the intermediate and old dark zones (Fig. 5). *Ochroconis* was present in 2 (new dark zone) or 5-7 modules (all other conditions). Both genera were present together in only two modules in the new and old dark zones, versus 4-5 modules in the other conditions.

Table 1. Comparison of co-occurrence networks for each rock surface condition.

Network characteristic	Distal unmarked surface	Proximal unmarked surface	New dark zone	Intermediate dark zone	Old dark zone
Number of nodes	685 (a)	656 (a)	397 (b)	495 (c)	575 (c)
Number of edges	6070 (a)	4983 (b)	1913 (c)	2799 (d)	3934 (d)
Number of positives edges	4386 (a)	3617 (b)	1405 (c)	1995 (d)	2828 (d)
Number of negatives edges	1684 (a)	1366 (a)	508 (b)	804 (c)	1106 (c)
Network diameter	6	7	6	6	6
Network density	2.5	2.3	2.4	2.2	2.3
Average inter-node distance	2.82	2.97	3.08	3.06	2.92
Centralized degree	17.72 (a)	15.19 (b)	9.64 (c)	11.31 (d)	13.68 (d)
Centralized betweenness	621.9 (a)	645.3 (a)	411.1 (b)	510.0 (c)	550.8 (c)
Centralized closeness	0.359	0.342	0.327	0.328	0.346
Hub score	476.6 (a)	370.9 (a)	118.6 (b)	312.1 (c)	272.1 (c)

Letters a to d indicate significant differences according to rock surface condition, based on post-hoc Wilcoxon test ($P < 0.05$).

The majority of network links were positive links in all rock surfaces (Table 1). *Pseudomonas* exhibited 70-176 links (depending on rock surface condition) versus only 31-92 for *Ochroconis* (Appendix S12 : Table S3). For *Pseudomonas* OTUs, the number of positive and negative links was higher (t test, $P = 0.009$) on unmarked surfaces than and on dark zone, whereas for *Ochroconis* OTUs the number of positive and negative links was higher (t test, $P = 0.04$) on unmarked surfaces than on altered surfaces. The new dark zone differed from the other rock surface conditions, with fewer OTUs (6 vs 8) and a lower number of positive and negative links. The taxonomic identity of the OTUs directly linked with *Ochroconis* or *Pseudomonas* differed greatly between rock surface conditions, and no link was maintained in all five conditions (Appendix S13 : Table S4). Co-occurrences between *Pseudomonas* and *Ochroconis* OTUs were more numerous under unmarked surface conditions than on dark zones (Appendix S14 : Table S5), and they involved

mainly unidentified *Pseudomonas* and *Ochroconis* species. *Ochroconis minima* was also evidenced, with positive links with *Pseudomonas* OTUs on unmarked surfaces, none in new dark zone and with negative links on intermediate and old dark zones (Appendix S14 : Table S5). A large part of the OTUs affiliated to *Ochroconis* and *Pseudomonas* did not occur together in the process of evolution/formation of dark zone.

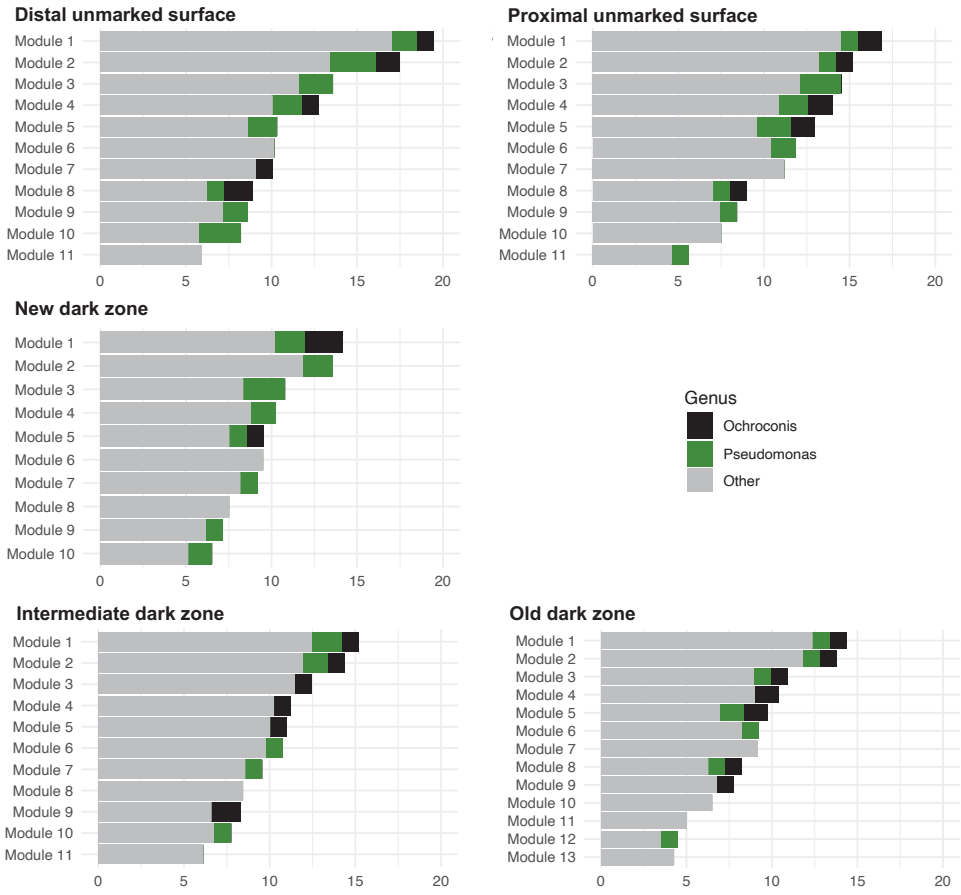

Fig 5. Number of *Ochroconis* and *Pseudomonas* OTUs in the co-occurrence network modules in each rock surface condition. Modules were identified using the Louvain clustering algorithm. *Pseudomonas* and *Ochroconis* genera are represented in green and black, respectively. The X axes represent the number of OTUs affiliated to the genera (i.e. *Pseudomonas*, *Ochroconis* and others) after square-root transformation.

Importance of neutral community assembly processes during dark zone growth

The frequency at which microbial taxa occurred in individual communities was described significantly by the neutral model (Appendix S6 : Figure S6). Overall, estimated migration rates exceeded the value of 0.25 on intermediate and old dark zones but were below 0.10 on newly-formed dark zone, meaning that communities are less dispersal-limited once dark zones are established. However, the fit of the model varied according to rock surface condition and marker gene. In all conditions, the neutral model outperformed the binomial distribution model, meaning that the processes of passive dispersal and ecological drift have a significant impact, without bias caused by randomness of community sampling (Appendix S15 : Table S6).

Quantitative estimates of community assembly processes during dark zone growth

The relative contributions of niche and neutral theories to community assembly in relation to dark zone dynamics was assessed as done by Stegen et al. (2013) (Appendix S7 : Figure S7 and Appendix S8 : Figure S8). For bacteria, the rate of deterministic processes was 21% on intermediate/old dark zones vs less than 10% on the other rock surface conditions (Fig. 6 and Appendix S9 : Figure S9). For archaea, this rate was 11-21% on old and intermediate dark zones vs 6% on new dark zone and less than 4% on unmarked surfaces. For microeukaryotes, the rate was higher than 8% on proximal unmarked surface, new and intermediate dark zones but less than 5% on distal unmarked surface and old dark zones.

For a deeper analysis, assembly processes were quantified for different taxa categories (Dominant taxa, Moderate taxa, Conditionally-rare taxa, Always-rare taxa). For dominant bacterial taxa, the rate of deterministic processes was null on unmarked surfaces, 2.6% on new dark zone and an average of 13.9% on intermediate and old dark zones (Fig. 6 and Appendix S9 : Figure S9). Dominant microeukaryotic taxa showed rates of deterministic processes between 6.9% (on the old dark zone) and 39.1% (on the intermediate dark zone). The number of archaeal dominant taxa was too low for quantification of community assembly processes.

Moderate taxa (all bacterial) exhibited a rate of deterministic processes of 13.6% on proximal unmarked surface, 1.6% on old dark zone and 0% for the other rock surface conditions (Fig. 6 and Appendix S9 : Figure S9). The numbers of archaeal moderate taxa and microeukaryotic moderate taxa were too low for analysis.

Bacterial conditionally-rare taxa displayed rates of deterministic processes of 39.1% on intermediate dark zone, 12.1% on old dark zone and <3.1% on the other rock surface conditions, whereas microeukaryotic conditionally-rare taxa had a rate of deterministic processes of 11.2% on unmarked surfaces but <5% on the other rock surface conditions (Fig. 6 and Appendix S9 : Figure S9). The number of archaeal conditionally-rare taxa was too low for analysis.

Bacterial always-rare taxa presented a rate of deterministic processes of 18.1% on new dark zone but <6.0% on the other rock surface conditions. Archaeal and microeukaryotic always-rare taxa presented a rate of deterministic processes of respectively 5.5% and 15.2% on proximal unmarked surface but <0.1% and 3.5% on the other rock surface conditions (Fig. 6 and Appendix S9 : Figure S9).

Discussion

Dark zones correspond to the most recent type of surface alteration taking place in Lascaux Cave (Alonso et al., submitted), one of the most anthropized Paleolithic caves. Whether such alterations also occur in other tourist caves is not known. Dark zones may be confounded with wet surfaces and in Lascaux they remained unnoticed for almost 5 years. Understanding the dynamics of dark zones could be important to guide cave management strategies.

This work aimed at testing the hypothesis that the formation of dark zones in tourist cave coincided with a rapid switch in microbial community. Indeed, NMDS and ANOSIM showed that microbial communities in distal vs proximal unmarked surfaces did not differ significantly, and likewise microbial communities in intermediate vs old dark zones did not differ. Therefore, at community level, the formation of dark zones implicated a single transition area at a centi-

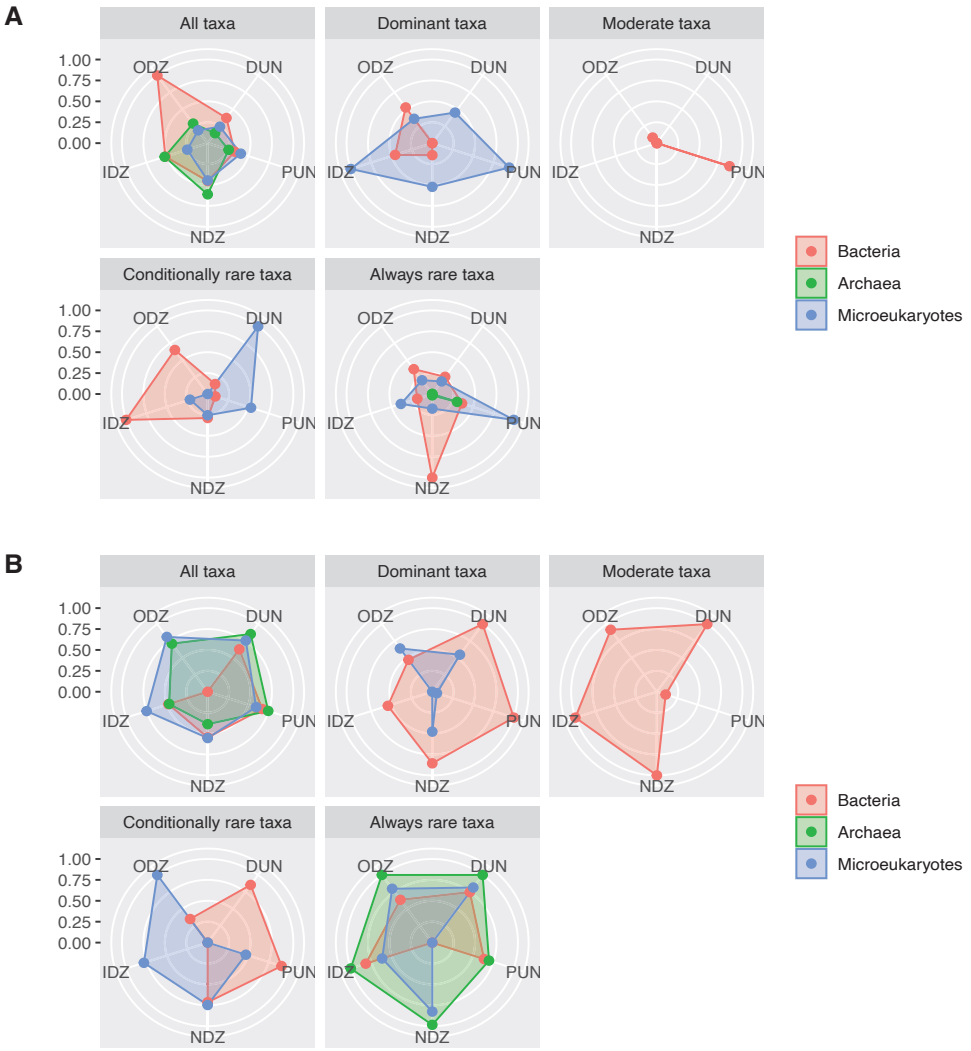

Fig 6. Radar chart of average logit-transformed intensity contributions of (A) deterministic processes and (B) stochastic processes in bacterial, archaeal and microeukaryotic communities. ODZ : Old Dark Zone ; IDZ : Intermediate Dark Zone ; NDZ : New Dark Zone ; PUN : Proximal Unmarked Surface ; DUN : Distal Unmarked Surface.

metric scale, which corresponded to the new dark zone condition. For microeukaryotes (but not bacteria), this transition area displayed reduced diversity, whereas NMDS difference between new vs intermediate/old dark zones was not significant for archaea, which means an absence of transition area for these microorganisms (i.e. the switch from unmarked surfaces to dark zone was direct). This dynamic was consistent in time, as microbial community for a given rock surface condition sampled at different dates did not show any significant change, even though that surface condition could occur at a further spatial distance. Arguably, the centimetric scale was perhaps too broad to monitor more subtle successions. However, in terms of feasibility, sampling at a finer geographic scale could not be performed and, in terms of community dynamics, dark zone formation is a rapid process against the usual context of cave microbiology (Barton and Jurado, 2007 ; Cuezva et al., 2009 ; Engel and Northup, 2008), as unmarked surfaces may transform into new dark zone at a rate of a few centimeters each year.

Brutal community change can be also illustrated with *Ochroconis*, as this fungal genus emblematic of dark zones (Alonso et al. submitted) was already well established in new dark

zones. Like certain other pigmented fungi (*Acremonium*, *Gliomastix*, etc.), it developed rapidly as alteration formed, suggesting that its proliferation does not require prior establishment of a preliminary dark-zone microbial community comprising helper taxa. This genus is also present on black stains, e.g. in Lascaux Cave and Castellana Cave (Italy) (De Hoog and Von Arx, 1973 ; Martin-Sanchez et al., 2012). Here, the black fungal genus *Exophiala* also identified in high abundance in Lascaux black stains (Alonso et al. submitted) represented less than 1% of the fungal sequences whatever the surface condition studied. This observation suggests that the formation of dark zone involves primarily the genus *Ochroconis*, unlike for black stains. The physico-chemical basis of dark-zone visual alterations is unknown. The high relative abundance of *Ochroconis* points towards melanin synthesis as one mechanism to consider, except that dark zones are not black. Because most microbial changes took place since the very start of the visual alteration, it suggests that microbial processes (i.e. gene expression patterns) leading to dark zone appearance are operational as soon as the corresponding microbial populations establish.

Sudden establishment of microbial taxa in dark zone was also found for certain bacteria e.g. *Sphingomonas*, a genus present in several anthropized caves and documented for manganese precipitation, pigment synthesis and aromatic compound catabolism (Barton and Jurado, 2007 ; Stegen et al., 2013). However, other taxa dynamics could also be evidenced. For certain taxa, the new dark zone represents a transition area where they display a transient higher abundance, pointing to minor microbial successions. This was found for *Pedobacter* and *Chitinophaga*, the latter Bacteroidetes being considered a potential bioindicator of cave anthropization (Bontemps et al., 2021 ; Cuezva et al., 2009 ; Engel and Northup, 2009. For others, increases (e.g. for *Nonomuraea*, *Bryobacter*) or decreases (e.g. for *Pseudomonas*, *Stenotrophomonas*) in relative abundance started in the new dark zone but these changes continued as dark zone aged. *Nonomuraea* cave isolates can synthesize antimicrobial compounds with possibly anti-*Pseudomonas* effects (Fang et al., 2017 ; Nazari et al., 2017 ; Nimaichand et al., 2015 ; Sungthong and Nakaew, 2015), whose potential contribution to *Pseudomonas* counter-selection in Lascaux deserves research attention. Among fungi, only *Mortierella* (a genus thriving on decaying organic matter including fecal pellets and exoskeletons of arthropods ; Deacon, 2005) exhibited a significant increase in relative abundance from new to old dark zones, suggesting that most microbial changes related to dark zone aging concern prokaryotes.

Unlike here, several steps can be required for some microbial community changes. For instance, in the establishment of certain biofilms, a thin film of organic and inorganic components starts forming, which changes surface properties and promotes microbial adhesion but without giving visual modifications (Berne et al., 2015 ; Crouzet et al., 2014 ; Donlan, 2002 ; Mortensen, 2014 ; Zheng et al., 2021). Here, however, the brutal community change during dark zone formation is also demonstrated by the lack of significant community difference between distal and proximal unmarked surfaces, even though the higher abundance of *Labrys* (Alphaproteobacteria known for halogenated compounds degradation and facultative methylotrophy ; Miller et al., 2005 ; Wong and Huyop, 2011) started in the proximal unmarked surface. Apart from that, it appears that preliminary community changes or early *Ochroconis* growth were not a prerequisite for dark zone formation, the dark zone facies appearing in phase with community changes. In particular, this applies to microbial counter-selection that takes place in parallel to

the establishment of dark zone taxa. The predominance of *Pseudomonas* on unmarked surfaces (Alonso et al., submitted) was confirmed here, but in addition we showed that the genus was still well present at the immediate proximity of dark zones, which raises the possibility that antifungal compounds (a typical trait in this genus, including in Lascaux isolates ; Alonso et al., submitted) might still be produced till the very start of dark zone formation. Such a possibility might also apply to the case of *Stenotrophomonas*, another gammaproteobacterial genus documented in various caves including Lascaux (Bastian et al., 2010 ; Northup et al., 2003 ; Tomova et al., 2013), and known for its synthesis of antifungal compounds as well as chitinolytic and proteolytic activities (Ryan et al., 2009). Brutal microbial community collapse was also shown in other ecosystems with anthropic disturbance (e.g. eroded land and hydrosphere) (Garris et al., 2018 ; Qiu et al., 2021), where (i) microbial populations had failed to implement the conditional regulation of genes required to adjust to perturbation (Prescott et al., 2003) or (ii) conditional gene regulation interfered with restoration of microbial functions and created conditions leading to collapse (Turkarslan et al., 2017).

The occurrence of three main microbiota conditions (on unmarked surfaces, new dark zone, and intermediate/old dark zones) was also highlighted by association network results. Newly-formed dark zone showed networks with particular global and linkage characteristics, with *Ochroconis* modules (but not *Pseudomonas* modules) in lower number. Similar reduced network complexity was also observed in degraded soils (Yun et al., 2021). The genus *Pseudomonas* having antifungal properties, this could partly explain why we observed both *Pseudomonas* and *Ochroconis* in several modules, as negative interactions of *Pseudomonas* with *Ochroconis* could be expected outside altered surfaces. However, a large part of the *Pseudomonas* and *Ochroconis* OTUs do not form interaction networks with respectively *Ochroconis* and *Pseudomonas* OTUs, pointing to a key role for other microorganisms in driving brutal microbial community switch during the formation/evolution of dark zones. More numerous positive associations were observed on unmarked surfaces than dark zones, which could mean lower cooperation (and higher competition) in the microbial community of dark zones, and suggests a lower influence of stochastic processes in community assembly of altered surfaces, as found in a long-term disturbance study (Yun et al., 2021).

Microbial dynamics underlying dark zone formation were investigated using the neutral community model (NCM), which considers random dispersal processes (Hubbell, 2001 ; Vellend, 2010). It showed here the best fit of the neutral model, highlighting the occurrence of stochasticity in our dataset. We evidenced different patterns of community assembly according to taxa category, with especially an important level of deterministic processes for the always-rare taxa category in the areas closest to alteration formation (i.e. proximal unmarked surface and new dark zone), raising the possibility of cooperative relations between these always-rare taxa during the switch from unmarked surface to dark zone.

Microbial switch can influence the microbial diversity-functioning relationship and lead to lower functional redundancy (Philippot et al., 2013 ; Saghaï et al., 2022), which is perhaps important here for the establishment of the new microbial community, whose development results in the dark zone facies. For example, this might apply to the case of antifungal functions relevant for inhibition of the black melanized fungi Ochroconis on the walls, and this issue deserves further

research attention.

Conclusion

Dark zones are rock alterations of high concern for conservation of Paleolithic art, but microbial dynamics during their formation were totally unknown. In this context, the current work fills a gap by revealing that dark zone formation involves brutal microbial community switch. Dark zone formation involves a single microbial transition stage initiated exactly where the new dark zone starts, and where the bacterial genera *Labrys*, *Nonomuraea* and *Sphingomonas* and the melanized fungus *Ochroconis* expand (among others). Community assembly processes suggested that cooperative relations between rare biosphere members may promote dark zone formation. Thus, this brutal microbial community switch involved rapid microbial successions, changes in microbial diversity and community assembly processes, as well as dynamic interaction networks leading to key changes in microbial functioning (i.e. in dark zone formation/evolution). A better understanding of the formation of Paleolithic cave wall alterations can be useful to guide cave management strategies.

Data accessibility

All data that support findings of this study have been deposited in EBI references PRJEB48913, PRJEB48916, PRJEB48919 and PRJEB48926 for bacterial 16S rRNA genes, archaeal 16S rRNA genes, microeukaryotic 18S rRNA genes and fungal ITS genes, respectively. The authors declare that the R (R 4.0.3) codes used to generate the results in this study are available in this paper. The R code supporting the finding presented here is available from the GitHub Repository https ://github.com/LascauxZelia/Bontempsetal20222

Acknowledgements

Funding was provided by DRAC Nouvelle Aquitaine (Bordeaux, France). We thank S. Géraud, J.C. Portais, M. Mauriac (DRAC Nouvelle Aquitaine) and D. Henry-Lormelle (restorer team) for information and help, and Lascaux Scientific Board for useful discussions.

CRediT authorship contributions statement

Zélia Bontemps : Resources, Formal analysis, Investigation, Data Curation, Visualization and Writing – Original draft preparation. **Mylène Hugoni** : Conceptualization, Visualisation, Validation. **Yvan Moënne-Loccoz** : Conceptualization, Resources, Investigation, Visualization, Supervision, Writing – Review and Editing, Project administration and funding acquisition.

Declaration of competing interest

The authors declare that they have no known competing financial interest or personal relationships that could have influenced the work reported in this paper.

References

Alonso, L., Pommier, T., Abrouk, D., Hugoni, M., Trân Van, V., Minard, G., Valiente Moro, V., Moënne-Loccoz, Y. Submitted. Microbiome analysis of new, insidious cave wall alterations in the Apse of Lascaux Cave. (provided for review)

Alonso, L., Pommier, T., Kaufmann, B., Dubost, A., Chapulliot, D., Doré, J., Douady, C.J., Moënne-Loccoz, Y., 2019. Anthropization level of Lascaux Cave microbiome shown by regional-scale comparisons of pristine and anthropized caves. Mol Ecol 28, 3383–3394.

Alonso, L., Pommier, T., Simon, L., Maucourt, F., Doré, J., Dubost, A., Trân Van, V., Minard, G., Valiente Moro, V., Douady, C.J., Moënne-Loccoz, Y., Submitted. Microbiome analysis in Lascaux Cave in relation to black stain alterations of rock surfaces and collembola. Environ. Microbiol. Rep. (provided for review).

Arbizu, P.M., 2021. pairwiseAdonis.

Barton, H.A., Jurado, V., 2007. What's up down there ? Microbial diversity in caves. Microbes 2, 132-138.

Bastian, F., Alabouvette, C., 2009. Lights and shadows on the conservation of a rock art cave : The case of Lascaux Cave. Int. J. Speleol. 38, 55-60

Bastian, F., Alabouvette, C., Jurado, V., Saiz-Jimenez, C., 2009. Impact of biocide treatments on the bacterial communities of the Lascaux Cave. Naturwissenschaften 96, 863–868.

Bastian, F., Jurado, V., Nováková, A., Alabouvette, C., Saiz-Jimenez, C., 2010. The microbiology of Lascaux Cave. Microbiology 156, 644–652.

Berne, C., Ducret, A., Hardy, G.G., Brun, Y.V., 2015. Adhesins involved in attachment to abiotic surfaces by Gram-negative bacteria. Microbiol. Spectr. 3, 10.1128 https ://doi.org/10.1128 /microbiolspec.MB-0018-2015

Bokulich, N.A., Subramanian, S., Faith, J.J., Gevers, D., Gordon, J.I., Knight, R., Mills, D.A., Caporaso, J.G., 2013. Quality-filtering vastly improves diversity estimates from Illumina amplicon sequencing. Nat. Methods 10, 57–59. https ://doi.org/10.1038/nmeth.2276

Bontemps, Z., Alonso, L., Pommier, T., Hugoni, M., Moënne-Loccoz, Y., 2021. Microbial ecology of tourist Paleolithic caves. Sci. Tot. Environ. 16, 151492. https ://doi.org/10.1016/j .scitotenv.2021.151492

Canveras, C.S.-J., Sanchez-Moral, S., Sloer, V., 2001. Microorganisms and microbially induced fabrics in cave walls. Geomicrobiol. J. 18, 223–240. https ://doi.org/10.1080/01490450152467769

Castresana, J., 2000. Selection of conserved blocks from multiple alignments for their use in phylogenetic analysis. Mol. Biol. Evol. 17, 540–552. https ://doi.org/10.1093/oxfordjournals.molbev.a026334

Chalmin, E., d'Orlyé, F., Zinger, L., Charlet, L., Geremia, R.A., Orial, G., Menu, M., Baffier, D., Reiche, I., 2007. Biotic versus abiotic calcite formation on prehistoric cave paintings : the Arcy-sur-Cure 'Grande Grotte' (Yonne, France) case. Geo. Soc. Lond. Spe. Pub. 279, 185–197.

Chao, A., 1987. Estimating the population size for capture-recapture data with unequal catchability. Biometrics 43, 783–791.

Clarke, K.R., 1993. Non-parametric multivariate analyses of changes in community structure. Aust. J. Ecol. 18, 117–143.

Crouzet, M., Le Senechal, C., Brözel, V.S., Costaglioli, P., Barthe, C., Bonneu, M., Garbay, B., Vilain, S., 2014. Exploring early steps in biofilm formation : set-up of an experimental system for molecular studies. BMC Microbiol 14, 253.

Csárdi, G., Nepusz, T., 2006. The igraph software package for complex network research.

Cuezva, S., Sanchez-Moral, S., Saiz-Jimenez, C., Cañaveras, J., 2009. Microbial communities and associated mineral fabrics in Altamira Cave, Spain. Int. J. Speleol 38, 83-92. http ://dx.doi.org /10.5038/1827-806X.38.1.9

De Hoog, G., Von Arx, J., 1973. Revision of Scolecobasidium and Pleurophragmium. Kavaka 1, 55–60.

De Leo, F., Iero, A., Zammit, G., Urzi, C.E., 2012. Chemoorganotrophic bacteria isolated from biodeteriorated surfaces in cave and catacombs. Int. J. Speleol. 41, 125–136.

De Mandal, S., Chatterjee, R., Kumar, N.S., 2017. Dominant bacterial phyla in caves and their predicted functional roles in C and N cycle. BMC Microbiol. 17, 90.

Deacon, J., 2005. Fungal Biology, 4th edn. Wiley-Blackwell.

Delmas, E., Besson, M., Brice, M.-H., Burkle, L.A., Dalla Riva, G.V., Fortin, M.-J., Gravel, D., Guimarães, P.R., Hembry, D.H., Newman, E.A., Olesen, J.M., Pires, M.M., Yeakel, J.D., Poisot, T., 2018. Analysing ecological networks of species interactions. Biol. Rev. Camb. Philos. Soc. 94, 16-36. https ://doi.org/10.1111/brv.12433

Diaz-Herraiz, M., Jurado, V., Cuezva, S., Laiz, L., Pallecchi, P., Tiano, P., Sanchez-Moral, S., Saiz-Jimenez, C., 2014. Deterioration of an Etruscan tomb by bacteria from the order Rhizobiales. Sci. Rep. 4, 3610.

Dini-Andreote, F., Stegen, J.C., Van Elsas, J.D., Salles, J.F., 2015. Disentangling mechanisms that mediate the balance between stochastic and deterministic processes in microbial succession. Proc. Natl. Acad. Sci. U. S. A. 112, E1326–E1332.

Dollive, S., Peterfreund, G.L., Sherrill-Mix, S., Bittinger, K., Sinha, R., Hoffmann, C., Nabel, C.S., Hill, D.A., Artis, D., Bachman, M.A., Custers-Allen, R., Grunberg, S., Wu, G.D., Lewis, J.D., Bushman, F.D., 2012. A tool kit for quantifying eukaryotic rRNA gene sequences from human microbiome samples. Genome Biol. 13, R60.

Donlan, R.M., 2002. Biofilms : microbial life on surfaces. Emerg. Infect. Dis. 8, 881–890. https ://doi.org/10.3201 /eid0809.020063

Elzhov, T.V., Mullen, K.M., Spiess, A.-N., Bolker, B., 2016. minpack.lm : R Interface to the Levenberg-Marquardt Nonlinear Least-Squares Algorithm Found in MINPACK, Plus Support for Bounds.

Engel, A.S., Northup, D.E., 2008. Caves and karst as model systems for advancing the microbial sciences. In : Frontiers of Karst Research, Special Publication 13. Karst Water Institute, Lewisburg, PA, pp. 37-48.

Escalas, A., Troussellier, M., Melayah, D., Bruto, M., Nicolas, S., Bernard, C., Ader, M., Leboulanger, C., Agogué, H., Hugoni, M., 2021. Strong reorganization of multi-domain microbial networks associated with primary producers sedimentation from oxic to anoxic conditions in an hypersaline lake. FEMS Microbiol. Ecol. 97, fiab163.

Escudié, F., Auer, L., Bernard, M., Mariadassou, M., Cauquil, L., Vidal, K., Maman, S., Hernandez-Raquet, G., Combes, S., Pascal, G., 2018. FROGS : Find, Rapidly, OTUs with Galaxy Solution. Bioinformatics 34, 1287–1294.

Espino del Castillo, A., Beraldi-Campesi, H., Amador-Lemus, P., Beltrán, H.I., Borgne, S.L., 2018. Bacterial diversity associated with mineral substrates and hot springs from caves and tunnels of the Naica Underground System (Chihuahua, Mexico). Int. J. Speleol. 47, 213–227.

Fang, B.-Z., Hua, Z.-S., Han, M.-X., Zhang, Z.-T., Wang, Y.-H., Yang, Z.-W., Zhang, W.-Q., Xiao, M., Li, W.-J. 2017, 2017. *Nonomuraea cavernae sp.* nov., a novel actinobacterium isolated from a karst cave sample. Int. J. Syst. Evol. Microbiol. 67, 4692–4697.

Garris, H.W., Baldwin, S.A., Taylor, J., Gurr, D.B., Denesiuk, D.R., Hamme, J.D.V., Fraser, L.H., 2018. Short-term microbial effects of a large-scale mine-tailing storage facility collapse on the local natural environment. PloS One 13, e0196032.

Hammer, Ø., Harper, D., Ryan, P., 2001. PAST : paleontological statistics software package for education and data analysis. Palaeontologia Electronica 4, 1-9.

Harrell, F., Dupont, C., 2018. Hmisc : Harrell Miscellaneous.

Herfort, L., Kim, J.-H., Coolen, M.J.L., Abbas, B., Schouten, S., Herndl, G.J., Damsté, J.S.S., 2009. Diversity of Archaea and detection of crenarchaeotal amoA genes in the rivers Rhine and Têt. Aqua. Microb. Ecol. 55, 189–201.

Herlemann, D.P., Labrenz, M., Jürgens, K., Bertilsson, S., Waniek, J.J., Andersson, A.F., 2011. Transitions in bacterial communities along the 2000 km salinity gradient of the Baltic Sea.

ISME J. 5, 1571–1579.

Hubbell, S., 2001. The unified neutral theory of biodiversity and biogeography, Princeton university press. Monographs in Population Biology.

Jurado, V., Porca, E., Cuezva, S., Fernandez-Cortes, A., Sanchez-Moral, S., Saiz-Jimenez, C., 2010. Fungal outbreak in a show cave. Sci. Tot. Environ. 408, 3632–3638.

Kembel, S.W., Cowan, P.D., Helmus, M.R., Cornwell, W.K., Morlon, H., Ackerly, D.D., Blomberg, S.P., Webb, C.O., 2010. Picante : R tools for integrating phylogenies and ecology. Bioinformatics 26, 1463–1464.

Kuraku, S., Zmasek, C.M., Nishimura, O., Katoh, K., 2013. aLeaves facilitates on-demand exploration of metazoan gene family trees on MAFFT sequence alignment server with enhanced interactivity. Nucleic Acids Res. 41, W22–W28.

Kurtz, Z., Mueller, C., Miraldi, E., 2019. SpiecEasi : Sparse inverse covariance for ecological statistical inference.

Kurtz, Z.D., Müller, C.L., Miraldi, E.R., Littman, D.R., Blaser, M.J., Bonneau, R.A., 2015. Sparse and compositionally robust inference of microbial ecological networks. PLoS Comput. Biol. 11, e1004226.

Leibold, M.A., McPeek, M.A., 2006. Coexistence of the niche and neutral perspectives in community ecology. Ecology 87, 1399–1410.

Liu, H., Roeder, K., Wasserman, L., 2010. Stability approach to regularization selection (StARS) for high dimensional graphical models, in : Advances in neural information processing systems 23, 1432-1440.

Magoč, T., Salzberg, S.L., 2011. FLASH : fast length adjustment of short reads to improve genome assemblies. Bioinformatics 27, 2957–2963. https ://doi.org/10.1093/bioinformatics/btr507

Mahé, F., Rognes, T., Quince, C., de Vargas, C., Dunthorn, M., 2014. Swarm : robust and fast clustering method for amplicon-based studies. PeerJ 2, e593 https ://doi.org/10.7717/peerj.593

Martin-Sanchez, Pedro M., Nováková, A., Bastian, F., Alabouvette, C., Saiz-Jimenez, C., 2012. Use of biocides for the control of Fungal Outbreaks in Subterranean Environments : The Case of the Lascaux Cave in France. Environ. Sci. Technol. 46, 3762–3770.

Martin-Sanchez, P.M., Nováková, A., Bastian, F., Alabouvette, C., Saiz-Jimenez, C., 2012. Two new species of the genus *Ochroconis*, *O. lascauxensis* and *O. anomala* isolated from black stains in Lascaux Cave, France. Fungal Biol. 116, 574–589.

McMurdie, P.J., Holmes, S., 2013. phyloseq : An R package for reproducible interactive analysis and graphics of microbiome census data. PloS One 8, e61217.

Miller, J.A., Kalyuzhnaya, M.G., Noyes, E., Lara, J.C., Lidstrom, M.E., Chistoserdova, L. 2005, 2005. *Labrys methylaminiphilus* sp. nov., a novel facultatively methylotrophic bacterium from a freshwater lake sediment. Int. J. Syst. Evol. Microbiol. 55, 1247–1253.

Minh, B.Q., Schmidt, H.A., Chernomor, O., Schrempf, D., Woodhams, M.D., von Haeseler, A., Lanfear, R., 2020. IQ-TREE 2 : New models and efficient methods for phylogenetic inference in the genomic era. Mol. Biol. Evol. 37, 1530–1534.

Mortensen, B.., 2014. Formation and detection of biofilms. Report from Bactoforce International 1-5.

Nazari, B., Forneris, C.C., Gibson, M.I., Moon, K., Schramma, K.R., Seyedsayamdost, M.R., 2017. *Nonomuraea* sp. ATCC 55076 harbours the largest actinomycete chromosome to date and the kistamicin biosynthetic gene cluster. Med. Chem. Commun. 8, 780–788.

Nilsson, R.H., Larsson, K.-H., Taylor, A.F.S., Bengtsson-Palme, J., Jeppesen, T.S., Schigel, D., Kennedy, P., Picard, K., Glöckner, F.O., Tedersoo, L., Saar, I., Kõljalg, U., Abarenkov, K., 2019. The UNITE database for molecular identification of fungi : handling dark taxa and parallel taxonomic classifications. Nucleic Acids Res. 47, D259–D264.

Nimaichand, S., Devi, A.M., Tamreihao, K., Ningthoujam, D.S., Li, W.-J., 2015. Actinobacterial diversity in limestone deposit sites in Hundung, Manipur (India) and their antimicrobial activities. Front Microbiol. 6, 413.

Ning, D., 2021. iCAMP : Infer community assembly mechanisms by phylogenetic-bin-based null model analysis.

Niquil, N., Haraldsson, M., Sime-Ngando, T., Huneman, P., Borrett, S.R., 2020. Shifting levels of ecological network's analysis reveals different system properties. Philos. Trans. R. Soc. Lond. B Biol. Sci. 375, 20190326.

Northup, D.E., Barns, S.M., Yu, L.E., Spilde, M.N., Schelble, R.T., Dano, K.E., Crossey, L.J., Connolly, C.A., Boston, P.J., Natvig, D.O., Dahm, C.N., 2003. Diverse microbial communities inhabiting ferromanganese deposits in Lechuguilla and Spider Caves. Environ. Microbiol. 5, 1071–1086.

Oksanen, J., Blanchet, F.G., Friendly, M., Kindt, R., Legendre, P., McGlinn, D., Minchin, P.R., O'Hara, R.B., Simpson, G.L., Solymos, P., Stevens, M.H.H., Szoecs, E., Wagner, H., 2020. vegan : Community ecology package.

Pasić, L., Kovce, B., Sket, B., Herzog-Velikonja, B., 2010. Diversity of microbial communities colonizing the walls of a karstic cave in Slovenia. FEMS Microbiol. Ecol. 71, 50–60.

Pellissier, L., Albouy, C., Bascompte, J., Farwig, N., Graham, C., Loreau, M., Maglianesi, M.A., Melián, C.J., Pitteloud, C., Roslin, T., Rohr, R., Saavedra, S., Thuiller, W., Woodward, G., Zimmermann, N.E., Gravel, D., 2018. Comparing species interaction networks along environmental gradients. Biol. Rev. 93, 785–800.

Pfendler, S., Karimi, B., Maron, P.-A., Ciadamidaro, L., Valot, B., Bousta, F., Alaoui-Sosse, L., Alaoui-Sosse, B., Aleya, L., 2018. Biofilm biodiversity in French and Swiss show caves using the metabarcoding approach : First data. Sci. Tot. Environ. 615, 1207–1217.

Philippot, L., Spor, A., Hénault, C., Bru, D., Bizouard, F., Jones, C.M., Sarr, A., Maron, P.-A., 2013. Loss in microbial diversity affects nitrogen cycling in soil. ISME J. 7, 1609–1619.

Portillo, M.C., Gonzalez, J.M., Saiz-Jimenez, C., 2008. Metabolically active microbial communities of yellow and grey colonizations on the walls of Altamira Cave, Spain. J. Appl. Microbiol. 104, 681–691.

Prescott, L.-M., Willey, J.M., Sherwood, L.M., Woolwerton, C.J., 2003. Microbiology, 5e edn. DeBoeck.

Qiu, L., Zhang, Q., Zhu, H., Reich, P.B., Banerjee, S., van der Heijden, M.G.A., Sadowsky, M.J., Ishii, S., Jia, X., Shao, M., Liu, B., Jiao, H., Li, H., Wei, X., 2021. Erosion reduces soil microbial diversity, network complexity and multifunctionality. ISME J. 15, 2474–2489.

Quast, C., Pruesse, E., Yilmaz, P., Gerken, J., Schweer, T., Yarza, P., Peplies, J., Glöckner, F.O., 2013. The SILVA ribosomal RNA gene database project : improved data processing and web-based tools. Nucleic Acids Res. 41, D590–D596.

R Core Team, 2020. R : A language and environment for statistical computing. R Foundation for Statistical Computing, Vienna, Austria.

Rognes, T., Flouri, T., Nichols, B., Quince, C., Mahé, F., 2016. VSEARCH : a versatile open source tool for metagenomics. PeerJ 4, e2584.

Russell, M.J., MacLean, V.L., 2008. Management issues in a Tasmanian tourist cave : potential microclimatic impacts of cave modifications. J. Environ. Manage. 87, 474–483.

Ryan, R.P., Monchy, S., Cardinale, M., Taghavi, S., Crossman, L., Avison, M.B., Berg, G., Van der Lelie, D., Dow, J.M., 2009. The versatility and adaptation of bacteria from the genus *Stenotrophomonas*. Nat. Rev. Microbiol. 7, 514–525.

Saghaï, A., Wittorf, L., Philippot, L., Hallin, S., 2022. Loss in soil microbial diversity constrains microbiome selection and alters the abundance of N-cycling guilds in barley rhizosphere. Appl. Soil Ecol. 169, 104224.

Shannon, C.E., 1948. A mathematical theory of communication. Bell Syst. Tech. J. 27, 623–656.

Simpson, E.H., 1949. Measurement of diversity. Nature 163, 688–688.

Stegen, J.C., Lin, X., Fredrickson, J.K., Chen, X., Kennedy, D.W., Murray, C.J., Rockhold, M.L., Konopka, A., 2013. Quantifying community assembly processes and identifying features

that impose them. ISME J. 7, 2069–2079.

Stegen, J.C., Lin, X., Fredrickson, J.K., Konopka, A.E., 2015. Estimating and mapping ecological processes influencing microbial community assembly. Front. Microbiol. 6, 370. https ://doi.org /10.3389/fmicb.2015.00370

Stegen, J.C., Lin, X., Konopka, A.E., Fredrickson, J.K., 2012. Stochastic and deterministic assembly processes in subsurface microbial communities. ISME J. 6, 1653–1664.

Stupar, M., Grbić, M.L., Džamić, A., Unković, N., Ristić, M., Jelikić, A., Vukojević, J., 2014. Antifungal activity of selected essential oils and biocide benzalkonium chloride against the fungi isolated from cultural heritage objects. S. Afr. J. Bot. 93, 118–124.

Sungthong, R., Nakaew, N., 2015. The genus *Nonomuraea* : A review of a rare actinomycete taxon for novel metabolites. J. Bas. Microbiol. 55, 554–565.

Talavera, G., Castresana, J., 2007. Improvement of phylogenies after removing divergent and ambiguously aligned blocks from protein sequence alignments. Syst. Biol. 56, 564–577.

Tipton, L., Müller, C.L., Kurtz, Z.D., Huang, L., Kleerup, E., Morris, A., Bonneau, R., Ghedin, E., 2018. Fungi stabilize connectivity in the lung and skin microbial ecosystems. Microbiome 6, 12.

Toju, H., Tanabe, A.S., Yamamoto, S., Sato, H., 2012. High-coverage ITS primers for the DNA-based identification of Ascomycetes and Basidiomycetes in environmental samples. PLoS One 7, e40863. https ://doi.org/10.1371 /journal.pone.0040863

Tomczyk-Żak, K., Zielenkiewicz, U., 2016. Microbial diversity in caves. Geomicrobiol. J. 33, 20–38.

Tomova, I., Lazarkevich, I., Tomova, A., Kambourova, M., Vasileva-Tonkova, E., 2013. Diversity and biosynthetic potential of culturable aerobic heterotrophic bacteria isolated from Magura Cave, Bulgaria. 42, 65-76. https ://doi.org/10.5038/1827-806X.42.1.8

Turkarslan, S., Raman, A.V., Thompson, A.W., Arens, C.E., Gillespie, M.A., von Netzer, F., Hillesland, K.L., Stolyar, S., López García de Lomana, A., Reiss, D.J., Gorman-Lewis, D., Zane, G.M., Ranish, J.A., Wall, J.D., Stahl, D.A., Baliga, N.S., 2017. Mechanism for microbial population collapse in a fluctuating resource environment. Mol. Syst. Biol. 13, 919.

Urzì, C., De Leo, F., Bruno, L., Albertano, P., 2010. Microbial diversity in Paleolithic caves : A Study case on the phototrophic biofilms of the Cave of Bats (Zuheros, Spain). Microb. Ecol. 60, 116–129.

Vellend, M., 2010. Conceptual synthesis in community ecology. Q. Rev. Biol. 85, 183–206.

Wong, W.-Y., Huyop, F., 2011. Characterization of a *Labrys* sp. strain Wy1 able to utilize 2,2-dichloropropionate (2,2-DCP) as sole source of carbon. Afr. J. Microbiol. Res. 5, 3282–3288.

Yun, Y., Gui, Z., Xie, J., Chen, Y., Tian, X., Li, G., Gu, J.-D., Ma, T., 2021. Stochastic assembly process dominates bacterial succession during a long-term microbial enhanced oil recovery. Sci. Tot. Environ. 790, 148203.

Zhang, J., Madden, T.L., 1997. PowerBLAST : a new network BLAST application for interactive or automated sequence analysis and annotation. Genome Res. 7, 649–656.

Zheng, S., Bawazir, M., Dhall, A., Kim, H.-E., He, L., Heo, J., Hwang, G., 2021. implication of surface properties, bacterial motility, and hydrodynamic conditions on bacterial surface sensing and their initial adhesion. Front. Bioeng. Biotech. 9, 82.

Zhou, J., Gu, Y., Zou, C., Mo, M., 2007. Phylogenetic diversity of bacteria in an earth-cave in Guizhou province, southwest of China. J. Microbiol. 45, 105–112.

Zhou, J., Ning, D., 2017. Stochastic community assembly : Does It matter in microbial ecology ? Microbiol. Mol. Biol. Rev. 81, e00002-17.

Supplementary data

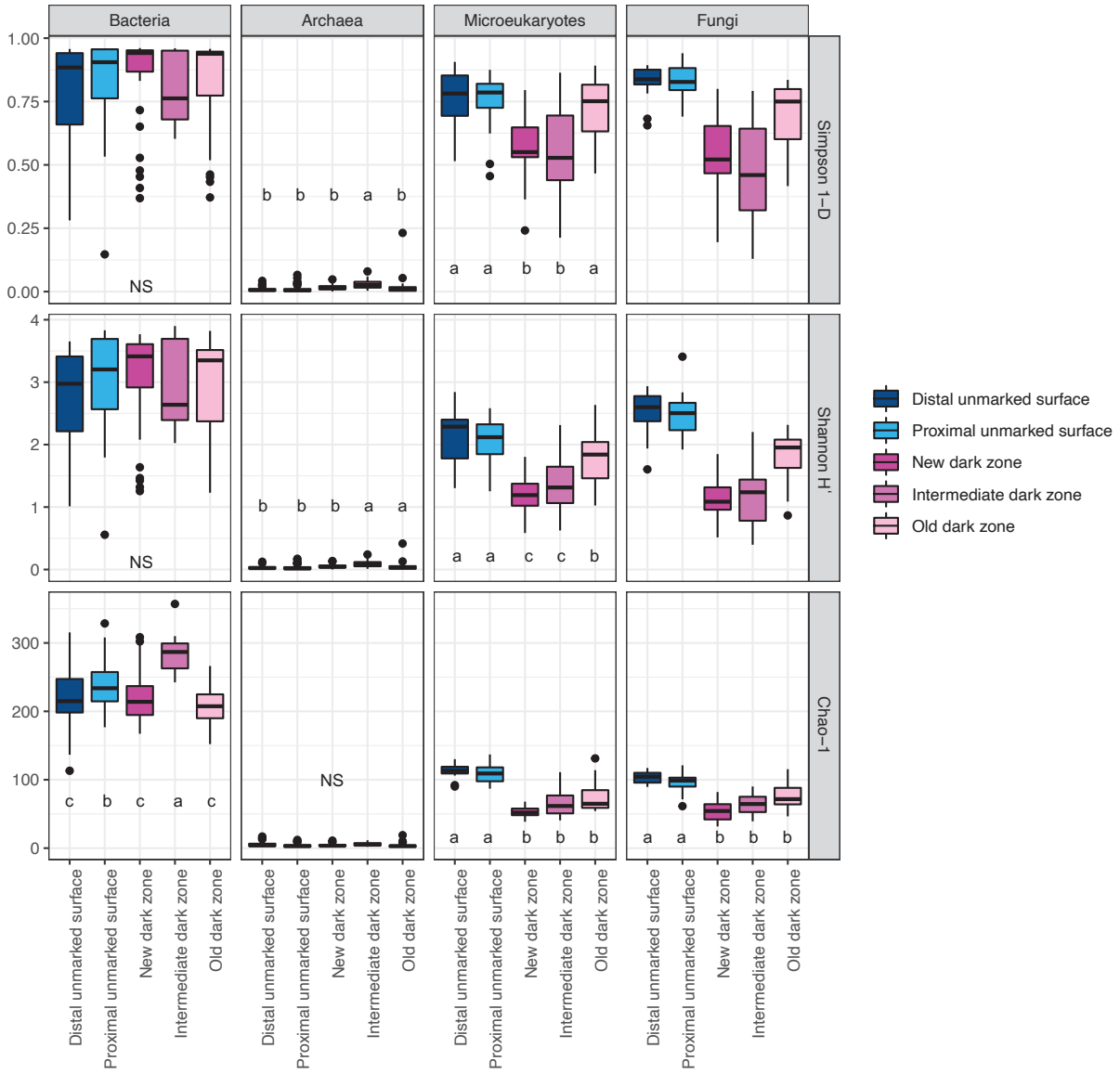

Appendix S1 : Figure S1. Alpha diversity indices of microbial communities according to rock surface condition, based on estimated richness (Chao-1 index), diversity (Shannon H' index), and evenness (Simpson 1-D index). For each index x microbial community combination, significant differences according to rock surface condition and post-hoc grouping are shown with letters (Wilcoxon test, $P < 0.05$).

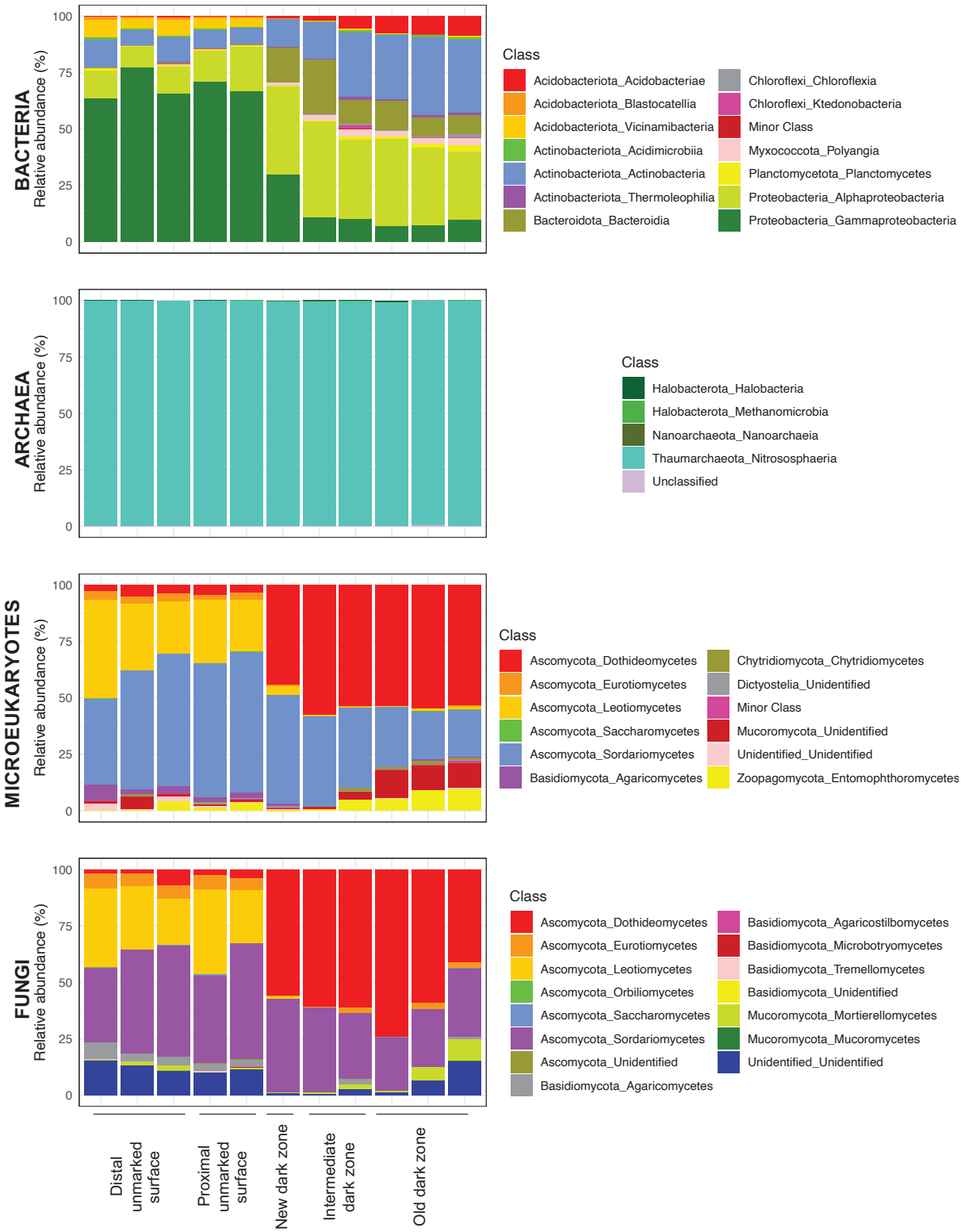

Appendix S2 : Figure S2. Distribution (% relative abundance) of the taxonomic classes according to rock surface condition and time. ODZ : Old Dark Zone ; IDZ : Intermediate Dark Zone ; NDZ : New Dark Zone ; PUN : Proximal Unmarked Surface ; DUN : Distal Unmarked Surface ; A19 : April 2019 ; D19 : December 2019 ; A21 : April 2021.

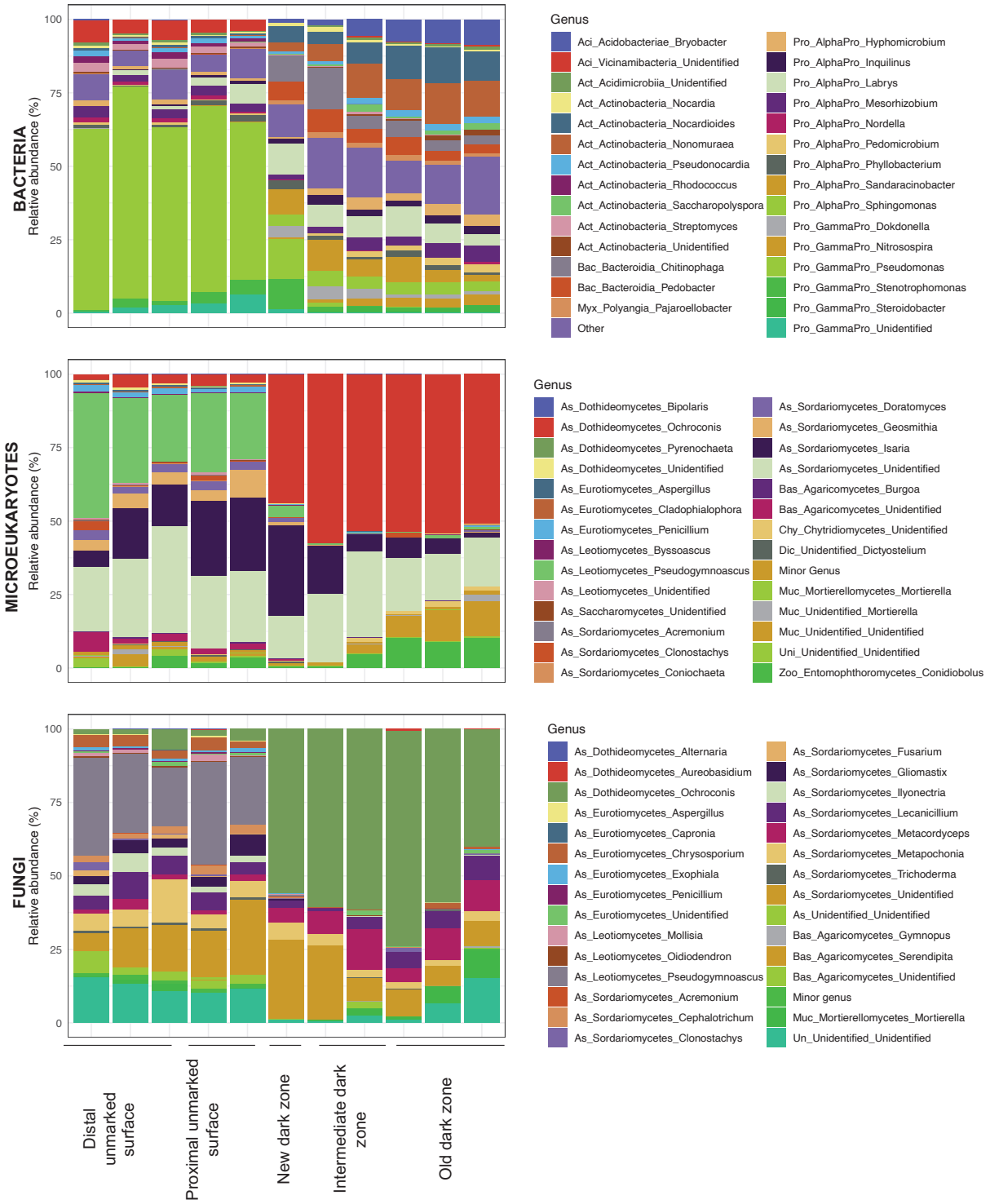

Appendix S3 : Figure S3. Distribution (% relative abundance) of the 30 most abundant genera according to rock surface condition and time. ODZ : Old Dark Zone ; IDZ : Intermediate Dark Zone ; NDZ : New Dark Zone ; PUN : Proximal Unmarked Surface ; DUN : Distal Unmarked Surface ; A19 : April 2019 ; D19 : December 2019 ; A21 : April 2021. Act : *Actinobacterota* ; Pro : *Proteobacteria* ; Aci : *Acidobacteria* ; Bac : *Bacteroidota* ; Myx : *Myxococcota* ; Pla : *Planctomycetes* ; Chl : *Chloroflexi* ; Asc : *Ascomycota* ; Bas : *Basidiomycota* ; Mur : *Mucoromycota* ; Un : Unidentified.

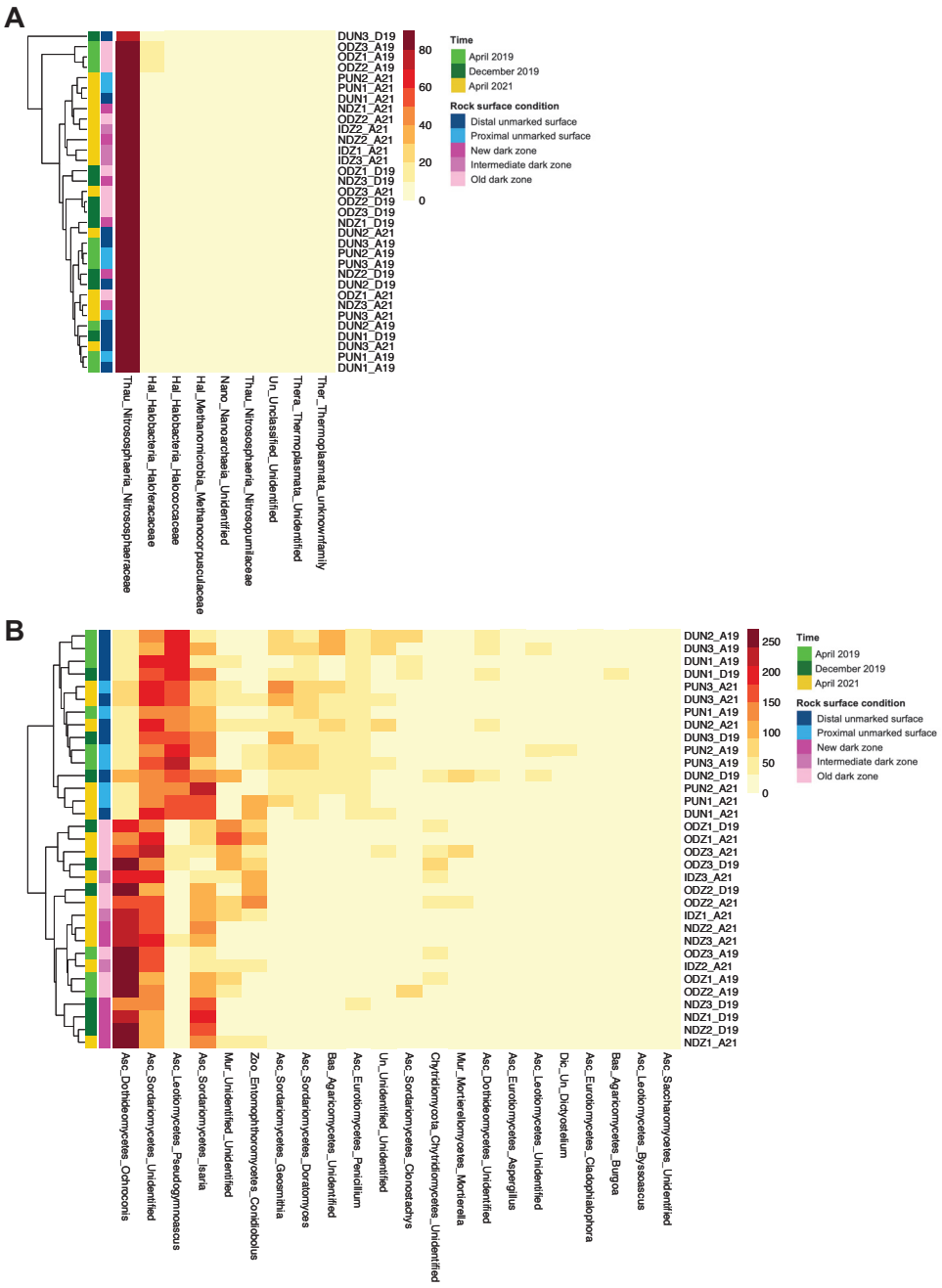

Appendix S4 : Figure S4. Distribution (% relative abundance) of the most abundant archaeal families (A) and microeukaryotic genera (B). The heatmap was coupled to a hierarchical clustering analysis of the most abundant genera (i.e. consisting of $> 0.05\%$ of total normalized sequences) in each rock surface condition. Community structure was analyzed using a matrix that was square root-transformed to minimize the impact of highly dominant families or genera. ODZ : Old Dark Zone ; IDZ : Intermediate Dark Zone ; NDZ : New Dark Zone ; PUN : Proximal Unmarked surface ; DUN : Distal Unmarked Surface ; A19 : April 2019 ; D19 : December 2019 ; A21 : April 2021 ; Thau : *Thaumarchaeota* ; Hal : *Halobacterota* ; Nano : *Nanoarchaeota* ; Ther : *Thermoplasmatota* ; Asc : *Ascomycota* ; Bas : *Basidiomycota* ; Mur : *Mucoromycota* ; Zoo : *Zoopagomycota* ; Dic : *Discosea* ; Chy : *Chytridiomycota* ; Un : Unidentified.

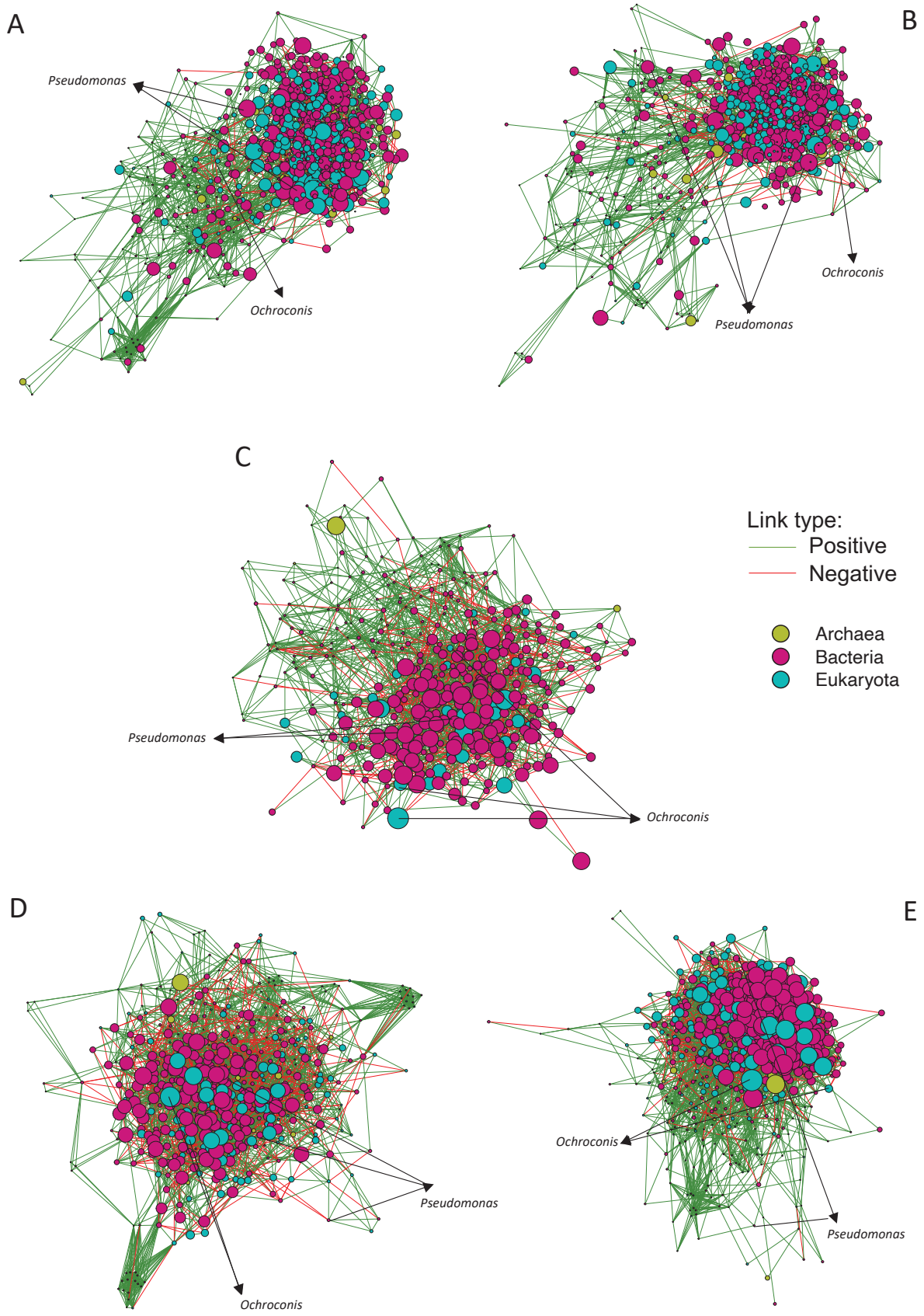

Appendix S5 : Figure S5. Co-occurrence networks in the five rock surfaces conditions. The size of the nodes is proportional to their abundance. Archaea are in green, bacteria in purple and microeukaryotes in blue. Positive links are in green and negative links in red. (A) Distal unmarked surface ; (B) Proximal unmarked surface, (C) New dark zone ; (D) Intermediate dark zone and (E) Old dark zone.

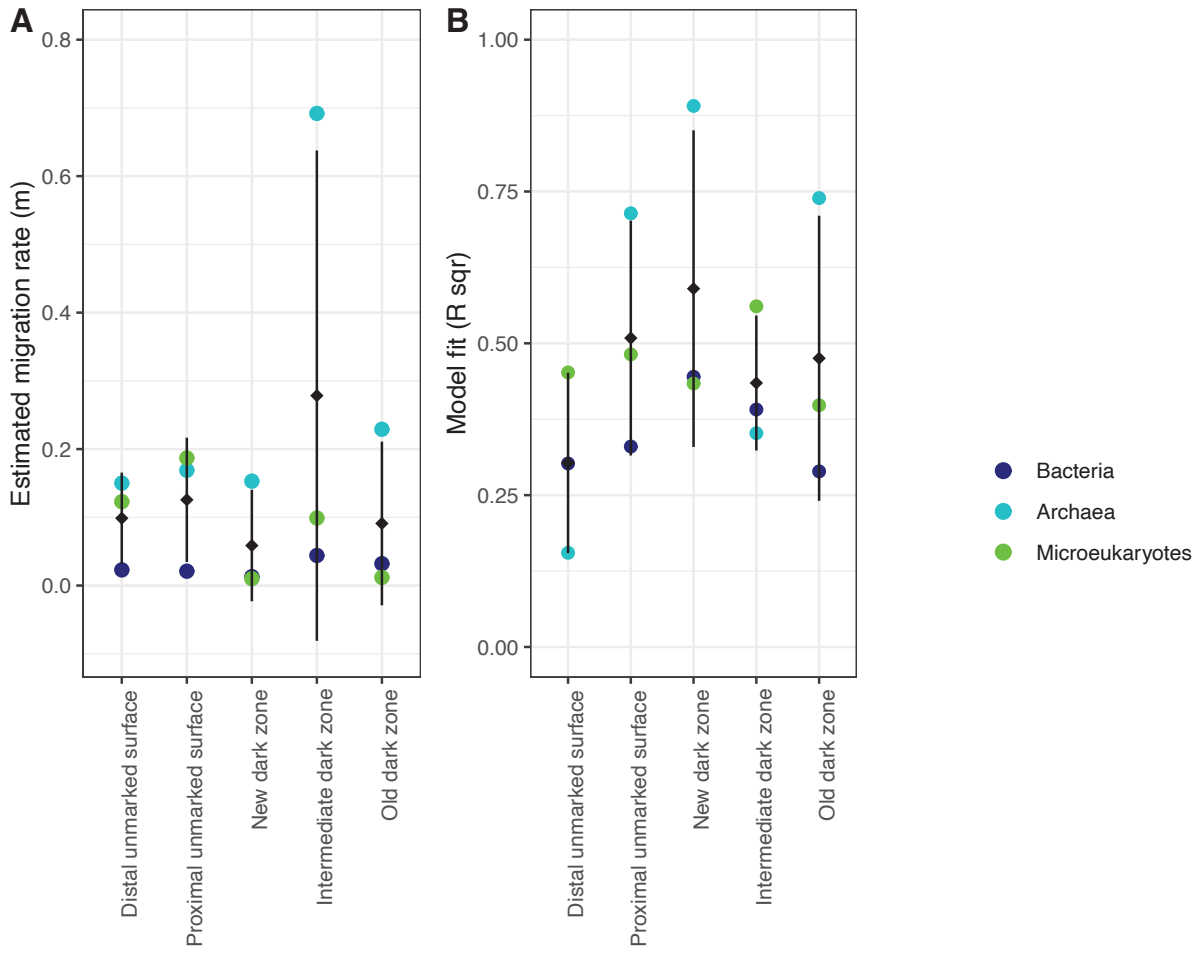

Appendix S6 : Figure S6. Neutral model across rock surfaces conditions. (A) Estimated migration rate (m) and (B) goodness-of-fit of the neutral model across rock surface conditions for the three domains of life. Comparison of the maximum likelihood fit of the neutral, binomial and Poisson models can be found in Appendix S14 : Table S5.

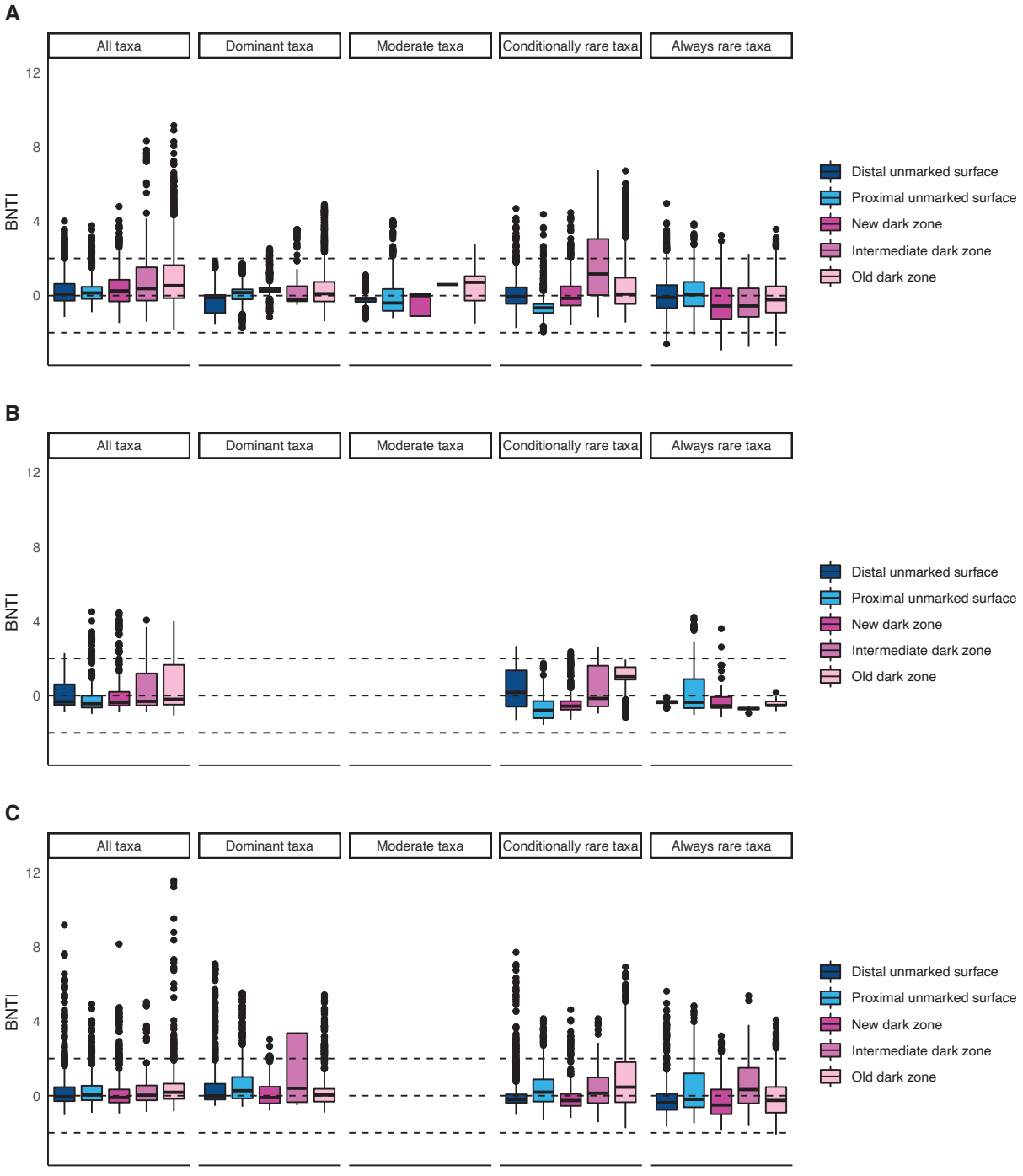

Appendix S7 : Figure S7. βNTI values for bacterial (A), archaeal (B) and microeukaryotic (C) communities according to taxa abundance category for different rock surface conditions. Horizontal dashed lines represent βNTI values of -2.0, 0.0 and +2.0.

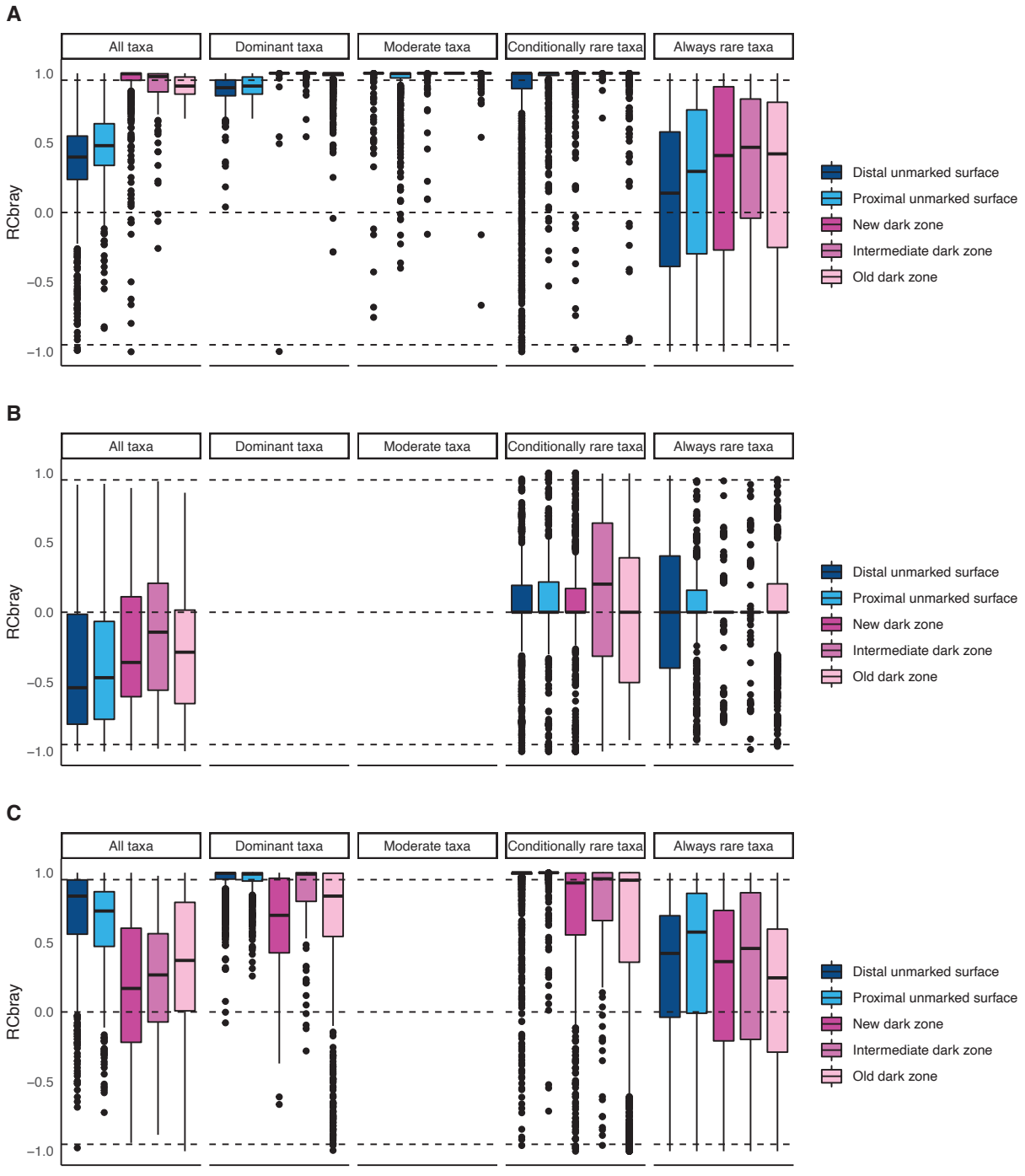

Appendix S8 : Figure S8. Bray-Curtis-based Raup-Crick (RC_bray) patterns for bacterial (A), archaeal (B) and microeukaryotic (C) communities according to taxa abundance category for different rock surface conditions. Horizontal dashed lines indicate the null value and significant thresholds of -0.95, 0.0 and +0.95.

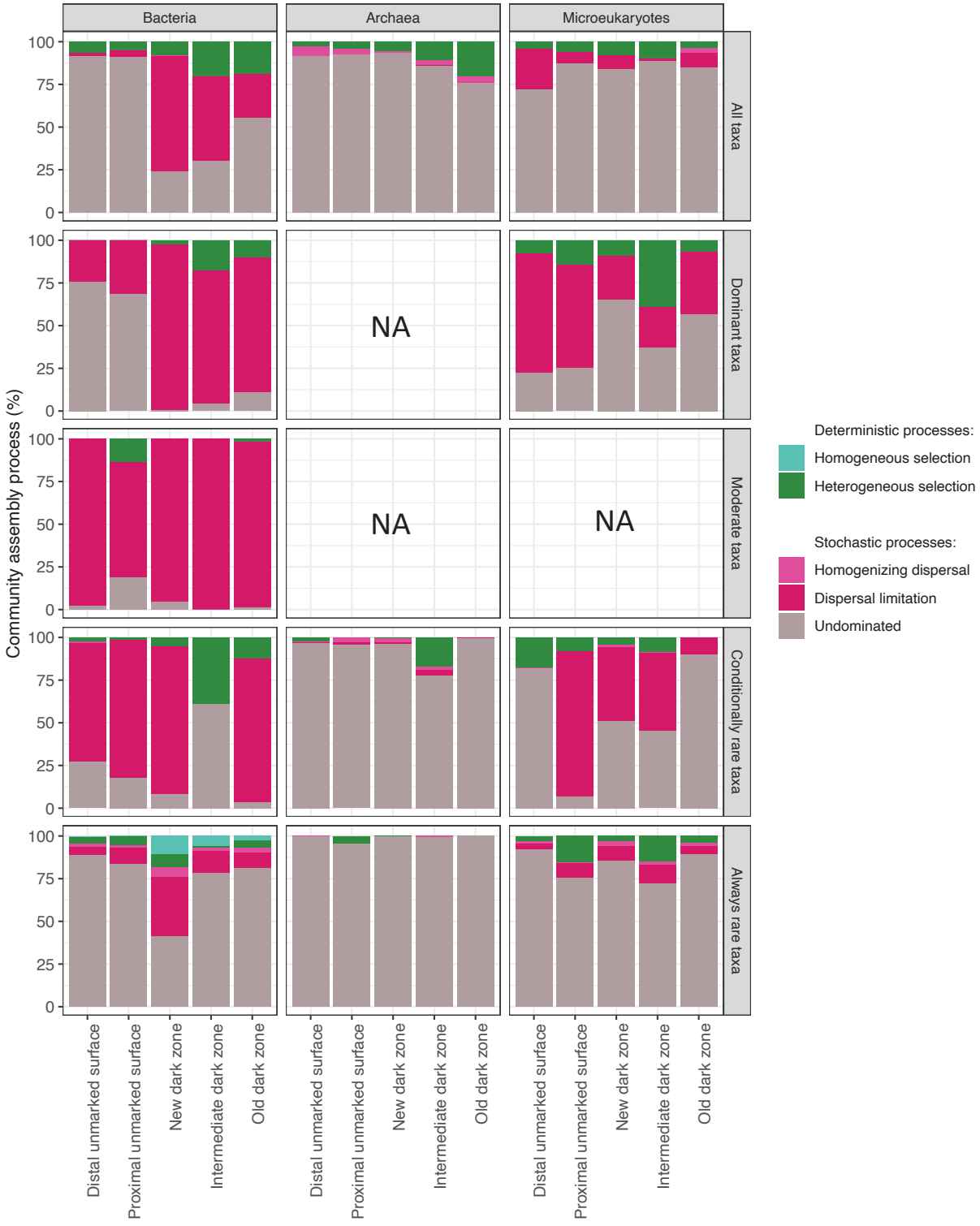

Appendix S9 : Figure S9. Contribution of deterministic and stochastic processes to the assembly of microbial communities. The percent turnover of bacterial, archaeal and microeukaryotic communities for each taxa category is shown for deterministic processes (including homogenous and heterogeneous selections) and stochastic processes (including homogenizing dispersal, dispersal limitation and undominated processes).

Appendix S10 : Table S1. Primers for amplification of taxonomic marker genes.

Marker gene	Region	Length	Name	Forward (F) or reverse (R)	Sequence	Reference
16S rRNA	V3-V4 Bacteria	550 bp	341F	F	5'-CCTACGGGNGGCWGCAG-3'	Herlemann *et al.*, 2011
			805R	R	5'-GACTACHVGGGTATCTAATCC-3'	
	V3-V4 Archaea	420 bp	515F	F	5'-CAGCCGCCGCGGTAA-3'	Herfort *et al.*, 2011
			915R	R	5'-GTGCTCCCCCGCCAATTCCT-3'	
18S rRNA	V4	350 bp	0067a_deg	F	5'-AAGCCATGCATGYCTAAGTATMA-3′	Dollive *et al.*, 2012
			NSR339	R	5'-TCTCAGGCTCCYTCTCCGG-3′	
ITS	ITS2	327 bp	ITS3_KYO2	F	5'-ATGAAGAACGYAGYRAA-3'	Toju *et al.*, 2012
			ITS4	R	5'-TCCTCCGCTTATTGATATGC- 3'	

Appendix S11 : Table S2. Number of modules identified in each rock surface condition using different clustering algorithms. The values are averages estimated across all samples from each rock surface condition. The Louvain system was preferably chosen in this work.

Algorithm	Distal unmarked surface	Proximal unmarked surface	New dark zone	Intermediate dark zone	Old dark zone
fast_greedy	5	6	7	7	7
leading_eigenvector	5	11	9	8	12
Spinglass	12	12	12	14	11
Louvain	11	11	10	13	11
Average :	8.3	10.0	9.5	10.5	10.3

Appendix S12 : Table S3. Shift in properties of *Pseudomonas* and *Ochroconis* (including the number of OTUs of these taxa) between rock surface conditions.

Taxa	**Rock surface condition**	**Number of OTUs**	**Links**			
			Positive		**Negative**	
			Number	**Weight**	**Number**	**Weight**
Pseudomonas	Distal unmarked surface	19	176	0.12	98	-0.07
	Proximal unmarked surface	20	181	0.13	88	-0.06
	New dark zone	18	100	0.17	44	-0.01
	Intermediate dark zone	8	70	0.17	20	-0.09
	Old dark zone	9	78	0.13	28	-0.06
Ochroconis	Distal unmarked surface	8	87	0.13	32	-0.04
	Proximal unmarked surface	8	92	0.14	42	-0.06
	New dark zone	6	31	0.17	10	-0.09
	Intermediate dark zone	8	55	0.16	25	-0.08
	Old dark zone	8	58	0.16	29	-0.05

Appendix S13 : Table S4. Shifts between rock surfaces conditions in the composition of networks containing *Pseudomonas* and/or *Ochroconis* OTUs.

Dominant taxa	Rock surface conditions	Domain	Phylum	Class	Order	Family	Genus	Link type
Pseudomonas	Distal unmarked surface	Bacteria	Bacteroidota	Bacteroidia	Cytophagales	Microscillaceae	Unknown genus	Negative
		Eukaryota	Ascomycota	Sordariomycetes	Xylariales	Xylariaceae	Kretzschmaria	Negative
		Bacteria	Acidobacteriota	Vicinamibacteria	Vicinamibacterales	Vicinamibacteraceae	Unknown genus	Negative
		Eukaryota	Ascomycota	Sordariomycetes	Xylariales	Xylariaceae	Ascotricha	Negative
		Eukaryota	Basidiomycota	Agaricomycetes	Russulales	Unidentified	Unidentified	Negative
		Eukaryota	Ascomycota	Saccharomycetes	Saccharomycetales	Pichiaceae	Martiniozyma	Negative
		Eukaryota	Amoebozoa	Discosea	Centramoebida	Unidentified	Unidentified	Negative
		Eukaryota	Ascomycota	Sordariomycetes	Hypocreales	Nectriaceae	Nectria	Negative
		Bacteria	Proteobacteria	Gammaproteobacteria	Pseudomonadales	Pseudomonadaceae	Pseudomonas	Negative
		Bacteria	Actinobacteriota	Actinobacteria	Streptosporangiales	Streptosporangiaceae	Nonomuraea	Negative
		Bacteria	Proteobacteria	Gammaproteobacteria	Xanthomonadales	Xanthomonadaceae	Luteimonas	Negative
		Bacteria	Actinobacteriota	Acidimicrobiia	Microtrichales	Unknown family	Unknown genus	Negative
		Bacteria	Acidobacteriota	Blastocatellia	45597	Unknown family	Unknown genus	Negative
		Bacteria	Actinobacteriota	Actinobacteria	Micrococcales	Promicromonosporaceae	Promicromonospora	Negative
		Bacteria	Proteobacteria	Gammaproteobacteria	Pseudomonadales	Moraxellaceae	Acinetobacter	Negative
		Bacteria	Actinobacteriota	Actinobacteria	Propionibacteriales	Nocardioidaceae	Aeromicrobium	Negative
		Bacteria	Actinobacteriota	Acidimicrobiia	Microtrichales	Ilumatobacteraceae	Unknown genus	Negative
		Eukaryota	Ascomycota	Dothideomycetes	Pleosporales	Cucurbitariaceae	Pyrenochaeta	Negative
		Bacteria	Proteobacteria	Alphaproteobacteria	Rhizobiales	Beijerinckiaceae	28-YEA-48	Negative
		Bacteria	Proteobacteria	Gammaproteobacteria	Xanthomonadales	Xanthomonadaceae	Stenotrophomonas	Negative
		Bacteria	Actinobacteriota	Actinobacteria	Pseudonocardiales	Pseudonocardiaceae	Pseudonocardia	Negative
		Bacteria	Proteobacteria	Gammaproteobacteria	Pseudomonadales	Pseudomonadaceae	Pseudomonas	Negative
		Bacteria	Proteobacteria	Gammaproteobacteria	Legionellales	Legionellaceae	Legionella	Negative
		Bacteria	Proteobacteria	Alphaproteobacteria	Rhizobiales	Hyphomicrobiaceae	Hyphomicrobium	Negative
		Eukaryota	Ascomycota	Leotiomycetes	Unidentified	Unidentified	Pseudogymnoascus	Negative
		Bacteria	Proteobacteria	Gammaproteobacteria	Pseudomonadales	Pseudomonadaceae	Pseudomonas	Negative
		Bacteria	Proteobacteria	Gammaproteobacteria	Pseudomonadales	Pseudomonadaceae	Pseudomonas	Negative
		Bacteria	Myxococcota	Polyangia	Nannocystales	Nannocystaceae	Unknown genus	Negative
		Bacteria	Proteobacteria	Alphaproteobacteria	Sphingomonadales	Sphingomonadaceae	Sphingopyxis	Negative
		Bacteria	Proteobacteria	Gammaproteobacteria	Burkholderiales	Burkholderiaceae	Ralstonia	Negative
		Eukaryota	Ascomycota	Dothideomycetes	Venturiales	Sympoventuriaceae	Ochroconis	Negative
		Eukaryota	Basidiomycota	Agaricomycetes	Unidentified	Unidentified	Unidentified	Negative
		Bacteria	Acidobacteriota	Blastocatellia	Blastocatellales	Blastocatellaceae	JGI0001001-H03	Negative
		Bacteria	Patescibacteria	Parcubacteria	Candidatus Adlerbacteria	Unknown family	Unknown genus	Negative
		Bacteria	Proteobacteria	Alphaproteobacteria	Reyranellales	Reyranellaceae	Unknown genus	Negative
		Bacteria	Acidobacteriota	Blastocatellia	Blastocatellales	Blastocatellaceae	Unidentified	Negative
		Bacteria	Myxococcota	Polyangia	Nannocystales	Nannocystaceae	Nannocystis	Negative
		Eukaryota	Zoopagomycota	Entomophthoromycetes	Entomophthorales	Ancylistaceae	Conidiobolus	Negative
		Eukaryota	Ascomycota	Leotiomycetes	Helotiales	Unidentified	Unidentified	Negative
		Bacteria	Proteobacteria	Alphaproteobacteria	Rhizobiales	Beijerinckiaceae	Unknown genus	Negative
		Eukaryota	Ascomycota	Eurotiomycetes	Chaetothyriales	Herpotrichiellaceae	Unidentified	Negative
		Bacteria	Proteobacteria	Gammaproteobacteria	Pseudomonadales	Pseudomonadaceae	Pseudomonas	Negative
		Bacteria	Actinobacteriota	Actinobacteria	Micrococcales	Microbacteriaceae	Agromyces	Negative
		Bacteria	Proteobacteria	Alphaproteobacteria	Rhizobiales	Rhizobiaceae	Phyllobacterium	Negative
		Bacteria	Proteobacteria	Gammaproteobacteria	Steroidobacterales	Steroidobacteraceae	Unidentified	Negative
		Bacteria	Actinobacteriota	Actinobacteria	Pseudonocardiales	Pseudonocardiaceae	Pseudonocardia	Negative
		Bacteria	Actinobacteriota	Actinobacteria	Streptomycetales	Streptomycetaceae	Streptomyces	Negative
		Bacteria	Actinobacteriota	Acidimicrobiia	Microtrichales	Unknown family	Unknown genus	Negative
		Eukaryota	Amoebozoa	Tubulinea	Echinamoebida	Unidentified	Unidentified	Negative
		Bacteria	Actinobacteriota	Actinobacteria	Propionibacteriales	Nocardioidaceae	Nocardioides	Negative
		Eukaryota	Cercozoa	Glissomonadida	Unidentified	Unidentified	Heteromita	Negative
		Bacteria	Acidobacteriota	Acidobacteriae	Bryobacterales	Bryobacteraceae	Bryobacter	Negative
		Bacteria	Bacteroidota	Bacteroidia	Sphingobacteriales	Sphingobacteriaceae	Olivibacter	Negative
		Bacteria	Proteobacteria	Gammaproteobacteria	Xanthomonadales	Xanthomonadaceae	Stenotrophomonas	Negative
		Bacteria	Proteobacteria	Alphaproteobacteria	Rickettsiales	Anaplasmataceae	Wolbachia	Negative
		Eukaryota	Ascomycota	Sordariomycetes	Hypocreales	Cordycipitaceae	Isaria	Negative
		Bacteria	Actinobacteriota	Actinobacteria	Propionibacteriales	Nocardioidaceae	Nocardioides	Negative
		Bacteria	Actinobacteriota	Actinobacteria	Micrococcales	Microbacteriaceae	Agromyces	Negative
		Eukaryota	Basidiomycota	Agaricomycetes	Polyporales	Unidentified	Burgoa	Negative
		Bacteria	Actinobacteriota	Acidimicrobiia	Microtrichales	Ilumatobacteraceae	Unknown genus	Negative
		Eukaryota	Basidiomycota	Agaricomycetes	Unidentified	Unidentified	Unidentified	Negative
		Bacteria	Proteobacteria	Alphaproteobacteria	Rhizobiales	Xanthobacteraceae	Pseudorhodoplanes	Negative
		Bacteria	Proteobacteria	Alphaproteobacteria	Rhizobiales	Labraceae	Labrys	Negative
		Eukaryota	Dictyostelia	Unidentified	Unidentified	Unidentified	Dictyostelium	Negative
		Bacteria	Proteobacteria	Gammaproteobacteria	Burkholderiales	Burkholderiaceae	Ralstonia	Negative
		Bacteria	Actinobacteriota	Actinobacteria	Corynebacteriales	Corynebacteriaceae	Unknown genus	Negative
		Bacteria	Acidobacteriota	Acidobacteriae	Unknown order	Unknown family	Unknown genus	Negative
		Bacteria	Actinobacteriota	Actinobacteria	Micrococcales	Intrasporangiaceae	Unidentified	Negative
		Bacteria	Bacteroidota	Bacteroidia	Chitinophagales	Chitinophagaceae	Chitinophaga	Negative
		Eukaryota	Ascomycota	Dothideomycetes	Venturiales	Sympoventuriaceae	Ochroconis	Negative
		Eukaryota	Ascomycota	Leotiomycetes	Helotiales	Leotiaceae	Pezoloma	Negative
		Bacteria	Actinobacteriota	Acidimicrobiia	Microtrichales	Unknown family	Unknown genus	Negative
		Bacteria	Acidobacteriota	Vicinamibacteria	Vicinamibacterales	Vicinamibacteraceae	Unknown genus	Negative
		Bacteria	Acidobacteriota	Vicinamibacteria	Vicinamibacterales	Vicinamibacteraceae	Unknown genus	Negative
		Bacteria	Proteobacteria	Alphaproteobacteria	Rhizobiales	Devosiaceae	Devosia	Negative
		Eukaryota	Ascomycota	Sordariomycetes	Hypocreales	Unidentified	Acremonium	Negative
		Eukaryota	Amoebozoa	Tubulinea	Echinamoebida	Unidentified	Vermamoeba	Negative
		Bacteria	Proteobacteria	Gammaproteobacteria	Pseudomonadales	Pseudomonadaceae	Pseudomonas	Negative
		Bacteria	Actinobacteriota	Actinobacteria	Pseudonocardiales	Pseudonocardiaceae	Pseudonocardia	Negative
		Eukaryota	Ascomycota	Dothideomycetes	Pleosporales	Unidentified	Unidentified	Negative
		Bacteria	Proteobacteria	Alphaproteobacteria	Rhizobiales	Beijerinckiaceae	Bosea	Negative
		Bacteria	Acidobacteriota	Vicinamibacteria	Vicinamibacterales	Vicinamibacteraceae	Unknown genus	Negative
		Bacteria	Proteobacteria	Alphaproteobacteria	Rhizobiales	Rhizobiaceae	Phyllobacterium	Negative
		Bacteria	Proteobacteria	Gammaproteobacteria	Pseudomonadales	Pseudomonadaceae	Pseudomonas	Negative
		Bacteria	Actinobacteriota	Actinobacteria	Propionibacteriales	Nocardioidaceae	Kribbella	Negative

Eukaryota	Ascomycota	Sordariomycetes	Glomerellales	Plectosphaerellaceae	Unidentified	Negative
Bacteria	Actinobacteriota	Actinobacteria	Propionibacteriales	Propionibacteriaceae	Jiangella	Negative
Bacteria	Acidobacteriota	Blastocatellia	Blastocatellales	Blastocatellaceae	Unidentified	Negative
Bacteria	Proteobacteria	Gammaproteobacteria	Legionellales	Legionellaceae	Legionella	Negative
Bacteria	Actinobacteriota	Actinobacteria	Micrococcales	Microbacteriaceae	Agromyces	Negative
Eukaryota	Ascomycota	Sordariomycetes	Glomerellales	Plectosphaerellaceae	Unidentified	Negative
Bacteria	Proteobacteria	Gammaproteobacteria	Xanthomonadales	Xanthomonadaceae	Luteimonas	Negative
Eukaryota	Ascomycota	Sordariomycetes	Hypocreales	Unidentified	Acremonium	Negative
Bacteria	Proteobacteria	Alphaproteobacteria	Acetobacterales	Acetobacteraceae	Roseomonas	Negative
Eukaryota	Unidentified	Unidentified	Unidentified	Unidentified	Mycamoeba	Negative
Bacteria	Dependentiae	Babeliae	Babeliales	Vermiphilaceae	Unknown genus	Negative
Bacteria	Actinobacteriota	Actinobacteria	Corynebacteriales	Nocardiaceae	Nocardia	Negative
Eukaryota	Ascomycota	Dothideomycetes	Pleosporales	Phaeosphaeriaceae	Phaeodothis	Negative
Eukaryota	Ascomycota	Leotiomycetes	Thelebolales	Thelebolaceae	Unidentified	Positive
Bacteria	Bacteroidota	Bacteroidia	Chitinophagales	Chitinophagaceae	Chitinophaga	Positive
Bacteria	Acidobacteriota	Vicinamibacteria	Subgroup17	Unknown family	Unknown genus	Positive
Bacteria	Bacteroidota	Bacteroidia	Sphingobacteriales	Sphingobacteriaceae	Pseudosphingobacterium	Positive
Bacteria	Acidobacteriota	Vicinamibacteria	Vicinamibacterales	Vicinamibacteraceae	Vicinamibacter	Positive
Bacteria	Chloroflexi	Chloroflexia	Thermomicrobiales	JG30-KF-CM45	Unknown genus	Positive
Eukaryota	Ascomycota	Sordariomycetes	Unidentified	Unidentified	Unidentified	Positive
Bacteria	Actinobacteriota	Actinobacteria	Propionibacteriales	Propionibacteriaceae	Jiangella	Positive
Bacteria	Acidobacteriota	Vicinamibacteria	Vicinamibacterales	Vicinamibacteraceae	Vicinamibacter	Positive
Bacteria	Proteobacteria	Alphaproteobacteria	Rhizobiales	Hyphomicrobiaceae	Hyphomicrobium	Positive
Bacteria	Proteobacteria	Gammaproteobacteria	Burkholderiales	Alcaligenaceae	Bordetella	Positive
Bacteria	Actinobacteriota	Actinobacteria	Frankiales	Acidothermaceae	Acidothermus	Positive
Eukaryota	Unidentified	Unidentified	Unidentified	Unidentified	Unidentified	Positive
Bacteria	Planctomycetota	Planctomycetes	Isosphaerales	Isosphaeraceae	Singulisphaera	Positive
Eukaryota	Ascomycota	Sordariomycetes	Unidentified	Unidentified	Unidentified	Positive
Bacteria	Proteobacteria	Alphaproteobacteria	Rhizobiales	Xanthobacteraceae	Unidentified	Positive
Bacteria	Actinobacteriota	Actinobacteria	Propionibacteriales	Propionibacteriaceae	Unidentified	Positive
Bacteria	Proteobacteria	Gammaproteobacteria	Legionellales	Legionellaceae	Legionella	Positive
Bacteria	Actinobacteriota	Acidimicrobiia	Microtrichales	Ilumatobacteraceae	Unknown genus	Positive
Eukaryota	Ascomycota	Eurotiomycetes	Eurotiales	Aspergillaceae	Aspergillus	Positive
Bacteria	Acidobacteriota	Acidobacteriae	Bryobacterales	Bryobacteraceae	Bryobacter	Positive
Eukaryota	Basidiomycota	Tremellomycetes	Cystofilobasidiales	Mrakiaceae	Itersonilia	Positive
Eukaryota	Chytridiomycota	Chytridiomycetes	Spizellomycetales	Unidentified	Unidentified	Positive
Bacteria	Proteobacteria	Gammaproteobacteria	Pseudomonadales	Pseudomonadaceae	Pseudomonas	Positive
Bacteria	Proteobacteria	Gammaproteobacteria	Burkholderiales	Alcaligenaceae	Unidentified	Positive
Eukaryota	Ascomycota	Dothideomycetes	Venturiales	Sympoventuriaceae	Ochroconis	Positive
Bacteria	Bacteroidota	Bacteroidia	Sphingobacteriales	Sphingobacteriaceae	Pedobacter	Positive
Bacteria	Actinobacteriota	Actinobacteria	Propionibacteriales	Propionibacteriaceae	Unknown genus	Positive
Eukaryota	Ascomycota	Sordariomycetes	Hypocreales	Cordycipitaceae	Isaria	Positive
Bacteria	Chloroflexi	Chloroflexia	Thermomicrobiales	JG30-KF-CM45	Unknown genus	Positive
Bacteria	Actinobacteriota	Actinobacteria	Pseudonocardiales	Pseudonocardiaceae	Pseudonocardia	Positive
Eukaryota	Ascomycota	Dothideomycetes	Pleosporales	Pleosporaceae	Bipolaris	Positive
Eukaryota	Ascomycota	Dothideomycetes	Venturiales	Sympoventuriaceae	Ochroconis	Positive
Eukaryota	Ascomycota	Sordariomycetes	Hypocreales	Hypocreaceae	Trichoderma	Positive
Bacteria	Proteobacteria	Alphaproteobacteria	Caulobacterales	Caulobacteraceae	Brevundimonas	Positive
Eukaryota	Ascomycota	Sordariomycetes	Unidentified	Unidentified	Unidentified	Positive
Bacteria	Actinobacteriota	Actinobacteria	Streptosporangiales	Streptosporangiaceae	Nonomuraea	Positive
Archaea	Thaumarchaeota	Nitrososphaeria	Nitrosopumilales	Nitrosopumilaceae	Multi-affiliation	Positive
Bacteria	Actinobacteriota	Acidimicrobiia	Microtrichales	Ilumatobacteraceae	Unknown genus	Positive
Bacteria	Actinobacteriota	Actinobacteria	Pseudonocardiales	Pseudonocardiaceae	Pseudonocardia	Positive
Bacteria	Actinobacteriota	Acidimicrobiia	Microtrichales	Iamiaceae	Iamia	Positive
Bacteria	Proteobacteria	Gammaproteobacteria	Xanthomonadales	Xanthomonadaceae	Stenotrophomonas	Positive
Bacteria	Bacteroidota	Bacteroidia	Chitinophagales	Chitinophagaceae	Chitinophaga	Positive
Eukaryota	Ascomycota	Leotiomycetes	Unidentified	Unidentified	Pseudogymnoascus	Positive
Bacteria	Actinobacteriota	Actinobacteria	Micrococcales	Promicromonosporaceae	Promicromonospora	Positive
Bacteria	Proteobacteria	Alphaproteobacteria	Sphingomonadales	Sphingomonadaceae	Sphingomonas	Positive
Eukaryota	Ascomycota	Leotiomycetes	Helotiales	Unidentified	Tetracladium	Positive
Eukaryota	Ascomycota	Sordariomycetes	Glomerellales	Plectosphaerellaceae	Unidentified	Positive
Bacteria	Actinobacteriota	Actinobacteria	Propionibacteriales	Nocardioidaceae	Aeromicrobium	Positive
Eukaryota	Ascomycota	Eurotiomycetes	Eurotiales	Unidentified	Unidentified	Positive
Archaea	Thaumarchaeota	Nitrososphaeria	Nitrososphaerales	Nitrososphaeraceae	Unknown genus	Positive
Bacteria	Proteobacteria	Alphaproteobacteria	Rhizobiales	Devosiaceae	Devosia	Positive
Eukaryota	Ascomycota	Sordariomycetes	Unidentified	Unidentified	Unidentified	Positive
Bacteria	Proteobacteria	Alphaproteobacteria	Rhizobiales	Xanthobacteraceae	Unknown genus	Positive
Bacteria	Proteobacteria	Alphaproteobacteria	Rhizobiales	Rhizobiaceae	Unidentified	Positive
Bacteria	Proteobacteria	Alphaproteobacteria	Sphingomonadales	Sphingomonadaceae	Sphingomonas	Positive
Bacteria	Bacteroidota	Bacteroidia	Sphingobacteriales	Sphingobacteriaceae	Pedobacter	Positive
Eukaryota	Ascomycota	Sordariomycetes	Hypocreales	Bionectriaceae	Geosmithia	Positive
Bacteria	Proteobacteria	Alphaproteobacteria	Rhizobiales	Hyphomicrobiaceae	Hyphomicrobium	Positive
Bacteria	Acidobacteriota	Acidobacteriae	Bryobacterales	Bryobacteraceae	Bryobacter	Positive
Bacteria	Actinobacteriota	Actinobacteria	Pseudonocardiales	Pseudonocardiaceae	Pseudonocardia	Positive
Bacteria	Proteobacteria	Gammaproteobacteria	Burkholderiales	Comamonadaceae	Variovorax	Positive
Bacteria	Bacteroidota	Bacteroidia	Chitinophagales	Chitinophagaceae	Chitinophaga	Positive
Bacteria	Chloroflexi	Chloroflexia	Thermomicrobiales	JG30-KF-CM45	Unknown genus	Positive
Bacteria	Proteobacteria	Alphaproteobacteria	Azospirillales	Inquilinaceae	Inquilinus	Positive
Bacteria	Proteobacteria	Gammaproteobacteria	Pseudomonadales	Pseudomonadaceae	Pseudomonas	Positive
Eukaryota	Basidiomycota	Agaricomycetes	Polyporales	Unidentified	Unidentified	Positive
Eukaryota	Ascomycota	Dothideomycetes	Venturiales	Sympoventuriaceae	Ochroconis	Positive
Bacteria	Proteobacteria	Alphaproteobacteria	Rhizobiales	Hyphomicrobiaceae	Pedomicrobium	Positive
Bacteria	Actinobacteriota	Actinobacteria	Streptomycetales	Streptomycetaceae	Streptomyces	Positive
Bacteria	Proteobacteria	Alphaproteobacteria	Rhizobiales	Methylopilaceae	Methylopila	Positive
Eukaryota	Basidiomycota	Agaricomycetes	Unidentified	Unidentified	Unidentified	Positive
Bacteria	Proteobacteria	Alphaproteobacteria	Caulobacterales	Hyphomonadaceae	SWB02	Positive

Bacteria	Proteobacteria	Alphaproteobacteria	Rhizobiales	Rhizobiaceae	Mesorhizobium	Positive
Eukaryota	Ascomycota	Sordariomycetes	Hypocreales	Unidentified	Unidentified	Positive
Bacteria	Acidobacteriota	Acidobacteriae	Bryobacterales	Bryobacteraceae	Bryobacter	Positive
Eukaryota	Ascomycota	Sordariomycetes	Microascales	Microascaceae	Doratomyces	Positive
Bacteria	Actinobacteriota	Actinobacteria	Corynebacteriales	Mycobacteriaceae	Mycobacterium	Positive
Bacteria	Proteobacteria	Alphaproteobacteria	Azospirillales	Inquilinaceae	Inquilinus	Positive
Bacteria	Acidobacteriota	Blastocatellia	45597	Unknown family	Unknown genus	Positive
Eukaryota	Ascomycota	Sordariomycetes	Unidentified	Unidentified	Unidentified	Positive
Bacteria	Acidobacteriota	Vicinamibacteria	Vicinamibacterales	Vicinamibacteraceae	Vicinamibacter	Positive
Eukaryota	Mucoromycota	Unidentified	Mortierellales	Mortierellaceae	Mortierella	Positive
Bacteria	Actinobacteriota	Thermoleophilia	Solirubrobacterales	67-14	Unknown genus	Positive
Bacteria	Proteobacteria	Alphaproteobacteria	Rhizobiales	Rhizobiaceae	Mesorhizobium	Positive
Eukaryota	Ascomycota	Eurotiomycetes	Eurotiales	Trichocomaceae	Talaromyces	Positive
Bacteria	Actinobacteriota	Actinobacteria	Propionibacteriales	Nocardioidaceae	Nocardioides	Positive
Bacteria	Actinobacteriota	Actinobacteria	Propionibacteriales	Nocardioidaceae	Nocardioides	Positive
Bacteria	Proteobacteria	Alphaproteobacteria	Reyranellales	Reyranellaceae	Unknown genus	Positive
Eukaryota	Ascomycota	Dothideomycetes	Capnodiales	Unidentified	Unidentified	Positive
Bacteria	Acidobacteriota	Acidobacteriae	Bryobacterales	Bryobacteraceae	Bryobacter	Positive
Eukaryota	Ascomycota	Sordariomycetes	Unidentified	Unidentified	Unidentified	Positive
Bacteria	Actinobacteriota	Actinobacteria	Propionibacteriales	Nocardioidaceae	Nocardioides	Positive
Bacteria	Proteobacteria	Alphaproteobacteria	Sphingomonadales	Sphingomonadaceae	Sphingobium	Positive
Bacteria	Acidobacteriota	Vicinamibacteria	Subgroup17	Unknown family	Unknown genus	Positive
Bacteria	Proteobacteria	Alphaproteobacteria	Rhizobiales	Xanthobacteraceae	Afipia	Positive
Bacteria	Actinobacteriota	Actinobacteria	Pseudonocardiales	Pseudonocardiaceae	Pseudonocardia	Positive
Bacteria	Proteobacteria	Alphaproteobacteria	Rhizobiales	Labraceae	Labrys	Positive
Archaea	Halobacterota	Halobacteria	Halobacterales	Haloferacaceae	Natronococcus	Positive
Bacteria	Proteobacteria	Alphaproteobacteria	Caulobacterales	Caulobacteraceae	Phenylobacterium	Positive
Eukaryota	Ascomycota	Sordariomycetes	Unidentified	Unidentified	Unidentified	Positive
Eukaryota	Ascomycota	Eurotiomycetes	Chaetothyriales	Cyphellophoraceae	Cyphellophora	Positive
Bacteria	Actinobacteriota	Actinobacteria	Pseudonocardiales	Pseudonocardiaceae	Pseudonocardia	Positive
Bacteria	Proteobacteria	Gammaproteobacteria	Burkholderiales	Alcaligenaceae	Bordetella	Positive
Bacteria	Myxococcota	bacteriap25	Unknown order	Unknown family	Unknown genus	Positive
Bacteria	Planctomycetota	Planctomycetes	Pirellulales	Pirellulaceae	Pir4lineage	Positive
Bacteria	Proteobacteria	Gammaproteobacteria	Legionellales	Legionellaceae	Legionella	Positive
Eukaryota	Ascomycota	Dothideomycetes	Venturiales	Sympoventuriaceae	Ochroconis	Positive
Eukaryota	Ascomycota	Dothideomycetes	Capnodiales	Unidentified	Unidentified	Positive
Bacteria	Proteobacteria	Gammaproteobacteria	Pseudomonadales	Pseudomonadaceae	Pseudomonas	Positive
Bacteria	Actinobacteriota	Actinobacteria	Pseudonocardiales	Pseudonocardiaceae	Saccharopolyspora	Positive
Bacteria	Actinobacteriota	Acidimicrobiia	IMCC26256	Unknown family	Unknown genus	Positive
Bacteria	Proteobacteria	Alphaproteobacteria	Rhizobiales	Xanthobacteraceae	Pseudorhodoplanes	Positive
Bacteria	Proteobacteria	Alphaproteobacteria	Rhizobiales	Rhizobiaceae	Mesorhizobium	Positive
Bacteria	Bacteroidota	Bacteroidia	Sphingobacteriales	Sphingobacteriaceae	Parapedobacter	Positive
Bacteria	Chloroflexi	Chloroflexia	Thermomicrobiales	JG30-KF-CM45	Unknown genus	Positive
Bacteria	Proteobacteria	Gammaproteobacteria	Burkholderiales	Alcaligenaceae	Unidentified	Positive
Bacteria	Actinobacteriota	Actinobacteria	Streptomycetales	Streptomycetaceae	Streptomyces	Positive
Bacteria	Proteobacteria	Gammaproteobacteria	Xanthomonadales	Xanthomonadaceae	Luteimonas	Positive
Bacteria	Actinobacteriota	Actinobacteria	Micrococcales	Microbacteriaceae	Agrococcus	Positive
Bacteria	Actinobacteriota	Actinobacteria	Propionibacteriales	Propionibacteriaceae	Unidentified	Positive
Eukaryota	Zoopagomycota	Entomophthoromycetes	Entomophthorales	Ancylistaceae	Conidiobolus	Positive
Eukaryota	Ascomycota	Eurotiomycetes	Eurotiales	Aspergillaceae	Aspergillus	Positive
Eukaryota	Ascomycota	Saccharomycetes	Saccharomycetales	Unidentified	Unidentified	Positive
Bacteria	Proteobacteria	Gammaproteobacteria	Xanthomonadales	Xanthomonadaceae	Stenotrophomonas	Positive
Eukaryota	Ascomycota	Leotiomycetes	Unidentified	Unidentified	Pseudogymnoascus	Positive
Bacteria	Actinobacteriota	Acidimicrobiia	Microtrichales	Ilumatobacteraceae	Unknown genus	Positive
Eukaryota	Ascomycota	Sordariomycetes	Hypocreales	Bionectriaceae	Geosmithia	Positive
Eukaryota	Amoebozoa	Discosea	Centramoebida	Unidentified	Unidentified	Positive
Eukaryota	Ascomycota	Pezizomycetes	Pezizales	Pyronemataceae	Tricharina	Positive
Bacteria	Bacteroidota	Bacteroidia	Chitinophagales	Chitinophagaceae	Chitinophaga	Positive
Eukaryota	Ascomycota	Eurotiomycetes	Eurotiales	Aspergillaceae	Penicillium	Positive
Bacteria	Proteobacteria	Gammaproteobacteria	Pseudomonadales	Pseudomonadaceae	Pseudomonas	Positive
Eukaryota	Ascomycota	Leotiomycetes	Helotiales	Sclerotiniaceae	Sclerotinia	Positive
Eukaryota	Ciliophora	Intramacronucleata	Conthreep	Colpodea	Bromeliothrix	Positive
Archaea	Thaumarchaeota	Nitrososphaeria	Nitrososphaerales	Nitrososphaeraceae	Unknown genus	Positive
Bacteria	Actinobacteriota	Actinobacteria	Pseudonocardiales	Pseudonocardiaceae	Pseudonocardia	Positive
Bacteria	Actinobacteriota	Actinobacteria	Frankiales	Frankiaceae	Jatrophihabitans	Positive
Eukaryota	Ascomycota	Sordariomycetes	Glomerellales	Plectosphaerellaceae	Unidentified	Positive
Bacteria	Acidobacteriota	Vicinamibacteria	Vicinamibacterales	Vicinamibacteraceae	Unknown genus	Positive
Bacteria	Myxococcota	Polyangia	Polyangiales	Polyangiaceae	Pajaroellobacter	Positive
Eukaryota	Mucoromycota	Unidentified	Unidentified	Unidentified	Unidentified	Positive
Bacteria	Proteobacteria	Alphaproteobacteria	Caulobacterales	Caulobacteraceae	Brevundimonas	Positive
Archaea	Nanoarchaeota	Nanoarchaeia	Woesearchaeales	Unidentified	Unknown genus	Positive
Bacteria	Proteobacteria	Alphaproteobacteria	Reyranellales	Reyranellaceae	Reyranella	Positive
Bacteria	Planctomycetota	Planctomycetes	Planctomycetales	Unknown family	Unknown genus	Positive
Eukaryota	Ascomycota	Sordariomycetes	Unidentified	Unidentified	Unidentified	Positive
Bacteria	Proteobacteria	Alphaproteobacteria	Rhizobiales	Labraceae	Labrys	Positive
Eukaryota	Unidentified	Unidentified	Unidentified	Unidentified	Unidentified	Positive
Bacteria	Proteobacteria	Gammaproteobacteria	Pseudomonadales	Pseudomonadaceae	Pseudomonas	Positive
Bacteria	Proteobacteria	Alphaproteobacteria	Rhizobiales	Hyphomicrobiaceae	Pedomicrobium	Positive
Bacteria	Acidobacteriota	Blastocatellia	45597	Unknown family	Unknown genus	Positive
Eukaryota	Mucoromycota	Mortierellomycetes	Mortierellales	Mortierellaceae	Mortierella	Positive
Bacteria	Actinobacteriota	Actinobacteria	Corynebacteriales	Nocardiaceae	Nocardia	Positive
Eukaryota	Ascomycota	Eurotiomycetes	Chaetothyriales	Herpotrichiellaceae	Cladophialophora	Positive
Bacteria	Proteobacteria	Gammaproteobacteria	Pseudomonadales	Pseudomonadaceae	Pseudomonas	Positive
Eukaryota	Ascomycota	Sordariomycetes	Microascales	Microascaceae	Cephalotrichum	Positive
Eukaryota	Ascomycota	Sordariomycetes	Hypocreales	Cordycipitaceae	Isaria	Positive
Bacteria	Proteobacteria	Gammaproteobacteria	Xanthomonadales	Xanthomonadaceae	Stenotrophomonas	Positive

	Bacteria	Proteobacteria	Gammaproteobacteria	Xanthomonadales	Xanthomonadaceae	Stenotrophomonas	Positive
	Bacteria	Actinobacteriota	Acidimicrobiia	Microtrichales	Ilumatobacteraceae	Unknown genus	Positive
	Eukaryota	Unclassified	Unclassified	Unclassified	Unclassified	Unclassified	Positive
	Bacteria	Actinobacteriota	Actinobacteria	Propionibacteriales	Propionibacteriaceae	Jiangella	Positive
	Bacteria	Actinobacteriota	Acidimicrobiia	Microtrichales	Ilumatobacteraceae	Unknown genus	Positive
	Bacteria	Actinobacteriota	Actinobacteria	Propionibacteriales	Nocardioidaceae	Nocardioides	Positive
	Bacteria	Proteobacteria	Gammaproteobacteria	Pseudomonadales	Pseudomonadaceae	Pseudomonas	Positive
	Bacteria	Actinobacteriota	Actinobacteria	Pseudonocardiales	Pseudonocardiaceae	Amycolatopsis	Positive
	Bacteria	Proteobacteria	Alphaproteobacteria	Rhizobiales	Xanthobacteraceae	Afipia	Positive
	Bacteria	Actinobacteriota	Actinobacteria	Streptomycetales	Streptomycetaceae	E1B-B3-114	Positive
	Archaea	Thaumarchaeota	Nitrososphaeria	Nitrososphaerales	Nitrososphaeraceae	Multi-affiliation	Positive
	Eukaryota	Ascomycota	Sordariomycetes	Sordariales	Chaetomiaceae	Chaetomium	Positive
	Bacteria	Proteobacteria	Alphaproteobacteria	Rhizobiales	Rhizobiaceae	Mesorhizobium	Positive
	Bacteria	Proteobacteria	Gammaproteobacteria	Burkholderiales	Burkholderiaceae	Ralstonia	Positive
	Bacteria	Chloroflexi	Chloroflexia	Thermomicrobiales	JG30-KF-CM45	Unknown genus	Positive
	Bacteria	Proteobacteria	Gammaproteobacteria	Pseudomonadales	Pseudomonadaceae	Pseudomonas	Positive
	Bacteria	Acidobacteriota	Blastocatellia	45597	Unknown family	Unknown genus	Positive
Proximal unmarked surfa	Eukaryota	Ascomycota	Dothideomycetes	Pleosporales	Cucurbitariaceae	Pyrenochaeta	Negative
	Bacteria	Proteobacteria	Gammaproteobacteria	Burkholderiales	Comamonadaceae	Variovorax	Negative
	Bacteria	Actinobacteriota	Acidimicrobiia	Microtrichales	Ilumatobacteraceae	Unknown genus	Negative
	Bacteria	Actinobacteriota	Thermoleophilia	Solirubrobacterales	67-14	Unknown genus	Negative
	Eukaryota	Ascomycota	Eurotiomycetes	Chaetothyriales	Cyphellophoraceae	Cyphellophora	Negative
	Bacteria	Proteobacteria	Gammaproteobacteria	Burkholderiales	Burkholderiaceae	Ralstonia	Negative
	Archaea	Thaumarchaeota	Nitrososphaeria	Nitrososphaerales	Nitrososphaeraceae	Unknown genus	Negative
	Archaea	Thaumarchaeota	Nitrososphaeria	Nitrososphaerales	Nitrososphaeraceae	Unknown genus	Negative
	Bacteria	Proteobacteria	Alphaproteobacteria	Caulobacterales	Caulobacteraceae	Brevundimonas	Negative
	Bacteria	Actinobacteriota	Actinobacteria	Propionibacteriales	Nocardioidaceae	Aeromicrobium	Negative
	Bacteria	Planctomycetota	Planctomycetes	Gemmatales	Gemmataceae	Gemmata	Negative
	Bacteria	Planctomycetota	Planctomycetes	Pirellulales	Pirellulaceae	Pir4lineage	Negative
	Eukaryota	Ascomycota	Dothideomycetes	Pleosporales	Phaeosphaeriaceae	Phaeodothis	Negative
	Eukaryota	Basidiomycota	Tremellomycetes	Filobasidiales	Piskurozymaceae	Solicoccozyma	Negative
	Bacteria	Actinobacteriota	Acidimicrobiia	Microtrichales	Unknown family	Unknown genus	Negative
	Bacteria	Acidobacteriota	Vicinamibacteria	Subgroup17	Unknown family	Unknown genus	Negative
	Bacteria	Proteobacteria	Alphaproteobacteria	Rhizobiales	Beijerinckiaceae	Unknown genus	Negative
	Eukaryota	Ascomycota	Eurotiomycetes	Chaetothyriales	Herpotrichiellaceae	Cladophialophora	Negative
	Bacteria	Actinobacteriota	Actinobacteria	Streptomycetales	Streptomycetaceae	Streptomyces	Negative
	Eukaryota	Ascomycota	Saccharomycetes	Saccharomycetales	Debaryomycetaceae	Unidentified	Negative
	Bacteria	Proteobacteria	Gammaproteobacteria	Pseudomonadales	Pseudomonadaceae	Pseudomonas	Negative
	Eukaryota	Ascomycota	Sordariomycetes	Unidentified	Unidentified	Unidentified	Negative
	Bacteria	Actinobacteriota	Actinobacteria	Corynebacteriales	Nocardiaceae	Rhodococcus	Negative
	Eukaryota	Ascomycota	Sordariomycetes	Unidentified	Unidentified	Unidentified	Negative
	Bacteria	Actinobacteriota	Actinobacteria	Streptosporangiales	Streptosporangiaceae	Unidentified	Negative
	Eukaryota	Ascomycota	Eurotiomycetes	Eurotiales	Aspergillaceae	Aspergillus	Negative
	Eukaryota	Ascomycota	Sordariomycetes	Unidentified	Unidentified	Unidentified	Negative
	Eukaryota	Basidiomycota	Tremellomycetes	Filobasidiales	Filobasidiaceae	Unidentified	Negative
	Bacteria	Actinobacteriota	Actinobacteria	Propionibacteriales	Nocardioidaceae	Nocardioides	Negative
	Bacteria	Acidobacteriota	Blastocatellia	Blastocatellales	Blastocatellaceae	Unidentified	Negative
	Eukaryota	Nematozoa	Chromadorea	Rhabditida	Unidentified	Unidentified	Negative
	Bacteria	Actinobacteriota	Actinobacteria	Propionibacteriales	Propionibacteriaceae	Unidentified	Negative
	Bacteria	Proteobacteria	Gammaproteobacteria	Xanthomonadales	Xanthomonadaceae	Stenotrophomonas	Negative
	Bacteria	Actinobacteriota	Actinobacteria	Propionibacteriales	Nocardioidaceae	Nocardioides	Negative
	Eukaryota	Ascomycota	Eurotiomycetes	Eurotiales	Aspergillaceae	Penicillium	Negative
	Bacteria	Actinobacteriota	Actinobacteria	Corynebacteriales	Mycobacteriaceae	Mycobacterium	Negative
	Bacteria	Proteobacteria	Gammaproteobacteria	Pseudomonadales	Pseudomonadaceae	Pseudomonas	Negative
	Eukaryota	Amoebozoa	Discosea	Centramoebida	Unidentified	Acanthamoeba	Negative
	Bacteria	Actinobacteriota	Acidimicrobiia	Microtrichales	Ilumatobacteraceae	Unknown genus	Negative
	Eukaryota	Ascomycota	Sordariomycetes	Hypocreales	Ophiocordycipitaceae	Tolypocladium	Negative
	Bacteria	Proteobacteria	Gammaproteobacteria	Pseudomonadales	Pseudomonadaceae	Pseudomonas	Negative
	Bacteria	Proteobacteria	Gammaproteobacteria	Pseudomonadales	Pseudomonadaceae	Pseudomonas	Negative
	Bacteria	Proteobacteria	Alphaproteobacteria	Rhizobiales	Rhizobiaceae	Mesorhizobium	Negative
	Eukaryota	Ascomycota	Sordariomycetes	Xylariales	Unidentified	Circinotrichum	Negative
	Bacteria	Proteobacteria	Alphaproteobacteria	Rhizobiales	Beijerinckiaceae	Bosea	Negative
	Eukaryota	Ascomycota	Eurotiomycetes	Eurotiales	Unidentified	Unidentified	Negative
	Eukaryota	Ascomycota	Leotiomycetes	Helotiales	Unidentified	Tetracladium	Negative
	Bacteria	Acidobacteriota	Blastocatellia	45597	Unknown family	Unknown genus	Negative
	Bacteria	Acidobacteriota	Vicinamibacteria	Vicinamibacterales	Vicinamibacteraceae	Unknown genus	Negative
	Bacteria	Actinobacteriota	Actinobacteria	Streptomycetales	Streptomycetaceae	Streptomyces	Negative
	Bacteria	Proteobacteria	Gammaproteobacteria	Pseudomonadales	Pseudomonadaceae	Pseudomonas	Negative
	Eukaryota	Ascomycota	Eurotiomycetes	Onygenales	Arthrodermataceae	Arthroderma	Negative
	Bacteria	Proteobacteria	Gammaproteobacteria	Pseudomonadales	Pseudomonadaceae	Pseudomonas	Negative
	Bacteria	Actinobacteriota	Actinobacteria	Pseudonocardiales	Pseudonocardiaceae	Pseudonocardia	Negative
	Bacteria	Actinobacteriota	Actinobacteria	Micrococcales	Intrasporangiaceae	Unidentified	Negative
	Eukaryota	Ascomycota	Eurotiomycetes	Eurotiales	Aspergillaceae	Aspergillus	Negative
	Bacteria	Actinobacteriota	Actinobacteria	Propionibacteriales	Nocardioidaceae	Nocardioides	Negative
	Bacteria	Actinobacteriota	Acidimicrobiia	Microtrichales	Unknown family	Unknown genus	Negative
	Eukaryota	Ascomycota	Dothideomycetes	Dothideales	Aureobasidiaceae	Unidentified	Negative
	Eukaryota	Cercozoa	Cercomonadidae	Unidentified	Unidentified	Cercomonas	Negative
	Bacteria	Proteobacteria	Alphaproteobacteria	Acetobacterales	Acetobacteraceae	Roseomonas	Negative
	Bacteria	Proteobacteria	Alphaproteobacteria	Sphingomonadales	Sphingomonadaceae	Sandaracinobacter	Negative
	Bacteria	Proteobacteria	Gammaproteobacteria	Xanthomonadales	Xanthomonadaceae	Luteimonas	Negative
	Bacteria	Actinobacteriota	Actinobacteria	Pseudonocardiales	Pseudonocardiaceae	Pseudonocardia	Negative
	Bacteria	Acidobacteriota	Vicinamibacteria	Vicinamibacterales	Unknown family	Unknown genus	Negative
	Bacteria	Actinobacteriota	Acidimicrobiia	Microtrichales	Ilumatobacteraceae	Unknown genus	Negative
	Bacteria	Actinobacteriota	Actinobacteria	Frankiales	Acidothermaceae	Acidothermus	Negative
	Archaea	Halobacterota	Methanomicrobia	Methanomicrobiales	Methanocorpusculaceae	Methanocalculus	Negative
	Eukaryota	Ascomycota	Dothideomycetes	Pleosporales	Unidentified	Unidentified	Negative

Bacteria	Acidobacteriota	Acidobacteriae	Bryobacterales	Bryobacteraceae	Bryobacter	Negative
Eukaryota	Unidentified	Unidentified	Unidentified	Unidentified	Unidentified	Negative
Bacteria	Proteobacteria	Alphaproteobacteria	Reyranellales	Reyranellaceae	Reyranella	Negative
Bacteria	Planctomycetota	Planctomycetes	Isosphaerales	Isosphaeraceae	Unknown genus	Negative
Bacteria	Proteobacteria	Gammaproteobacteria	Burkholderiales	Alcaligenaceae	Bordetella	Negative
Bacteria	Actinobacteriota	Actinobacteria	Propionibacteriales	Nocardioidaceae	Kribbella	Negative
Eukaryota	Ascomycota	Eurotiomycetes	Eurotiales	Trichocomaceae	Talaromyces	Negative
Bacteria	Actinobacteriota	Thermoleophilia	Solirubrobacterales	Solirubrobacteraceae	Solirubrobacter	Negative
Bacteria	Acidobacteriota	Acidobacteriae	Bryobacterales	Bryobacteraceae	Bryobacter	Negative
Bacteria	Acidobacteriota	Vicinamibacteria	Vicinamibacterales	Vicinamibacteraceae	Vicinamibacter	Negative
Bacteria	Actinobacteriota	Actinobacteria	Propionibacteriales	Propionibacteriaceae	Unidentified	Negative
Eukaryota	Ascomycota	Sordariomycetes	Hypocreales	Bionectriaceae	Geosmithia	Negative
Eukaryota	Basidiomycota	Agaricomycetes	Agaricales	Lyophyllaceae	Asterophora	Negative
Eukaryota	Ascomycota	Leotiomycetes	Unidentified	Unidentified	Pseudogymnoascus	Negative
Bacteria	Actinobacteriota	Actinobacteria	Corynebacteriales	Mycobacteriaceae	Mycobacterium	Negative
Eukaryota	Ascomycota	Sordariomycetes	Coniochaetales	Coniochaetaceae	Coniochaeta	Negative
Eukaryota	Ascomycota	Sordariomycetes	Hypocreales	Cordycipitaceae	Isaria	Negative
Bacteria	Actinobacteriota	Acidimicrobiia	Microtrichales	Ilumatobacteraceae	Unknown genus	Negative
Bacteria	Acidobacteriota	Vicinamibacteria	Vicinamibacterales	Vicinamibacteraceae	Unknown genus	Negative
Bacteria	Acidobacteriota	Vicinamibacteria	Vicinamibacterales	Vicinamibacteraceae	Unknown genus	Positive
Archaea	Unclassified	Unclassified	Unclassified	Unidentified	Unclassified	Positive
Bacteria	Verrucomicrobiota	Verrucomicrobiae	Verrucomicrobiales	Verrucomicrobiaceae	Verrucomicrobium	Positive
Eukaryota	Ascomycota	Sordariomycetes	Microascales	Microascaceae	Doratomyces	Positive
Eukaryota	Dictyostelia	Unidentified	Unidentified	Unidentified	Dictyostelium	Positive
Bacteria	Proteobacteria	Gammaproteobacteria	Pseudomonadales	Pseudomonadaceae	Pseudomonas	Positive
Bacteria	Actinobacteriota	Actinobacteria	Streptosporangiales	Streptosporangiaceae	Nonomuraea	Positive
Bacteria	Actinobacteriota	Actinobacteria	Propionibacteriales	Propionibacteriaceae	Marinilutecoccus	Positive
Bacteria	Proteobacteria	Alphaproteobacteria	Rhizobiales	Xanthobacteraceae	Pseudorhodoplanes	Positive
Bacteria	Acidobacteriota	Blastocatellia	45597	Unknown family	Unknown genus	Positive
Bacteria	Actinobacteriota	Actinobacteria	Pseudonocardiales	Pseudonocardiaceae	Pseudonocardia	Positive
Bacteria	Proteobacteria	Gammaproteobacteria	Pseudomonadales	Pseudomonadaceae	Pseudomonas	Positive
Bacteria	Proteobacteria	Gammaproteobacteria	Pseudomonadales	Pseudomonadaceae	Pseudomonas	Positive
Eukaryota	Ascomycota	Eurotiomycetes	Eurotiales	Aspergillaceae	Penicillium	Positive
Bacteria	Actinobacteriota	Actinobacteria	Corynebacteriales	Unknown family	Unknown genus	Positive
Eukaryota	Ascomycota	Dothideomycetes	Pleosporales	Unidentified	Unidentified	Positive
Bacteria	Bacteroidota	Bacteroidia	Sphingobacteriales	Sphingobacteriaceae	Anseongella	Positive
Bacteria	Actinobacteriota	Actinobacteria	Pseudonocardiales	Pseudonocardiaceae	Actinophytocola	Positive
Bacteria	Actinobacteriota	Thermoleophilia	Solirubrobacterales	67-14	Unknown genus	Positive
Bacteria	Actinobacteriota	Actinobacteria	Pseudonocardiales	Pseudonocardiaceae	Pseudonocardia	Positive
Bacteria	Proteobacteria	Gammaproteobacteria	Xanthomonadales	Xanthomonadaceae	Stenotrophomonas	Positive
Bacteria	Proteobacteria	Alphaproteobacteria	Reyranellales	Reyranellaceae	Unknown genus	Positive
Bacteria	Actinobacteriota	Actinobacteria	Pseudonocardiales	Pseudonocardiaceae	Pseudonocardia	Positive
Bacteria	Proteobacteria	Alphaproteobacteria	Rhizobiales	Rhizobiaceae	Unidentified	Positive
Eukaryota	Ascomycota	Sordariomycetes	Unidentified	Unidentified	Unidentified	Positive
Eukaryota	Chytridiomycota	Chytridiomycetes	Spizellomycetales	Unidentified	Unidentified	Positive
Bacteria	Actinobacteriota	Actinobacteria	Streptomycetales	Streptomycetaceae	E1B-B3-114	Positive
Bacteria	Proteobacteria	Gammaproteobacteria	Burkholderiales	Burkholderiaceae	Burkholderia	Positive
Bacteria	Actinobacteriota	Actinobacteria	Streptomycetales	Streptomycetaceae	Streptomyces	Positive
Bacteria	Bacteroidota	Bacteroidia	Chitinophagales	Chitinophagaceae	Chitinophaga	Positive
Eukaryota	Mucoromycota	Mortierellomycetes	Mortierellales	Mortierellaceae	Mortierella	Positive
Bacteria	Actinobacteriota	Actinobacteria	Propionibacteriales	Nocardioidaceae	Nocardioides	Positive
Bacteria	Proteobacteria	Alphaproteobacteria	Rhizobiales	Devosiaceae	Devosia	Positive
Eukaryota	Mucoromycota	Unidentified	Unidentified	Unidentified	Unidentified	Positive
Bacteria	Proteobacteria	Alphaproteobacteria	Rhizobiales	Rhodobiaceae	Afifella	Positive
Eukaryota	Basidiomycota	Agaricomycetes	Unidentified	Unidentified	Unidentified	Positive
Bacteria	Proteobacteria	Alphaproteobacteria	Rhizobiales	Rhizobiaceae	Phyllobacterium	Positive
Bacteria	Planctomycetota	Planctomycetes	Pirellulales	Pirellulaceae	Pir4lineage	Positive
Eukaryota	Ascomycota	Dothideomycetes	Venturiales	Sympoventuriaceae	Ochroconis	Positive
Bacteria	Actinobacteriota	Actinobacteria	Propionibacteriales	Nocardioidaceae	Nocardioides	Positive
Eukaryota	Ascomycota	Sordariomycetes	Unidentified	Unidentified	Unidentified	Positive
Bacteria	Actinobacteriota	Acidimicrobiia	Microtrichales	Ilumatobacteraceae	Unknown genus	Positive
Bacteria	Chloroflexi	Chloroflexia	Thermomicrobiales	JG30-KF-CM45	Unknown genus	Positive
Eukaryota	Basidiomycota	Agaricomycetes	Polyporales	Unidentified	Unidentified	Positive
Bacteria	Proteobacteria	Alphaproteobacteria	Rhizobiales	Xanthobacteraceae	Rhodopseudomonas	Positive
Eukaryota	Ascomycota	Sordariomycetes	Hypocreales	Cordycipitaceae	Isaria	Positive
Eukaryota	Unclassified	Unclassified	Unclassified	Unclassified	Unclassified	Positive
Eukaryota	Basidiomycota	Tremellomycetes	Tremellales	Sirobasidiaceae	Sirobasidium	Positive
Bacteria	Actinobacteriota	Thermoleophilia	Solirubrobacterales	Solirubrobacteraceae	Solirubrobacter	Positive
Bacteria	Proteobacteria	Alphaproteobacteria	Sphingomonadales	Sphingomonadaceae	Sphingopyxis	Positive
Bacteria	Acidobacteriota	Blastocatellia	45597	Unknown family	Unknown genus	Positive
Eukaryota	Ascomycota	Dothideomycetes	Venturiales	Sympoventuriaceae	Ochroconis	Positive
Eukaryota	Ascomycota	Dothideomycetes	Botryosphaeriales	Botryosphaeriaceae	Lasiodiplodia	Positive
Bacteria	Proteobacteria	Gammaproteobacteria	Legionellales	Legionellaceae	Legionella	Positive
Bacteria	Actinobacteriota	Actinobacteria	Micrococcales	Promicromonosporaceae	Promicromonospora	Positive
Bacteria	Actinobacteriota	Actinobacteria	Propionibacteriales	Nocardioidaceae	Nocardioides	Positive
Bacteria	Proteobacteria	Alphaproteobacteria	Rhizobiales	Labraceae	Labrys	Positive
Eukaryota	Ascomycota	Sordariomycetes	Hypocreales	Cordycipitaceae	Cordyceps	Positive
Bacteria	Actinobacteriota	Actinobacteria	Propionibacteriales	Nocardioidaceae	Kribbella	Positive
Bacteria	Bacteroidota	Bacteroidia	Chitinophagales	Chitinophagaceae	Terrimonas	Positive
Eukaryota	Basidiomycota	Agaricostilbomycetes	Agaricostilbales	Chionosphaeraceae	Kurtzmanomyces	Positive
Bacteria	Actinobacteriota	Actinobacteria	Corynebacteriales	Nocardiaceae	Nocardia	Positive
Bacteria	Actinobacteriota	Acidimicrobiia	Microtrichales	Unknown family	Unknown genus	Positive
Eukaryota	Ascomycota	Dothideomycetes	Venturiales	Sympoventuriaceae	Ochroconis	Positive
Bacteria	Proteobacteria	Alphaproteobacteria	Rhizobiales	Hyphomicrobiaceae	Pedomicrobium	Positive
Eukaryota	Ascomycota	Dothideomycetes	Venturiales	Sympoventuriaceae	Ochroconis	Positive
Eukaryota	Ascomycota	Unidentified	Unidentified	Unidentified	Unidentified	Positive

Bacteria	Proteobacteria	Gammaproteobacteria	Xanthomonadales	Xanthomonadaceae	Stenotrophomonas	Positive
Bacteria	Acidobacteriota	Vicinamibacteria	Vicinamibacterales	Vicinamibacteraceae	Vicinamibacter	Positive
Bacteria	Bacteroidota	Bacteroidia	Sphingobacteriales	Sphingobacteriaceae	Pedobacter	Positive
Bacteria	Proteobacteria	Alphaproteobacteria	Sphingomonadales	Sphingomonadaceae	Sphingomonas	Positive
Bacteria	Proteobacteria	Alphaproteobacteria	Rhizobiales	Hyphomicrobiaceae	Pedomicrobium	Positive
Bacteria	Actinobacteriota	Actinobacteria	Pseudonocardiales	Pseudonocardiaceae	Pseudonocardia	Positive
Eukaryota	Ascomycota	Sordariomycetes	Hypocreales	Unidentified	Unidentified	Positive
Eukaryota	Ascomycota	Sordariomycetes	Unidentified	Unidentified	Unidentified	Positive
Bacteria	Myxococcota	Polyangia	Polyangiales	Polyangiaceae	Pajaroellobacter	Positive
Bacteria	Actinobacteriota	Acidimicrobiia	Microtrichales	Iamiaceae	Iamia	Positive
Eukaryota	Ascomycota	Dothideomycetes	Pleosporales	Pleosporaceae	Bipolaris	Positive
Bacteria	Actinobacteriota	Acidimicrobiia	Microtrichales	Ilumatobacteraceae	Unknown genus	Positive
Eukaryota	Ciliophora	Intramacronucleata	Conthreep	Colpodea	Bromeliothrix	Positive
Bacteria	Proteobacteria	Alphaproteobacteria	Sphingomonadales	Sphingomonadaceae	Sphingobium	Positive
Bacteria	Proteobacteria	Gammaproteobacteria	Pseudomonadales	Pseudomonadaceae	Pseudomonas	Positive
Bacteria	Acidobacteriota	Acidobacteriae	Bryobacterales	Bryobacteraceae	Bryobacter	Positive
Eukaryota	Ascomycota	Sordariomycetes	Glomerellales	Plectosphaerellaceae	Unidentified	Positive
Bacteria	Proteobacteria	Gammaproteobacteria	Xanthomonadales	Xanthomonadaceae	Stenotrophomonas	Positive
Bacteria	Proteobacteria	Alphaproteobacteria	Rhizobiales	Xanthobacteraceae	Unknown genus	Positive
Eukaryota	Basidiomycota	Tremellomycetes	Cystofilobasidiales	Mrakiaceae	Itersonilia	Positive
Bacteria	Proteobacteria	Alphaproteobacteria	Rickettsiales	Anaplasmataceae	Wolbachia	Positive
Bacteria	Proteobacteria	Alphaproteobacteria	Rhizobiales	Rhizobiaceae	Unidentified	Positive
Bacteria	Proteobacteria	Alphaproteobacteria	Azospirillales	Inquilinaceae	Inquilinus	Positive
Bacteria	Proteobacteria	Alphaproteobacteria	Rhizobiales	Rhizobiaceae	Allorhizobium	Positive
Bacteria	Actinobacteriota	Acidimicrobiia	IMCC26256	Unknown family	Unknown genus	Positive
Eukaryota	Ascomycota	Dothideomycetes	Capnodiales	Unidentified	Unidentified	Positive
Eukaryota	Unidentified	Unidentified	Unidentified	Unidentified	Unidentified	Positive
Bacteria	Actinobacteriota	Actinobacteria	Pseudonocardiales	Pseudonocardiaceae	Pseudonocardia	Positive
Bacteria	Proteobacteria	Gammaproteobacteria	Burkholderiales	Alcaligenaceae	Unidentified	Positive
Bacteria	Proteobacteria	Alphaproteobacteria	Caulobacterales	Caulobacteraceae	Brevundimonas	Positive
Bacteria	Bacteroidota	Bacteroidia	Sphingobacteriales	Sphingobacteriaceae	Pedobacter	Positive
Bacteria	Bacteroidota	Bacteroidia	Sphingobacteriales	Sphingobacteriaceae	Pedobacter	Positive
Bacteria	Actinobacteriota	Actinobacteria	Streptosporangiales	Streptosporangiaceae	Nonomuraea	Positive
Bacteria	Actinobacteriota	Actinobacteria	Micromonosporales	Micromonosporaceae	Catelliglobosispora	Positive
Bacteria	Bacteroidota	Bacteroidia	Chitinophagales	Chitinophagaceae	Chitinophaga	Positive
Bacteria	Chloroflexi	Chloroflexia	Thermomicrobiales	JG30-KF-CM45	Unknown genus	Positive
Bacteria	Acidobacteriota	Blastocatellia	45597	Unknown family	Unknown genus	Positive
Bacteria	Proteobacteria	Alphaproteobacteria	Sphingomonadales	Sphingomonadaceae	Sphingomonas	Positive
Eukaryota	Basidiomycota	Agaricomycetes	Boletales	Unidentified	Hygrophoropsis	Positive
Eukaryota	Mucoromycota	Unidentified	Unidentified	Unidentified	Unidentified	Positive
Bacteria	Proteobacteria	Gammaproteobacteria	Xanthomonadales	Xanthomonadaceae	Stenotrophomonas	Positive
Eukaryota	Ascomycota	Saccharomycetes	Saccharomycetales	Pichiaceae	Martiniozyma	Positive
Eukaryota	Basidiomycota	Agaricomycetes	Polyporales	Unidentified	Burgoa	Positive
Bacteria	Proteobacteria	Alphaproteobacteria	Reyranellales	Reyranellaceae	Reyranella	Positive
Bacteria	Proteobacteria	Gammaproteobacteria	Pseudomonadales	Pseudomonadaceae	Pseudomonas	Positive
Bacteria	Chloroflexi	Ktedonobacteria	Ktedonobacterales	Ktedonobacteraceae	1959-1	Positive
Bacteria	Actinobacteriota	Actinobacteria	Micrococcales	Microbacteriaceae	Agromyces	Positive
Eukaryota	Ascomycota	Eurotiomycetes	Eurotiales	Aspergillaceae	Aspergillus	Positive
Bacteria	Proteobacteria	Gammaproteobacteria	Pseudomonadales	Pseudomonadaceae	Pseudomonas	Positive
Bacteria	Proteobacteria	Alphaproteobacteria	Rhizobiales	Devosiaceae	Devosia	Positive
Eukaryota	Ascomycota	Sordariomycetes	Glomerellales	Plectosphaerellaceae	Unidentified	Positive
Eukaryota	Ascomycota	Sordariomycetes	Hypocreales	Cordycipitaceae	Isaria	Positive
Eukaryota	Ascomycota	Sordariomycetes	Unidentified	Unidentified	Unidentified	Positive
Bacteria	Chloroflexi	Chloroflexia	Thermomicrobiales	JG30-KF-CM45	Unknown genus	Positive
Eukaryota	Ascomycota	Sordariomycetes	Hypocreales	Unidentified	Unidentified	Positive
Bacteria	Bacteroidota	Bacteroidia	Chitinophagales	Chitinophagaceae	Chitinophaga	Positive
Bacteria	Proteobacteria	Gammaproteobacteria	Pseudomonadales	Pseudomonadaceae	Pseudomonas	Positive
Eukaryota	Ascomycota	Eurotiomycetes	Eurotiales	Aspergillaceae	Penicillium	Positive
Bacteria	Planctomycetota	Planctomycetes	Isosphaerales	Isosphaeraceae	Tundrisphaera	Positive
Bacteria	Acidobacteriota	Vicinamibacteria	Vicinamibacterales	Vicinamibacteraceae	Unknown genus	Positive
Bacteria	Actinobacteriota	Actinobacteria	Streptomycetales	Streptomycetaceae	Streptomyces	Positive
Bacteria	Actinobacteriota	Actinobacteria	Propionibacteriales	Nocardioidaceae	Nocardioides	Positive
Eukaryota	Mucoromycota	Unidentified	Mortierellales	Mortierellaceae	Mortierella	Positive
Bacteria	Proteobacteria	Alphaproteobacteria	Rhizobiales	Methylopilaceae	Methylopila	Positive
Eukaryota	Ascomycota	Eurotiomycetes	Chaetothyriales	Herpotrichiellaceae	Cladophialophora	Positive
Bacteria	Chloroflexi	Chloroflexia	Thermomicrobiales	JG30-KF-CM45	Unknown genus	Positive
Eukaryota	Ascomycota	Sordariomycetes	Glomerellales	Plectosphaerellaceae	Unidentified	Positive
Bacteria	Proteobacteria	Alphaproteobacteria	Rhizobiales	Labraceae	Labrys	Positive
Eukaryota	Ascomycota	Leotiomycetes	Unidentified	Unidentified	Pseudogymnoascus	Positive
Bacteria	Actinobacteriota	Actinobacteria	Pseudonocardiales	Pseudonocardiaceae	Lechevalieria	Positive
Eukaryota	Ascomycota	Eurotiomycetes	Eurotiales	Aspergillaceae	Aspergillus	Positive
Bacteria	Proteobacteria	Alphaproteobacteria	Rhizobiales	Xanthobacteraceae	Afipia	Positive
Bacteria	Proteobacteria	Gammaproteobacteria	Burkholderiales	Nitrosomonadaceae	Nitrosospira	Positive
Bacteria	Proteobacteria	Gammaproteobacteria	Pseudomonadales	Pseudomonadaceae	Pseudomonas	Positive
Bacteria	Bacteroidota	Bacteroidia	Chitinophagales	Chitinophagaceae	Chitinophaga	Positive
Bacteria	Proteobacteria	Alphaproteobacteria	Rhizobiales	Rhizobiaceae	Mesorhizobium	Positive
Bacteria	Bacteroidota	Bacteroidia	Chitinophagales	Chitinophagaceae	Chitinophaga	Positive
Bacteria	Proteobacteria	Alphaproteobacteria	Rhizobiales	Rhizobiaceae	Mesorhizobium	Positive
Bacteria	Actinobacteriota	Actinobacteria	Propionibacteriales	Propionibacteriaceae	Jiangella	Positive
Bacteria	Proteobacteria	Gammaproteobacteria	Pseudomonadales	Pseudomonadaceae	Pseudomonas	Positive
Bacteria	Actinobacteriota	Actinobacteria	Streptomycetales	Streptomycetaceae	E1B-B3-114	Positive
Eukaryota	Ascomycota	Dothideomycetes	Venturiales	Sympoventuriaceae	Ochroconis	Positive
Eukaryota	Zoopagomycota	Entomophthoromycetes	Entomophthorales	Ancylistaceae	Conidiobolus	Positive
Bacteria	Proteobacteria	Alphaproteobacteria	Rhizobiales	Rhizobiaceae	Phyllobacterium	Positive
Eukaryota	Ascomycota	Sordariomycetes	Hypocreales	Unidentified	Unidentified	Positive
Bacteria	Proteobacteria	Alphaproteobacteria	Rhizobiales	Xanthobacteraceae	Pseudorhodoplanes	Positive

	Eukaryota	Ascomycota	Sordariomycetes	Xylariales	Xylariaceae	Ascotricha	Positive
	Bacteria	Proteobacteria	Alphaproteobacteria	Rhizobiales	Hyphomicrobiaceae	Hyphomicrobium	Positive
	Eukaryota	Ascomycota	Sordariomycetes	Hypocreales	Nectriaceae	Fusarium	Positive
	Eukaryota	Ochrophyta	Chrysophyceae	Unidentified	Unidentified	Chlamydomyxa	Positive
	Bacteria	Actinobacteriota	Actinobacteria	Corynebacteriales	Nocardiaceae	Nocardia	Positive
	Eukaryota	Ascomycota	Sordariomycetes	Hypocreales	Unidentified	Acremonium	Positive
	Bacteria	Actinobacteriota	Actinobacteria	Frankiales	Unknown family	Unknown genus	Positive
	Eukaryota	Ascomycota	Sordariomycetes	Hypocreales	Nectriaceae	Nectria	Positive
	Eukaryota	Ascomycota	Dothideomycetes	Venturiales	Sympoventuriaceae	Ochroconis	Positive
	Bacteria	Proteobacteria	Alphaproteobacteria	Rhizobiales	Labraceae	Labrys	Positive
	Bacteria	Actinobacteriota	Acidimicrobiia	Microtrichales	Ilumatobacteraceae	Unknown genus	Positive
	Bacteria	Chloroflexi	Dehalococcoidia	S085	Unknown family	Unknown genus	Positive
	Bacteria	Bacteroidota	Bacteroidia	Sphingobacteriales	Sphingobacteriaceae	Olivibacter	Positive
	Bacteria	Actinobacteriota	Actinobacteria	Propionibacteriales	Propionibacteriaceae	Jiangella	Positive
	Bacteria	Proteobacteria	Gammaproteobacteria	Pseudomonadales	Pseudomonadaceae	Pseudomonas	Positive
	Bacteria	Bacteroidota	Bacteroidia	Cytophagales	Microscillaceae	Unknown genus	Positive
	Archaea	Thaumarchaeota	Nitrososphaeria	Nitrososphaerales	Nitrososphaeraceae	Unknown genus	Positive
	Eukaryota	Ascomycota	Leotiomycetes	Thelebolales	Thelebolaceae	Unidentified	Positive
	Archaea	Thaumarchaeota	Nitrososphaeria	Nitrososphaerales	Nitrososphaeraceae	Candidatus Nitrocosmicus	Positive
	Bacteria	Proteobacteria	Gammaproteobacteria	Pseudomonadales	Pseudomonadaceae	Pseudomonas	Positive
	Bacteria	Myxococcota	Polyangia	Nannocystales	Nannocystaceae	Unknown genus	Positive
	Bacteria	Proteobacteria	Gammaproteobacteria	Xanthomonadales	Xanthomonadaceae	Stenotrophomonas	Positive
	Bacteria	Actinobacteriota	Actinobacteria	Pseudonocardiales	Pseudonocardiaceae	Pseudonocardia	Positive
	Bacteria	Actinobacteriota	Actinobacteria	Pseudonocardiales	Pseudonocardiaceae	Pseudonocardia	Positive
	Bacteria	Proteobacteria	Gammaproteobacteria	Burkholderiales	Alcaligenaceae	Bordetella	Positive
	Eukaryota	Ascomycota	Sordariomycetes	Hypocreales	Unidentified	Nectriopsis	Positive
	Bacteria	Proteobacteria	Gammaproteobacteria	Burkholderiales	Alcaligenaceae	Unidentified	Positive
	Bacteria	Actinobacteriota	Actinobacteria	Micrococcales	Microbacteriaceae	Unidentified	Positive
New dark zone	Eukaryota	Ascomycota	Saccharomycetes	Saccharomycetales	Debaryomycetaceae	Unidentified	Negative
	Bacteria	Actinobacteriota	Actinobacteria	Micromonosporales	Micromonosporaceae	Unknown genus	Negative
	Bacteria	Proteobacteria	Alphaproteobacteria	Rhizobiales	Hyphomicrobiaceae	Pedomicrobium	Negative
	Bacteria	Proteobacteria	Gammaproteobacteria	Burkholderiales	Comamonadaceae	Variovorax	Negative
	Eukaryota	Ascomycota	Eurotiomycetes	Eurotiales	Trichocomaceae	Talaromyces	Negative
	Bacteria	Proteobacteria	Alphaproteobacteria	Rhizobiales	Rhizobiaceae	Mesorhizobium	Negative
	Bacteria	Proteobacteria	Alphaproteobacteria	Rhizobiales	Xanthobacteraceae	Afipia	Negative
	Bacteria	Verrucomicrobiota	Chlamydiae	Chlamydiales	Parachlamydiaceae	Candidatus Protochlamydi	Negative
	Bacteria	Acidobacteriota	Vicinamibacteria	Subgroup17	Unknown family	Unknown genus	Negative
	Bacteria	Actinobacteriota	Actinobacteria	Propionibacteriales	Nocardioidaceae	Kribbella	Negative
	Bacteria	Actinobacteriota	Actinobacteria	Pseudonocardiales	Pseudonocardiaceae	Pseudonocardia	Negative
	Bacteria	Actinobacteriota	Thermoleophilia	Solirubrobacterales	67-14	Unknown genus	Negative
	Bacteria	Acidobacteriota	Blastocatellia	45597	Unknown family	Unknown genus	Negative
	Bacteria	Actinobacteriota	Actinobacteria	Pseudonocardiales	Pseudonocardiaceae	Actinophytocola	Negative
	Bacteria	Bacteroidota	Bacteroidia	Sphingobacteriales	Sphingobacteriaceae	Pedobacter	Negative
	Bacteria	Acidobacteriota	Vicinamibacteria	Vicinamibacterales	Vicinamibacteraceae	Unknown genus	Negative
	Bacteria	Proteobacteria	Gammaproteobacteria	Burkholderiales	Burkholderiaceae	Ralstonia	Negative
	Bacteria	Proteobacteria	Alphaproteobacteria	Rhizobiales	RhizobialesIncertaeSedis	Nordella	Negative
	Bacteria	Actinobacteriota	Actinobacteria	Frankiales	Acidothermaceae	Acidothermus	Negative
	Bacteria	Bacteroidota	Bacteroidia	Chitinophagales	Chitinophagaceae	Chitinophaga	Negative
	Bacteria	Acidobacteriota	Acidobacteriae	Bryobacterales	Bryobacteraceae	Bryobacter	Negative
	Bacteria	Proteobacteria	Gammaproteobacteria	Burkholderiales	Unidentified	Unidentified	Negative
	Bacteria	Proteobacteria	Gammaproteobacteria	Burkholderiales	Nitrosomonadaceae	Nitrosospira	Negative
	Bacteria	Planctomycetota	Planctomycetes	Isosphaerales	Isosphaeraceae	Tundrisphaera	Negative
	Bacteria	Actinobacteriota	Actinobacteria	Propionibacteriales	Nocardioidaceae	Nocardioides	Negative
	Bacteria	Proteobacteria	Gammaproteobacteria	Xanthomonadales	Xanthomonadaceae	Stenotrophomonas	Negative
	Eukaryota	Mucoromycota	Unidentified	Mortierellales	Mortierellaceae	Mortierella	Negative
	Bacteria	Myxococcota	Polyangia	Polyangiales	Polyangiaceae	Pajaroellobacter	Negative
	Bacteria	Myxococcota	Polyangia	Polyangiales	Phaselicystidaceae	Phaselicystis	Negative
	Bacteria	Actinobacteriota	Actinobacteria	Corynebacteriales	Unknown family	Unknown genus	Negative
	Bacteria	Proteobacteria	Gammaproteobacteria	Steroidobacterales	Steroidobacteraceae	Steroidobacter	Negative
	Eukaryota	Ascomycota	Sordariomycetes	Unidentified	Unidentified	Unidentified	Negative
	Bacteria	Actinobacteriota	Actinobacteria	Corynebacteriales	Nocardiaceae	Rhodococcus	Negative
	Bacteria	Proteobacteria	Alphaproteobacteria	Caulobacterales	Caulobacteraceae	Brevundimonas	Negative
	Eukaryota	Unclassified	Unclassified	Unclassified	Unclassified	Unclassified	Negative
	Bacteria	Actinobacteriota	Actinobacteria	Corynebacteriales	Nocardiaceae	Rhodococcus	Negative
	Eukaryota	Ascomycota	Sordariomycetes	Microascales	Microascaceae	Doratomyces	Negative
	Bacteria	Proteobacteria	Gammaproteobacteria	Burkholderiales	Alcaligenaceae	Bordetella	Negative
	Bacteria	Actinobacteriota	Actinobacteria	Pseudonocardiales	Pseudonocardiaceae	Saccharopolyspora	Negative
	Bacteria	Chloroflexi	Ktedonobacteria	Ktedonobacterales	Ktedonobacteraceae	1959-1	Negative
	Bacteria	Planctomycetota	Planctomycetes	Isosphaerales	Isosphaeraceae	Paludisphaera	Negative
	Bacteria	Proteobacteria	Alphaproteobacteria	Acetobacterales	Acetobacteraceae	Roseomonas	Negative
	Bacteria	Myxococcota	Polyangia	Polyangiales	Polyangiaceae	Pajaroellobacter	Negative
	Bacteria	Proteobacteria	Alphaproteobacteria	Rhizobiales	Beijerinckiaceae	Bosea	Negative
	Bacteria	Planctomycetota	Planctomycetes	Gemmatales	Gemmataceae	Unknown genus	Positive
	Bacteria	Actinobacteriota	Actinobacteria	Streptomycetales	Streptomycetaceae	Streptomyces	Positive
	Bacteria	Proteobacteria	Alphaproteobacteria	Rhizobiales	Hyphomicrobiaceae	Hyphomicrobium	Positive
	Bacteria	Actinobacteriota	Acidimicrobiia	Microtrichales	Ilumatobacteraceae	Unknown genus	Positive
	Bacteria	Proteobacteria	Alphaproteobacteria	Sphingomonadales	Sphingomonadaceae	Sandaracinobacter	Positive
	Bacteria	Chloroflexi	Chloroflexia	Thermomicrobiales	JG30-KF-CM45	Unknown genus	Positive
	Bacteria	Planctomycetota	Planctomycetes	Isosphaerales	Isosphaeraceae	Singulisphaera	Positive
	Bacteria	Chloroflexi	Dehalococcoidia	S085	Unknown family	Unknown genus	Positive
	Bacteria	Proteobacteria	Alphaproteobacteria	Reyranellales	Reyranellaceae	Reyranella	Positive
	Eukaryota	Ascomycota	Sordariomycetes	Unidentified	Unidentified	Unidentified	Positive
	Bacteria	Actinobacteriota	Actinobacteria	Micrococcales	Promicromonosporaceae	Promicromonospora	Positive
	Eukaryota	Ascomycota	Eurotiomycetes	Eurotiales	Aspergillaceae	Aspergillus	Positive
	Bacteria	Actinobacteriota	Actinobacteria	Pseudonocardiales	Pseudonocardiaceae	Pseudonocardia	Positive
	Bacteria	Actinobacteriota	Actinobacteria	Streptomycetales	Streptomycetaceae	Streptomyces	Positive

Bacteria	Actinobacteriota	Actinobacteria	Pseudonocardiales	Pseudonocardiaceae	Pseudonocardia	Positive
Bacteria	Actinobacteriota	Actinobacteria	Propionibacteriales	Propionibacteriaceae	Jiangella	Positive
Bacteria	Actinobacteriota	Actinobacteria	Streptomycetales	Streptomycetaceae	Streptomyces	Positive
Bacteria	Verrucomicrobiota	Chlamydiae	Chlamydiales	Parachlamydiaceae	Neochlamydia	Positive
Bacteria	Proteobacteria	Gammaproteobacteria	Pseudomonadales	Pseudomonadaceae	Pseudomonas	Positive
Bacteria	Proteobacteria	Alphaproteobacteria	Sphingomonadales	Sphingomonadaceae	Unidentified	Positive
Bacteria	Proteobacteria	Alphaproteobacteria	Caulobacterales	Caulobacteraceae	Brevundimonas	Positive
Bacteria	Acidobacteriota	Vicinamibacteria	Vicinamibacterales	Vicinamibacteraceae	Unknown genus	Positive
Bacteria	Proteobacteria	Alphaproteobacteria	Rhizobiales	Hyphomicrobiaceae	Hyphomicrobium	Positive
Bacteria	Proteobacteria	Alphaproteobacteria	Rhizobiales	Labraceae	Labrys	Positive
Bacteria	Proteobacteria	Alphaproteobacteria	Sphingomonadales	Sphingomonadaceae	Unidentified	Positive
Bacteria	Bacteroidota	Bacteroidia	Chitinophagales	Chitinophagaceae	Chitinophaga	Positive
Bacteria	Actinobacteriota	Actinobacteria	Unidentified	Unidentified	Unidentified	Positive
Bacteria	Chloroflexi	Chloroflexia	Thermomicrobiales	JG30-KF-CM45	Unknown genus	Positive
Bacteria	Proteobacteria	Alphaproteobacteria	Rhizobiales	Devosiaceae	Devosia	Positive
Bacteria	Bacteroidota	Bacteroidia	Sphingobacteriales	Sphingobacteriaceae	Pedobacter	Positive
Bacteria	Proteobacteria	Alphaproteobacteria	Sphingomonadales	Sphingomonadaceae	Novosphingobium	Positive
Bacteria	Bacteroidota	Bacteroidia	Chitinophagales	Chitinophagaceae	Chitinophaga	Positive
Bacteria	Proteobacteria	Alphaproteobacteria	Rhizobiales	Xanthobacteraceae	Pseudorhodoplanes	Positive
Bacteria	Proteobacteria	Gammaproteobacteria	Pseudomonadales	Pseudomonadaceae	Pseudomonas	Positive
Bacteria	Proteobacteria	Gammaproteobacteria	Pseudomonadales	Pseudomonadaceae	Pseudomonas	Positive
Bacteria	Acidobacteriota	Acidobacteriae	Unknown order	Unknown family	Unknown genus	Positive
Bacteria	Proteobacteria	Alphaproteobacteria	Rhizobiales	Devosiaceae	Devosia	Positive
Bacteria	Actinobacteriota	Actinobacteria	Pseudonocardiales	Pseudonocardiaceae	Pseudonocardia	Positive
Bacteria	Actinobacteriota	Actinobacteria	Micrococcales	Microbacteriaceae	Galbitalea	Positive
Bacteria	Proteobacteria	Alphaproteobacteria	Sphingomonadales	Sphingomonadaceae	Sphingobium	Positive
Bacteria	Proteobacteria	Alphaproteobacteria	Rhizobiales	Labraceae	Labrys	Positive
Bacteria	Proteobacteria	Gammaproteobacteria	Xanthomonadales	Xanthomonadaceae	Stenotrophomonas	Positive
Bacteria	Actinobacteriota	Actinobacteria	Pseudonocardiales	Pseudonocardiaceae	Pseudonocardia	Positive
Bacteria	Proteobacteria	Gammaproteobacteria	Pseudomonadales	Pseudomonadaceae	Pseudomonas	Positive
Bacteria	Actinobacteriota	Acidimicrobiia	IMCC26256	Unknown family	Unknown genus	Positive
Bacteria	Proteobacteria	Gammaproteobacteria	Legionellales	Legionellaceae	Legionella	Positive
Bacteria	Actinobacteriota	Acidimicrobiia	Microtrichales	Ilumatobacteraceae	Unknown genus	Positive
Bacteria	Proteobacteria	Alphaproteobacteria	Sphingomonadales	Sphingomonadaceae	Sphingomonas	Positive
Bacteria	Actinobacteriota	Actinobacteria	Micrococcales	Microbacteriaceae	Agromyces	Positive
Bacteria	Proteobacteria	Gammaproteobacteria	Xanthomonadales	Rhodanobacteraceae	Dokdonella	Positive
Bacteria	Proteobacteria	Alphaproteobacteria	Sphingomonadales	Sphingomonadaceae	Sandaracinobacter	Positive
Bacteria	Proteobacteria	Gammaproteobacteria	Burkholderiales	Burkholderiaceae	Ralstonia	Positive
Bacteria	Actinobacteriota	Actinobacteria	Pseudonocardiales	Pseudonocardiaceae	Pseudonocardia	Positive
Bacteria	Proteobacteria	Gammaproteobacteria	Pseudomonadales	Pseudomonadaceae	Pseudomonas	Positive
Bacteria	Actinobacteriota	Acidimicrobiia	Microtrichales	Unknown family	Unknown genus	Positive
Bacteria	Proteobacteria	Alphaproteobacteria	Rhizobiales	Rhizobiaceae	Phyllobacterium	Positive
Bacteria	Proteobacteria	Alphaproteobacteria	Rhizobiales	Hyphomicrobiaceae	Pedomicrobium	Positive
Bacteria	Actinobacteriota	Actinobacteria	Propionibacteriales	Propionibacteriaceae	Unidentified	Positive
Bacteria	Chloroflexi	Chloroflexia	Thermomicrobiales	JG30-KF-CM45	Unknown genus	Positive
Bacteria	Proteobacteria	Alphaproteobacteria	Azospirillales	Inquilinaceae	Inquilinus	Positive
Bacteria	Actinobacteriota	Acidimicrobiia	Microtrichales	Ilumatobacteraceae	Unknown genus	Positive
Eukaryota	Ascomycota	Dothideomycetes	Venturiales	Sympoventuriaceae	Ochroconis	Positive
Bacteria	Proteobacteria	Gammaproteobacteria	Pseudomonadales	Pseudomonadaceae	Pseudomonas	Positive
Bacteria	Proteobacteria	Gammaproteobacteria	Pseudomonadales	Moraxellaceae	Acinetobacter	Positive
Bacteria	Acidobacteriota	Acidobacteriae	Bryobacterales	Bryobacteraceae	Bryobacter	Positive
Bacteria	Proteobacteria	Gammaproteobacteria	Xanthomonadales	Xanthomonadaceae	Luteimonas	Positive
Eukaryota	Ascomycota	Dothideomycetes	Venturiales	Sympoventuriaceae	Ochroconis	Positive
Bacteria	Actinobacteriota	Actinobacteria	Propionibacteriales	Nocardioidaceae	Nocardioides	Positive
Bacteria	Actinobacteriota	Actinobacteria	Streptomycetales	Streptomycetaceae	Streptomyces	Positive
Bacteria	Proteobacteria	Gammaproteobacteria	Xanthomonadales	Xanthomonadaceae	Stenotrophomonas	Positive
Bacteria	Actinobacteriota	Actinobacteria	Pseudonocardiales	Pseudonocardiaceae	Lechevalieria	Positive
Bacteria	Actinobacteriota	Actinobacteria	Streptomycetales	Streptomycetaceae	E1B-B3-114	Positive
Bacteria	Proteobacteria	Gammaproteobacteria	Pseudomonadales	Pseudomonadaceae	Pseudomonas	Positive
Bacteria	Chloroflexi	Chloroflexia	Thermomicrobiales	JG30-KF-CM45	Unknown genus	Positive
Bacteria	Actinobacteriota	Actinobacteria	Corynebacteriales	Nocardiaceae	Nocardia	Positive
Bacteria	Actinobacteriota	Actinobacteria	Corynebacteriales	Nocardiaceae	Nocardia	Positive
Bacteria	Actinobacteriota	Thermoleophilia	Solirubrobacterales	67-14	Unknown genus	Positive
Bacteria	Actinobacteriota	Actinobacteria	Propionibacteriales	Propionibacteriaceae	Microlunatus	Positive
Bacteria	Proteobacteria	Alphaproteobacteria	Rhizobiales	Rhizobiaceae	Mesorhizobium	Positive
Bacteria	Acidobacteriota	Vicinamibacteria	Subgroup17	Unknown family	Unknown genus	Positive
Eukaryota	Mucoromycota	Unidentified	Unidentified	Unidentified	Unidentified	Positive
Bacteria	Bacteroidota	Bacteroidia	Chitinophagales	Chitinophagaceae	Chitinophaga	Positive
Bacteria	Actinobacteriota	Actinobacteria	Propionibacteriales	Nocardioidaceae	Nocardioides	Positive
Bacteria	Proteobacteria	Gammaproteobacteria	Burkholderiales	Alcaligenaceae	Bordetella	Positive
Bacteria	Proteobacteria	Gammaproteobacteria	Xanthomonadales	Xanthomonadaceae	Stenotrophomonas	Positive
Bacteria	Proteobacteria	Alphaproteobacteria	Rhizobiales	Beijerinckiaceae	28-YEA-48	Positive
Bacteria	Proteobacteria	Alphaproteobacteria	Rhizobiales	Hyphomicrobiaceae	Pedomicrobium	Positive
Bacteria	Proteobacteria	Alphaproteobacteria	Sphingomonadales	Sphingomonadaceae	Sandaracinobacter	Positive
Bacteria	Acidobacteriota	Acidobacteriae	Bryobacterales	Bryobacteraceae	Bryobacter	Positive
Bacteria	Proteobacteria	Gammaproteobacteria	Pseudomonadales	Pseudomonadaceae	Pseudomonas	Positive
Bacteria	Proteobacteria	Gammaproteobacteria	Pseudomonadales	Pseudomonadaceae	Pseudomonas	Positive
Eukaryota	Ascomycota	Dothideomycetes	Pleosporales	Unidentified	Unidentified	Positive
Bacteria	Actinobacteriota	Thermoleophilia	Solirubrobacterales	Solirubrobacteraceae	Solirubrobacter	Positive
Bacteria	Proteobacteria	Gammaproteobacteria	Pseudomonadales	Pseudomonadaceae	Pseudomonas	Positive
Bacteria	Proteobacteria	Gammaproteobacteria	Burkholderiales	Alcaligenaceae	Bordetella	Positive
Bacteria	Proteobacteria	Alphaproteobacteria	Rhizobiales	Hyphomicrobiaceae	Pedomicrobium	Positive
Bacteria	Proteobacteria	Gammaproteobacteria	Xanthomonadales	Xanthomonadaceae	Stenotrophomonas	Positive
Bacteria	Proteobacteria	Alphaproteobacteria	Sphingomonadales	Sphingomonadaceae	Sphingopyxis	Positive
Bacteria	Proteobacteria	Gammaproteobacteria	Pseudomonadales	Pseudomonadaceae	Pseudomonas	Positive
Bacteria	Proteobacteria	Alphaproteobacteria	Reyranellales	Reyranellaceae	Unknown genus	Positive

Intermediate dark zone	Bacteria	Actinobacteriota	Actinobacteria	Pseudonocardiales	Pseudonocardiaceae	Pseudonocardia	Negative
	Bacteria	Actinobacteriota	Actinobacteria	Pseudonocardiales	Pseudonocardiaceae	Pseudonocardia	Negative
	Bacteria	Chloroflexi	Chloroflexia	Thermomicrobiales	JG30-KF-CM45	Unknown genus	Negative
	Bacteria	Actinobacteriota	Actinobacteria	Micromonosporales	Micromonosporaceae	Hamadaea	Negative
	Archaea	Crenarchaeota	Nitrososphaeria	Nitrososphaerales	Nitrososphaeraceae	Unidentified	Negative
	Bacteria	Planctomycetota	Planctomycetes	Gemmatales	Gemmataceae	Gemmata	Negative
	Eukaryota	Unidentified	Unidentified	Unidentified	Unidentified	Mycamoeba	Negative
	Bacteria	Myxococcota	Polyangia	Nannocystales	Nannocystaceae	Nannocystis	Negative
	Bacteria	Proteobacteria	Alphaproteobacteria	Azospirillales	Inquilinaceae	Inquilinus	Negative
	Bacteria	Bacteroidota	Bacteroidia	Chitinophagales	Chitinophagaceae	Niabella	Negative
	Bacteria	Actinobacteriota	Acidimicrobiia	Microtrichales	Ilumatobacteraceae	Unknown genus	Negative
	Eukaryota	Ascomycota	Eurotiomycetes	Eurotiales	Trichocomaceae	Talaromyces	Negative
	Bacteria	Actinobacteriota	Actinobacteria	Unknown order	Unknown family	Unknown genus	Negative
	Bacteria	Actinobacteriota	Acidimicrobiia	Microtrichales	Unknown family	Unknown genus	Negative
	Bacteria	Proteobacteria	Gammaproteobacteria	Burkholderiales	Burkholderiaceae	Ralstonia	Negative
	Bacteria	Actinobacteriota	Actinobacteria	Propionibacteriales	Nocardioidaceae	Nocardioides	Negative
	Bacteria	Actinobacteriota	Actinobacteria	Pseudonocardiales	Pseudonocardiaceae	Pseudonocardia	Negative
	Bacteria	Proteobacteria	Alphaproteobacteria	Rhizobiales	Xanthobacteraceae	Pseudorhodoplanes	Negative
	Bacteria	Bacteroidota	Bacteroidia	Sphingobacteriales	Sphingobacteriaceae	Anseongella	Negative
	Eukaryota	Ascomycota	Dothideomycetes	Venturiales	Sympoventuriaceae	Ochroconis	Negative
	Bacteria	Proteobacteria	Alphaproteobacteria	Sphingomonadales	Sphingomonadaceae	Sphingomonas	Positive
	Eukaryota	Amoebozoa	Discosea	Centramoebida	Unidentified	Unidentified	Positive
	Bacteria	Actinobacteriota	Actinobacteria	Corynebacteriales	Corynebacteriaceae	Unknown genus	Positive
	Bacteria	Proteobacteria	Alphaproteobacteria	Sphingomonadales	Sphingomonadaceae	Sphingomonas	Positive
	Bacteria	Bacteroidota	Bacteroidia	Sphingobacteriales	Sphingobacteriaceae	Pedobacter	Positive
	Bacteria	Planctomycetota	Planctomycetes	Pirellulales	Pirellulaceae	Pir4lineage	Positive
	Eukaryota	Ascomycota	Sordariomycetes	Microascales	Microascaceae	Doratomyces	Positive
	Bacteria	Proteobacteria	Alphaproteobacteria	Sphingomonadales	Sphingomonadaceae	Novosphingobium	Positive
	Bacteria	Proteobacteria	Gammaproteobacteria	Burkholderiales	Unidentified	Unidentified	Positive
	Eukaryota	Unclassified	Unclassified	Unclassified	Unclassified	Unclassified	Positive
	Bacteria	Actinobacteriota	Actinobacteria	Propionibacteriales	Nocardioidaceae	Nocardioides	Positive
	Bacteria	Actinobacteriota	Actinobacteria	Micromonosporales	Micromonosporaceae	Longispora	Positive
	Bacteria	Bacteroidota	Bacteroidia	Cytophagales	Microscillaceae	Unknown genus	Positive
	Bacteria	Bacteroidota	Bacteroidia	Sphingobacteriales	Sphingobacteriaceae	Olivibacter	Positive
	Bacteria	Actinobacteriota	Thermoleophilia	Solirubrobacterales	67-14	Unknown genus	Positive
	Bacteria	Chloroflexi	Chloroflexia	Thermomicrobiales	JG30-KF-CM45	Unknown genus	Positive
	Bacteria	Actinobacteriota	Actinobacteria	Streptosporangiales	Streptosporangiaceae	Nonomuraea	Positive
	Archaea	Thaumarchaeota	Nitrososphaeria	Nitrososphaerales	Nitrososphaeraceae	Unknown genus	Positive
	Eukaryota	Ascomycota	Sordariomycetes	Hypocreales	Unidentified	Unidentified	Positive
	Eukaryota	Basidiomycota	Agaricomycetes	Corticiales	Corticiaceae	Haplotrichum	Positive
	Eukaryota	Ascomycota	Dothideomycetes	Venturiales	Sympoventuriaceae	Ochroconis	Positive
	Bacteria	Bacteroidota	Bacteroidia	Chitinophagales	Chitinophagaceae	Chitinophaga	Positive
	Eukaryota	Ascomycota	Dothideomycetes	Dothideales	Aureobasidiaceae	Unidentified	Positive
	Bacteria	Actinobacteriota	Actinobacteria	Pseudonocardiales	Pseudonocardiaceae	Pseudonocardia	Positive
	Bacteria	Proteobacteria	Alphaproteobacteria	Reyranellales	Reyranellaceae	Reyranella	Positive
	Bacteria	Actinobacteriota	Actinobacteria	Micrococcales	Microbacteriaceae	Agromyces	Positive
	Bacteria	Proteobacteria	Alphaproteobacteria	Caulobacterales	Hyphomonadaceae	SWB02	Positive
	Bacteria	Bacteroidota	Bacteroidia	Chitinophagales	Chitinophagaceae	Chitinophaga	Positive
	Bacteria	Proteobacteria	Alphaproteobacteria	Rhizobiales	Hyphomicrobiaceae	Hyphomicrobium	Positive
	Bacteria	Bacteroidota	Bacteroidia	Chitinophagales	Chitinophagaceae	Terrimonas	Positive
	Eukaryota	Ascomycota	Dothideomycetes	Capnodiales	Unidentified	Unidentified	Positive
	Bacteria	Acidobacteriota	Blastocatellia	Blastocatellales	Blastocatellaceae	Unidentified	Positive
	Bacteria	Actinobacteriota	Actinobacteria	Propionibacteriales	Propionibacteriaceae	Unidentified	Positive
	Archaea	Thaumarchaeota	Nitrososphaeria	Nitrososphaerales	Nitrososphaeraceae	Unknown genus	Positive
	Bacteria	Proteobacteria	Alphaproteobacteria	Sphingomonadales	Sphingomonadaceae	Sandaracinobacter	Positive
	Eukaryota	Mucoromycota	Unidentified	Unidentified	Unidentified	Unidentified	Positive
	Bacteria	Actinobacteriota	Actinobacteria	Frankiales	Frankiaceae	Jatrophihabitans	Positive
	Eukaryota	Ascomycota	Eurotiomycetes	Eurotiales	Aspergillaceae	Penicillium	Positive
	Bacteria	Chloroflexi	Ktedonobacteria	Ktedonobacterales	Ktedonobacteraceae	1959-1	Positive
	Bacteria	Bacteroidota	Bacteroidia	Sphingobacteriales	Sphingobacteriaceae	Pseudosphingobacterium	Positive
	Bacteria	Actinobacteriota	Thermoleophilia	Solirubrobacterales	67-14	Unknown genus	Positive
	Bacteria	Proteobacteria	Alphaproteobacteria	Azospirillales	Inquilinaceae	Inquilinus	Positive
	Eukaryota	Ascomycota	Sordariomycetes	Unidentified	Unidentified	Unidentified	Positive
	Bacteria	Desulfobacterota	Unknown class	Unknown order	Unknown family	Unknown genus	Positive
	Bacteria	Actinobacteriota	Actinobacteria	Micrococcales	Microbacteriaceae	Agromyces	Positive
	Bacteria	Actinobacteriota	Actinobacteria	Streptosporangiales	Streptosporangiaceae	Nonomuraea	Positive
	Bacteria	Proteobacteria	Alphaproteobacteria	Rhizobiales	Devosiaceae	Devosia	Positive
	Bacteria	Actinobacteriota	Actinobacteria	Pseudonocardiales	Pseudonocardiaceae	Pseudonocardia	Positive
	Bacteria	Actinobacteriota	Actinobacteria	Micromonosporales	Micromonosporaceae	Unknown genus	Positive
	Bacteria	Myxococcota	Polyangia	Polyangiales	Phaselicystidaceae	Phaselicystis	Positive
	Bacteria	Actinobacteriota	Acidimicrobiia	Microtrichales	Ilumatobacteraceae	Unknown genus	Positive
	Bacteria	Proteobacteria	Alphaproteobacteria	Rhodobacterales	Rhodobacteraceae	Amaricoccus	Positive
	Bacteria	Proteobacteria	Alphaproteobacteria	Rhizobiales	Rhizobiaceae	Mesorhizobium	Positive
	Bacteria	Actinobacteriota	Actinobacteria	Propionibacteriales	Nocardioidaceae	Nocardioides	Positive
	Eukaryota	Basidiomycota	Tremellomycetes	Cystofilobasidiales	Mrakiaceae	Itersonilia	Positive
	Bacteria	Actinobacteriota	Actinobacteria	Propionibacteriales	Propionibacteriaceae	Microlunatus	Positive
	Bacteria	Acidobacteriota	Vicinamibacteria	Vicinamibacterales	Vicinamibacteraceae	Vicinamibacter	Positive
	Bacteria	Actinobacteriota	Acidimicrobiia	Microtrichales	Unknown family	Unknown genus	Positive
	Bacteria	Proteobacteria	Alphaproteobacteria	Rhizobiales	Xanthobacteraceae	Unknown genus	Positive
	Eukaryota	Ascomycota	Sordariomycetes	Hypocreales	Cordycipitaceae	Isaria	Positive
	Eukaryota	Basidiomycota	Agaricomycetes	Polyporales	Unidentified	Unidentified	Positive
	Bacteria	Proteobacteria	Alphaproteobacteria	Acetobacterales	Acetobacteraceae	Roseomonas	Positive
	Bacteria	Bacteroidota	Bacteroidia	Sphingobacteriales	Sphingobacteriaceae	Parapedobacter	Positive
	Eukaryota	Ascomycota	Dothideomycetes	Pleosporales	Pleosporaceae	Bipolaris	Positive
	Bacteria	Planctomycetota	Planctomycetes	Isosphaerales	Isosphaeraceae	Aquisphaera	Positive
	Eukaryota	Ascomycota	Leotiomycetes	Thelebolales	Thelebolaceae	Unidentified	Positive

	Eukaryota	Ascomycota	Eurotiomycetes	Eurotiales	Aspergillaceae	Penicillium	Positive
	Eukaryota	Basidiomycota	Tremellomycetes	Filobasidiales	Filobasidiaceae	Unidentified	Positive
	Bacteria	Bacteroidota	Bacteroidia	Sphingobacteriales	Sphingobacteriaceae	Anseongella	Positive
	Bacteria	Bacteroidota	Bacteroidia	Chitinophagales	Chitinophagaceae	Chitinophaga	Positive
Old dark zone	Eukaryota	Ascomycota	Sordariomycetes	Hypocreales	Ophiocordycipitaceae	Tolypocladium	Negative
	Archaea	Halobacterota	Halobacteria	Halobacterales	Haloferacaceae	Natronococcus	Negative
	Bacteria	Planctomycetota	Planctomycetes	Isosphaerales	Isosphaeraceae	Paludisphaera	Negative
	Bacteria	Proteobacteria	Alphaproteobacteria	Rhizobiales	Hyphomicrobiaceae	Pedomicrobium	Negative
	Bacteria	Proteobacteria	Gammaproteobacteria	Xanthomonadales	Xanthomonadaceae	Luteimonas	Negative
	Bacteria	Actinobacteriota	Actinobacteria	Corynebacteriales	Nocardiaceae	Nocardia	Negative
	Bacteria	Actinobacteriota	Actinobacteria	Micrococcales	Intrasporangiaceae	Unidentified	Negative
	Bacteria	Actinobacteriota	Actinobacteria	Corynebacteriales	Nocardiaceae	Rhodococcus	Negative
	Eukaryota	Ascomycota	Sordariomycetes	Glomerellales	Plectosphaerellaceae	Unidentified	Negative
	Bacteria	Actinobacteriota	Actinobacteria	Streptosporangiales	Streptosporangiaceae	Nonomuraea	Negative
	Bacteria	Proteobacteria	Alphaproteobacteria	Rhizobiales	Xanthobacteraceae	Pseudorhodoplanes	Negative
	Bacteria	Proteobacteria	Alphaproteobacteria	Rhizobiales	Xanthobacteraceae	Unknown genus	Negative
	Bacteria	Actinobacteriota	Actinobacteria	Pseudonocardiales	Pseudonocardiaceae	Saccharopolyspora	Negative
	Bacteria	Proteobacteria	Alphaproteobacteria	Reyranellales	Reyranellaceae	Unknown genus	Negative
	Bacteria	Acidobacteriota	Acidobacteriae	Bryobacterales	Bryobacteraceae	Bryobacter	Negative
	Bacteria	Proteobacteria	Alphaproteobacteria	Azospirillales	Inquilinaceae	Inquilinus	Negative
	Bacteria	Proteobacteria	Gammaproteobacteria	Pseudomonadales	Pseudomonadaceae	Pseudomonas	Negative
	Bacteria	Actinobacteriota	Acidimicrobiia	Microtrichales	Unknown family	Unknown genus	Negative
	Bacteria	Proteobacteria	Alphaproteobacteria	Rhizobiales	Xanthobacteraceae	Rhodopseudomonas	Negative
	Bacteria	Bacteroidota	Bacteroidia	Chitinophagales	Chitinophagaceae	Flavihumibacter	Negative
	Eukaryota	Mucoromycota	Mortierellomycetes	Mortierellales	Mortierellaceae	Mortierella	Negative
	Eukaryota	Ascomycota	Saccharomycetes	Saccharomycetales	Unidentified	Unidentified	Negative
	Bacteria	Proteobacteria	Gammaproteobacteria	Pseudomonadales	Pseudomonadaceae	Pseudomonas	Negative
	Bacteria	Proteobacteria	Gammaproteobacteria	Pseudomonadales	Pseudomonadaceae	Pseudomonas	Negative
	Bacteria	Acidobacteriota	Acidobacteriae	Bryobacterales	Bryobacteraceae	Bryobacter	Negative
	Archaea	Thaumarchaeota	Nitrososphaeria	Nitrososphaerales	Nitrososphaeraceae	Unknown genus	Negative
	Bacteria	Proteobacteria	Alphaproteobacteria	Rhizobiales	Rhizobiaceae	Mesorhizobium	Negative
	Bacteria	Actinobacteriota	Actinobacteria	Pseudonocardiales	Pseudonocardiaceae	Actinophytocola	Negative
	Bacteria	Proteobacteria	Alphaproteobacteria	Rhizobiales	Rhizobiaceae	Mesorhizobium	Positive
	Eukaryota	Basidiomycota	Agaricomycetes	Agaricales	Crepidotaceae	Crepidotus	Positive
	Bacteria	Myxococcota	Polyangia	Polyangiales	Polyangiaceae	Pajaroellobacter	Positive
	Eukaryota	Ascomycota	Unidentified	Unidentified	Unidentified	Unidentified	Positive
	Bacteria	Proteobacteria	Alphaproteobacteria	Sphingomonadales	Sphingomonadaceae	Sandaracinobacter	Positive
	Bacteria	Acidobacteriota	Acidobacteriae	Bryobacterales	Bryobacteraceae	Bryobacter	Positive
	Bacteria	Actinobacteriota	Actinobacteria	Pseudonocardiales	Pseudonocardiaceae	Pseudonocardia	Positive
	Bacteria	Acidobacteriota	Vicinamibacteria	Vicinamibacterales	Vicinamibacteraceae	Vicinamibacter	Positive
	Eukaryota	Ascomycota	Eurotiomycetes	Eurotiales	Aspergillaceae	Penicillium	Positive
	Bacteria	Acidobacteriota	Acidobacteriae	Bryobacterales	Bryobacteraceae	Bryobacter	Positive
	Eukaryota	Mucoromycota	Mortierellomycetes	Mortierellales	Mortierellaceae	Mortierella	Positive
	Bacteria	Proteobacteria	Gammaproteobacteria	Xanthomonadales	Xanthomonadaceae	Stenotrophomonas	Positive
	Bacteria	Proteobacteria	Gammaproteobacteria	Xanthomonadales	Xanthomonadaceae	Stenotrophomonas	Positive
	Eukaryota	Ascomycota	Sordariomycetes	Glomerellales	Plectosphaerellaceae	Unidentified	Positive
	Bacteria	Chloroflexi	Unknown class	Unknown order	Unknown family	Unknown genus	Positive
	Eukaryota	Basidiomycota	Agaricomycetes	Corticiales	Corticiaceae	Haplotrichum	Positive
	Bacteria	Actinobacteriota	Actinobacteria	Propionibacteriales	Nocardioidaceae	Kribbella	Positive
	Eukaryota	Ascomycota	Dothideomycetes	Venturiales	Sympoventuriaceae	Ochroconis	Positive
	Bacteria	Bacteroidota	Bacteroidia	Sphingobacteriales	Sphingobacteriaceae	Pedobacter	Positive
	Bacteria	Bacteroidota	Bacteroidia	Chitinophagales	Chitinophagaceae	Chitinophaga	Positive
	Eukaryota	Ascomycota	Sordariomycetes	Hypocreales	Bionectriaceae	Geosmithia	Positive
	Eukaryota	Ascomycota	Eurotiomycetes	Eurotiales	Unidentified	Unidentified	Positive
	Bacteria	Proteobacteria	Alphaproteobacteria	Rhizobiales	Labraceae	Labrys	Positive
	Eukaryota	Ascomycota	Dothideomycetes	Venturiales	Sympoventuriaceae	Ochroconis	Positive
	Bacteria	Myxococcota	Polyangia	Polyangiales	Phaselicystidaceae	Phaselicystis	Positive
	Bacteria	Bacteroidota	Bacteroidia	Sphingobacteriales	Sphingobacteriaceae	Pedobacter	Positive
	Bacteria	Actinobacteriota	Actinobacteria	Frankiales	Sporichthyaceae	hgcIclade	Positive
	Bacteria	Chloroflexi	Chloroflexia	Thermomicrobiales	JG30-KF-CM45	Unknown genus	Positive
	Bacteria	Proteobacteria	Alphaproteobacteria	Rhizobiales	Rhizobiaceae	Mesorhizobium	Positive
	Bacteria	Actinobacteriota	Acidimicrobiia	Microtrichales	Ilumatobacteraceae	Unknown genus	Positive
	Bacteria	Actinobacteriota	Actinobacteria	Pseudonocardiales	Pseudonocardiaceae	Pseudonocardia	Positive
	Bacteria	Proteobacteria	Alphaproteobacteria	Rhizobiales	RhizobialesIncertaeSedis	Phreatobacter	Positive
	Bacteria	Chloroflexi	Chloroflexia	Thermomicrobiales	JG30-KF-CM45	Unknown genus	Positive
	Eukaryota	Ascomycota	Eurotiomycetes	Eurotiales	Trichocomaceae	Talaromyces	Positive
	Bacteria	Actinobacteriota	Actinobacteria	Frankiales	Acidothermaceae	Acidothermus	Positive
	Bacteria	Myxococcota	Polyangia	Polyangiales	Polyangiaceae	Pajaroellobacter	Positive
	Bacteria	Actinobacteriota	Actinobacteria	Micromonosporales	Micromonosporaceae	Unknown genus	Positive
	Eukaryota	Ascomycota	Sordariomycetes	Hypocreales	Cordycipitaceae	Isaria	Positive
	Eukaryota	Ascomycota	Sordariomycetes	Hypocreales	Cordycipitaceae	Cordyceps	Positive
	Eukaryota	Ascomycota	Sordariomycetes	Hypocreales	Cordycipitaceae	Isaria	Positive
	Bacteria	Proteobacteria	Gammaproteobacteria	Xanthomonadales	Rhodanobacteraceae	Dokdonella	Positive
	Eukaryota	Ascomycota	Sordariomycetes	Unidentified	Unidentified	Unidentified	Positive
	Bacteria	Actinobacteriota	Acidimicrobiia	Microtrichales	Ilumatobacteraceae	Unknown genus	Positive
	Bacteria	Proteobacteria	Alphaproteobacteria	Sphingomonadales	Sphingomonadaceae	Sandaracinobacter	Positive
	Bacteria	Actinobacteriota	Actinobacteria	Propionibacteriales	Nocardioidaceae	Nocardioides	Positive
	Bacteria	Actinobacteriota	Actinobacteria	Propionibacteriales	Nocardioidaceae	Nocardioides	Positive
	Eukaryota	Cercozoa	Cercomonadidae	Unidentified	Unidentified	Cercomonas	Positive
	Bacteria	Myxococcota	Polyangia	Polyangiales	Sandaracinaceae	Sandaracinus	Positive
	Eukaryota	Ascomycota	Eurotiomycetes	Eurotiales	Aspergillaceae	Penicillium	Positive
	Eukaryota	Amoebozoa	Discosea	Centramoebida	Unidentified	Acanthamoeba	Positive
	Bacteria	Actinobacteriota	Thermoleophilia	Solirubrobacterales	67-14	Unknown genus	Positive
	Eukaryota	Ascomycota	Sordariomycetes	Hypocreales	Unidentified	Unidentified	Positive
	Bacteria	Chloroflexi	Chloroflexia	Thermomicrobiales	JG30-KF-CM45	Unknown genus	Positive
	Bacteria	Actinobacteriota	Actinobacteria	Micrococcales	Microbacteriaceae	Agromyces	Positive

	Bacteria	Proteobacteria	Gammaproteobacteria	Pseudomonadales	Pseudomonadaceae	Pseudomonas	Positive
	Bacteria	Chloroflexi	Chloroflexia	Thermomicrobiales	JG30-KF-CM45	Unknown genus	Positive
	Bacteria	Actinobacteriota	Actinobacteria	Pseudonocardiales	Pseudonocardiaceae	Pseudonocardia	Positive
	Eukaryota	Ascomycota	Dothideomycetes	Pleosporales	Pleosporaceae	Bipolaris	Positive
	Eukaryota	Ascomycota	Dothideomycetes	Venturiales	Sympoventuriaceae	Ochroconis	Positive
	Bacteria	Actinobacteriota	Acidimicrobiia	Microtrichales	Ilumatobacteraceae	Unknown genus	Positive
	Bacteria	Proteobacteria	Alphaproteobacteria	Sphingomonadales	Sphingomonadaceae	Sphingomonas	Positive
	Bacteria	Actinobacteriota	Actinobacteria	Propionibacteriales	Nocardioidaceae	Aeromicrobium	Positive
	Bacteria	Proteobacteria	Alphaproteobacteria	Rhizobiales	Hyphomicrobiaceae	Hyphomicrobium	Positive
	Bacteria	Actinobacteriota	Acidimicrobiia	Microtrichales	Iamiaceae	Iamia	Positive
	Bacteria	Bacteroidota	Bacteroidia	Sphingobacteriales	Sphingobacteriaceae	Pedobacter	Positive
	Eukaryota	Chytridiomycota	Chytridiomycetes	Spizellomycetales	Unidentified	Unidentified	Positive
	Bacteria	Bacteroidota	Bacteroidia	Chitinophagales	Chitinophagaceae	Chitinophaga	Positive
	Bacteria	Proteobacteria	Alphaproteobacteria	Rhizobiales	Hyphomicrobiaceae	Pedomicrobium	Positive
	Eukaryota	Basidiomycota	Agaricomycetes	Polyporales	Unidentified	Unidentified	Positive
	Eukaryota	Ascomycota	Dothideomycetes	Venturiales	Sympoventuriaceae	Ochroconis	Positive
	Eukaryota	Ascomycota	Sordariomycetes	Glomerellales	Plectosphaerellaceae	Unidentified	Positive
	Bacteria	Actinobacteriota	Actinobacteria	Propionibacteriales	Nocardioidaceae	Nocardioides	Positive
	Archaea	Halobacterota	Halobacteria	Halobacterales	Haloferacaceae	Natronococcus	Positive
	Eukaryota	Ascomycota	Sordariomycetes	Hypocreales	Unidentified	Unidentified	Positive
	Eukaryota	Ascomycota	Sordariomycetes	Microascales	Microascaceae	Doratomyces	Positive
	Eukaryota	Ascomycota	Eurotiomycetes	Chaetothyriales	Cyphellophoraceae	Cyphellophora	Positive
	Bacteria	Actinobacteriota	Actinobacteria	Corynebacteriales	Mycobacteriaceae	Mycobacterium	Positive
	Bacteria	Actinobacteriota	Actinobacteria	Propionibacteriales	Nocardioidaceae	Nocardioides	Positive
	Bacteria	Actinobacteriota	Actinobacteria	Propionibacteriales	Nocardioidaceae	Nocardioides	Positive
	Bacteria	Proteobacteria	Gammaproteobacteria	Pseudomonadales	Pseudomonadaceae	Pseudomonas	Positive
	Eukaryota	Ascomycota	Sordariomycetes	Unidentified	Unidentified	Unidentified	Positive
	Bacteria	Proteobacteria	Alphaproteobacteria	Sphingomonadales	Sphingomonadaceae	Sphingobium	Positive
	Eukaryota	Ascomycota	Leotiomycetes	Unidentified	Unidentified	Pseudogymnoascus	Positive
	Eukaryota	Ascomycota	Sordariomycetes	Unidentified	Unidentified	Unidentified	Positive
	Bacteria	Proteobacteria	Alphaproteobacteria	Caulobacterales	Caulobacteraceae	Phenylobacterium	Positive
	Eukaryota	Ascomycota	Eurotiomycetes	Eurotiales	Aspergillaceae	Penicillium	Positive
	Bacteria	Planctomycetota	Planctomycetes	Pirellulales	Pirellulaceae	Pir4lineage	Positive
	Bacteria	Actinobacteriota	Actinobacteria	Pseudonocardiales	Pseudonocardiaceae	Pseudonocardia	Positive
	Bacteria	Proteobacteria	Gammaproteobacteria	Legionellales	Legionellaceae	Legionella	Positive
	Eukaryota	Ascomycota	Dothideomycetes	Venturiales	Sympoventuriaceae	Ochroconis	Positive
	Eukaryota	Ascomycota	Dothideomycetes	Capnodiales	Unidentified	Unidentified	Positive
	Bacteria	Bacteroidota	Bacteroidia	Sphingobacteriales	Sphingobacteriaceae	Parapedobacter	Positive
	Bacteria	Chloroflexi	Chloroflexia	Thermomicrobiales	JG30-KF-CM45	Unknown genus	Positive
	Eukaryota	Ascomycota	Sordariomycetes	Hypocreales	Bionectriaceae	Geosmithia	Positive
	Eukaryota	Ciliophora	Intramacronucleata	Conthreep	Colpodea	Bromeliothrix	Positive
	Eukaryota	Ascomycota	Leotiomycetes	Helotiales	Sclerotiniaceae	Sclerotinia	Positive
	Bacteria	Proteobacteria	Alphaproteobacteria	Caulobacterales	Caulobacteraceae	Brevundimonas	Positive
	Bacteria	Actinobacteriota	Actinobacteria	Pseudonocardiales	Pseudonocardiaceae	Pseudonocardia	Positive
	Bacteria	Actinobacteriota	Actinobacteria	Frankiales	Frankiaceae	Jatrophihabitans	Positive
	Eukaryota	Ascomycota	Eurotiomycetes	Chaetothyriales	Herpotrichiellaceae	Cladophialophora	Positive
	Eukaryota	Ascomycota	Sordariomycetes	Glomerellales	Plectosphaerellaceae	Unidentified	Positive
	Bacteria	Acidobacteriota	Blastocatellia	45597	Unknown family	Unknown genus	Positive
	Archaea	Nanoarchaeota	Nanoarchaeia	Woesearchaeales	Unidentified	Unknown genus	Positive
	Eukaryota	Ascomycota	Sordariomycetes	Unidentified	Unidentified	Unidentified	Positive
	Eukaryota	Mucoromycota	Unidentified	Unidentified	Unidentified	Unidentified	Positive
	Eukaryota	Unidentified	Unidentified	Unidentified	Unidentified	Unidentified	Positive
	Eukaryota	Ascomycota	Sordariomycetes	Microascales	Microascaceae	Doratomyces	Positive
	Eukaryota	Unclassified	Unclassified	Unclassified	Unclassified	Unclassified	Positive
	Eukaryota	Mucoromycota	Mortierellomycetes	Mortierellales	Mortierellaceae	Mortierella	Positive
	Bacteria	Chloroflexi	Chloroflexia	Thermomicrobiales	JG30-KF-CM45	Unknown genus	Positive
	Bacteria	Proteobacteria	Alphaproteobacteria	Rhizobiales	Rhizobiaceae	Mesorhizobium	Positive
Proximal unmarked surfa	Eukaryota	Nematozoa	Chromadorea	Rhabditida	Unidentified	Unidentified	Negative
	Bacteria	Actinobacteriota	Thermoleophilia	Solirubrobacterales	67-14	Unknown genus	Negative
	Eukaryota	Amoebozoa	Discosea	Centramoebida	Unidentified	Acanthamoeba	Negative
	Eukaryota	Ascomycota	Leotiomycetes	Unidentified	Unidentified	Pseudogymnoascus	Negative
	Bacteria	Proteobacteria	Alphaproteobacteria	Rhizobiales	Rhizobiaceae	Phyllobacterium	Negative
	Bacteria	Acidobacteriota	Vicinamibacteria	Vicinamibacterales	Vicinamibacteraceae	Vicinamibacter	Negative
	Eukaryota	Mucoromycota	Mortierellomycetes	Mortierellales	Mortierellaceae	Mortierella	Negative
	Bacteria	Actinobacteriota	Actinobacteria	Propionibacteriales	Propionibacteriaceae	Jiangella	Negative
	Eukaryota	Ascomycota	Sordariomycetes	Coniochaetales	Coniochaetaceae	Coniochaeta	Negative
	Archaea	Thaumarchaeota	Nitrososphaeria	Nitrososphaerales	Nitrososphaeraceae	Unknown genus	Negative
	Bacteria	Acidobacteriota	Vicinamibacteria	Vicinamibacterales	Vicinamibacteraceae	Vicinamibacter	Negative
	Eukaryota	Ascomycota	Sordariomycetes	Hypocreales	Cordycipitaceae	Cordyceps	Negative
	Bacteria	Actinobacteriota	Actinobacteria	Pseudonocardiales	Pseudonocardiaceae	Pseudonocardia	Negative
	Bacteria	Proteobacteria	Alphaproteobacteria	Caulobacterales	Caulobacteraceae	Phenylobacterium	Negative
	Bacteria	Actinobacteriota	Thermoleophilia	Solirubrobacterales	67-14	Unknown genus	Negative
	Bacteria	Proteobacteria	Alphaproteobacteria	Rhodobacterales	Rhodobacteraceae	Amaricoccus	Negative
	Bacteria	Proteobacteria	Alphaproteobacteria	Sphingomonadales	Sphingomonadaceae	Sphingopyxis	Negative
	Eukaryota	Unidentified	Discosea	Centramoebida	Unidentified	Acanthamoeba	Negative
	Eukaryota	Unidentified	Unidentified	Unidentified	Unidentified	Mycamoeba	Negative
	Bacteria	Actinobacteriota	Actinobacteria	Streptomycetales	Streptomycetaceae	Streptomyces	Negative
	Bacteria	Proteobacteria	Alphaproteobacteria	Reyranellales	Reyranellaceae	Unknown genus	Negative
	Bacteria	Actinobacteriota	Actinobacteria	Pseudonocardiales	Pseudonocardiaceae	Pseudonocardia	Negative
	Bacteria	Bacteroidota	Bacteroidia	Chitinophagales	Chitinophagaceae	Flavihumibacter	Negative
	Bacteria	Actinobacteriota	Actinobacteria	Propionibacteriales	Propionibacteriaceae	Unidentified	Negative
	Bacteria	Proteobacteria	Gammaproteobacteria	Burkholderiales	Comamonadaceae	Variovorax	Negative
	Bacteria	Proteobacteria	Gammaproteobacteria	Pseudomonadales	Moraxellaceae	Acinetobacter	Negative
	Bacteria	Actinobacteriota	Acidimicrobiia	Microtrichales	Unknown family	Unknown genus	Negative
	Bacteria	Bacteroidota	Bacteroidia	Sphingobacteriales	Sphingobacteriaceae	Pedobacter	Negative
	Eukaryota	Ascomycota	Eurotiomycetes	Onygenales	Arthrodermataceae	Unidentified	Negative

Bacteria	Actinobacteriota	Acidimicrobiia	Microtrichales	Ilumatobacteraceae	Unknown genus	Negative
Bacteria	Myxococcota	Polyangia	Nannocystales	Nannocystaceae	Nannocystis	Negative
Eukaryota	Ascomycota	Sordariomycetes	Hypocreales	Cordycipitaceae	Parengyodontium	Negative
Bacteria	Actinobacteriota	Actinobacteria	Streptomycetales	Streptomycetaceae	Streptomyces	Negative
Bacteria	Proteobacteria	Alphaproteobacteria	Rhizobiales	Hyphomicrobiaceae	Hyphomicrobium	Negative
Eukaryota	Ascomycota	Sordariomycetes	Microascales	Microascaceae	Doratomyces	Negative
Eukaryota	Ascomycota	Sordariomycetes	Glomerellales	Plectosphaerellaceae	Unidentified	Negative
Bacteria	Actinobacteriota	Actinobacteria	Streptosporangiales	Streptosporangiaceae	Nonomuraea	Negative
Bacteria	Actinobacteriota	Actinobacteria	Pseudonocardiales	Pseudonocardiaceae	Pseudonocardia	Negative
Eukaryota	Ascomycota	Dothideomycetes	Pleosporales	Unidentified	Unidentified	Negative
Bacteria	Actinobacteriota	Acidimicrobiia	Microtrichales	Ilumatobacteraceae	Unknown genus	Negative
Bacteria	Proteobacteria	Alphaproteobacteria	Rhizobiales	Methylopilaceae	Methylopila	Negative
Bacteria	Actinobacteriota	Actinobacteria	Corynebacteriales	Nocardiaceae	Nocardia	Negative
Bacteria	Actinobacteriota	Actinobacteria	Streptomycetales	Streptomycetaceae	E1B-B3-114	Positive
Bacteria	Proteobacteria	Gammaproteobacteria	Pseudomonadales	Pseudomonadaceae	Pseudomonas	Positive
Bacteria	Chloroflexi	Chloroflexia	Thermomicrobiales	JG30-KF-CM45	Unknown genus	Positive
Bacteria	Acidobacteriota	Acidobacteriae	Bryobacterales	Bryobacteraceae	Bryobacter	Positive
Bacteria	Planctomycetota	Planctomycetes	Gemmatales	Gemmataceae	Unknown genus	Positive
Bacteria	Actinobacteriota	Acidimicrobiia	Microtrichales	Unknown family	Unknown genus	Positive
Bacteria	Actinobacteriota	Actinobacteria	Corynebacteriales	Nocardiaceae	Nocardia	Positive
Bacteria	Proteobacteria	Alphaproteobacteria	Rhizobiales	Rhizobiaceae	Mesorhizobium	Positive
Bacteria	Chloroflexi	Chloroflexia	Thermomicrobiales	JG30-KF-CM45	Unknown genus	Positive
Bacteria	Actinobacteriota	Acidimicrobiia	Microtrichales	Unknown family	Unknown genus	Positive
Bacteria	Bacteroidota	Bacteroidia	Chitinophagales	Chitinophagaceae	Chitinophaga	Positive
Bacteria	Proteobacteria	Alphaproteobacteria	Rhizobiales	Hyphomicrobiaceae	Pedomicrobium	Positive
Bacteria	Proteobacteria	Alphaproteobacteria	Rhizobiales	Devosiaceae	Devosia	Positive
Bacteria	Proteobacteria	Gammaproteobacteria	Pseudomonadales	Pseudomonadaceae	Pseudomonas	Positive
Bacteria	Proteobacteria	Alphaproteobacteria	Rhizobiales	RhizobialesIncertaeSedis	Phreatobacter	Positive
Eukaryota	Cercozoa	Cercomonadidae	Unidentified	Unidentified	Cercomonas	Positive
Bacteria	Proteobacteria	Alphaproteobacteria	Rhizobiales	Xanthobacteraceae	Pseudorhodoplanes	Positive
Bacteria	Planctomycetota	Planctomycetes	Gemmatales	Gemmataceae	Gemmata	Positive
Eukaryota	Basidiomycota	Agaricomycetes	Agaricales	Unidentified	Baeospora	Positive
Bacteria	Proteobacteria	Alphaproteobacteria	Rhizobiales	Hyphomicrobiaceae	Hyphomicrobium	Positive
Bacteria	Actinobacteriota	Actinobacteria	Micrococcales	Promicromonosporaceae	Promicromonospora	Positive
Bacteria	Actinobacteriota	Acidimicrobiia	Microtrichales	Ilumatobacteraceae	Unknown genus	Positive
Bacteria	Proteobacteria	Gammaproteobacteria	Pseudomonadales	Pseudomonadaceae	Pseudomonas	Positive
Bacteria	Actinobacteriota	Actinobacteria	Streptomycetales	Streptomycetaceae	Streptomyces	Positive
Bacteria	Planctomycetota	Planctomycetes	Gemmatales	Gemmataceae	Unknown genus	Positive
Bacteria	Gemmatimonadota	Gemmatimonadetes	Gemmatimonadales	Gemmatimonadaceae	Unknown genus	Positive
Eukaryota	Ascomycota	Leotiomycetes	Thelebolales	Thelebolaceae	Unidentified	Positive
Archaea	Thaumarchaeota	Nitrososphaeria	Nitrososphaerales	Nitrososphaeraceae	Unknown genus	Positive
Eukaryota	Ascomycota	Unidentified	Unidentified	Unidentified	Unidentified	Positive
Bacteria	Proteobacteria	Gammaproteobacteria	Pseudomonadales	Pseudomonadaceae	Pseudomonas	Positive
Bacteria	Actinobacteriota	Actinobacteria	Streptosporangiales	Streptosporangiaceae	Unidentified	Positive
Eukaryota	Ascomycota	Sordariomycetes	Hypocreales	Unidentified	Unidentified	Positive
Bacteria	Actinobacteriota	Actinobacteria	Pseudonocardiales	Pseudonocardiaceae	Pseudonocardia	Positive
Bacteria	Proteobacteria	Gammaproteobacteria	Pseudomonadales	Pseudomonadaceae	Pseudomonas	Positive
Bacteria	Actinobacteriota	Actinobacteria	Pseudonocardiales	Pseudonocardiaceae	Pseudonocardia	Positive
Bacteria	Actinobacteriota	Thermoleophilia	Solirubrobacterales	Solirubrobacteraceae	Solirubrobacter	Positive
Bacteria	Proteobacteria	Alphaproteobacteria	Caulobacterales	Caulobacteraceae	Brevundimonas	Positive
Bacteria	Proteobacteria	Alphaproteobacteria	Azospirillales	Inquilinaceae	Inquilinus	Positive
Bacteria	Proteobacteria	Gammaproteobacteria	Pseudomonadales	Pseudomonadaceae	Pseudomonas	Positive
Bacteria	Actinobacteriota	Thermoleophilia	Solirubrobacterales	67-14	Unknown genus	Positive
Eukaryota	Ascomycota	Sordariomycetes	Hypocreales	Bionectriaceae	Clonostachys	Positive
Eukaryota	Ascomycota	Eurotiomycetes	Eurotiales	Aspergillaceae	Aspergillus	Positive
Bacteria	Actinobacteriota	Acidimicrobiia	Microtrichales	Unknown family	Unknown genus	Positive
Bacteria	Proteobacteria	Alphaproteobacteria	Rhizobiales	Beijerinckiaceae	Bosea	Positive
Bacteria	Bacteroidota	Bacteroidia	Chitinophagales	Chitinophagaceae	Unknown genus	Positive
Eukaryota	Basidiomycota	Agaricomycetes	Agaricales	Crepidotaceae	Crepidotus	Positive
Bacteria	Chloroflexi	Chloroflexia	Thermomicrobiales	JG30-KF-CM45	Unknown genus	Positive
Bacteria	Proteobacteria	Alphaproteobacteria	Rhizobiales	Xanthobacteraceae	Unknown genus	Positive
Eukaryota	Ascomycota	Sordariomycetes	Unidentified	Unidentified	Unidentified	Positive
Eukaryota	Ascomycota	Eurotiomycetes	Chaetothyriales	Herpotrichiellaceae	Cladophialophora	Positive
Eukaryota	Ascomycota	Sordariomycetes	Hypocreales	Unidentified	Unidentified	Positive
Bacteria	Proteobacteria	Alphaproteobacteria	Rhizobiales	Xanthobacteraceae	Unknown genus	Positive
Bacteria	Chloroflexi	Chloroflexia	Thermomicrobiales	JG30-KF-CM45	Unknown genus	Positive
Bacteria	Proteobacteria	Gammaproteobacteria	Pseudomonadales	Pseudomonadaceae	Pseudomonas	Positive
Bacteria	Acidobacteriota	Vicinamibacteria	Subgroup17	Unknown family	Unknown genus	Positive
Bacteria	Actinobacteriota	Actinobacteria	Micrococcales	Microbacteriaceae	Microbacterium	Positive
Bacteria	Proteobacteria	Gammaproteobacteria	Xanthomonadales	Xanthomonadaceae	Stenotrophomonas	Positive
Bacteria	Actinobacteriota	Actinobacteria	Micrococcales	Microbacteriaceae	Agromyces	Positive
Bacteria	Proteobacteria	Gammaproteobacteria	Xanthomonadales	Rhodanobacteraceae	Dokdonella	Positive
Eukaryota	Basidiomycota	Tremellomycetes	Filobasidiales	Filobasidiaceae	Unidentified	Positive
Bacteria	Acidobacteriota	Acidobacteriae	Bryobacterales	Bryobacteraceae	Bryobacter	Positive
Eukaryota	Amoebozoa	Discosea	Centramoebida	Unidentified	Acanthamoeba	Positive
Eukaryota	Ochrophyta	Chrysophyceae	Unidentified	Unidentified	Chlamydomyxa	Positive
Eukaryota	Ascomycota	Sordariomycetes	Unidentified	Unidentified	Unidentified	Positive
Bacteria	Proteobacteria	Gammaproteobacteria	Pseudomonadales	Pseudomonadaceae	Pseudomonas	Positive
Eukaryota	Ascomycota	Dothideomycetes	Venturiales	Sympoventuriaceae	Ochroconis	Positive
Eukaryota	Ascomycota	Dothideomycetes	Venturiales	Sympoventuriaceae	Ochroconis	Positive
Eukaryota	Ascomycota	Sordariomycetes	Hypocreales	Unidentified	Acremonium	Positive
Bacteria	Proteobacteria	Alphaproteobacteria	Rhizobiales	Devosiaceae	Devosia	Positive
Eukaryota	Unidentified	Unidentified	Unidentified	Unidentified	Unidentified	Positive
Bacteria	Proteobacteria	Alphaproteobacteria	Azospirillales	Inquilinaceae	Inquilinus	Positive
Bacteria	Acidobacteriota	Acidobacteriae	Bryobacterales	Bryobacteraceae	Bryobacter	Positive
Eukaryota	Ascomycota	Leotiomycetes	Unidentified	Myxotrichaceae	Byssoascus	Positive

	Eukaryota	Ascomycota	Sordariomycetes	Glomerellales	Plectosphaerellaceae	Unidentified	Positive
	Bacteria	Proteobacteria	Alphaproteobacteria	Sphingomonadales	Sphingomonadaceae	Sphingomonas	Positive
	Eukaryota	Ascomycota	Sordariomycetes	Xylariales	Unidentified	Unidentified	Positive
	Bacteria	Actinobacteriota	Actinobacteria	Propionibacteriales	Propionibacteriaceae	Microlunatus	Positive
	Eukaryota	Mucoromycota	Unidentified	Unidentified	Unidentified	Unidentified	Positive
	Bacteria	Actinobacteriota	Actinobacteria	Micrococcales	Microbacteriaceae	Agromyces	Positive
	Bacteria	Actinobacteriota	Actinobacteria	Propionibacteriales	Propionibacteriaceae	Marinilutecoccus	Positive
	Bacteria	Proteobacteria	Gammaproteobacteria	Pseudomonadales	Pseudomonadaceae	Pseudomonas	Positive
	Eukaryota	Ascomycota	Sordariomycetes	Glomerellales	Plectosphaerellaceae	Unidentified	Positive
	Archaea	Thaumarchaeota	Nitrososphaeria	Nitrosopumilales	Nitrosopumilaceae	Multi-affiliation	Positive
	Eukaryota	Amoebozoa	Discosea	Centramoebida	Unidentified	Unidentified	Positive
	Eukaryota	Ascomycota	Eurotiomycetes	Eurotiales	Aspergillaceae	Penicillium	Positive
	Bacteria	Bacteroidota	Bacteroidia	Chitinophagales	Chitinophagaceae	Niabella	Positive
	Bacteria	Proteobacteria	Gammaproteobacteria	Steroidobacterales	Steroidobacteraceae	Steroidobacter	Positive
	Archaea	Unclassified	Unclassified	Unclassified	Unidentified	Unclassified	Positive
	Archaea	Thaumarchaeota	Nitrososphaeria	Nitrososphaerales	Nitrososphaeraceae	Candidatus Nitrocosmicus	Positive
	Eukaryota	Ascomycota	Sordariomycetes	Glomerellales	Plectosphaerellaceae	Unidentified	Positive
	Bacteria	Bacteroidota	Bacteroidia	Chitinophagales	Chitinophagaceae	Chitinophaga	Positive
	Eukaryota	Amoebozoa	Tubulinea	Echinamoebida	Unidentified	Unidentified	Positive
New dark zone	Eukaryota	Ascomycota	Sordariomycetes	Hypocreales	Bionectriaceae	Geosmithia	Negative
	Eukaryota	Ascomycota	Sordariomycetes	Microascales	Microascaceae	Doratomyces	Negative
	Bacteria	Myxococcota	Polyangia	Nannocystales	Nannocystaceae	Nannocystis	Negative
	Eukaryota	Ascomycota	Sordariomycetes	Glomerellales	Plectosphaerellaceae	Unidentified	Negative
	Eukaryota	Ascomycota	Eurotiomycetes	Eurotiales	Trichocomaceae	Talaromyces	Negative
	Bacteria	Proteobacteria	Alphaproteobacteria	Sphingomonadales	Sphingomonadaceae	Sandaracinobacter	Negative
	Bacteria	Bacteroidota	Bacteroidia	Chitinophagales	Chitinophagaceae	Chitinophaga	Negative
	Eukaryota	Mucoromycota	Unidentified	Unidentified	Unidentified	Unidentified	Negative
	Eukaryota	Unidentified	Unidentified	Unidentified	Unidentified	Unidentified	Negative
	Bacteria	Proteobacteria	Gammaproteobacteria	Pseudomonadales	Pseudomonadaceae	Pseudomonas	Negative
	Eukaryota	Ascomycota	Sordariomycetes	Unidentified	Unidentified	Unidentified	Positive
	Bacteria	Bacteroidota	Bacteroidia	Sphingobacteriales	Sphingobacteriaceae	Pedobacter	Positive
	Bacteria	Actinobacteriota	Actinobacteria	Streptomycetales	Streptomycetaceae	Streptomyces	Positive
	Bacteria	Proteobacteria	Alphaproteobacteria	Holosporales	Holosporaceae	Unknown genus	Positive
	Bacteria	Proteobacteria	Alphaproteobacteria	Reyranellales	Reyranellaceae	Reyranella	Positive
	Bacteria	Proteobacteria	Alphaproteobacteria	Rhizobiales	Xanthobacteraceae	Afipia	Positive
	Bacteria	Actinobacteriota	Actinobacteria	Micrococcales	Microbacteriaceae	Rudaibacter	Positive
	Bacteria	Myxococcota	Polyangia	Polyangiales	Polyangiaceae	Pajaroellobacter	Positive
	Bacteria	Bacteroidota	Bacteroidia	Chitinophagales	Chitinophagaceae	Chitinophaga	Positive
	Eukaryota	Ascomycota	Dothideomycetes	Pleosporales	Unidentified	Unidentified	Positive
	Eukaryota	Ascomycota	Dothideomycetes	Venturiales	Sympoventuriaceae	Ochroconis	Positive
	Bacteria	Proteobacteria	Alphaproteobacteria	Reyranellales	Reyranellaceae	Unknown genus	Positive
	Bacteria	Proteobacteria	Gammaproteobacteria	Burkholderiales	Alcaligenaceae	Bordetella	Positive
	Bacteria	Myxococcota	Polyangia	Polyangiales	Polyangiaceae	Pajaroellobacter	Positive
	Bacteria	Acidobacteriota	Vicinamibacteria	Vicinamibacterales	Vicinamibacteraceae	Unknown genus	Positive
	Bacteria	Actinobacteriota	Actinobacteria	Micrococcales	Microbacteriaceae	Agromyces	Positive
	Bacteria	Proteobacteria	Alphaproteobacteria	Rhizobiales	Hyphomicrobiaceae	Hyphomicrobium	Positive
	Bacteria	Proteobacteria	Gammaproteobacteria	Pseudomonadales	Pseudomonadaceae	Pseudomonas	Positive
	Bacteria	Proteobacteria	Gammaproteobacteria	Pseudomonadales	Pseudomonadaceae	Pseudomonas	Positive
	Bacteria	Proteobacteria	Gammaproteobacteria	Burkholderiales	Unidentified	Unidentified	Positive
	Bacteria	Bacteroidota	Bacteroidia	Chitinophagales	Chitinophagaceae	Chitinophaga	Positive
	Bacteria	Proteobacteria	Alphaproteobacteria	Sphingomonadales	Sphingomonadaceae	Sphingomonas	Positive
	Bacteria	Proteobacteria	Alphaproteobacteria	Rhizobiales	Beijerinckiaceae	28-YEA-48	Positive
	Eukaryota	Mucoromycota	Unidentified	Mortierellales	Mortierellaceae	Mortierella	Positive
	Bacteria	Actinobacteriota	Actinobacteria	Pseudonocardiales	Pseudonocardiaceae	Pseudonocardia	Positive
	Bacteria	Actinobacteriota	Actinobacteria	Pseudonocardiales	Pseudonocardiaceae	Pseudonocardia	Positive
	Bacteria	Actinobacteriota	Actinobacteria	Pseudonocardiales	Pseudonocardiaceae	Saccharopolyspora	Positive
	Bacteria	Actinobacteriota	Actinobacteria	Streptosporangiales	Streptosporangiaceae	Nonomuraea	Positive
	Bacteria	Actinobacteriota	Actinobacteria	Pseudonocardiales	Pseudonocardiaceae	Pseudonocardia	Positive
	Eukaryota	Ascomycota	Dothideomycetes	Venturiales	Sympoventuriaceae	Ochroconis	Positive
	Eukaryota	Ascomycota	Dothideomycetes	Venturiales	Sympoventuriaceae	Ochroconis	Positive
Intermediate dark zone	Bacteria	Bacteroidota	Bacteroidia	Chitinophagales	Chitinophagaceae	Chitinophaga	Negative
	Bacteria	Actinobacteriota	Actinobacteria	Micromonosporales	Micromonosporaceae	Hamadaea	Negative
	Eukaryota	Basidiomycota	Agaricomycetes	Boletales	Unidentified	Hygrophoropsis	Negative
	Bacteria	Chloroflexi	Chloroflexia	Thermomicrobiales	JG30-KF-CM45	Unknown genus	Negative
	Bacteria	Proteobacteria	Alphaproteobacteria	Rhizobiales	Hyphomicrobiaceae	Pedomicrobium	Negative
	Bacteria	Actinobacteriota	Actinobacteria	Propionibacteriales	Propionibacteriaceae	Jiangella	Negative
	Eukaryota	Ascomycota	Sordariomycetes	Glomerellales	Plectosphaerellaceae	Unidentified	Negative
	Eukaryota	Unidentified	Unidentified	Unidentified	Unidentified	Unidentified	Negative
	Bacteria	Proteobacteria	Alphaproteobacteria	Rhizobiales	Rhizobiaceae	Mesorhizobium	Negative
	Eukaryota	Mucoromycota	Unidentified	Mortierellales	Mortierellaceae	Mortierella	Negative
	Bacteria	Actinobacteriota	Actinobacteria	Corynebacteriales	Nocardiaceae	Nocardia	Negative
	Archaea	Thaumarchaeota	Nitrososphaeria	Nitrososphaerales	Nitrososphaeraceae	Unknown genus	Negative
	Bacteria	Proteobacteria	Alphaproteobacteria	Sphingomonadales	Sphingomonadaceae	Sphingomonas	Negative
	Bacteria	Actinobacteriota	Actinobacteria	Propionibacteriales	Nocardioidaceae	Aeromicrobium	Negative
	Bacteria	Actinobacteriota	Thermoleophilia	Solirubrobacterales	67-14	Unknown genus	Negative
	Bacteria	Proteobacteria	Gammaproteobacteria	Burkholderiales	Burkholderiaceae	Ralstonia	Negative
	Bacteria	Actinobacteriota	Actinobacteria	Propionibacteriales	Propionibacteriaceae	Unidentified	Negative
	Eukaryota	Unclassified	Unclassified	Unclassified	Unclassified	Unclassified	Negative
	Bacteria	Proteobacteria	Alphaproteobacteria	Rhodobacterales	Rhodobacteraceae	Amaricoccus	Negative
	Bacteria	Actinobacteriota	Actinobacteria	Propionibacteriales	Propionibacteriaceae	Unidentified	Negative
	Bacteria	Actinobacteriota	Actinobacteria	Corynebacteriales	Nocardiaceae	Nocardia	Negative
	Eukaryota	Ascomycota	Saccharomycetes	Saccharomycetales	Unidentified	Unidentified	Negative
	Bacteria	Planctomycetota	Planctomycetes	Isosphaerales	Isosphaeraceae	Isosphaera	Negative
	Eukaryota	Ascomycota	Pezizomycetes	Pezizales	Unidentified	Unidentified	Negative
	Bacteria	Proteobacteria	Alphaproteobacteria	Sphingomonadales	Sphingomonadaceae	Sphingomonas	Negative
	Bacteria	Actinobacteriota	Actinobacteria	Micrococcales	Microbacteriaceae	Galbitalea	Positive

	Bacteria	Proteobacteria	Alphaproteobacteria	Rhizobiales	Beijerinckiaceae	Bosea	Positive
	Archaea	Unclassified	Unclassified	Unclassified	Unidentified	Unclassified	Positive
	Eukaryota	Ascomycota	Sordariomycetes	Hypocreales	Ophiocordycipitaceae	Tolypocladium	Positive
	Eukaryota	Unidentified	Unidentified	Unidentified	Unidentified	Unidentified	Positive
	Bacteria	Proteobacteria	Alphaproteobacteria	Rhizobiales	Labraceae	Labrys	Positive
	Archaea	Crenarchaeota	Nitrososphaeria	Nitrososphaerales	Nitrososphaeraceae	Unidentified	Positive
	Bacteria	Proteobacteria	Alphaproteobacteria	Rhizobiales	Methylopilaceae	Methylopila	Positive
	Bacteria	Actinobacteriota	Acidimicrobiia	Microtrichales	Unknown family	Unknown genus	Positive
	Bacteria	Actinobacteriota	Actinobacteria	Micromonosporales	Micromonosporaceae	Catelliglobosispora	Positive
	Bacteria	Chloroflexi	Chloroflexia	Thermomicrobiales	JG30-KF-CM45	Unknown genus	Positive
	Bacteria	Acidobacteriota	Vicinamibacteria	Vicinamibacterales	Vicinamibacteraceae	Unknown genus	Positive
	Bacteria	Actinobacteriota	Actinobacteria	Frankiales	Sporichthyaceae	Sporichthya	Positive
	Bacteria	Proteobacteria	Gammaproteobacteria	Legionellales	Legionellaceae	Legionella	Positive
	Bacteria	Proteobacteria	Gammaproteobacteria	Pseudomonadales	Pseudomonadaceae	Pseudomonas	Positive
	Bacteria	Proteobacteria	Gammaproteobacteria	Burkholderiales	Nitrosomonadaceae	Nitrosospira	Positive
	Bacteria	Actinobacteriota	Actinobacteria	Micrococcales	Microbacteriaceae	Rudaibacter	Positive
	Bacteria	Actinobacteriota	Actinobacteria	Propionibacteriales	Nocardioidaceae	Nocardioides	Positive
	Bacteria	Actinobacteriota	Thermoleophilia	Solirubrobacterales	Solirubrobacteraceae	Solirubrobacter	Positive
	Eukaryota	Ascomycota	Eurotiomycetes	Eurotiales	Aspergillaceae	Penicillium	Positive
	Eukaryota	Mucoromycota	Mortierellomycetes	Mortierellales	Mortierellaceae	Mortierella	Positive
	Bacteria	Actinobacteriota	Actinobacteria	Micrococcales	Microbacteriaceae	Microbacterium	Positive
	Bacteria	Myxococcota	Polyangia	Polyangiales	Polyangiaceae	Pajaroellobacter	Positive
	Bacteria	Proteobacteria	Alphaproteobacteria	Rhizobiales	Xanthobacteraceae	Rhodopseudomonas	Positive
	Bacteria	Proteobacteria	Gammaproteobacteria	Xanthomonadales	Xanthomonadaceae	Stenotrophomonas	Positive
	Bacteria	Proteobacteria	Alphaproteobacteria	Rhizobiales	Xanthobacteraceae	Unknown genus	Positive
	Bacteria	Actinobacteriota	Actinobacteria	Pseudonocardiales	Pseudonocardiaceae	Pseudonocardia	Positive
	Bacteria	Proteobacteria	Alphaproteobacteria	Rhizobiales	Hyphomicrobiaceae	Pedomicrobium	Positive
	Bacteria	Bacteroidota	Bacteroidia	Chitinophagales	Chitinophagaceae	Chitinophaga	Positive
	Bacteria	Proteobacteria	Alphaproteobacteria	Acetobacterales	Acetobacteraceae	Roseomonas	Positive
	Eukaryota	Ascomycota	Eurotiomycetes	Eurotiales	Aspergillaceae	Aspergillus	Positive
	Bacteria	Proteobacteria	Gammaproteobacteria	Burkholderiales	Alcaligenaceae	Bordetella	Positive
	Bacteria	Bacteroidota	Bacteroidia	Sphingobacteriales	Sphingobacteriaceae	Pseudosphingobacterium	Positive
	Bacteria	Planctomycetota	Planctomycetes	Isosphaerales	Isosphaeraceae	Aquisphaera	Positive
	Bacteria	Proteobacteria	Alphaproteobacteria	Rhizobiales	Labraceae	Labrys	Positive
	Bacteria	Actinobacteriota	Actinobacteria	Propionibacteriales	Nocardioidaceae	Kribbella	Positive
	Bacteria	Actinobacteriota	Actinobacteria	Pseudonocardiales	Pseudonocardiaceae	Amycolatopsis	Positive
	Bacteria	Actinobacteriota	Actinobacteria	Propionibacteriales	Nocardioidaceae	Nocardioides	Positive
	Eukaryota	Chytridiomycota	Chytridiomycetes	Spizellomycetales	Unidentified	Unidentified	Positive
	Eukaryota	Ascomycota	Dothideomycetes	Venturiales	Sympoventuriaceae	Ochroconis	Positive
	Bacteria	Bacteroidota	Bacteroidia	Chitinophagales	Chitinophagaceae	Niabella	Positive
	Bacteria	Actinobacteriota	Actinobacteria	Micromonosporales	Micromonosporaceae	Unidentified	Positive
	Bacteria	Chloroflexi	Chloroflexia	Thermomicrobiales	JG30-KF-CM45	Unknown genus	Positive
	Bacteria	Actinobacteriota	Actinobacteria	Pseudonocardiales	Pseudonocardiaceae	Pseudonocardia	Positive
	Bacteria	Actinobacteriota	Actinobacteria	Pseudonocardiales	Pseudonocardiaceae	Pseudonocardia	Positive
	Eukaryota	Ascomycota	Dothideomycetes	Venturiales	Sympoventuriaceae	Ochroconis	Positive
	Archaea	Nanoarchaeota	Nanoarchaeia	Woesearchaeales	Unidentified	Unknown genus	Positive
	Eukaryota	Ascomycota	Sordariomycetes	Unidentified	Unidentified	Unidentified	Positive
	Bacteria	Patescibacteria	Parcubacteria	Candidatus Adlerbacteria	Unknown family	Unknown genus	Positive
	Eukaryota	Cercozoa	Cercomonadidae	Unidentified	Unidentified	Cercomonas	Positive
	Bacteria	Actinobacteriota	Actinobacteria	Pseudonocardiales	Pseudonocardiaceae	Pseudonocardia	Positive
	Eukaryota	Ascomycota	Dothideomycetes	Venturiales	Sympoventuriaceae	Ochroconis	Positive
	Bacteria	Actinobacteriota	Actinobacteria	Unidentified	Unidentified	Unidentified	Positive
	Eukaryota	Ascomycota	Sordariomycetes	Unidentified	Unidentified	Unidentified	Positive
	Eukaryota	Ascomycota	Leotiomycetes	Helotiales	Leotiaceae	Pezoloma	Positive
Old dark zone	Bacteria	Bacteroidota	Bacteroidia	Chitinophagales	Chitinophagaceae	Chitinophaga	Negative
	Eukaryota	Ascomycota	Eurotiomycetes	Onygenales	Arthrodermataceae	Arthroderma	Negative
	Bacteria	Actinobacteriota	Actinobacteria	Micromonosporales	Micromonosporaceae	Hamadaea	Negative
	Bacteria	Bacteroidota	Bacteroidia	Sphingobacteriales	Sphingobacteriaceae	Anseongella	Negative
	Bacteria	Actinobacteriota	Actinobacteria	Corynebacteriales	Unknown family	Unknown genus	Negative
	Eukaryota	Ascomycota	Sordariomycetes	Glomerellales	Plectosphaerellaceae	Unidentified	Negative
	Bacteria	Proteobacteria	Alphaproteobacteria	Rhizobiales	Hyphomicrobiaceae	Pedomicrobium	Negative
	Eukaryota	Zoopagomycota	Entomophthoromycetes	Entomophthorales	Ancylistaceae	Conidiobolus	Negative
	Bacteria	Myxococcota	Polyangia	Polyangiales	Phaselicystidaceae	Phaselicystis	Negative
	Eukaryota	Amoebozoa	Discosea	Centramoebida	Unidentified	Unidentified	Negative
	Eukaryota	Ascomycota	Sordariomycetes	Unidentified	Unidentified	Unidentified	Negative
	Eukaryota	Mucoromycota	Unidentified	Unidentified	Unidentified	Unidentified	Negative
	Bacteria	Actinobacteriota	Actinobacteria	Propionibacteriales	Nocardioidaceae	Nocardioides	Negative
	Bacteria	Actinobacteriota	Actinobacteria	Propionibacteriales	Propionibacteriaceae	Jiangella	Negative
	Eukaryota	Mucoromycota	Unidentified	Unidentified	Unidentified	Unidentified	Negative
	Eukaryota	Basidiomycota	Agaricomycetes	Unidentified	Unidentified	Unidentified	Negative
	Bacteria	Proteobacteria	Alphaproteobacteria	Rhizobiales	Rhizobiaceae	Allorhizobium	Negative
	Bacteria	Bacteroidota	Bacteroidia	Chitinophagales	Chitinophagaceae	Flavihumibacter	Negative
	Archaea	Nanoarchaeota	Nanoarchaeia	Woesearchaeales	Unidentified	Unknown genus	Negative
	Bacteria	Actinobacteriota	Actinobacteria	Propionibacteriales	Propionibacteriaceae	Unidentified	Negative
	Bacteria	Chloroflexi	Ktedonobacteria	Ktedonobacterales	Ktedonobacteraceae	1959-1	Negative
	Bacteria	Actinobacteriota	Thermoleophilia	Solirubrobacterales	67-14	Unknown genus	Negative
	Eukaryota	Ascomycota	Sordariomycetes	Glomerellales	Plectosphaerellaceae	Unidentified	Negative
	Archaea	Thaumarchaeota	Nitrososphaeria	Nitrososphaerales	Nitrososphaeraceae	Unknown genus	Negative
	Bacteria	Proteobacteria	Alphaproteobacteria	Rhizobiales	Labraceae	Labrys	Negative
	Bacteria	Proteobacteria	Alphaproteobacteria	Sphingomonadales	Sphingomonadaceae	Sandaracinobacter	Negative
	Bacteria	Bacteroidota	Bacteroidia	Chitinophagales	Chitinophagaceae	Flavihumibacter	Negative
	Eukaryota	Ascomycota	Sordariomycetes	Microascales	Microascaceae	Doratomyces	Negative
	Bacteria	Actinobacteriota	Acidimicrobiia	Microtrichales	Ilumatobacteraceae	Unknown genus	Negative
	Eukaryota	Mucoromycota	Mortierellomycetes	Mortierellales	Mortierellaceae	Mortierella	Positive
	Bacteria	Acidobacteriota	Acidobacteriae	Bryobacterales	Bryobacteraceae	Bryobacter	Positive
	Eukaryota	Ascomycota	Saccharomycetes	Saccharomycetales	Debaryomycetaceae	Unidentified	Positive

Bacteria	Verrucomicrobiota	Verrucomicrobiae	Verrucomicrobiales	Verrucomicrobiaceae	Verrucomicrobium	Positive
Bacteria	Proteobacteria	Alphaproteobacteria	Rhizobiales	Rhizobiaceae	Phyllobacterium	Positive
Eukaryota	Ascomycota	Sordariomycetes	Hypocreales	Unidentified	Unidentified	Positive
Bacteria	Proteobacteria	Alphaproteobacteria	Rhizobiales	Xanthobacteraceae	Unidentified	Positive
Archaea	Unclassified	Unclassified	Unclassified	Unidentified	Unclassified	Positive
Bacteria	Actinobacteriota	Actinobacteria	Propionibacteriales	Nocardioidaceae	Nocardioides	Positive
Bacteria	Proteobacteria	Gammaproteobacteria	Burkholderiales	Alcaligenaceae	Unidentified	Positive
Eukaryota	Basidiomycota	Agaricomycetes	Unidentified	Unidentified	Unidentified	Positive
Bacteria	Proteobacteria	Gammaproteobacteria	Pseudomonadales	Pseudomonadaceae	Pseudomonas	Positive
Eukaryota	Ascomycota	Dothideomycetes	Venturiales	Sympoventuriaceae	Ochroconis	Positive
Bacteria	Actinobacteriota	Acidimicrobiia	Microtrichales	Unknown family	Unknown genus	Positive
Eukaryota	Ascomycota	Eurotiomycetes	Eurotiales	Trichocomaceae	Talaromyces	Positive
Bacteria	Actinobacteriota	Actinobacteria	Streptosporangiales	Streptosporangiaceae	Nonomuraea	Positive
Bacteria	Planctomycetota	Planctomycetes	Gemmatales	Gemmataceae	Gemmata	Positive
Bacteria	Proteobacteria	Gammaproteobacteria	Pseudomonadales	Pseudomonadaceae	Pseudomonas	Positive
Bacteria	Bacteroidota	Bacteroidia	Chitinophagales	Chitinophagaceae	Pseudoflavitalea	Positive
Eukaryota	Ascomycota	Eurotiomycetes	Chaetothyriales	Herpotrichiellaceae	Cladophialophora	Positive
Eukaryota	Amoebozoa	Discosea	Centramoebida	Unidentified	Unidentified	Positive
Bacteria	Bacteroidota	Bacteroidia	Chitinophagales	Chitinophagaceae	Chitinophaga	Positive
Eukaryota	Ascomycota	Eurotiomycetes	Chaetothyriales	Cyphellophoraceae	Cyphellophora	Positive
Eukaryota	Ascomycota	Sordariomycetes	Unidentified	Unidentified	Unidentified	Positive
Bacteria	Actinobacteriota	Actinobacteria	Streptosporangiales	Streptosporangiaceae	Nonomuraea	Positive
Bacteria	Actinobacteriota	Actinobacteria	Pseudonocardiales	Pseudonocardiaceae	Actinophytocola	Positive
Eukaryota	Ascomycota	Unidentified	Unidentified	Unidentified	Calcarisporiella	Positive
Eukaryota	Ascomycota	Sordariomycetes	Glomerellales	Plectosphaerellaceae	Unidentified	Positive
Bacteria	Proteobacteria	Alphaproteobacteria	Azospirillales	Inquilinaceae	Inquilinus	Positive
Eukaryota	Ascomycota	Leotiomycetes	Unidentified	Unidentified	Pseudogymnoascus	Positive
Eukaryota	Ascomycota	Eurotiomycetes	Onygenales	Arthrodermataceae	Unidentified	Positive
Bacteria	Proteobacteria	Gammaproteobacteria	Burkholderiales	Nitrosomonadaceae	Nitrosospira	Positive
Eukaryota	Basidiomycota	Agaricomycetes	Polyporales	Unidentified	Burgoa	Positive
Eukaryota	Zoopagomycota	Entomophthoromycetes	Entomophthorales	Ancylistaceae	Conidiobolus	Positive
Bacteria	Proteobacteria	Alphaproteobacteria	Rhizobiales	Rhizobiaceae	Mesorhizobium	Positive
Eukaryota	Ascomycota	Dothideomycetes	Venturiales	Sympoventuriaceae	Ochroconis	Positive
Bacteria	Bacteroidota	Bacteroidia	Sphingobacteriales	Sphingobacteriaceae	Pseudosphingobacterium	Positive
Bacteria	Proteobacteria	Alphaproteobacteria	Rhizobiales	Beijerinckiaceae	28-YEA-48	Positive
Bacteria	Actinobacteriota	Actinobacteria	Pseudonocardiales	Pseudonocardiaceae	Pseudonocardia	Positive
Bacteria	Proteobacteria	Alphaproteobacteria	Rhizobiales	Hyphomicrobiaceae	Pedomicrobium	Positive
Bacteria	Proteobacteria	Alphaproteobacteria	Sphingomonadales	Sphingomonadaceae	Sandaracinobacter	Positive
Bacteria	Proteobacteria	Alphaproteobacteria	Sphingomonadales	Sphingomonadaceae	Sandaracinobacter	Positive
Bacteria	Actinobacteriota	Actinobacteria	Propionibacteriales	Nocardioidaceae	Nocardioides	Positive
Bacteria	Acidobacteriota	Acidobacteriae	Bryobacterales	Bryobacteraceae	Bryobacter	Positive
Bacteria	Proteobacteria	Alphaproteobacteria	Rhizobiales	Hyphomicrobiaceae	Hyphomicrobium	Positive
Eukaryota	Unidentified	Unidentified	Unidentified	Unidentified	Unidentified	Positive
Bacteria	Actinobacteriota	Actinobacteria	Micrococcales	Intrasporangiaceae	Unidentified	Positive
Bacteria	Proteobacteria	Alphaproteobacteria	Rhizobiales	Rhizobiaceae	Phyllobacterium	Positive
Eukaryota	Ascomycota	Dothideomycetes	Venturiales	Sympoventuriaceae	Ochroconis	Positive
Bacteria	Proteobacteria	Alphaproteobacteria	Rhizobiales	Hyphomicrobiaceae	Pedomicrobium	Positive
Bacteria	Myxococcota	Polyangia	Polyangiales	Polyangiaceae	Pajaroellobacter	Positive
Eukaryota	Ascomycota	Leotiomycetes	Unidentified	Unidentified	Pseudogymnoascus	Positive
Eukaryota	Unidentified	Unidentified	Unidentified	Unidentified	Unidentified	Positive
Bacteria	Actinobacteriota	Actinobacteria	Frankiales	Sporichthyaceae	Sporichthya	Positive
Bacteria	Proteobacteria	Alphaproteobacteria	Sphingomonadales	Sphingomonadaceae	Sandaracinobacter	Positive
Bacteria	Proteobacteria	Gammaproteobacteria	Xanthomonadales	Xanthomonadaceae	Stenotrophomonas	Positive
Eukaryota	Ascomycota	Dothideomycetes	Venturiales	Sympoventuriaceae	Ochroconis	Positive
Eukaryota	Ascomycota	Dothideomycetes	Venturiales	Sympoventuriaceae	Ochroconis	Positive

Appendix S14 : Table S5. Direct association between *Pseudomonas* and *Ochroconis* genera according to the rock surface conditions. The % interaction of *Pseudomonas* (or *Ochroconis*) is obtained by dividing the number of associations by the number of OTUs affiliated to *Pseudomonas* (or *Ochroconis*) from each rock surface condition.

Type of association	Rock surface condition	Genus	Species	OTU	Link type	% interaction (Number of associations/Number of OTUs)
Association with *Pseudomonas*	Distal unmarked surface	*Ochroconis*	Unidentified	OTU 1	Negative	75% (6/8)
		Ochroconis	Unidentified	OTU 45	Negative	
		Ochroconis	*Ochroconis minima*	OTU 38	Positive	
		Ochroconis	Unidentified	OTU 57	Positive	
		Ochroconis	Unidentified	OTU 76	Positive	
		Ochroconis	Unidentified	OTU 123	Positive	
	Proximal unmarked surface	*Ochroconis*	Unidentified	OTU 1	Positive	62% (5/8)
		Ochroconis	Unidentified	OTU 45	Positive	
		Ochroconis	*Ochroconis minima*	OTU 38	Positive	
		Ochroconis	Unidentified	OTU 57	Positive	
		Ochroconis	Unidentified	OTU 123	Positive	
	New dark zone	*Ochroconis*	Unidentified	OTU 1	Positive	33% (2/6)
		Ochroconis	Unidentified	OTU 57	Positive	
	Intermediate dark zone	*Ochroconis*	*Ochroconis minima*	OTU 38	Negative	25% (2/8)
		Ochroconis	Unidentified	OTU 392	Positive	
	Old dark zone	*Ochroconis*	*Ochroconis minima*	OTU 38	Negative	25% (2/8)
		Ochroconis	Unidentified	OTU 392	Positive	
Association with *Ochroconis*	Distal unmarked surface	*Pseudomonas*	Unidentified	OTU 1	Negative	26% (5/19)
		Pseudomonas	Unidentified	OTU 7	Negative	
		Pseudomonas	Unidentified	OTU 8	Negative	
		Pseudomonas	Unidentified	OTU 75	Positive	
		Pseudomonas	Unidentified	OTU 165	Positive	
	Proximal unmarked surface	*Pseudomonas*	Unidentified	OTU 212	Positive	20% (4/20)
		Pseudomonas	Unidentified	OTU 389	Positive	
		Pseudomonas	Unidentified	OTU 426	Positive	
		Pseudomonas	Unidentified	OTU 475	Positive	
	New dark zone	*Pseudomonas*	Unidentified	OTU 7	Negative	16% (3/18)
		Pseudomonas	Unidentified	OTU 654	Positive	
		Pseudomonas	Unidentified	OTU 562	Positive	
	Intermediate dark zone	*Pseudomonas*	Unidentified	OTU 1437	Positive	12% (1/8)
	Old dark zone	*Pseudomonas*	Unidentified	OTU 764	Positive	11% (1/9)

Appendix S15 : Table S6. Model fit comparison of the neutral, binomial and Poisson models for each rock surface condition and the three domains of life. m : estimated migration rate ; Rsqr : R square ; AIC : Akaike Information Criterion ; BIC : Bayesian Information Criterion.

Domain	Rock surface condition	*m*	Rsqr neutral	Rsqr binomial	Rsqr Poisson	AIC neutral	BIC neutral	AIC binomial	BIC binomial	AIC Poisson	BIC Poisson
Bacteria	Distal unmarked surface	0.023	0.302	NA	-0.430	223.0	229.9	NA	NA	161.9	168.9
	Proximal unmarked surface	0.021	0.330	NA	-0.519	219.8	226.7	NA	NA	179.6	186.4
	New dark zone	0.013	0.445	NA	-0.985	43.70	50.28	NA	NA	122.7	129.2
	Intermediate dark zone	0.044	0.391	NA	-0.065	76.85	83.44	NA	NA	80.77	87.36
	Old dark zone	0.032	0.289	NA	-0.287	121.8	128.64	NA	NA	118.1	124.8
Archaea	Distal unmarked surface	0.15	0.155	-0.285	-0.285	0.191	-1.991	6.774	7.904	6.769	7.899
	Proximal unmarked surface	0.169	0.714	-0.736	-0.735	-20.85	-19.19	-0.300	1.366	-0.309	1.356
	New dark zone	0.153	0.891	-0.663	-0.662	-33.12	-31.57	-4.177	-2.632	-4.188	-2.642
	Intermediate dark zone	0.692	0.352	0.501	0.502	1.308	2.586	-3.441	-2.162	-3.446	-2.168
	Old dark zone	0.229	0.739	-0.306	-0.305	-11.88	-10.60	-1.859	-0.581	-1.865	-0.587
Micro-eukaryotes	Distal unmarked surface	0.123	0.452	-0.311	-0.311	11.95	18.52	46.07	52.64	46.06	52.63
	Proximal unmarked surface	0.187	0.482	-0.052	-0.052	-0.275	6.218	11.47	17.97	11.47	17.96
	New dark zone	0.010	0.434	-2.759	-2.759	-4.015	2.109	59.68	65.80	59.67	65.80
	Intermediate dark zone	0.099	0.561	-1.508	-1.508	50.92	56.79	70.43	76.30	70.43	76.30
	Old dark zone	0.012	0.398	-2.400	-2.40	6.113	12.32	79.31	85.52	79.30	85.52

Article 3. Dark-zone alterations expand throughout Paleolithic Lascaux Cave despite spatial heterogeneity of the cave microbiome

ZELIA BONTEMPS[1], ALICE GUILLMOT[1], MYLENE HUGONI[1,2,3] AND YVAN MOENNE-LOCCOZ[1]

[1]Univ Lyon, Université Claude Bernard Lyon 1, CNRS, INRAE, VetAgro Sup, UMR Ecologie Microbienne, F-69622 Villeurbanne, France
[2]Univ Lyon, Université Claude Bernard Lyon 1, CNRS, INSA de Lyon, UMR Microbiologie Adaptation et Pathogénie, F-69622 Villeurbanne, France
[3] Institut Universitaire de France (IUF)

Current address for Mylène Hugoni : Univ Lyon, INSA Lyon, CNRS, UMR 5240 Microbiologie Adaptation et Pathogénie, F-69621 Villeurbanne, France

Corresponding author
Yvan MOENNE-LOCCOZ
Univ Lyon, Université Claude Bernard Lyon 1, CNRS, INRAE, VetAgro Sup, UMR5557 Ecologie Microbienne, 43 bd du 11 novembre 1918, F-69622 Villeurbanne, France
yvan.moenne-loccoz@univ-lyon1.fr

Abstract

Cave anthropization related to rock art tourism can lead to cave microbiota imbalance and microbial alterations threatening Paleolithic artwork, but the underpinning microbial changes are poorly understood. In heterogeneous caves, certain rock wall alterations develop in different rooms despite probable spatial heterogeneity of the cave microbiome, raising the possibility that a same surface alteration can involve cosmopolitan taxa as well as taxa endemic to each cave room. We tested this hypothesis in Lascaux, by comparing recent alterations (dark zones) and nearby unmarked surfaces in nine locations within the cave. Illumina MiSeq metabarcoding of unmarked surfaces confirmed microbiome heterogeneity. The microbial communities of unmarked and altered surfaces differed at each location. The use of a decision matrix showed that microbiota changes relation to dark zone formation could differ according to location, but dark zones from different locations displayed microbial similarities. Thus, dark zones harbor Lascaux-cosmopolitan bacterial and fungal taxa as well as dark zone-specific taxa present at all locations (especially bacteria) or at particular locations within Lascaux. This probably explains why dark zones could form in various areas of the cave and suggests that the spread of these alterations might continue according to the area of distribution of cosmopolitan taxa.

Key words

Lascaux Cave ; Cave alteration ; Decisional matrix ; Anthropization ; Unbalanced microbiota ; Dark zones

Introduction

Karst environments have attracted tourist interest for several centuries, especially when caves harbor Paleolithic art forms (Cigna, 2016). Rock art tourism has intensified in the last century and has significantly altered environmental conditions in several underground systems. The impact of tourism results from the initial opening of the caves to the outside environment (initiation of air exchange) as well as the developments implemented to facilitate tourism, such as floor excavations (e.g. King Salomon Cave in Tasmania and Lascaux Cave in France), installation of air management machinery (operated from 1958 to early 2015 in Lascaux Cave), stairs, concrete paths, and artificial light (Brunet et al., 1987 ; Dupont et al., 2007 ; Russell and MacLean, 2008 ; Bastian et al., 2010 ; Martin-Sanchez et al., 2015 ; Bontemps et al., 2021). Visitors themselves can cause strong environmental imbalance in karst ecosystems, with an increase in temperature ($\pm$ 0.20°C in Tito Bustillo cave in Spain and $\pm$ 1.5°C in Lascaux Cave compared with the original temperatures ; (Cañveras, 2001 ; Dupont et al., 2007)), CO_2 concentrations and water vapor levels (Cañveras, 2001 ; Russell and MacLean, 2008 ; Fabiola Bastian et al., 2009 ; Diaz-Herraiz et al., 2014). As a result, the ecological disturbance suffered by show caves has impacted the structure, species richness and functioning of microbial communities (Ikner et al., 2007 ; Alonso et al., 2019 ; Bontemps et al., 2021).

Cave microbiota imbalance due to anthropization can cause microbial alteration of rock surfaces, which may threaten Paleolithic artwork. These alterations include (i) biodeterioration of the walls (implicating e.g. Actinobacteria and Ascomycota phyla) (He et al., 2022), (ii) Lampenflora related to light systems, which is mainly composed of Cyanobacteria, Chysophytes and algae (Chlorophyta), and termed green disease in the 1960s in Lascaux (Lefèvre, 1974 ; Bastian and Alabouvette, 2009 ; Baquedano Estévez et al., 2019), (iii) the development of calcite veil, possibly involving bacterial genera such as *Pseudomonas*, *Bacillus* and *Myxococcus* and masking art on the walls of the Great cave of Arcy-sur-Cure in France (Chalmin et al., 2007), (iv) gypsum efflorescence (Lepinay et al., 2018) and (v) stains of different colors e.g. white, yellow and gray stains in Altamira Cave (Spain) (Portillo et al., 2008 ; Portillo and Gonzalez, 2010), red stains attributed to the outgrowth of bacteria (e.g. Xanthomonodales, *Thauera*, etc.) and fungi (e.g. *Exophiala*, *Acremonium*, etc.)(Portillo et al., 2008 ; Bontemps et al., 2021) in the Cave of Bats (Spain) (Urzì et al., 2010), white stains caused by *Fusarium solani* early 2001 (Bastian et al., 2010) and black stains (termed black disease) since the end of 2001 and attributed to black melanized fungi such as *Ochroconis lascauxensis* (Bastian et al., 2010) in Lascaux Cave. In several caves, stain mitigation was attempted by spraying antibiotics and chemical treatments (e.g. benzalkonium chloride) on cave walls, which can accentuate further the imbalance of the cave microbiota as found in Lascaux (Bastian et al., 2010 ; Martin-Sanchez et al., 2015). In the case of Lascaux Cave, the most recent surface alteration, termed dark zone, has developed in the Apse room over the past 15 years (Alonso et al. submitted, Bontemps et al. *in prep*).

Lascaux Cave is a model of particular interest, as it is arguably the most anthropized Paleolithic cave, and knowledge on surface alteration processes there can provide baseline information for the understanding and management of Paleolithic caves elsewhere. Among surface alterations, dark zones are the main threats currently as they keep growing, at the rate of a few cm each year. In comparison with unaltered surfaces, dark zones showed differences in the rela-

tive abundance of many genera, as *Ochroconis* fungi proliferate and *Pseudomonas* bacteria are counter-selected (Alonso et al. submitted). These changes are concomitant with the development of Bacteroidota and the bacterial genus *Labrys* (among others) from the onset of dark zone formation (Bontemps et al. *in prep*). These findings point towards a brutal community switch in relation to dark zone formation, with rapid microbial successions leading to variations in microbial diversity and interaction networks (Bontemps et al. *in prep*).

Till recently, Lascaux's dark zones were thought to be restricted to the Apse. However, close monitoring in several other rooms of the cave (e.g. Nave, Passage, Hall of Bulls, etc.) evidenced visual changes resembling those of the Apse's dark zones on several rock walls (as well as on artificial limestone walls built to organize visits), leading to the hypothesis that similar microbiota changes (associated to dark zone formation) could be taking place in these different rooms. Yet, previous results showed that Lascaux's microbiota was spatially heterogeneous when comparing different surfaces within a room (Alonso et al., 2018) or a same type of surface in two different rooms (Alonso et al., 2019), despite strong uniformity of climatic conditions. This probably applies at a wider scale within Lascaux (and other caves), and it raises the hypothesis that at least part of the changes in microbial community related to the formation of dark zones are room or surface specific, in line with microbiota specificities of the different rooms or surfaces.

The objective of this study was to assess microbiota particularities of cave wall alterations in heterogeneous caves, using the model case of dark zone alterations in Lascaux Cave. First, we compared the microbial communities of unmarked limestone surfaces in nine areas of the cave. Second, we explored the microbial communities associated to dark zones in these nine areas, in comparison with the corresponding communities of unmarked surfaces nearby. Third, we assessed using a decisional matrix the level of similarity of the different dark zones relatively to the reference situation of the Apse, where dark zones appeared first and have already been characterized. Fourth, we investigated to which extent the formation of dark zones involved microbial proliferation, based on qPCR and (where permitted) scanning electron microscopy.

Materials and Methods

Sample collection

Lascaux Cave is located near Montignac in Périgord, South-West France (N 45°03'13.087" and E 1°10'12.362"). Touristic visits were stopped in 1963. Human presence is now highly restricted and restrained to scientific campaigns and official visits. The upper inclined plane at the left side of the Apse (hereafter termed 'Apse') was selected for reference sampling due to the first identification of a dark zone in June 2008 (based on photographic archives).

Other dark zones, similar to Apse's dark zones, were sampled in eight other different areas (Figure 1A), i.e. (i) two natural calcareous surfaces in the upper inclined planes (hereafter termed 'Nave high') and the low vertical wall ('Nave low') of the right side of the Nave (dark zones first noticed in July 2011 for both), (ii) four masonry benches made of local limestone particles and mortar, in the vertical part ('Passage vertical'; dark zones first noticed in September 2016) and the horizontal part ('Passage horizontal'; dark zones first noticed in March 2016) of the left bench (built in 1957 and modified in 1963) at the end of the Passage, and the vertical parts of the left bench ('Bulls left'; built in 1957-1958) and central bench ('Bulls center'; built in

1947-1948) at the back of the Hall of the Bulls (dark zones first noticed in April 2016 for both), and (iii) the two sides of the left stone wall (built in 1957-1958 using Santonian limestone blocks from a local quarry, with joints made of sand mixed with lime and/or cement) separating the Hall of the Bulls and the Airlock-2 entrance zone ('Airlock-2 wall' and 'Bulls wall' ; dark zones first noticed in October 2016 and June 2013, respectively) (Figure 1B). All areas sampled had received chemical treatments in the past, but none since the formation of dark zones.

Sampling of the nine areas for molecular analyses was performed in September 2020, using sterile swabs. Samples (n = 6 for each condition) were placed immediately into liquid nitrogen and later transferred at -80°C until DNA extraction. For electron microscopy, samples were taken in March 2021 with a small chisel, and authorization for sampling was granted only for masonry benches. Bulls center and Passage vertical were studied, and samples were placed in tubes containing 0.1M sodium cacodylate buffer with 2% glutaraldehyde and kept à 4°C.

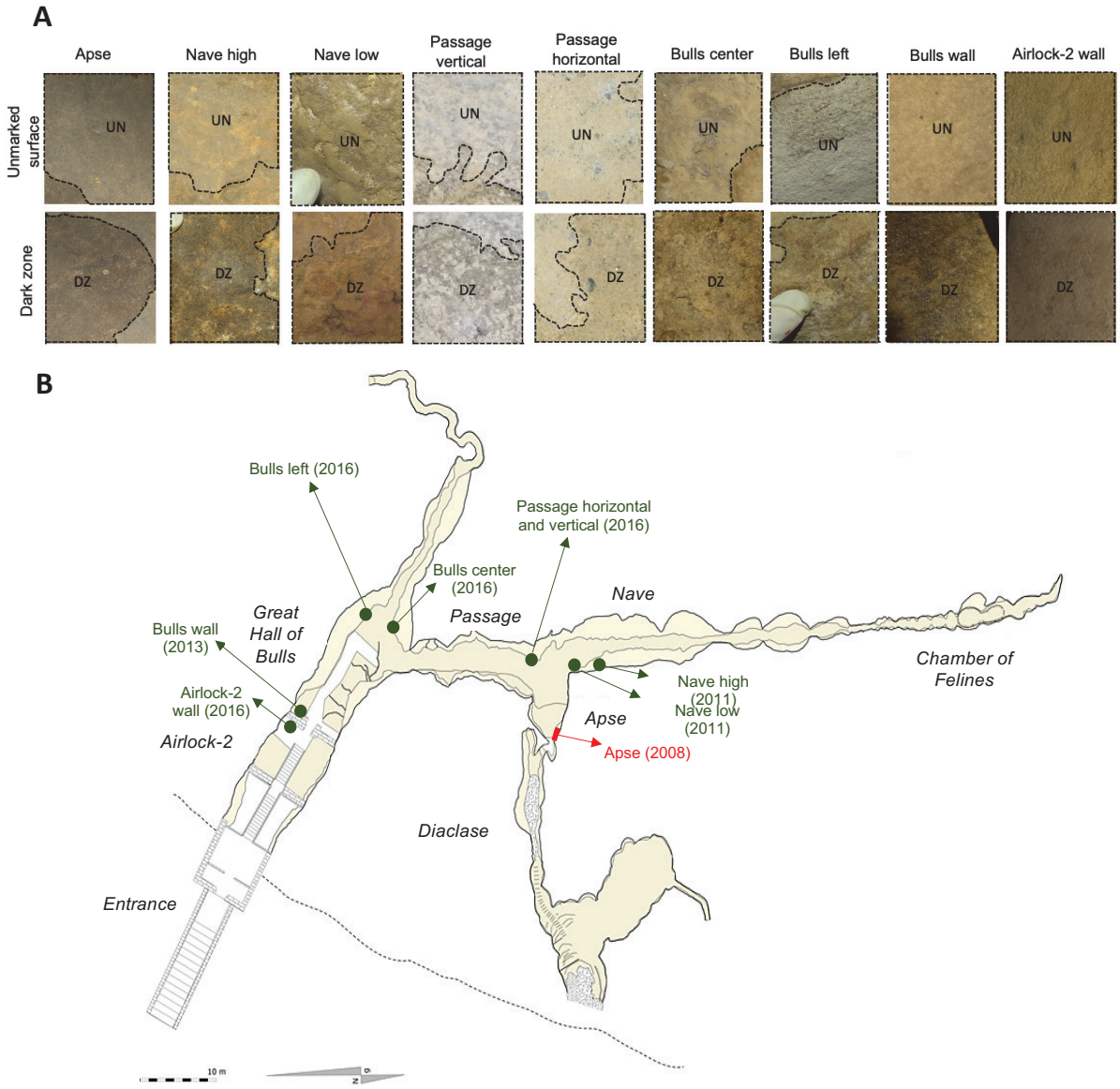

Figure 1. Map of Lascaux Cave with location of the dark zones studied (A) and photographs of dark zones sampled. In (B), the reference situation in the Apse in indicated in red, and the others in dark green (source of the map : S. Konik, Centre National de la Préhistoire). The year in which dark zones were first noticed is indicated in parenthesis.

DNA extraction and high-throughput sequencing

Extraction of total genomic DNA was carried out with the FastDNA SPIN kit for Soil (MP Biomedicals, Illkirch, France), following the manufacturer's instructions. The lysis solution was added to the tube containing the sample matrix. Elution was performed using 80 µl volume for each sample, and the final DNA concentration was measured using the Qubit dsDNA Hs Assay Kit (Invitrogen, Carlsbad, USA) following the manufacturer's instructions. The DNA extracts were kept at -20°C.

Three gene markers were analyzed in each sample. The V3-V4 region of the 16S rRNA genes was amplified for Bacteria and Archaea using the universal primers 341F/805R (Herlemann et al. 2011) and 515F/915R (Herfort et al. 2009), respectively. The fungal ITS2 region was amplified using the universal primers ITS3 KYO2/ITS4 (Toju et al. 2012) (Supplementary Table S1). The PCR mix consisted in 5 µl of 5X Hot BioAmp Blend Master Mix RTL (Biofidal, Vaulx-en-Velin, France), 0.1 μM of each primer, 0.1X of GC-rich-enhancer (Biofidal), 0.2 ng.μl^{-1} of Bovine Serum Albumin (Promega, Madison, USA) and 0.2-1.0 ng of template DNA. All amplifications were performed in triplicate, in a Bio-Rad T1000 thermal cycler (Bio-Rad, Hercules, USA). The PCR program for Bacteria was 3 min at 95°C, 28 cycles of 45 s at 95°C, 45 s at 50°C and 90 s at 72°C, followed by 7 min at 72°C. For Archaea, it consisted in 10 min at 94°C, 30 cycles of 1 min at 94°C, 1 min at 58°C and 90 s at 72°C, followed by 10 min at 72°C. For Fungi, PCR was done with 10 min at 95°C, 28 cycles of 20 s at 94°C, 30 s at 47°C and 20 s at 72°C, followed by 7 min at 72°C. Primers were tagged with the Illumina adapters TCG TCG GCA GCG TCA GAT GTG TAT AAG AGA CAG and GTC TCG TGG GCT CGG AGA TGT GTA TAA GAG ACA G, enabling a two-step PCR construction of amplicon libraries. DNA extraction was also carried out without any biological matrix and this was considered a negative control to evaluate ambient contamination. Amplicons were checked by electrophoresis on 1.5% agarose 20 min at 100 V and UV visualization, and the correct lengths were obtained with samples (and no signal with the blanks, as expected). Illumina MiSeq (2 x 300 bp, paired-end chemistry v3) was done after pooling PCR triplicates, and was performed by Biofidal, aiming (for each sample) at 40,000 sequences for the bacterial 16S rRNA gene and the ITS, and 70,000 sequences for the archaeal 16S rRNA gene.

Bioinformatic treatment of Illumina sequence data

For each of the three datasets (i.e. bacterial 16S rRNA genes, archaeal 16S rRNA genes and fungal ITS2), paired-end reads were demultiplexed in the different samples according to exact match adaptors (subsequently removed). The reads obtained were merged using Fast Length Adjustment of Short reads (FLASh) (Magoc and Salzberg 2011), based on a maximum of 10% mismatches in the overlap region. Denoising was carried out by discarding reads without the expected 200-500 bp length or that displayed ambiguous bases (N). Once sequence dereplication was done, clusterization was performed using SWARM (Mahé et al. 2014), based on a local clustering threshold (rather than a global threshold) and an aggregation distance of 3 for identification of operational taxonomic units (OTUs). Chimeric OTUs were discarded using VSEARCH (Rognes et al. 2016) and sequences of low abundance were filtered at 0.005% of all sequences (Bokulich et al. 2013). OTU affiliation was carried out with both RDP Classifier and BLASTn

(Zhang and Madden 1997) against the 138.1 SILVA database (Quast et al. 2013) for bacterial and archaeal 16S rRNA genes and the 8.2 UNITE database for fungal ITS markers (Nilsson et al. 2019), which was automated in the FROGS pipeline (Escudié et al. 2018). Contaminant OTUs identified from the negative controls (blanks) samples were removed. Normalization for sample comparison was implemented by randomly resampling down to 13,467 and 12,753 sequences in the bacterial and fungal datasets, respectively, whereas the archaeal dataset was not normalized due to very low numbers of reads in dark zones.

Quantitative PCR

To assess the numbers of bacterial 16S rRNA gene, archaeal 16S rRNA gene and fungal ITS2 region, quantitative PCR (qPCR) was performed using primers 519F (5'-CCGTCAATTCMTTTR AGTTT-3') / 907R (5'-AAGGAAGGCAGCAGGCG-3') (Laiz et al. 2003), 787F (5'- ATTA-GATACCCSBGT AGTCC-3') / 1059R (5'- GCCATGCACCWCCTCT-3') (Nehmé et al. 2009) ITS7F (5'-GTGYCAGCMGCCGCGGGTA-3') / ITS4R (5'-TCCTCCGCTTATTGATATGC-3') (Hugoni et al. 2018), respectively. Briefly, qPCR assays were conducted using 10 µL of LightCycler 480 SYBR Green I Master mix, 2 μL of sample DNA, 2 μL (final concentration 0.3 μM) of each primer in a final volume of 20 μL, with a thermocycling CFX-96 Connect (Biorad, California). PCR was done with denaturation at 95°C for 10 min, followed by 40 cycles of 15 s (bacteria) or 30 s (fungi) denaturation at 95°C, hybridization 60 s at 63°C (bacteria) or 45 s at 57°C (fungi), and 30 s (bacteria) or 90 s (fungi) elongation at 72°C. For archaea, PCR was done with denaturation at 37°C for 10 min and 95°C for 15 min, followed by 45 cycles of 15 s denaturation at 95°C and 60 s hybridization at 60°C. Melting curve calculation and Tm determination were done using the Tm Calling Analysis module of CFX Maestro Software v 2.3 (Biorad, California).

Definition of dark zone reference criteria based on Apse data

For the three domains of Life, a range of criteria were defined for subsequent quantification of similarity level with the Apse's dark zones. First, genus-centered criteria were computed for bacteria and fungi, as follows. For the Apse's dark zone and control, the mean numbers of reads for individual genera were log transformed, and the variation in relative abundance between limestone (control) and dark zone was calculated as Δlog = log(control) - log(dark zone). All taxa with a Δlog value > 1 or < -1 (arbitrarily-chosen thresholds) were selected as reference criteria, making 41 reference taxa. Second, the number of reads for archaea were log-transformed, and the variation between control and dark zone was calculated as Δlog = log(control) - log(dark zone). Third, the Bray-Curtis distance between control and dark zone was calculated separately for Bacteria and Fungi. Fourth, qPCR levels for bacteria, archaea and fungi (expressed as numbers of gene copies per ng of extracted DNA) were also used.

Construction of the decision matrix

To determine the extent to which dark zones from different Lascaux rooms correspond to those present in the Apse, a decision matrix was built on the basis of the reference criteria defined

above, using data from each dark zone studied (and its corresponding control). Computation was done as follows (illustrated in Figure 2 for *Ochroconis* and *Pseudomonas* genera). First, for each of the 41 reference taxa, the Δlog value was computed (Supplementary Table S2), and the fold change value between this Δlog value and the corresponding Δlog value for the Apse (i.e., ΔFold-change) was scored as 1 (when |Δfold change| was below one tenth of the Δlog value for the Apse), 0.9 (when |Δfold change| was between one and two tenths of the Δlog value for the Apse), . . ., 0.1 (when |Δfold change| was between eight and nine tenths of the Δlog value for the Apse) and 0 (when |Δfold change| was above nine tenths of the Δlog value for the Apse) (Figure 2). The comparisons were implemented using a script in Python version 3.10.1 (Van Rossum and Drake, 2009). Second, the same approach was followed with the number of archaeal reads. Third, for the criterion based on the Bray-Curtis distance (computed with 'vegdist' package in R ; (Oksanen et al., 2020) a measurement of the difference between the Apse and each of the other situations studied was done, by computing α = Bray-Curtis distance between the controls in the Apse and the controls in the other sampling areas, β = Bray-Curtis distance between the dark zones in the Apse and the dark zones in the other sampling areas, and $(\beta - \alpha) \div \alpha$ representing the differential dark zone evolution between the Apse and the other sampling areas. On this basis, a decimal score was obtained, ranging from 1 (when $(\beta$ - $\alpha) \div \alpha < 0.1$) to 0 (when $(\beta$ - $\alpha) \div \alpha > 0.9$). Finally, the sum of the 44 scores was computed.

Statistical analysis

The efficacy of sampling and sequencing was evaluated using rarefactions curves. Alpha diversity at OTU level was measured with Chao-1 index (Chao, 1987), Shannon's H' index (Shannon, 1948) and Simpson 1-D index (Simpson, 1949), using Paleontological Statistics (PAST) software (version 4.04) (Hammer et al., 2001). The diversity indices were assessed with Kruskal-Wallis tests and post-hoc Wilcoxon pairwise tests, or with ANOVA and post-hoc Tukey-HSD using 'vegan' package in R (version 4.0.3) (Oksanen et al., 2020). Comparison of microbial communities was done by non-metric multidimensional scaling (NMDS), which was performed using 'phyloseq' package in R (McMurdie and Holmes, 2013 ; Husson et al., 2020 ; Kassambara and Mundt, 2020). Replicates of each situation (i.e. room and rock surface condition) were grouped into one condition, and NMDS was vectorized from unmarked surface (control) to altered surface (dark zone), which was done using 'phyloseq', 'vegan' and 'dplyr' package in R (McMurdie and Holmes, 2013 ; Oksanen et al., 2020 ; Wickham et al., 2021). The stress value was calculated to measure the difference between the ranks on the ordination configuration and the ranks in the original similarity matrix for each replicate. Stress values below 0.1 are considered without risk and those not exceeding 0.2 are acceptable (Clarke, 1993). Then, analysis of variance using distance matrices (Adonis) was performed using 'vegan' and 'pairwiseAdonis' packages, to assess differences at $P < 0.05$ and at $P < 0.10$ in overall microbial community composition. A Holm-Bonferroni correction was applied on P values to lower alpha risk. All statistical analyses were performed using R software (version 4.0.3) (R Core Team, 2020).

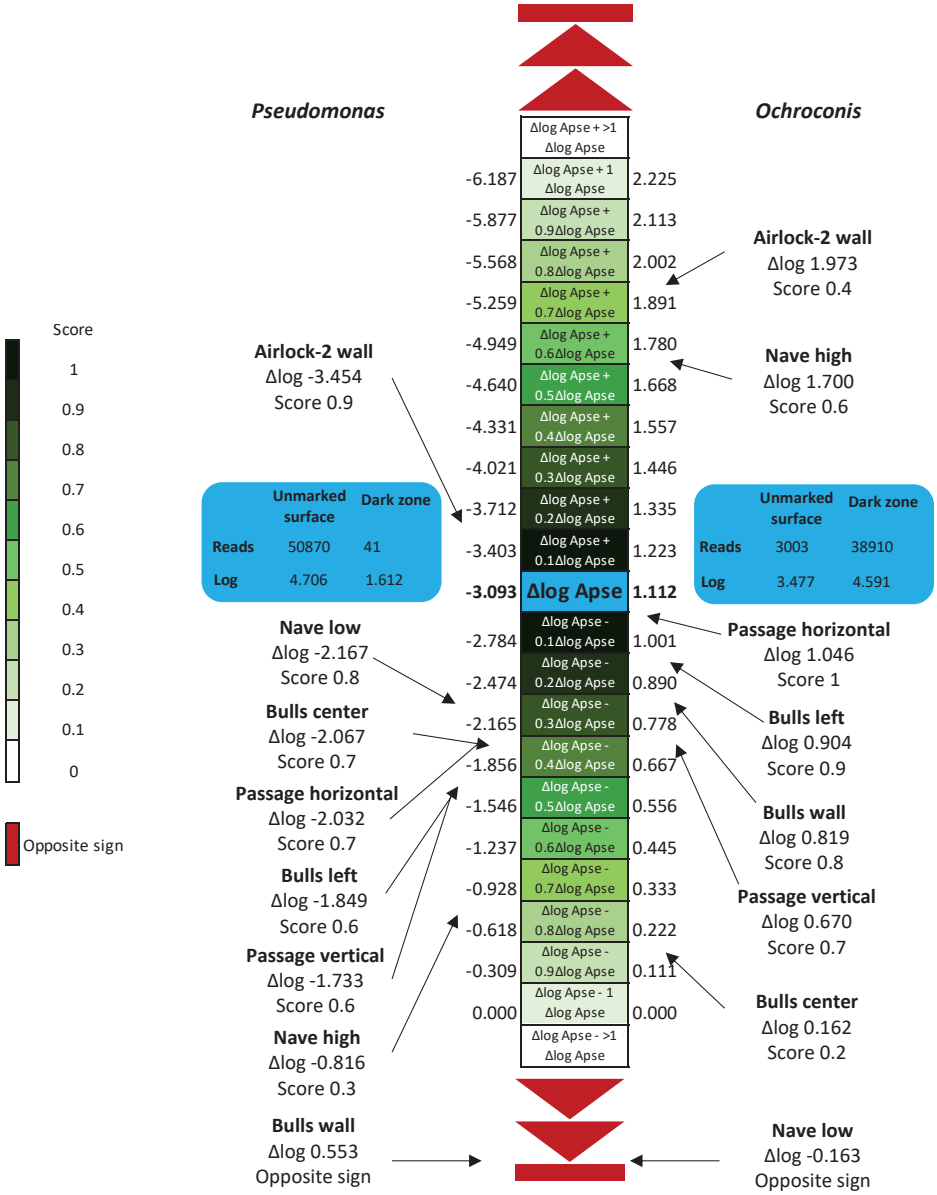

Figure 2. Determination of the scores assigned for each similarity criterion based on their Δlog values (Δlog = log(control) - log(dark zone)) with the data obtained for the Apse reference situation (in blue). The data (higher or lower) obtained for the other dark zones are positioned according to the different intervals of values, each corresponding to a given scale of gap with the Apse reference situation, resulting into a score between 0 and 1 (with increments of 0.1, according to the green gradient), whereas data for which the gap falls outside of the scale or with an opposite sign are represented in red. The Δlog value are computed, and the fold change value between this Δlog value and the corresponding Δlog value for the Apse (i.e., ΔFold-change) is scored as 1 (when |Δfold change| is below one tenth of the Δlog value for the Apse), 0.9 (when |Δfold change| is between one and two tenths of the Δlog value for the Apse), . . ., and 0 (when |Δfold change| is above nine tenths of the Δlog value for the Apse). Δlog values and score assignations are illustrated for *Ochroconis* and *Pseudomonas* criteria in all sample locations.

Scanning electron microscopy

Glutaraldehyde-fixed samples were serially washed in 0.1M sodium cacodylate baths over two days, and were dehydrated using ethanol solutions at 30%, 50%, 70%, 80%, 95% (30 min each), and 100% ethanol (three times 30 min). The samples were placed in a mixture of 50% ethanol and 50% hexamethyldisilazane for 30 min and again for 60 min (twice), and in 100% hexame-

thyldisilazane overnight, till total evaporation was achieved. The samples were then metalized with carbon and analyzed by Scanning Electron Microscopy (SEM) using a FEG FEI Quanta 250 SEM microscope equipped with an Everhart-Thornley Detector (ETD, secondary electrons).

Results

Microbial community structure on unmarked rock surfaces

NMDS and ANOSIM tests indicated that the effect of the sampling location on community structure was significant on unmarked surfaces for bacteria ($P = 0.001$, $R^2 = 0.70$, Figure 3A) and fungi ($P = 0.007$, $R^2 = 0.63$, Figure 3B), meaning that Lascaux's microbiota is spatially heterogeneous (Supplementary Table S3).

For bacteria on unmarked surfaces, Bulls left ($R^2 = 0.60$), Bulls wall ($R^2 = 0.51$) and Nave low ($R^2 = 0.47$) showed significant differences compared with the Apse ($P = 0.036$) (Supplementary Table S3). Bacterial communities were different between Passage horizontal and Passage vertical ($P = 0.036$, $R^2 = 0.28$), but significance level was only $P = 0.072$ for Bulls wall compared with Airlock-2 wall ($R^2 = 0.41$), Nave low ($R^2 = 0.44$) and Passage horizontal ($R^2 = 0.52$).

For fungi on unmarked surfaces, the Apse differed from Bulls wall ($P = 0.036$, $R^2 = 0.53$) but but significance level was only $P = 0.072$ for the Apse vs Airlock-2 wall ($R^2 = 0.46$). In addition, there was also a trend ($P = 0.072$) for a difference between Bulls center and Nave high ($R^2 = 0.54$), Passage horizontal ($R^2 = 0.38$), Passage vertical ($R^2 = 0.37$) and Airlock-2 wall ($R^2 = 0.71$) (Supplementary Table S3).

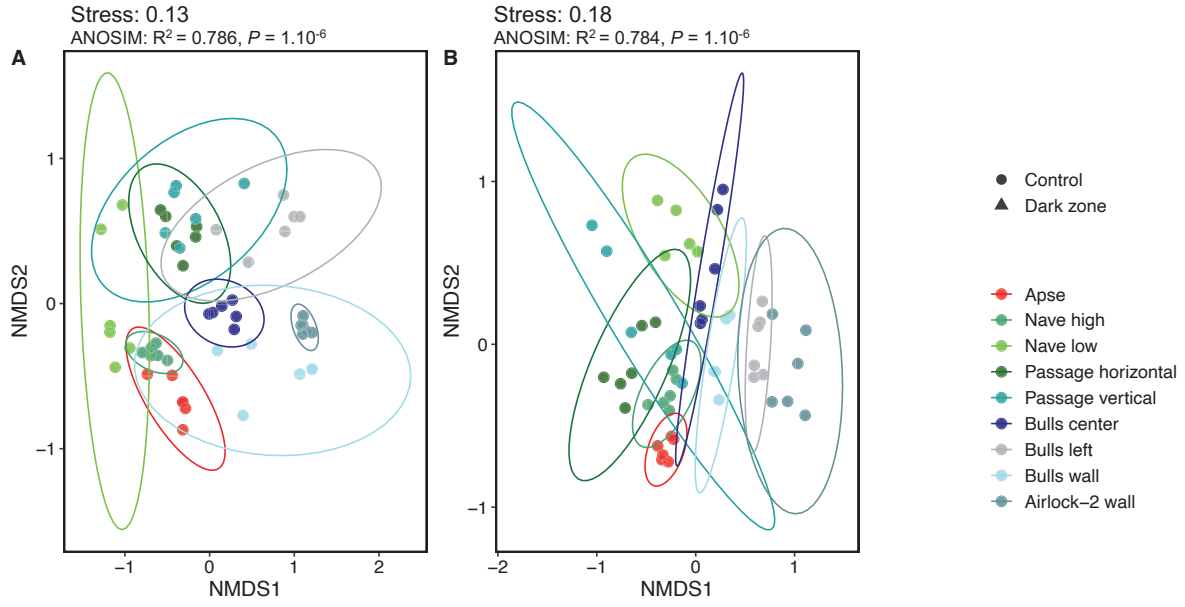

Figure 3. Non-metric multidimensional scaling (NMDS) analysis of microbial community structure in unmarked surfaces of Lascaux Cave according to sampling position (i.e. location in the cave). Ellipses (95% confidence intervals) indicate the different sampling positions for bacterial (A) and fungal (B) communities.

Microbial community composition on unmarked rock surfaces

The bacterial community was composed from 16 to 24 classes (depending on location) on unmarked surfaces, with high variations for the most abundant classes Gammaproteobacteria (from 7.7% to 91.3%), Alphaproteobacteria (4.4%-51.0%) and Actinobacteria (2.8%-22.9%) (Figure 4A). Notably, the Apse differed from Passage vertical, Bulls left and Airlock-2 wall, as follows. The Actinobacteria amounted to 7.2% in the Apse versus 28.6% in Bulls left and 23.0% in Airlock-2 wall, and the Alphaproteobacteria to 14.0% versus 51.0% in Passage vertical, 26.0% in Bulls left and 31.6% in Airlock-2 wall. The Planctomycetes reached 5.75% and Acidimicrobiia 8.25% in Airlock-2 but lower values (<0.1-0.3%) and 0.1-2.2%, respectively) in the other locations, whereas the Gammaproteobacteria reached only 7.6% in Airlock-2 versus 37.1-91.3% elsewhere. The Bacteroidia accounted for 16.4% of sequences in Bulls left versus only <0.1-6.5% in the other locations, and the Bacili 3.1% in Bulls center versus <0.1-0.4% elsewhere.

The fungal community was composed from 12-17 classes on unmarked surfaces. The Sordariomycetes (51.3-76.2%), Eurotiomycetes (1.02-30.0%) and Leotiomycetes (0.09-25.0%) were the most abundant classes on all unmarked surfaces (Figure 4B). Compared with other locations, the reference area (Apse) and Nave displayed a lower proportion of Sordariomycetes (respectively 51.3% and 55.2%, versus 63.4-85.4% elsewhere) and higher proportions of Leotiomycetes (respectively 23.3% and 18.4%, versus <0.1-9.0%) and Dothideomycetes (respectively 4.4% and 3.0%, versus 0.1-1.8%). The Agaromycetes reached 8.1% and Mortierellomycetes 8.0% in Bulls wall but lower values (0.4-3.3% and <0.1-2.5%, respectively) in the other locations. Nave low and Bulls left showed a higher proportion of Eurotiomycetes (13.8% and 22.3%, respectively) compared with the other locations (0.9-8.4%). The Leotiomycetes accounted for 1.6% of sequences in Bulls wall and 0.09% in Airlock-2 versus 6.1-25.4% in the other locations, and the Saccharomycetes 8.0% in Nave low but only 0.1-1.6% elsewhere (Figure 4B).

Microbial community size on unmarked surfaces

The effect of sampling location on qPCR levels on unmarked surfaces differed for bacteria, archaea and fungi (Supplementary Table S4). For bacteria, community size in the Apse differed significantly from all other sample locations excepted Airlock-2 wall ($P = 0.42$). In addition, it also was different between Nave low and Nave right ($P = 0.001$), and between Passage vertical and Passage horizontal ($P = 0.001$). For archaea, community size was higher in the Apse than in all other sample locations (all $P = 0.001$). It also differed between each sample locations (all at $P \leq 0.001$) excepted between Nave high and Nave low ($P = 0.47$). For fungi, community size was lower in the Apse compared with all other sample locations (all at $P \leq 0.005$), and all sample locations differed from one another (all at $P \leq 0.001$).

Microbial community structure of dark zones compared with unmarked surfaces

NMDS and ANOSIM tests indicated that the effect of rock surface condition (control vs dark zone) on community structure was significant for bacteria ($P = 0.009$, $R^2 = 0.17$, Figure 5A) and fungi ($P = 0.009$, $R^2 = 0.08$, Figure 5B). The interaction between location in Lascaux Cave and rock surface condition was significant for bacterial ($P = 0.001$, $R^2 = 0.23$) and fungal

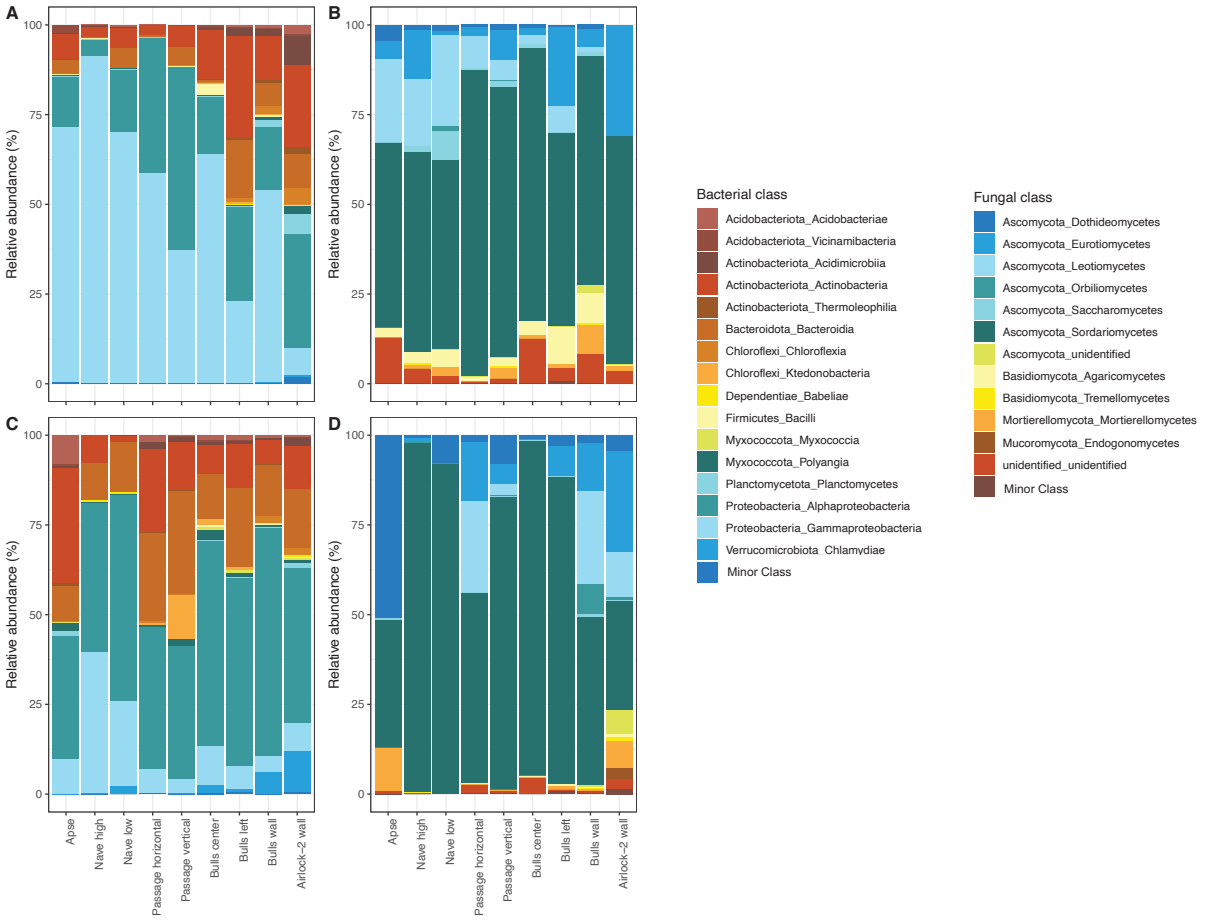

Figure 4. Relative abundance (% of sequences) of bacterial (A, C) and fungal (B, D) classes for the controls (A, B) and dark zones (C, D). Phyla or classes of relative abundance < 0.1% were considered as minor phyla or minor classes, respectively.

communities ($P = 0.001$, $R^2 = 0.18$) (Supplementary Table S5).

For both taxonomic markers, dark zones differed from their adjacent unmarked surfaces at each location in Lascaux Cave (Supplementary Table S5), and the interaction between location and rock surface condition was significant both for bacterial ($P = 0.001$, $R^2 = 0.23$) and fungal communities ($P = 0.001$, $R^2 = 0.18$). For the bacterial community, the difference between dark zone and control was the largest in the Apse ($P = 0.001$, $R^2 = 0.80$) and the smallest in Bull left ($P = 0.011$, $R^2 = 0.24$). For the fungal community, the difference between dark zone and control was of less significance in Passage horizontal ($P = 0.011$, $R^2 = 0.29$), Passage vertical ($P = 0.005$, $R^2 = 0.27$) and Airlock-2 ($P = 0.009$, $R^2 = 0.22$) than in other locations (all at $P = 0.003$, $R^2 = 0.39$-0.72).

Microbial community composition of dark zones compared with unmarked surfaces

Bacterial classes of Gammaproteobacteria, Alphaproteobacteria, Bacteroidia and Actinobacteria showed the most important variations (positive or negative) between unmarked and dark zone conditions overall (-40%, +23%, +12% and +1.8%, respectively) (Figure 4AC). When considering locations, the highest variation between unmarked and dark zone was observed for Gammaproteobacteria in the Apse (71.0% in dark zone vs 9.4% in the control), whereas this

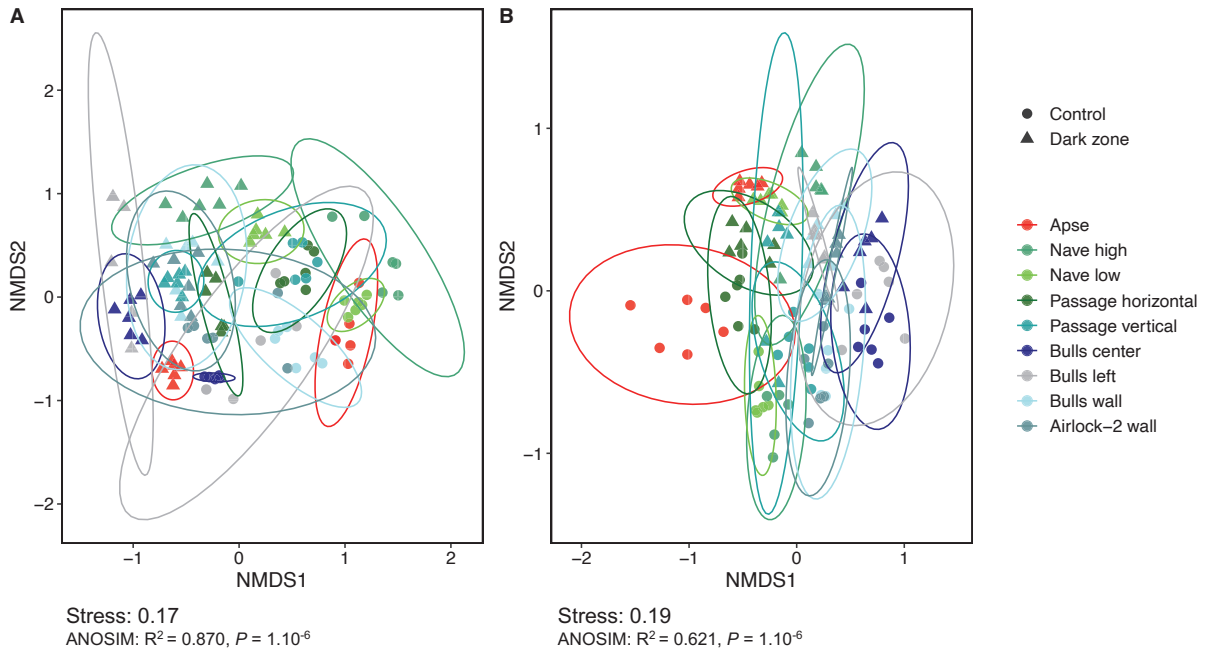

Figure 5. Non-metric multidimensional scaling (NMDS) analysis of microbial community structure in Lascaux Cave according both to sampling position (i.e. location in the cave) and rock surface condition (i.e. control or dark zone). Controls and dark zone are represented by circles and triangles, respectively. Ellipses (95% confidence intervals) indicate the different sampling positions for bacterial (A) and fungal (B) communities.

class reached similar levels in Airlock-2 wall (8.1% vs 7.6%, respectively) (Figure 4AC). The Alphaproteobacteria were at higher level in dark zone in Bulls wall (57.2% in dark zone vs 15.8% in the control), unlike in Passage vertical (37.1% in dark zone vs 50.9% in the control). The Bacteroidia displayed higher levels in dark zone compared with unmarked surface, notably in Passage horizontal (24.7% in dark zone vs 0.6% in the control) and Passage vertical (28.2% vs 5.1%, respectively), as found with the Chlamydiae in Bulls walls (2.1% in dark zone vs 0.1% in the control) and Airlock-2 wall (11.4% vs 0.5%, respectively). The Actinobacteria reached higher levels in dark zones in the Apse (32.1% in dark zone vs 7.2% in the control), Passage horizontal (23.1% vs 2.7%, respectively) and Passage vertical (13.5% vs 5.6%, respectively), but the opposite was found in Bulls left (8.1% in dark zone vs 13.6% in the control), Airlock-2 wall (12.3% vs 22.9%, respectively), Bulls wall (6.8% vs 12.4%, respectively) and Bulls center (12.1% vs 28.6%, respectively).

Variations (positive or negative) between dark zone and unmarked surface were of lower magnitude for fungal classes, the most important ones concerning the Dothideomycetes (+7.6%), Sordariomycetes (+4.2%), Agaromycetes (-3.8%) and Leotiomycetes (-2.9%) (Figure 4BD). Taking into consideration the various sampling locations within Lascaux, the Dothideomycetes were at higher level in dark zone in the Apse (50.9% in dark zone vs 4.4% in the control), unlike in Nave high (0.9% and 1.5%, respectively) (Figure 4BD). The Leotiomycetes were in higher amounts in dark zones for Passage horizontal (25.2% in dark zone vs 8.9% in the control), Bulls wall (26.1% vs 1.6%, respectively) and Airlock-2 wall (12.4% vs 0.1%, respectively), but the opposite was found for Apse (0.1% in dark zone vs 23.3% in the control), Nave high (0.2% vs 18.4%, respectively), Nave low (<0.1% vs 25.4%, respectively) and Bulls center (<0.1% vs 7.1%, respectively).

Microbial community size of dark zones compared with unmarked surfaces

qPCR levels for the bacterial community were significantly higher in dark zones compared with unmarked surfaces for all locations excepted Airlock-2 wall ($P = 0.49$) and Bulls left ($P = 0.47$) (Supplementary Table S6), while archaeal community size was higher in unmarked surfaces compared with dark zones for all sample locations (all at $P = 0.001$). Fungal community size was higher in dark zones compared with unmarked surfaces for all locations (all at $P \leq 0.001$) excepted in Bulls wall, where it was higher in unmarked surface compared with dark zone ($P = 0.003$).

The occurrence of microorganisms was further assessed based on scanning electron microscopy, at the only locations were we were allowed to take samples using a blade (small chisel). Bacteria or archaea could be seen outside of dark zones, essentially as individual cells, and a few filament were also found (illustrated in Figure 6A-D). In contrast, prokaryote cells were readily observed in dark zone samples, sometimes as individual cells or small clusters of a few cells, but more often as large clusters of many more cells (illustrated in Figure 6E-H). Filamentous microorganisms were seen. Filaments (putatively polysaccharides) were sometimes observed in the vicinity of microorganisms. Overall, qualitative observations of samples from Passage vertical and Bulls central supported the higher levels of bacteria and fungi in dark zones that were determined by qPCR.

Comparisons with reference dark zone from the Apse

When the decisional matrix was built to assess similarity level of various dark zones to the reference dark zone in the Apse, 5 of the 47 criteria (i.e. for the bacterial genera *Niabella, Steroidobacter, Acidothermus, Rhodopseudomonas* and fungal genus *Serendipita*) were scored 0 in all other dark zones whereas similarities were found for the 42 other criteria (Figure 7 ; Supplementary Table S8). When considering the three domains of Life together, Passage horizontal, Bulls center, Bulls left, Nave high and Passage vertical obtained global scores of respectively 18.9, 18.8, 17.6, 15.1 and 14.6 when adding positive scores for the 47 criteria, i.e. similarities of respectively 40.2%, 40.0%, 37.4%, 32.1% and 31.1% to the reference dark zone in the Apse based on the 47 criteria (Figure 7). Scores for Nave low, Airlock-2 wall and Bulls wall were only 11.8, 11.3 and 9.8, respectively, i.e. similarities of respectively 25.1%, 24.0% and 20.8%.

Some of the criteria are of particular interest, e.g. because they displayed large variations or were identified as potentially important to explain dark zone formation (Bontemps et al., *in prep*). For the bacterial community (Figure 7 ; Supplementary Table S8), the *Pseudomonas* genus was the bacterial criterion with the biggest variation in the Apse (Δlog Apse = -3.093) ; except for Bulls wall (opposite sign), all other dark zones showed also *Pseudomonas* counter-selection, with a score of 0.3 in Nave high to 0.9 in Airlock-2 wall (an average of 0.66). *Sphingopyxis* and *Afipia* genera displayed moderate variation in the Apse (Δlog Apse = 1.054 and 1.029, respectively), and the eight other dark zones had the same variation sign with high score 0.5 to 1 (excepted for Nave high with score of 0) and 0.6 to 1, respectively. For genera *Nonomuraea* (Δlog Apse = 1.652) and *Bryobacter* (Δlog Apse = 1.633), thought to play a role in dark zone evolution (Bontemps et al., *in prep*), we found (i) high scores in Nave high (1 and 0.5, respectively) and Passage horizontal (0.5 and 1, respectively), (ii) moderate scores in Bulls back

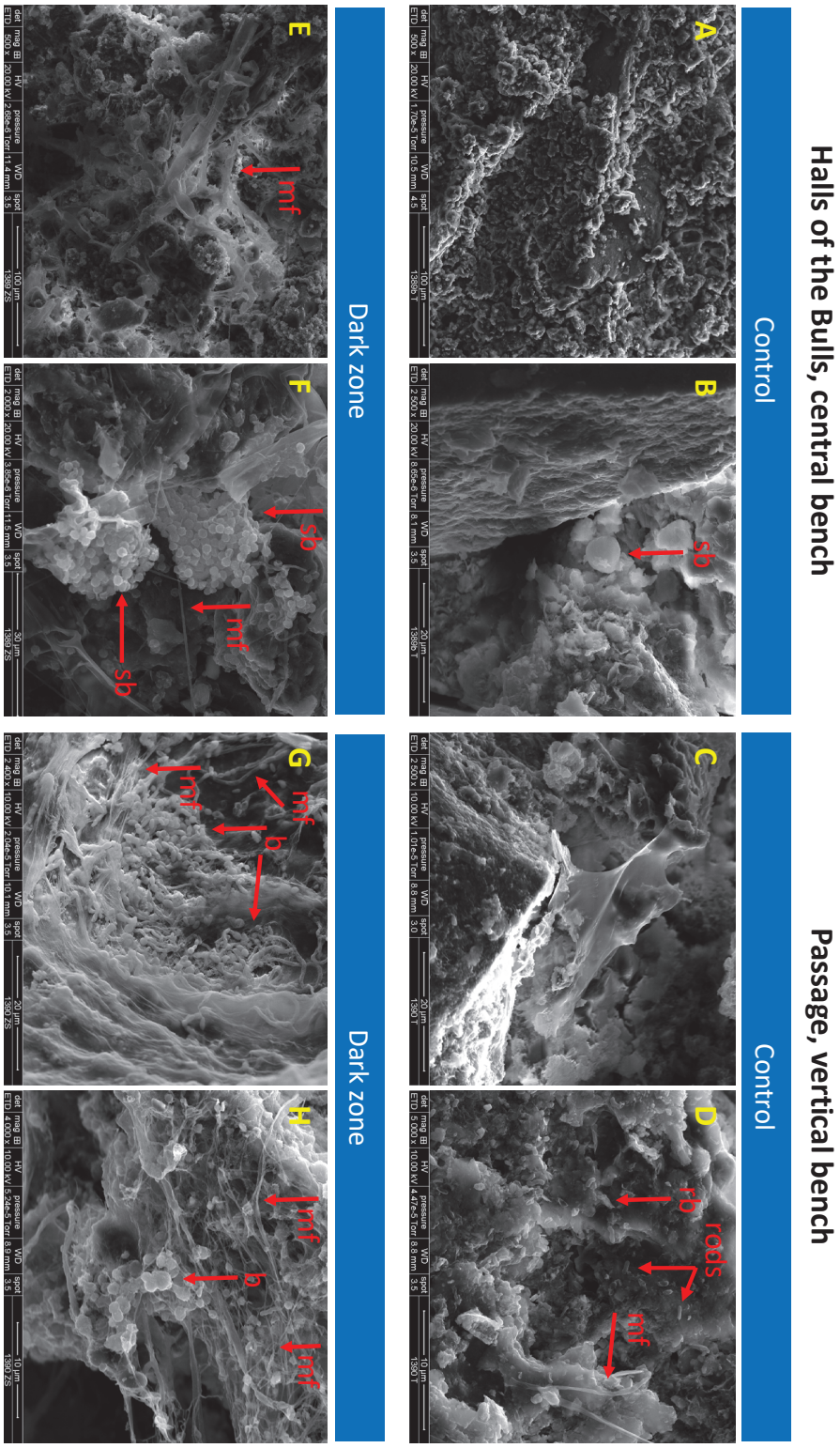

Figure 6. Scanning electron microscopy pictures of dark zones (E-H) and unmarked surfaces nearby (A-D) at various magnifications, in the Hall of the Bulls (central bench) and the Passage (vertical bench). Spherical bacteria are indicated by sb (one in B, many in F), rotini-shaped bacteria by rb (in D), bacteria of various shapes by b (in G and H), and microbial filament by mf (in B, E, F, G).

(0.3 and 0.8, respectively) and Passage vertical (0.2 and 0.1, respectively), and (iii) on the contrary an opposite variation (i.e. with opposite sign) in Nave low and Bulls wall. At the entire

bacterial community level, the Bray-Curtis distance gave scores of 1 (Passage horizontal and Bulls left), 0.9 (Passage vertical), 0.8 (Bulls wall), 0.7 (Bulls back), 0.5 (Nave low) and 0 (Nave high and Airlock-2 wall). qPCR data for bacteria gave a similarity score of 0.6 for Nave low, 0.3 for Nave high, Bulls center and Airlock-2 wall, 0.1 for Passage horizontal and Bulls left, but 0 for Passage vertical and the variation was even opposite for Bulls wall.

For the archaeal community, only the Δlog number of reads (with Δlog Apse = -1.037) and the copy number of archaeal 16S rRNA genes (Δlog Apse = -2.860) were considered to assign similarity scores, because of the strong counter-selection of archaea (Figure 7 ; Supplementary Table S8). Nave high and Bulls center had a same variation (with scores > 0.9) for both criteria, Nave low and Airlock-2 wall showed scores between 0.5 and 0.7, whereas Passage horizontal and Bulls wall had a score of 0 for the number of reads and 1 and 0.3 (respectively) for qPCR levels.

For the fungal community (Figure 7 ; Supplementary Table S8), the *Pseudogymnoascus* genus (Δlog Apse = -2.987) had a score of 1 in Nave low, 0.8 in Nave high, Passage vertical, Bulls back and Bulls left, 0.7 in Passage horizontal and 0.6 in Bulls wall, but of 0 in Airlock-2 wall. The black-melanized fungi *Ochroconis* proliferating in the Apse's dark zones (Δlog Apse = 1.112) was also observed in all other dark zones excepted in Nave high ; Passage vertical, Bulls left, Bulls wall and Passage horizontal had scores of respectively 1, 0.9, 0.8 and 0.7, and Airlock-2 wall and Bulls center only of 0.4 and 0.2, respectively. *Mortierella* (Δlog Apse = 2.218) gave a score of 0.3 in Passage horizontal but all the other dark zones displayed an opposite variation. The *Chrysosporium* genus was the fungal criterion with the biggest variation (Δlog Apse = -3.425), and the other dark zones had scores between 0 and 0.8 or displayed an opposite variation (for Passage). For the Bray-Curtis distance criterion, Bulls center, Passage vertical, Bulls wall, Bulls left, Nave high and Nave low had scores of 1, 0.9, 0.9, 0.8, 0.6 and 0.5, respectively, whereas Passage horizontal and Airlock-2 wall had scores of 0. With qPCR data of fungi, scores were 0.7 for Nave low, 0.5 for Passage vertical, 0.3 for Nave high and Bulls center, 0.2 for Airlock-2 wall, 0 for Passage vertical and Bulls left, but the variation was opposite for Bulls wall.

Cosmopolitan taxa vs taxa specific and/or endemic to dark zones

Out of the 197 genera evidenced here, 50 cosmopolitan genera (36 bacteria and 14 fungi) were identified for unmarked surfaces and dark zones together, i.e. taxa evidenced in all replicates of both types of samples at each of the nine locations (Figure 8). They included taxa already documented in Lascaux Cave, such as the bacterial genera *Pseudomonas, Bryobacter, Afipia, Labrys, Chitinophaga*, and the fungal genera *Ochroconis, Pseudogymnoascus, Nonomuraea, Mortierella* and *Gliomastix* (Bontemps et al., *in prep* ; Alonso et al., 2018)

Six dark zone-specific taxa (i.e. taxa present in dark zones at all nine locations and not detected in any unmarked surface sample) were identified, all of them bacterial (*Microbacterium, Actinophytocola, Lactobacillus, Bosea, Neochlamydia* and *Tsukamurella*) (Figure 8). In addition, a few dark zone-specific taxa endemic to a particular sampling location were found for 5 of the 9 sampling locations, i.e. the Apse (the fungi *Bipolaris, Xylodon* and *Itersonilia*), Nave high (the bacteria *Achromobacter, Phytomonospora* and the fungi *Nectria* and *Plagiostoma*), Bulls center (the bacteria *Nitriliruptor* and *Phytoactinopolyspora*), Bulls left (the bacteria *Aliihoeflea*, *Flindersiella, Arenibacter* and the fungus *Basidiobolus*) and Bulls wall (the bacteria *Hirschia*

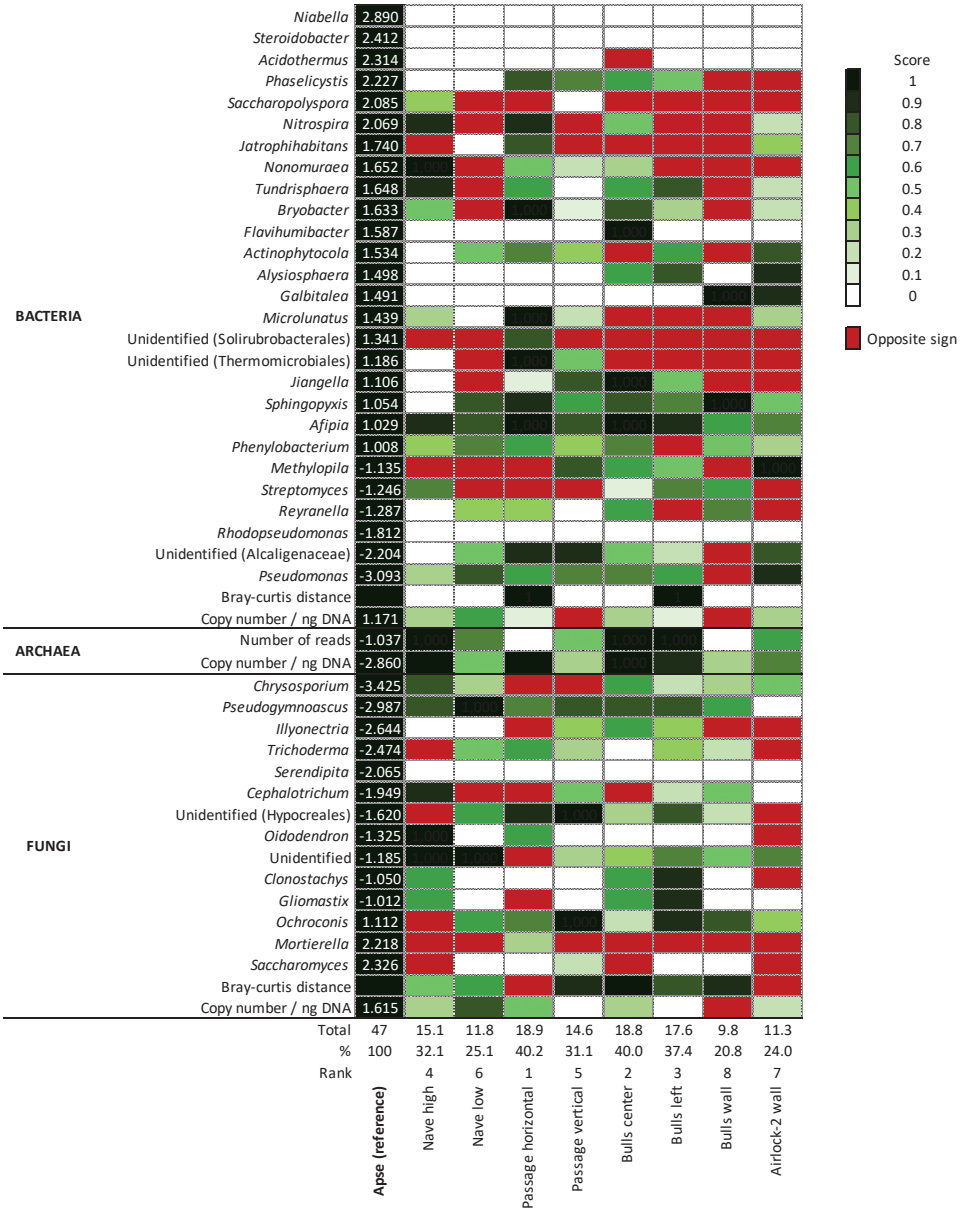

Figure 7. Decisional matrix based on the dark zone reference (in the Apse) for 47 criteria corresponding to 27 bacterial genera, 14 fungal genera, 1 bacterial and 1 fungal Bray-Curtis distance, the number of archaeal reads, and the copy number of marker genes (per ng of DNA) for bacteria, archaea and fungi. The Δlog Apse value is indicated in white (when applicable). Scores between 0 and 1 are shown with a green color intensity (gradient for each 0.1 increment ; see Materials and Methods section for more details), and red is used when changes were opposite to those for the Apse (i.e. Δlog was of opposite sign compared with Δlog Apse). The total score as well as the % of similarity to the dark zone reference were calculated for each dark zone, and the ranking based on the % similarity is indicated. Detailed calculation is provide in Table S8.

and the fungus *Vulleminia*). No dark zone-specific, endemic taxa were observed in Nave low, Passsage horizontal, Passage vertical and Airlock 2.

Discussion

Dark zone formation on wall surfaces of Lascaux's Apse coincides with major shifts in microbial community composition (Bontemps et al., *in prep*), and the current work aimed at understanding how dark zones could expand to different locations of the cave despite the presumed spatial

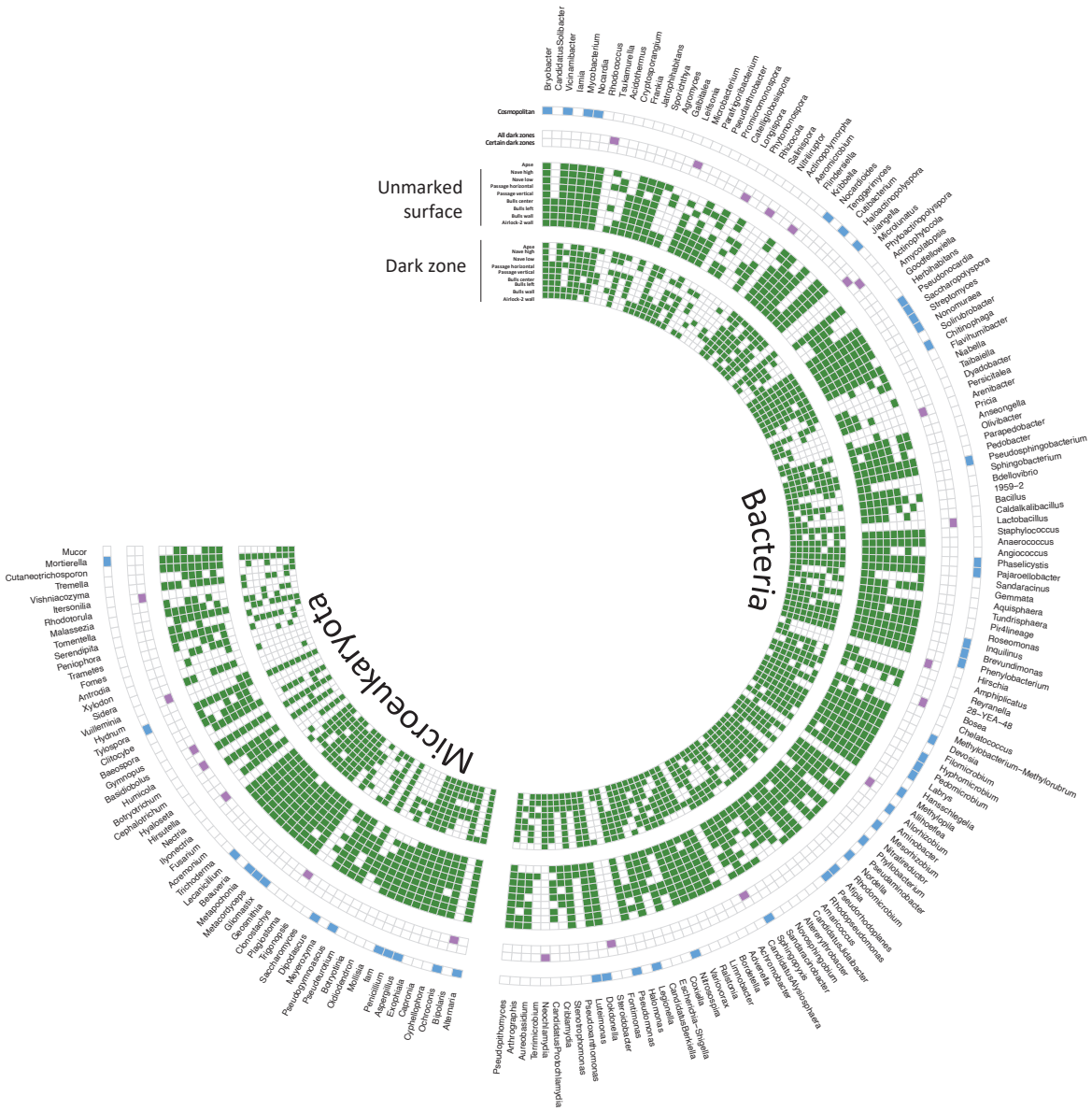

Figure 8. Occurrence of bacterial and fungal genera in unmarked surface and dark zone across nine sample locations in the Lascaux Cave. Presence of these genera in each condition is represented by green squares. In the outer circles, blue indicates cosmopolitan genera i.e. present in all dark zone samples and all unmarked surface samples in all locations ('Cosmopolitan'), and purple the dark zone-specific genera found in all dark zone samples in all locations ('All dark zones') and dark zone-specific genera found in all samples of certain dark zone locations ('Certain dark zones').

heterogeneity of Lascaux Cave microbiome.

In a first stage, we clarified the level of spatial heterogeneity of the microbial community in Lascaux. In various caves, microbiota heterogeneity has been documented in relation to (i) the distance to the cave entrance for bacteria (Wu et al., 2015 ; Buresova-Faitova et al., 2022), fungi (Man et al., 2018) or bacteria, archaea and microeukaryotes (Alonso et al., 2019), (ii) different mineral surfaces e.g. weathered rock vs sediment (for bacteria ; (Ma et al., 2021)), rock, sediment vs cave floor (for bacteria and fungi ; Alonso et al. 2018), or various types of speleothems (for bacteria ; (Dhami et al., 2018 ; Tok et al., 2021)), and (iii) more contrasted types of environmental samples e.g. rock wall deposit, water sediment vs sinkhole soil (for bacteria ; (Wu et al., 2015)),

or drip water, weathered rock, bat guano, sediment vs air (for fungi ; (Man et al., 2018)). Here, NMDS and ANOSIM analysis showed that the microbial community on unmarked wall surfaces differed significantly across locations. The distance to the entrance might be a significant factor (Bourges et al., 2014 ; Bednarik et al., 2016), with differences for Acidimicrobiia, Planctomycetes, Gammaproteobacteria, Eurotiomycetes, etc. between Airlock-2 wall (near the entrance) and the furthest areas e.g. Apse, Nave high and Nave low. However, climatic heterogeneity within the cave (Lacanette et al., 2009 ; Bourges et al., 2014) is likely limited by the existence of a door and several entry locks (Figure 1B). A second key factor (largely confounding with the previous one) could be the type of limestone surface, with differences between natural cave limestone (e.g. higher relative abundance of Gammaproteobacteria), calcareous masonry benches (e.g. higher relative abundance of Alphaproteobacteria and Actinobacteria) and quarry limestone blocks (e.g. higher relative abundance of Chloroflexia and Planctomycetes). Mineral substrate particularities influence microbial communities (Uroz et al., 2015 ; Alonso et al., 2018 ; Brewer and Fierer, 2018 ; Dhami et al., 2018). A third factor is the application of chemical treatments aiming at curbing microbial outgrowth, which differed among locations in Lascaux Cave (Martin-Sanchez et al., 2015). Perhaps the January 2008' treatments in the Passage, Apse and Nave walls contributed to the higher abundance there of Gammaproteobacteria (in accordance with Bastian et al.), as many of them are resistant to the chemicals used (Merchel Piovesan Pereira and Tagkopoulos, 2019).

In a second stage, we compared dark zones and unmarked surfaces nearby. NMDS and ANOSIM analysis indicated that their microbiota differed at each of the nine locations. All dark zone alterations displayed counter-selection of the Gammaproteobacteria class, as already described in Lascaux Cave for the gammaproteobacterial genus *Pseudomonas*, (Alonso et al. submitted, Bontemps et al. *in prep*). Alphaproteobacteria selected on all dark zones (except on Passage vertical) included the Rhizobiales order, involved in alteration of paintings in Tomba Del Colle (Italy) (Diaz-Herraiz et al., 2014). It is interesting to note that dark zones started in the Apse in 2008, and disseminated progressively towards the cave entrance, with those on Airlock-2 wall appearing late 2016. Obviously, dark zone formation did not involve microbial invaders having made it into the cave via the entrance, and the occurrence of multiple taxa changes point to community-level modifications. *Folsomia candida* collembola have the potential to disseminate microorganisms (Bastian et al., 2009 ; Alonso et al., submitted), but they are mainly observed in the Apse. Since microbiota variations associated with dark zones could differ from one location to the other, it suggests that changes in environmental conditions triggered these microbial dynamics. This might entail (i) long-term effects of previous chemical treatments, (ii) progressive changes in climatic conditions perhaps resulting from global warming and (since January 2015) the phasing-out of the air management system, or (iii) a combination of these factors. Further research will be needed to clarify this issue.

Many microorganisms may deteriorate materials by excretion of metabolites or extracellular enzymes (Sand, 1997 ; Uroz et al., 2015), adhesion mechanisms, or penetration of hyphae into microporous surfaces. (Riding, 2000 ; Gorbushina, 2007 ; Zucconi et al., 2012 ; Bontemps et al., 2021). This is likely to be promoted by mere microbial proliferation, and indeed qPCR levels of bacteria and fungi (but not of archaea, which were strongly counter-selected) were

significantly higher in dark zones than unmarked surfaces in all locations but on quarry limestone blocks of Airlock-2 wall and the masonry bench in Bulls left. Microbial proliferation is also indicated by direct, microscopy observations for the few samples of larger size that could be taken. Accordingly, the extensive use of chemical treatments also meant the introduction of organic carbon and nitrogen (Martin-Sanchez et al., 2015), and chemical analysis of cave floor samples did not point to N limitation (Alonso et al., 2019).

In a third stage, we assessed the similarity of the various dark zones to the reference dark zones in the Apse, thanks to a decisional matrix based on criteria of the three domains of Life stemming from observations of Bontemps et al. (*in prep*). They included the counter-selection of *Pseudomonas* and the selection of *Ochroconis*, which are important criteria for the reference dark zones of the Apse (Bontemps et al. *in prep*, Alonso et al. submitted). On the basis of the decisional matrix, there was not a strong relationship with spatial distance/dark zone age or mineral surface, as distant masonry benches such as Bulls center and Bulls left (dark zones from 2016 on) displayed an overall similarity of respectively 40.0% and 37.4% with the Apse (where dark zones develop since 2008), whereas nearby natural surfaces of Nave high and Nave (dark zones from 2011 on) low had a similarity of 32.1% and 25.1%, respectively. Yet, the quarry limestone blocks in Airlock-2 wall and Bulls wall, also the most distant from the Apse and where dark zones were among the most recent ones (from 2016 and 2013, respectively), displayed only 24.0% and 20.8% similarity, respectively. Similarity levels were not high overall (none exceeding the 40.2% value of Passage horizontal), especially since the contribution of individual criteria showing opposite dynamics were not accounted for. Therefore, in comparison with taxa associated with dark zone formation in the Apse, it suggests that key dark zone taxa at other Lascaux locations (i) may be endemic to these locations or at least present at higher population levels, and/or (ii) may correspond to cosmopolitan taxa but whose growth and contribution to alteration could be location-specific.

In a fourth stage, we assessed taxa based on biogeographic patterns. As many as 50 cosmopolitan genera were found, as well as 6 dark zone-specific genera found in all dark zone locations. The latter were only bacteria, including *Microbacterium* and *Bosea* described as producers of pigments such as carotenoids (Meddeb-Mouelhi et al., 2016 ; Albert et al., 2019). The lack of dark zone-specific fungi found in all dark zone locations suggests that bacteria may play a particular role in triggering dark zone formation. Perhaps dark zone formation involves also more location-specific contributions of other dark zone-specific microorganisms, i.e. (i) bacteria such as *Achromobacter* and *Nectria* in Nave high, *Hirschia* in Bulls wall, *Aliihoeflea* and *Arenibacter* in Bulls left, which may produce pigments (Duerre and Buckley, 1965 ; Parisot et al., 1983 ; Ivanova et al., 2001 ; Kang and Lee, 2009 ; Jung et al., 2013), and (ii) fungi e.g. *Bipolaris, Xylodon* and *Itersonilia* pointed in the Apse (Bontemps et al. *in prep*) and known for yellow-brown pigment production (Sharma et al., 2014 ; Riebesehl et al., 2019).

Conclusion

Dark zone alterations are a major concern for Paleolithic art conservation in Lascaux, as they can form in various locations of the cave despite spatial heterogeneity of the microbial community. Microbiota differences between dark zones and unmarked surfaces at different locations present

some similarities as well as location-specific properties. Microbial biogeographic patterns lead to the hypothesis that dark zone formation could entail proliferation of (i) a wide range of cosmopolitan bacterial and fungal taxa, (ii) six dark zone-specific bacterial genera found in all dark zone locations, and (iii) perhaps also other dark zone-specific bacteria and fungi found in certain but not all dark zone locations. Further work will target this issue. A better understanding of cave alteration dynamics may be useful to guide conservation strategies in Lascaux and other Paleolithic caves.

Data accessibility

All data that support findings of this study have been deposited in NCBI SRA database PRJNA798658, PRJNA799195 and PRJNA798756 for bacterial 16S rRNA genes, archaeal 16S rRNA genes and fungal ITS genes, respectively. The authors declare that the R (R 4.0.3) codes used to generate the results in this study are available in this paper. The R code supporting the finding presented here is available from the GitHub Repository https ://github.com/LascauxZelia /BontempsetalDZ

Acknowledgements

We thank S. Géraud, J.C. Portais, T. Baritaud, M. Mauriac (DRAC Nouvelle Aquitaine) and D. Henry-Lormelle (restorer team) for information and help, and Lascaux Scientific Board for useful discussions.

Author contributions

ZB contributed to sampling, acquired data, interpreted results, wrote the manuscript and prepared figures and tables ; MH contributed to conceptualization and revised the manuscript ; YML obtained funding, managed the project, designed the experiments, contributed to sampling, interpreted results and revised the manuscript.

Funding

Funding was provided by DRAC Nouvelle Aquitaine (Bordeaux, France).

References

Albert, R.A., McGuine, M., Pavlons, S.C., Roecker, J., Bruess, J., Mossman, S., et al. (2019) *Bosea psychrotolerans* sp. nov., a psychrotrophic alphaproteobacterium isolated from Lake Michigan water. Int J Syst Evol Microbiol 69 : 1376–1383.

Alonso, L., Creuzé-des-Châtelliers, C., Trabac, T., Dubost, A., Moënne-Loccoz, Y., and Pommier, T. (2018) Rock substrate rather than black stain alterations drives microbial community structure in the passage of Lascaux Cave. Microbiome 6 : 216-232.

Alonso, L., Pommier, T., Kaufmann, B., Dubost, A., Chapulliot, D., Doré, J., et al. (2019) Anthropization level of Lascaux Cave microbiome shown by regional-scale comparisons of pristine and anthropized caves. Mol Ecol 28 : 3383–3394.

Alonso, L., Pommier, T., Simon, L., Maucourt, F., Doré, J., Dubost, A., et al. (Submitted) Microbiome analysis in Lascaux Cave in relation to black stain alterations of rock surfaces and collembola. Environ Microbiol Rep.

Alonso, L., Pommier, T., Abrouk, D., Hugoni, H., Tran Van, V., Minard, G., Valiente Moro, C., Moënne-Loccoz, Y. (Submitted) Microbial analysis of recent cave wall alterations in the Apse of Lascaux Cave.

Baquedano Estévez, C., Merino, L.M., de la Losa Román, A., and Valsero, J.D. (2019) The lampenflora in show caves and its treatment : an emerging ecological problem. Int J Speleol 48 : 4.

Bastian, F. and Alabouvette, C. (2009a) Lights and shadows on the conservation of a rock art cave : The case of Lascaux Cave. Int J Speleol 38 : 1-6.

Bastian, Fabiola, Alabouvette, C., Jurado, V., and Saiz-Jimenez, C. (2009b) Impact of biocide treatments on the bacterial communities of the Lascaux Cave. Naturwissenschaften 96 : 863–868.

Bastian, F., Alabouvette, C., and Saiz-Jimenez, C. (2009) The impact of arthropods on fungal community structure in Lascaux Cave. J Appl Microbiol 106 : 1456–1462.

Bastian, F., Jurado, V., Nováková, A., Alabouvette, C., and Saiz-Jimenez, C. (2010) The microbiology of Lascaux Cave. Microbiology 156 : 644–652.

Bednarik, R.G., Fiore, D., and Basile, M. (2016) Paleoart and materiality : The scientific study of rock art, Archaeopress Publishing Ltd 211–325.

Bokulich, N.A., Subramanian, S., Faith, J.J., Gevers, D., Gordon, J.I., Knight, R., et al. (2013) Quality-filtering vastly improves diversity estimates from Illumina amplicon sequencing. Nat Methods 10 : 57–59.

Bontemps, Z., Alonso, L., Pommier, T., Hugoni, M., and Moënne-Loccoz, Y. (2021) Microbial ecology of tourist Paleolithic caves. Sci Tot Environ 816 : 151492.

Bontemps, Z., Hugoni, M., and Moënne-Loccoz, Y. (*in prep*) Microscale dynamics of dark zone alterations in anthropized karstic cave shows brutal microbial community switch.

Bourges, F., Genthon, P., Genty, D., Lorblanchet, M., Mauduit, E., and D'Hulst, D. (2014) Conservation of prehistoric caves and stability of their inner climate : Lessons from Chauvet and other French caves. Sci Tot Environ 493 : 79–91.

Brewer, T.E. and Fierer, N. (2018) Tales from the tomb : the microbial ecology of exposed rock surfaces. Environ Microbiol 20 : 958–970.

Brunet, J., Vidal, P., and Vouvé, J. (1987) The conservation of rock art. Studies and documents on the cultural heritage.

Buresova-Faitova, A., Kopecky, J., Sagova-Mareckova, M., Alonso, L., Vautrin, F., Moënne-Loccoz, Y., and Rodriguez-Nava, V. (2022) Comparison of Actinobacteria communities from human-impacted and pristine karst caves. MicrobiologyOpen 11 : e1276.

Cañveras, C.S.-J., S. Sanchez-Moral and V. Sloer (2001) Microorganisms and microbially induced fabrics in cave walls. Geomicrobiol J 18 : 223–240.

Chalmin, E., d'Orlyé, F., Zinger, L., Charlet, L., Geremia, R.A., Orial, G., et al. (2007) Biotic versus abiotic calcite formation on prehistoric cave paintings : the Arcy-sur-Cure 'Grande Grotte' (Yonne, France) case. Geol Soc Lond Spec Publ 279 : 185–197.

Chao, A. (1987) Estimating the population size for capture-recapture data with unequal catchability. Biometrics 43 : 783–791.

Cigna, A. (2016) Tourism and show caves. Geomorphol Suppl Issues 60 : 217–233.

Clarke, K.R. (1993) Non-parametric multivariate analyses of changes in community structure. Aust J Ecol 18 : 117–143.

Dhami, N.K., Mukherjee, A., and Watkin, E.L.J. (2018) Microbial diversity and mineralogical-mechanical properties of calcitic cave speleothems in natural and in vitro biomineralization conditions. Front Microbiol 9 : 40.

Diaz-Herraiz, M., Jurado, V., Cuezva, S., Laiz, L., Pallecchi, P., Tiano, P., et al. (2014) Deterioration of an Etruscan tomb by bacteria from the order Rhizobiales. Sci Rep 4 : 3610.

Duerre, J.A. and Buckley, P.J. (1965) Pigment production from tryptophan by an *Achromobacter* species. J Bacteriol 90 : 1686–1691.

Dupont, J., Jacquet, C., Dennetière, B., Lacoste, S., Bousta, F., Orial, G., et al. (2007) Invasion of the French Paleolithic painted cave of Lascaux by members of the *Fusarium solani* species complex. Mycologia 99 : 526–533.

Escudié, F., Auer, L., Bernard, M., Mariadassou, M., Cauquil, L., Vidal, K., et al. (2018) FROGS : Find, Rapidly, OTUs with Galaxy Solution. Bioinformatics 34 : 1287–1294.

Gorbushina, A.A. (2007) Life on the rocks. Environ Microbiol 9 : 1613–1631.

Hammer, Ø., Harper, D.., and Ryan, P. (2001) PAST : paleontological statis- tics software package for education and data analysis. Palaeontol Electron 4 : 1-9.

He, J., Zhang, N., Muhammad, A., Shen, X., Sun, C., Li, Q., et al. (2022) From surviving to thriving, the assembly processes of microbial communities in stone biodeterioration : A case study of the West Lake UNESCO World Heritage area in China. Sci Tot Environ 805 : 150395.

Herfort, L., Kim, J.-H., Coolen, M.J.L., Abbas, B., Schouten, S., Herndl, G.J., and Damsté, J.S.S. (2009) Diversity of Archaea and detection of crenarchaeotal *amoA* genes in the rivers Rhine and Têt. Aquat Microb Ecol 55 : 189–201.

Herlemann, D.P., Labrenz, M., Jürgens, K., Bertilsson, S., Waniek, J.J., and Andersson, A.F. (2011) Transitions in bacterial communities along the 2000 km salinity gradient of the Baltic Sea. ISME J 5 : 1571–1579.

Hugoni, M., Luis, P., Guyonnet, J., and Haichar, F. el Z. (2018) Plant host habitat and root exudates shape fungal diversity. Mycorrhiza 28 : 451–463.

Husson, F., Josse, J., Le, S., and Mazet, J. (2020) FactoMineR : Multivariate Exploratory Data Analysis and Data Mining.

Ikner, L.A., Toomey, R.S., Nolan, G., Neilson, J.W., Pryor, B.M., and Maier, R.M. (2007) Culturable microbial diversity and the impact of tourism in Kartchner Caverns, Arizona. Microb Ecol 53 : 30–42.

Ivanova, E.P., Nedashkovskaya, O.I., Chun, J., Lysenko, A.M., Frolova, G.M., Svetashev, V.I., et al. (2001) *Arenibacter* gen. nov., new genus of the family Flavobacteriaceae and description of a new species, *Arenibacter latericius* sp. nov. Int J Syst Evol Microbiol 51 : 1987–1995.

Jung, M.-Y., Shin, K.-S., Kim, S., Kim, S.-J., Park, S.-J., Kim, J.-G., et al. (2013) *Hoeflea halophila* sp. nov., a novel bacterium isolated from marine sediment of the East Sea, Korea. Antoni Leeuw Int J 103 : 971–978.

Kang, H.S. and Lee, S.D. 2009 (2009) Hirschia maritima sp. nov., isolated from seawater. Int J Syst Evol Microbiol 59 : 2264–2268.

Kassambara, A. and Mundt, F. (2020) factoextra : Extract and visualize the results of multivariate data analyses.

Lacanette, D., Vincent, S., Sarthou, A., Malaurent, P., and Caltagirone, J.-P. (2009) An Eulerian/Lagrangian method for the numerical simulation of incompressible convection flows interacting with complex obstacles : Application to the natural convection in the Lascaux Cave. Int J Heat Mass Transf 52 : 2528–2542.

Laiz, L., Piñar, G., Lubitz, W., and Saiz-Jimenez, C. (2003) Monitoring the colonization of monuments by bacteria : cultivation versus molecular methods. Environ Microbiol 5 : 72–74.

Lefèvre, M. (1974) La 'Maladie Verte' de Lascaux. Stud Conserv 19 : 126–156.

Lepinay, C., Mihajlovski, A., Touron, S., Seyer, D., Bousta, F., and Di Martino, P. (2018) Bacterial diversity associated with saline efflorescences damaging the walls of a French decorated prehistoric cave registered as a World Cultural Heritage Site. Int Biodeterior Biodegrad 130 : 55–64.

Ma, L., Huang, X., Wang, H., Yun, Y., Cheng, X., Liu, D., et al. (2021) Microbial interactions drive distinct taxonomic and potential metabolic responses to habitats in karst cave ecosystem. Microbiol Spectr 9 : e0115221.

Magoč, T. and Salzberg, S.L. (2011) FLASH : fast length adjustment of short reads to improve genome assemblies. Bioinformatics 27 : 2957–2963.

Mahé, F., Rognes, T., Quince, C., de Vargas, C., and Dunthorn, M. (2014) Swarm : robust and fast clustering method for amplicon-based studies. PeerJ 2 : e593.

Man, B., Wang, H., Yun, Y., Xiang, X., Wang, R., Duan, Y., and Cheng, X. (2018) Diversity of fungal communities in Heshang Cave of central China revealed by mycobiome-sequencing. Front Microbiol 9 : 1400.

Martin-Sanchez, P.M., Miller, A.Z., and Saiz-Jimenez, C. (2015) Lascaux Cave : An example of fragile ecological balance in subterranean environments, De Gruyter, Berlin/Boston, 279–301.

McMurdie, P.J. and Holmes, S. (2013) phyloseq : An R package for reproducible interactive analysis and graphics of microbiome census data. PLoS ONE 8 : e61217.

Meddeb-Mouelhi, F., Moisan, J.K., Bergeron, J., Daoust, B., and Beauregard, M. (2016) Structural characterization of a novel antioxidant pigment produced by a photochromogenic *Microbacterium oxydans* strain. Appl Biochem Biotechnol 180 : 1286–1300.

Merchel Piovesan Pereira, B. and Tagkopoulos, I. (2019) Benzalkonium chlorides : Uses, regulatory status, and microbial resistance. Appl Environ Microbiol 85 : e00377-19.

Nehme, C. (2013) The use of passive seismological imaging in speleogenetic studies ; an example from Kanaan Cave, Lebanon. Int J Speleol 42 : 97–108.

Nilsson, R.H., Larsson, K.-H., Taylor, A.F.S., Bengtsson-Palme, J., Jeppesen, T.S., Schigel, D., et al. (2019) The UNITE database for molecular identification of fungi : handling dark taxa and parallel taxonomic classifications. Nucleic Acids Res 47 : D259–D264.

Oksanen, J., Blanchet, F.G., Friendly, M., Kindt, R., Legendre, P., McGlinn, D., et al. (2020) vegan : Community ecology package.

Parisot, D., Devys, M., Férézou, J.-P., and Barbier, M. (1983) Pigments from *Nectria haematococca* : Anhydrofusarubin lactone and nectriafurone. Phytochemistry 22 : 1301–1303.

Portillo, M.C. and Gonzalez, J.M. (2010) Differential effects of distinct bacterial biofilms in a cave environment. Curr Microbiol 60 : 435–438.

Portillo, M.C., Gonzalez, J.M., and Saiz-Jimenez, C. (2008) Metabolically active microbial communities of yellow and grey colonizations on the walls of Altamira Cave, Spain. J Appl Microbiol 104 : 681–691.

Quast, C., Pruesse, E., Yilmaz, P., Gerken, J., Schweer, T., Yarza, P., et al. (2013) The SILVA ribosomal RNA gene database project : improved data processing and web-based tools. Nucleic Acids Res 41 : D590–D596.

R Core Team (2020) R : A language and environment for statistical computing., Vienna, Austria : R Foundation for Statistical Computing.

Riding, R. (2000) Microbial carbonates : the geological record of calcified bacterial–algal mats and biofilms. Sedimentology 47 : 179–214.

Riebesehl, J., Yurchenko, E., Nakasone, K.K., and Langer, E. (2019) Phylogenetic and morphological studies in *Xylodon* (Hymenochaetales, Basidiomycota) with the addition of four new species. MycoKeys 47 : 97–137.

Rognes, T., Flouri, T., Nichols, B., Quince, C., and Mahé, F. (2016) VSEARCH : a versatile open source tool for metagenomics. PeerJ 4 : e2584.

Russell, M.J. and MacLean, V.L. (2008) Management issues in a Tasmanian tourist cave : potential microclimatic impacts of cave modifications. J Environ Manage 87 : 474–483.

Sand, W. (1997) Microbial mechanisms of deterioration of inorganic substrates—A general mechanistic overview. Int Biodeterior Biodegrad 40 : 183–190.

Shannon, C.E. (1948) A mathematical theory of communication. Bell Syst Tech J 27 : 623–656.

Simpson, E.H. (1949) Measurement of diversity. Nature 163 : 688–688.

Toju, H., Tanabe, A.S., Yamamoto, S., and Sato, H. (2012) High-coverage ITS primers for the DNA-based identification of Ascomycetes and Basidiomycetes in environmental samples. PLoS ONE 7 :11-18.

Tok, E., Olgun, N., and Dalfes, H.N. (2021) Profiling bacterial diversity in relation to different habitat types in a limestone cave : İnsuyu Cave, Turkey. Geomicrobiol J 38 : 776–790.

Uroz, S., Kelly, L.C., Turpault, M.-P., Lepleux, C., and Frey-Klett, P. (2015) The mineralosphere concept : Mineralogical control of the distribution and function of mineral-associated bacterial communities. Trends Microbiol 23 : 751–762.

Urzì, C., De Leo, F., Bruno, L., and Albertano, P. (2010) Microbial diversity in Paleolithic caves : A study case on the phototrophic biofilms of the Cave of Bats (Zuheros, Spain). Microb Ecol 60 : 116–129.

Van Rossum, G. and Drake, F. (2009) Python 3 Reference Manual, Scotts Valley : CA : CreateSpace.

Wickham, H., François, R., Henry, L., Müller, K., and RStudio (2021) dplyr : A grammar of data manipulation.

Wu, Y., Tan, L., Liu, W., Wang, B., Wang, J., Cai, Y., and Lin, X. (2015) Profiling bacterial diversity in a limestone cave of the western Loess Plateau of China. Front Microbiol 6 : 244.

Zhang, J. and Madden, T.L. (1997) PowerBLAST : a new network BLAST application for interactive or automated sequence analysis and annotation. Genome Res 7 : 649–656.

Zucconi, L., Gagliardi, M., Isola, D., Onofri, S., Andaloro, M.C., Pelosi, C., et al. (2012) Biodeterioration agents dwelling in or on the wall paintings of the Holy Saviour's cave (Vallerano, Italy). Int Biodeterior Biodegrad 70 : 40–46.

Supplementary data

Supplementary Table S1. Primers for amplification of taxonomic marker genes.

Marker gene	Region	Length	Name	Forward (F) or reverse (R)	Sequence	Reference
16S rRNA	V3-V4 Bacteria	550 bp	341F	F	5'-CCTACGGGNGGCWGCAG-3'	Herlemann et al. 2011
			805R	R	5'-GACTACHVGGGTATCTAATCC-3'	
	V3-V4 Archaea	420 bp	515F	F	5'-CAGCCGCCGCGGTAA-3'	Herfort et al. 2011
			915R	R	5'-GTGCTCCCCCGCCAATTCCT-3'	
18S rRNA	V4	350 bp	0067a_deg	F	5'-AAGCCATGCATGYCTAAGTATMA-3′	Dollive et al. 2012
			NSR339	R	5'-TCTCAGGCTCCYTCTCCGG-3′	
ITS	ITS2	327 bp	ITS3_KYO2	F	5'-ATGAAGAACGYAGYRAA-3'	Toju et al. 2012
			ITS4	R	5'-TCCTCCGCTTATTGATATGC- 3'	

Supplementary Table S2. Δlog Apse interval for score attribution for each criterion.

Criteria	Δlog Apse + 1 Δlog Apse	Δlog Apse + 0.9Δlog Apse	Δlog Apse + 0.8Δlog Apse	Δlog Apse + 0.7Δlog Apse	Δlog Apse + 0.6Δlog Apse	Δlog Apse + 0.5Δlog Apse	Δlog Apse + 0.4Δlog Apse	Δlog Apse + 0.3Δlog Apse	Δlog Apse + 0.2Δlog Apse	Δlog Apse + 0.1Δlog Apse	Δlog Apse
Niabella	5.781	5.492	5.203	4.914	4.625	4.336	4.047	3.758	3.469	3.180	2.890
Steroidobacter	4.824	4.583	4.342	4.100	3.859	3.618	3.377	3.135	2.894	2.653	2.412
Acidothermus	4.629	4.398	4.166	3.935	3.703	3.472	3.240	3.009	2.777	2.546	2.314
Phaselicystis	4.454	4.231	4.008	3.785	3.563	3.340	3.117	2.895	2.672	2.449	2.227
Saccharopolyspora	4.171	3.963	3.754	3.546	3.337	3.128	2.920	2.711	2.503	2.294	2.085
Nitrospira	4.139	3.932	3.725	3.518	3.311	3.104	2.897	2.690	2.483	2.276	2.069
Jatrophihabitans	3.480	3.306	3.132	2.958	2.784	2.610	2.436	2.262	2.088	1.914	1.740
Nonomuraea	3.305	3.140	2.975	2.809	2.644	2.479	2.3144	2.148	1.983	1.818	1.652
Tundrisphaera	3.296	3.131	2.966	2.802	2.637	2.472	2.307	2.142	1.977	1.812	1.648
Bryobacter	3.267	3.104	2.941	2.777	2.614	2.450	2.287	2.124	1.960	1.797	1.633
Flavihumibacter	3.175	3.016	2.857	2.699	2.540	2.381	2.222	2.064	1.905	1.746	1.587
Actinophytocola	3.069	2.916	2.762	2.609	2.455	2.302	2.148	1.995	1.841	1.688	1.534
Alysiosphaera	2.996	2.846	2.696	2.547	2.397	2.247	2.097	1.947	1.797	1.648	1.498
Galbitalea	2.982	2.833	2.684	2.535	2.386	2.237	2.087	1.938	1.789	1.640	1.491
Microlunatus	2.878	2.734	2.590	2.446	2.302	2.158	2.015	1.871	1.727	1.583	1.439
Unidentified (Solirubrobacterales)	2.683	2.549	2.415	2.280	2.146	2.012	1.878	1.744	1.610	1.475	1.341
Unidentified (Thermomicrobiales)	2.373	2.255	2.136	2.017	1.899	1.780	1.661	1.543	1.424	1.305	1.186
Jiangella	2.212	2.102	1.991	1.880	1.770	1.659	1.549	1.438	1.327	1.217	1.106
Sphingopyxis	2.109	2.003	1.898	1.792	1.687	1.581	1.476	1.371	1.265	1.160	1.054
Afipia	2.059	1.956	1.853	1.750	1.647	1.544	1.441	1.338	1.235	1.132	1.029
Phenylobacterium	2.017	1.916	1.815	1.714	1.613	1.512	1.412	1.311	1.210	1.109	1.008
Methylopila	-2.271	-2.157	-2.044	-1.930	-1.817	-1.703	-1.589	-1.476	-1.362	-1.249	-1.135
Streptomyces	-2.492	-2.367	-2.242	-2.118	-1.993	-1.869	-1.744	-1.619	-1.495	-1.370	-1.246
Reyranella	-2.574	-2.445	-2.316	-2.188	-2.059	-1.930	-1.801	-1.673	-1.544	-1.415	-1.287
Rhodopseudomonas	-3.625	-3.444	-3.263	-3.081	-2.900	-2.719	-2.538	-2.356	-2.175	-1.994	-1.812
Unidentified (Alcaligenaceae)	-4.408	-4.188	-3.967	-3.747	-3.526	-3.306	-3.085	-2.865	-2.645	-2.424	-2.204
Pseudomonas	-6.187	-5.877	-5.568	-5.259	-4.949	-4.640	-4.331	-4.021	-3.712	-3.403	-3.093
16S Copy number / ng DNA	2.342	2.225	2.108	1.991	1.873	1.756	1.639	1.522	1.405	1.288	1.171
Number of reads	-2.076	-1.971	-1.868	-1.764	-1.660	-1.550	-1.453	-1.349	-1.245	-1.141	-1.037
16S Copy number / ng DNA	-5.722	-5.436	-5.150	-4.863	-4.577	-4.291	-4.005	-3.719	-3.433	-3.147	-2.861
Chrysosporium	-6.851	-6.509	-6.166	-5.823	-5.481	-5.138	-4.796	-4.453	-4.111	-3.768	-3.425
Pseudogymnoascus	-5.974	-5.676	-5.377	-5.078	-4.779	-4.481	-4.182	-3.883	-3.584	-3.286	-2.987
Illyonectria	-5.288	-5.024	-4.759	-4.495	-4.231	-3.966	-3.702	-3.437	-3.173	-2.908	-2.644
Trichoderma	-4.949	-4.702	-4.454	-4.207	-3.959	-3.712	-3.464	-3.217	-2.969	-2.722	-2.474
Serendipita	-4.130	-3.924	-3.717	-3.510	-3.304	-3.097	-2.891	-2.684	-2.478	-2.271	-2.065
Cephalotrichum	-3.899	-3.703	-3.508	-3.313	-3.119	-2.924	-2.729	-2.534	-2.339	-2.144	-1.949
Unidentified (Hypocreales)	-3.241	-3.079	-2.917	-2.755	-2.593	-2.431	-2.269	-2.107	-1.945	-1.782	-1.620
Oidodendron	-2.650	-2.517	-2.385	-2.252	-2.120	-1.987	-1.855	-1.722	-1.590	-1.457	-1.325
Unidentified	-2.370	-2.252	-2.133	-2.015	-1.896	-1.778	-1.659	-1.541	-1.422	-1.304	-1.185
Clonostachys	-2.101	-1.996	-1.891	-1.785	-1.680	-1.575	-1.470	-1.365	-1.260	-1.155	-1.050
Gliomastix	-2.024	-1.923	-1.822	-1.720	-1.619	-1.518	-1.417	-1.315	-1.214	-1.113	-1.012
Ochroconis	2.225	2.113	2.002	1.891	1.780	1.668	1.557	1.446	1.335	1.223	1.112
Mortierella	4.437	4.215	3.993	3.771	3.549	3.328	3.106	2.884	2.662	2.440	2.218
Saccharomyces	4.652	4.420	4.187	3.954	3.722	3.489	3.256	3.024	2.791	2.558	2.326
ITS Copy number / ng DNA	3.230	3.068	2.907	2.745	2.584	2.422	2.261	2.099	1.938	1.776	1.615

Δlog Apse - 0.1Δlog Apse	Δlog Apse - 0.2Δlog Apse	Δlog Apse - 0.3Δlog Apse	Δlog Apse - 0.4Δlog Apse	Δlog Apse - 0.5Δlog Apse	Δlog Apse - 0.6Δlog Apse	Δlog Apse - 0.7Δlog Apse	Δlog Apse - 0.8Δlog Apse	Δlog Apse - 0.9Δlog Apse	Δlog Apse - 1 Δlog Apse
2.601	2.312	2.023	1.734	1.445	1.156	0.867	0.578	0.289	0.000
2.171	1.929	1.688	1.447	1.206	0.964	0.723	0.482	0.241	0.000
2.083	1.851	1.620	1.388	1.157	0.925	0.694	0.462	0.231	0.000
2.004	1.781	1.558	1.336	1.113	0.890	0.668	0.445	0.222	0.000
1.877	1.668	1.460	1.251	1.042	0.834	0.625	0.417	0.208	0.000
1.862	1.655	1.448	1.241	1.034	0.827	0.620	0.413	0.206	0.000
1.566	1.392	1.218	1.044	0.870	0.696	0.522	0.348	0.174	0.000
1.487	1.322	1.157	0.991	0.826	0.661	0.495	0.330	0.165	0.000
1.483	1.318	1.153	0.988	0.824	0.659	0.494	0.329	0.164	0.000
1.470	1.307	1.143	0.980	0.816	0.653	0.490	0.326	0.163	0.000
1.428	1.270	1.111	0.952	0.793	0.635	0.476	0.317	0.158	0.000
1.381	1.227	1.074	0.920	0.767	0.613	0.460	0.306	0.153	0.000
1.348	1.198	1.048	0.898	0.749	0.599	0.449	0.299	0.149	0.000
1.342	1.193	1.043	0.894	0.745	0.596	0.447	0.298	0.149	0.000
1.295	1.151	1.007	0.863	0.719	0.575	0.431	0.287	0.143	0.000
1.207	1.073	0.939	0.805	0.670	0.536	0.402	0.268	0.134	0.000
1.068	0.949	0.830	0.712	0.593	0.474	0.356	0.237	0.118	0.000
0.995	0.885	0.774	0.663	0.553	0.442	0.331	0.221	0.110	0.000
0.949	0.843	0.738	0.632	0.527	0.421	0.316	0.210	0.105	0.000
0.926	0.823	0.720	0.617	0.514	0.411	0.308	0.205	0.102	0.000
0.907	0.806	0.706	0.605	0.504	0.403	0.302	0.201	0.100	0.000
-1.022	-0.908	-0.794	-0.681	-0.567	-0.454	-0.340	-0.227	-0.113	0.000
-1.121	-0.996	-0.872	-0.747	-0.623	-0.498	-0.373	-0.249	-0.124	0.000
-1.158	-1.029	-0.900	-0.772	-0.643	-0.514	-0.386	-0.257	-0.128	0.000
-1.631	-1.450	-1.269	-1.087	-0.906	-0.725	-0.543	-0.362	-0.181	0.000
-1.983	-1.763	-1.542	-1.322	-1.102	-0.881	-0.661	-0.440	-0.220	0.000
-2.784	-2.474	-2.165	-1.856	-1.546	-1.237	-0.928	-0.618	-0.309	0.000
1.054	0.936	0.819	0.702	0.585	0.468	0.351	0.234	0.117	0.000
-0.934	-0.830	-0.726	-0.622	-0.518	-0.415	-0.311	-0.207	-0.103	0.000
-2.575	-2.288	-2.002	-1.716	-1.430	-1.144	-0.858	-0.572	-0.286	0.000
-3.083	-2.740	-2.398	-2.055	-1.712	-1.370	-1.027	-0.685	-0.342	0.000
-2.688	-2.389	-2.091	-1.792	-1.493	-1.194	-0.896	-0.597	-0.298	0.000
-2.379	-2.115	-1.851	-1.586	-1.322	-1.057	-0.793	-0.528	-0.264	0.000
-2.227	-1.979	-1.732	-1.484	-1.237	-0.989	-0.742	-0.494	-0.247	0.000
-1.858	-1.652	-1.445	-1.239	-1.032	-0.826	-0.619	-0.413	-0.206	0.000
-1.754	-1.559	-1.364	-1.169	-0.974	-0.779	-0.584	-0.389	-0.194	0.000
-1.458	-1.296	-1.134	-0.972	-0.810	-0.648	-0.486	-0.324	-0.162	0.000
-1.192	-1.060	-0.927	-0.795	-0.662	-0.530	-0.397	-0.265	-0.132	0.000
-1.066	-0.948	-0.829	-0.711	-0.592	-0.474	-0.355	-0.237	-0.118	0.000
-0.945	-0.840	-0.735	-0.630	-0.525	-0.420	-0.315	-0.210	-0.105	0.000
-0.911	-0.809	-0.708	-0.607	-0.506	-0.404	-0.303	-0.202	-0.101	0.000
1.001	0.890	0.778	0.667	0.556	0.445	0.333	0.222	0.111	0.000
1.996	1.774	1.553	1.331	1.109	0.887	0.665	0.443	0.221	0.000
2.093	1.861	1.628	1.395	1.163	0.930	0.697	0.465	0.232	0.000
1.453	1.292	1.130	0.969	0.807	0.640	0.484	0.323	0.161	0.000

Supplementary Table S3. Adonis comparison of sampling location for bacterial 16S rRNA genes and for fungal ITS region, separately for control and dark zone conditions.

		Bacterial 16S rRNA gene				Fungal ITS region			
		Df	**F**	***P***	**R^2**	**Df**	**F**	***P***	**R^2**
Control	*Effect :* Location	8	12.835	**0.001**	0.695	8	9.338	**0.007**	0.629
	Residuals	53				53			
Dark zone	*Effect :* Location	8	9.784	**0.008**	0.634	8	7.005	**0.010**	0.560
	Residuals	53				53			

Supplementary Table S4. qPCR results (gene copies number / ng of total DNA) for bacterial, archaeal and fungal communities for control and dark zone conditions at each location in Lascaux Cave.

	Bacteria 16S rRNA				Archaea 16S rRNA				Fungi ITS			
	Control		Dark zone		Control		Dark zone		Control		Dark zone	
Sampling location	Mean	SD	Mean	SD	Mean	SD	Mean	SD	Mean	SD	Mean	SD
Apse	2.94E+08	1.93E+02	4.36E+09	3.78E+02	6.61E+09	1.96E+02	2.66E+08	1.96E+02	1.33E+08	1.85E+03	5.48E+09	9.76E+02
Bulls center	1.06E+09	2.73E+02	2.73E+09	2.56E+02	3.31E+08	3.49E+01	4.72E+07	4.13E+02	4.64E+08	1.25E+02	1.21E+09	4.49E+01
Bulls left	4.50E+09	9.48E+01	6.12E+09	1.20E+03	2.83E+09	7.93E+02	8.18E+07	5.33E+01	5.16E+09	2.16E+02	6.64E+09	6.12E+02
Bulls wall	2.79E+09	8.10E+02	1.99E+08	1.40E+02	3.53E+09	4.48E+02	8.65E+06	6.15E+01	1.95E+09	1.85E+01	1.19E+08	5.01E+02
Airlock-2 wall	1.93E+09	6.53E+01	4.20E+09	8.05E+01	5.51E+09	8.67E+01	9.64E+07	8.66E+02	1.59E+09	7.47E+01	3.57E+09	8.63E+02
Nave high	3.68E+09	9.64E+01	7.75E+09	4.77E+02	2.20E+09	4.01E+02	8.53E+07	4.59E+02	1.50E+09	4.59E+02	2.40E+09	4.59E+02
Nave low	5.19E+09	1.72E+02	2.38E+11	3.35E+02	1.47E+09	2.32E+02	5.62E+08	8.47E+03	1.62E+09	7.65E+02	1.44E+11	8.74E+01
Passage horizontal	2.46E+09	2.12E+02	3.40E+09	1.36E+01	5.35E+08	1.84E+01	8.73E+07	1.09E+02	5.44E+08	9.20E+01	2.86E+09	1.02E+02
Passage vertical	2.56E+10	1.19E+02	2.44E+09	3.36E+01	2.64E+10	1.28E+02	3.30E+07	1.28E+03	2.63E+09	5.11E+03	3.44E+09	1.29E+01

Supplementary Table S5. Pairwise-Adonis comparisons of sample locations for bacterial 16S rRNA genes and for fungal ITS region, separately for control and dark zone conditions.

	Bacterial 16S rRNA gene						Fungal ITS region					
Sampling location	Df	F Model	R^2	*P*	*P* adjusted		Df	F Model	R^2	*P*	*P* adjusted	
Apse	1	40.23	0.80	0.001	0.001	***	1	9.9	0.50	0.003	0.003	*
Bulls center	1	15.26	0.60	0.004	0.004	*	1	6.49	0.39	0.003	0.003	*
Bulls left	1	3.16	0.24	0.011	0.011	NS	1	25.14	0.72	0.003	0.003	*
Bulls wall	1	6.81	0.40	0.003	0.003	*	1	3.84	0.30	0.003	0.003	*
Airlok-2 wall	1	9.72	0.49	0.004	0.004	*	1	4.07	0.29	0.011	0.011	NS
Nave high	1	55.94	0.85	0.003	0.003	*	1	13.02	0.57	0.003	0.003	*
Nave low	1	16.58	0.62	0.006	0.006	*	1	7.94	0.47	0.003	0.003	*
Passage horizontal	1	13.82	0.58	0.006	0.006	*	1	3.65	0.27	0.005	0.005	*
Passage vertical	1	34.84	0.78	0.004	0.004	*	1	2.89	0.22	0.009	0.009	*

Supplementary Table S6. Adonis comparison of rock surface conditions (control vs dark zone) and sample locations across the whole dataset for bacterial 16S rRNA genes and for fungal ITS region.

	Bacterial 16S rRNA gene				Fungal ITS region			
	Df	F	*P*	R^2	Df	F	*P*	R^2
Effect :								
Location	8	13.059	**0.004**	0.32	8	10.792	**0.001**	0.36
Rock surface condition	1	53.516	**0.009**	0.17	1	20.818	**0.009**	0.08
Location × Rock surface condition	8	5.460	**0.001**	0.23	8	5.460	**0.001**	0.18
Residuals	107				105			

Supplementary Table S7. Pairwise-Adonis comparisons of control and dark zone conditions for bacterial 16S rRNA genes and for fungal ITS region, separately for each.

		16S Bacterial rRNA gene						**Fungal ITS region**					
Rock surface condition	pairs	Df	Sums Of Sqs	F	R^2	*P*	*P* adjusted	Df	Sums Of Sqs	F	R^2	*P*	*P* adjusted
CONTROL	Apse Bulls_center	1	0.78	10.96	0.52	0.004	0.144	1	1.76	13.05	0.57	0.004	0.144
	Apse Bulls_left	1	2.01	14.95	0.60	0.002	0.072	1	1.55	12.89	0.56	0.005	0.180
	Apse Airlock-2_Bulls	1	1.24	10.52	0.51	0.001	0.036	1	1.37	10.30	0.53	0.001	0.036
	Apse Airlock-2	1	2.27	25.61	0.72	0.003	0.108	1	1.44	8.60	0.46	0.002	0.072
	Apse Nave_high	1	0.11	2.68	0.21	0.046	1.000	1	0.62	3.52	0.26	0.006	0.216
	Apse Nave_low	1	0.78	8.78	0.47	0.001	0.036	1	0.75	3.55	0.26	0.013	0.468
	Apse Passage_horizontal	1	1.35	24.38	0.71	0.007	0.252	1	1.18	7.11	0.42	0.003	0.108
	Apse Passage_vertical	1	1.51	23.10	0.70	0.004	0.144	1	1.20	7.99	0.44	0.003	0.108
	Bulls_center Bulls_left	1	1.63	11.04	0.52	0.002	0.072	1	1.74	22.40	0.69	0.003	0.108
	Bulls_center Airlock-2_Bulls	1	1.06	8.06	0.45	0.003	0.108	1	0.55	6.50	0.42	0.004	0.144
	Bulls_center Airlock-2	1	2.01	19.74	0.66	0.002	0.072	1	2.06	16.50	0.62	0.006	0.216
	Bulls_center Nave_high	1	0.71	12.71	0.56	0.005	0.180	1	1.60	11.92	0.54	0.002	0.072
	Bulls_center Nave_low	1	0.88	8.56	0.46	0.003	0.108	1	1.52	9.06	0.48	0.003	0.108
	Bulls_center Passage_horizontal	1	0.74	10.83	0.52	0.002	0.072	1	0.75	6.12	0.38	0.002	0.072
	Bulls_center Passage_vertical	1	1.25	15.85	0.61	0.004	0.144	1	0.62	5.85	0.37	0.002	0.072
	Bulls_left Airlock-2_Bulls	1	1.34	6.86	0.41	0.004	0.144	1	1.50	21.52	0.71	0.002	0.072
	Bulls_left Airlock-2	1	1.13	6.81	0.41	0.002	0.072	1	0.99	8.94	0.47	0.003	0.108
	Bulls_left Nave_high	1	2.14	17.97	0.64	0.002	0.072	1	1.91	15.97	0.61	0.004	0.144
	Bulls_left Nave_low	1	1.89	11.44	0.53	0.005	0.180	1	1.80	11.71	0.54	0.004	0.144
	Bulls_left Passage_horizontal	1	1.49	11.32	0.53	0.002	0.072	1	1.73	15.89	0.61	0.003	0.108
	Bulls_left Passage_vertical	1	1.39	9.77	0.49	0.005	0.180	1	1.53	16.49	0.62	0.004	0.144
	Airlock-2_Bulls Airlock-2	1	1.04	6.99	0.41	0.002	0.072	1	1.59	13.00	0.59	0.003	0.108
	Airlock-2_Bulls Nave_high	1	1.26	12.27	0.55	0.003	0.108	1	1.35	10.23	0.53	0.003	0.108
	Airlock-2_Bulls Nave_low	1	1.18	7.90	0.44	0.002	0.072	1	1.19	7.02	0.44	0.002	0.072
	Airlock-2_Bulls Passage_horizontal	1	1.27	10.95	0.52	0.002	0.072	1	1.45	12.07	0.57	0.008	0.288
	Airlock-2_Bulls Passage_vertical	1	1.33	10.53	0.51	0.005	0.180	1	1.11	10.88	0.55	0.002	0.072
	Airlock-2 Nave_high	1	2.48	33.73	0.77	0.003	0.108	1	1.92	11.47	0.53	0.004	0.144
	Airlock-2 Nave_low	1	2.26	18.83	0.65	0.005	0.180	1	1.76	8.76	0.47	0.004	0.144
	Airlock-2 Passage_horizontal	1	2.16	25.01	0.71	0.003	0.108	1	2.01	12.84	0.56	0.003	0.108
	Airlock-2 Passage_vertical	1	2.13	22.01	0.69	0.004	0.144	1	1.90	13.57	0.58	0.004	0.144
	Nave_high Nave_low	1	0.58	7.84	0.44	0.004	0.144	1	0.52	2.49	0.20	0.040	1.000
	Nave_high Passage_horizontal	1	1.12	27.77	0.74	0.005	0.180	1	1.10	6.63	0.40	0.005	0.180
	Nave_high Passage_vertical	1	1.40	27.68	0.73	0.004	0.144	1	1.12	7.51	0.43	0.003	0.108
	Nave_low Passage_horizontal	1	0.54	6.29	0.39	0.001	0.036	1	1.17	5.89	0.37	0.005	0.180
	Nave_low Passage_vertical	1	0.81	8.31	0.45	0.003	0.108	1	1.20	6.58	0.40	0.004	0.144

	Passage_horizontal	Passage_vertical	1	0.24	3.85	0.28	0.010	0.360	1	0.10	0.75	0.07	0.582	1.000
	Apse	Bulls_center	1	1.35	12.06	0.55	0.006	0.216	1	1.92	19.70	0.66	0.004	0.144
	Apse	Bulls_left	1	1.41	9.50	0.49	0.002	0.072	1	1.81	17.60	0.64	0.003	0.108
	Apse	Airlock-2_Bulls	1	1.87	12.93	0.56	0.002	0.072	1	1.31	6.27	0.41	0.002	0.072
	Apse	Airlock-2	1	2.01	26.64	0.73	0.003	0.108	1	1.33	7.22	0.42	0.003	0.108
	Apse	Nave_high	1	1.84	38.73	0.79	0.007	0.252	1	1.53	9.90	0.50	0.002	0.072
	Apse	Nave_low	1	1.80	20.37	0.67	0.002	0.072	1	1.50	12.97	0.56	0.005	0.180
	Apse	Passage_horizontal	1	1.42	12.64	0.56	0.004	0.144	1	1.28	6.23	0.38	0.005	0.180
	Apse	Passage_vertical	1	1.99	39.76	0.80	0.003	0.108	1	1.52	15.30	0.60	0.002	0.072
	Bulls_center	Bulls_left	1	0.42	2.09	0.17	0.025	0.900	1	0.05	0.68	0.06	0.496	1.000
	Bulls_center	Airlock-2_Bulls	1	0.88	4.44	0.31	0.001	0.036	1	1.01	5.86	0.39	0.001	0.036
	Bulls_center	Airlock-2	1	1.31	10.09	0.50	0.005	0.180	1	1.67	10.94	0.52	0.004	0.144
	Bulls_center	Nave_high	1	1.30	12.78	0.56	0.005	0.180	1	0.56	4.58	0.31	0.009	0.324
	Bulls_center	Nave_low	1	0.62	4.35	0.30	0.001	0.036	1	0.54	6.53	0.40	0.004	0.144
	Bulls_center	Passage_horizontal	1	0.99	5.90	0.37	0.001	0.036	1	0.75	4.32	0.30	0.005	0.180
	Bulls_center	Passage_vertical	1	0.91	8.74	0.47	0.004	0.144	1	0.39	5.81	0.37	0.004	0.144
	Bulls_left	Airlock-2_Bulls	1	0.84	3.57	0.26	0.010	0.360	1	1.09	6.08	0.40	0.005	0.180
	Bulls_left	Airlock-2	1	0.91	5.47	0.35	0.003	0.108	1	1.65	10.41	0.51	0.002	0.072
DARK	Bulls_left	Nave_high	1	1.41	10.23	0.51	0.004	0.144	1	0.50	3.94	0.28	0.012	0.432
ZONE	Bulls_left	Nave_low	1	0.78	4.35	0.30	0.005	0.180	1	0.43	4.81	0.32	0.015	0.540
	Bulls_left	Passage_horizontal	1	0.63	3.11	0.24	0.027	0.972	1	0.76	4.28	0.30	0.004	0.144
	Bulls_left	Passage_vertical	1	0.50	3.55	0.26	0.003	0.108	1	0.37	5.09	0.34	0.006	0.216
	Airlock-2_Bulls	Airlock-2	1	0.74	4.54	0.31	0.015	0.540	1	0.77	2.85	0.24	0.005	0.180
	Airlock-2_Bulls	Nave_high	1	1.66	12.34	0.55	0.004	0.144	1	1.02	4.30	0.32	0.012	0.432
	Airlock-2_Bulls	Nave_low	1	0.82	4.68	0.32	0.003	0.108	1	1.19	6.17	0.41	0.002	0.072
	Airlock-2_Bulls	Passage_horizontal	1	1.36	6.80	0.40	0.003	0.108	1	0.85	2.91	0.24	0.003	0.108
	Airlock-2_Bulls	Passage_vertical	1	1.27	9.21	0.48	0.005	0.180	1	1.05	6.00	0.40	0.003	0.108
	Airlock-2	Nave_high	1	2.01	30.92	0.76	0.003	0.108	1	1.11	5.30	0.35	0.016	0.576
	Airlock-2	Nave_low	1	1.40	13.18	0.57	0.003	0.108	1	1.58	9.26	0.48	0.006	0.216
	Airlock-2	Passage_horizontal	1	1.36	10.44	0.51	0.004	0.144	1	0.94	3.59	0.26	0.007	0.252
	Airlock-2	Passage_vertical	1	1.33	19.70	0.66	0.001	0.036	1	1.29	8.29	0.45	0.007	0.252
	Nave_high	Nave_low	1	1.21	15.43	0.61	0.003	0.108	1	0.21	1.53	0.13	0.099	1.000
	Nave_high	Passage_horizontal	1	1.79	17.46	0.64	0.003	0.108	1	1.07	4.63	0.32	0.005	0.180
	Nave_high	Passage_vertical	1	2.05	51.32	0.84	0.001	0.036	1	1.20	9.58	0.49	0.003	0.108
	Nave_low	Passage_horizontal	1	1.24	8.66	0.46	0.005	0.180	1	1.23	6.41	0.39	0.003	0.108
	Nave_low	Passage_vertical	1	1.11	13.74	0.58	0.001	0.036	1	1.35	15.79	0.61	0.007	0.252
	Passage_horizontal	Passage_vertical	1	0.64	6.12	0.38	0.003	0.108	1	0.56	3.21	0.24	0.006	0.216

Supplementary Table S8. Computation of the 47 similarity scores for dark zones of Lascaux, in relation to the situation of the Apse's dark zones. For individual taxa, the raw data correspond to the mean number of sequences. SD, standard deviation (n = 6). Cell colors for scores correspond to the color code in Figure 2. Scores without positive values are not indicated and the corresponding cell is displayed with a reddish color.

	Apse							Nave high						
	Raw data			Log data				Raw data			Log data			
	Unmarked surface	Unmarked surfaces (SD)	Dark zone	Dark zone (SD)	Unmarked surface (log)	Dark zone (log)	Delta log	Score	Unmarked surface	Unmarked surfaces (SD)	Dark zone	Dark zone (SD)	Unmarked surface (log)	Dark zone (log)	Delta log	Score
Bacteria																
Niabella	1	0.0	778	13.1	0.000	2.890	2.890	1	1	0.0	1	0.0	0.000	0.000	0.000	0.0
Steroidobacter	8	3.2	2067	172.9	0.903	3.315	2.412	1	0	0.0	0	0.0	NA	NA	NA	0.0
Acidothermus	4	1.0	826	103.2	0.602	2.916	2.314	1	0	0.0	0	0.0	NA	NA	NA	0.0
Phaselicystis	3	0.0	506	58.4	0.477	2.704	2.227	1	2	0.5	2	0.8	0.301	0.301	0.000	0.0
Saccharopolyspora	8	1.8	975	168.8	0.903	2.989	2.085	1	5	0.0	14	0.0	0.698	1.146	0.447	0.4
Nitrospira	21	7.6	2467	220.4	1.322	3.392	2.069	1	2	0.0	400	115.7	0.301	2.602	2.301	0.9
Jatrophihabitans	2	0.0	110	5.6	0.301	2.041	1.740	1	13	1.8	4	1.2	1.113	0.602	-0.511	
Nonomuraea	245	89.2	11017	354.9	2.389	4.042	1.652	1	16	1.6	448	110.1	1.204	2.651	1.447	1.0
Tundrisphaera	23	5.7	1023	142.3	1.361	3.009	1.648	1	2	0.0	50	0.0	0.301	1.698	1.397	0.9
Bryobacter	154	54.1	6629	214.8	2.187	3.821	1.633	1	9	1.2	29	7.0	0.954	1.462	0.508	0.5
Flavihumibacter	17	6.9	658	94.2	1.230	2.818	1.587	1	0	0.0	1	0.0	NA	0.000	NA	0.0
Actinophytocola	19	6.8	651	42.0	1.278	2.813	1.534	1	0	0.0	7	1.1	NA	0.845	NA	0.0
Alysiosphaera	4	0.0	126	0.0	0.602	2.100	1.498	1	0	0.0	5	0.0	NA	0.698	NA	0.0
Galbitalea	1	0.4	31	4.2	0.000	1.491	1.491	1	0	0.0	2	0.8	NA	0.301	NA	0.0
Microlunatus	2	0.4	55	5.4	0.301	1.740	1.439	1	1	0.0	2	0.8	0.000	0.301	0.301	0.3
Unidentified (Solirubrobacterales)	29	0.0	637	5.4	1.462	2.804	1.341	1	110	0.8	21	0.5	2.041	1.322	-0.719	
Unidentified (Thermomicrobiales)	21	0.0	323	0.0	1.322	2.509	1.186	1	164	0.0	194	0.0	2.214	2.287	0.0729	0.0
Jiangella	18	2.5	230	48.5	1.255	2.361	1.106	1	2	0.5	482	174.5	0.301	2.683	2.382	0.0
Sphingopyxis	323	2.5	3663	48.5	2.509	3.563	1.054	1	15	0.5	4054	84.5	1.176	3.607	2.431	0.0
Afipia	72	10.8	771	18.0	1.857	2.887	1.029	1	57	5.8	1115	95.2	1.755	3.047	1.291	0.9
Phenylobacterium	25	2.7	255	41.0	1.397	2.406	1.008	1	9	1.2	22	8.5	0.954	1.342	0.388	0.4
Methylopila	205	61.4	15	3.0	2.311	1.176	-1.135	1	75	20.4	961	62.2	1.875	2.982	1.107	
Streptomyces	1163	161.5	66	1.8	3.065	1.819	-1.246	1	394	20.6	77	7.2	2.595	1.886	-0.709	0.7
Reyranella	368	28.5	19	6.7	2.565	1.278	-1.287	1	7	1.6	0	0.0	0.845	NA	NA	0.0
Rhodopseudomonas	195	49.1	3	0.8	2.290	0.477	-1.812	1	0	0.0	0	0.0	NA	NA	NA	0.0
Unidentified (Alcaligenaceae)	2721	6.8	17	2.0	3.434	1.230	-2.204	1	8578	0.0	7891	1.1	3.933	3.897	-0.036	0.0
Pseudomonas	50870	3896.6	41	4.7	4.706	1.612	-3.093	1	63810	1056.8	9753	758.3	4.804	3.989	-0.815	0.3
Bray-curtis distance	NA	NA	NA	NA	NA	NA	NA	1	0.36	NA	0.77	NA	NA	NA	0.403	0.0
16S Copy number / ng DNA	2.94E+08	193.2	4.36E+09	378.1	8.468	9.639	1.171	1	3.68E+09	96.4	7.75E+09	477.0	0.322	9.889	0.411	0.4
Archaea																
Number of reads	8129	431.2	745	5.2	3.910	2.872	-1.037	1	17770	732.8	1798	16.1	4.249	3.254	-0.994	1.0
16S Copy number / ng DNA	6.61E+9	195.8	2.66E+08	195.8	9.820	6.958	-2.861	1	2.20E+09	400.7	8.53E+07	458.9	9.341	6.209	-2.666	0.0
Fungi																
Chrysosporium	2666	542.5	1	0.0	3.425	0.000	-3.425	1	2413	378.1	8	5.4	3.382	0.903	-2.479	0.8
Pseudogymnoascus	17486	1910.9	18	0.8	4.242	1.255	-2.987	1	13827	684.5	90	19.0	4.140	1.954	-2.186	0.8
Illyonectria	882	190.1	2	0.0	2.945	0.301	-2.644	1	10	2.8	0	0.0	1.000	NA	NA	0.0
Trichoderma	597	77.7	2	0.8	2.775	0.301	-2.474	1	309	32.3	2827	18.1	2.489	3.451	0.961	
Serendipita	1046	338.0	9	0.0	3.019	0.954	-2.065	1	8	0.0	0	0.0	0.903	NA	NA	0.0
Cephalotrichum	1068	114.4	12	1.8	3.028	1.079	-1.949	1	1651	209.1	27	9.8	3.217	1.431	-1.786	0.9
Unidentified (Hypocreales)	1086	178.0	26	7.1	3.035	1.414	-1.620	1	4337	632.1	4567	235.6	3.637	3.659	0.022	
Oidodendron	296	39.0	14	3.0	2.471	1.146	-1.325	1	25	2.5	1	0.0	1.397	0.000	-1.397	1.0
Unidentified	9764	3235.6	637	74.8	3.989	2.804	-1.185	1	3178	668.6	184	8.8	3.502	2.264	-1.237	1.0
Clonostachys	719	107.5	64	15.4	2.856	1.806	-1.050	1	200	38.7	6	0.6	2.301	0.778	-1.522	0.6
Gliomastix	895	63.2	87	13.6	2.951	1.939	-1.012	1	355	58.8	13	8.6	2.550	1.113	-1.436	0.6
Ochroconis	3003	57.5	38910	765.0	3.477	4.590	1.112	1	913	210.9	627	213.3	2.960	2.797	-0.163	
Mortierella	55	10.5	9100	1408.1	1.740	3.959	2.218	1	774	90.1	67	2.3	2.888	1.826	-1.062	
Saccharomyces	1	0.0	212	1.7	0.000	2.326	2.326	1	173	0.0	1	0.0	2.238	0.000	-2.238	
Bray-curtis distance	NA	NA	NA	NA	NA	NA	NA	1	0.54	NA	0.847	NA	NA	NA	0.568	0.5
ITS Copy number / ng DNA	1.33E+08	1851.8	5.48E+09	975.8	8.123	9.738	1.615	1	1.50E+09	458.9	2.40E+09	458.9	9.176	9.380	0.416	0.0

Nave low								Passage horizontal										
Raw data				Log data				Raw data				Log data				Raw data		
Unmarked surface	Unmarked surfaces (SD)	Dark zone	Dark zone (SD)	Unmarked surface (log)	Dark zone (log)	Delta log	Score	Unmarked surface	Unmarked surfaces (SD)	Dark zone	Dark zone (SD)	Unmarked surface (log)	Dark zone (log)	Delta log	Score	Unmarked surface	Unmarked surfaces (SD)	Dark zone
0	0.0	0	0.0	NA	NA	NA	0.0	0	0.0	0	0.0	NA	NA	NA	0.0	0	0.0	0
1	0.0	0	0.0	NA	NA	NA	0.0	1	0.0	0	0.0	0.000	NA	NA	0.0	0	0.0	0
3	0.8	0	0.0	0.477	NA	NA	0.0	0	0.0	0	0.0	NA	NA	NA	0.0	0	0.0	0
36	14.6	55	21.9	1.556	1.740	0.184	0.0	2	0.8	102	29.5	0.301	2.008	1.707	0.8	29	11.8	1029
25	10.2	3	0.0	1.397	0.477	-0.920		30	0.0	24	0.0	1.477	1.380	-0.096		20	5.6	24
104	11.8	21	0.0	2.017	1.322	-0.694		33	1.6	838	161.2	1.518	2.923	1.404	0.9	15	1.2	2
3	1.2	0	0.0	0.477	NA	NA	0.0	27	6.8	351	75.9	1.431	2.545	1.113	0.8	167	27.1	8
772	312.1	50	8.6	2.887	1.690	-1.188		6	1.1	19	2.8	0.778	1.278	0.500	0.5	60	20.7	114
72	2.8	3	0.4	1.857	0.477	-1.380		2	0.0	10	0.0	0.301	1.000	0.698	0.6	2	0.4	0
448	182.8	73	22.0	2.651	1.863	-0.787		41	10.9	1583	202.5	1.612	3.199	1.586	1.0	160	62.3	266
164	66.9	170	69.4	2.214	2.230	0.015	0.0	0	0.0	0	0.0	NA	NA	NA	0.0	0	0.0	0
36	14.2	154	41.1	1.556	2.187	0.631	0.5	5	0.7	46	6.5	0.698	1.662	0.963	0.7	104	39.0	249
1	0.0	0	0.0	NA	NA	NA	0.0	2	0.0	0	1.1	0.301	NA	NA	0.0	0	0.0	16
0	0.0	0	0.0	NA	NA	NA	0.0	0	0.0	0	0.0	NA	NA	NA	0.0	0	0.0	0
8	3.2	0	0.0	NA	NA	NA	0.0	18	3.1	397	74.0	1.255	2.598	1.343	1.0	5	0.5	9
8	0.0	1	0.0	0.903	0.000	-0.903		15	0.9	173	7.8	1.176	2.238	1.061	0.8	8	0.8	3
69	0.0	34	0.0	1.838	1.531	-0.307		24	0.0	329	0.0	1.380	2.517	1.136	1.0	58	0.0	174
161	65.7	18	4.3	2.206	1.255	-0.951		6	1.5	715	126.7	0.778	2.854	2.076	0.1	95	35.8	2783
722	65.8	18024	45.0	2.858	4.255	1.397	0.8	411	1.5	7439	126.7	2.613	3.871	1.257	0.9	1685	5.6	6916
407	159.8	9101	630.0	2.609	3.959	1.349	0.8	146	21.6	2001	209.3	2.164	3.301	1.136	1.0	229	70.1	5435
29	10.8	135	40.0	1.462	2.130	0.667	0.7	172	19.8	562	114.4	2.235	2.749	0.514	0.6	70	9.6	139
163	66.5	431	38.7	2.212	2.634	0.422		13	1.9	36	10.6	1.113	1.556	0.442		244	65.2	7
56	8.9	142	26.8	1.748	2.152	0.404		177	23.3	1034	151.9	2.247	3.014	0.766		104	8.7	188
12	3.5	4	1.6	1.079	0.602	-0.477	0.4	3	0.8	1	0.0	0.477	0.000	-0.477	0.4	1	0.0	1
0	0.0	0	0.0	NA	NA	NA	0.0	0	0.0	0	0.0	NA	NA	NA	0.0	0	0.0	0
16947	14.2	1447	41.1	4.229	3.160	-1.068	0.5	13201	0.7	87	6.5	4.120	1.939	-2.181	0.9	6622	39.0	15
34436	4598.8	235	21.3	4.537	2.371	-2.165	0.8	31674	1524.5	586	114.6	4.500	2.767	-1.732	0.6	18412	1867.6	171
0.523	NA	0.829	NA	NA	NA	21.500	0.0	0.712	NA	0.848	NA	NA	NA	1.026	1.0	0.556	NA	0.733
5.19E+09	171.5	2.33E+11	335.3	1.661	11.377	0.133	0.0	2.46E+09	211.5	3.40E+09	13.5	0.139	9.531	-1.146	0.0	2.56E+10	119.4	2.44E+09
14482	1919.7	433	25.9	4.160	2.636	-1.524	0.7	14048	6561.0	11757	103.8	4.147	4.070	-0.077	0.0	12375	484.6	244
1.47E+09	232.4	5.62E+08	8471.4	9.166	7.497	-3.266	0.5	5.35E+08	18.4	8.73E+07	109.4	8.728	6.224	-4.608	0.0	2.64E+10	127.9	3.30E+07
13	3.0	2.4	0.0	1.113	0.380	-0.733	0.3	135	42.7	5763	29.6	2.130	3.760	1.630		340	11.0	1312
19252	4113.5	4.8	3.5	4.284	0.681	-3.603	1.0	6731	3.9	103	51.4	3.828	2.012	-1.815	0.7	3876	9.6	17
138	42.0	0	0.0	2.139	NA	NA	0.0	42	5.1	87	58.4	1.623	1.939	0.316		78	21.6	8
6245	467.0	474	26.6	3.795	2.675	-1.119	0.5	3313	729.8	144	37.9	3.520	2.158	-1.361	0.6	955	10.3	287
0	0.0	0	0.0	NA	NA	NA	0.0	0	0.0	0	0.0	NA	NA	NA	0.0	4	0.0	0
5856	63.2	9775.2	68.5	3.767	3.990	0.222		298	70.7	711	73.3	2.474	2.851	0.377		465	104.5	70
1658	126.0	188.4	66.4	3.219	2.275	-0.944	0.6	3882	101.9	161	22.7	3.589	2.206	-1.382	0.9	1369	132.5	32
20	0.0	0	0.0	1.301	NA	NA	0.0	6	2.0	1	0.0	0.778	0.000	-0.778	0.6	11	4.4	0
1425	436.1	93.6	3.9	3.153	1.971	-1.182	1.0	400	72.2	1777	92.5	2.602	3.249	0.647		1008	52.7	463
326	123.8	2.4	0.0	2.513	0.380	-2.133	0.0	4127	447.7	3	0.0	3.615	0.477	-3.138	0.0	866	91.4	0
548	81.8	3.6	1.4	2.738	0.556	-2.182	0.0	78	9.6	332	11.7	1.892	2.521	0.629		450	75.2	32
121	58.0	6066	3.8	2.082	3.782	1.700	0.6	267	1.1	1248	64.0	2.426	3.096	0.669	0.7	562	4.8	6243
1921	154.6	32.4	3.1	3.283	1.510	-1.772		70	6.8	298	65.0	1.845	2.474	0.629	0.3	2285	835.4	181
985	318.0	0	0.0	2.993	NA	NA	0.0	7	2.4	0	0.0	0.845	NA	NA	0.0	128	6.4	218
0.546	NA	0.806	NA	NA	NA	0.485	0.6	0.762	NA	0.733	NA	NA	NA	-0.037		0.668	NA	0.751
1.62E+09	765.4	1.44E+11	87.4	9.209	11.156	0.1099	0.8	5.44E+08	91.9	2.89E+09	101.9	8.735	9.457	-1.214	0.5	2.63E+09	5112.9	3.44E+09

Passage vertical					Bulls center								Bulls left					
	Log data				Raw data				Log data				Raw data				Log data	
Dark zone (SD)	Unmarked surface (log)	Dark zone (log)	Delta log	Score	Unmarked surface	Unmarked surfaces (SD)	Dark zone	Dark zone (SD)	Unmarked surface (log)	Dark zone (log)	Delta log	Score	Unmarked surface	Unmarked surfaces (SD)	Dark zone	Dark zone (SD)	Unmarked surface (log)	Dark zone (log)
0.0	NA	NA	NA	0.0	0	0.0	0	0.0	NA	NA	NA	0.0	0	0.0	0	0.0	NA	NA
0.0	NA	NA	NA	0.0	0	0.0	0	0.0	NA	NA	NA	0.0	2	0.5	0	0.0	0.301	NA
0.8	NA	NA	NA	0.0	3	0.8	1	0.0	0.477	0.000	-0.477		0	0.0	0	0.0	NA	NA
85.4	1.462	3.012	1.550	0.7	11	2.0	160	28.5	1.041	2.204	1.162	0.6	111	31.2	545	75.0	2.045	2.736
0.5	1.301	1.380	0.079	0.0	64	1.2	17	0.5	1.806	1.230	-0.575		168	1.2	36	0.0	2.225	1.556
0.8	1.176	0.301	-0.875		5	0.8	27	1.0	0.698	1.431	0.732	0.5	39	11.3	35	14.2	1.591	1.544
1.0	2.222	0.903	-1.319		42	8.2	9	1.3	1.623	0.954	-0.669		802	55.9	65	18.2	2.904	1.812
22.7	1.778	2.056	0.278	0.0	27	2.7	74	11.3	1.431	1.869	0.437	0.3	35	10.1	11	0.7	1.544	1.041
0.0	0.301		NA	0.0	10	0.0	56	0.0	1.000	1.748	0.748	0.6	14	0.8	156	0.0	1.146	2.193
16.9	2.204	2.424	0.220	0.1	106	16.7	1242	147.4	2.025	3.094	1.068	0.8	534	96.5	1162	194.1	2.727	3.065
0.0	NA	NA	NA	0.0	1	0.4	28	8.6	0.000	1.447	1.447	1.0	0	0.0	0	0.0	NA	NA
24.3	2.017	2.396	0.379	0.4	98	2.3	2	0.0	1.991	0.301	-1.690		86	4.0	480	126.3	1.934	2.681
0.0	NA	1.204	NA	0.0	2	0.8	11	0.0	0.301	1.041	0.740	0.6	40	2.1	319	2.5	1.602	2.503
0.0	NA	NA	NA	0.0	0	0.0	0	0.0	NA	NA	NA	0.0	0	0.0	0	0.0	NA	NA
0.3	0.698	0.954	0.255	0.0	14	1.6	8	2.8	1.146	0.903	-0.243		410	94.2	38	4.5	2.612	1.579
0.5	0.903	0.477	-0.425		38	2.2	6	2.4	1.579	0.778	-0.801		20	36.0	11	8.0	1.301	1.041
0.0	1.763	2.240	0.477	0.5	224	0.0	105	0.4	2.350	2.021	-0.329		707	0.0	192	0.0	2.849	2.283
208.5	1.977	3.444	1.466	0.8	145	20.0	1818	407.8	2.161	3.259	1.098	1.0	437	66.4	1216	232.1	2.640	3.084
8.5	3.226	3.839	0.613	0.6	602	20.0	17174	407.8	2.779	4.234	1.455	0.8	2025	66.4	11420	232.1	3.306	4.057
276.9	2.359	3.735	1.375	0.8	339	45.0	4699	607.6	2.530	3.670	1.141	1.0	137	23.1	2553	336.2	2.136	3.407
12.4	1.845	2.143	0.297	0.4	112	18.0	487	52.5	2.049	2.687	0.638	0.7	181	17.3	160	12.1	2.257	2.204
1.1	2.387	0.845	-1.542	0.8	998	87.0	19	4.9	2.999	1.278	-1.720	0.6	195	31.8	76	25.6	2.290	1.880
23.1	2.017	2.274	0.257		439	46.8	290	82.1	2.642	2.462	-0.180	0.1	583	140.1	106	25.3	2.765	2.025
0.0	0.000	0.000	0.000	0.0	131	20.6	25	5.4	2.117	1.397	-0.719	0.6	20	4.7	33	10.1	1.301	1.518
0.0	0.000	0.000	0.000	0.0	62	16.1	0	0.0	1.792	NA	NA	0.0	1	0.0	0	0.0	0.000	NA
24.3	3.820	1.176	-2.644	0.9	2703	2.3	270	0.4	3.431	2.431	-1.000	0.5	1569	4.0	703	126.3	3.195	2.846
16.6	4.265	2.232	-2.032	0.7	46213	790.6	396	79.2	4.664	2.597	-2.067	0.7	15890	4418.1	225	33.6	4.201	2.352
NA	NA	NA	-0.205	0.0	0.769	NA	0.781	NA	NA	NA	-0.231	0.0	0.769	NA	0.781	NA	NA	NA
33.5	-1.021	9.386	0.338	0.3	1.06E+09	272.7	2.73E+09	255.9	0.411	9.436	0.322	0.3	4.5E+09	94.8	6.12E+09	1202.2	0.133	9.786
76.7	4.092	2.387	-1.705	0.5	13455	699.3	1006	65.3	4.128	3.002	-1.126	1.0	5736	3913.5	437	39.1	3.758	2.640
1275.9	10.421	5.646	-3.454	0.3	3.31E+08	34.8	4.72E+07	412.8	8.520	5.853	-3.131	1.0	2.83E+09	793.3	8.18E+07	53.3	9.451	6.184
80.4	2.531	3.117	0.586		1207	66.2	24	6.4	3.081	1.380	-1.701	0.6	14749	94.2	4151	653.0	4.168	3.618
2.6	3.588	1.230	-2.357	0.8	1935	626.8	11	7.7	3.286	1.041	-2.245	0.8	5397	81.0	18	8.7	3.732	1.255
6.7	1.892	0.903	-0.989	0.4	26	2.0	1	0.0	1.414	0.000	-1.414	0.6	35	4.7	5	0.2	1.544	0.698
3.0	2.980	2.457	-0.522	0.3	441	95.6	0	0.0	2.644	NA	NA	0.0	626	132.8	78	15.2	2.796	1.892
0.0	0.602	0.000	NA	0.0	0	0.0	0	0.0	NA	NA	NA	0.0	0	0.0	0	0.0	NA	NA
18.8	2.667	1.845	-0.822	0.5	169	18.2	302	21.8	2.227	2.480	0.252		59	9.8	26	6.4	1.770	1.414
4.7	3.136	1.505	-1.631	1.0	1256	811.3	502	81.2	3.098	2.700	-0.398	0.3	281	19.0	16	2.9	2.448	1.204
0.0	1.041	0.000	NA	0.0	0	0.0	0	0.0	NA	NA	NA	0.0	6	0.0	0	0.0	0.778	NA
42.0	3.003	2.665	-0.337	0.3	9347	1211.4	3304	84.4	3.970	3.519	-0.451	0.4	2706	889.6	359	10.2	3.432	2.555
0.0	2.937	0.000	NA	0.0	38	8.0	1	0.0	1.579	0.000	-1.579	0.6	16	1.1	2	0.3	1.204	0.301
9.9	2.653	1.505	-1.148	0.0	153	41.2	85	30.1	2.184	1.929	-0.255	0.6	318	65.1	130	58.4	2.502	2.113
891.9	2.749	3.795	1.045	1.0	540	30.4	784	172.1	2.732	2.894	0.161	0.0	274	89.5	2198	196.7	2.437	3.342
20.8	3.358	2.257	-1.101		676	88.1	260	48.4	2.829	2.414	-0.414		946	12.8	770	334.8	2.975	2.886
9.8	2.107	2.338	0.231	0.0	12	2.9	1	0.5	1.079	0.000	-1.079		3	0.8	0	0.0	0.477	NA
NA	NA	NA	0.122	0.0	0.837	NA	0.89	NA	NA	NA	0.063	0.0	0.704	NA	0.847	NA	NA	NA
12.9	9.420	9.536	0.350	0.0	4.64E+08	124.8	1.21E+09	44.8	8.666	9.082	0.204	0.3	5.19E+09	216.3	6.64E+09	612.3	9.712	9.821

		Bulls wall								Airlock-2 wall							
		Raw data				Log data				Raw data				Log data			
Delta log	Score	Unmarked surface	Unmarked surfaces (SD)	Dark zone	Dark zone (SD)	Unmarked surface (log)	Dark zone (log)	Delta log	Score	Unmarked surface	Unmarked surfaces (SD)	Dark zone	Dark zone (SD)	Unmarked surface (log)	Dark zone (log)	Delta log	Score
NA	0.0	0	0.0	0	0.0	NA	NA	NA	0.0	0	0.0	0	0.0	0.000	0.000	NA	0.0
NA	0.0	1	0.0	0	0.0	0.000	NA	NA	0.0	0	0.0	0	0.0	0.000	0.000	NA	0.0
NA	0.0	0	0.0	0	0.0	NA	NA	NA	0.0	1	0.0	0	0.0	0.000	0.000	NA	0.0
0.691	0.5	728	45.2	16	4.2	2.862	1.204	-1.658		150	55.9	18	4.9	2.176	1.255	-0.920	
-0.669		405	4.2	3	0.0	2.607	0.477	-2.130		33	3.6	13	0.4	1.519	1.113	-0.404	
-0.046		1617	80.7	126	48.9	3.208	2.100	-1.108		351	21.7	703	142.8	2.545	2.846	0.301	0.0
-1.091		1471	21.6	160	48.1	3.167	2.204	-0.963		116	1.7	342	42.8	2.064	2.534	0.469	0.4
-0.502		1656	66.2	4	0.8	3.219	0.602	-2.617		194	27.1	40	6.1	2.287	1.602	-0.685	
1.046	0.8	1316	0.4	261	0.4	3.119	2.416	-0.702		240	3.9	577	0.4	2.380	2.761	0.380	0.0
0.337	0.3	818	75.2	629	194.1	2.912	2.798	-0.114		282	8.8	496	42.2	2.450	2.695	0.245	0.0
NA	0.0	0	0.0	0	0.0	0.000	0.000	0.000	0.0	0	0.0	51	10.4	0.000	1.707	NA	0.0
0.746	0.6	2170	38.7	1156	318.5	3.336	3.062	-0.273		210	42.9	2366	235.2	2.322	3.374	1.051	0.8
0.901	0.8	27	0.4	29	0.0	1.431	1.462	0.031	0.0	12	2.0	227	1.9	1.079	2.356	1.276	0.9
NA	0.0	1	0.0	16	6.0	0.000	1.204	1.204	1.0	6	0.4	80	5.6	0.778	1.903	1.124	0.9
-1.033		233	3.7	98	9.6	2.367	1.991	-0.376		25	4.1	63	14.0	1.397	1.799	0.401	0.3
-0.259		649	7.6	95	2.0	2.812	1.977	-0.834		453	55.8	25	6.0	2.656	1.397	-1.258	
-0.566		3638	0.0	1616	0.8	3.560	3.208	-0.352		1954	0.9	1657	19.3	3.290	3.219	-0.071	
0.444	0.5	1787	185.3	214	41.7	3.252	2.330	-0.921		790	197.1	430	27.2	2.897	2.633	-0.264	
0.751	0.7	2239	185.3	28979	41.7	3.350	4.462	1.112	1.0	1824	197.1	6075	27.2	3.261	3.783	0.522	0.5
1.270	0.9	1820	212.6	6926	579.1	3.260	3.840	0.580	0.6	1398	162.3	6459	575.6	3.145	3.810	0.664	0.7
-0.053		65	29.5	180	31.0	1.812	2.255	0.442	0.5	111	11.1	199	31.7	2.045	2.298	0.253	0.3
-0.409	0.5	1	0.0	118	31.2	0.000	2.071	2.071		149	0.4	12	2.2	2.173	1.079	-1.094	1.0
-0.740	0.7	580	87.2	2407	628.2	2.763	3.381	0.618	0.6	480	50.8	1490	128.2	2.681	3.173	0.491	
0.217		402	3.4	52	20.3	2.604	1.716	-0.888	0.7	32	4.5	134	5.9	1.505	2.127	0.621	
NA	0.0	0	0.0	0	0.0	NA	NA	NA	0.0	132	0.0	0	0.0	0.000	0.000	NA	0.0
-0.348	0.0	21	8.7	90	8.5	1.322	1.954	0.632		7051	342.9	19	5.2	3.848	1.278	-2.569	0.8
-1.848	0.6	14	6.0	50	12.2	1.146	1.698	0.552		28456	2.0	10	1.2	4.454	1,000	-3.454	0.9
1.066	1.0	0.713	NA	0.869	NA	NA	NA	4.302	0.0	0.912	NA	0.863	NA	NA	NA	-0.125	0.0
1.661	0.6	2.79E+09	809.8	1.99E+08	140.1	-1.146	8.299	0.139	0.0	1.93E+09	65.2	4.20E+09	80.4	0.338	9.623	-1.021	0.0
-1.118	1.0	33226	16971.3	267	245.3	4.521	2.426	-2.094	0.0	14926	2664.6	3928	201.9	4.173	3.594	-0.579	0.6
-1.669	0.9	3.53E+09	448.4	8.65E+06	61.4	9.548	4.939	-2.503	0.3	5.51E+09	86.6	9.64E+07	865.6	9.741	6.286	-4.775	0.7
-0.550	0.0	50.4	6.1	5	2.8	1.702	0.698	-1.003	0.3	135	37.9	4	1.8	2.130	0.602	-1.528	0.5
-2.476	0.8	514.8	86.7	9	2.5	2.711	0.954	-1.757	0.6	32	6.1	17	3.7	1.505	1.230	-0.274	0.0
-0.845	0.4	117.6	45.7	564	183.7	2.070	2.751	0.680		3	2.1	704	281.6	0.477	2.847	2.370	
-0.904	0.4	12792	398.5	6872	519.7	4.106	3.837	-0.269	0.0	24	3.1	967	90.2	1.380	2.985	1.605	
NA	0.0	0	0.0	0	0.0	NA	NA	NA	0.0	0	0.0	0	0.0	0.000	0.000	NA	0.0
-0.355	0.0	13.2	2.7	2	0.0	1.120	0.301	-0.819	0.5	298	.5581348741	0	0.0	2.474	0.000	NA	0.0
-1.244	0.8	362.4	32.5	195	59.4	2.559	2.290	-0.269	0.0	186	21.3	414	0.0	2.269	2.617	0.347	
NA	0.0	13.2	0.0	0	0.0	1.120	NA	NA	0.0	0	0.0	0	0.0	0.000	0.000	NA	
-0.877	0.7	6174	222.5	2058	287.4	3.790	3.313	-0.477	0.5	2689	116.5	407	154.2	3.429	2.609	-0.819	0.7
-0.903	0.9	49.2	5.3	0	0.0	1.691	NA	NA	0.0	17	7.5	19	5.4	1.230	1.278	0.048	
-0.388	0.9	1116	99.3	175	17.4	3.047	2.243	-0.804	0.0	222	50.9	98	3.4	2.346	1.991	-0.355	0.0
0.904	0.9	512.4	16.6	3375	873.8	2.709	3.528	0.818	0.8	19	7.3	1784	428.4	1.278	3.251	1.972	0.4
-0.089		6126	222.4	5711	164.8	3.787	3.756	-0.030		974	212.4	567	40.7	2.988	2.753	-0.234	
NA	0.0	7.2	0.8	0	0.0	0.857	NA	NA	0.0	84	20.9	1	0.0	1.924	0.000	-1.924	
0.203	0.0	0.755	NA	0.848	NA	NA	NA	0.123	0.0	0.847	NA	0.736	NA	NA	NA	-0.137	0.0
1.947	0.0	1.95E+09	18.4	1.19E+08	501.4	9.290	8.076	0.721	0.0	1.59E+09	74.6	3.57E+09	862.6	9.201	9.552	0.115	0.3

CHAPITRE 3

Identification des successions microbiennes associées aux phénomènes de régression et de recolonisation des taches noires

Avant-propos

Dans le chapitre précédent, nous nous sommes intéressés aux dynamiques microbiennes des zones sombres, mais les dynamiques des taches noires, second type majeur d'altération retrouvé dans la grotte de Lascaux, restent encore non caractérisées à ce jour. Les taches noires ont été identifiées sur les parois dès 2001, elles sont réparties de manière hétérogène sur les parois et se sont développées en grand nombre dans la grotte depuis 2006. Par le passé, la structure et la composition de ces taches ont été étudiées à plusieurs reprises soit par des méthodes de clonage/séquençage Sanger [Bastian *et al.*, 2010, Sáiz-Jiménez, 1995] soit par des méthodes de séquençage à haut-débit d'amplicons [Alonso *et al.*, 2018, Alonso, 2018]. Ces méthodes ont mis en évidence une abondance relative élevée (i) des champignons mélanisés (e.g. *Ochroconis*, *Exophiala*, etc.) dans les taches noires et (ii) du genre bactérien *Pseudomonas* dans les parties non tachées de certaines salles (e.g. Abside, Nef). Ces genres sont rarement prédominants dans les grottes naturelles, et l'hypothèse est faite qu'ils ont été sélectionnés en conséquence des traitements chimiques et antibiotiques [Bastian *et al.*, 2009a]. En effet, la mélanine fongique peut conférer une résistance à de nombreux types de stress environnementaux. Cependant, les champignons noirs colonisent également les zones non tachées mais avec une abondance relative beaucoup plus faible [Alonso *et al.*, 2018]. Cela suggère donc que la présence de champignons noirs n'est pas suffisante pour engendrer la formation de taches mais que l'ensemble des interactions de ces champignons avec la communauté microbienne dans son entier est à prendre en compte pour comprendre les phénomènes de formation et/ou évolution des taches noires. Dans ce contexte, deux dynamiques microbiennes particulières, associées aux taches noires ont été étudiées, (i) la régression de certaines taches noires, qui a lieu uniquement dans le Cabinet des Félins, salle terminale de la grotte de Lascaux **(Article 4)** et (ii) la recolonisation après nettoyage mécanique de certaines taches noires dans l'Abside **(Article 5)**.

Les échantillons ont été prélevés par la restauratrice Diane Henry-Lormelle avec le support technique de l'UMR Écologie Microbienne, et analysés en suivant le protocole décrit page 86 compatible avec les contraintes de conservation de la grotte.

La première étude **(Article 4)**, concernant l'identification des dynamiques microbiennes associées au phénomène de régression (atténuation) des taches noires a été réalisée grâce à 18 échantillons prélevés avant le début de ma thèse (février 2017), complété par 18 autres échantillons en 2022 et qui sont toujours en cours de séquençage. Ces échantillons proviennent de l'entrée du Cabinet des Félins, seule salle ou une régression naturelle des taches noires est observée. Le Cabinet des Félins est une salle terminale de la grotte avec des teneurs en CO_2 importantes et la présence de champs ornés très proches du cheminement, ce qui rend cette salle difficile d'accès. Prenant en considération la perturbation anthropique (chimique, vaporisation de Vitalub 5% sur les parois) survenue dans les années 2000 dans le Cabinet des Félins, trois conditions de surfaces ont été prélevées illustrant trois types de réponses à cette perturbation : (i) le calcaire non taché correspondant à la communauté résistante à cette perturbation, (ii) les taches noires correspondant à la communauté impactée par cette perturbation et (iii) les taches atténuées correspondant à la communauté résiliente à cette perturbation. Les résultats de cette

étude ont permis la reconstruction de scenarii écologiques basés sur les processus d'assemblage des communautés microbiennes des trois domaines du vivant en réponse à une perturbation. Quatre scenarii ont été identifiés dont trois sont déjà décrits dans la littérature. Plus précisément, nous avons proposé l'existence d'un quatrième scenario qui concerne les taxons microbiens toujours rares, pour lesquels les processus stochastiques prédominent même après perturbation, mais sont remplacés par des processus déterministes lors de la phase de résilience à cette perturbation. Cela suggère donc un rôle majeur de la biosphère rare dans la résilience, dû à des fonctions clés nécessaires au rétablissement de l'écosystème.

Mon rôle dans ce travail a été le suivant : j'ai participé à la réflexion sur les objectifs scientifiques et à la démarche expérimentale. J'ai réalisé les étapes de biologie moléculaire avant séquençage (extraction ADN, PCR1). J'ai traité les données de séquençage brutes, j'ai ensuite analysé ces données, notamment en réalisant des statistiques multivariées et de la modélisation déterminant les processus d'assemblage des communautés.

La deuxième étude **(Article 5)**, qui concerne l'identification des dynamiques microbiennes associées au phénomène de recolonisation des taches noires, a été réalisée suite à un nettoyage mécanique (utilisation d'un scalpel stérile et finitions dans certaines zones avec une éponge) effectué par la restauratrice en septembre 2020 pour six taches noires de l'Absidiole. Six conditions de surface altérées ont été étudiées en septembre 2020, octobre 2020, décembre 2020, janvier 2022 et avril 2022, correspondant à des échantillons prélevés (i) avant nettoyage, (ii) juste après le nettoyage, (iii) 3 semaines après le nettoyage, (iv) 4 mois après le nettoyage, (v) 16 mois après le nettoyage et (vi) 19 mois après le nettoyage. La partie nettoyée avec un scalpel et une éponge, correspondant à la sixième condition a été prélevée 19 mois après ce nettoyage. Les témoins de cette étude correspondent aux éponges seules, au calcaire non marqué et aux taches noires non nettoyées prélevées le jour du nettoyage et 19 mois après le nettoyage. Au total, 72 échantillons ont été prélevés pour cette étude. Les résultats de cette étude ont montré que le nettoyage mécanique des taches noires permettait de générer artificiellement une succession microbienne dont les principaux représentants sont affiliés aux genres *Pseudomonas*, *Pedomicrobium* et *Ochroconis*. Des différences microbiennes ont été observées entre les surfaces nettoyées au scalpel et les surfaces nettoyées à l'éponge, probablement en raison de modifications des propriétés de surface induites par les éponges qui peut donc engendrer une colonisation différentielle du substrat par les microorganismes. Certains taxons allochtones, i.e. potentiellement des contaminants, ont été identifiés (*Filomicrobium*, *Isaria*, *Cephalotrichum*) dans les éponges et sur les surfaces nettoyées à l'éponge. Ces taxons sont cités dans la littérature comme acteurs de la biodégradation de peintures dans les milieux souterrains [Nováková, 2009, Diaz-Herraiz *et al.*, 2014].

Mon rôle dans ce travail a été le suivant : j'ai participé à la réflexion sur les objectifs scientifiques, à la démarche expérimentale ainsi qu'aux différentes missions d'échantillonnage. J'ai réalisé les étapes de biologie moléculaire avant séquençage (extraction ADN, PCR1). J'ai traité les données de séquençage brutes, j'ai ensuite analysé ces données permettant d'observer les dynamiques de recolonisation microbiennes.

L'ensemble de ce travail a permis la rédaction de deux publications 'Microbiome facing

disturbance : common response of the rare biosphere from the three domains of life' (soumission prévue début 2023) et 'Experimental assessment of microbial successions following mechanical removal of black stain alterations on Paleolithic cave walls' (soumission prévue fin 2022).

Article 4. Microbiome facing disturbance : common response of the rare biosphere from the three domains of life

ZELIA BONTEMPS[1], YVAN MOENNE-LOCCOZ[1] AND MYLENE HUGONI[1,2]

[1]Univ Lyon, Université Claude Bernard Lyon 1, CNRS, INRAE, VetAgro Sup, UMR Ecologie Microbienne, F-69622 Villeurbanne, France
[2] Institut Universitaire de France (IUF)

Current address for Mylène Hugoni : Univ Lyon, INSA Lyon, CNRS, UMR 5240 Microbiologie Adaptation et Pathogénie, F-69621 Villeurbanne, France

Short running title : Common response of the rare biosphere to disturbance

Corresponding author
Mylène HUGONI
Univ Lyon, Université Claude Bernard Lyon 1, CNRS, INRAE, VetAgro Sup, UMR5557 Ecologie Microbienne, 43 bd du 11 novembre 1918, F-69622 Villeurbanne, France
mylene.hugoni@univ-lyon1.fr

Abstract

Community assembly processes are complex and understanding them represent a challenge in microbial ecology. Here, we used Lascaux Cave as a stable, confined environment to quantify the importance of stochastic vs deterministic processes during microbial community dynamics across the three domains of life, in relation to an anthropogenic disturbance that had resulted in side-by-side occurrence of a resistant community (unstained limestone), an impacted community (present in black stains) and a resilient community (attenuated stains). Unexpectedly, we found four scenarios to explain community response to disturbance in stable conditions for the three domains of life. Specifically, we proposed the existence of a fourth, not-documented yet scenario that concerns the always-rare microbial taxa, where stochastic processes predominate even after disturbance, but are replaced by deterministic processes during post-disturbance recovery. This points to a major role of always-rare taxa in resilience, perhaps because they provide key functions required for ecosystem recovery.

Keywords

Community assembly processes ; Disturbance ; Rare biosphere ; Microbial ecology.

Introduction

The relevance of community assembly rules for predicting and modelling how communities face different environmental scenarios, based on events controlling the presence and abundance of species in a community, is a key issue in ecology. According to the niche-based theory, deterministic processes linked to abiotic and biotic factors dictate community assembly, making environmental filtering and/or niche selection the prevalent mechanisms underpinning ecological selection (Vellend 2010 ; Zhou and Ning 2017). Conversely, the neutral theory emphasizes the role of stochastic processes (Hubbell 2001 ; Sloan et al. 2006 ; Vellend 2010 ; Chase and Myers 2011 ; Zhou and Ning 2017), with a major part played by ecological drift, dispersal limitation and probabilistic dispersal (Zhou and Ning 2017 ; Corline et al. 2021). While the consensus is that both deterministic and stochastic processes simultaneously influence the assembly of communities, along a continuum (Chase and Myers 2011 ; Zhou and Ning 2017), the challenge is now to quantify their importance in various ecosystems. While these ecological concepts have been historically applied to macroorganisms (Chase 2007 ; Hartmann et al. 2012 ; Kardol et al. 2013 ; Burns et al. 2016 ; Mi et al. 2016 ; Ning et al. 2020), they have hardly been considered for microbial communities.

In natural ecosystems, microorganisms are highly diversified, growing and evolving fast, depending on horizontal gene transfers or mutation (Prescott et al. 2003), and they form complex assemblages of Archaea, Bacteria and Microeukaryota. Most studies have focused on a single domain-of-life instead of taking into account the entire microbiome (Ferrenberg et al. 2013 ; Tripathi et al. 2018 ; Gao et al. 2020 ; Jiao and Lu 2020 ; Luan et al. 2020). As key contributors to biogeochemical cycles, microorganisms represent a biosphere compartment that must be considered to model and predict global changes (Madsen 2011). Microbial communities exposed to disturbance may display (i) resistance, involving plasticity (Maurice et al. 2013) ; (ii) resilience, based on functional redundancy (Allison and Martiny 2008 ; Shade et al. 2012) and/or (iii) an alternative state where new taxa harboring different functions arise, inducing a new community functioning (Shade et al. 2012 ; Zaneveld et al. 2017). Many studies focusing on microbial responses to disturbance have used experimental set-ups that lacked realism and complexity (i.e. lab conditions, simplified consortia), but stable ecosystems experiencing ecological disturbance are more relevant to assess community assembly patterns in natural conditions.

Cave ecosystems provide a unique set of stable environmental variables including absence of light, high relative humidity and CO_2 concentrations, almost-constant temperature and oligotrophy (0.5 mg organic carbon/L) (Di Russo et al. 1997 ; Cañveras 2001 ; Barton and Northup 2007 ; Bastian et al. 2009 ; Cuezva et al. 2009 ; Engel 2010 ; Pasić et al. 2010 ; De Leo et al. 2012 ; Hüppop 2012 ; Banerjee and Joshi 2013). Interestingly, many are rather confined, implying slow exchanges with surrounding karst (Bourges et al. 2014). This is the case today for Lascaux Cave, which has been monitored from a climatic, hydrogeological and microbiological standpoint for over a decade (Lacanette et al. 2007 ; Bastian et al. 2010 ; Alabouvette and Saiz-Jiménez 2011 ; Bourges et al. 2014 ; Alonso 2018). Within caves, terminal rooms are particularly stable, such as Lascaux's Chamber of Felines, which also was never visited by the public. During the 2000s, Lascaux Cave has been the theater of chemical treatments to prevent fungal outgrowth problems related to past tourism activities (Lefèvre 1974 ; Bastian et al. 2010 ; Martin-Sanchez et al. 2015).

This anthropization constituted a disturbance for microbial communities initially established, prompted the development of melanin-producing fungi on cave surfaces, and resulted in the formation of black stains, many still present (Bastian et al. 2010 ; Alabouvette and Saiz-Jiménez 2011 ; Martin-Sanchez et al. 2012a, 2015 ; Alonso 2018).

In the Chamber of Felines, three rock surface conditions (Fig 1.) are present on the same walls, i.e. (i) limestone that has never been stained (microbial community considered resistant to anthropization ; control), (ii) black stains present since 2002 (impacted community), and (iii) former black stains, now greyish, where black pigmentation has progressively disappeared since 2007. These greyish, attenuated stains differ little from unstained limestone and correspond to a resilient status. We aimed at testing whether community assembly patterns were similar for Archaea, Bacteria and Microeukaryota retrieved during the resistant, impacted, and resilient states. By assessing the abundant and rare biospheres, we demonstrated for the first time that always-rare taxa, shaped by stochastic processes in control and impacted communities, were the only microbial fraction selected among the three domains of life during the resilient state.

Materials and Methods

Sampling. Lascaux Cave is located in the South-West of France (N 45°03'13.087" and E 1°10'12.362"). Samples were collected in February 2017 from the walls of the Chamber of Felines, in areas devoid of Paleolithic paintings and engravings, with special authorization (from Ministry of Culture, DRAC Nouvelle-Aquitaine). Six black stains, six control zones (i.e. unstained surface) and six attenuated stains were sampled using swabs gently rubbed against the rock wall. Samples were conserved at -80°C until DNA extraction.

Illumina sequencing and bioinformatics analysis. Total genomic DNA extraction was performed using the FastDNA SPIN Kit For Soil (MP Biomedicals, Illkirch, France), following the manufacturer's instructions. DNA concentration was quantified using the Qubit dsDNA HS Assay Kit (Invitrogen, Carlsbad, CA) following the manufacturer's preconisation.

Three gene markers were analyzed in each individual sample. The V3-V4 region of the 16S rRNA genes was amplified in triplicate for Bacteria and Archaea using the universal primers 341F (CCTACGGGNGGCWGCAG) and 805R (GACTACHVGGGTATCTAATCC) (Herlemann et al. 2011), and 515F (CAGCCGCCGCGGTAA) and 915R (GTGCTCCCCCGCCAATTCCT) (Herfort et al. 2009), respectively. For Eukaryota, the V4 region of the 18S rRNA genes was amplified in triplicate using the universal primers 0067a deg (AAGCCATGCATGYCTAAGTATMA) and NSR399 (TCTCAGGCTCCYTCTCCGG) (Dollive et al. 2012). The PCR mix consisted in 5 µl of 5× Hot BioAmp Blend Master Mix RTL (Biofidal, Vaux-en-Velin, France), 0.1 µM of the two primers, 0.1× GC-rich-enhancer (Biofidal), 0.2 ng.µl-1 of bovine serum albumin (Promega, Madison, WI) and 0.2-1.0 ng DNA. All amplifications were performed in a Bio-Rad T1000 thermal cycler (Bio-Rad, Hercules, CA). The PCR program for Bacteria was 3 min at 95°C, 28 cycles of 45 s at 95°C, 45 s at 50°C and 90 s at 72°C, followed by 7 min at 72°C. For Archaea, it consisted in 10 min at 94°C, 30 cycles of 1 min at 94°C, 1 min at 58°C and 90 s at 72°C, followed by 10 min at 72°C. For the 18S rRNA gene, it consisted in 10 min at 95°C, 30 cycles of 1 min at 94°C, 1 min at 55°C and 90 s at 72°C, followed by 10 min at

72°C. For the ITS2 region, it consisted in 10 min at 95°C, 28 cycles of 20 s at 94°C, 30 s at 47°C and 20 s at 72°C, followed by 7 min at 72°C. All primers were tagged with the Illumina adapter sequences (TCG TCG GCA GCG TCA GAT GTG TAT AAG AGA CAG and GTC TCG TGG GCT CGG AGA TGT GTA TAA GAG ACA G), allowing the construction of amplicon libraries by a two-step PCR. DNA extraction was also carried out from tubes without any biological matrix, and this negative control was used to evaluate and subtract ambient and kit products contamination. Amplification signals were checked by electrophoresis on 1.5% agarose gel. High-throughput sequencing was achieved after pooling PCR triplicates, using Illumina MiSeq with 2 x 300 bp, paired-end chemistry v3.

For each of the three datasets (i.e. bacterial 16S rRNA genes, archaeal 16S rRNA genes and eukaryotic, 18S rRNA genes), paired-end reads were merged with a maximum of 10% mismatches in the overlap region using FLASh (Fast Length Adjustment of Short reads) (Magoč and Salzberg 2011). Denoising procedures were carried out by discarding reads without the expected length (200-500 bp) or containing any ambiguous bases (N). After dereplication of sequences, the clusterisation tool was run with Swarm (Mahé et al. 2014), which uses a local clustering threshold rather than a global threshold and an aggregation distance of 3 for identification of OTUs. Chimeric OTUs were removed using VSEARCH (Rognes et al. 2016). Moreover, low abundance sequences were filtered to keep OTUs representing at least 0.005% of all sequences (Bokulich et al. 2013). Taxonomic affiliation was performed with both RDP Classifier and BLASTn (Zhang and Madden 1997) against the 138.1 SILVA database (Quast et al. 2013) for bacterial 16S rRNA genes, archaeal 16S rRNA genes and microeukaryotic 18S rRNA genes and against the 8.2 UNITE database for fungal ITS markers (Nilsson et al. 2019). This procedure was automated in the FROGS pipeline (Escudié et al. 2018). Contaminant OTUs identified from the negative control samples were removed. To compare samples, a normalization procedure was applied by randomly resampling down to 12,105, 6,209, 31,981 and 25,821 sequences in the bacterial, archaeal, microeukaryotic and fungal datasets, respectively.

Rarefaction curves were calculated to assess sequencing effort, using Paleontological Statistics (PAST) software v4.02 (Hammer et al. 2001). OTU richness and diversity were estimated using Chao 1 index (Chao 1987), Shannon's H' (Shannon 1948), and Simpson (1-D) index (Supplementary Table 3) (Simpson 1949). Communities were primarily compared with NMDS, using vegan package35 in R (R Core Team 2020). The procedure computes a stress value, which measures the difference between the ranks on the ordination configuration and the ranks in the original similarity matrix for each replicate (Clarke 1993). Analysis of similarity (ANOSIM) was conducted using the vegan package in R (Oksanen et al. 2020), to test differences ($P < 0.05$) in overall community composition between the three rock surface conditions i.e. resistant, impacted and resilient, and to further confirm the results observed in the NMDS plot. A Bonferroni correction was applied to P values to lower alpha risk. All analyses were based on abundance dissimilarity matrices with the Bray-Curtis index (Bray and Curtis 1957), using R.

Definition of abundant and rare taxa. In this study, OTUs were classified into four categories according to their relative abundance (Chen et al. 2019), as described (Supplementary Fig. 4) : (i) always-rare taxa, with an abundance $< 0.01\%$ in all samples, (ii) conditionally-rare

taxa, with an abundance $< 1\%$ in all samples and $< 0.01\%$ in some samples (maximum 33% of samples), (iii) moderate taxa, with an abundance $< 1\%$ and $> 0.01\%$ in all samples, and (iv) dominant taxa, with an abundance $\geq 1\%$ of all sequences in all samples or that fluctuates strongly, i.e. $< 0.01\%$ in certain samples and $\leq 1\%$ in others.

Assessment of community dispersal rate : neutral model. Sloan's Neutral Community Model (NCM) was used to estimate the importance of passive dispersal on community assembly by assessing the relationship between the frequency at which taxa occur in a set of local communities and their abundance across the wider meta-community (Sloan et al. 2006). In this model, the migration rate (m) is a parameter used to evaluate the probability of a random lost of an individual in a local community, to be replaced by an immigrant from the meta-community (Hubbell 2001). It is calculated as follows :

$$Freq_i = 1 - I(1 \div N | N \times m \times p_i, N \times m \times (1 - p_i)) \tag{3.1}$$

where Freq_i is the occurrence frequency of taxa i across communities ; N is the number of individuals per community ; m is the estimated dispersal rate ; p_i is the average relative abundance of taxa i across communities ; and I() is the probability density function of beta distribution (Luan et al. 2020). This analysis was performed using nonlinear least-square fitting, and calculation of 95% confidence interval for the model predictions was conducted using the Wilson score interval ('minpack.lm' and 'Hmisc' package in R (Elzhov et al. 2016 ; Harrell and Dupont 2018)). The overall fit of the model to observed data was done by comparing the sum of squares of residuals (SS_err) with the total sum of squares (SS_total), with model fit = 1 - $\text{SS}_err/\text{SS}_total$ (generalized R-squared). The Akaike Information Criterion (AIC) and Bayesian Information Criterion (BIC) were calculated based on 1000 bootstrap replicates for the neutral, binomial and Poisson distribution models to determine the best model fit and whether the model was based on only the random sampling of the source meta-community.

Phylogenetic analysis and estimated assembly community processes. For each taxonomic marker, sequences were aligned using MAFFT (Kuraku et al. 2013), then gaps and poorly conserved regions were eliminated using Gblocks (Castresana 2000 ; Talavera and Castresana 2007). Finally, phylogeny was reconstructed using IQ-TREE-2 (Minh et al. 2020) (default parameters), with the best model being automatically chosen by the program according to the BIC. Node support was estimated using the bootstrap method (1000 replicates). To quantify the relative importance of stochastic and deterministic processes that drive microbial community assembly, βNTI and RC_bray were calculated using R software v4.0.2, using scripts from Stegen et al. (Stegen et al. 2012), based on the phylogenetic distance and OTU abundance (n > 6 OTUs) (Stegen et al. 2012). βNTI is the number of standard deviations of the beta mean nearest taxon distance (βMNTD) from the mean of the null distribution (Stegen et al. 2012). The RCbray value was used to further partition pairwise comparisons that were assigned to stochastic processes (Zhou and Ning 2017). The βNTI values between –2 and 2 indicate dominance of the stochastic processes, whereas βNTI values smaller than –2 or larger than 2 indicate that deterministic processes (i.e., homogeneous selection and heterogeneous selection) play a

more important role in community assembly than stochastic processes (Zhou and Ning 2017). For $|\beta\text{NTI}| < 2$, $\text{RC}_b ray < -0.95$ and $\text{R}_b ray > 0.95$ indicate relative dominant influence of homogenizing dispersal and dispersal limitation, respectively ; and |RCbray| < 0.95 indicates a crucial role of "Undominated" assembly, including weak selection, weak dispersal, diversification, and/or drift (Stegen et al. 2015). The major factors that influence the assembly of dominant taxa, conditionally-rare taxa, and always-rare taxa were explored separately.

Statistical analyses.

All statistical analyses were performed in R (R 4.0.2), using "phyloseq" (McMurdie and Holmes 2013), "minipack.lm" (Elzhov et al. 2016), "hmisc" (Harrell and Dupont 2018), "vegan" (Oksanen et al. 2020), "stats" (Bolar 2019), "ade4" (Dray and Dufour 2007), "picante" (Kembel et al. 2010), "iCAMP" (Ning 2021) packages.

Results

Quantified importance of community assembly processes. Non-metric multidimensional scaling (NMDS) (Fig. 1) and permutational multivariate analysis of variance (Supplementary Table 1) showed that microbial communities in the three rock surface conditions differed. Therefore, community assembly patterns were evaluated to understand the relative importance of stochastic vs deterministic processes, using Neutral-Community Model (NCM). The NCM fitted well for archaeal, bacterial and microeukaryotic communities (Supplementary Fig. 1), outperforming binomial and Poisson distribution models (Supplementary Table 2). This points to the prevalence of stochastic processes (passive dispersal or ecological drift) independently of the random sampling performed within each of the three rock surface conditions. For the three domains of life combined, the community migration rate (m) reached an average of 0.47 in resistant communities, versus 0.06 in impacted communities and 0.19 in resilient communities (Fig. 2), pointing to more extensive dispersal and ecological drift in resistant communities compared with the others.

We quantified the relative contribution of stochastic and deterministic processes shaping microbial community assembly, by calculating the β-nearest taxon index (βNTI) (Supplementary Fig. 2) and Bray-Curtis-based Raup-Crick ($\text{RC}_b ray$) (Supplementary Fig. 3) from the abundance of operational taxonomic units (OTUs) and phylogenetic distances. The βNTI is the difference between the observed β-mean nearest taxon index (βMNTD) and the mean of the null distribution of βMNTD normalized by its standard deviation. βNTI values $> +2$ indicate significantly more phylogenetic turnover than expected (heterogeneous selection), and βNTI values < -2 less phylogenetic turnover than expected (homogeneous selection) (Stegen et al. 2013). As the observed βMNTD value did not significantly deviate from the null βMNTD distribution (i.e. $|\beta\text{NTI}| < 2$), it meant stochastic turnover in phylogenetic composition. Since this stochasticity could entail dispersal limitation, homogenizing dispersal, or the lack of a single dominant process (termed the undominated fraction) (Hardy 2008 ; Stegen et al. 2012), this was clarified by calculating the $\text{RC}_b ray$ on pairwise comparisons with $|\beta\text{NTI}| < 2$, as follows : $|\text{RC}_b ray| > +0.95$ means dispersal limitation, $|\text{RC}_b ray| <$ -0.95 means homogenizing dispersal, and -0.95 $< |\text{RC}_b ray| < 0.95$ means the undominated fraction (Chase et al. 2011 ; Stegen et al. 2012 ; Zhou

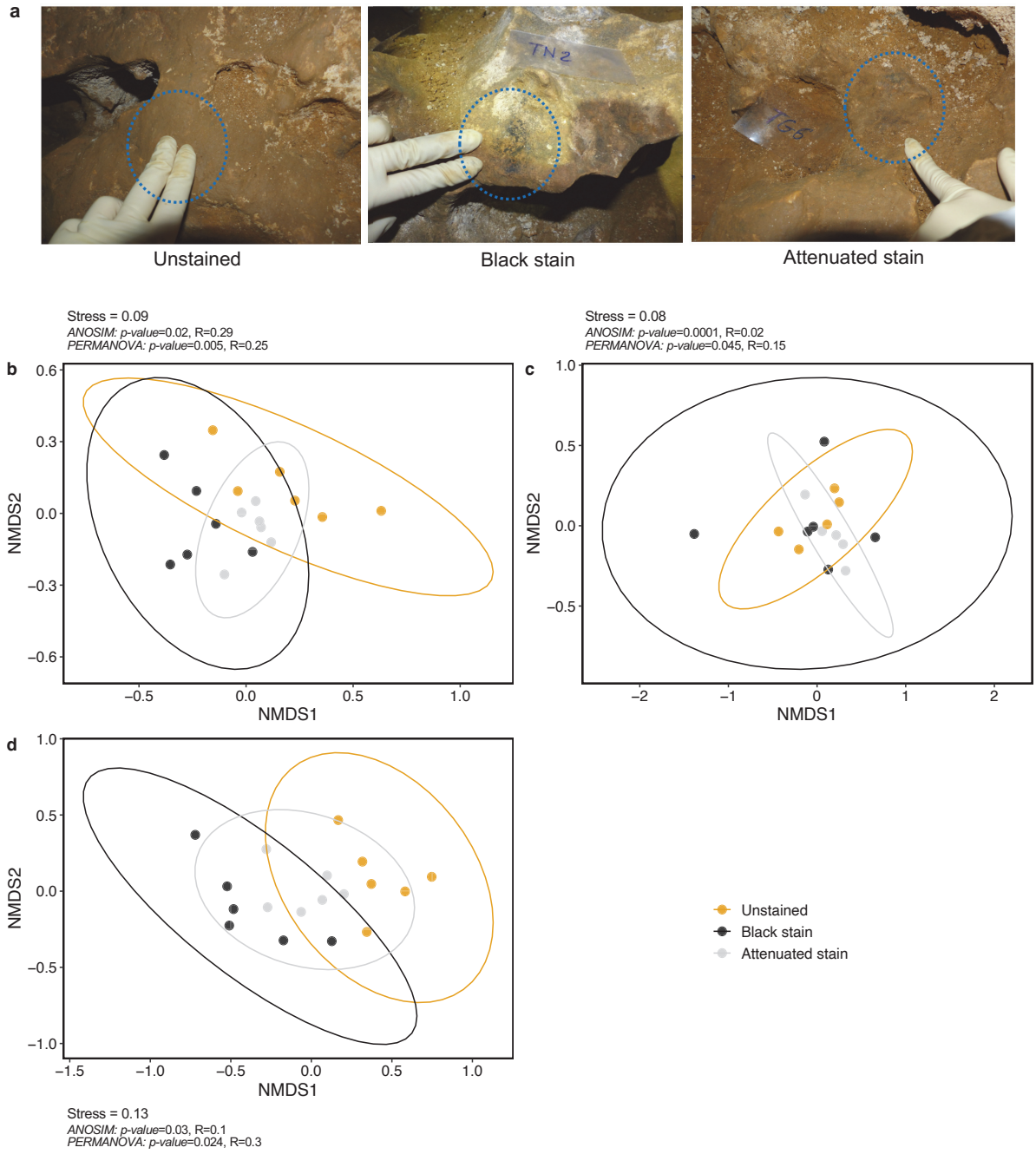

Fig. 1. Comparison of rock surface conditions in Lascaux's Chamber of Felines. a. Photographs of unstained limestone (resistant microbial community), black stain (impacted community) and attenuated stain (resilient status) (Credit : DRAC Nouvelle Aquitaine). bcd. Differences in bacterial (b), archaeal (c) and microeukaryotic communities (d) indicated by Non-Metric Dimensional Scaling (NMDS) ordination based on Bray-Curtis dissimilarity index calculated on abundance matrices at the OTU level. Permutational analysis of variance (PERMANOVA), stress value and analysis of similarities (ANOSIM) are presented in each case.

and Ning 2017). The identified assembly processes showed contrasted patterns among the three domains of life. Indeed, the contribution of stochastic processes to bacterial community assembly amounted to 93.3% on unstained limestone and 80.0% in attenuated stains, versus only 53.3% in black stains (Fig. 3). For the archaeal community, in contrast, stochastic processes accounted for

80.0% of community assembly on unstained limestone, 90.0% in attenuated stains and 100% in black stains. Assembly patterns were exclusively stochastic for the microeukaryotic community, regardless of rock surface condition.

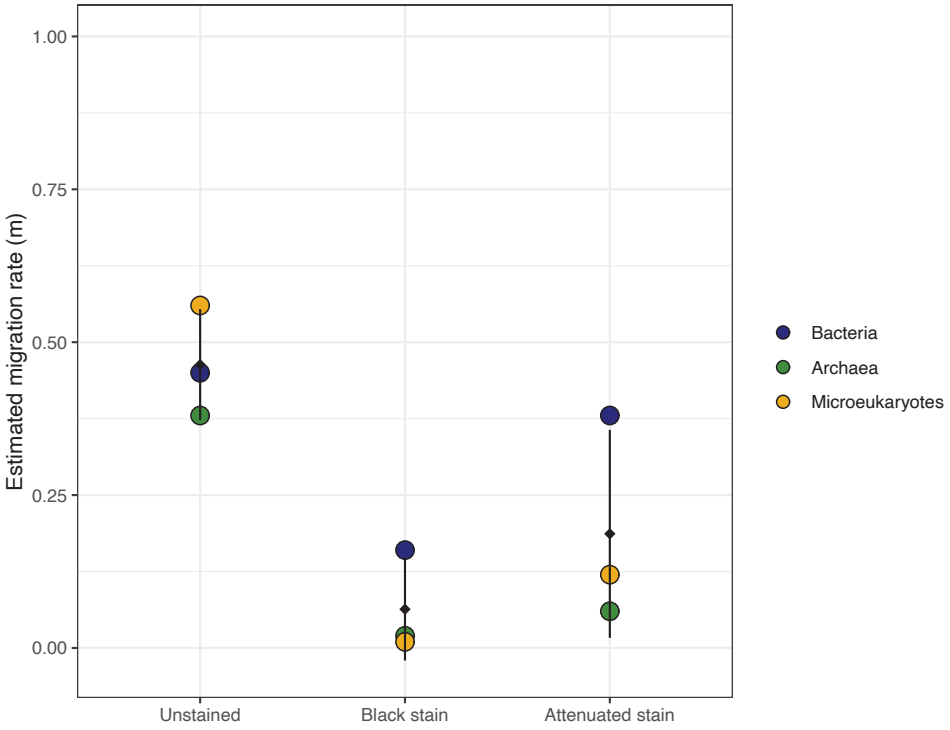

Fig. 2. Estimated migration rate (m) of neutral model during microbial dynamics for the three domains of life. The goodness-of-fit of the neutral model and the comparison of the maximum likelihood fit of the neutral, binomial and Poisson models for each community can be found in Supplementary Fig. 1 and Supplementary Table 1.

Assembly processes for abundant vs rare biosphere. To go beyond classical analyses considering microbial diversity as a whole, the abundance of taxa (i.e. abundant versus rare biosphere) was also taken into account for each domain of life, to decipher community assembly patterns in more details. To this end, OTUs were classified (Liu et al. 2015 ; Dai et al. 2016) as always-rare taxa, conditionally-rare taxa or dominant taxa (Supplementary Fig. 4), and assembly processes were reassessed for each taxa category. Bacterial dominant taxa showed a high level of heterogeneous selection in black stains (66.7%) but exhibited dispersal limitation in attenuated stains and on unstained surfaces. In contrast, microeukaryotic dominant taxa mostly displayed stochastic properties, with mainly undominated processes on the unstained surfaces and in black stains, but only dispersal limitation in the attenuated stains. However, heterogeneous selection also occurred in impacted communities (33.3%), as for Bacteria. Analysis was not possible with Archaea, as only two dominant taxa were found.

In conditionally-rare taxa, dispersal limitation predominated for Bacteria (75.5%) and microeukaryotes (60.0%) in all three surface conditions, whereas such taxa were rare in Archaea. Heterogeneous selection also contributed to the assembly of Bacteria (in all conditions) and microeukaryotes (but only in black stains).

On unstained surfaces and in black stains, always-rare taxa from the three domains of life

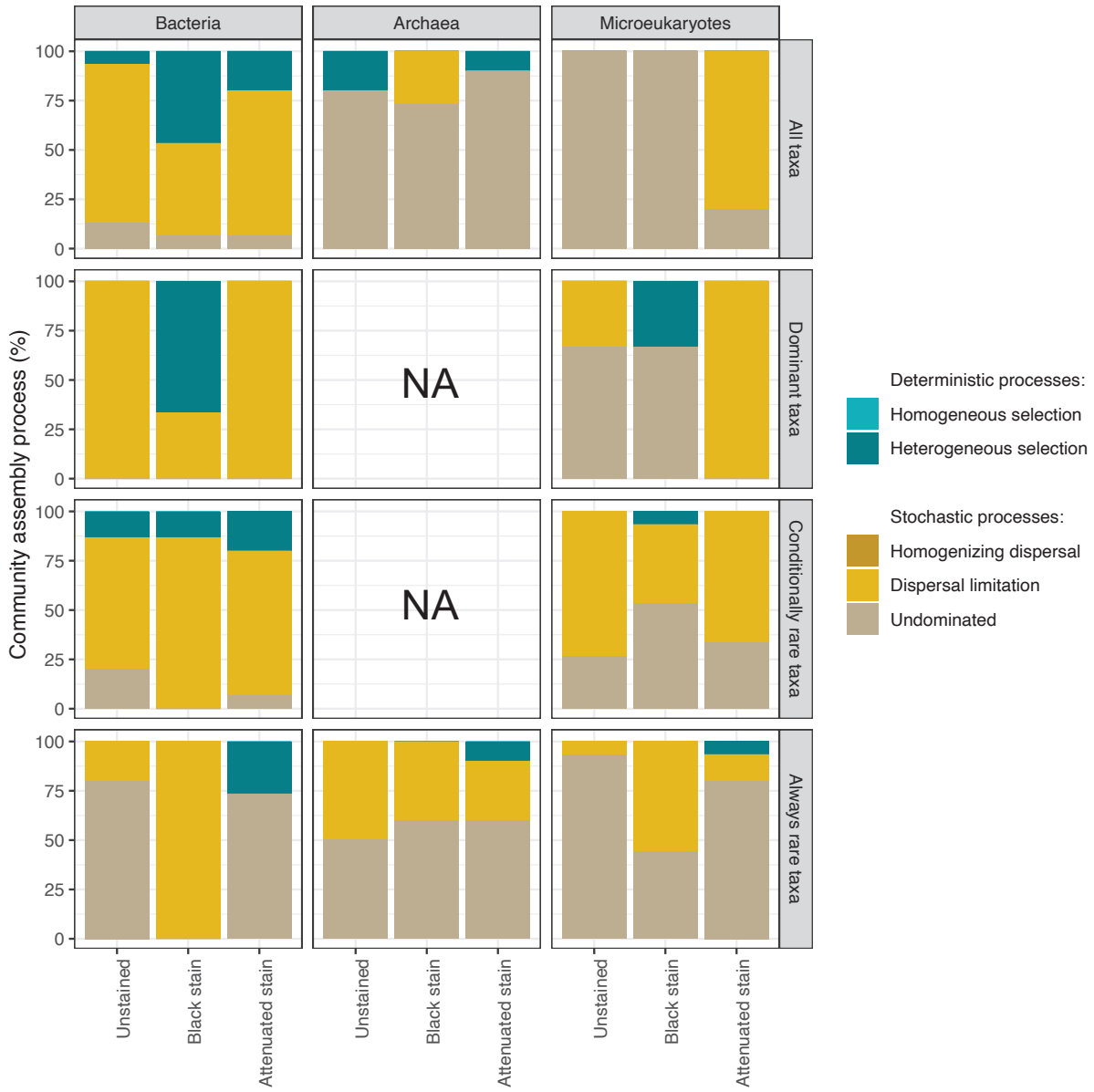

Fig. 3. Contribution of deterministic and stochastic processes for all taxa, dominant taxa, conditionally-rare taxa and always-rare taxa of the three microbial communities. Community assembly processes were calculated for deterministic processes (including homogenous and heterogeneous selection) and stochastic processes (including homogenizing dispersal, dispersal limitation, and undominated processes). NA, Not available.

were associated to stochastic assembly, mostly by undominated processes. The latter means that the underlying assembly mechanisms are not quantifiable yet, all the more as the rare biosphere in caves is particularly undocumented. The same trend was found in the attenuated stains, with also a contribution of deterministic processes amounting to 6.7, 10.0 and 26.7% for heterogeneous selection in microeukaryotic, archaeal and bacterial communities, respectively (Fig. 3). This result clearly shows that always-rare taxa from the three domains of life were selected only in the resilient status, suggesting their importance in ecosystem functioning.

Always-rare taxa composition across rock surface conditions. We investigated the

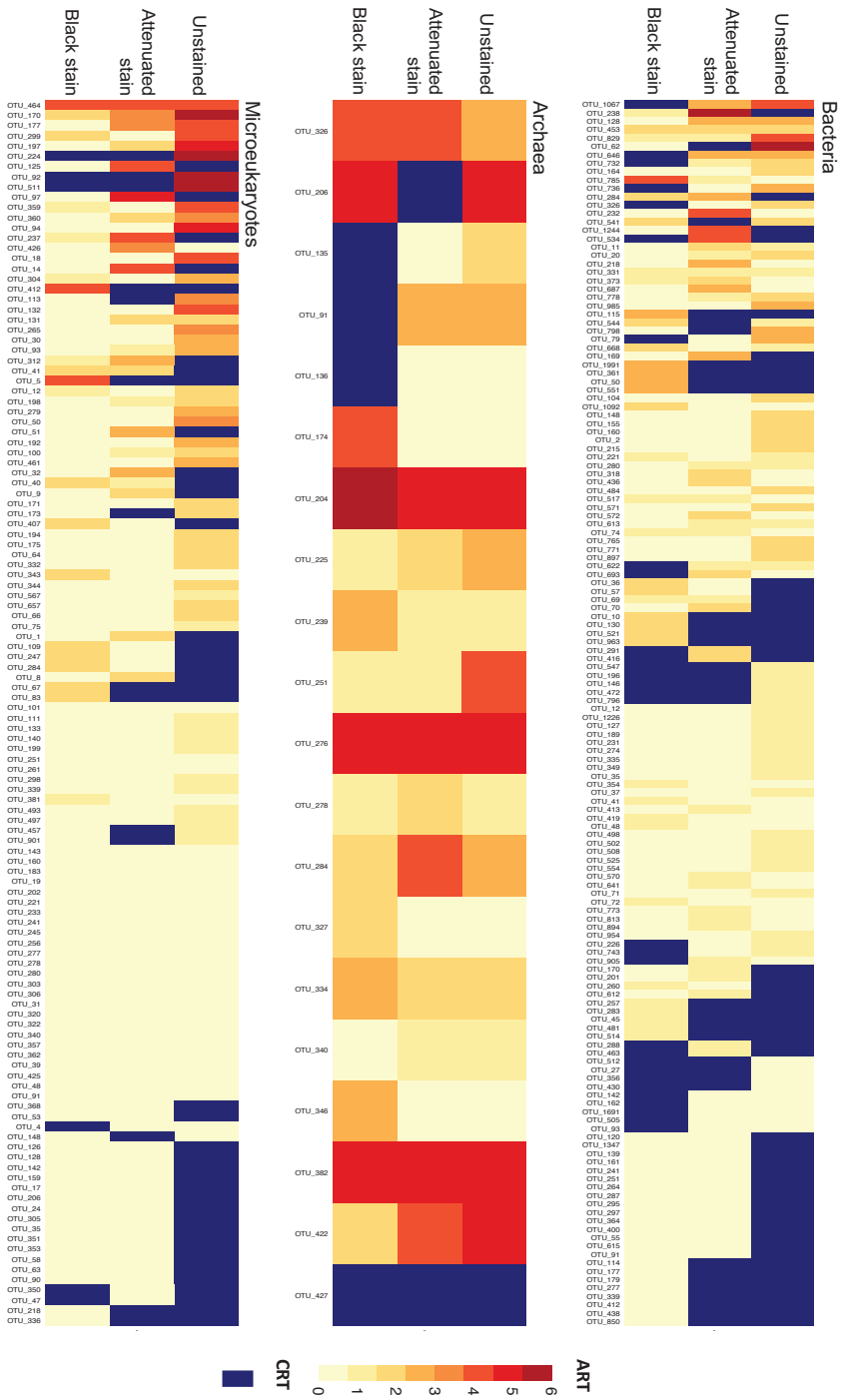

Fig. 4. Distribution of always-rare taxa affiliated with Bacteria, Archaea or microeukaryotes for each rock surface condition. The heatmap was performed using OTU abundance of always-rare taxa (represented with a yellow-red gradient) and conditionally-rare taxa (in blue).

taxonomic identity of the 286 always-rare taxa since they were the only OTU category that had undergone deterministic assembly processes in attenuated stains. Among them, 150 OTUs displayed the always-rare status in all three rock surface conditions and 136 in one or two rock surface conditions (Fig. 4). In these 286 OTUs, 15 were retrieved only in attenuated stains and they belonged to Acidobacteria (3 OTUs), Actinobacteria (3 OTUs), Chloroflexi, Alphaproteobacteria, Planctomycetota, Thaumarchaeota and Ascomycota. In addition, 42 other OTUs including

Actinobacteria (12 OTUs), Alphaproteobacteria (5 OTUs) and Ascomycota (20 OTUs) were common to attenuated stains and unstained surfaces. Among these 42 rare microbial members, *Mycobacterium*, *Sphingobium*, *Phyllobacterium*, *Vicinamibacter* (known as degraders of polycyclic aromatic hydrocarbons or chloroaromatic compounds (Teng et al. 2017 ; Vieira et al. 2017 ; Dudhagara and Dave 2018)) have been identified, which might be relevant for biodegradation of black melanin pigments in stains.

Discussion

In the present work, the response of microbial communities to disturbance was assessed in relation to predictive scenarios by considering explicitly the ecological differences between taxa categories (dominant taxa, conditionally-rare taxa, always-rare taxa) and the assembly processes identified (Fig. 5). Interestingly, several scenarios proved relevant to describe microbial responses.

Scenario 1 : Disturbance imposes selection. In the resistant state (unstained surface), stochastic assembly processes (neutral theory) dominated. In the impacted state (black stains), deterministic assembly processes became predominant, but lessened in the resilient state (attenuated stains). This scenario was demonstrated for Bacteria (considering all taxa together, or only the dominant taxa or the conditionally-rare taxa) and microeukaryotes (for dominant taxa and conditionally-rare taxa). These results are conceptually consistent with previous findings on macroorganisms (in the cases of drought in ponds (Chase 2007) and forest evolution after fire disturbance (Myers and Harms 2011)) and microorganisms (e.g. bacterial succession within pH soil gradients or across microbial desiccation processes (Valverde et al. 2014 ; Tripathi et al. 2018)).

Scenario 2 : Disturbance leads to selection relaxed. Here, resistant communities (unstained surface) have undergone strong variable selection. Indeed, the disturbance weakens selection, which will lead to stochastic community assembly. As resilience develops (from black stains to attenuated stains), deterministic processes will increase in importance, as found for Archaea (all taxa together). The relevance of this scenario is supported by analysis of forest harvesting (Hartmann et al. 2012 ; Zhou et al. 2014), which leads to depletion of soil organic matter and soil compaction. Hartmann et al. found that soil microbial communities were significantly different between such disturbed forests and non-harvested forests, even 15 years after harvest (Hartmann et al. 2012). Such a scenario was also observed for bacterial communities in agricultural soils affected by tillage (Zhou et al. 2014).

Scenario 3 : Absence of selection. This scenario reflects the neutral theory and highlights that some microbial systems are constantly dominated by stochastic processes (Dini-Andreote et al. 2015). This might be linked to abundant resource supply and high levels of organismal dispersal (Zhou and Ning 2017). In the present work, it was the case for microeukaryotic dominant taxa. This concept has been previous reported in fluidic systems with constant resource supply (Zhou et al. 2014), where only a few microbial taxa were prevented from growing.

Scenario 4 : Disturbance removal leads to selection. Unexpectedly, the first three scenarios proved insufficient to depict the diversity of microbial responses documented. Therefore, it resulted in the proposition of a novel scenario applicable to the always-rare taxa. In this fourth scenario, the resistant and impacted states (unstained surface and black stain, respecti-

vely) displayed strong stochastic signatures, probably because perturbation was either minor for all taxa including always-rare taxa (in the resistant state) or strong for dominant taxa, thereby alleviating competition towards always-rare taxa (in the impacted state). In the resilient state, selection processes are important for always-rare taxa, perhaps because dominant taxa become better adapted and impose selection pressures. Alternatively, certain always-rare taxa may be positively selected by trophic opportunities, such as the fungus Ochroconis lascauxensis able to degrade benzalkonium chloride previously used in chemical treatments in Lascaux Cave (Bastian et al. 2009 ; Galand et al. 2009 ; Martin-Sanchez et al. 2012b, Pedrós-Alió 2012). A previous rhizosphere study showed that rare bacterial taxa had undergone strong selection processes as well (Jiao and Lu 2020). Importantly, we found that scenario 4 was relevant for always-rare taxa from the three domains of life, suggesting common ecological behaviours as well as cooperative relations promoted by disturbance. It is probably of major significance for ecosystem functioning.

To conclude, we propose a novel scenario to predict the dynamics of always-rare taxa, which was validated in the case of Lascaux's Chamber of Felines. We showed the necessity to consider the rare biosphere (and its functions) to fully assess microbial responses to environmental change and their involvement in ecosystem functioning. The conceptual model reported in this work (scenario 4) needs now to be tested in diverse environments to better predict and model ecosystem functioning.

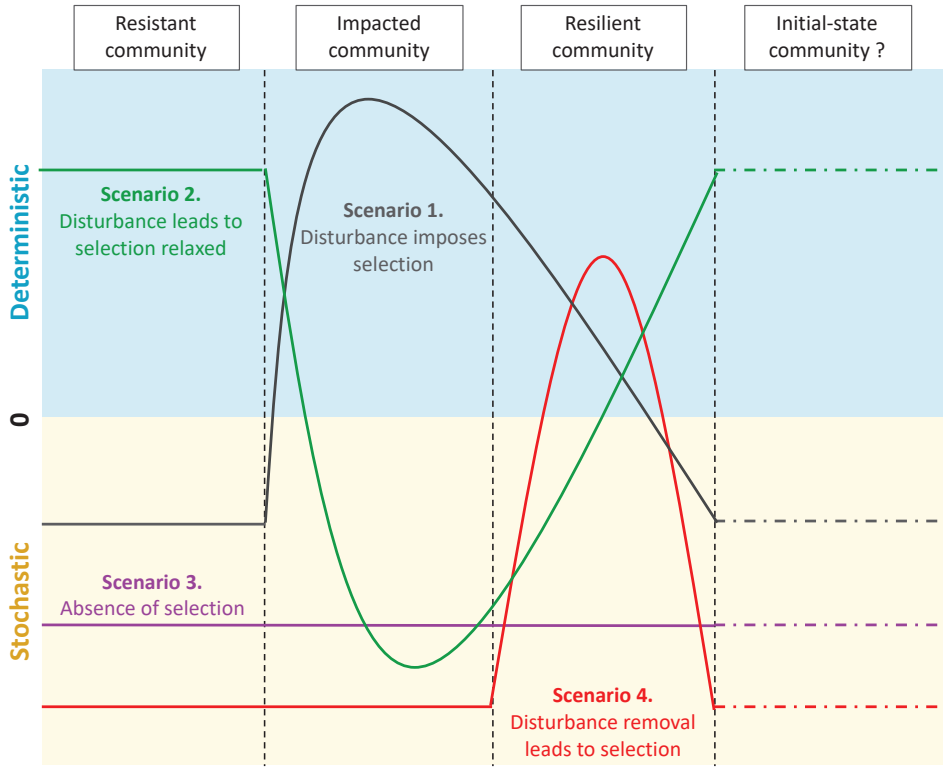

Fig. 5. Four-scenario conceptual model integrating the three domains of life along the stochastic-deterministic continuum. Neutral hypothesis model (stochastic processes) and niche-based theory (deterministic processes) are represented in yellow and blue, respectively. Scenarios 1, 2, 3 and 4 are represented in black, green, purple and red, respectively.

Data accessibility

All data that support findings of this study have been deposited in EBI under reference PRJEB46483, PRJEB46545 and PRJEB46546 for bacterial 16S rRNA genes, archaeal 16S rRNA genes and microeukaryotic 18S rRNA genes, respectively.

Code availability

The authors declare that the R (R 4.0.2) codes used to generate the results reported in this study are available in this paper. The R code supporting the finding presented here is available from the GitHub Repository https ://github.com/LascauxZelia/Bontempsetal2022

Acknowledgments

Funding was provided by DRAC Nouvelle Aquitaine (Bordeaux, France). We are very grateful to S. Géraud, J.C. Portais and M. Mauriac (DRAC Nouvelle Aquitaine) for key information and help, D. Henry-Lormelle and colleagues for technical help with Lascaux sampling, Lascaux Scientific Board for helpful discussions and L. Alonso for help in technical analysis.

Author contributions

Y.M.L. obtained funding and coordinated the project, Y.M.L. and M.H. designed the research, Z.B. analyzed data, Z.B., Y.M.L. and M.H. wrote the paper. All authors were involved in writing and approved the manuscript.

References

Alabouvette, C. and Saiz-Jiménez, C. (2011). Écologie microbienne de la Grotte de Lascaux. CSIC-Instituto de Recursos Naturales y Agrobiología de Sevilla (IRNAS).

Allison, S.D. and Martiny, J.B.H. (2008). Resistance, resilience, and redundancy in microbial communities. Proceedings National Academy of Sciences USA., 105, 11512–11519.

Alonso, L. (2018). Hétérogénéité spatio-temporelle du microbiote de la grotte de Lascaux. These de doctorat. Université de Lyon, France.

Banerjee, S. and Joshi, S.R. (2013). Insights into cave architecture and the role of bacterial Biofilm. Proceedings National Academy of Sciences USA., 83, 277–290.

Barton, H.A. and Northup, D.E. (2007). Geomicrobiology in cave environments : past, current and future perspectives. Journal of Cave Karst Stuties, 69, 163–178.

Bastian, F., Alabouvette, C., Jurado, V. and Saiz-Jimenez, C. (2009). Impact of biocide treatments on the bacterial communities of the Lascaux Cave. Naturwissenschaften, 96, 863–868.

Bastian, F., Jurado, V., Nováková, A., Alabouvette, C. and Saiz-Jimenez, C. (2010). The microbiology of Lascaux Cave. Microbiology, 156, 644–652.

Bokulich, N.A., Subramanian, S., Faith, J.J., Gevers, D., Gordon, J.I., Knight, R., et al. (2013). Quality-filtering vastly improves diversity estimates from Illumina amplicon sequencing. Nature Methods, 10, 57–59.

Bolar, K. (2019). STAT : Interactive Document for Working with Basic Statistical Analysis.

Bourges, F., Genthon, P., Genty, D., Lorblanchet, M., Mauduit, E. and D'Hulst, D. (2014). Conservation of prehistoric caves and stability of their inner climate : Lessons from Chauvet and other French caves. Sciences of the Total Environment., 493, 79–91.

Bray, J. and Curtis, J. (1957). An ordination of the upland forest com- munities of southern Wisconsin. Ecological Monographs, 27, 325–349.

Burns, A.R., Stephens, W.Z., Stagaman, K., Wong, S., Rawls, J.F., Guillemin, K., et al. (2016). Contribution of neutral processes to the assembly of gut microbial communities in the zebrafish over host development. ISME Journal, 10, 655–664.

Cañveras, C., Sain-Jimenez, C., S. Sanchez-Moral and V. Sloer. (2001). Microorganisms and microbially induced fabrics in cave walls. Geomicrobiology Journal, 18, 223–240.

Castresana, J. (2000). Selection of conserved blocks from multiple alignments for their use in phylogenetic analysis. Molecular Biology and Evolution, 17, 540–552.

Chao, A. (1987). Estimating the Population Size for Capture-Recapture Data with Unequal Catchability. Biometrics, 43, 783–791.

Chase, J.M. (2007). Drought mediates the importance of stochastic community assembly. Proceedings National Academy of Sciences USA., 104, 17430–17434.

Chase, J.M., Kraft, N.J.B., Smith, K.G., Vellend, M. and Inouye, B.D. (2011). Using null models to disentangle variation in community dissimilarity from variation in /*alpha*-diversity. Ecosphere, 2, 1-11.

Chase, J.M. and Myers, J.A. (2011). Disentangling the importance of ecological niches from stochastic processes across scales. Philosophical Transactions of the Royal Society. 366, 2351–2363.

Chen, W., Ren, K., Isabwe, A., Chen, H., Liu, M. and Yang, J. (2019). Stochastic processes shape microeukaryotic community assembly in a subtropical river across wet and dry seasons. Microbiome, 7, 1-16.

Clarke, K.R. (1993). Non-parametric multivariate analyses of changes in community structure. Aust. Journal of Ecology., 18, 117–143.

Corline, N.J., Peek, R.A., Montgomery, J., Katz, J.V.E. and Jeffres, C.A. (2021). Understanding community assembly rules in managed floodplain food webs. Ecosphere, 12, e03330.

Cuezva, S., Sanchez-Moral, S., Saiz-Jimenez, C. and Cañaveras, J. (2009). Microbial communities and associated mineral fabrics in Altamira Cave, Spain. International Journal of Speleology, 38, 83-92.

Dai, T., Zhang, Y., Tang, Y., Bai, Y., Tao, Y., Huang, B., et al. (2016). Identifying the key taxonomic categories that characterize microbial community diversity using full-scale classification : a case study of microbial communities in the sediments of Hangzhou Bay. FEMS Microbiology Ecology., 92, fiw150.

De Leo, F., Iero, A., Zammit, G. and Urzi, C.E. (2012). Chemoorganotrophic bacteria isolated from biodeteriorated surfaces in cave and catacombs. International Journal of Speleology, 41, 125–136.

Di Russo, C., Carchini, G., Rampini, M., Lucarelli, M. and Sbordoni, V. (1997). Long term stability of a terrestrial cave community. International Journal of Speleology, 26.

Dini-Andreote, F., Stegen, J.C., van Elsas, J.D. and Salles, J.F. (2015). Disentangling mechanisms that mediate the balance between stochastic and deterministic processes in microbial succession. Proceedings National Academy of Sciences USA., 112, 1326–1332.

Dollive, S., Peterfreund, G.L., Sherrill-Mix, S., Bittinger, K., Sinha, R., Hoffmann, C., et al. (2012). A tool kit for quantifying eukaryotic rRNA gene sequences from human microbiome samples. Genome Biology, 13, 1-13.

Dray, S. and Dufour, A.-B. (2007). The ade4 package : Implementing the duality diagram for ecologists. Journal of Statistical Software, 22, 1–20.

Dudhagara, D.R. and Dave, B.P. (2018). Mycobacterium as Polycyclic Aromatic Hydrocarbons (PAHs) Degrader. Mycobacterium-Research and Development.

Elzhov, T.V., Mullen, K.M., Spiess, A.-N. and Bolker, B. (2016). minpack.lm : R nterface to the Levenberg-Marquardt Nonlinear Least-Squares Algorithm Found in MINPACK, Plus Support for Bounds.

Engel, A.S. (2010). Microbial diversity of cave ecosystems. In : Geomicrobiology : Molecular and Environmental Perspective (eds. Barton, L.L., Mandl, M. and Loy, A.). Springer Netherlands, Dordrecht, pp. 219–238.

Escudié, F., Auer, L., Bernard, M., Mariadassou, M., Cauquil, L., Vidal, K., et al. (2018). FROGS : Find, Rapidly, OTUs with Galaxy Solution. Bioinformatics, 34, 1287–1294.

Ferrenberg, S., O'Neill, S.P., Knelman, J.E., Todd, B., Duggan, S., Bradley, D., et al. (2013). Changes in assembly processes in soil bacterial communities following a wildfire disturbance. ISME Journal, 7, 1102–1111.

Galand, P.E., Casamayor, E.O., Kirchman, D.L. and Lovejoy, C. (2009). Ecology of the rare microbial biosphere of the Arctic Ocean. Proceedings National Academy of Sciences USA., 106, 22427–22432

Gao, C., Montoya, L., Xu, L., Madera, M., Hollingsworth, J., Purdom, E., et al. (2020). Fungal community assembly in drought-stressed sorghum shows stochasticity, selection, and universal ecological dynamics. Nature Communication, 11, 1-14.

Hammer, Ø., Harper, D.. and Ryan, P. (2001). PAST : paleontological statis- tics software package for education and data analysis. Palaeontologia Electronica, 4.

Hardy, O.J. (2008). Testing the spatial phylogenetic structure of local communities : statistical performances of different null models and test statistics on a locally neutral community. Journal of Ecology, 96, 914–926.

Harrell, F. and Dupont, C. (2018). Hmisc : Harrell Miscellaneous.

Hartmann, M., Howes, C.G., VanInsberghe, D., Yu, H., Bachar, D., Christen, R., et al. (2012). Significant and persistent impact of timber harvesting on soil microbial communities in Northern coniferous forests. ISME Journal, 6, 2199–2218.

Herfort, L., Kim, J.-H., Coolen, M.J.L., Abbas, B., Schouten, S., Herndl, G.J., et al. (2009). Diversity of Archaea and detection of crenarchaeotal amoA genes in the rivers Rhine and Têt. Aquatic Microbial Ecology, 55, 189–201.

Herlemann, D.P., Labrenz, M., Jürgens, K., Bertilsson, S., Waniek, J.J. and Andersson, A.F. (2011). Transitions in bacterial communities along the 2000 km salinity gradient of the Baltic Sea. ISME Journal, 5, 1571–1579.

Hubbell, S. (2001). The Unified Neutral Theory of Biodiversity and Biogeography. Monographs in Population Biology. Princeton University Press.

Hüppop, K. (2012). Adaptation to low food. In : Encyclopedia of Caves (Second Edition) (eds. White, W.B. and Culver, D.C.). Academic Press, Amsterdam, pp. 1–9.

Jiao, S. and Lu, Y. (2020). Soil pH and temperature regulate assembly processes of abundant and rare bacterial communities in agricultural ecosystems. Environmental Microbiology, 22, 1052–1065.

Kardol, P., Souza, L. and Classen, A.T. (2013). Resource availability mediates the importance of priority effects in plant community assembly and ecosystem function. Oikos, 122, 84–94.

Kembel, S.W., Cowan, P.D., Helmus, M.R., Cornwell, W.K., Morlon, H., Ackerly, D.D., et al. (2010). Picante : R tools for integrating phylogenies and ecology. Bioinformatics, 26, 1463–1464.

Kuraku, S., Zmasek, C.M., Nishimura, O. and Katoh, K. (2013). aLeaves facilitates on-demand exploration of metazoan gene family trees on MAFFT sequence alignment server with enhanced interactivity. Nucleic Acids Research, 41, 22–28.

Lacanette, D., Malaurent, P., Caltagirone, J.-P. and Brunet, J. (2007). Étude des transferts de masse et de chaleur dans la grotte de Lascaux : le suivi climatique et le simulateur. Karstologia, 50, 19–30.

Lefèvre, M. (1974). La 'Maladie Verte' De Lascaux. Studies in Conservation, 19, 126–156.

Liu, L., Yang, J., Yu, Z. and Wilkinson, D.M. (2015). The biogeography of abundant and rare bacterioplankton in the lakes and reservoirs of China. ISME Journal, 9, 2068–2077.

Luan, L., Jiang, Y., Cheng, M., Dini-Andreote, F., Sui, Y., Xu, Q., et al. (2020). Organism body size structures the soil microbial and nematode community assembly at a continental and global scale. Nature Communication, 11, 6406.

Madsen, E.L. (2011). Microorganisms and their roles in fundamental biogeochemical cycles. Curr. Opin. Biotechnol., Energy biotechnology – Environmental biotechnology, 22, 456–464.

Magoč, T. and Salzberg, S.L. (2011). FLASH : fast length adjustment of short reads to improve genome assemblies. Bioinformatics, 27, 2957–2963.

Mahé, F., Rognes, T., Quince, C., de Vargas, C. and Dunthorn, M. (2014). Swarm : robust and fast clustering method for amplicon-based studies. PeerJ, 2, e593.

Martin-Sanchez, P.M., Miller, A.Z. and Saiz-Jimenez, C. (2015). 13. Lascaux Cave : An Example of Fragile Ecological Balance in Subterranean Environments. De Gruyter.

Martin-Sanchez, P.M., Nováková, A., Bastian, F., Alabouvette, C. and Saiz-Jimenez, C. (2012a). Two new species of the genus Ochroconis, O. lascauxensis and O. anomala isolated from black stains in Lascaux Cave, France. Fungal Biology, 116, 574–589.

Martin-Sanchez, P.M., Nováková, A., Bastian, F., Alabouvette, C. and Saiz-Jimenez, C. (2012b). Use of biocides for the control of fungal outbreaks in subterranean environments : The case of the Lascaux Cave in France. Environmental Science and Technology, 46, 3762–3770.

Maurice, C.F., Haiser, H.J. and Turnbaugh, P.J. (2013). Xenobiotics shape the physiology and gene expression of the active human gut microbiome. Cell, 152, 39–50.

McMurdie, P.J. and Holmes, S. (2013). phyloseq : An R package for reproducible interactive analysis and graphics of microbiome census data. PLoS ONE, 8, e61217.

Mi, X., Swenson, N.G., Jia, Q., Rao, M., Feng, G., Ren, H., et al. (2016). Stochastic assembly in a subtropical forest chronosequence : evidence from contrasting changes of species, phylogenetic and functional dissimilarity over succession. Scientific Reports, 6, 3259-3269.

Minh, B.Q., Schmidt, H.A., Chernomor, O., Schrempf, D., Woodhams, M.D., von Haeseler, A., et al. (2020). IQ-TREE 2 : New Models and Efficient Methods for Phylogenetic Inference in the Genomic Era. Molecular Biology and Evolution, 37, 1530–1534.

Myers, J.A. and Harms, K.E. (2011). Seed arrival and ecological filters interact to assemble high-diversity plant communities. Ecology, 92, 676–686.

Nilsson, R.H., Larsson, K.-H., Taylor, A.F.S., Bengtsson-Palme, J., Jeppesen, T.S., Schigel, D., et al. (2019). The UNITE database for molecular identification of fungi : handling dark taxa and parallel taxonomic classifications. Nucleic Acids Research, 47, 259–264.

Ning, D. (2021). iCAMP : Infer Community Assembly Mechanisms by Phylogenetic-Bin-Based Null Model Analysis.

Ning, D., Yuan, M., Wu, L., Zhang, Y., Guo, X., Zhou, X., et al. (2020). A quantitative framework reveals ecological drivers of grassland microbial community assembly in response to warming. Nature Communication, 11, 4717-4719.

Oksanen, J., Blanchet, F.G., Friendly, M., Kindt, R., Legendre, P., McGlinn, D., et al. (2020). vegan : Community Ecology Package.

Pasić, L., Kovce, B., Sket, B. and Herzog-Velikonja, B. (2010). Diversity of microbial communities colonizing the walls of a Karstic cave in Slovenia. FEMS Microbiology and Ecology, 71, 50–60.

Pedrós-Alió, C. (2012). The rare bacterial biosphere. Annual Review of Marine Science, 4, 449–466.

Prescott, L.-M., Willey, J.M., Sherwood, L.M. and Woolwerton, C.J. (2003). Microbiology. 5e edn. DeBoeck.

Quast, C., Pruesse, E., Yilmaz, P., Gerken, J., Schweer, T., Yarza, P., et al. (2013). The SILVA ribosomal RNA gene database project : improved data processing and web-based tools. Nucleic Acids Research, 41, 590–596.

R Core Team. (2020). R : A language and environment for statistical computing. R Foundation for Statistical Computing, Vienna, Austria. URL https ://www.R-project.org/.

Rognes, T., Flouri, T., Nichols, B., Quince, C. and Mahé, F. (2016). VSEARCH : a versatile open source tool for metagenomics. PeerJ, 4, e2584.

Shade, A., Peter, H., Allison, S.D., Baho, D., Berga, M., Buergmann, H., et al. (2012). Fundamentals of Microbial Community Resistance and Resilience. Frontiers in Microbiology, 3, 1-19.

Shannon, C.E. (1948). A Mathematical Theory of Communication. Bell Labs Technical Journal, 27, 623–656.

Simpson, E.H. (1949). Measurement of Diversity. Nature, 163, 688–688.

Sloan, W.T., Lunn, M., Woodcock, S., Head, I.M., Nee, S. and Curtis, T.P. (2006). Quantifying the roles of immigration and chance in shaping prokaryote community structure. Environmental Microbiology, 8, 732–740.

Stegen, J.C., Lin, X., Fredrickson, J.K., Chen, X., Kennedy, D.W., Murray, C.J., et al. (2013). Quantifying community assembly processes and identifying features that impose them. ISME Journal, 7, 2069–2079.

Stegen, J.C., Lin, X., Fredrickson, J.K. and Konopka, A.E. (2015). Estimating and mapping ecological processes influencing microbial community assembly. Frontiers in Microbiology, 6, 1-15.

Stegen, J.C., Lin, X., Konopka, A.E. and Fredrickson, J.K. (2012). Stochastic and deterministic assembly processes in subsurface microbial communities. ISME Journal, 6, 1653–1664.

Talavera, G. and Castresana, J. (2007). Improvement of phylogenies after removing divergent and ambiguously aligned blocks from protein sequence alignments. Systematic Biology, 56, 564–577.

Teng, Y., Feng, S., Ren, W., Zhu, L., Ma, W., Christie, P., et al. (2017). Phytoremediation of diphenylarsinic-acid-contaminated soil by Pteris vittata associated with Phyllobacterium myrsinacearum RC6b. International Journal Phytoremediation, 19, 463–469.

Tripathi, B.M., Stegen, J.C., Kim, M., Dong, K., Adams, J.M. and Lee, Y.K. (2018). Soil pH mediates the balance between stochastic and deterministic assembly of bacteria. ISME Journal, 12, 1072–1083.

Valverde, A., Makhalanyane, T.P. and Cowan, D.A. (2014). Contrasting assembly processes in a bacterial metacommunity along a desiccation gradient. Frontiers in Microbiology, 5.

Vellend, M. (2010). Conceptual synthesis in community ecology. Quarterly Review Biology, 85, 183–206.

Vieira, S., Luckner, M., Wanner, G. and Overmann, J. (2017). Luteitalea pratensis gen. nov., sp. nov. a new member of subdivision 6 Acidobacteria isolated from temperate grassland soil. International Journal of Systematic Evolutionary Microbiology, 67, 1408–1414.

Zaneveld, J.R., McMinds, R. and Vega Thurber, R. (2017). Stress and stability : applying the Anna Karenina principle to animal microbiomes. Nature Microbiology, 2, 1–8.

Zhang, J. and Madden, T.L. (1997). PowerBLAST : a new network BLAST application for interactive or automated sequence analysis and annotation. Genome Research, 7, 649–656.

Zhou, J., Deng, Y., Zhang, P., Xue, K., Liang, Y., Van Nostrand, J.D., et al. (2014). Stochasticity, succession, and environmental perturbations in a fluidic ecosystem. Proceedings National Academy of Sciences USA., 111, 836–845.

Zhou, J. and Ning, D. (2017). Stochastic Community Assembly : Does It Matter in Microbial Ecology ? Microbiology Molecular Biology Reviews, 81, e0002-17.

Supplementary data

Supplementary table 1. Effect of rock surface condition (unstained surface, black stain, attenuated stain) on microbial community composition.

Gene	Effect	Df	F	p-value	R^2
Bacterial 16S rRNA	Status	2	2.544	**0.001**	0.25
	Residuals	15			
Archaeal 16S rRNA	Status	2	1.064	**0.035**	0.14
	Residuals	15			
Microeukaryotic 18S rRNA	Status	2	3.216	**0.001**	0.25
	Residuals	15			

Supplementary table 2. Comparison of the maximum likelihood fit of the neutral, binomial and Poisson models for each gene and each rock surface condition. m : estimated migration rate ; AIC : Akaike Information Criterion ; BIC : Bayesian Information Criterion ; BS : Black stain ; AT : Attenuated stain ; UN : Unstained ; All : All rock surface conditions.

Gene	Zone	*m*	R^2 neutral	R^2 binomial	R^2 Poisson	AIC neutral	AIC binomial	AIC Poisson	BIC neutral	BIC binomial	BIC Poisson
Bacterial 16S rRNA	BS	0.161	0.689	0.401	0.399	-177.8	-104.5	-104.5	-170.6	-97.20	-97.21
	AT	0.383	0.695	0.613	0.613	-194.7	-194.3	-194.3	-187.3	-186.9	-186.9
	UN	0.451	0.629	0.619	0.609	-112.7	-150.4	-150.4	-105.1	-142.8	-142.8
	All	0.259	0.888	0.758	0.759	-482.7	-394.1	-394.1	-474.9	-386.2	-386.3
Archaeal 16S rRNA	BS	0.017	0.150	-1.075	-1.075	11.67	9.360	9.360	14.13	11.79	11.79
	AT	0.055	0.465	0.083	0.089	0.338	9.360	9.360	2.427	11.79	6.019
	UN	0.385	0.180	0.006	0.006	0.338	9.360	9.360	2.427	11.79	6.019
	All	0.168	0.100	-0.777	-0.777	0.338	9.360	17.46	2.427	11.79	19.98
Microeukaryotic 18S rRNA	BS	0.012	0.315	-0.763	-0.763	29.87	45.56	45.56	34.97	50.67	50.67
	AT	0.121	0.594	0.247	0.247	-16.83	-12.64	-12.64	-11.48	-7.297	-7.298
	UN	0.556	0.735	0.720	0.720	-51.72	-101.8	-101.9	-45.49	-95.65	-95.66
	All	0.061	0.759	0.345	0.345	-119.5	-52.20	-52.20	-113.2	-45.86	-45.86

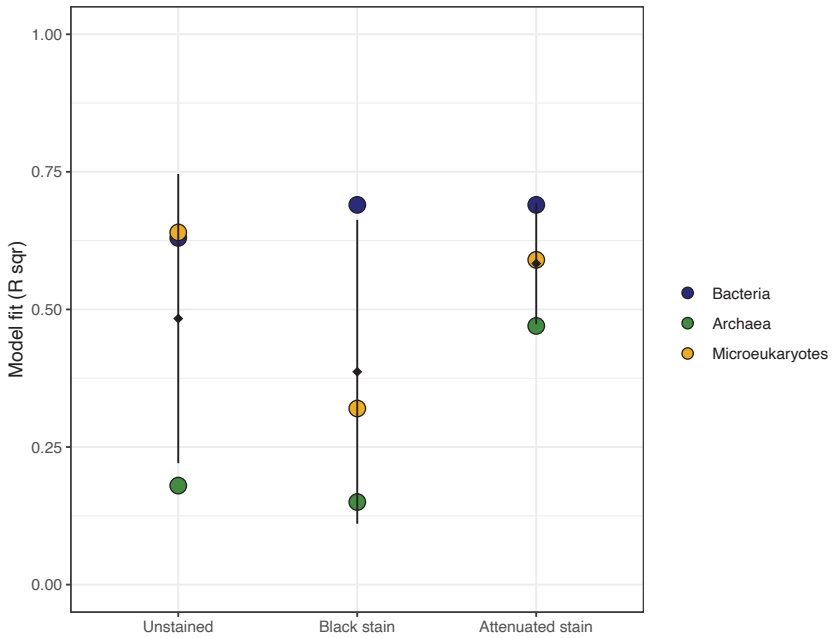

Supplementary figure 1. The goodness-of-fit of the neutral model during microbial dynamics for the three domains of life.

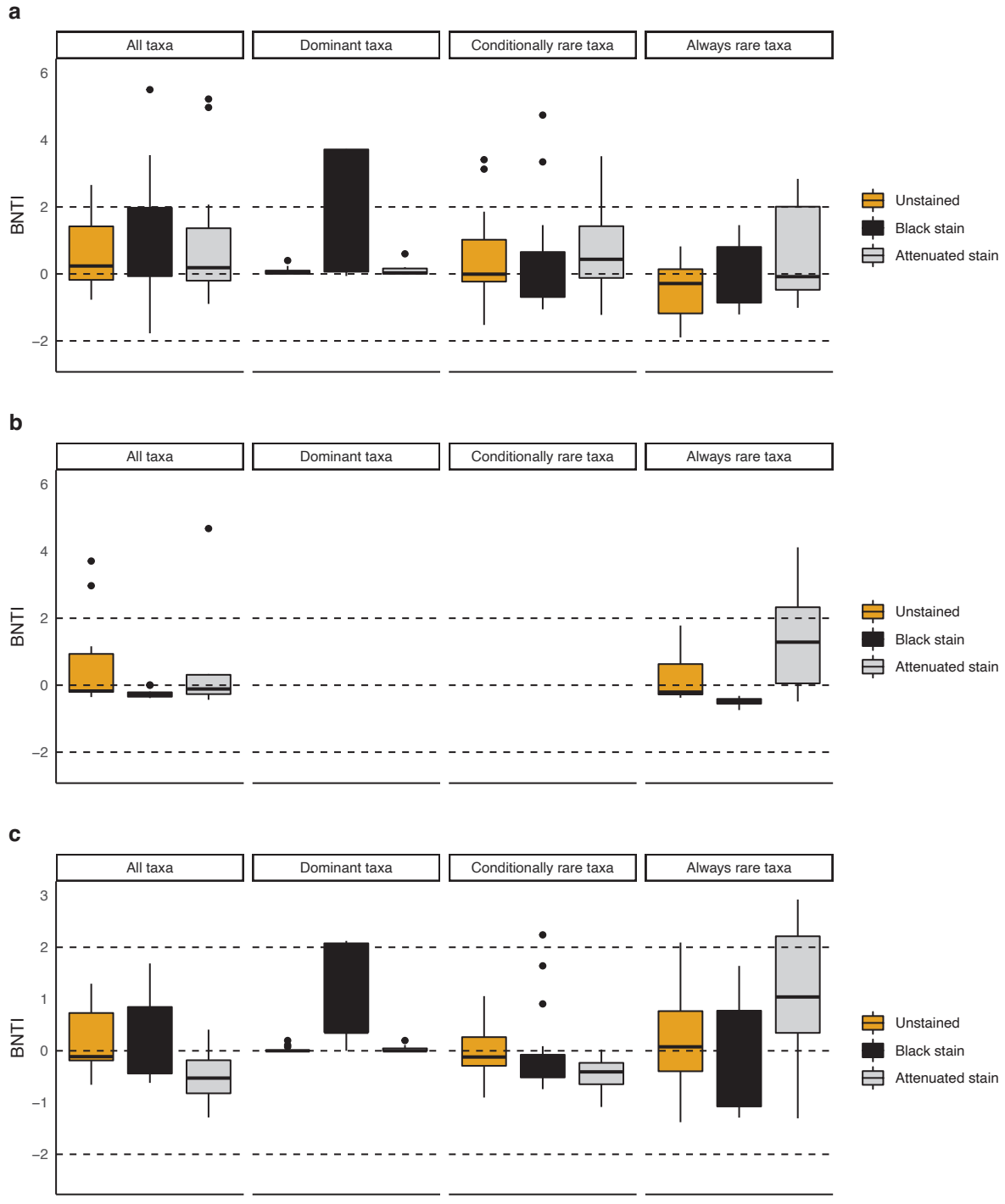

Supplementary figure 2. βNTI patterns for bacterial, archaeal and microeukaryotic communities across rock surface conditions. Horizontal dashed lines indicate null values as well as upper and lower significant thresholds of -2 and +2. In b, no data is shown for dominant taxa and conditionally-rare taxa because the number of OTUs in these categories was low (< 6).

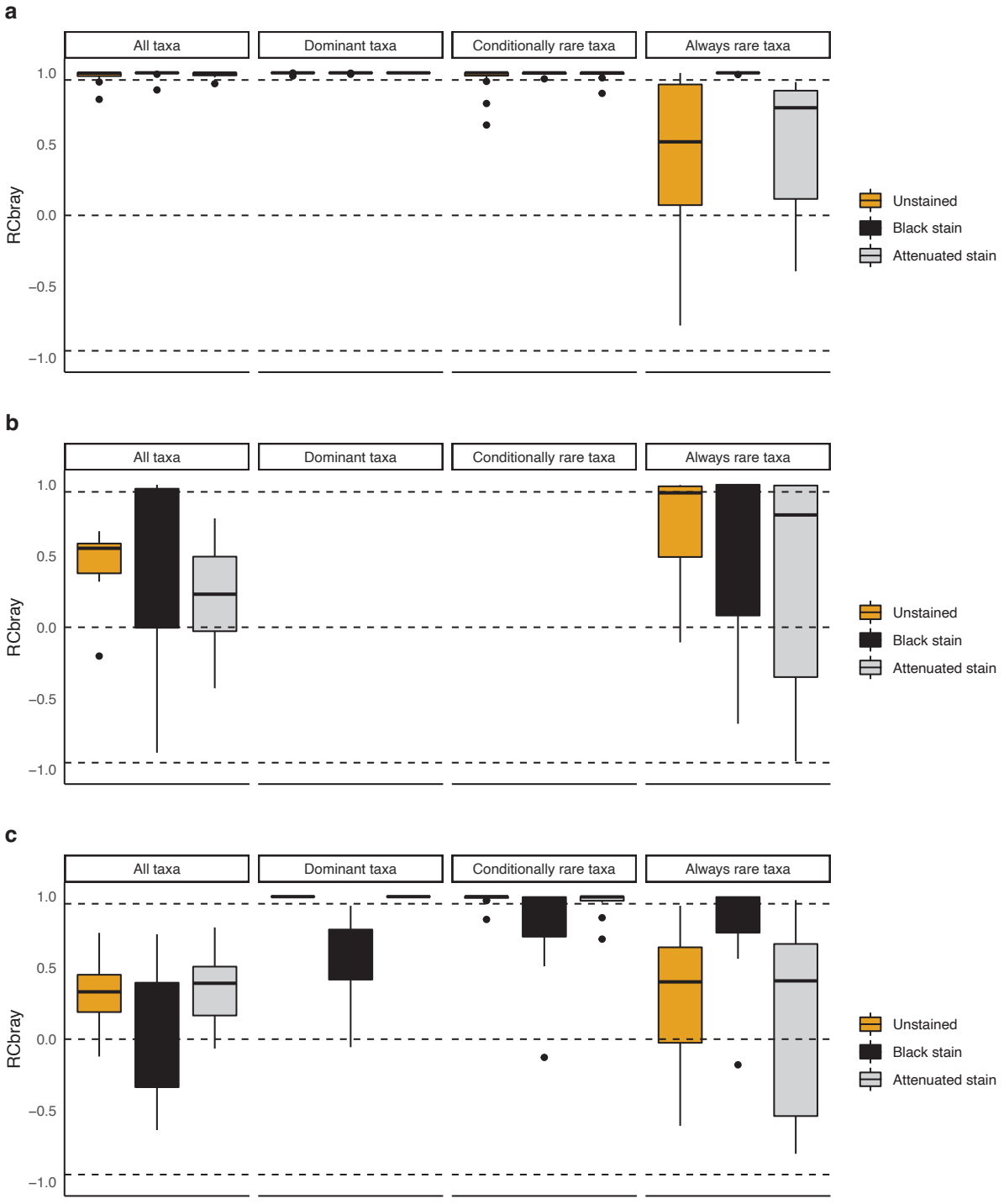

Supplementary figure 3. Bray-Curtis-based Raup-Crick (RC_bray) values for bacterial, archaeal and microeukaryotic communities across rock surface conditions. Horizontal dashed lines indicate null values as well as upper and lower significant thresholds of -0.95 and +0.95. In b, no data is shown for dominant taxa and conditionally-rare taxa because the number of OTUs in these categories was low (< 6).

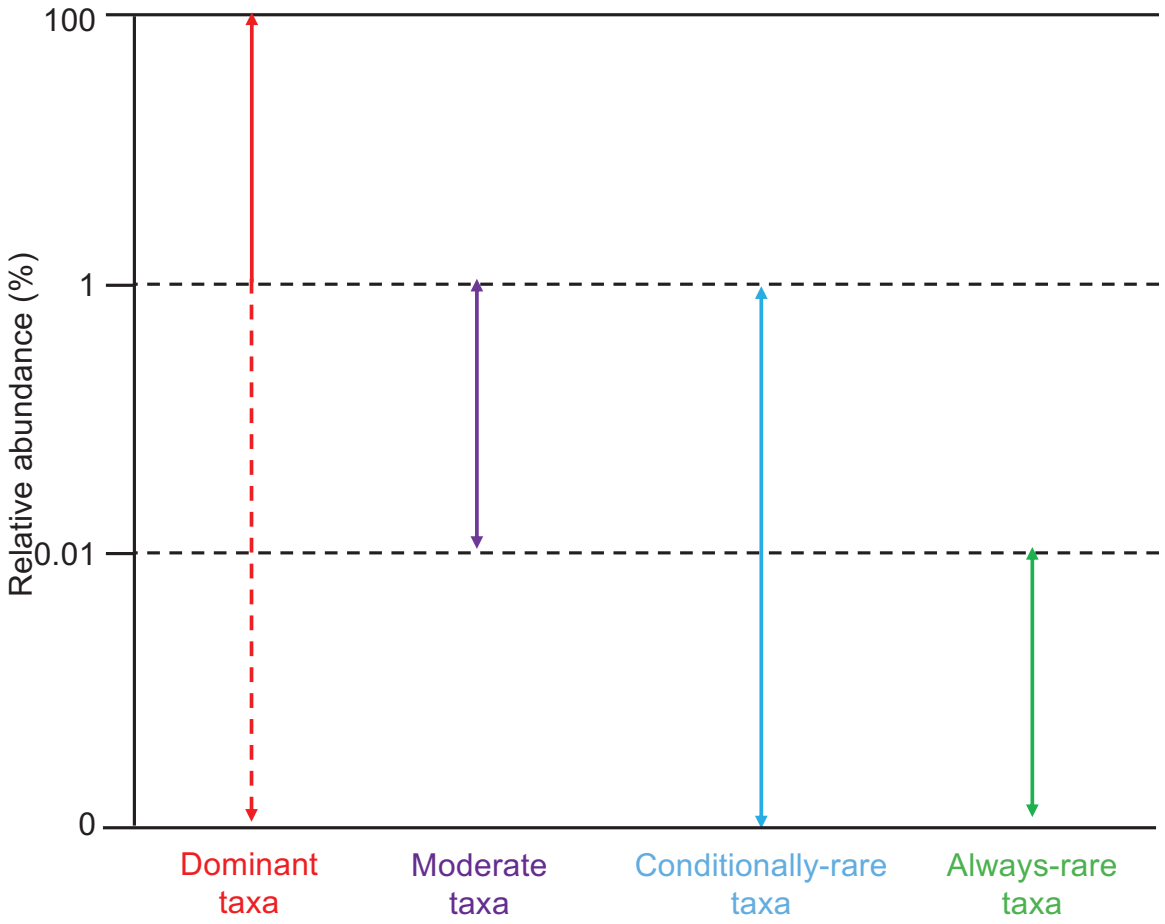

Supplementary figure 4. Thresholds used to define abundant and rare taxa categories in this study. Dominant taxa were (i) OTUs with a relative abundance between 1% and 100% in all samples or (ii) OTUs with a relative abundance varying from rare ($< 0.01\%$) to abundant ($\geq 1\%$). Moderate taxa were the OTUs with relative abundance between 0.01% and 1% in all samples. Conditionally-rare taxa were the OTUs with a relative abundance $< 0.01\%$ in no more than 33% of all samples but never $\geq 1\%$ in all samples. Always-rare taxa were the OTUs with a relative abundance $< 0.01\%$ in all samples.

Article 5. Experimental assessment of microbial successions following mechanical removal of black strain alterations on Paleolithic cave walls

ZELIA BONTEMPS[1], MYLENE HUGONI[1,2,3] AND YVAN MOENNE-LOCCOZ[1]

[1]Univ Lyon, Université Claude Bernard Lyon 1, CNRS, INRAE, VetAgro Sup, UMR Ecologie Microbienne, F-69622 Villeurbanne, France
[2]Univ Lyon, Université Claude Bernard Lyon 1, CNRS, INSA de Lyon, UMR Microbiologie Adaptation et Pathogénie, F-69622 Villeurbanne, France
[3]Institut Universitaire de France (IUF)

Current address for Mylène Hugoni : Univ Lyon, INSA Lyon, CNRS, UMR 5240 Microbiologie Adaptation et Pathogénie, F-69621 Villeurbanne, France

Corresponding author
Yvan MOENNE-LOCCOZ
Univ Lyon, Université Claude Bernard Lyon 1, CNRS, INRAE, VetAgro Sup, UMR5557 Ecologie Microbienne, 43 bd du 11 novembre 1918, F-69622 Villeurbanne, France
yvan.moenne-loccoz@univ-lyon1.fr

Highlights

- Cave anthropization can result in the formation of microbial alterations on walls
- Mechanical cleaning of black stains artificially generated a pioneer community
- Recolonization started with genera *Pseudomonas*, *Pedomicrobium* and *Ochroconis*
- Recolonizing microbial communities depended on stain cleaning method
- Sponges used for cleaning are not sterile and contaminate cave surfaces durably

Abstract

Anthropization of Paleolithic karstic caves can cause an imbalance of cave microbiota and may result in the formation of wall alterations including black stains. In Lascaux Cave, a previous attempt to mechanically remove black stains was followed by reformation of the stain in months, suggesting that microbial recolonization had taken place as in the initial colonization process. On this basis, we hypothesized that microbial successions involved in black stain formation implicate specific taxa from the very early stages (pioneer taxa) of recolonization on, and that mechanical cleaning was a useful experimental approach to generate artificially a pioneer community and monitor subsequent microbial successions. We assessed microbial recolonization in the Apse of Lascaux Cave (France), with two methods of mechanical cleaning (scalpel or scalpel + sponge), across 19 months of microbial recolonization. Illumina MiSeq metabarcoding evidenced various taxa i.e. bacteria *Pseudomonas*, *Pedomicrobium* and black-melanized fungi *Ochroconis* during early recolonization of cleaned surfaces and later the bacteria *Luteimonas*, *Chitinophaga* and fungi *Exophiala* etc. Surfaces at 19 months after cleaning were visually and microbiologically different from unstained surfaces and non-cleaned stained surfaces, probably because microbial succession differed from the original succession during stain formation. Variations of Bacteroidota and Eurotiomycetes classes and Exophiala genus were higher when the sponge was used in addition to the scalpel. The bacteria *Filomicrobium* and the fungi *Isaria* and *Cephalotrichum* were identified on sponge-cleaned surfaces and on the sponge itself, pointing to a contaminant status. Taken together, these findings suggest that pioneer communities may play an important role in orienting stain (re)formation in caves, and that sponges routinely used by restorers for cleaning stains in cultural heritage sites may bring microbial contaminants.

Graphical abstract

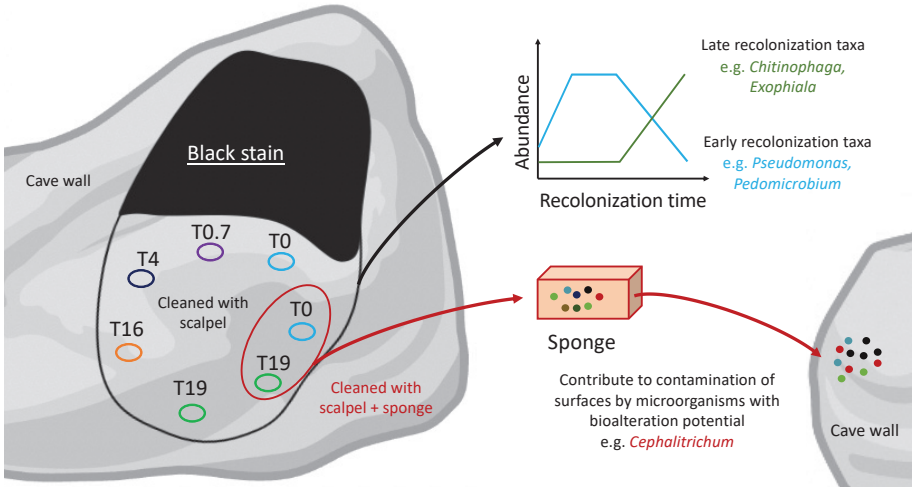

Key words

Paleolithic cave ; Cave alteration ; Conservation strategy ; Microbial successions, Metabarcoding

1. Introduction

Limestone regions display karstic underground ecosystems resulting from bedrock dissolution by percolating water (Cuezva et al., 2012). Many caves have been used by prehistoric humans for shelter or parietal art, including paintings, drawings and carvings (Dupont et al., 2007 ; Mohen and Taborin, 2019), leading to contemporary touristic activities in many of them. Tourism is also significant in a broad range of karstic caves with outstanding geological features, such as speleothems or underground water bodies (Cigna et al., 2013).

Show caves have undergone substantial environmental changes, first as a consequence of transformations implemented to manage tourist access and visits, i.e. building of staircases, installation of a light systems, etc. (Bontemps et al., 2021 ; Cañveras, 2001). Second, the visitors themselves have an impact by consuming oxygen, releasing carbon dioxide, depositing organic matter and dust from the outside via their shoes, loss of hair or skin, etc. (Cañveras, 2001 ; Dupont et al., 2007 ; Jurado et al., 2010 ; Russell and MacLean, 2008). These anthropic effects may cause an imbalance in the cave microbiota (Pfendler et al., 2018). In some cases, it leads to abnormal microbial growth, resulting in the formation of surface alterations on cave walls. Consequently, several show caves had to be closed to the public, in particular the iconic UNESCO caves Altamira (Spain) and Lascaux (France), whereas others were never opened to the public as a precaution to avoid cave degradation, e.g. Chauvet and Cussac in France (Barton and Jurado, 2007 ; Bastian et al., 2010 ; Cañveras, 2001 ; Cigna, 2016).

Various types of surface alterations have been reported on cave walls, with stains corresponding to microbial constituents e.g. melanin pigments (black) from fungal cell walls (De la Rosa et al., 2017), carotenoid pigments (brown/orange) from fungal and bacterial species including *Streptomyces* spp. (Sakr et al., 2020), or to the outcome of microbial transformations, such as manganese precipitation by many different bacterial and fungal species (from the phyla Proteobacteria, Firmicutes, Actinobacteria, Ascomycota and Basidiomycota) (Alabouvette and Saiz-Jiménez, 2011 ; Carmichael et al., 2015) and calcite deposition by various bacteria (e.g. *Pseudomonas*, *Bacillus* and *Myxococcus*) (Chalmin et al., 2007). Stains are commonly managed using mechanical removal and/or targeted chemical treatments, and the latter manage (or sometimes fail) to control microbial outbreaks (Bastian et al., 2009a ; Diaz-Herraiz et al., 2014 ; Mitova et al., 2017). In fact, the chemical treatments themselves may trigger the formation of cave wall alterations in certain cases, as illustrated with benzalkonium chloride and black stains in Lascaux Cave (Bastian et al., 2010 ; Martin-Sanchez et al., 2015), perhaps the most anthropized of all show caves. In Lascaux Cave, black stains represent one of the most extreme alterations, as they may develop after previous types of stains were removed by chemical treatments (Martin-Sanchez et al., 2015) and they are hard to eradicate chemically (Bastian et al., 2009a), probably because melanin pigments are an effective protection of microorganisms against strong chemical stress (El-Bialy et al., 2019 ; Plonka and Grabacka, 2006). Black stains are also documented in other caves than Lascaux, e.g. in Holly Saviour's cave (Zucconi et al., 2012) and Grotta del Cervo (Bernardini et al., 2021) in Italy, Driny Cave in Slovakia (Ogórek et al., 2016), or Cova Eirós in Spain (Steelman et al., 2017).

Certain microorganisms possibly involved in cave wall alterations have been evidenced, e.g. Xanthomonodales and *Thauera* in Altamira (Portillo et al., 2008) or *Ochroconis* pigmented fungi

in Lascaux (Alonso, 2018)(Bontemps et al. *in prep*), but they are not always well documented in most caves. Furthermore, microbial successions leading to their proliferation are essentially unknown, because the advent of high-throughput sequencing methods is rather recent. In 2015, mechanical removal of a black stain was carried out in the Apse room of Lascaux, and a new black stain started to form in the following months, with the same size, shape and contour as the previous one, suggesting that removal of black stain microorganisms had been incomplete and that microbial recolonization was fast. On this basis, we hypothesized that microbial successions involved in black stain formation implicate specific taxa (possibly from the three domains of Life) from the very early stages (pioneer taxa) of recolonization on, and that mechanical cleaning (incomplete in microbial terms, as some microorganisms remain) was a useful experimental approach to generate artificially a pioneer community and monitor subsequent microbial successions.

The objective of the current work was to test this hypothesis by characterizing the microbial successions taking place once black stains are removed by mechanical means, using black stains present in the Apse of Lascaux Cave. To this end, six black stains were manually cleaned by an accredited restorer and microbial recolonization was monitored during 19 months. In addition to the identification of taxa associated with microbial recolonization, mechanical cleaning methods were compared, i.e. using sterile scalpel only vs sterile scalpel + sponges. MiSeq Illumina sequencing for all three domains of life was used to assess the structure and composition of microbial communities.

2. Materials and Methods

2.1 Sampling and nucleic acid extraction

Lascaux Cave in South-West of France (N 45°03'13.087" and E 1°10'12.362") has been closed for tourist visits since 1963 due to cave wall alterations. Since then, access to the cave has been limited to scientists and official visits, to preserve the integrity of the cave. One major room inside Lascaux is the Apse (30 m^2), which contains more than a thousand Paleolithic figures, and where black stains and dark zones were identified on limestone wall surfaces. To study the natural reformation of black stains, six black stains located at the back of the Apse, in a small area termed the Absidiole, were subjected to mechanical cleaning on 23 September 2020, using sterile disposable scalpels (Paramount 3 ; MDSS GmbH, Hannover, Germany) treated by gamma irradiation (Figure 1A).

Samples from stains were collected immediately before (Stain T0 samples) and immediately after scalpel cleaning (CStain T0 - 23 September 2020), at 3 weeks (CStain T0.7 - 13 October 2020), 4 months (CStain T4 - 7 December 2020), 16 months (CStain T16 - 4 January 2022) and 19 months (CStain T19 - 28 April 2022), according to the authorizations given by the DRAC Nouvelle-Aquitaine (Bordeaux office, Ministry of Culture) (Figure 1B). One sample was taken per stain and separate areas of each stain were sampled at the different dates. In addition, a control sample was taken near each black stain and on black stain on the day of mechanical cleaning and at 19 months (samples Control T0, Control T19, Stain T0 and Stain T19, respectively). Finally, one part of each black stain was cleaned with both scalpel and sponges AION D3 (AION, Japan) made of polyvinyl formal (PVFM) resin, as often done by cave restorers. Before

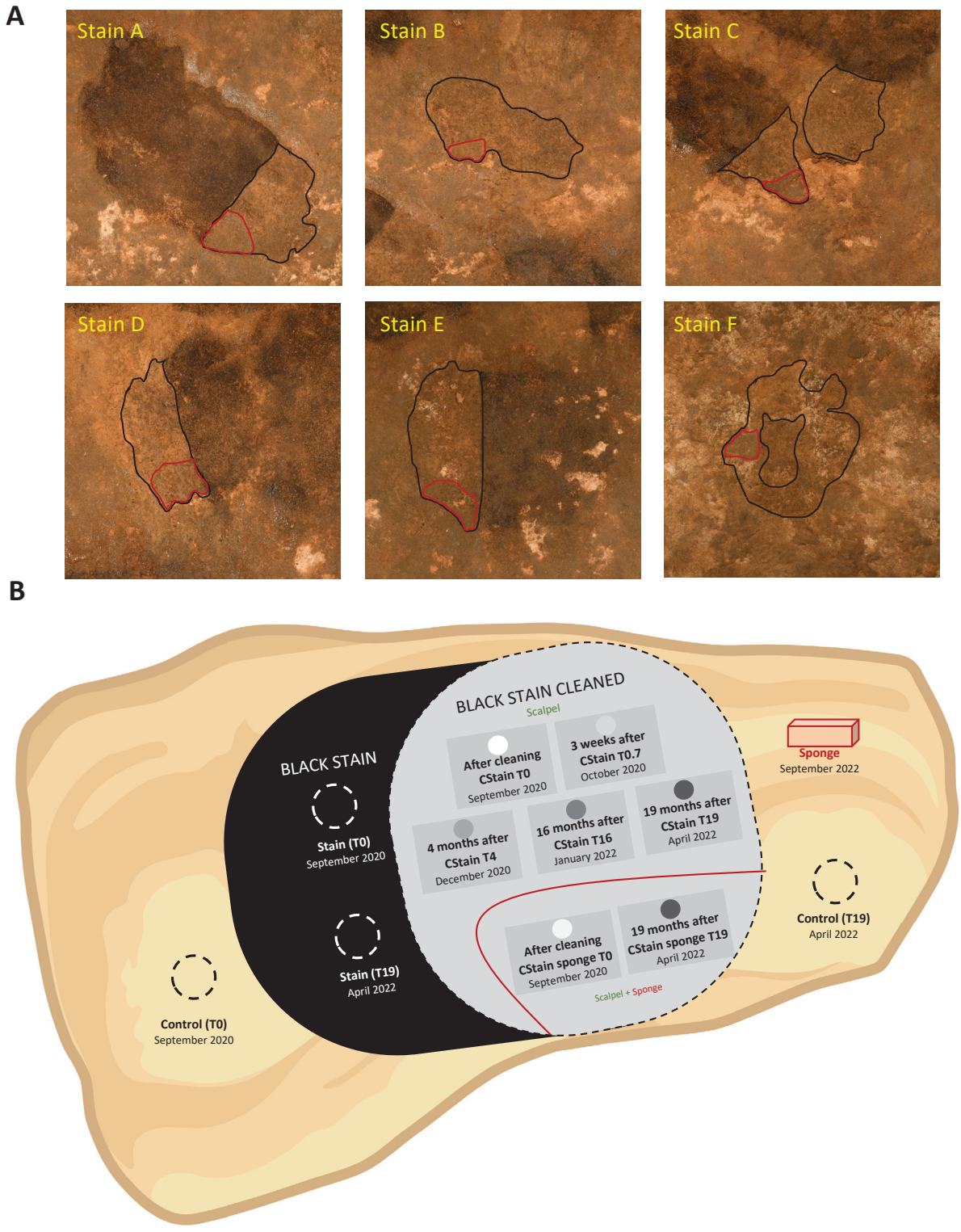

Figure 1. (A) Photography of black stains after mechanical cleaning. The green line delimits the area cleaned with a scalpel + sponge, while the grey zone delimits the area cleaned only with a scalpel. (B) Schematic layout of the samples in each rock surface condition at different sampling time, for the six replicates of black stains cleaned. Controls conditions are represented with dotted circle.

use, the sponges had been rinsed with tap water (to remove preservatives), cut into 3 cm × 1 cm × 2 cm pieces, disinfected in boiling water for 20 min and packed in aluminum foil. Parts

cleaned with scalpel and sponges AION D3 were sampled immediately after mechanical cleaning and 19 months after cleaning (samples CStain sponge T0 and CStain sponge T19) (Figure 1B), and the surface of six unused sponges was also sampled on 23 September 2020 (samples Sponge), using scalpels. To avoid a scalpel finish after sampling of sponge-cleaned surfaces, the restorator used sponges again on these areas to reinstall a sponge finish. In total, 54 samples were collected for this study. To avoid any modification of the microbial community in the samples, they were immediately placed in liquid nitrogen and transferred to -80°C at the laboratory, until DNA extraction.

2.2 Total DNA extraction, PCR amplification and high-throughput sequencing

Total genomic DNA extraction was performed using the FastDNA SPIN Kit For Soil (MP Biomedicals, Illkirch, France), based on manufacturer's instructions and adjusted to small samples. Broken swab heads or sponge surface samples (about 200 mg) were placed in lysis tube, and lysis solution was added. The elution step was achieved using 90 µl of elution buffer for each sample. The DNA concentrations were quantified using the Qubit dsDNA HS Assay Kit (Invitrogen, Carlsbad, USA) following the manufacturer's instructions.

Three gene markers were analyzed in each individual sample. The V3-V4 region of the 16S rRNA genes was amplified in triplicate for Bacteria and Archaea using the universal primers 341F and 805R (Herlemann et al., 2011) and 515F and 915R (Herfort et al., 2009), respectively (Supplementary Table S1). For Eukaryota, the V4 region of the 18S rRNA genes was amplified in triplicate using the universal : primer 0067a deg and NSR399 (Dollive et al., 2012). The PCR mix consisted in 5 µl of 5X Hot BioAmp Blend Master Mix RTL (Biofidal - now Microsynth France, Vaulx-en-Velin, France), 0.1 µM of each primer, 0.1X of GC-rich-enhancer (Microsynth France), 0.2 ng.µl-1 of bovine serum albumin (Promega, Madison, USA) and 0.2-1 ng DNA. All amplifications were performed in a Biorad T1000 thermal cycler (Biorad, Hercules, USA) using a PCR program for Bacteria composed of 3 min at 95°C, 28 cycles of 45 s at 95°C, 45 s at 50°C and 90 s at 72°C, followed by 7 min at 72°C. For Archaea, it consisted in 10 min at 94°C, 30 cycles of 1 min at 94°C, 1 min at 58°C and 90 s at 72°C, followed by 10 min at 72°C. For Eukarya, it consisted in 10 min at 95°C, 30 cycles of 1 min at 94°C, 1 min at 55°C and 90 s at 72°C, followed by 10 min at 72°C. All primers were tagged with the Illumina adapter sequences (TCG TCG GCA GCG TCA GAT GTG TAT AAG AGA CAG and GTC TCG TGG GCT CGG AGA TGT GTA TAA GAG ACA G) allowing the construction of amplicon libraries by a two-step PCR. Additionally, DNA extraction was carried out without any biological matrix and was considered a negative control to evaluate ambient and kit products contamination. Amplification signals were verified by electrophoresis on agarose gel 1.5%. High-throughput sequencing was achieved after pooling PCR triplicates using Illumina MiSeq (2 × 300 bp, paired-end chemistry v3), and was performed by Microsynth (Balgach, Switzerland), aiming (for each sample) at 40,000 sequences for the bacterial 16S rRNA gene, the 18S rRNA gene and the ITS, and 70,000 sequences for the archaeal 16S rRNA gene.

2.3 Sequence processing

For each dataset i.e. bacterial 16S rRNA genes, archaeal 16S rRNA genes, 18S rRNA genes and ITS2 regions, paired-ends reads obtained were demultiplexed in the samples according to exact match adaptors (removed) and reads were merged with a maximum of 10% mismatches in the overlap region using FLASh (Magoč and Salzberg, 2011). Denoising procedures was carried out by discarding reads without the expected length (200-500 bp) or containing any ambiguous base (N). After dereplication of sequences, clusterization was performed using SWARM (Mahé et al., 2014), which uses a local clustering threshold (rather than a global clustering threshold) and an aggregation distance of 3 for identification of operational taxonomic units (OTUs). The lower taxonomic level reached to define OTUs corresponded to (depending on taxa considered) the genus or the species ('genus/species' level). Chimeric sequences were discarded using VSEARCH (Rognes et al., 2016), and low-abundance sequences were filtered at 0.005% of all sequences. Taxonomic affiliation was preformed with both RDP Classifier and BLASTn (Zhang and Madden, 1997) against the 138.1 SILVA database (Quast et al., 2013) for bacteria, archaea and microeukaryotes (18S rRNA genes) and the 8.2 UNITE database for fungi (ITS region), which was automated in the FROGS pipeline (Escudié et al., 2018). Contaminant OTUs identified from the negative controls (blank samples) were removed and the eukaryotic dataset was manually curated for metazoan sequences (data not shown). To compare samples, a normalization procedure was applied by randomly resampling down to 15,196, 1,220 and 25,646 sequences in the bacterial, archaeal and microeukaryotic 18S data sets, respectively.

2.4 Statistical analyses

Rarefaction curves were calculated to assess sampling efficacy, using Paleontological Statistics (PAST) software v4.02 (Hammer et al., 2001). OTU richness and diversity were estimated using Chao 1 index (Chao, 1987), Shannon's H' (Shannon, 1948), Evenness $E^{h/s}$ index (Harper, 1999) , and Simpson (1-D) index (Simpson, 1949). Communities were primarily compared with NMDS, using VEGAN package in R v4.0.2 (R Core Team, 2020). The procedure computes a stress value, which measures the difference between the ranks on the ordination configuration and the ranks in the original similarity matrix for each replicate. Stress values below 0.1 are considered without risk of drawing false inferences, values below 0.2 acceptable (especially those close to 0.1), while values above 0.2 indicate limited interpretation potential (Clarke, 1993). Analysis of similarity (ANOSIM) was conducted using the VEGAN package in R, to test differences ($P \leq 0.05$) in overall community composition between different sampling conditions (see above) and to further confirm the results observed in the NMDS plot. A Bonferroni correction was applied on P values to lower alpha risk. All analyses were based on similarity matrices calculated with the Bray-Curtis similarity index (Bray and Curtis, 1957), using R.

3. Results

3.1 Contaminants associated to cleaning tools

The scalpels used for cleaning were sterile, but not the sponges. Analysis of sponges prepared for cleaning operations evidenced 199 bacterial OTUs, 10 archaeal OTUs and 103 microeukaryotic

OTUs. Bacterial OTUs belonged mainly to the phylum Proteobacteria (102 OTUs) followed by Actinobacteria (51 OTUs) and Myxococcota (8 OTUs). All 10 archaeal OTUs were affiliated to the phylum Thaumarchaeota. The microeukaryotic OTUs belonged mainly to the phylum Ascomycota (83 OTUs), followed by the Mucoromycota (8 OTUs).

3.2 Visual dynamics upon stain cleaning

The visual aspect of black stains and of unmarked surfaces did not change during the 19-month study. Mechanical cleaning of black stains was effective to removed black constituents, leading to a surface visually similar to unmarked surfaces located nearby (Supplementary Figure S1). Essentially no change in visual properties was identified at 3 weeks and 4 months after cleaning. At 16 and 19 months after cleaning, black stains had not reformed, but (i) cleaned areas had became heterogeneous, with the appearance of darker spots, and (ii) a black border, thin and discontinuous (which was preferentially sampled at 16 and 19 months), had started forming at the periphery of several of them, following the shape of the 'old stain'.

3.3 Community structure

NMDS and ANOSIM analyses indicated that the effect of rock surface condition (i.e. stain, stain after cleaning, or unstained surface × cleaning method if applicable × sampling time) on community structure was significant for bacteria ($P = 0.001$, $R^2 = 0.55$, Figure 2A and Supplementary Table S2), archaea ($P = 0.001$, $R^2 = 0.32$, Figure 2B and Supplementary Table S3) and microeukaryotes ($P = 0.001$, $R^2 = 0.44$, Figure 2C and Supplementary Table S4). In particular, data showed that black stain cleaning has a significant effect on the bacterial ($P = 0.001$, $R^2 = 0.13$) and microeukaryotic communities ($P = 0.001$, $R^2 = 0.11$), but not the archaeal community ($P = 0.34$, $R^2 = 0.03$). In this context, there was no difference between cleaning methods (i.e scapel vs scalpel/sponge) at T0, for bacteria ($P = 0.89$, $R^2 = 0.05$), archaea ($P = 0.39$, $R^2 = 0.10$) and microeukaryotes ($P = 0.38$, $R^2 = 0.10$).

Afterwards, the effect of recolonization time on community structure was not significant for bacteria ($P = 0.06$, $R^2 = 0.04$), archaea ($P = 0.06$, $R^2 = 0.02$) and microeukaryotes ($P = 0.07$, $R^2 = 0.06$). In addition, there was no difference between cleaning methods at T19, for bacteria ($P = 0.70$, $R^2 = 0.07$), archaea ($P = 0.71$, $R^2 = 0.05$) and microeukaryotes ($P = 0.47$, $R^2 = 0.08$).

3.4 Microbial richness and diversity levels

For bacteria, Chao-1 richness index, Simpson 1-D and Shannon H' diversity indices were lower for control conditions (Control T0 and Control T19 samples) than (i) all other rock surface conditions for Simpson 1-D (Wilcoxon test : $P = 1.9 \times 10^{-5}$ and $P = 3.1 \times 10^{-4}$, respectively) and Chao-1 ($P = 7.3 \times 10^{-5}$ and $P = 2.2 \times 10^{-4}$, respectively), or (ii) most other rock surface conditions (for Shannon H'; $P = 0.002$ and $P = 0.001$, respectively), without any effect of cleaning or recolonization time (Figure 3). The evenness diversity index was higher for cleaned surface conditions at T0 (CStain T0 and CStain sponge T0 samples) than for the other rock surface conditions ($P = 1.5 \times 10^{-4}$ and $P = 1.7 \times 10^{-4}$, respectively), therefore the effects of

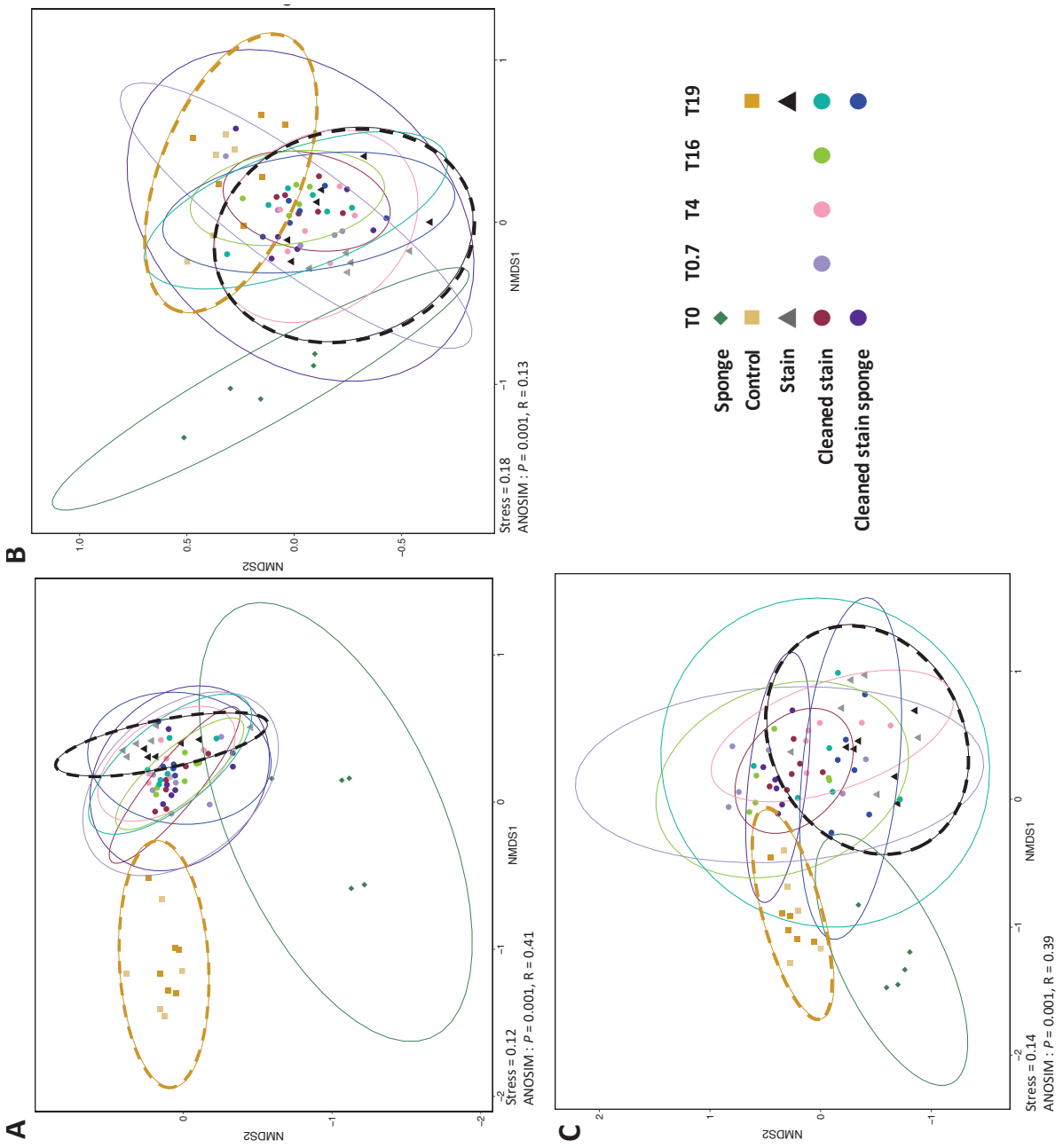

Figure 1. Non-metric Multidimensional scaling (NMDS) analysis of microbial community structure in Lascaux's Cave according to rock surface condition and time. Ellipse (95% confidence interval) indicate the different rock surface condition for bacteria (A), archaea (B) and microeukaryotes (C). Controls conditions are represented with dotted circle.

cleaning and of recolonization time were significant based on this criterion, and for both effects it was without a difference between cleaning methods.

For archaea, the differences in Chao-1 richness index, Simpson 1-D and Shannon H' diversity indices, and Evenness diversity index between rock surface conditions were not significant (Figure 3), pointing to a lack of effect of cleaning and of recolonization time.

For microeukaryotes, differences in Simpson 1-D diversity index between rock surface conditions were not significant, whereas Shannon index was higher for control conditions (T0 and T19 samples) than all other rock surface conditions ($P = 0.001$ and $P = 4.5 \times 10^{-4}$, respectively)

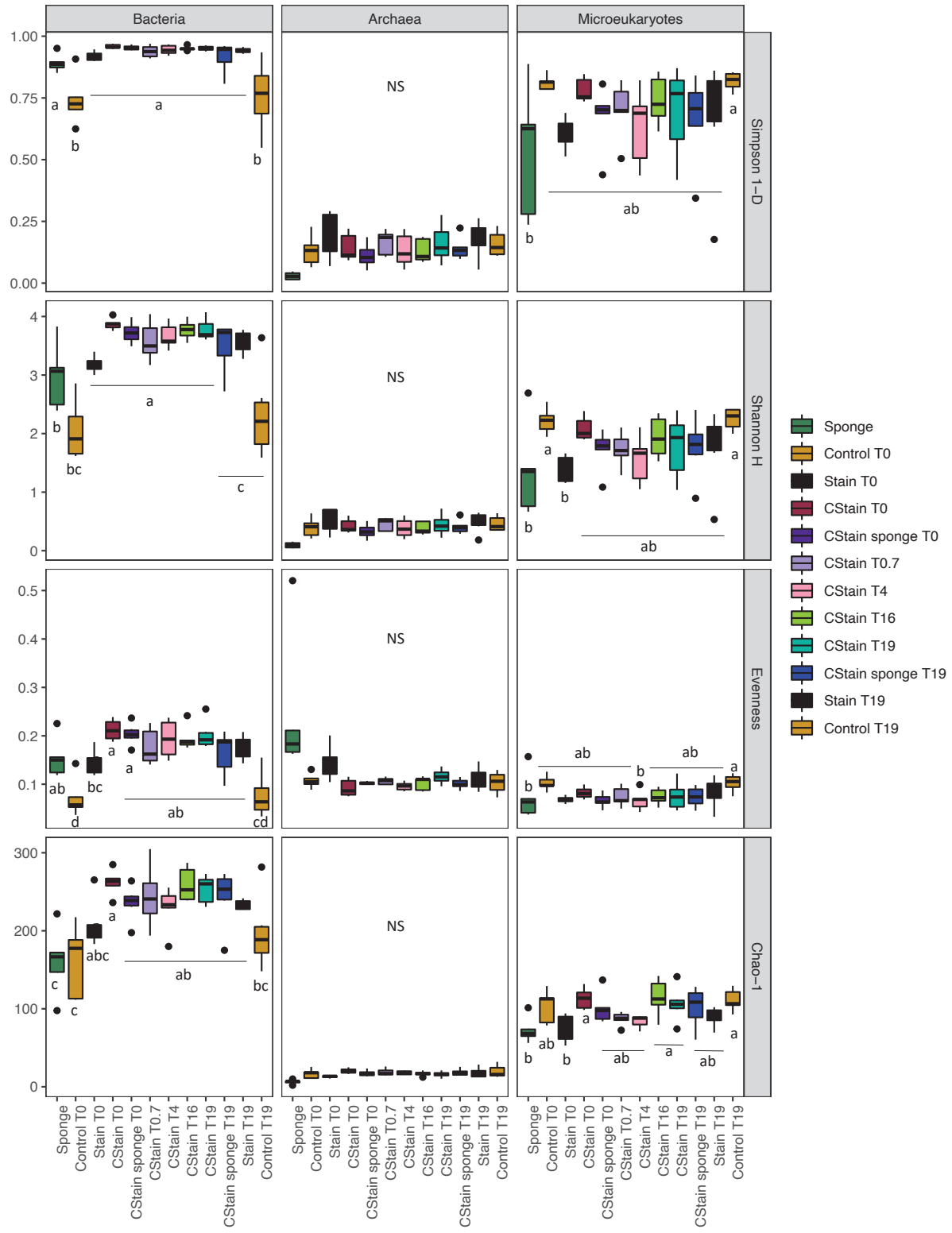

Figure 3. Alpha diversity indices of microbial community according to rock surface condition, based on estimated evenness (Simpson 1-D index and Evenness index), richness (Chao-1 index) and diversity (Shannon H' index). For each index, microbial community combination, significant differences according to rock surface condition and post-hoc grouping are shown with letters (Wilcoxon test, $P > 0.05$).

(Figure 3). Chao-1 index for black stains at T0 (Stain T0 samples) and Evenness index for cleaned surfaces at 4 months (CStain T4 samples) were lower than for the other rock surface conditions ($P = 1.1 \times 10^{-4}$ and $P = 0.001$, respectively). Thus, there was some impact of black stain cleaning (for both cleaning methods) but essentially none of recolonization time.

3.5 Microbial community composition in black stains vs unmarked surfaces

Unmarked surfaces (control) had similar bacterial, archaeal and microeukaryotic communities (Pairwise Adonis : $P = 0.882$, $R^2 = 0.4$; $P = 0.479$, $R^2 = 0.08$ and $P = 0.325$, $R^2 = 0.12$, respectively) across time (T0 vs T19) (Supplementary Tables S3, S4 and S5). The bacterial community was composed of 19 classes with predominantly Gammaproteobacteria (82.4% of bacterial sequences), highly represented by the *Pseudomonas* genus (73.9%) following by Alphaproteobacteria (9.9%) and Actinobacteria (2.3%) (Figures 4A and 5A). Archaeal community composition was characterized by the dominance of the Nitrososphaeria class (100% of archaeal sequences) (Figure 4B). The microeukaryotic community was composed of 21 classes including Sordariomycetes (43.0% of microeukaryotic sequences), Leotiomycetes (18.7%) mostly affiliated to the *Pseudogymnoascus* genus (18.3%) and Dothideomycetes (7.9%) (Figures 4C and 5B).

Black stains had similar bacterial, archaeal and microeukaryotic communities (Pairwise Adonis : $P = 0.386$, $R^2 = 0.10$; $P = 0.198$, $R^2 = 0.13$ and $P = 0.766$, $R^2 = 0.04$, respectively) across time (T0 vs T19) (Supplementary Tables S3, S4 and S5). The bacterial community of black stains was composed of 19 classes including Alphaprotebacteria (37.4%), Actinobacteria (18.6%), Bacteroidia (16.8%) highly represented by the *Chitinophaga* genus (8.2%) and Acidobacteriae (12.9%) mostly affiliated to the *Bryobacter* genus (12.2%) (Figures 4A and 5A). The archaeal community was composed of the two classes Nitrososphaeria (97.6%) and Halobacterota (2.4%) (Figure 4B). The microeukaryotic community consisted in 19 classes with predominantly the Eurotiomycetes class (65.9%) and especially the *Exophiala* genus (25.4%), followed by Sordariomycetes (21.0%) and Dothideomycetes (1.7%) (Figures 4C and 5B).

Unmarked surfaces showed significant differences compared with black stains for bacterial (whatever the sampling time), archaeal and microeukaryotic communities (Supplementary Tables S3, S4 and S5). For the three domains of life, community composition showed strong variations between stained and unmarked surfaces for the most abundant classes or genera, notably for the Gammaproteobacteria (an average of -72% in black stains compared with unstained surfaces based on T0 and T19 data), Alphaproteobacteria (+28%), Bacteroidia (-15%), Sordaryomycetes (-22%), Leotiomycetes (-19%) and Eurotiomycetes (+59%) classes (Figures 4A and 4C). Similarly, strong variations were also observed at genus level, especially for *Pseudomonas* (an average of -74% in black stains compared with unstained surfaces), *Chitinophaga* (+6%), *Pseudogymnoascus* (-18%) and Exophiala genera (+24%) (Figure 5).

3.6 Microbial community composition after scalpel cleaning and across recolonization states

Scalpel cleaning of black stain changed microbial community composition for bacteria and microeukaryotes, as the bacteria *Nonomuraea* and fungi *Exophiala* and *Ochroconis* amounted to respectively 5.9%, 24.3% and 0.8% in stained surfaces vs 2.4%, 9.8% and 10% in cleaned sur-

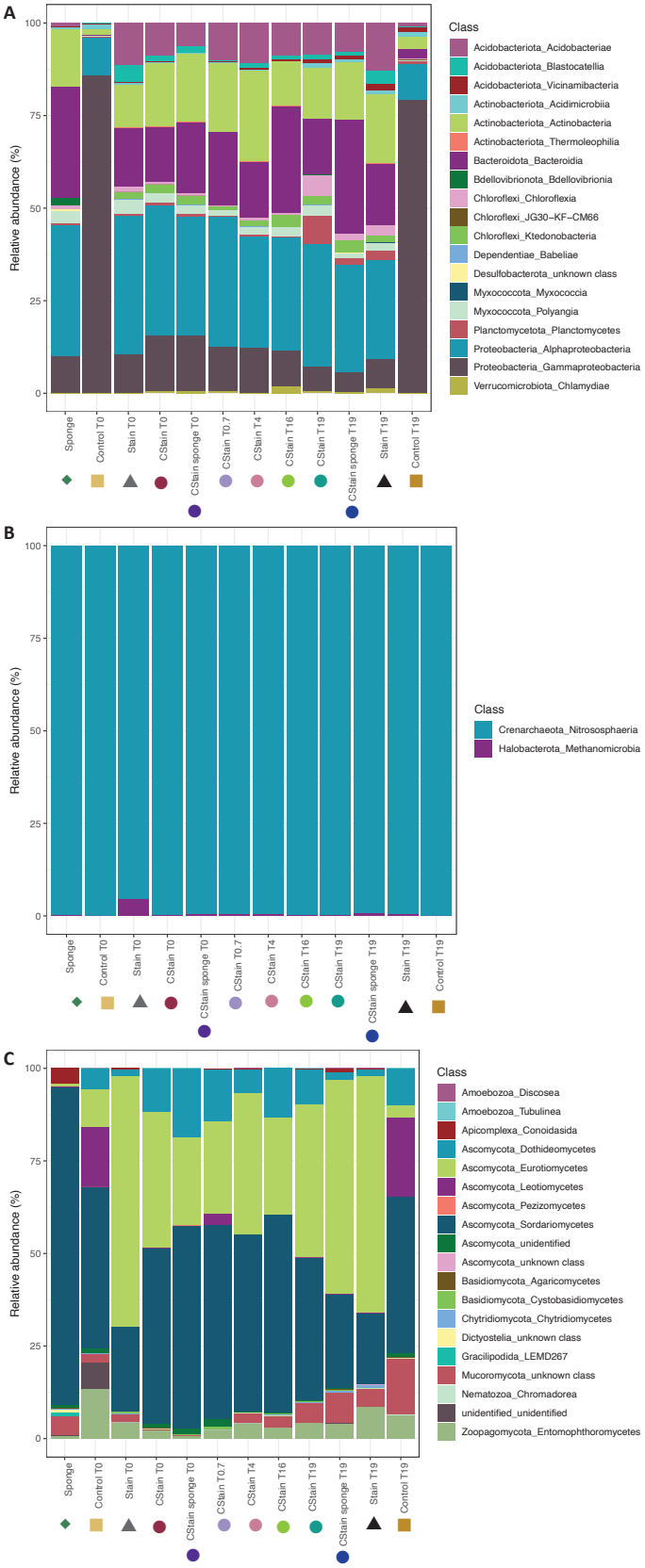

Figure 4. Relative abundance (% of sequences) of bacterial (A), archaeal (B) and microeukaryotic (C) classes according to rock surface condition.The symbols represent each surface condition studied, as used in Figure 2.

faces (Figure 5B). Cleaning had resulted in removal of black surface constituents, but without reaching the community composition of unmarked surfaces, as for instance Luteimonas reached 9.0% on cleaned surfaces, Nocardioides 5.7% and *Chitinophaga* 18.0%, vs only 0.1%, 0.07% and 0.7%, respectively, in unmarked surfaces (Figure 5A).

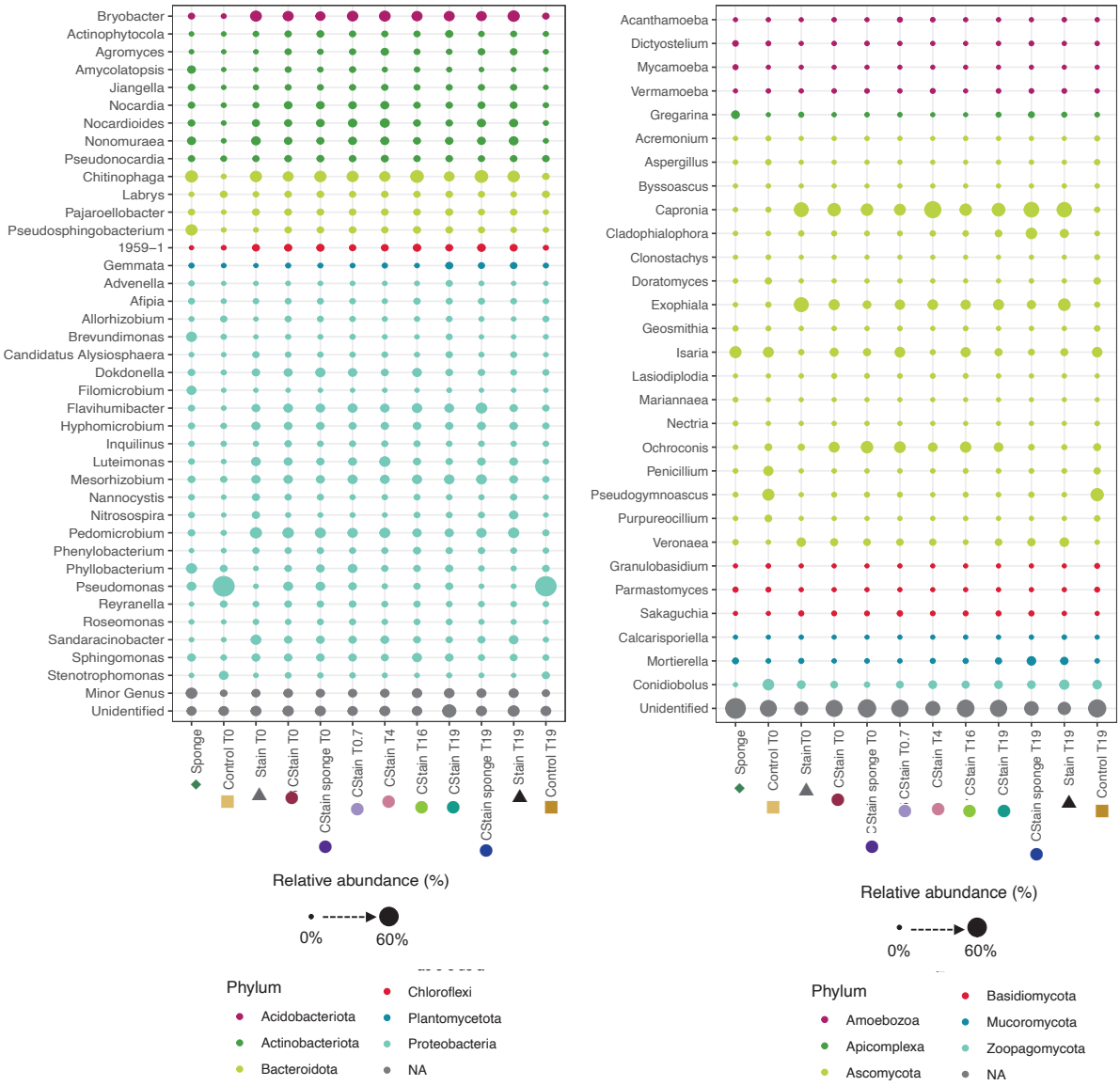

Figure 5. Distribution of the most abundant bacterial (A) and microeukaryotic (B) genera according to rock surface condition (also indicated with the symbols used in Figures 2 and 4). Within the panel, the relative abundance of the genera is proportional to the diameter of the circles, all genera consisting of $> 0.05\%$ of total normalized sequences were considered as minor genera, and the color of the circles represents the taxonomic affiliation at phylum level.

Immediately after cleaning, microbial communities were mainly composed of Alphaproteobacteria, Actinobacteria, Nitrososphaeria and Sordariomycetes classes (Figure 4), but community composition changed during the next 19 months for bacteria and microeukaryotes (Supplementary Tables S3, S4 and S5). In the bacterial community, the gammaproteobacterial class (mainly the *Pseudomonas* genus) decreased from 15.2% of sequences to 6.7% (and *Pseudomonas* from 5.6% to 0.9%) between T0 and T19 (Figures 4A and 5A). The Chloroflexia and Planc-

tomycetota bacterial classes (about 0.6% and 0.5% from T0 to T16, respectively) increased to 5.8% and 7.8%, respectively, at T19 (Figure 4A). The Actinobacteria class reached 17.5% at T0 and T0.7, 24.5% at T4 but only 12.7% at T16 and T19. At genus level, *Luteimonas* and Nocardioides genera amounted to respectively 3.3% and 3.0% at T0 and T0.7, 9.3% at T4, but only 1.6% and 1.7% at T16 and T19 (Figure 5A), whereas *Chitinophaga* increased from 9.9% (at T0, T0.7 and T4) to 18.5% (at T16 and T19) and *Pedomicrobium* decreased from 8.9% (at T0, T0.7 and T4) but to about 4.1% (at T16 and T19).

In the microeukaryotic community, the Sordariomycetes reached 50.4% at T0, T0.7, T4 and T16, but only 38.0% at T19 (Figure 4C). The relative abundance of Dothideomycetes and Eurotiomycetes fluctuated, as the Dothideomycetes reached 11.7% at T0, 14.0% at T0.7, 6.4% at T4, 13.3% at T16 and 9.6% at T19, whereas the Eurotiomycetes amounted to 36.6% at T0, 25.1% at T0.7, 38.1% at T4, 26.3% at T16 and 41.1% at T19. At genus level, *Exophiala* was stable (8.9-11.2%), *Ochroconis* fluctuated (10.9% at T0, 13.8% at T0.7, 6.3% at T4, 6.4% at T16 and 6.5% at T19), and *Capronia*, *Conidiobolus* and Unidentified genera amounted to 19.1%, 2.6% and 47.2% at T0, T0.7, T16 and T19 but at T4 they reached 46.1%, 4.3% and 30.6%, respectively (Figure 5B).

3.7 Cleaning method comparison

Unlike the bacterial community (Figure 4A), class composition of the fungal community immediately after cleaning depended on the cleaning method (Figure 4C). The Dothideomycetes reached 11.7% (scalpel) versus 18.5% (scalpel/sponge) (Figure 4C), whereas the Eurotiomycetes amounted to 36.6% (scalpel) vs 23.6% (scalpel/sponge) and the Sordariomycetes 47.3% (scalpel) vs 54.9% (scalpel/sponge). These contrasted abundances were also visible at the genus level, as *Exophiala* and *Ochroconis* amounted to 11.2% and 11.0% (sponge) vs 4.0% and 17.2% (scalpel/sponge), respectively (Figure 5B). At that level, some differences were seen also with bacteria, e.g. with *Chitinophaga* at 13.0% (sponge) vs only 8.3% (scalpel/sponge) (Figure 5A).

At 19 months after cleaning (T19), the Bacteroidota amounted for 15.0% (scalpel cleaning) versus as much as 30.6% where scalpel and sponge had been used (Figure 4A), and the Chloroflexia reached 5.8% (scalpel) vs 1.8% (scalpel/sponge). The Dothideomycetes class accounted for 9.5% of sequences (scalpel) vs only 1.9% (scalpel/sponge) and the Sordariomycetes for 38.6% (scalpel) vs only 25.3% (scalpel/sponge) (Figure 4C), whereas the Eurotiomycetes amounted to 41.1% (scalpel) vs 57.7% (scalpel/sponge). At genus level, *Pedomicrobium* amounted to 4.0% (scalpel) and 6.9% (scalpel/sponge) (Figure 5A), whereas *Chitinophaga* reached 18.8% (scalpel) vs only 8.0% (scalpel/sponge) and Phyllobacterium 2.0% (scalpel) vs only 0.4% (scalpel/sponge), and *Flavihumibacter* amounted to 5.2% (scalpel) vs as much as 10.7% (scalpel/sponge). *Exophiala* and *Ochroconis* amounted to 10.9% and 6.4% (scalpel) vs only 5.4% and 0.7% (scalpel/sponge), respectively (Figure 5B). In contrast, *Capronia*, *Cladophialophora* and *Veronaea* reached 23.2%, 2.1% and 1.9% (scalpel) vs as much as 35.4%, 13.2% and 3.4% (scalpel/sponge), respectively.

3.8 Fate of microbial contaminants from sponge

Microbial OTUs present in sponge samples but not in black stain or unstained surfaces were mainly affiliated to Bacteroidia (OTU_617), Alphaproteobacteria (OTU_65 = *Brevundimonas*) and Sordariomycetes class (i.e. OTU_332 = *Isaria* and OTU_455 = *Nectria*), while other sponge OTUs were also present in black stains or unstained surfaces, i.e. Acidimicrobiia (OTU_627, OTU_251), Bacteroidia (OTU_246, OTU_259, OTU_245), Alphaproteobacteria (OTU_981, OTU_810, OTU_441), Planctomycetes (OTU_1027), Eurotiomycetes (OTU_19, OTU_3, OTU_14), Enthromophtoromycetes (OTU_6), Sordariomycetes (OTU_24, OTU_7, OTU_8), etc. (Figure 6).

Figure 6A. Occurrence of all bacterial OTUs according to rock surface condition. OTU name are shown on the outer circle, while phyla affiliation is shown in inner circle. OTU presence is in blue and absence in lightblue.

OTUs found in sponge and sponge-cleaned samples at T0 and T19 but not in black stains, unstained surfaces or scalpel-cleaned stains were OTU_582 (unidentified Planctomycete), OTU_747

(unidentified Gammaproteobacteria), OTU_106 (*Veronaea*, Eurotiomycetes), OTU_488 (unidentified Eurotiomycete), OTU_304 (*Isaria*, Sordariomycete) and OTU_354 (unidentified Sordariomycete) (Figure 6). Overall, these OTUs represented respectively 0.15% and 0.08% (at T0) and 0.10% and 0.10% (at T19) of the bacterial and microeukaryotic sequences in sponge-cleaned samples. In addition, OTU_432 affiliated to *Cephalotrichum* genus (Sordariomycetes) and associated with sponge was also present in scalpel-cleaned stain at T4 (Figure 6B).

Figure 6B. Occurrence of all microeukaryotic OTUs according to rock surface condition. OTU name are shown on the outer circle, while phyla affiliation is shown in inner circle. OTU presence is in blue and absence in lightblue.

On the first day of the study, taxa evidenced in sponges corresponded to 89% and 96% of the bacterial and microeukaryotic sequences, respectively, on surfaces immediately after scalpel/sponge cleaning, vs 88% and 97% in black stains, 81% and 97% on unmarked surfaces and 86% and 96% on surfaces immediately after scalpel cleaning. Overall, these taxa present on sponges corresponded, at 19 months, to 90% and 98% of the bacterial and microeukaryotic

sequences, on surfaces that had undergone scalpel/sponge cleaning, vs 86% and 96% in black stains, 82% and 98% on unmarked surfaces and 82% and 96% on surfaces that had been cleaning with scalpel only. This means that taxa present on sponges were already well represented on Lascaux surfaces.

4. Discussion

In the present work, we aimed at testing the hypothesis that mechanical cleaning of black stains would lead to a pioneer-like community likely to undergo further microbial dynamics and perhaps microbial successions leading to the reformation of black stains. NMDS and Adonis analysis showed that the microbial communities of black stains and unstained surfaces differed significantly from each other and were stable. This parallels the stability of cave environmental conditions (Barton and Northup, 2007 ; Bourges et al., 2014 ; Cañveras, 2001 ; Di Russo et al., 1997 ; Engel, 2010) and especially the stability of black stains (once formed) in this part of the cave. Black stains in the Absidiole displayed counter-selection of *Pseudomonas* bacteria (from 73.9% of bacterial sequences to 0.03%) and selection of *Exophiala* fungi (from 0.4% to 30.4% of fungal sequences), as in Lascaux's Passage (Alonso et al., 2018), but surprisingly the relative abundance of *Ochroconis* fungi was of the same level in unmarked and stained surfaces (an average of 2%). *Exophiala* fungi have been found in environments rich in aromatic compounds (i.e. arsenic mine, creosote-treated wood and soil contaminated with aromatic hydrocarbons), where they can use alkybenzene as the sole carbon source (Cox et al., 1993 ; Schnitzler et al., 1999 ; Zhao et al., 2010). Also, these fungi have the potential to produce melanin pigment, which gives this black color to the stains in tombs (Isola et al., 2021) or caves (Martin-Sanchez et al., 2012)(Bontemps et al. *in prep*). Thus, selection of *Exophiala* black fungi was likely to have been promoted by the availability of residues of aromatic biocides used at Lascaux (Martin-Sanchez et al., 2015).

Against this background, mechanical cleaning of black stains with sterile scalpels resulted in a more richer community (with 462 taxa instead of 383), probably because dominant taxa were trimmed during stain removal. It was not the same community as in neighboring unmarked surfaces, even though the surface was not black anymore. Immediately after scalpel cleaning, the microbial community was mainly composed of Alphaproteobacteria, Actinobacteria, Nitrososphaeria and Sordariomycetes classes, and the relative abundance of *Pedomicrobium*, *Ochroconis*, *Pseudomonas* genera was significant.

The community thus obtained by scalpel cleaning was not stable, as microbial changes took place subsequently. Early successional stages are expected to include r-strategy taxa (Odum, 1969), with fast growth, high turnover rates and copiotrophy, which promote colonization (Barbault, 1995 ; Zhou and Ning, 2017). This is the case of many Proteobacteria, such as *Pseudomonas* (Jurburg et al., 2017). Early taxa may change surface conditions and facilitate microbial successions (Boston et al., 2009 ; Uroz et al., 2009). In Lechuguilla Cave (New Mexico) pioneer microorganisms (unidentified) produce organic acids that promote dissolution of cemented bedrock (Northup, 1997 ; Spilde et al., 2005). Here, microbial succession was observed only for bacterial and microeukaryotic communities, over the 19 months following cleaning. Several patterns of microbial dynamics were observed, i.e. (i) a linear decrease from T0 to T19, for instance

for Gammaproteobacteria and mainly the *Pseudomonas* genus, (ii) a decrease from T4 to T19 (for *Ochroconis*), (iii) stable abundance from T0 to T19 (e.g. for *Exophiala*), (iv) stable abundance with a peak only at T4 (for *Luteimonas*, Nocardioides and *Capronia*), and (v) an increase from T4 to T19 (for *Chitinophaga*, Dothideomycetes). Thus, most changes are observed at 4 months and after, with the selection of certain taxa that could correspond to K-strategy species. This is the case of many Actinobacteria (Bastian et al., 2009b). After the initial stages of colonization, K strategists with high competitive ability are expected to be preferentially selected (Yin et al., 2022).

Microbial communities 19 months after scalpel cleaning were not yet similar to those of black stains, with *Chitinophaga* (harboring genes for melanin synthesis ; Chapter 4) at 18% (vs 8% in black stains) and the black fungus *Ochroconis* at 10% vs 0.8%.This was surprising, as the original black stains as such did not reform. Perhaps black stains reformation requires other pigmented taxa. Black stains in the Apse typically display *Folsomia candida* collembola, which can feed on black fungi and disseminate them (Alonso et al., submitted ; Bastian et al., 2009). These collembola were back within weeks of stain cleaning in 2015 but were sparsely seen in this work, suggesting that melanin synthesis may be a response to grazing. Monitoring of *F. candida* populations in various areas of the cave showed that their dynamics can be erratic (personal communication from S. Géraud). Here, the microbial community on cleaned surfaces did not change much between 16 and 19 months, pointing that secondary succession could lead to a paraclimax. Microbial recolonization depends on the disturbance regime, microbial legacy and microbial dynamics related to species regrowth, immigration and recruitment (Cox et al., 1993 ; Schnitzler et al., 1999 ; Zhao et al., 2010).

In addition to representing a useful experimental approach to generate artificially a pioneer community for subsequent monitoring, this experiment was also based on the rationale that mechanical cleaning is a routine procedure followed by restorers to remove stains in show caves as well as historical buildings. Therefore, we included a standard cleaning procedure in which sponges are also used, for stain removal and final smoothing of cleaned surfaces. Here, however, we showed that sponges, despite disinfection in boiling water, displayed a microbial community. Three issues are raised. First, as expected, this community differed from that of rock surface conditions in Lascaux, but it included Bacteroidota, which have been proposed as bioindicators of anthropization in caves (Alonso et al., 2018 ; Pfendler et al., 2018) as well as the black fungus Exophiala. This raises the possibility that allochthonous strains from these taxa could actually contribute to cave populations following routine cleaning procedures. Second, some taxa present on the sponge were found only on surfaces cleaned with the sponge, pointing to microbial contamination via the sponge (but at modest levels of relative abundance). This is the case of the bacterial genus *Filomicrobium* and fungal genera *Isaria* and *Cephalotrichum*, which have been also identified in other anthropized subsurface environments (Diaz-Herraiz et al., 2014 ; Miller et al., 2020 ; Novakova et al., 2005). These microorganisms might be significant for cave conservation issues, as *Filomicrobium* and *Cephalotrichum* were pointed at in biodegradation of respectively the Tomba del Coll Etruscan tomb (Diaz-Herraiz et al., 2014) and the Takamatsuzuka Tumulus stone chamber in Japan ((Kiyuna et al., 2017) but here scalpel/sponge cleaning did not lead to darker surfaces than scalpel cleaning at 19 months. Therefore, cosmopolitan taxa with surface

alteration potential may be disseminated during cleaning procedures, and more care is needed when selecting these procedures for cultural heritage sites. Third, Finally, the sponge treatment can modify rock surface properties, selecting certain species with particular adhesion properties and able to thrive (Barton and Jurado, 2007 ; Uroz et al., 2015). This may also contribute to changes in microbial community composition.

5. Conclusion

Rock surface alterations by microorganisms in Paleolithic caves are of high concern for conservation of artwork, and here we show that mechanical cleaning of black stains leads to subsequent microbial successions. Early recolonization involved specific taxa e.g. *Pseudomonas*, *Pedomicrobium* and black-melanized fungi *Ochroconis*, followed by *Chitinophaga* members of the Dothideomycetes class, probably leading to a paraclimax. In addition, we identified that the use of sponge for mechanical cleaning, a routine procedure in heritage sites, can have a significant impact on microbial communities and contribute to contamination of cave surfaces by microorganisms with bioalteration potential. Thus, our work provides a better understanding of microbial dynamics associated with surface alterations in Paleolithic caves and highlights shortcomings in current cave conservation procedures.

Data accessibility

All data that support findings of this study have been deposited in NCBI SRA database PRJNA860522, PRJNA60527 and PRJNA860536 for bacterial 16S rRNA genes, archaeal 16S rRNA genes and 18S rRNA genes, respectively. The authors declare that the R (R 4.0.3) codes used to generate the results in this study are available in this paper.

Acknowledgements

Funding was provided by DRAC Nouvelle Aquitaine (Bordeaux, France). We thank S. Géraud, J.C. Portais, T. Baritaud, M. Mauriac (DRAC Nouvelle Aquitaine) and D. Henry-Lormelle (restorer team) for information and help, and Lascaux Scientific Board for useful discussions.

CRediT authorship contributions statement

Zélia Bontemps : Resources, Formal analysis, Investigation, Data Curation, Visualization and Writing – Original draft preparation. **Mylène Hugoni** : Visualization, Validation. **Yvan Moënne-Loccoz** : Conceptualization, Resources, Investigation, Visualization, Supervision, Writing – Review and Editing, Project administration and funding acquisition.

Declaration of competing interest

The authors declare that they have no known competing financial interest or personal relationships that could have influenced the work reported in this paper.

References

Alabouvette, C., Saiz-Jiménez, C., 2011. Écologie microbienne de la Grotte de Lascaux. CSIC-Instituto de Recursos Naturales y Agrobiología de Sevilla (IRNAS).

Alonso, L., 2018. Hétérogénéité spatio-temporelle du microbiote de la grotte de Lascaux (Ph.D. thesis). University of Lyon.

Alonso, L., Creuzé-des-Châtelliers, C., Trabac, T., Dubost, A., Moënne-Loccoz, Y., Pommier, T., 2018. Rock substrate rather than black stain alterations drives microbial community structure in the passage of Lascaux Cave. Microbiome 6, 216.

Alonso, L., Pommier, T., Simon, L., Maucourt, F., Doré, J., Dubost, A., Trân Van, V., Minard, G., Valiente Moro, C., Douady, C.J., Moënne-Loccoz, Y.,. Microbiome analysis in Lascaux Cave in relation to black stain alterations of rock surfaces and collembola. Environmental Microbiology Reports. Submitted.

Barbault, R., 1995. Biodiversity dynamics : from population and community ecology approaches to a landscape ecology point of view. Landscape and Urban Planning 31, 89–98.

Barton, H.A., Jurado, V., 2007. What's up down there ? Microbial diversity in caves microorganisms in caves survive under nutrient-poor conditions and are metabolically versatile and unexpectedly diverse. Microbes 2, 132–138.

Barton, H.A., Northup, D.E., 2007. Geomicrobiology in cave environments : past, current and future perspectives. Journal of Cave and Karst Studies 69, 163–178.

Bastian, F., Alabouvette, C., Saiz-Jimenez, C., 2009. The impact of arthropods on fungal community structure in Lascaux Cave. Journal of Applied Microbiology 106, 1456–1462.

Bastian, F., Alabouvette, C., Jurado, V., Saiz-Jimenez, C., 2009a. Impact of biocide treatments on the bacterial communities of the Lascaux Cave. Naturwissenschaften 96, 863–868.

Bastian, F., Bouziri, L., Nicolardot, B., Ranjard, L., 2009b. Impact of wheat straw decomposition on successional patterns of soil microbial community structure. Soil Biology and Biochemistry 41, 262–275.

Bastian, F., Jurado, V., Nováková, A., Alabouvette, C., Saiz-Jimenez, C., 2010. The microbiology of Lascaux Cave. Microbiology 156, 644–652.

Bernardini, S., Bellatreccia, F., Columbu, A., Vaccarelli, I., Pellegrini, M., Jurado, V., Del Gallo, M., Saiz-Jimenez, C., Sodo, A., Millo, C., Jovane, L., De Waele, J., 2021. Morpho-mineralogical and bio-geochemical description of cave manganese stromatolite-like patinas (Grotta del Cervo, Central Italy) and hints on their paleohydrological-driven genesis. Frontiers in Earth Science 9, 642667.

Bontemps, Z., Alonso, L., Pommier, T., Hugoni, M., Moënne-Loccoz, Y., 2021. Microbial ecology of tourist Paleolithic caves. Science of The Total Environment 816, 151492.

Boston, P.J., Spilde, M.N., Northup, D.E., Curry, M.D., Melim, L.A., Rosales-Lagarde, L., 2009. Microorganisms as speleogenetic agents : geochemical diversity but geomicrobial unity. hypogene speleogenesis and karst hydrogeology of artesian basins. Ukranian Institute of Speleology and Karstology 1, 51–58.

Bourges, F., Genthon, P., Genty, D., Lorblanchet, M., Mauduit, E., D'Hulst, D., 2014. Conservation of prehistoric caves and stability of their inner climate : Lessons from Chauvet and other French caves. Science of The Total Environment 493, 79–91.

Bray, J.., Curtis, J.., 1957. An ordination of the upland forest communities of southern Wisconsin. Ecological Monogrqphs 27, 325–349.

Cañveras, C.S.-J., S. Sanchez-Moral, V. Sloer, 2001. Microorganisms and microbially induced fabrics in cave walls. Geomicrobiology Journal 18, 223–240.

Carmichael, S.K., Zorn, B.T., Santelli, C.M., Roble, L.A., Carmichael, M.J., Bräuer, S.L., 2015. Nutrient input influences fungal community composition and size and can stimulate manganese (II) oxidation in caves. Environmental Microbiology Reports 7, 592–605.

Chalmin, E., d'Orlyé, F., Zinger, L., Charlet, L., Geremia, R.A., Orial, G., Menu, M., Baffier, D., Reiche, I., 2007. Biotic versus abiotic calcite formation on prehistoric cave paintings : the

Arcy-sur-Cure 'Grande Grotte' (Yonne, France) case. Geological Society, 279, 185–197.

Chao, A., 1987. Estimating the population size for capture-recapture data with unequal catchability. Biometrics 43, 783–791.

Cigna, A., 2016. Tourism and show caves. Geomorphology 60, 217–233.

Cigna, A., Forti, P., Moreira, J.C., Carvalho, C.N. de, 2013. Caves : the most important geotouristic feature in the world. Tourism and Karst Areas 6, 9–26.

Clarke, K.R., 1993. Non-parametric multivariate analyses of changes in community structure. Australian Journal of Ecology 18, 117–143.

Cox, H.H.J., Houtman, J.H.M., Doddema, H.J., Harder, W., 1993. Growth of the black yeast *Exophiala jeanselmei* on styrene and styrene-related compounds. Applied Microbiology and Biotechnology 39, 372–376.

Cuezva, S., Fernandez-Cortes, A., Porca, E., Pašić, L., Jurado, V., Hernandez-Marine, M., Serrano-Ortiz, P., Hermosin, B., Cañaveras, J.C., Sanchez-Moral, S., 2012. The biogeochemical role of Actinobacteria in Altamira cave, Spain. FEMS Microbiology Ecology 81, 281–290.

De la Rosa, J.M., Martin-Sanchez, P.M., Sanchez-Cortes, S., Hermosin, B., Knicker, H., Saiz-Jimenez, C., 2017. Structure of melanins from the fungi *Ochroconis lascauxensis* and *Ochroconis anomala* contaminating rock art in the Lascaux Cave. Scientific Reports 7, 13441.

Di Russo, C., Carchini, G., Rampini, M., Lucarelli, M., Sbordoni, V., 1997. Long term stability of a terrestrial cave community. International Journal of Speleology 26, 7. Diaz-Herraiz, M., Jurado, V., Cuezva, S., Laiz, L., Pallecchi, P., Tiano, P., Sanchez-Moral, S., Saiz-Jimenez, C., 2014. Deterioration of an Etruscan tomb by bacteria from the order Rhizobiales. Scientific Reports 4, 3610.

Dollive, S., Peterfreund, G.L., Sherrill-Mix, S., Bittinger, K., Sinha, R., Hoffmann, C., Nabel, C.S., Hill, D.A., Artis, D., Bachman, M.A., Custers-Allen, R., Grunberg, S., Wu, G.D., Lewis, J.D., Bushman, F.D., 2012. A tool kit for quantifying eukaryotic rRNA gene sequences from human microbiome samples. Genome Biology 13, R60.

Dupont, J., Jacquet, C., Dennetière, B., Lacoste, S., Bousta, F., Orial, G., Cruaud, C., Couloux, A., Roquebert, M.-F., 2007. Invasion of the French Paleolithic painted cave of Lascaux by members of the *Fusarium solani* species complex. Mycologia 99, 526–533.

El-Bialy, H.A., El-Gamal, M.S., Elsayed, M.A., Saudi, H.A., Khalifa, M.A., 2019. Microbial melanin physiology under stress conditions and gamma radiation protection studies. Radiation Physics and Chemistry 162, 178–186.

Engel, A.S., Northup, D.E., 2008. Caves and karst as model systems for advancing the microbial sciences. In : Frontiers of Karst Research, Special Publication 13. Karst Water Institute, Lewisburg, PA, pp. 37-48.

Escudié, F., Auer, L., Bernard, M., Mariadassou, M., Cauquil, L., Vidal, K., Maman, S., Hernandez-Raquet, G., Combes, S., Pascal, G., 2018. FROGS : Find, Rapidly, OTUs with Galaxy Solution. Bioinformatics 34, 1287–1294.

Hammer, Ø., Harper, D.., Ryan, P., 2001. PAST : paleontological statistics software package for education and data analysis. Palaeontologia Electronica 4, 1–9.

Harper, D.A.T., 1999. Numerical palaeobiology. Computer-based modelling and analysis of fossils and their distributions. Geological Magazine 137, 463–479.

Herfort, L., Kim, J.-H., Coolen, M.J.L., Abbas, B., Schouten, S., Herndl, G.J., Damsté, J.S.S., 2009. Diversity of Archaea and detection of crenarchaeotal *amoA* genes in the rivers Rhine and Têt. Aquatic Microbial Ecology 55, 189–201.

Herlemann, D.P., Labrenz, M., Jürgens, K., Bertilsson, S., Waniek, J.J., Andersson, A.F., 2011. Transitions in bacterial communities along the 2000 km salinity gradient of the Baltic Sea. The ISME Journal 5, 1571–1579.

Isola, D., Zucconi, L., Cecchini, A., Caneva, G., 2021. Dark-pigmented biodeteriogenic fungi in Etruscan hypogeal tombs : New data on their culture-dependent diversity, favouring conditions, and resistance to biocidal treatments. Fungal Biology 125, 609–620.

Jurado, V., Porca, E., Cuezva, S., Fernandez-Cortes, A., Sanchez-Moral, S., Saiz-Jimenez, C., 2010. Fungal outbreak in a show cave. Science of The Total Environment 408, 3632–3638.

Jurburg, S.D., Nunes, I., Stegen, J.C., Le Roux, X., Priemé, A., Sørensen, S.J., Salles, J.F., 2017. Autogenic succession and deterministic recovery following disturbance in soil bacterial communities. Scientific Reports 7, 45691.

Kiyuna, T., An, K.-D., Kigawa, R., Sano, C., Sugiyama, J., 2017. Noteworthy anamorphic fungi, *Cephalotrichum verrucisporum*, *Sagenomella striatispora*, and *Sagenomella griseoviridis*, isolated from biodeteriorated samples in the Takamatsuzuka and Kitora Tumuli, Nara, Japan. Mycoscience 58, 320–327.

Magoč, T., Salzberg, S.L., 2011. FLASH : fast length adjustment of short reads to improve genome assemblies. Bioinformatics 27, 2957–2963.

Mahé, F., Rognes, T., Quince, C., de Vargas, C., Dunthorn, M., 2014. Swarm : robust and fast clustering method for amplicon-based studies. PeerJ 2, e593.

Martin-Sanchez, P.M., Miller, A.Z., Saiz-Jimenez, C., 2015. Lascaux Cave : An example of fragile ecological balance in subterranean environments. In : Microbial Life of Cave Systems. eds. De Gruyter pp. 279-302.

Martin-Sanchez, P.M., Nováková, A., Bastian, F., Alabouvette, C., Saiz-Jimenez, C., 2012. Use of biocides for the control of fungal outbreaks in subterranean environments : The case of the Lascaux Cave in France. Environmental Science and Technology 46, 3762–3770.

Miller, A.Z., García-Sánchez, A.M., L. Coutinho, M., Costa Pereira, M.F., Gázquez, F., Calaforra, J.M., Forti, P., Martínez-Frías, J., Toulkeridis, T., Caldeira, A.T., Saiz-Jimenez, C., 2020. Colored microbial coatings in show caves from the Galapagos Islands (Ecuador) : First microbiological approach. Coatings 10, 1134.

Mitova, M., Iliev, M., Nováková, A., Gorbushina, A., Groudeva, V., Martin-Sanchez, P., 2017. Diversity and biocide susceptibility of fungal assemblages dwelling in the Art Gallery of Magura Cave, Bulgaria. International Journal of Speleology 46, 8.

Mohen, J., Taborin, Y., 2019. Les sociétés de la préhistoire, Hachette éducation. ed. Hachette.

Northup, D.E., 1997. Balancing conservation of unusual cave microbial communities with exploration and research in Lechuguilla Cave, Carlsbad Caverns national park, New Mexico. Final report to the Lindburgh foundation and the national park service.

Novakova, A., Elhottová, D., Kristufek, V., Lukesova, A., Hill, P., Kovac, L., Mock, A., Luptacik, P., 2005. Feeding sources of invertebrates in Ardovská Cave and Domica Cave systems – preliminary results. Institute of Soil Biology AS CR 107–112.

Odum, E.P., 1969. The strategy of ecosystem development. Science 164, 262–270.

Ogórek, R., Višňovská, Z., Tančinová, D., 2016. Mycobiota of underground habitats : Case study of Harmanecká Cave in Slovakia. Microbial Ecology 71, 87–99.

Pfendler, S., Karimi, B., Maron, P.-A., Ciadamidaro, L., Valot, B., Bousta, F., Alaoui-Sosse, L., Alaoui-Sosse, B., Aleya, L., 2018. Biofilm biodiversity in French and Swiss show caves using the metabarcoding approach : First data. Science of The Total Environment 615, 1207–1217.

Plonka, P.M., Grabacka, M., 2006. Melanin synthesis in microorganisms-biotechnological and medical aspects. Acta Biochimica Polonica 53, 429–443.

Portillo, M.C., Gonzalez, J.M., Saiz-Jimenez, C., 2008. Metabolically active microbial communities of yellow and grey colonizations on the walls of Altamira Cave, Spain. Journal of Applied Microbiology 104, 681–691.

Quast, C., Pruesse, E., Yilmaz, P., Gerken, J., Schweer, T., Yarza, P., Peplies, J., Glöckner, F.O., 2013. The SILVA ribosomal RNA gene database project : improved data processing and web-based tools. Nucleic Acids Research 41, D590–D596.

R Core Team, 2020. R : A language and environment for statistical computing. R Foundation for Statistical Computing, Vienna, Austria.

Rognes, T., Flouri, T., Nichols, B., Quince, C., Mahé, F., 2016. VSEARCH : a versatile open-source tool for metagenomics. PeerJ 4, e2584.

Russell, M.J., MacLean, V.L., 2008. Management issues in a Tasmanian tourist cave : potential microclimatic impacts of cave modifications. Journal of Environmental Management 87, 474–483.

Sakr, A.A., Ghaly, M.F., Edwards, H.G.M., Ali, M.F., Abdel-Haliem, M.E.F., 2020. Involvement of *Streptomyces* in the deterioration of cultural heritage materials through biomineralization and bio-pigment production pathways : A review. Geomicrobiology Journal 37, 653–662.

Schnitzler, N., Peltroche-Llacsahuanga, H., Bestier, N., Zündorf, J., Lütticken, R., Haase, G., 1999. Effect of melanin and carotenoids of *Exophiala dermatitidis* on Phagocytosis, oxidative burst, and killing by human neutrophils. Infection and Immunity 67, 94–101.

Shannon, C.E., 1948. A mathematical theory of communication. Bell System Technical Journal 27, 623–656.

Simpson, E.H., 1949. Measurement of diversity. Nature 163, 688–688.

Spilde, M.N., Northup, D.E., Boston, P.J., Schelble, R.T., Dano, K.E., Crossey, L.J., Dahm, C.N., 2005. Geomicrobiology of cave ferromanganese deposits : A field and laboratory investigation. Geomicrobiology Journal 22, 99–116.

Steelman, K.L., Lombera-Hermida, A. de, Viñas-Vallverdú, R., Rodríguez-Álvarez, X.P., Carrera-Ramírez, F., Rubio-Mora, A., Fábregas-Valcarce, R., 2017. Cova Eirós : An integrated approach to dating the earliest known cave art in NW Iberia. Radiocarbon 59, 151–164.

Toju, H., Tanabe, A.S., Yamamoto, S., Sato, H., 2012. High-Coverage ITS primers for the DNA-Based identification of Ascomycetes and Basidiomycetes in environmental samples. PLoS One 7, e40863.

Uroz, S., Calvaruso, C., Turpault, M.-P., Frey-Klett, P., 2009. Mineral weathering by bacteria : ecology, actors and mechanisms. Trends in Microbiology 17, 378–387.

Uroz, S., Kelly, L.C., Turpault, M.-P., Lepleux, C., Frey-Klett, P., 2015. The mineralosphere concept : Mineralogical control of the distribution and function of mineral-associated bacterial communities. Trends in Microbiology 23, 751–762.

Yin, Q., Sun, Y., Li, B., Feng, Z., Wu, G., 2022. The r/K selection theory and its application in biological wastewater treatment processes. Science of The Total Environment 824, 153836.

Zhang, J., Madden, T.L., 1997. PowerBLAST : a new network BLAST application for interactive or automated sequence analysis and annotation. Genome Research 7, 649–656.

Zhao, J., Zeng, J., de Hoog, G.S., Attili-Angelis, D., Prenafeta-Boldú, F.X., 2010. Isolation and Identification of black yeasts by enrichment on atmospheres of monoaromatic hydrocarbons. Microbial Ecology 60, 149–156.

Zhou, J., Ning, D., 2017. Stochastic community assembly : Does it matter in microbial ecology ? Microbiology Molecular Biology Review 81, e00002-17.

Zucconi, L., Gagliardi, M., Isola, D., Onofri, S., Andaloro, M.C., Pelosi, C., Pogliani, P., Selbmann, L., 2012. Biodeterioration agents dwelling in or on the wall paintings of the Holy Saviour's cave (Vallerano, Italy). International Biodeterioration and Biodegradation 70, 40–46.

Supplementary data

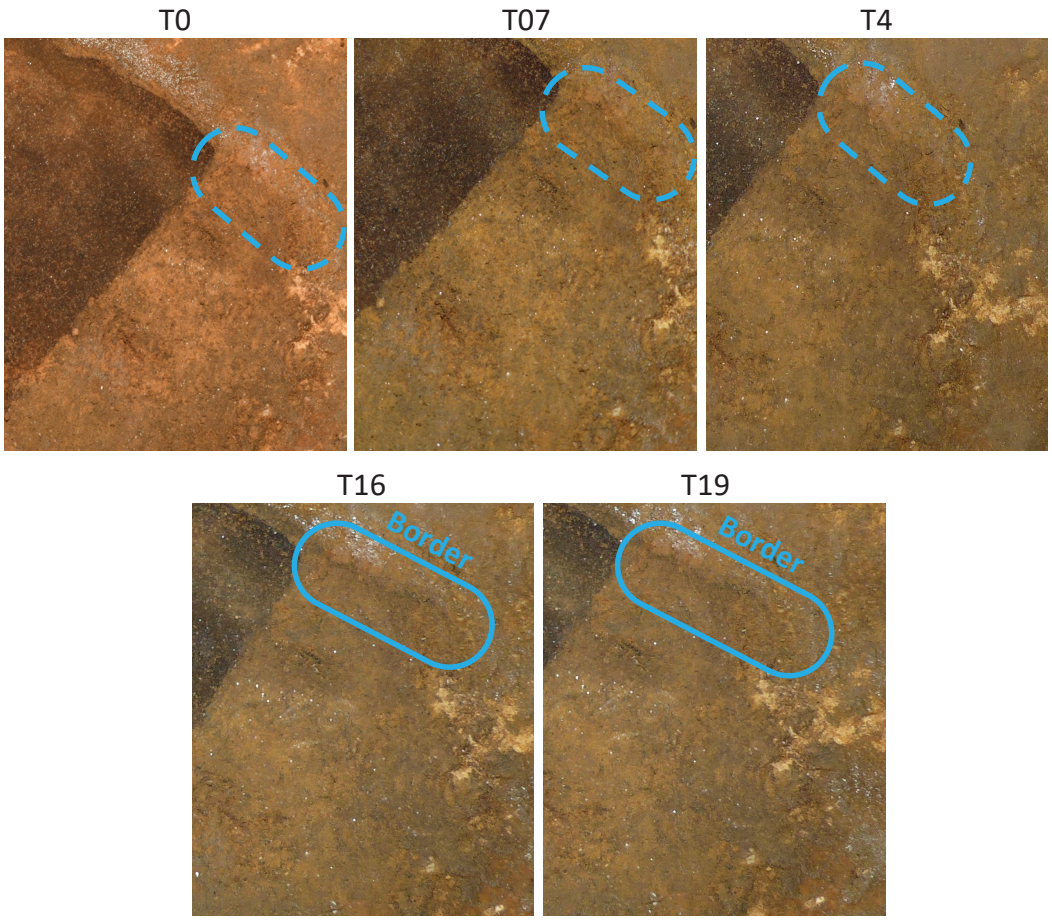

Supplementary figure S1. Photography of surfaces after stain cleaning (Source : S. Géraud, DRAC Nouvelle Aquitaine). The development of a darker border (indicated with a blue frame) starts to be visible at later samplings (T16 and T19).

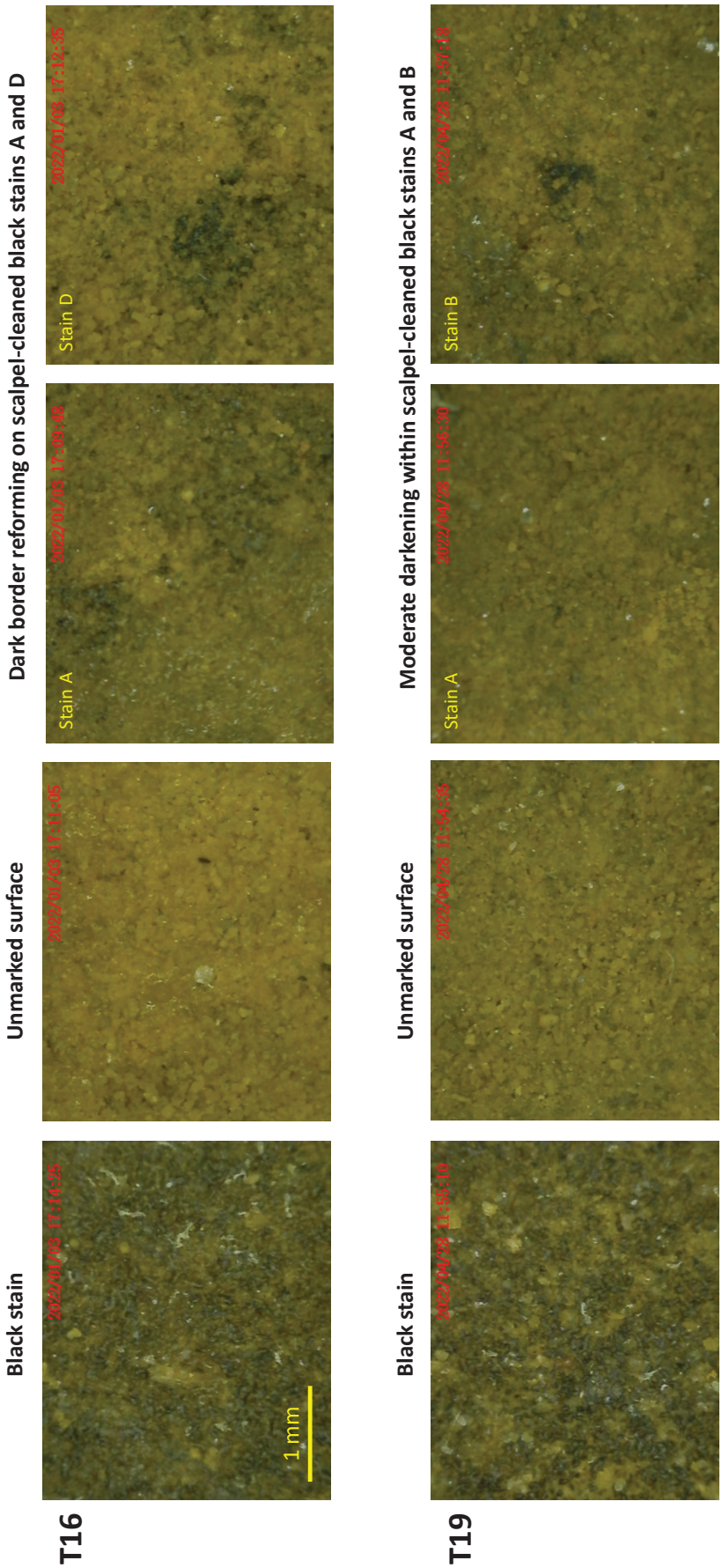

Supplementary figure S2. Dinolite microscope photographs showing the darkening taking place on surfaces where black stains had been cleaned with a scalpel.

Supplementary table S1. Primers for amplification of taxonomic marker genes.

Marker gene	Region	Length	Name	Forward (F) or reverse (R)	Sequence	Reference
16S rRNA	V3-V4 Bacteria	550 bp	341F	F	5'-CCTACGGGNGGCWGCAG-3'	Herlemann *et al.*, 2011
			805R	R	5'-GACTACHVGGGTATCTAATCC-3'	
	V3-V4 Archaea	420 bp	515F	F	5'-CAGCCGCCGCGGTAA-3'	Herfort *et al.*, 2011
			915R	R	5'-GTGCTCCCCCGCCAATTCCT-3'	
18S rRNA	V4	350 bp	0067a_deg	F	5'-AAGCCATGCATGYCTAAGTATMA-3′	Dollive *et al.*, 2012
			NSR339	R	5'-TCTCAGGCTCCYTCTCCGG-3′	
ITS	ITS2	327 bp	ITS3_KYO2	F	5'-ATGAAGAACGYAGYRAA-3'	Toju *et al.*, 2012
			ITS4	R	5'-TCCTCCGCTTATTGATATGC- 3'	

Supplementary table S2. Bacteria 16S rRNA gene, Archaeal rRNA gene and 18S rRNA gene Adonis test for whole dataset.

Microbial group	Factors	Df	F	*P*	R^2
Bacteria	Rock surface condition	11	7.968	**0.001**	0.55
	Residuals	58			
Archaea	Rock surface condition	11	2.388	**0.001**	0.32
	Residuals	55			
Microeukaryotes	Rock surface condition	11	5.198	**0.001**	0.44
	Residuals	58			

Supplementary table S3. Pairwise adonis test for bacterial communities between each rock surface condition.

Test	Pairwise comparison	Df	Sums of squares	F model	R^2	*P*
1	Sponge vs Stain T0	1	1.37	6.76	0.43	**0.002**
2	Sponge vs CStain T0	1	1.35	7.67	0.46	**0.002**
3	Sponge vs CStain sponge T0	1	1.29	7.00	0.44	**0.002**
4	Sponge vs Control T0	1	1.67	10.49	0.57	**0.007**
5	Sponge vs CStain T0.7	1	1.22	5.64	0.39	**0.004**
6	Sponge vs CStain T4	1	1.42	8.17	0.48	**0.004**
7	Sponge vs CStain T16	1	1.38	7.85	0.47	**0.002**
8	Sponge vs Stain T19	1	1.42	8.04	0.50	**0.004**
9	Sponge vs Control T19	1	1.79	12.02	0.57	**0.002**
10	Sponge vs CStain T19	1	1.29	6.74	0.43	**0.003**
11	Sponge vs CStain sponge T19	1	1.25	6.08	0.40	**0.004**
12	Stain T0 vs CStain T0	1	0.28	2.01	0.17	**0.017**
13	Stain T0 vs CStain sponge T0	1	0.32	2.16	0.18	**0.027**
14	Stain T0 vs Control T0	1	2.09	17.28	0.66	**0.002**
15	Stain T0 vs CStain T0.7	1	0.31	1.78	0.15	**0.050**
16	Stain T0 vs CStain T4	1	0.25	1.79	0.15	**0.070**
17	Stain T0 vs CStain T16	1	0.39	2.83	0.22	**0.004**
18	Stain T0 vs Stain T19	1	0.14	1.05	0.10	0.386
19	Stain T0 vs Control T19	1	2.22	19.21	0.66	**0.002**
20	Stain T0 vs CStain T19	1	0.25	1.60	0.14	0.121
21	Stain T0 vs CStain sponge T19	1	0.29	1.72	0.15	0.052
22	CStain T0 vs CStain sponge T0	1	0.06	0.51	0.05	0.892
23	CStain T0 vs Control T0	1	1.76	18.82	0.68	**0.004**
24	CStain T0 vs CStain T0.7	1	0.10	0.67	0.06	0.743
25	CStain T0 vs CStain T4	1	0.13	1.17	0.10	0.328
26	CStain T0 vs CStain T16	1	0.24	2.10	0.17	0.051
27	CStain T0 vs Stain T19	1	0.33	3.02	0.25	**0.007**
28	CStain T0 vs Control T19	1	1.86	20.52	0.67	**0.003**
29	CStain T0 vs CStain T19	1	0.15	1.16	0.10	0.358
30	CStain T0 vs CStain sponge T19	1	0.23	1.61	0.14	0.052
31	CStain sponge T0 vs Control T0	1	1.76	17.23	0.66	**0.003**
32	CStain sponge T0 vs CStain T0.7	1	0.10	0.64	0.06	0.814
33	CStain sponge T0 vs CStain T4	1	0.21	1.69	0.14	0.097
34	CStain sponge T0 vs CStain T16	1	0.19	1.57	0.14	0.127
35	CStain sponge T0 vs Stain T19	1	0.40	3.38	0.27	**0.004**
36	CStain sponge T0 vs Control T19	1	1.87	19.00	0.66	**0.004**
37	CStain sponge T0 vs CStain T19	1	0.18	1.31	0.12	0.198
38	CStain sponge T0 vs CStain sponge T19	1	0.24	1.58	0.14	0.067
39	Control T0 vs CStain T0.7	1	1.77	13.26	0.60	**0.001**
40	Control T0 vs CStain T4	1	2.10	22.80	0.72	**0.005**

41	Control T0 vs CStain T16	1	2.04	21.70	0.71	**0.005**
42	Control T0 vs Stain T19	1	2.04	24.29	0.75	**0.008**
43	Control T0 vs Control T19	1	0.02	0.37	0.04	0.882
44	Control T0 vs CStain T19	1	2.04	18.58	0.67	**0.002**
45	Control T0 vs CStain sponge T19	1	2.01	16.25	0.64	**0.007**
46	CStain T0.7 vs CStain T4	1	0.15	0.98	0.09	0.469
47	CStain T0.7 vs CStain T16	1	0.14	0.94	0.09	0.532
48	CStain T0.7 vs Stain T19	1	0.32	2.12	0.19	**0.036**
49	CStain T0.7 vs Control T19	1	1.89	14.89	0.60	**0.001**
50	CStain T07 vs CStain T19	1	0.16	0.97	0.09	0.507
51	CStain T07 vs CStain sponge T19	1	0.18	1.02	0.09	0.461
52	CStain T4 vs CStain T16	1	0.31	2.71	0.21	**0.026**
53	CStain T4 vs Stain T19	1	0.20	1.89	0.17	**0.035**
54	CStain T4 vs Control T19	1	2.22	24.76	0.71	**0.002**
55	CStain T4 vs CStain T19	1	0.15	1.21	0.11	0.229
56	CStain T4 vs CStain sponge T19	1	0.15	1.04	0.09	0.421
57	CStain T16 vs Stain T19	1	0.36	3.29	0.27	**0.007**
58	CStain T16 vs Control T19	1	2.14	23.59	0.70	**0.004**
59	CStain T16 vs CStain T19	1	0.14	1.11	0.10	0.319
60	CStain T16 vs CStain sponge T19	1	0.21	1.47	0.13	0.128
61	Stain T19 vs Control T19	1	2.14	26.13	0.74	**0.004**
62	Stain T19 vs CStain T19	1	0.24	1.94	0.18	**0.033**
63	Stain T19 vs CStain sponge T19	1	0.21	1.54	0.15	**0.026**
64	Control T19 vs CStain T19	1	2.13	20.27	0.67	**0.002**
65	Control T19 vs CStain sponge T19	1	2.11	17.87	0.64	**0.002**
66	CStain T19 vs CStain sponge T19	1	0.11	0.71	0.07	0.702

Supplementary table S4. Pairwise adonis test for archaeal communities between each rock surface condition.

Test	Pairwise comparison	Df	Sums of squares	F model	R^2	*P*
1	Sponge vs Stain T0	1	0.02	8.34	0.51	**0.006**
2	Sponge vs CStain T0	1	0.01	11.09	0.55	**0.005**
3	Sponge vs CStain sponge T0	1	0.01	8.05	0.47	**0.006**
4	Sponge vs Control T0	1	0.01	12.05	0.60	**0.008**
5	Sponge vs CStain T0.7	1	0.01	12.73	0.61	**0.010**
6	Sponge vs CStain T4	1	0.01	9.54	0.51	**0.006**
7	Sponge vs CStain T16	1	0.01	15.47	0.66	**0.010**
8	Sponge vs Stain T19	1	0.02	8.73	0.49	**0.004**
9	Sponge vs Control T19	1	0.02	16.28	0.64	**0.004**
10	Sponge vs CStain T19	1	0.02	10.65	0.54	**0.007**
11	Sponge vs CStain sponge T19	1	0.01	14.56	0.62	**0.003**
12	Stain T0 vs CStain T0	1	0.01	2.25	0.20	0.087
13	Stain T0 vs CStain sponge T0	1	0.01	3.14	0.26	**0.036**
14	Stain T0 vs Control T0	1	0.01	3.06	0.28	**0.046**
15	Stain T0 vs CStain T0.7	1	0.01	1.65	0.17	0.171
16	Stain T0 vs CStain T4	1	0.01	2.21	0.20	0.091
17	Stain T0 vs CStain T16	1	0.01	2.78	0.26	0.076
18	Stain T0 vs Stain T19	1	0.01	1.36	0.13	0.198
19	Stain T0 vs Control T19	1	0.01	3.72	0.29	**0.011**
20	Stain T0 vs CStain T19	1	0.01	1.77	0.16	0.137
21	Stain T0 vs CStain sponge T19	1	0.01	2.37	0.21	0.075
22	CStain T0 vs CStain sponge T0	1	0.00	1.08	0.10	0.386
23	CStain T0 vs Control T0	1	0.00	1.77	0.16	0.162
24	CStain T0 vs CStain T0.7	1	0.00	0.39	0.04	0.842
25	CStain T0 vs CStain T4	1	0.00	0.12	0.01	0.886
26	CStain T0 vs CStain T16	1	0.00	0.35	0.04	0.701
27	CStain T0 vs Stain T19	1	0.00	0.64	0.06	0.659
28	CStain T0 vs Control T19	1	0.00	1.94	0.16	0.125
29	CStain T0 vs CStain T19	1	0.00	0.38	0.04	0.693
30	CStain T0 vs CStain sponge T19	1	0.00	0.03	0.00	1.000
31	CStain sponge T0 vs Control T0	1	0.00	1.22	0.12	0.328
32	CStain sponge T0 vs CStain T0.7	1	0.00	1.55	0.15	0.193
33	CStain sponge T0 vs CStain T4	1	0.00	1.10	0.10	0.323
34	CStain sponge T0 vs CStain T16	1	0.00	1.03	0.10	0.388
35	CStain sponge T0 vs Stain T19	1	0.01	2.09	0.17	0.069
36	CStain sponge T0 vs Control T19	1	0.00	2.46	0.20	0.088
37	CStain sponge T0 vs CStain T19	1	0.00	1.79	0.15	0.133
38	CStain sponge T0 vs CStain sponge T19	1	0.00	1.21	0.11	0.308
39	Control T0 vs CStain T0.7	1	0.00	1.53	0.16	0.220
40	Control T0 vs CStain T4	1	0.00	1.80	0.17	0.171
41	Control T0 vs CStain T16	1	0.00	1.53	0.16	0.227
42	Control T0 vs Stain T19	1	0.01	2.23	0.20	0.068
43	Control T0 vs Control T19	1	0.00	0.73	0.08	0.479
44	Control T0 vs CStain T19	1	0.00	1.77	0.16	0.164
45	Control T0 vs CStain sponge T19	1	0.00	2.40	0.21	**0.038**
46	CStain T0.7 vs CStain T4	1	0.00	0.62	0.06	0.526
47	CStain T0.7 vs CStain T16	1	0.00	0.80	0.09	0.444
48	CStain T0.7 vs Stain T19	1	0.00	0.63	0.07	0.775
49	CStain T0.7 vs Control T19	1	0.00	1.29	0.13	0.248
50	CStain T0.7 vs CStain T19	1	0.00	0.38	0.04	0.909

51	CStain T0.7 vs CStain sponge T19	1	0.00	0.76	0.08	0.590
52	CStain T4 vs CStain T16	1	0.00	0.54	0.06	0.522
53	CStain T4 vs Stain T19	1	0.00	0.88	0.08	0.426
54	CStain T4 vs Control T19	1	0.00	2.61	0.21	0.054
55	CStain T4 vs CStain T19	1	0.00	0.69	0.06	0.513
56	CStain T4 vs CStain sponge T19	1	0.00	0.41	0.04	0.757
57	CStain T16 vs Stain T19	1	0.00	1.27	0.12	0.240
58	CStain T16 vs Control T19	1	0.00	1.66	0.16	0.191
59	CStain T16 vs CStain T19	1	0.00	0.58	0.06	0.598
60	CStain T16 vs CStain sponge T19	1	0.00	0.38	0.04	0.826
61	Stain T19 vs Control T19	1	0.01	2.22	0.18	**0.029**
62	Stain T19 vs CStain T19	1	0.00	0.63	0.06	0.689
63	Stain T19 vs CStain sponge T19	1	0.00	0.97	0.09	0.422
64	Control T19 vs CStain T19	1	0.00	1.76	0.15	0.139
65	Control T19 vs CStain sponge T19	1	0.00	2.57	0.20	0.054
66	CStain T19 vs CStain sponge T19	1	0.00	0.49	0.05	0.708

Supplementary table S5. Pairwise adonis test for microeukaryotic communities between each rock surface condition.

Test	Pairwise comparison	Df	Sums of squares	F model	R^2	*P*
1	Sponge vs Stain T0	1	1.66	8.90	0.50	**0.003**
2	Sponge vs CStain T0	1	1.83	15.91	0.64	**0.005**
3	Sponge vs CStain sponge T0	1	1.81	13.35	0.60	**0.003**
4	Sponge vs Control T0	1	1.33	7.12	0.47	**0.012**
5	Sponge vs CStain T0.7	1	1.58	7.85	0.47	**0.002**
6	Sponge vs CStain T4	1	1.78	12.45	0.58	**0.002**
7	Sponge vs CStain T16	1	1.77	12.61	0.58	**0.002**
8	Sponge vs Stain T19	1	1.57	8.15	0.48	**0.002**
9	Sponge vs Control T19	1	1.53	11.23	0.56	**0.007**
10	Sponge vs CStain T19	1	1.48	7.27	0.45	**0.002**
11	Sponge vs CStain sponge T19	1	1.47	7.90	0.47	**0.003**
12	Stain T0 vs CStain T0	1	0.48	3.21	0.24	**0.026**
13	Stain T0 vs CStain sponge T0	1	0.85	5.08	0.34	**0.010**
14	Stain T0 vs Control T0	1	1.21	5.58	0.38	**0.004**
15	Stain T0 vs CStain T0.7	1	0.53	2.33	0.19	0.071
16	Stain T0 vs CStain T4	1	0.24	1.36	0.12	0.248
17	Stain T0 vs CStain T16	1	0.70	4.05	0.29	1.000
18	Stain T0 vs Stain T19	1	0.10	0.46	0.04	0.766
19	Stain T0 vs Control T19	1	1.60	9.50	0.49	**0.004**
20	Stain T0 vs CStain T19	1	0.28	1.23	0.11	0.279
21	Stain T0 vs CStain sponge T19	1	0.34	1.59	0.14	0.146
22	CStain T0 vs CStain sponge T0	1	0.11	1.07	0.10	0.383
23	CStain T0 vs Control T0	1	1.04	7.11	0.44	**0.002**
24	CStain T0 vs CStain T0.7	1	0.04	0.27	0.03	0.915
25	CStain T0 vs CStain T4	1	0.25	2.26	0.18	0.104
26	CStain T0 vs CStain T16	1	0.08	0.72	0.07	0.507
27	CStain T0 vs Stain T19	1	0.52	3.34	0.25	**0.019**
28	CStain T0 vs Control T19	1	1.47	14.02	0.58	**0.004**
29	CStain T0 vs CStain T19	1	0.10	0.59	0.06	0.778
30	CStain T0 vs CStain sponge T19	1	0.43	2.90	0.22	**0.020**
31	CStain sponge T0 vs Control T0	1	0.99	5.96	0.40	**0.004**
32	CStain sponge T0 vs CStain T0.7	1	0.09	0.50	0.05	0.776
33	CStain sponge T0 vs CStain T4	1	0.51	3.97	0.28	**0.038**
34	CStain sponge T0 vs CStain T16	1	0.12	0.94	0.09	0.502
35	CStain sponge T0 vs Stain T19	1	0.93	5.37	0.35	**0.006**
36	CStain sponge T0 vs Control T19	1	1.30	10.61	0.51	**0.001**
37	CStain sponge T0 vs CStain T19	1	0.25	1.38	0.12	0.239
38	CStain sponge T0 vs CStain sponge T19	1	0.69	4.11	0.29	**0.004**
39	Control T0 vs CStain T0.7	1	0.84	3.63	0.29	**0.005**
40	Control T0 vs CStain T4	1	1.18	6.77	0.43	**0.004**

41	Control T0 vs CStain T16	1	0.86	5.03	0.36	**0.004**
42	Control T0 vs Stain	1	1.00	4.50	0.33	**0.004**
43	Control T0 vs Control T19	1	0.20	1.17	0.12	0.325
44	Control T0 vs CStain T19	1	0.89	3.80	0.30	**0.007**
45	Control T0 vs CStain sponge T19	1	0.94	4.35	0.33	**0.005**
46	CStain T0.7 vs CStain T4	1	0.32	1.71	0.15	0.187
47	CStain T0.7 vs CStain T16	1	0.05	0.24	0.02	0.852
48	CStain T0.7 vs Stain T19	1	0.56	2.42	0.19	0.057
49	CStain T0.7 vs Control T19	1	1.28	7.02	0.41	**0.001**
50	CStain T0.7 vs CStain T19	1	0.11	0.43	0.04	0.833
51	CStain T0.7 vs CStain sponge T19	1	0.48	2.13	0.18	0.087
52	CStain T4 vs CStain T16	1	0.39	2.92	0.23	**0.017**
53	CStain T4 vs Stain T19	1	0.22	1.23	0.11	0.277
54	CStain T4 vs Control T19	1	1.59	12.26	0.55	**0.002**
55	CStain T4 vs CStain T19	1	0.16	0.84	0.08	0.515
56	CStain T4 vs CStain sponge T19	1	0.20	1.15	0.10	0.345
57	CStain T16 vs Stain T19	1	0.67	3.78	0.27	**0.019**
58	CStain T16 vs Control T19	1	1.29	10.15	0.50	**0.001**
59	CStain T16 vs CStain T19	1	0.16	0.83	0.08	0.458
60	CStain T16 vs CStain sponge T19	1	0.59	3.44	0.26	0.050
61	Stain vs Control T19	1	1.48	8.50	0.46	**0.004**
62	Stain vs CStain T19	1	0.26	1.12	0.10	0.383
63	Stain vs CStain sponge T19	1	0.13	0.59	0.06	0.683
64	Control vs CStain T19	1	1.24	6.73	0.40	**0.004**
65	Control vs CStain sponge T19	1	1.32	7.88	0.44	**0.002**
66	CStain T19 vs CStain sponge T19	1	0.20	0.90	0.08	0.469

Supplementary table S6. Taxonomic details of OTU codes in Figure 6.

OTU_ID	Domain	Phylum	Class	Genus
OTU_1	Bacteria	Acidobacteriota	Acidobacteriae	Bryobacter
OTU_228	Bacteria	Actinobacteriota	Acidimicrobiia	Unidentified
OTU_507	Bacteria	Actinobacteriota	Acidimicrobiia	Unidentified
OTU_490	Bacteria	Actinobacteriota	Acidimicrobiia	Unidentified
OTU_627	Bacteria	Actinobacteriota	Acidimicrobiia	Unidentified
OTU_251	Bacteria	Actinobacteriota	Acidimicrobiia	Unidentified
OTU_199	Bacteria	Actinobacteriota	Acidimicrobiia	Unidentified
OTU_769	Bacteria	Actinobacteriota	Acidimicrobiia	Unidentified
OTU_116	Bacteria	Actinobacteriota	Acidimicrobiia	Unidentified
OTU_205	Bacteria	Actinobacteriota	Acidimicrobiia	Unidentified
OTU_369	Bacteria	Actinobacteriota	Acidimicrobiia	Unidentified
OTU_829	Bacteria	Actinobacteriota	Acidimicrobiia	Unidentified
OTU_993	Bacteria	Actinobacteriota	Acidimicrobiia	Iamia
OTU_239	Bacteria	Actinobacteriota	Actinobacteria	Acidothermus
OTU_410	Bacteria	Actinobacteriota	Actinobacteria	Acidothermus
OTU_35	Bacteria	Actinobacteriota	Actinobacteria	Actinophytocola
OTU_266	Bacteria	Actinobacteriota	Actinobacteria	Actinophytocola
OTU_22	Bacteria	Actinobacteriota	Actinobacteria	Agromyces
OTU_486	Bacteria	Actinobacteriota	Actinobacteria	Agromyces
OTU_99	Bacteria	Actinobacteriota	Actinobacteria	Amycolatopsis
OTU_173	Bacteria	Actinobacteriota	Actinobacteria	Amycolatopsis
OTU_212	Bacteria	Acidobacteriota	Acidobacteriae	Bryobacter
OTU_36	Bacteria	Acidobacteriota	Acidobacteriae	Bryobacter
OTU_2123	Bacteria	Acidobacteriota	Acidobacteriae	Bryobacter
OTU_139	Bacteria	Acidobacteriota	Acidobacteriae	Bryobacter
OTU_242	Bacteria	Actinobacteriota	Actinobacteria	Catelliglobosispora
OTU_623	Bacteria	Actinobacteriota	Actinobacteria	Catelliglobosispora
OTU_645	Bacteria	Actinobacteriota	Actinobacteria	Dactylosporangium
OTU_64	Bacteria	Actinobacteriota	Actinobacteria	Jiangella
OTU_290	Bacteria	Actinobacteriota	Actinobacteria	Jiangella
OTU_70	Bacteria	Actinobacteriota	Actinobacteria	Jiangella
OTU_175	Bacteria	Actinobacteriota	Actinobacteria	Jiangella
OTU_178	Bacteria	Actinobacteriota	Actinobacteria	Jiangella
OTU_183	Bacteria	Actinobacteriota	Actinobacteria	Jiangella
OTU_578	Bacteria	Actinobacteriota	Actinobacteria	Jiangella
OTU_759	Bacteria	Actinobacteriota	Actinobacteria	Jiangella
OTU_294	Bacteria	Actinobacteriota	Actinobacteria	Kribbella
OTU_761	Bacteria	Actinobacteriota	Actinobacteria	Kribbella
OTU_206	Bacteria	Actinobacteriota	Actinobacteria	Microbacterium
OTU_321	Bacteria	Actinobacteriota	Actinobacteria	Microbacterium
OTU_807	Bacteria	Actinobacteriota	Actinobacteria	Microlunatus
OTU_943	Bacteria	Actinobacteriota	Actinobacteria	Mycobacterium
OTU_1288	Bacteria	Actinobacteriota	Actinobacteria	Mycobacterium
OTU_427	Bacteria	Actinobacteriota	Actinobacteria	Mycobacterium
OTU_567	Bacteria	Actinobacteriota	Actinobacteria	Mycobacterium
OTU_961	Bacteria	Actinobacteriota	Actinobacteria	Mycobacterium
OTU_23	Bacteria	Actinobacteriota	Actinobacteria	Nocardia
OTU_53	Bacteria	Actinobacteriota	Actinobacteria	Nocardia
OTU_97	Bacteria	Actinobacteriota	Actinobacteria	Nocardia
OTU_283	Bacteria	Actinobacteriota	Actinobacteria	Nocardia
OTU_15	Bacteria	Actinobacteriota	Actinobacteria	Nocardioides
OTU_46	Bacteria	Actinobacteriota	Actinobacteria	Nocardioides
OTU_91	Bacteria	Actinobacteriota	Actinobacteria	Nocardioides
OTU_890	Bacteria	Actinobacteriota	Actinobacteria	Nocardioides
OTU_3972	Bacteria	Actinobacteriota	Actinobacteria	Nocardioides
OTU_7	Bacteria	Actinobacteriota	Actinobacteria	Nonomuraea
OTU_479	Bacteria	Actinobacteriota	Actinobacteria	Nonomuraea
OTU_606	Bacteria	Actinobacteriota	Actinobacteria	Nonomuraea
OTU_712	Bacteria	Actinobacteriota	Actinobacteria	Nonomuraea
OTU_857	Bacteria	Actinobacteriota	Actinobacteria	Nonomuraea
OTU_792	Bacteria	Actinobacteriota	Actinobacteria	Nonomuraea
OTU_108	Bacteria	Actinobacteriota	Actinobacteria	Phytomonospora

OTU_ID	Domain	Phylum	Class	Genus
OTU_1	Bacteria	Acidobacteriota	Acidobacteriae	Bryobacter
OTU_228	Bacteria	Actinobacteriota	Acidimicrobiia	Unidentified
OTU_507	Bacteria	Actinobacteriota	Acidimicrobiia	Unidentified
OTU_490	Bacteria	Actinobacteriota	Acidimicrobiia	Unidentified
OTU_627	Bacteria	Actinobacteriota	Acidimicrobiia	Unidentified
OTU_251	Bacteria	Actinobacteriota	Acidimicrobiia	Unidentified
OTU_199	Bacteria	Actinobacteriota	Acidimicrobiia	Unidentified
OTU_769	Bacteria	Actinobacteriota	Acidimicrobiia	Unidentified
OTU_116	Bacteria	Actinobacteriota	Acidimicrobiia	Unidentified
OTU_205	Bacteria	Actinobacteriota	Acidimicrobiia	Unidentified
OTU_369	Bacteria	Actinobacteriota	Acidimicrobiia	Unidentified
OTU_829	Bacteria	Actinobacteriota	Acidimicrobiia	Unidentified
OTU_993	Bacteria	Actinobacteriota	Acidimicrobiia	Iamia
OTU_239	Bacteria	Actinobacteriota	Actinobacteria	Acidothermus
OTU_410	Bacteria	Actinobacteriota	Actinobacteria	Acidothermus
OTU_35	Bacteria	Actinobacteriota	Actinobacteria	Actinophytocola
OTU_266	Bacteria	Actinobacteriota	Actinobacteria	Actinophytocola
OTU_22	Bacteria	Actinobacteriota	Actinobacteria	Agromyces
OTU_486	Bacteria	Actinobacteriota	Actinobacteria	Agromyces
OTU_99	Bacteria	Actinobacteriota	Actinobacteria	Amycolatopsis
OTU_173	Bacteria	Actinobacteriota	Actinobacteria	Amycolatopsis
OTU_212	Bacteria	Acidobacteriota	Acidobacteriae	Bryobacter
OTU_36	Bacteria	Acidobacteriota	Acidobacteriae	Bryobacter
OTU_2123	Bacteria	Acidobacteriota	Acidobacteriae	Bryobacter
OTU_139	Bacteria	Acidobacteriota	Acidobacteriae	Bryobacter
OTU_242	Bacteria	Actinobacteriota	Actinobacteria	Catelliglobosispora
OTU_623	Bacteria	Actinobacteriota	Actinobacteria	Catelliglobosispora
OTU_645	Bacteria	Actinobacteriota	Actinobacteria	Dactylosporangium
OTU_64	Bacteria	Actinobacteriota	Actinobacteria	Jiangella
OTU_290	Bacteria	Actinobacteriota	Actinobacteria	Jiangella
OTU_70	Bacteria	Actinobacteriota	Actinobacteria	Jiangella
OTU_175	Bacteria	Actinobacteriota	Actinobacteria	Jiangella
OTU_178	Bacteria	Actinobacteriota	Actinobacteria	Jiangella
OTU_183	Bacteria	Actinobacteriota	Actinobacteria	Jiangella
OTU_578	Bacteria	Actinobacteriota	Actinobacteria	Jiangella
OTU_759	Bacteria	Actinobacteriota	Actinobacteria	Jiangella
OTU_294	Bacteria	Actinobacteriota	Actinobacteria	Kribbella
OTU_761	Bacteria	Actinobacteriota	Actinobacteria	Kribbella
OTU_206	Bacteria	Actinobacteriota	Actinobacteria	Microbacterium
OTU_321	Bacteria	Actinobacteriota	Actinobacteria	Microbacterium
OTU_807	Bacteria	Actinobacteriota	Actinobacteria	Microlunatus
OTU_943	Bacteria	Actinobacteriota	Actinobacteria	Mycobacterium
OTU_1288	Bacteria	Actinobacteriota	Actinobacteria	Mycobacterium
OTU_427	Bacteria	Actinobacteriota	Actinobacteria	Mycobacterium
OTU_567	Bacteria	Actinobacteriota	Actinobacteria	Mycobacterium
OTU_961	Bacteria	Actinobacteriota	Actinobacteria	Mycobacterium
OTU_23	Bacteria	Actinobacteriota	Actinobacteria	Nocardia
OTU_53	Bacteria	Actinobacteriota	Actinobacteria	Nocardia
OTU_97	Bacteria	Actinobacteriota	Actinobacteria	Nocardia
OTU_283	Bacteria	Actinobacteriota	Actinobacteria	Nocardia
OTU_15	Bacteria	Actinobacteriota	Actinobacteria	Nocardioides
OTU_46	Bacteria	Actinobacteriota	Actinobacteria	Nocardioides
OTU_91	Bacteria	Actinobacteriota	Actinobacteria	Nocardioides
OTU_890	Bacteria	Actinobacteriota	Actinobacteria	Nocardioides
OTU_3972	Bacteria	Actinobacteriota	Actinobacteria	Nocardioides
OTU_7	Bacteria	Actinobacteriota	Actinobacteria	Nonomuraea
OTU_479	Bacteria	Actinobacteriota	Actinobacteria	Nonomuraea
OTU_606	Bacteria	Actinobacteriota	Actinobacteria	Nonomuraea
OTU_712	Bacteria	Actinobacteriota	Actinobacteria	Nonomuraea
OTU_857	Bacteria	Actinobacteriota	Actinobacteria	Nonomuraea
OTU_792	Bacteria	Actinobacteriota	Actinobacteria	Nonomuraea
OTU_108	Bacteria	Actinobacteriota	Actinobacteria	Phytomonospora

OTU_ID	Domain	Phylum	Class	Genus
OTU_1	Bacteria	Acidobacteriota	Acidobacteriae	Bryobacter
OTU_228	Bacteria	Actinobacteriota	Acidimicrobiia	Unidentified
OTU_507	Bacteria	Actinobacteriota	Acidimicrobiia	Unidentified
OTU_490	Bacteria	Actinobacteriota	Acidimicrobiia	Unidentified
OTU_627	Bacteria	Actinobacteriota	Acidimicrobiia	Unidentified
OTU_251	Bacteria	Actinobacteriota	Acidimicrobiia	Unidentified
OTU_199	Bacteria	Actinobacteriota	Acidimicrobiia	Unidentified
OTU_769	Bacteria	Actinobacteriota	Acidimicrobiia	Unidentified
OTU_116	Bacteria	Actinobacteriota	Acidimicrobiia	Unidentified
OTU_205	Bacteria	Actinobacteriota	Acidimicrobiia	Unidentified
OTU_369	Bacteria	Actinobacteriota	Acidimicrobiia	Unidentified
OTU_829	Bacteria	Actinobacteriota	Acidimicrobiia	Unidentified
OTU_993	Bacteria	Actinobacteriota	Acidimicrobiia	Iamia
OTU_239	Bacteria	Actinobacteriota	Actinobacteria	Acidothermus
OTU_410	Bacteria	Actinobacteriota	Actinobacteria	Acidothermus
OTU_35	Bacteria	Actinobacteriota	Actinobacteria	Actinophytocola
OTU_266	Bacteria	Actinobacteriota	Actinobacteria	Actinophytocola
OTU_22	Bacteria	Actinobacteriota	Actinobacteria	Agromyces
OTU_486	Bacteria	Actinobacteriota	Actinobacteria	Agromyces
OTU_99	Bacteria	Actinobacteriota	Actinobacteria	Amycolatopsis
OTU_173	Bacteria	Actinobacteriota	Actinobacteria	Amycolatopsis
OTU_212	Bacteria	Acidobacteriota	Acidobacteriae	Bryobacter
OTU_36	Bacteria	Acidobacteriota	Acidobacteriae	Bryobacter
OTU_2123	Bacteria	Acidobacteriota	Acidobacteriae	Bryobacter
OTU_139	Bacteria	Acidobacteriota	Acidobacteriae	Bryobacter
OTU_242	Bacteria	Actinobacteriota	Actinobacteria	Catelliglobosispora
OTU_623	Bacteria	Actinobacteriota	Actinobacteria	Catelliglobosispora
OTU_645	Bacteria	Actinobacteriota	Actinobacteria	Dactylosporangium
OTU_64	Bacteria	Actinobacteriota	Actinobacteria	Jiangella
OTU_290	Bacteria	Actinobacteriota	Actinobacteria	Jiangella
OTU_70	Bacteria	Actinobacteriota	Actinobacteria	Jiangella
OTU_175	Bacteria	Actinobacteriota	Actinobacteria	Jiangella
OTU_178	Bacteria	Actinobacteriota	Actinobacteria	Jiangella
OTU_183	Bacteria	Actinobacteriota	Actinobacteria	Jiangella
OTU_578	Bacteria	Actinobacteriota	Actinobacteria	Jiangella
OTU_759	Bacteria	Actinobacteriota	Actinobacteria	Jiangella
OTU_294	Bacteria	Actinobacteriota	Actinobacteria	Kribbella
OTU_761	Bacteria	Actinobacteriota	Actinobacteria	Kribbella
OTU_206	Bacteria	Actinobacteriota	Actinobacteria	Microbacterium
OTU_321	Bacteria	Actinobacteriota	Actinobacteria	Microbacterium
OTU_807	Bacteria	Actinobacteriota	Actinobacteria	Microlunatus
OTU_943	Bacteria	Actinobacteriota	Actinobacteria	Mycobacterium
OTU_1288	Bacteria	Actinobacteriota	Actinobacteria	Mycobacterium
OTU_427	Bacteria	Actinobacteriota	Actinobacteria	Mycobacterium
OTU_567	Bacteria	Actinobacteriota	Actinobacteria	Mycobacterium
OTU_961	Bacteria	Actinobacteriota	Actinobacteria	Mycobacterium
OTU_23	Bacteria	Actinobacteriota	Actinobacteria	Nocardia
OTU_53	Bacteria	Actinobacteriota	Actinobacteria	Nocardia
OTU_97	Bacteria	Actinobacteriota	Actinobacteria	Nocardia
OTU_283	Bacteria	Actinobacteriota	Actinobacteria	Nocardia
OTU_15	Bacteria	Actinobacteriota	Actinobacteria	Nocardioides
OTU_46	Bacteria	Actinobacteriota	Actinobacteria	Nocardioides
OTU_91	Bacteria	Actinobacteriota	Actinobacteria	Nocardioides
OTU_890	Bacteria	Actinobacteriota	Actinobacteria	Nocardioides
OTU_3972	Bacteria	Actinobacteriota	Actinobacteria	Nocardioides
OTU_7	Bacteria	Actinobacteriota	Actinobacteria	Nonomuraea
OTU_479	Bacteria	Actinobacteriota	Actinobacteria	Nonomuraea
OTU_606	Bacteria	Actinobacteriota	Actinobacteria	Nonomuraea
OTU_712	Bacteria	Actinobacteriota	Actinobacteria	Nonomuraea
OTU_857	Bacteria	Actinobacteriota	Actinobacteria	Nonomuraea
OTU_792	Bacteria	Actinobacteriota	Actinobacteria	Nonomuraea
OTU_108	Bacteria	Actinobacteriota	Actinobacteria	Phytomonospora

OTU_ID	Domain	Phylum	Class	Genus
OTU_1	Bacteria	Acidobacteriota	Acidobacteriae	Bryobacter
OTU_228	Bacteria	Actinobacteriota	Acidimicrobiia	Unidentified
OTU_507	Bacteria	Actinobacteriota	Acidimicrobiia	Unidentified
OTU_490	Bacteria	Actinobacteriota	Acidimicrobiia	Unidentified
OTU_627	Bacteria	Actinobacteriota	Acidimicrobiia	Unidentified
OTU_251	Bacteria	Actinobacteriota	Acidimicrobiia	Unidentified
OTU_199	Bacteria	Actinobacteriota	Acidimicrobiia	Unidentified
OTU_769	Bacteria	Actinobacteriota	Acidimicrobiia	Unidentified
OTU_116	Bacteria	Actinobacteriota	Acidimicrobiia	Unidentified
OTU_205	Bacteria	Actinobacteriota	Acidimicrobiia	Unidentified
OTU_369	Bacteria	Actinobacteriota	Acidimicrobiia	Unidentified
OTU_829	Bacteria	Actinobacteriota	Acidimicrobiia	Unidentified
OTU_993	Bacteria	Actinobacteriota	Acidimicrobiia	Iamia
OTU_239	Bacteria	Actinobacteriota	Actinobacteria	Acidothermus
OTU_410	Bacteria	Actinobacteriota	Actinobacteria	Acidothermus
OTU_35	Bacteria	Actinobacteriota	Actinobacteria	Actinophytocola
OTU_266	Bacteria	Actinobacteriota	Actinobacteria	Actinophytocola
OTU_22	Bacteria	Actinobacteriota	Actinobacteria	Agromyces
OTU_486	Bacteria	Actinobacteriota	Actinobacteria	Agromyces
OTU_99	Bacteria	Actinobacteriota	Actinobacteria	Amycolatopsis
OTU_173	Bacteria	Actinobacteriota	Actinobacteria	Amycolatopsis
OTU_212	Bacteria	Acidobacteriota	Acidobacteriae	Bryobacter
OTU_36	Bacteria	Acidobacteriota	Acidobacteriae	Bryobacter
OTU_2123	Bacteria	Acidobacteriota	Acidobacteriae	Bryobacter
OTU_139	Bacteria	Acidobacteriota	Acidobacteriae	Bryobacter
OTU_242	Bacteria	Actinobacteriota	Actinobacteria	Catelliglobosispora
OTU_623	Bacteria	Actinobacteriota	Actinobacteria	Catelliglobosispora
OTU_645	Bacteria	Actinobacteriota	Actinobacteria	Dactylosporangium
OTU_64	Bacteria	Actinobacteriota	Actinobacteria	Jiangella
OTU_290	Bacteria	Actinobacteriota	Actinobacteria	Jiangella
OTU_70	Bacteria	Actinobacteriota	Actinobacteria	Jiangella
OTU_175	Bacteria	Actinobacteriota	Actinobacteria	Jiangella
OTU_178	Bacteria	Actinobacteriota	Actinobacteria	Jiangella
OTU_183	Bacteria	Actinobacteriota	Actinobacteria	Jiangella
OTU_578	Bacteria	Actinobacteriota	Actinobacteria	Jiangella
OTU_759	Bacteria	Actinobacteriota	Actinobacteria	Jiangella
OTU_294	Bacteria	Actinobacteriota	Actinobacteria	Kribbella
OTU_761	Bacteria	Actinobacteriota	Actinobacteria	Kribbella
OTU_206	Bacteria	Actinobacteriota	Actinobacteria	Microbacterium
OTU_321	Bacteria	Actinobacteriota	Actinobacteria	Microbacterium
OTU_807	Bacteria	Actinobacteriota	Actinobacteria	Microlunatus
OTU_943	Bacteria	Actinobacteriota	Actinobacteria	Mycobacterium
OTU_1288	Bacteria	Actinobacteriota	Actinobacteria	Mycobacterium
OTU_427	Bacteria	Actinobacteriota	Actinobacteria	Mycobacterium
OTU_567	Bacteria	Actinobacteriota	Actinobacteria	Mycobacterium
OTU_961	Bacteria	Actinobacteriota	Actinobacteria	Mycobacterium
OTU_23	Bacteria	Actinobacteriota	Actinobacteria	Nocardia
OTU_53	Bacteria	Actinobacteriota	Actinobacteria	Nocardia
OTU_97	Bacteria	Actinobacteriota	Actinobacteria	Nocardia
OTU_283	Bacteria	Actinobacteriota	Actinobacteria	Nocardia
OTU_15	Bacteria	Actinobacteriota	Actinobacteria	Nocardioides
OTU_46	Bacteria	Actinobacteriota	Actinobacteria	Nocardioides
OTU_91	Bacteria	Actinobacteriota	Actinobacteria	Nocardioides
OTU_890	Bacteria	Actinobacteriota	Actinobacteria	Nocardioides
OTU_3972	Bacteria	Actinobacteriota	Actinobacteria	Nocardioides
OTU_7	Bacteria	Actinobacteriota	Actinobacteria	Nonomuraea
OTU_479	Bacteria	Actinobacteriota	Actinobacteria	Nonomuraea
OTU_606	Bacteria	Actinobacteriota	Actinobacteria	Nonomuraea
OTU_712	Bacteria	Actinobacteriota	Actinobacteria	Nonomuraea
OTU_857	Bacteria	Actinobacteriota	Actinobacteria	Nonomuraea
OTU_792	Bacteria	Actinobacteriota	Actinobacteria	Nonomuraea
OTU_108	Bacteria	Actinobacteriota	Actinobacteria	Phytomonospora

OTU_ID	Domain	Phylum	Class	Genus
OTU_1	Bacteria	Acidobacteriota	Acidobacteriae	Bryobacter
OTU_228	Bacteria	Actinobacteriota	Acidimicrobiia	Unidentified
OTU_507	Bacteria	Actinobacteriota	Acidimicrobiia	Unidentified
OTU_490	Bacteria	Actinobacteriota	Acidimicrobiia	Unidentified
OTU_627	Bacteria	Actinobacteriota	Acidimicrobiia	Unidentified
OTU_251	Bacteria	Actinobacteriota	Acidimicrobiia	Unidentified
OTU_199	Bacteria	Actinobacteriota	Acidimicrobiia	Unidentified
OTU_769	Bacteria	Actinobacteriota	Acidimicrobiia	Unidentified
OTU_116	Bacteria	Actinobacteriota	Acidimicrobiia	Unidentified
OTU_205	Bacteria	Actinobacteriota	Acidimicrobiia	Unidentified
OTU_369	Bacteria	Actinobacteriota	Acidimicrobiia	Unidentified
OTU_829	Bacteria	Actinobacteriota	Acidimicrobiia	Unidentified
OTU_993	Bacteria	Actinobacteriota	Acidimicrobiia	Iamia
OTU_239	Bacteria	Actinobacteriota	Actinobacteria	Acidothermus
OTU_410	Bacteria	Actinobacteriota	Actinobacteria	Acidothermus
OTU_35	Bacteria	Actinobacteriota	Actinobacteria	Actinophytocola
OTU_266	Bacteria	Actinobacteriota	Actinobacteria	Actinophytocola
OTU_22	Bacteria	Actinobacteriota	Actinobacteria	Agromyces
OTU_486	Bacteria	Actinobacteriota	Actinobacteria	Agromyces
OTU_99	Bacteria	Actinobacteriota	Actinobacteria	Amycolatopsis
OTU_173	Bacteria	Actinobacteriota	Actinobacteria	Amycolatopsis
OTU_212	Bacteria	Acidobacteriota	Acidobacteriae	Bryobacter
OTU_36	Bacteria	Acidobacteriota	Acidobacteriae	Bryobacter
OTU_2123	Bacteria	Acidobacteriota	Acidobacteriae	Bryobacter
OTU_139	Bacteria	Acidobacteriota	Acidobacteriae	Bryobacter
OTU_242	Bacteria	Actinobacteriota	Actinobacteria	Catelliglobosispora
OTU_623	Bacteria	Actinobacteriota	Actinobacteria	Catelliglobosispora
OTU_645	Bacteria	Actinobacteriota	Actinobacteria	Dactylosporangium
OTU_64	Bacteria	Actinobacteriota	Actinobacteria	Jiangella
OTU_290	Bacteria	Actinobacteriota	Actinobacteria	Jiangella
OTU_70	Bacteria	Actinobacteriota	Actinobacteria	Jiangella
OTU_175	Bacteria	Actinobacteriota	Actinobacteria	Jiangella
OTU_178	Bacteria	Actinobacteriota	Actinobacteria	Jiangella
OTU_183	Bacteria	Actinobacteriota	Actinobacteria	Jiangella
OTU_578	Bacteria	Actinobacteriota	Actinobacteria	Jiangella
OTU_759	Bacteria	Actinobacteriota	Actinobacteria	Jiangella
OTU_294	Bacteria	Actinobacteriota	Actinobacteria	Kribbella
OTU_761	Bacteria	Actinobacteriota	Actinobacteria	Kribbella
OTU_206	Bacteria	Actinobacteriota	Actinobacteria	Microbacterium
OTU_321	Bacteria	Actinobacteriota	Actinobacteria	Microbacterium
OTU_807	Bacteria	Actinobacteriota	Actinobacteria	Microlunatus
OTU_943	Bacteria	Actinobacteriota	Actinobacteria	Mycobacterium
OTU_1288	Bacteria	Actinobacteriota	Actinobacteria	Mycobacterium
OTU_427	Bacteria	Actinobacteriota	Actinobacteria	Mycobacterium
OTU_567	Bacteria	Actinobacteriota	Actinobacteria	Mycobacterium
OTU_961	Bacteria	Actinobacteriota	Actinobacteria	Mycobacterium
OTU_23	Bacteria	Actinobacteriota	Actinobacteria	Nocardia
OTU_53	Bacteria	Actinobacteriota	Actinobacteria	Nocardia
OTU_97	Bacteria	Actinobacteriota	Actinobacteria	Nocardia
OTU_283	Bacteria	Actinobacteriota	Actinobacteria	Nocardia
OTU_15	Bacteria	Actinobacteriota	Actinobacteria	Nocardioides
OTU_46	Bacteria	Actinobacteriota	Actinobacteria	Nocardioides
OTU_91	Bacteria	Actinobacteriota	Actinobacteria	Nocardioides
OTU_890	Bacteria	Actinobacteriota	Actinobacteria	Nocardioides
OTU_3972	Bacteria	Actinobacteriota	Actinobacteria	Nocardioides
OTU_7	Bacteria	Actinobacteriota	Actinobacteria	Nonomuraea
OTU_479	Bacteria	Actinobacteriota	Actinobacteria	Nonomuraea
OTU_606	Bacteria	Actinobacteriota	Actinobacteria	Nonomuraea
OTU_712	Bacteria	Actinobacteriota	Actinobacteria	Nonomuraea
OTU_857	Bacteria	Actinobacteriota	Actinobacteria	Nonomuraea
OTU_792	Bacteria	Actinobacteriota	Actinobacteria	Nonomuraea
OTU_108	Bacteria	Actinobacteriota	Actinobacteria	Phytomonospora

OTU_ID	Domain	Phylum	Class	Genus
OTU_1	Bacteria	Acidobacteriota	Acidobacteriae	Bryobacter
OTU_228	Bacteria	Actinobacteriota	Acidimicrobiia	Unidentified
OTU_507	Bacteria	Actinobacteriota	Acidimicrobiia	Unidentified
OTU_490	Bacteria	Actinobacteriota	Acidimicrobiia	Unidentified
OTU_627	Bacteria	Actinobacteriota	Acidimicrobiia	Unidentified
OTU_251	Bacteria	Actinobacteriota	Acidimicrobiia	Unidentified
OTU_199	Bacteria	Actinobacteriota	Acidimicrobiia	Unidentified
OTU_769	Bacteria	Actinobacteriota	Acidimicrobiia	Unidentified
OTU_116	Bacteria	Actinobacteriota	Acidimicrobiia	Unidentified
OTU_205	Bacteria	Actinobacteriota	Acidimicrobiia	Unidentified
OTU_369	Bacteria	Actinobacteriota	Acidimicrobiia	Unidentified
OTU_829	Bacteria	Actinobacteriota	Acidimicrobiia	Unidentified
OTU_993	Bacteria	Actinobacteriota	Acidimicrobiia	Iamia
OTU_239	Bacteria	Actinobacteriota	Actinobacteria	Acidothermus
OTU_410	Bacteria	Actinobacteriota	Actinobacteria	Acidothermus
OTU_35	Bacteria	Actinobacteriota	Actinobacteria	Actinophytocola
OTU_266	Bacteria	Actinobacteriota	Actinobacteria	Actinophytocola
OTU_22	Bacteria	Actinobacteriota	Actinobacteria	Agromyces
OTU_486	Bacteria	Actinobacteriota	Actinobacteria	Agromyces
OTU_99	Bacteria	Actinobacteriota	Actinobacteria	Amycolatopsis
OTU_173	Bacteria	Actinobacteriota	Actinobacteria	Amycolatopsis
OTU_212	Bacteria	Acidobacteriota	Acidobacteriae	Bryobacter
OTU_36	Bacteria	Acidobacteriota	Acidobacteriae	Bryobacter
OTU_2123	Bacteria	Acidobacteriota	Acidobacteriae	Bryobacter
OTU_139	Bacteria	Acidobacteriota	Acidobacteriae	Bryobacter
OTU_242	Bacteria	Actinobacteriota	Actinobacteria	Catelliglobosispora
OTU_623	Bacteria	Actinobacteriota	Actinobacteria	Catelliglobosispora
OTU_645	Bacteria	Actinobacteriota	Actinobacteria	Dactylosporangium
OTU_64	Bacteria	Actinobacteriota	Actinobacteria	Jiangella
OTU_290	Bacteria	Actinobacteriota	Actinobacteria	Jiangella
OTU_70	Bacteria	Actinobacteriota	Actinobacteria	Jiangella
OTU_175	Bacteria	Actinobacteriota	Actinobacteria	Jiangella
OTU_178	Bacteria	Actinobacteriota	Actinobacteria	Jiangella
OTU_183	Bacteria	Actinobacteriota	Actinobacteria	Jiangella
OTU_578	Bacteria	Actinobacteriota	Actinobacteria	Jiangella
OTU_759	Bacteria	Actinobacteriota	Actinobacteria	Jiangella
OTU_294	Bacteria	Actinobacteriota	Actinobacteria	Kribbella
OTU_761	Bacteria	Actinobacteriota	Actinobacteria	Kribbella
OTU_206	Bacteria	Actinobacteriota	Actinobacteria	Microbacterium
OTU_321	Bacteria	Actinobacteriota	Actinobacteria	Microbacterium
OTU_807	Bacteria	Actinobacteriota	Actinobacteria	Microlunatus
OTU_943	Bacteria	Actinobacteriota	Actinobacteria	Mycobacterium
OTU_1288	Bacteria	Actinobacteriota	Actinobacteria	Mycobacterium
OTU_427	Bacteria	Actinobacteriota	Actinobacteria	Mycobacterium
OTU_567	Bacteria	Actinobacteriota	Actinobacteria	Mycobacterium
OTU_961	Bacteria	Actinobacteriota	Actinobacteria	Mycobacterium
OTU_23	Bacteria	Actinobacteriota	Actinobacteria	Nocardia
OTU_53	Bacteria	Actinobacteriota	Actinobacteria	Nocardia
OTU_97	Bacteria	Actinobacteriota	Actinobacteria	Nocardia
OTU_283	Bacteria	Actinobacteriota	Actinobacteria	Nocardia
OTU_15	Bacteria	Actinobacteriota	Actinobacteria	Nocardioides
OTU_46	Bacteria	Actinobacteriota	Actinobacteria	Nocardioides
OTU_91	Bacteria	Actinobacteriota	Actinobacteria	Nocardioides
OTU_890	Bacteria	Actinobacteriota	Actinobacteria	Nocardioides
OTU_3972	Bacteria	Actinobacteriota	Actinobacteria	Nocardioides
OTU_7	Bacteria	Actinobacteriota	Actinobacteria	Nonomuraea
OTU_479	Bacteria	Actinobacteriota	Actinobacteria	Nonomuraea
OTU_606	Bacteria	Actinobacteriota	Actinobacteria	Nonomuraea
OTU_712	Bacteria	Actinobacteriota	Actinobacteria	Nonomuraea
OTU_857	Bacteria	Actinobacteriota	Actinobacteria	Nonomuraea
OTU_792	Bacteria	Actinobacteriota	Actinobacteria	Nonomuraea
OTU_108	Bacteria	Actinobacteriota	Actinobacteria	Phytomonospora

OTU_ID	Domain	Phylum	Class	Genus
OTU_1	Bacteria	Acidobacteriota	Acidobacteriae	Bryobacter
OTU_228	Bacteria	Actinobacteriota	Acidimicrobiia	Unidentified
OTU_507	Bacteria	Actinobacteriota	Acidimicrobiia	Unidentified
OTU_490	Bacteria	Actinobacteriota	Acidimicrobiia	Unidentified
OTU_627	Bacteria	Actinobacteriota	Acidimicrobiia	Unidentified
OTU_251	Bacteria	Actinobacteriota	Acidimicrobiia	Unidentified
OTU_199	Bacteria	Actinobacteriota	Acidimicrobiia	Unidentified
OTU_769	Bacteria	Actinobacteriota	Acidimicrobiia	Unidentified
OTU_116	Bacteria	Actinobacteriota	Acidimicrobiia	Unidentified
OTU_205	Bacteria	Actinobacteriota	Acidimicrobiia	Unidentified
OTU_369	Bacteria	Actinobacteriota	Acidimicrobiia	Unidentified
OTU_829	Bacteria	Actinobacteriota	Acidimicrobiia	Unidentified
OTU_993	Bacteria	Actinobacteriota	Acidimicrobiia	Iamia
OTU_239	Bacteria	Actinobacteriota	Actinobacteria	Acidothermus
OTU_410	Bacteria	Actinobacteriota	Actinobacteria	Acidothermus
OTU_35	Bacteria	Actinobacteriota	Actinobacteria	Actinophytocola
OTU_266	Bacteria	Actinobacteriota	Actinobacteria	Actinophytocola
OTU_22	Bacteria	Actinobacteriota	Actinobacteria	Agromyces
OTU_486	Bacteria	Actinobacteriota	Actinobacteria	Agromyces
OTU_99	Bacteria	Actinobacteriota	Actinobacteria	Amycolatopsis
OTU_173	Bacteria	Actinobacteriota	Actinobacteria	Amycolatopsis
OTU_212	Bacteria	Acidobacteriota	Acidobacteriae	Bryobacter
OTU_36	Bacteria	Acidobacteriota	Acidobacteriae	Bryobacter
OTU_2123	Bacteria	Acidobacteriota	Acidobacteriae	Bryobacter
OTU_139	Bacteria	Acidobacteriota	Acidobacteriae	Bryobacter
OTU_242	Bacteria	Actinobacteriota	Actinobacteria	Catelliglobosispora
OTU_623	Bacteria	Actinobacteriota	Actinobacteria	Catelliglobosispora
OTU_645	Bacteria	Actinobacteriota	Actinobacteria	Dactylosporangium
OTU_64	Bacteria	Actinobacteriota	Actinobacteria	Jiangella
OTU_290	Bacteria	Actinobacteriota	Actinobacteria	Jiangella
OTU_70	Bacteria	Actinobacteriota	Actinobacteria	Jiangella
OTU_175	Bacteria	Actinobacteriota	Actinobacteria	Jiangella
OTU_178	Bacteria	Actinobacteriota	Actinobacteria	Jiangella
OTU_183	Bacteria	Actinobacteriota	Actinobacteria	Jiangella
OTU_578	Bacteria	Actinobacteriota	Actinobacteria	Jiangella
OTU_759	Bacteria	Actinobacteriota	Actinobacteria	Jiangella
OTU_294	Bacteria	Actinobacteriota	Actinobacteria	Kribbella
OTU_761	Bacteria	Actinobacteriota	Actinobacteria	Kribbella
OTU_206	Bacteria	Actinobacteriota	Actinobacteria	Microbacterium
OTU_321	Bacteria	Actinobacteriota	Actinobacteria	Microbacterium
OTU_807	Bacteria	Actinobacteriota	Actinobacteria	Microlunatus
OTU_943	Bacteria	Actinobacteriota	Actinobacteria	Mycobacterium
OTU_1288	Bacteria	Actinobacteriota	Actinobacteria	Mycobacterium
OTU_427	Bacteria	Actinobacteriota	Actinobacteria	Mycobacterium
OTU_567	Bacteria	Actinobacteriota	Actinobacteria	Mycobacterium
OTU_961	Bacteria	Actinobacteriota	Actinobacteria	Mycobacterium
OTU_23	Bacteria	Actinobacteriota	Actinobacteria	Nocardia
OTU_53	Bacteria	Actinobacteriota	Actinobacteria	Nocardia
OTU_97	Bacteria	Actinobacteriota	Actinobacteria	Nocardia
OTU_283	Bacteria	Actinobacteriota	Actinobacteria	Nocardia
OTU_15	Bacteria	Actinobacteriota	Actinobacteria	Nocardioides
OTU_46	Bacteria	Actinobacteriota	Actinobacteria	Nocardioides
OTU_91	Bacteria	Actinobacteriota	Actinobacteria	Nocardioides
OTU_890	Bacteria	Actinobacteriota	Actinobacteria	Nocardioides
OTU_3972	Bacteria	Actinobacteriota	Actinobacteria	Nocardioides
OTU_7	Bacteria	Actinobacteriota	Actinobacteria	Nonomuraea
OTU_479	Bacteria	Actinobacteriota	Actinobacteria	Nonomuraea
OTU_606	Bacteria	Actinobacteriota	Actinobacteria	Nonomuraea
OTU_712	Bacteria	Actinobacteriota	Actinobacteria	Nonomuraea
OTU_857	Bacteria	Actinobacteriota	Actinobacteria	Nonomuraea
OTU_792	Bacteria	Actinobacteriota	Actinobacteria	Nonomuraea
OTU_108	Bacteria	Actinobacteriota	Actinobacteria	Phytomonospora

OTU_ID	Domain	Phylum	Class	Genus
OTU_1	Bacteria	Acidobacteriota	Acidobacteriae	Bryobacter
OTU_228	Bacteria	Actinobacteriota	Acidimicrobiia	Unidentified
OTU_507	Bacteria	Actinobacteriota	Acidimicrobiia	Unidentified
OTU_490	Bacteria	Actinobacteriota	Acidimicrobiia	Unidentified
OTU_627	Bacteria	Actinobacteriota	Acidimicrobiia	Unidentified
OTU_251	Bacteria	Actinobacteriota	Acidimicrobiia	Unidentified
OTU_199	Bacteria	Actinobacteriota	Acidimicrobiia	Unidentified
OTU_769	Bacteria	Actinobacteriota	Acidimicrobiia	Unidentified
OTU_116	Bacteria	Actinobacteriota	Acidimicrobiia	Unidentified
OTU_205	Bacteria	Actinobacteriota	Acidimicrobiia	Unidentified
OTU_369	Bacteria	Actinobacteriota	Acidimicrobiia	Unidentified
OTU_829	Bacteria	Actinobacteriota	Acidimicrobiia	Unidentified
OTU_993	Bacteria	Actinobacteriota	Acidimicrobiia	Iamia
OTU_239	Bacteria	Actinobacteriota	Actinobacteria	Acidothermus
OTU_410	Bacteria	Actinobacteriota	Actinobacteria	Acidothermus
OTU_35	Bacteria	Actinobacteriota	Actinobacteria	Actinophytocola
OTU_266	Bacteria	Actinobacteriota	Actinobacteria	Actinophytocola
OTU_22	Bacteria	Actinobacteriota	Actinobacteria	Agromyces
OTU_486	Bacteria	Actinobacteriota	Actinobacteria	Agromyces
OTU_99	Bacteria	Actinobacteriota	Actinobacteria	Amycolatopsis
OTU_173	Bacteria	Actinobacteriota	Actinobacteria	Amycolatopsis
OTU_212	Bacteria	Acidobacteriota	Acidobacteriae	Bryobacter
OTU_36	Bacteria	Acidobacteriota	Acidobacteriae	Bryobacter
OTU_2123	Bacteria	Acidobacteriota	Acidobacteriae	Bryobacter
OTU_139	Bacteria	Acidobacteriota	Acidobacteriae	Bryobacter
OTU_242	Bacteria	Actinobacteriota	Actinobacteria	Catelliglobosispora
OTU_623	Bacteria	Actinobacteriota	Actinobacteria	Catelliglobosispora
OTU_645	Bacteria	Actinobacteriota	Actinobacteria	Dactylosporangium
OTU_64	Bacteria	Actinobacteriota	Actinobacteria	Jiangella
OTU_290	Bacteria	Actinobacteriota	Actinobacteria	Jiangella
OTU_70	Bacteria	Actinobacteriota	Actinobacteria	Jiangella
OTU_175	Bacteria	Actinobacteriota	Actinobacteria	Jiangella
OTU_178	Bacteria	Actinobacteriota	Actinobacteria	Jiangella
OTU_183	Bacteria	Actinobacteriota	Actinobacteria	Jiangella
OTU_578	Bacteria	Actinobacteriota	Actinobacteria	Jiangella
OTU_759	Bacteria	Actinobacteriota	Actinobacteria	Jiangella
OTU_294	Bacteria	Actinobacteriota	Actinobacteria	Kribbella
OTU_761	Bacteria	Actinobacteriota	Actinobacteria	Kribbella
OTU_206	Bacteria	Actinobacteriota	Actinobacteria	Microbacterium
OTU_321	Bacteria	Actinobacteriota	Actinobacteria	Microbacterium
OTU_807	Bacteria	Actinobacteriota	Actinobacteria	Microlunatus
OTU_943	Bacteria	Actinobacteriota	Actinobacteria	Mycobacterium
OTU_1288	Bacteria	Actinobacteriota	Actinobacteria	Mycobacterium
OTU_427	Bacteria	Actinobacteriota	Actinobacteria	Mycobacterium
OTU_567	Bacteria	Actinobacteriota	Actinobacteria	Mycobacterium
OTU_961	Bacteria	Actinobacteriota	Actinobacteria	Mycobacterium
OTU_23	Bacteria	Actinobacteriota	Actinobacteria	Nocardia
OTU_53	Bacteria	Actinobacteriota	Actinobacteria	Nocardia
OTU_97	Bacteria	Actinobacteriota	Actinobacteria	Nocardia
OTU_283	Bacteria	Actinobacteriota	Actinobacteria	Nocardia
OTU_15	Bacteria	Actinobacteriota	Actinobacteria	Nocardioides
OTU_46	Bacteria	Actinobacteriota	Actinobacteria	Nocardioides
OTU_91	Bacteria	Actinobacteriota	Actinobacteria	Nocardioides
OTU_890	Bacteria	Actinobacteriota	Actinobacteria	Nocardioides
OTU_3972	Bacteria	Actinobacteriota	Actinobacteria	Nocardioides
OTU_7	Bacteria	Actinobacteriota	Actinobacteria	Nonomuraea
OTU_479	Bacteria	Actinobacteriota	Actinobacteria	Nonomuraea
OTU_606	Bacteria	Actinobacteriota	Actinobacteria	Nonomuraea
OTU_712	Bacteria	Actinobacteriota	Actinobacteria	Nonomuraea
OTU_857	Bacteria	Actinobacteriota	Actinobacteria	Nonomuraea
OTU_792	Bacteria	Actinobacteriota	Actinobacteria	Nonomuraea
OTU_108	Bacteria	Actinobacteriota	Actinobacteria	Phytomonospora

OTU_ID	Domain	Phylum	Class	Genus
OTU_1	Bacteria	Acidobacteriota	Acidobacteriae	Bryobacter
OTU_228	Bacteria	Actinobacteriota	Acidimicrobiia	Unidentified
OTU_507	Bacteria	Actinobacteriota	Acidimicrobiia	Unidentified
OTU_490	Bacteria	Actinobacteriota	Acidimicrobiia	Unidentified
OTU_627	Bacteria	Actinobacteriota	Acidimicrobiia	Unidentified
OTU_251	Bacteria	Actinobacteriota	Acidimicrobiia	Unidentified
OTU_199	Bacteria	Actinobacteriota	Acidimicrobiia	Unidentified
OTU_769	Bacteria	Actinobacteriota	Acidimicrobiia	Unidentified
OTU_116	Bacteria	Actinobacteriota	Acidimicrobiia	Unidentified
OTU_205	Bacteria	Actinobacteriota	Acidimicrobiia	Unidentified
OTU_369	Bacteria	Actinobacteriota	Acidimicrobiia	Unidentified
OTU_829	Bacteria	Actinobacteriota	Acidimicrobiia	Unidentified
OTU_993	Bacteria	Actinobacteriota	Acidimicrobiia	Iamia
OTU_239	Bacteria	Actinobacteriota	Actinobacteria	Acidothermus
OTU_410	Bacteria	Actinobacteriota	Actinobacteria	Acidothermus
OTU_35	Bacteria	Actinobacteriota	Actinobacteria	Actinophytocola
OTU_266	Bacteria	Actinobacteriota	Actinobacteria	Actinophytocola
OTU_22	Bacteria	Actinobacteriota	Actinobacteria	Agromyces
OTU_486	Bacteria	Actinobacteriota	Actinobacteria	Agromyces
OTU_99	Bacteria	Actinobacteriota	Actinobacteria	Amycolatopsis
OTU_173	Bacteria	Actinobacteriota	Actinobacteria	Amycolatopsis
OTU_212	Bacteria	Acidobacteriota	Acidobacteriae	Bryobacter
OTU_36	Bacteria	Acidobacteriota	Acidobacteriae	Bryobacter
OTU_2123	Bacteria	Acidobacteriota	Acidobacteriae	Bryobacter
OTU_139	Bacteria	Acidobacteriota	Acidobacteriae	Bryobacter
OTU_242	Bacteria	Actinobacteriota	Actinobacteria	Catelliglobosispora
OTU_623	Bacteria	Actinobacteriota	Actinobacteria	Catelliglobosispora
OTU_645	Bacteria	Actinobacteriota	Actinobacteria	Dactylosporangium
OTU_64	Bacteria	Actinobacteriota	Actinobacteria	Jiangella
OTU_290	Bacteria	Actinobacteriota	Actinobacteria	Jiangella
OTU_70	Bacteria	Actinobacteriota	Actinobacteria	Jiangella
OTU_175	Bacteria	Actinobacteriota	Actinobacteria	Jiangella
OTU_178	Bacteria	Actinobacteriota	Actinobacteria	Jiangella
OTU_183	Bacteria	Actinobacteriota	Actinobacteria	Jiangella
OTU_578	Bacteria	Actinobacteriota	Actinobacteria	Jiangella
OTU_759	Bacteria	Actinobacteriota	Actinobacteria	Jiangella
OTU_294	Bacteria	Actinobacteriota	Actinobacteria	Kribbella
OTU_761	Bacteria	Actinobacteriota	Actinobacteria	Kribbella
OTU_206	Bacteria	Actinobacteriota	Actinobacteria	Microbacterium
OTU_321	Bacteria	Actinobacteriota	Actinobacteria	Microbacterium
OTU_807	Bacteria	Actinobacteriota	Actinobacteria	Microlunatus
OTU_943	Bacteria	Actinobacteriota	Actinobacteria	Mycobacterium
OTU_1288	Bacteria	Actinobacteriota	Actinobacteria	Mycobacterium
OTU_427	Bacteria	Actinobacteriota	Actinobacteria	Mycobacterium
OTU_567	Bacteria	Actinobacteriota	Actinobacteria	Mycobacterium
OTU_961	Bacteria	Actinobacteriota	Actinobacteria	Mycobacterium
OTU_23	Bacteria	Actinobacteriota	Actinobacteria	Nocardia
OTU_53	Bacteria	Actinobacteriota	Actinobacteria	Nocardia
OTU_97	Bacteria	Actinobacteriota	Actinobacteria	Nocardia
OTU_283	Bacteria	Actinobacteriota	Actinobacteria	Nocardia
OTU_15	Bacteria	Actinobacteriota	Actinobacteria	Nocardioides
OTU_46	Bacteria	Actinobacteriota	Actinobacteria	Nocardioides
OTU_91	Bacteria	Actinobacteriota	Actinobacteria	Nocardioides
OTU_890	Bacteria	Actinobacteriota	Actinobacteria	Nocardioides
OTU_3972	Bacteria	Actinobacteriota	Actinobacteria	Nocardioides
OTU_7	Bacteria	Actinobacteriota	Actinobacteria	Nonomuraea
OTU_479	Bacteria	Actinobacteriota	Actinobacteria	Nonomuraea
OTU_606	Bacteria	Actinobacteriota	Actinobacteria	Nonomuraea
OTU_712	Bacteria	Actinobacteriota	Actinobacteria	Nonomuraea
OTU_857	Bacteria	Actinobacteriota	Actinobacteria	Nonomuraea
OTU_792	Bacteria	Actinobacteriota	Actinobacteria	Nonomuraea
OTU_108	Bacteria	Actinobacteriota	Actinobacteria	Phytomonospora

CHAPITRE 4

Potentiel génétique et reconstruction génomique des communautés microbiennes présentes sur les surfaces altérées et non-altérées

Avant-propos

Les chapitres précédents étaient orientés sur l'analyse des dynamiques microbiennes associées à différents phénomènes d'évolution des altérations (zones sombres et taches noires) avec un focus sur les assemblages microbiens d'un point de vue de leur taxonomie, sans prendre en compte le potentiel fonctionnel de la communauté. Ces précédentes études montrent que (i) l'effet du temps d'échantillonnage n'est pas significatif, (ii) les zones sombres sont majoritairement composées du champignon noir *Ochroconis* tandis que les taches noires sont composées majoritairement de l'assemblage *Exophiala/Ochroronis*, (iii) quel que soit le type d'altération, la surface non altérée associée présente une forte proportion du genre bactérien *Pseudomonas* dans certaines salles (e.g. Abside, Passage) et que (iv) le microbiote de la grotte est spatialement hétérogène et sa composition dépend de la salle et du substrat géologique. Malgré les informations apportées par cette thèse sur les processus permettant la formation et/ou l'évolution des altérations, à ce jour peu d'information est disponible sur le fonctionnement des communautés microbiennes de la grotte de Lascaux [Alonso, 2018]. Ainsi, en étudiant la dynamique fonctionnelle par une approche de séquençage non ciblé (i.e. métagénomique) de différentes salles de la grotte à différentes dates et pour différentes situations (taches noires, zones sombres et parois non marquées) nous avons pris en compte l'hétérogénéité présente dans la grotte pour comprendre le fonctionnement de la communauté microbienne. L'hypothèse est que les gènes impliqués dans les voies métaboliques de la biosynthèse de pigments (mélanines) sont davantage présents dans les zones altérées (taches noires et zones sombres) en comparaison avec les zones non marquées.

Les échantillons ont été prélevés par la restauratrice Diane Henry-Lormelle avec le support technique de l'UMR Écologie microbienne, compatible avec les contraintes de conservation de la grotte. Pour chaque échantillon de microbiologie une extraction ADN a été réalisée à l'aide du kit FastDNA SPIN kit for Soil (MP Biomedical, Illkirch, France), les concentrations d'ADN ont été quantifiées en utilisant le kit Qubit DNAdb HS (Thermo Fisher Scientific, Waltham, Etats-Unis). Les métagénomes des communautés présentes dans les altérations et les zones non altérées associées, ont été séquencés par la technologie Illumina NovaSeq 6000, en vue de l'obtention de 60 millions de séquences par échantillon.

La première étude **(Article 6)** s'est focalisée sur l'étude du potentiel génétique des communautés microbiennes retrouvées dans les taches noires. Pour cela, trois taches noires et leurs surfaces non altérées associées ont été prélevées en septembre 2020 dans la Nef. Au total, 6 métagénomes ont été analysés pour cette étude et ont permis l'analyse du potentiel génétique d'une part et la reconstruction de génomes d'autre part. D'autres échantillons étaient également prévus pour cette étude mais ils ont été perdus par le prestataire de séquençage. Des analyses moléculaires complémentaires ont été réalisées sur ces échantillons : métabarcoding et PCR quantitative ciblant le gène de l'ARN 16S bactéries, 16S archées et le gène de l'ARN 18S microeucaryotes. Les résultats de cette étude ont montré une composition des communautés microbiennes et des potentiels génétiques très contrastés entre les échantillons provenant des surfaces non altérées ou des taches noires. Ce travail a permis pour la première fois de mettre en évidence que la couleur noire des taches pourrait être due à la présence de voies métaboliques

impliquées dans la biosynthèse de différents pigments organiques tels que des caroténoïdes et des mélanines (catéchol-mélanine, DHN mélanine et DOPA mélanine) produits par des champignons (e.g. champignon noir *Exophiala*) et des bactéries (e.g. *Chitinophaga*). De plus, le potentiel génétique de la communauté permet de pointer un lien entre la synthèse de mélanine et la dégradation des produits chimiques précédemment appliqués sur les parois de la grotte, ce qui suggère que les micro-organismes producteurs de pigments sont favorisés par l'application de biocides.

La deuxième étude **(Article 7)**, concerne la comparaison de métagénomes provenant de zones sombres dont le temps d'échantillonnage et le substrat géologique étaient différents. L'échantillonnage a été réalisé en septembre 2020 et avril 2021 sur le plan incliné droit de l'Abside et en avril 2021 sur les banquettes maçonnées du Passage, au total 18 échantillons ont été prélevés. Les résultats des profils taxonomiques en métagénomique étaient largement convergents avec les données précédentes obtenues par métabarcoding. Des similarités entre 2020 et 2021 ont été mises en évidence, associées à des différences en fonction de la situation étudiée. Pour autant, nous avons montré que dans les deux salles où ont été appliqués des biocides par le passé, les gènes et les voies métaboliques associés à la dégradation des composés aromatiques étaient présents dans et hors des zones sombres. En outre, les zones sombres coïncident avec la présence de voies métabolique impliquées dans la biosynthèse de pigments. Des gènes ou des voies de production d'antimicrobiens ont également été mis en évidence sur les surfaces non marquées, ce qui pourrait limiter le développement des micro-organismes pigmentés. Ce travail propose un cadre conceptuel de formation des zones sombres en relation avec le métabolisme secondaire microbien, qui peut aider à comprendre les altérations des parois lors d'une anthropisation sévère des grottes.

Mon rôle dans ces deux études a été le suivant : j'ai participé à la réflexion sur les objectifs scientifiques et à la démarche expérimentale ainsi qu'aux différentes missions d'échantillonnage. J'ai réalisé l'extraction d'ADN avant séquençage et les amplifications pour le séquençage metabarcoding. J'ai traité les données de séquençage brutes, j'ai ensuite analysé ces données permettant d'observer le profil taxonomique et métabolique des métagénomes associés à chaque condition à l'aide notamment de statistiques multivariées. Des génomes ont été reconstruits et leur potentiel métabolique a été étudié.

L'ensemble de ce travail a permis la rédaction de deux publications 'Functional characterization of microbial communities related to black stain formation in Lascaux Cave' et 'Microbial diversity and secondary metabolism potential in relation to dark alterations in Paleolithic Lascaux Cave' (soumissions prévues en 2023).

Article 6. Functional characterization of microbial communities related to black stain formation in Lascaux Cave

ZELIA BONTEMPS[1], DANIS ABROUK[1], YVAN MOENNE-LOCCOZ[1] AND MYLENE HUGONI[1,2,3]

[1]Univ Lyon, Université Claude Bernard Lyon 1, CNRS, INRAE, VetAgro Sup, UMR Ecologie Microbienne, F-69622 Villeurbanne, France
[2]Univ Lyon, Université Claude Bernard Lyon 1, CNRS, INSA de Lyon, UMR Microbiologie Adaptation et Pathogénie, F-69622 Villeurbanne, France
[3]Institut Universitaire de France (IUF)
Corresponding author : Mylene HUGONI - Univ Lyon, INSA Lyon, CNRS, UMR 5240 Microbiologie Adaptation et Pathogénie, F-69621 Villeurbanne, France - mylene.hugoni@univ-lyon1.fr

Abstract

Background : Paleolithic caves attract a million tourists per year, which may cause imbalance of cave microbiota and promote the development of microbial stains on cave walls. In certain cases, chemical biocides e.g. benzalkonium chloride (BAC) have been applied on cave walls to mitigate rock alterations, but without success. In Lascaux Cave, metabarcoding showed that pigmented fungi were selected and Pseudomonas bacteria counter-selected in black stains. Findings to date point to a model of black stain formation, but its functional relevance remains to be clarified, and the objective of this work was to test this model.

Results : Based on metabarcoding and PCR quantification of bacteria, archaea and microeukaryotes, as well as metagenomics, we expanded the range of microbial taxa documented to differ between black stains and neighboring unmarked surfaces. Genes for synthesis of melanin or carotenoid pigments were more prevalent in black stains and were identified in several reconstructed genomes. They were evidenced not only in fungi (as expected) but also in bacteria. Genes for degradation of aromatic compounds and presumably of biocides used in the cave were also found, strengthening that chemical treatments could have selected melanin-producing microorganisms as well as melanin synthesis. Finally, genes for synthesis of antimicrobial secondary compounds were identified, including for antifungal phenazines, both on unmarked surfaces and black stains.

Conclusion : Our findings complete previous predictions regarding black stain formation in anthropized Lascaux Cave ecosystem, by documenting a broader range of (i) microorganisms involved, (ii) potential biotransformations (including of chemical biocides), (iii) pathways for synthesis of melanins as well as carotenoid pigments, and (iv) possible antagonistic interactions to consider to understand microbial dynamics during cave wall alterations. These different aspects may be important to take into account for conservation of underground Paleolithic art.

Key words : Paleolithic Cave, Benzalkonium chloride, melanin, catechol, *Pseudomonas*, Metagenomics

Introduction

The microbiology of subterranean environments has received increasing attention in the last decade, notably because microorganisms have been identified as key players in the biodeterioration processes that may affect the integrity of speleothems and parietal art in caves subjected to excessive tourism [1–4]. Underground ecosystems are well developed in calcareous areas, and many caves have been used by humans for parietal artwork [4]. In hundreds of caves, facilities (e.g. artificial light, stairs, elevators) have been set up to promote touristic activities and human frequentation has been significant, thereby changing environmental and possibly microbiota conditions [5–7]. This was reported in iconic painted caves such as Altamira (Spain) and Lascaux (France), where microbial outgrowth led to cave wall alterations and resulted in closure of the caves to the public [8–12]. In Lascaux, microbial alterations were treated mechanically and/or using chemical biocides, mostly antibiotics and quaternary ammonium compounds, especially aromatic ones such as benzalkonium chloride (BAC) [13,14]. BAC affects bacteria by disturbing the electronic charge and alkyl chains in the bilayered membrane [15]. However, resistance exists in various bacterial taxa, for instance by modifying fatty acid composition and stabilizing membrane electronic charge in *Pseudomonas* spp. [16], and certain bacteria e.g. *Pseudomonas* spp. can even degrade BAC by dealkylation into benzyldimenthylamine, benzylamine and benzoic acid [16,17]. Accordingly, exposure to BAC can decrease community diversity [17,18], but subsequent BAC degradation may reduce environmental toxicity and trigger microbial community changes [17,19], but this was not shown in caves.

Black stains are often the most advanced stage of rock wall alterations, and they are documented in many locations including Cave of Bats (Spain ; [20]), the Monterozzi Etruscan tomb (Italy ; [21,22]), Driny Cave (Slovakia ; [23]), Adjanta Cave (India ; [24]), Castellana Cave (Italy ; [25]) and Lascaux Cave (France ; [10]). In Lascaux Cave, black stains are wall alterations related to past touristic exploitation of the cave [14] as well as chemical treatments used to mitigate previous microbial outbreaks, i.e. (i) green algal biofilms formed in 1960 and due to *Brateoccocus minor*, which was treated with a combination of antibiotics and formaldehyde [26], and (ii) white mycelium of the fungus *Fusarium solani* in early 2001, which was treated using benzalkonium chloride [14] and antibiotics [27,28]. These black alterations were first noticed on cave walls in late 2001 and developed strongly from 2006 on. They are typically attributed to melanin-producing pigmented fungi such as *Ochroconis lascauxensis* [29], based on (i) the isolation of *Ochroconis* fungi that produce melanin *in vitro* [30], (ii) cloning-sequencing data of ITS and RPB2 regions pointing to melanized fungi [29], and (iii) the prevalence of pigmented fungi [31]. Melanin pigments derive from the oxidation and polymerization of 3,4-hydroxyphenylalanine (DOPA), 5,6-dihydroxyindole, catechol or 1,8-dihydroxynaphthalene (DHN) precursors [32]. Chemical treatments were used against Lascaux black stains but proved ineffective. This is consistent with the fact that melanins confer resistance to toxic chemicals (Jacobson 2000, Nosanchuck et al. 2006) (and are difficult to degrade [33]), and the possibility that aromatic chemicals such as BAC might even undergo microbial degradation (and generate compounds used for microbial synthesis of black pigments perhaps [33]). In Lascaux Cave, therefore, melanin-producing microorganisms were probably favored by the application of chemical treatments.

The assessments made to date point to a likely scenario for the formation of black stains

[10,29–31,34], but several questions remain unanswered : Our vision of Lascaux microbial diversity is based on the use of PCR tools, but does it reflect correctly the main differences in community related to the presence of black stains ? Melanin has been evidenced *in vitro*, using fungal isolates, but which biosynthetic processes are involved in situ, and in which microorganisms ? Which other metabolic pathways might be implicated as well, to yield substrates for melanin synthesis, and what is the contribution of past chemical treatments ? Certain microorganisms (i.e. *Pseudomonas*) isolated outside of black stains inhibit pigmented fungi *in vitro* [35], but what is the significance of this inhibition potential for control of black stain growth ?

Against this background, and taking into account previous findings (e.g. selection of black pigmented fungi and counter-selection of *Pseudomonas* in black stains, etc.), the current work was carried out to test the hypotheses that (i) metabarcoding and metagenomics would give convergent diversity findings, based on the facts that previous diversity differences between black stains and unmarked surfaces were large, (ii) genetic pathways for melanin synthesis would be prevalent in black stains, perhaps also in a wider range of microorganisms than those identified so far, (iii) melanin synthesis would be fueled by degradation products of chemicals previously applied to cave walls (which also implicates that melanin-producing microorganisms were probably favored by the application of chemical treatments), and (iv) pathways involved in synthesis of antimicrobial compounds should occur, particularly outside black stains. Thus, we investigated the diversity and especially the genetic potential of the communities in black stains and unmarked surfaces by a metagenomic approach coupled with genome-resolved metagenomics (i.e. metagenome-assembled genomes also named bins reconstruction).

Materials and Methods

Sampling and nucleic acid extraction

Lascaux Cave is located in the South-West of France in Périgord (N 45°03'13.087" and E 1°10'12.362"). This cave has been closed for tourist visits since 1963 due to cave wall alterations and access is limited to scientist with special authorization from DRAC Nouvelle-Aquitaine (Ministry of Culture). One major room inside Lascaux Cave is the Nave, containing outstanding Paleolithic paintings (e.g. Seven Ibexes, Great Black Cow, Crossed Bison), and where black stains started to form in March 2006 on limestone walls. Samples of stains that developed from January 2019 on were collected in September 2020 from the lower part of the left walls of the Nave, an area devoid of Paleolithic art (Supplementary Fig. S1). Three black stains (three replicates) and unmarked limestone surfaces nearby were sampled with sterile scalpels, for each sample on a small area (< 1 cm^2), and were immediately placed into liquid nitrogen and transferred to -80°C in the laboratory, before DNA extraction.

Total DNA was extracted using the FastDNA SPIN Kit For Soil (MP Biomedicals, Illkirch, France) with modification of the FastPrep step, i.e. 80 s at a speed setting of 6.0 m/s and 15 min at 4°C for centrifugation. The elution step was achieved using 50 µl elution buffer for each sample. The DNA concentrations were quantified using the Qubit dsDNA HS Assay Kit (Invitrogen, Carlsbad, USA) following the manufacturer's instructions. The DNA extracts were stored at -20°C until library preparation.

Quantitative PCR

To assess the number of bacterial 16S rRNA genes, archaeal 16S rRNA genes and microeukaryotic 18S rRNA genes, quantitative PCR (qPCR) was performed using primers 519F (5'-CCGTCAATTCMTTTRAGTTT-3') / 907R (5'-AAGGAAGGCAGCAGGCG-3') [36], 787F (5'-ATTAGATACCCSBGTAGTCC-3') / 1059R (5'- GCCATGCACCWCCTCT-3') [37], and Euk34-5F (5'- AGGAAGGCAGCAGGCG-3') / Euk499R (5'-CACCAGACTTGCCCTCYAAT-3') [38], respectively. Briefly, qPCR assays were conducted using 10 µl of LightCycler 480 SYBR Green I Master mix, 2 µl of sample DNA, 2 µl (final concentration 0.3 µM) of each primer in a final volume of 20 µl, in the thermocycler CFX-96 Connect (Bio-Rad, Hercules, United States). qPCR programs for bacteria and eukaryotes consisted in an initial denaturation at 95°C for 10 min, followed by 40 cycles of 15 s denaturation at 95°C, hybridization 60 s at 63°C (16S) or 15 s at 60°C (18S), and 30 s (16S) or 15 s (18S) elongation at 72°C. qPCR for archaea was done with an initial denaturation at 37°C for 10 min and 95°C for 15 min, followed by 45 cycles of 15 s denaturation at 95°C and 60 s hybridization at 60°C. Standard curves for targeted genes (bacterial 16S rRNA gene, archaeal 16S RNA gene and microeukaryotic 18S rRNA gene) were generated from a mix of plasmids representative of the environment studied (NucleoSpin® Plasmid, Macherey-Nagel, Hoerdt, France). Melting curve calculation and Tm determination were done using the Tm Calling Analysis module of CFX Maestro Software v 2.3 (Bio-Rad).

Illumina MiSeq amplicon libraries, sequencing and analysis

Microbial composition of altered and unmarked surfaces in Lascaux Cave was determined using high throughput sequencing of bacterial 16S rRNA genes, archaeal 16S rRNA genes and eukaryotic 18S rRNA genes using primers targeting bacterial V3-V4 region (341F and 805R ; 550 bp product) [39], archaeal V3-V4 region (515F and 915R ; 420 bp product) [40] and V2 eukaryotic region (18S 0067a deg and 18S NSR399 ; 350 bp product) [41], respectively. All primers were tagged with the Illumina adapter sequences (TCG TCG GCA GCG TCA GAT GTG TAT AAG AGA CAG and GTC TCG TGG GCT CGG AGA TGT GTA TAA GAG ACA G) allowing the construction of amplicon libraries by a two-step PCR. All PCR reactions were carried out following Bontemps et al. (*in prep*). High-throughput sequencing was achieved after pooling PCR triplicates using Illumina MiSeq (2 x 300 bp, chemistry v3), and was performed by Microsynth (Balgach, Switzerland), aiming for each sample at 40,000 sequences for bacterial 16S rRNA gene and eukaryotic 18S rRNA gene, and 70,000 sequences for archaeal 16S rRNA gene (to compensate for some primer aspecificity).

For each dataset, paired-end reads were demultiplexed according to exact match adaptors (removed) and reads were merged with a maximum of 10% mismatches in the overlap region using FLASh [42]. Denoising procedures were carried out by discarding reads without the expected length (200-500 bp) or containing any ambiguous bases (N). After dereplication of sequences, clusterisation of sequences into OTUs was performed using SWARM [43], which uses a local clustering threshold (rather than a global clustering threshold) and an aggregation distance of 3.0 for identification of operational taxonomic units (OTUs). Chimeric sequences were discarded using VSEARCH [44]. OTUs with low abundance ($\leq 0.0005\%$) were filtered, i.e. keeping OTUs representing at least 0.005% of the dataset, along with singletons that were also removed from

the datasets. Taxonomic affiliation was performed using both RDP Classifier and BLASTn [45] against the 138.1 SILVA database [46] for Bacteria, Archaea and Eukaryotes, which was automated in the FROGS pipeline [47]. Contaminant OTUs identified from the negative control samples (blanks) were removed and the eukaryotic dataset was manually curated for metazoan sequences (data not shown). Finally, samples were randomly resampled to lowest number of sequences retrieved per sample, that is 127,994, 11,353 and 210,384 sequences for bacterial, archaeal and microeukaryotic datasets, respectively, to allow comparisons between samples (Supplementary Table S2). Raw sequences were deposited in the NCBI public database under Bioproject PRJNA860536.

Illumina NovaSeq 6000 metagenomic library preparation, sequencing and analysis

Three metagenomic libraries were constructed for limestone samples and three others for black stains, using NEBNext Ultra^{tm} DNA Library Prep Kit (fragment size $\approx$ 350 bp, Illumina, San Diego, United States) according to the manufacturer's recommendations. Sequencing was performed by Genewiz company (Germany) using Illumina NovaSeq 6000 system 2 x 150 bp. Adapter sequences were removed from the metagenomic data on the instrument and sequence data were exported in FASTQ files. Datasets were quality filtered using Trimmomatic [48] with default settings. All metagenomes were then pooled and co-assembled using MEGAHIT [49]. Reads were mapped against contigs using Bowtie to estimate coverage [50]. Assembly quality was evaluated using prinseq [51] and presented in Supplementary Table S2. Gene prediction was achieved using Prodigal [52] and rRNA detected using barrnap [53], before classification using RDP classifier [54]. The latest versions of KEGG [55], MetaCyc [56] and COG [57] databases (April 2022) were used for functional annotation. To allow sample comparisons, metagenomes were normalized to the lowest number of sequences (151,801,037 reads, see Supplementary Table S1 for details).

In addition, reconstruction of genomic bins was performed, using the two binning algorithms MetaBAT-2 [58] and Maxbin 2.0 [59] and contigs longer than 2000 bp. Redundant bins obtained from both binning algorithms were identified and removed using DAS Tool [60]. The completeness and contamination level of the combined genomic bins were then evaluated using CheckM for prokaryotic bins [61] and Busco for microeukaryotic bins [62]. Only bins with a contamination level under 5% and completeness above 75% were analyzed and represented using 'circlize' package in R software [63]. Genetic composition of bins was then explored using KEGG [55], MetaCyc [56] and COG [57] databases, based on genes identified in the co-assembly. Metabolic pathways in which 75% of the genes were present were considered and represented using '*circlize*' and '*CircleHeatmap*' packages in R software [63]. Raw sequences were deposited in the NCBI public database under Bioproject PRJNA860536 and bin files are available in FigShare ($doi.org/10.6084/m9.figshare.20626854.v1$).

Statistical analyses

Rarefaction curves were calculated to assess sequencing efficacy, using Paleontological Statistics (PAST) software v4.02 [64]. OTU richness and diversity were estimated using Chao 1 index [65] and Shannon H' [66]. Communities were primarily compared with Non-metric MultiDimensional Scaling (NMDS) based on the Bray-Curtis dissimilarity matrix, using '*vegan*' package in R

v4.0.2 [67,68]. The procedure computes a stress value, which measures the difference between the ranks on the ordination configuration and the ranks in the original dissimilarity matrix for each replicate. Stress values below 0.1 are ideal, those below 0.2 acceptable (especially if close to 0.1), while values above 0.2 point to limited interpretation potential [69]. Analysis of similarity (ANOSIM) was conducted using the '*vegan*' package in R, to test differences ($P \leq 0.05$) in overall community composition between different sampling zones (unmarked surfaces vs dark zones) and to further confirm the results observed in the NMDS plot. Student *t*-tests and Wilcoxon tests were performed using '*stats*' package in R [67], to test differences ($P \leq 0.05$) in diversity index and metabolic classes between different sampling zones (unmarked surfaces vs dark zones). The radar plot was performed using '*plotly*' package [70]. Enrichment plot was made using the '*enrichplot*' and '*fcros*' packages in R [71,72], and *P* value was estimated by a hypergeometric distribution.

Results

Microbial community structure and composition in black stains vs unmarked surfaces

Metabarcoding analysis of bacterial 16S rRNA genes indicated that bacterial community structure strongly differed between black stains and unmarked surfaces, but variability also occurred between black stains and between unmarked surfaces (Fig 1A). The bacterial community in unmarked surfaces was richer (evaluated through Chao-1 ; $P = 0.009$) but less diverse (evaluated through Shannon H' ; $P = 0.003$) compared with black stains. Bacterial community composition at the taxonomic class level was similar for the three unmarked surface replicates and especially the three black stain replicates, but unmarked surfaces and black stains differed. In particular, the relative abundance of Gammaproteobacteria class showed the highest variation (-26.4% in black stains compared with unmarked surfaces) followed by Alphaproteobacteria (+9.9%), Bacteroidia (+4.4%), Actinobacteria (+3.6%) and Chloroflexia (+2.2%).

Metabarcoding analysis of archaeal 16S rRNA genes indicated that archaeal community structure of black stains and unmarked surfaces differed statistically despite replicate variability, as for bacteria, but differences between diversity indices were not significant (both for richness and diversity) (Fig 1B). The *Nitrososphaeraceae* family dominated, with more than 99% of sequences in black stains and in unmarked surfaces, but lower taxonomic levels could not be investigated due to database limitation.

Metabarcoding analysis of microeukaryotic 18S rRNA genes evidenced a difference in microeukaryotic community structure between black stains and unmarked surfaces (Fig 1C). Shannon H' (diversity) was higher in black stains ($P = 0.022$) but Chao-1 (richness) did not differ. Community composition at the class level was similar for the three unmarked surface replicates and especially the three black stain replicates, but unmarked surfaces and black stains differed significantly. Most microeukaryotic sequences were affiliated to Ascomycota fungi (83.2% of 18S rRNA sequences). Strong variation in relative abundance was found for the Eurotiomycetes class (+70.5% in black stains compared with unmarked surfaces) and the Sordariomycetes class (-64.5%), followed by the Conoidasida (-5.6%).

Metagenomic analysis of the whole community showed variability between replicates, and

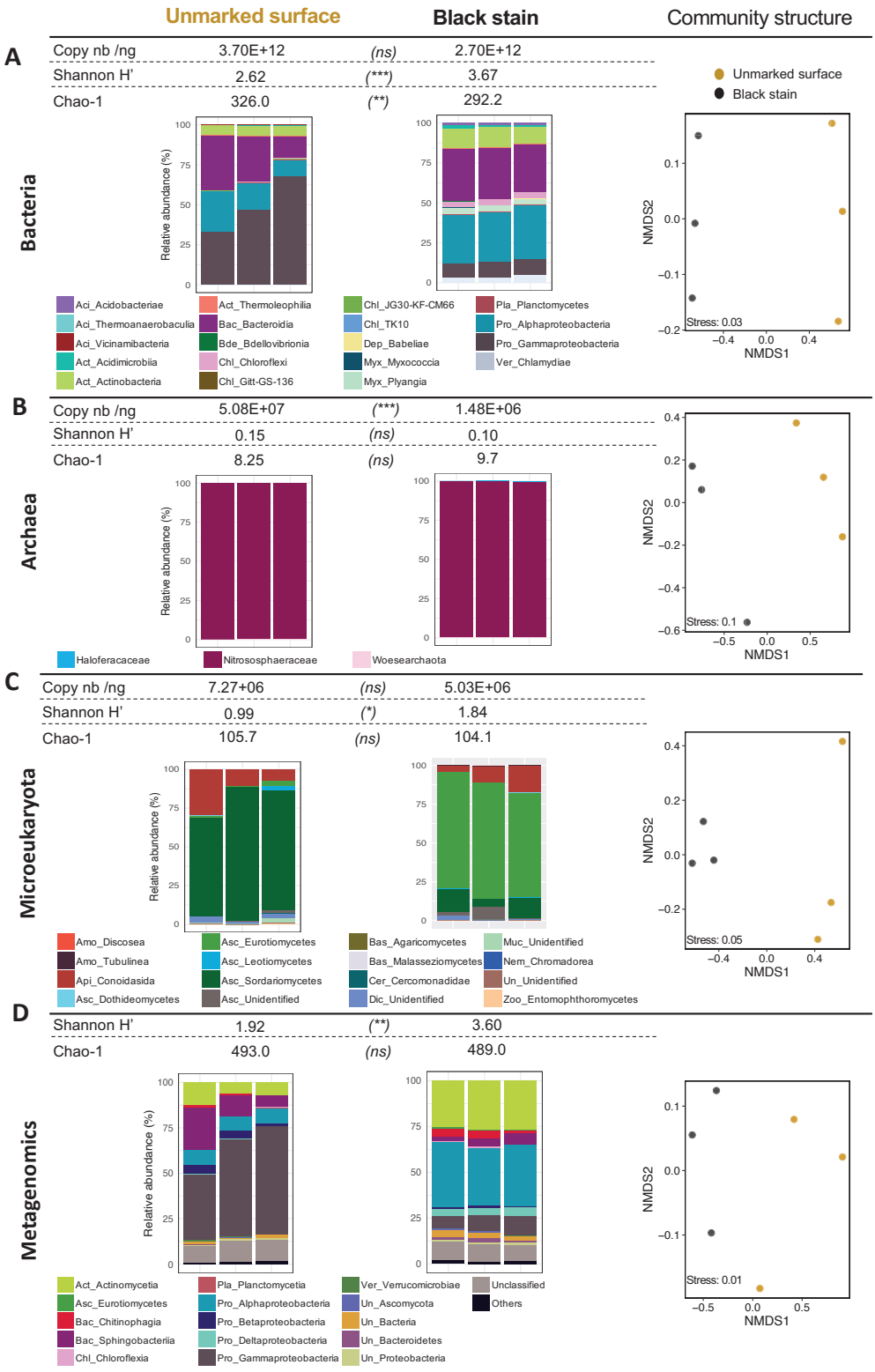

Fig 1. Abundance, diversity and community structure in unmarked surfaces and black stains of Lascaux Cave. Data are shown for bacteria (A) archaea (B), microeukaryotes (C) and the total community by shotgun metagenomics (D). Microbial abundance (qPCR) is shown in A-C, diversity (Shannon H' and Chao-1 indices), the distribution of the most abundant classes (i.e. consisting in $> 0.01\%$ of total normalized sequences) and NMDS analysis of microbial communities in A-D. Copy nb/ng : Gene copy number / ng ADNg in sample. Significance of t tests : (ns), not-significant ; (*),$P < 0.05$; (**),$P < 0.01$; (***),$P < 0.005$.

overall community structure differed significantly between black stains and unmarked surfaces (Fig 1D). Shannon H' diversity index (but not Chao-1 index) was significantly higher in black stains ($P = 0.007$). In metagenomes, 85.5%, 0.7% and 0.5% of sequences were affiliated with Bacteria, Microeukaryotes and Archaea, respectively (Supplementary Table S2). Black stain replicates rather than unmarked surface replicates displayed similarities in whole community composition. Overall, the highest variation in relative abundance was found for bacterial classes, i.e. Gammaproteobacteria (-42.8% in black stains compared with unmarked surfaces), Alphaproteobacteria (+24.9%), Actinomycetia (+17.0%), Sphingobacteriia (-7.3%), Deltaproteobacteria (+4.0%) and Chitinophagia (+2.6%), followed by fungal classes Eurotiomycetes (+0.47%) and Sordariomycetes (-0.4%).

Microbial community size in black stains vs unmarked surfaces

Quantification of bacterial 16S rRNA genes did not show any difference between black stains and unmarked surfaces ($P = 0.13$), with $2.7 \pm 4.3 \times 10^{12}$ and $3.7 \pm 2.6 \times 10^{12}$ gene copies / ng of total DNA, respectively (Fig 1A). The difference was not significant either for microeukaryotic 18S rRNA genes ($P = 0.423$), with $5.0 \pm 3.6 \times 10^{6}$ (black stains) and $7.3 \pm 2.4 \times 10^{6}$ (unmarked surfaces) gene copies / ng of total DNA (Fig 1C). However, archaeal 16S rRNA genes showed lower copy number ($P = 0.001$) in black stains ($1.5 \pm 1.8 \times 10^{6}$ copies / ng of total DNA) than unmarked surfaces ($5.1 \pm 2.8 \times 10^{7}$ copies / ng of total DNA) (Fig 1B).

Genetic potential in black stains vs unmarked surfaces

Shotgun metagenomes from unmarked surfaces and black stains allowed the identification of 9,822 different genes (KEGG orthologues). Certain genes involved in metabolic categories of type B (in reference to the BRITE hierarchy ; Kaneisha and Goto 2000) were significantly enriched in black stains compared with unmarked surfaces (Fig 2A), i.e. Environmental adaptation (fold change ratio of 1.18, $P = 0.027$), Antimicrobial (drug resistance) (ratio 1.11, $P = 0.0001$), Amino acids metabolism (ratio 1.05, $P = 0.025$), Metabolisms of cofactors and vitamins (ratio 1.03, $P = 0.0001$) and Cell motility (1.03, $P = 0.0001$). On the contrary, other metabolic categories displayed a fold change ratio lower than 1.0 but this was not significant at $P \leq 0.05$, i.e. Development (ratio 0.53, $P = 0.60$), Signaling molecules and interaction (ratio 0.73, $P = 0.45$) and Cell growth and death (ratio 0.90, $P = 0.81$).

A more in-depth analysis of pathways classes (category C) showed that several of their genes were less abundant in black stain communities compared with unmarked surface conditions, i.e. Bacterial motility (87,671 vs 173,764 genes ; $P = 0.0001$), Antimicrobial resistance (14,994 vs 96,993 genes ; $P = 0.002$), Biofilm formation (160,815 vs 260,746 genes ; $P = 0.012$) and Phenazine biosynthesis (8,950 vs 77,907 genes ; $P = 0.009$) (Fig 2B). Conversely, genes involved in pathway class Phenylpropanoid biosynthesis were more abundant in black stains than in unmarked surfaces (1,410 vs 304 genes ; $P = 0.04$).

Genes involved in melanin synthesis were not identified. A focus made on Aromatic compounds degradation indicated that functional genes were comparatively more abundant in black stains when considering Aminobenzoate degradation (69,113 vs 41,386 genes ; $P = 0.003$), Polycyclic aromatic hydrocarbon degradation (15,777 vs 8,099 genes ; $P = 0.004$) and Styrene

Fig 2. Functional capacity in unmarked surfaces and black stains of Lascaux Cave. (A) Functional capacity enrichment analysis of all KEGG pathways showing community enrichment in black stains vs unmarked surfaces. The values on the X axis indicate the fold enrichment ratio of the relative percentages of metabolic pathways upregulated on black stains. Dark green circles indicate categories for which enrichment was significant (P $<$ 0.05 in a one-sided hypergeometric test) and light green circles indicate categories with $P > 0.05$. (B) Relative proportion of metabolic pathways from unmarked surfaces (yellow) and black stains (grey). The relative abundance of selected pathways was analyzed using a matrix that was square-root-transformed to minimize the impact of highly dominant functional classes. Significance of Wilcoxon tests : -, not-significant ; *,$P < 0.05$; **,$P < 0.01$; ***,$P < 0.005$. PAH : Polycyclic Aromatic Hydrocarbons.

degradation (29,052 vs 12,713 genes ; $P = 0.0002$) (Fig 2B). Black stains and unmarked surfaces displayed similar numbers of genes ($P = 0.002$) associated to Benzoate degradation (188,814 vs 174,155 genes ; $P = 0.47$) and Dioxin degradation (24,180 vs 25,940 genes ; $P = 0.91$), whereas

Xylene degradation was the only pathway class less abundant in black stains (38,380 genes) than unmarked surfaces (68,026 genes).

Metagenome-assembled genomes in black stains vs unmarked surfaces

A total of 31 bins with > 75% completeness and < 5% contamination levels were reconstructed from metagenomes of Lascaux Cave (Supplementary Table S3 and Fig. 3). The most represented lineages in reconstructed bins were Alphaproteobacteria (9 different bins), Actinobacteria (4 bins), Bacteroidetes (4 bins) and Gammaproteobacteria (4 bins) (Figs. 3 and Supplementary figure S2). Metabolic capabilities were inferred from these genomic bins, as follows.

First, the focus was on pigment biosynthetic pathways that could account for the black shade of altered surfaces, and that would be expected in bins reconstructed from black stains rather than unmarked surfaces. Accordingly, a genetic potential for carotenoid and melanin biosynthesis was detected in black stain bins, but not in bins from unmarked surfaces (Fig. 3 and Supplementary figure S2). More specifically, the Carotenoid biosynthesis pathway (with *crt* genes) was identified in the bin for the pigmented fungus *Exophiala*, whereas the L-DOPA degradation pathway (with a tyrosinase-encoding gene) was found in four bins affiliated to bacteria (Actinomycetia class, Bacteroidetes phylum, and *Chitinophaga* genus) and the fungus *Exophiala*.

Second, due to the past application of biocides, genes involved in aromatic compound degradation were expected in and outside black stains. Several bins from black stains, two affiliated with Actinobacteria and one with Ascomycota, included genes for Xylene degradation (*xylA, xylB, xylC* and *xylM*) not found in bins from unmarked surfaces (Figs. 3 and Supplementary figure S2). Genes encoding Phenylethylamine degradation I pathway (*maoA* and *padA*) were the only ones present exclusively in unmarked surface bins (affiliated to *Pseudomonas* genus). The genes *xylEFJK* and *todGHI* of the catechol degradation pathway were identified only in Alphaproteobacteria (*Hyphomicrobium*) and Actinobacteria bins from black stains. The Catechol degradation III pathway and Catechol degradation to β-ketoadipate pathway (genes *catABC* and *pcaDJF* present in both metabolic pathways) were found in three bins, i.e. two Alphaproteobacteria reconstructed from both rock surface conditions (*Phyllobacterium* and *Bradyrhizobium*) and one Ascomycota reconstructed from black stains (Fig. 3). Benzoate degradation I pathway (*benABCD* and *xylLXYZ* genes) was identified in bins affiliated with Betaproteobacteria (from both rock surface conditions) and Actinobacteria (from black stains). In contrast, Phenol degradation I metabolic pathway was found in two bins reconstructed only from black stain samples (*Hyphomicrobium* and Actinobacteria) (Fig. 3). Chloride compound degradation was also widespread in the community, and it corresponded to many metabolic pathways for degradation of (i) 3-chlorocatechol, (ii) 3,4-dichlorocatechol, (iii) 3,4,6-trichlorocatechol, (iv) 4-sulfocatechol, (v) 1,4-dichlorobenzene and (vi) 2,4,6-trichlorotoluene. These pathways were always retrieved together in 6 bins affiliated to the bacteria *Pseudomonas* (from unmarked surfaces), *Sphingomonas*, *Chitinophaga*, *Phyllobacterium* and *Mezorhizobium* (reconstructed from both rock surface conditions), or the fungus *Exophiala* (from black stains). Therefore, the hypothesis that genes for aromatic compound degradation would be well present both in and outside black stains proved correct.

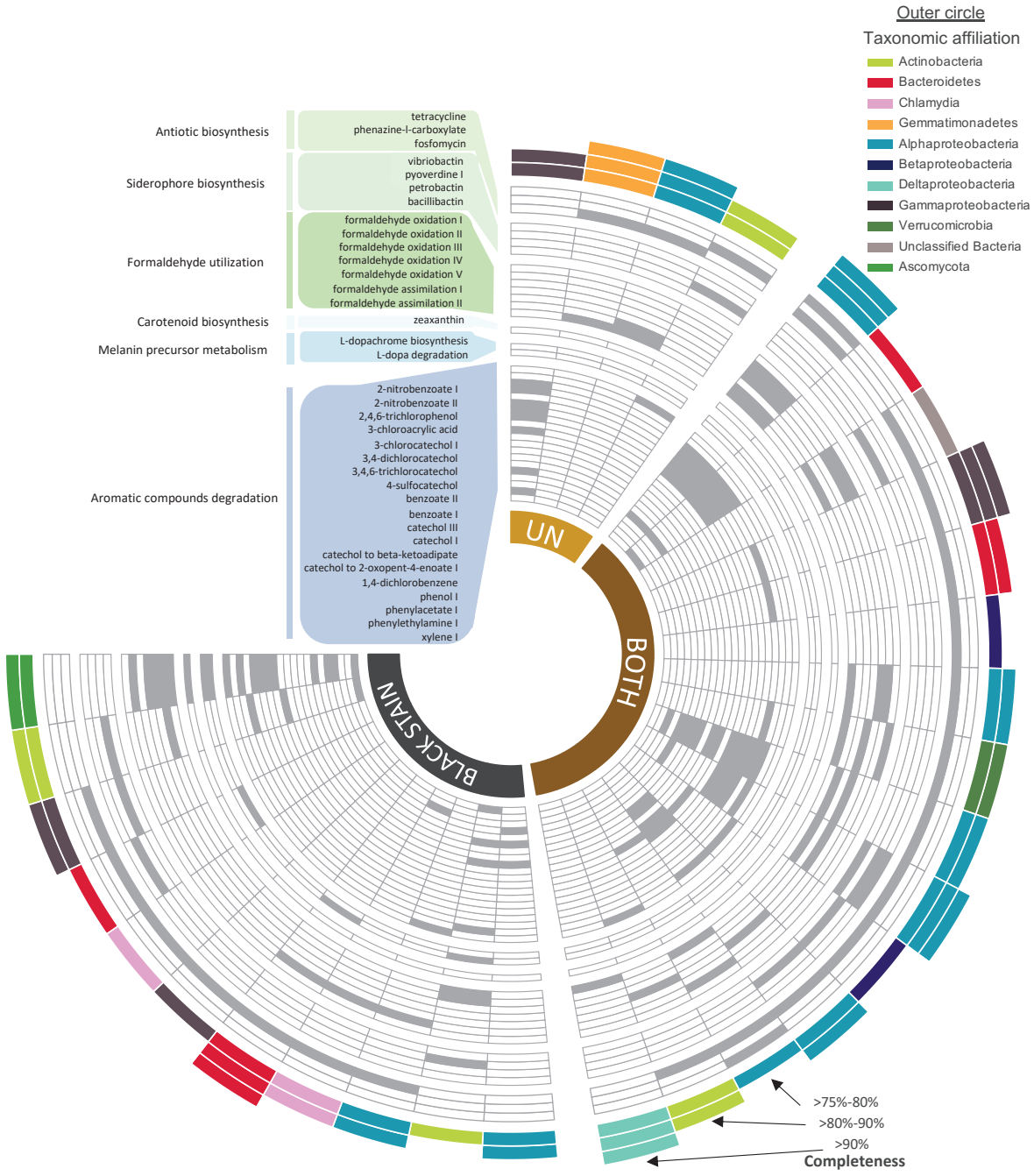

Fig 3. Key metabolic pathways identified in reconstructed genomic bins. Six metabolic classes are represented : Antibiotic biosynthesis, Siderophore biosynthesis, Formaldehyde utilization, Carotenoid biosynthesis, Melanin precursor metabolism and Aromatic compounds degradation. Colors in the outer circle represent the taxonomic affiliation of the bins. Details of genomic bins (ID, completeness, contamination, taxonomy and coverage) are presented in Supplementary Table S3.

Third, we considered metabolic pathways involved in synthesis of antimicrobial compounds that might inhibit pigmented microorganisms on the unmarked surfaces. Pathways associated to antibiotic biosynthesis were detected in 23 bins reconstructed from all rock surface conditions, mainly affiliated with Alphaproteobacteria (9 bins) and Bacteroidetes (4 bins) (Figs. 3 and Supplementary figure S2). More precisely, Fosfomycin biosynthesis potential was detected in the bins BIN 8 *Sphingomonas* and BIN 62 *Agrobacterium* reconstructed from unmarked sur-

faces and black stains. In contrast, Tetracycline biosynthesis potential was detected in 22 bins from all rock surface conditions and thus widespread in the community. In unmarked surfaces, Siderophore biosynthesis (Pyoverdine I) was detected only once in an Actinobacteria bin. Pyoverdine biosynthesis was detected in 3 bins reconstructed from both rock surfaces (affiliated to Alphaproteobacteria, Betaproteobacteria and unidentified Bacteria) and 3 bins from black stains (affiliated to Actinobacteria, Actinomycetia and *Pseudomonas*). Potential for Bacillibactin, Petrobactin and Vibriobactin biosynthesis was evidenced in an Alphaproteobacteria (*Mesorhizobium*) bin reconstructed from unmarked surfaces and black stains. Therefore, in contrast to our hypothesis, biosynthesis pathways for antimicrobials were found not only in bins reconstructed from unmarked surfaces but also in bins for black stains.

Comparison of *Pseudomonas* bins

Previous work on Lascaux black stains highlighted that *Pseudomonas* bacteria were counter-selected (34-63% of 16S rRNA sequences in unmarked surfaces compared with 0.01-0.11% in black stains ; [35]), prompting a focus on *Pseudomonas* bins to determine whether *Pseudomonas* from black stains (i.e. having resisted counter-selection effects) vs unmarked surfaces have different ecological strategies because of the particularities of their respective environments. Here, two bins affiliated to the *Pseudomonas* genus were reconstructed in Lascaux Cave microbial community. One bin (BIN 27) named *Pseudomonas* sp. was retrieved only in black stain samples, while another bin (BIN 1) affiliated to *Pseudomonas spelaei* was reconstructed only from unmarked surface samples (Fig. 4, Supplementary Table S1). The *Pseudomonas* sp. bin harbored 208 metabolic pathways, while only 118 pathways were detected in the *Pseudomonas spelaei* bin, and these differences were observed in several pathway classes.

Only 4 of 18 aromatic compound degradation pathways (i.e. 22%) were identified in the two reconstructed *Pseudomonas* bins (e.g. 3-amino-5-hydroxybenzoate biosynthesis, 3-dehydroquinate biosynthesis I), while 61% of Aromatic compounds degradation pathways (e.g. 4-aminobutyrate degradation I, Benzoate degradation I, Xylene degradation, etc.) were detected only in the *Pseudomonas* sp. bin (Fig. 4). In the *Pseudomonas spelaei* bin, only two Aromatic compound degradation pathways (2-nitrobenzoate degradation I and Gentisate degradation) were identified.

A total of 29 of 37 Carbohydrate pathways (i.e. 78%) were detected only in the *Pseudomonas* sp. bin (e.g. Sucrose degradation IV, GDP-mannose biosynthesis, dTDP-L-rhamnose biosynthesis I, etc.) while only 4 pathways affiliated to this metabolic class (Trehalose biosynthesis IV, 2-amino-3-carboxymuconate semialdehyde degradation, UDP-D-galacturonate biosynthesis I) were identified in the *Pseudomonas spelaei* bin (Fig. 4). Fermentation (e.g. Heterolactic fermentation), Formaldehyde (e.g. Formaldehyde oxidation IV) and Inorganic nutrients (e.g. Phosphonoacetate degradation) metabolic pathway classes were identified only in the *Pseudomonas* sp. bin (Fig. 4).

As many as 6 of 11 secondary metabolite biosynthesis pathways were detected only in the *Pseudomonas* sp. bin (Biosynthesis of vancomycin group antibiotics, Inositol metabolism, Isoprene biosynthesis, Phenazine biosynthesis, etc.), while only 2 of them were identified in the *Pseudomonas spelaei* bin (β-carboline biosynthesis) (Fig. 4). Thus, as expected, the overall

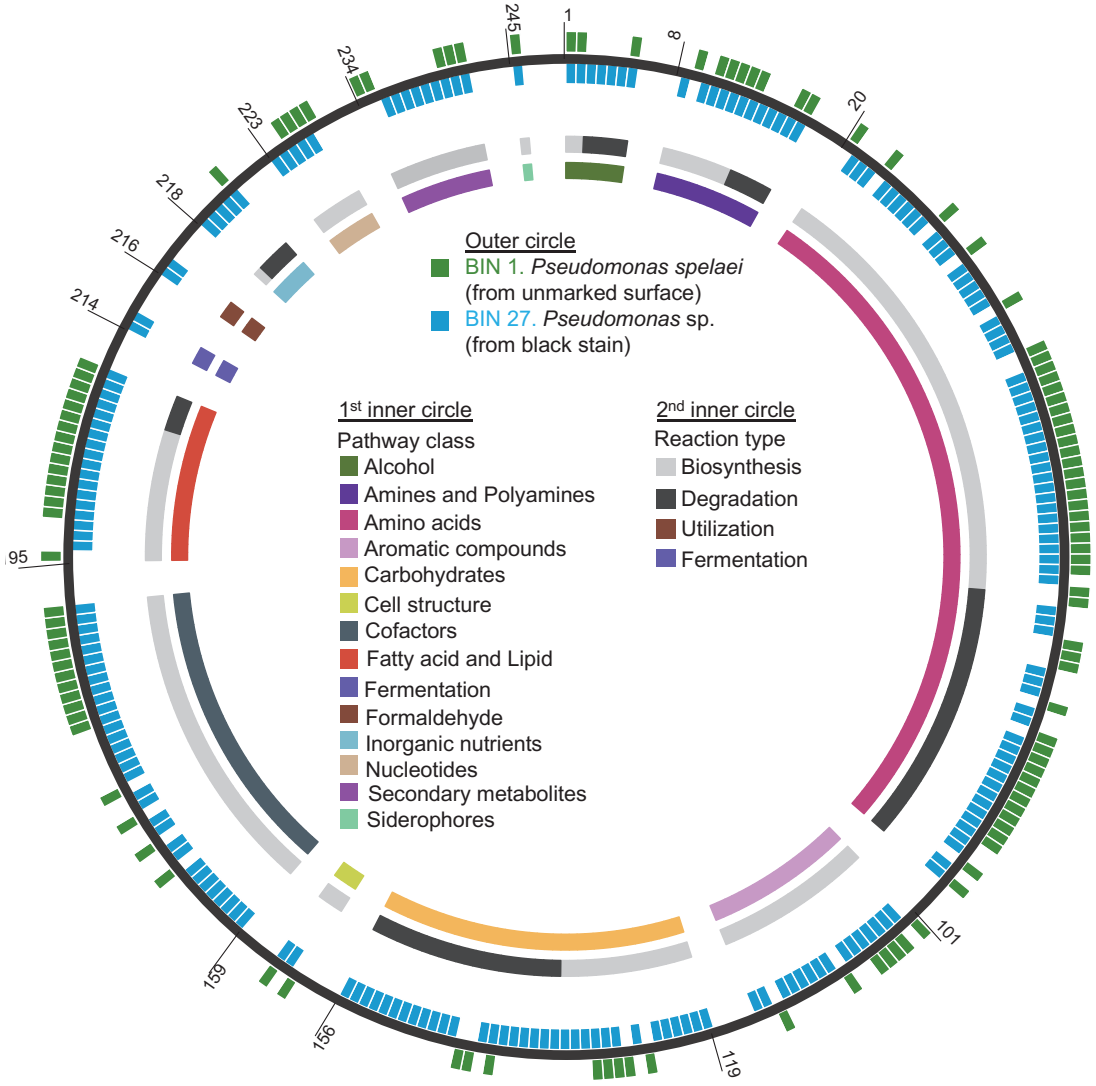

Fig 4. Metabolic profile comparison of two genomic bins affiliated with *Pseudomonas* genus in unmarked surfaces (BIN 1) and black stains (BIN 27). Colors in the inner circles represent (i) pathway class affiliation and (ii) reaction type. Presence of metabolic pathways in BIN 1 (in green) and BIN 27 (in blue) is represented by squares in the outer circle. Details of metabolic pathways are presented in Supplementary Table S4 (name, class and type of reaction).

functional potential of the two *Pseudomonas* reconstructed genomes differed, with 118 metabolic pathways in the bin from unmarked surfaces vs as many as 209 in the bin from black stains.

Discussion

This work was undertaken to test whether key hypotheses put forward on the formation of Lascaux black stains during pioneering work [10,33] and more recent investigations [31,35] could be strengthened by a metagenomic approach focusing on the diversity and especially the genetic potential of microbial communities. Several bacterial classes notably Actinomycetia, Sphingobacteriia, Chitinophagia, Betaproteobacteria and Deltaproteobacteria, collectively representing a quarter of microbial sequences, were identified only by PCR-free metagenomic sequencing (Fig. 1), highlighting that metabarcoding primers may introduce a bias. On one hand, metagenomics

expanding the range of microbial diversity documented so far in Lascaux. On the other hand, metagenomics was not effective to analyze microeukaryotic and archaeal communities, probably because their abundance was very low in comparison with bacterial sequences, both in and outside stains. This suggests that the bacterial community might play a predominant role in the processes leading to the formation of black stains. As in previous studies [10,31,35], strong community changes were observed from unmarked surfaces to black stains, with e.g. the selection of Alphaproteobateria and Eurotiomycetes and counter-selection of Gammaproteobacteria and Sordariomycetes in black stains. These modifications took place without significant changes in bacterial or microeukaryotic abundance, according to previous findings in another Lascaux room [31] (Fig. 1). Here, however, qPCR analyses were extended to the case of archaea, which evidenced a smaller archaeal community in black stains but without apparent taxonomic change community still dominated by the Nitrososphaeraceae family).

Previous studies have suggested that the black shade of the stains was due to melanin from pigmented fungi (*Ochroconis*, *Exophiala*, *Acremonium* etc.) [31,33]. Accordingly, metabolic pathways for synthesis of melanin (or its precursors) were more prevalent in black stains. In particular, tyr genes (tyroninase) were identified only in black stains and in bins from black stains. These bins were bacterial (*Chitinophaga*, Actinomycetia, Bacteroidetes) or fungal (*Exophiala*). Indeed, melanins can be produced both by bacteria (catechol melanin, DHN-melanin and pyomelanin) and fungi (DHN-melanin, GHB-melanin and DOPA-melanin), and they can be evidenced in laboratory colonies presenting black or dark brown colors and corresponding to various microbial species [30,32,73]. Tyrosinase is a key regulator and rate-limiting melanogenic enzyme [74], which uses molecular oxygen to catalyze (i) the ortho-hydroxylation of monophenols to ortho-diphenols and (ii) the oxidation of ortho-diphenols to ortho-quinones [75,76]. These reactions convert L-tyrosine to L-dopa and L-dopa to dopaquinone, respectively. Dopaquinone can spontaneously react to form the eumelanin precursor L-dopachrome [77,78]. Genes for L-dopa metabolism were detected in the bacterial genus Chitinophagia. For the first time in Lascaux Cave, we show that bacteria present in black stains have the potential to synthesize melanin. The fungal genus *Exophiala* is known for its production of melanin [10,14], and here it was identified in higher abundance in black stains than in unmarked surfaces based on 18S rRNA metabarcoding. In addition, the *Exophiala* bin reconstructed from black stains presented the genetic potential for synthesis of carotenoid pigments in particular zeaxanthin, a yellow-brown pigment documented in fungi [80]. Therefore, *Exophiala* might be a major player in black stain formation through synthesis of both melanin and carotenoids. Overall, our results strengthen the hypothesis that genetic pathways for melanin synthesis are prevalent in black stains, while extending the range of microorganisms potentially involved in their synthesis.

Previous laboratory studies on Lascaux isolates have pointed that melanin synthesis was likely stimulated by the degradation of aromatic biocides previously applied onto cave walls, which probably favored melanin-producing microorganisms. Accordingly, genes and pathways for degradation of aromatic compounds were found both in and outside black stains, but were more prevalent in black stains. This concerned the genetic potential for Aminobenzoate degradation, Polycyclic Aromatic Hydrocarbon (PAHs) degradation, and Styrene degradation, which might be useful for the metabolism of catechol, a melanin precursor [81,82]. Thus, the *xyl*, *cat* and *tod*

gene clusters involved in catechol degradation were identified in bins reconstructed only from black stains (Actinobacteria, *Hyphomicrobium*, *Exophiala*) or from both rock surface conditions (*Phyllobacterium*, *Bradyrhizobium*). The catechol meta-cleavage pathway involves conversion of benzoate into catechol, while the catechol ortho-cleavage pathway allows the production of succinyl-CoA and acetyl-CoA, necessary for the biosynthesis of DHN-melanin [77]. To allow the formation of catechol-melanin, a disproportionation reaction between catechol and a benzoquinone (produced either by catechol oxidase or by degradation of 2,4,6-trichlorotoluene, as observed here in the *Pseudomonas spelaei* bin) can generate radical semi-quinones. Alternatively, benzoquinones can react with H_2O to generate 1,2,4-trihydroxybenzene [77,83]. Spontaneous reactions (still not well understood) generate aromatic biphenolic dimers or diphenylene-dioxide-2,3-quinone, resulting in an undefined catechol-melanin polymer [32,84].

One major biocide used in Lascaux was BAC [1]. Exposure of microbial communities to BAC can result in lower diversity and the enrichment of BAC-resistant taxa, especially *Pseudomonas* species [85]. Here, we evidenced that *Pseudomonas* abundance was lower in black stains than unmarked surfaces, based on metabarcoding and shotgun metagenomics, in agreement with previous studies in Lascaux Cave [31,35](Bontemps et al. *in prep*). Certain *Pseudomonas* strains can degrade BAC by dealkylation [18,79], yielding the degradation products benzyldimenthylamine, benzylamine and benzoic acid [87]. In this work, functional genes involved in benzoate, dioxin and xylene degradation were found in several taxa (e.g. *Pseudomonas*, Betaproteobacteria) from unmarked surfaces. This might be relevant also for degradation of BAC, which also possesses a benzene structure [16]. Indeed, degradation of benzene compounds by soil isolates from these taxa has been demonstrated [88,89]. Microbial degradation is effective to reduce environmental toxicity of BAC [18,79], which can promote community changes (24). In Lascaux, such processes are perhaps important for the selection of pigmented microorganisms and counter-selection of *Pseudomonas* in black stains, where these bacteria are in lower numbers and genetically different compared with *Pseudomonas* strains outside strains. For instance, the reconstructed genome of *Pseudomonas spelaei* from unmarked surfaces harbored a lower genetic repertory compared with the bin of *Pseudomonas* reconstructed in black stains.

Pseudomonas isolates from unmarked surfaces could inhibit pigmented fungi on plates [90], suggesting that microbial inhibition could be one factor accounting for limited spread of black stains in Lascaux. Metagenomics provided a wider appraisal of this possibility. On one hand, genes for biosynthesis of antifungal phenazines (as well as genes for resistance to antimicrobials and for biofilm formation) were indeed more prevalent in unmarked surfaces than in black stains. On the other hand, biosynthesis pathways for antimicrobials were identified both in bins from unmarked surfaces and bins from black stains, indicating that this hypothesis deserves further work.

Conclusion

Black stains resulting from tourism-related anthropization threaten the Paleolithic heritage of Lascaux Cave, and it is important to better understand their formation. Our metagenomic analyses reinforced previous findings and hypotheses that (i) community differences between black stains and unmarked surfaces are major, (ii) a wide range of black stain microorganisms - inclu-

ding also bacteria - may participate to pigmentation of rock surfaces (based on genes relevant for synthesis of undefined catechol melanin, DHN-melanin and DOPA-melanin or carotenoid pigments), (iii) degradation of biocide residues could have favored melanin-producing microorganisms and melanin synthesis, and (iv) microbial dynamics may be influenced significantly by antimicrobial secondary compounds, on unmarked surfaces as anticipated but probably also in black stains. Understanding microbial functioning can be important to guide future conservation strategies for Lascaux Cave.

Acknowledgements

Funding was provided by DRAC Nouvelle Aquitaine (Bordeaux, France). We thank S. Géraud, J.C. Portais, M. Mauriac (DRAC Nouvelle Aquitaine) and D. Henry-Lormelle (restorer team) for information and help, and Lascaux Scientific Board for useful discussions.

Authorship contributions statement

ZB contributed to sampling, acquired data, interpreted results, wrote the manuscript, and prepared figures and tables ; DB acquired data ; YML obtained funding, managed the project, designed the experiments, contributed to sampling, interpreted results, and revised the manuscript ; MH interpreted results and revised the manuscript.

Declaration of competing interest

The authors declare that they have no known competing financial interest or personal relationships that could have influenced the work reported in this paper.

References

1. Martin-Sanchez PM, Nováková A, Bastian F, Alabouvette C, Saiz-Jimenez C. Use of biocides for the control of fungal outbreaks in subterranean environments : The case of the Lascaux Cave in France. Environ Sci Technol. 2012 ;46 :3762–70.

2. Barton HA, Jurado V. What's up down there ? Microbial diversity in caves microorganisms in caves survive under nutrient-poor conditions and are metabolically versatile and unexpectedly diverse. 2007 ;2 :132–8.

3. Northup D, Lavoie K. Geomicrobiology of caves : Review. Geomicrobiol J. 2001 ;18 :199–222.

4. Jaubert J, Verheyden S, Genty D, Soulier M, Cheng H, Blamart D, et al. Early neanderthal constructions deep in Bruniquel Cave in southwestern France. Nature. 2016 ;534 :111–4.

5. Bastian F, Alabouvette C, Jurado V, Saiz-Jimenez C. Impact of biocide treatments on the bacterial communities of the Lascaux Cave. Naturwissenschaften. 2009 ;96 :863–8.

6. Bontemps Z, Alonso L, Pommier T, Hugoni M, Moënne-Loccoz Y. Microbial ecology of tourist Paleolithic caves. Sci Tot Environ. 2021 ;816 :151492.

7. Gauchon C, Jaillet S, Prud'homme F. Dynamique de la construction topographique et toponymique à l'aven d'Orgnac (Ardèche, France). Collection EDYTEM Cah. Géog. 2012 ;13 :157–76.

8. Chalmin E, d'Orlyé F, Zinger L, Charlet L, Geremia RA, Orial G, et al. Biotic versus abiotic calcite formation on prehistoric cave paintings : the Arcy-sur-Cure 'Grande Grotte' (Yonne, France) case. Geol Soc. 2007 ;279 :185–97.

9. Lepinay C, Mihajlovski A, Touron S, Seyer D, Bousta F, Di Martino P. Bacterial diversity associated with saline efflorescences damaging the walls of a French decorated prehistoric cave registered as a World Cultural Heritage Site. Int Biodet Biodeg. 2018 ;130 :55–64.

10. Bastian F, Jurado V, Nováková A, Alabouvette C, Saiz-Jimenez C. The microbiology of Lascaux Cave. Microbiology. 2010 ;156 :644–52.

11. Pasić L, Kovce B, Sket B, Herzog-Velikonja B. Diversity of microbial communities colonizing the walls of a karstic cave in Slovenia. FEMS Microbiol Ecol. 2010 ;71 :50–60.

12. Portillo MC, Gonzalez JM, Saiz-Jimenez C. Metabolically active microbial communities of yellow and grey colonizations on the walls of Altamira Cave, Spain. J Appl Microbiol. 2008 ;104 :681–91.

13. Mitova M, Iliev M, Nováková A, Gorbushina A, Groudeva V, Martin-Sanchez P. Diversity and biocide susceptibility of fungal assemblages dwelling in the art gallery of Magura Cave, Bulgaria. Int J Speleol. 2017 ;46.

14. Martin-Sanchez PM, Miller AZ, Saiz-Jimenez C. Lascaux Cave : An example of fragile ecological balance in subterranean environments. Berlin, Germany : De Gruyter, Inc. :2015.

15. Wessels S, Ingmer H. Modes of action of three disinfectant active substances : A review. Regul Tox Pharm. 2013 ;67 :456–67.

16. Merchel Piovesan Pereira B, Tagkopoulos I. Benzalkonium chlorides : Uses, regulatory status, and microbial resistance. Appl Environ Microbiol. 2019 ;85 :e00377-19.

17. Ertekin E, Hatt JK, Konstantinidis KT, Tezel U. Similar microbial consortia and genes are involved in the biodegradation of benzalkonium chlorides in different environments. Environ Sci Technol. 2016 ;50 :4304–13.

18. Tandukar M, Oh S, Tezel U, Konstantinidis KT, Pavlostathis SG. Long-term exposure to benzalkonium chloride disinfectants results in change of microbial community structure and increased antimicrobial resistance. Environ Sci Technol. 2013 ;47 :9730–8.

19. Patrauchan MA, Oriel PJ. Degradation of benzyldimethylalkylammonium chloride by *Aeromonas hydrophila* sp. K. J Appl Microbiol. 2003 ;94 :266–72.

20. Urzì C, De Leo F, Bruno L, Albertano P. Microbial diversity in Paleolithic caves : A study case on the phototrophic biofilms of the Cave of Bats (Zuheros, Spain). Microb Ecol. 2010 ;60 :116–29.

21. Isola D, Zucconi L, Cecchini A, Caneva G. Dark-pigmented biodeteriogenic fungi in Etruscan hypogeal tombs : New data on their culture-dependent diversity, favouring conditions, and resistance to biocidal treatments. Fungal Biol. 2021 ;125 :609–20.

22. Diaz-Herraiz M, Jurado V, Cuezva S, Laiz L, Pallecchi P, Tiano P, et al. Deterioration of an Etruscan tomb by bacteria from the order Rhizobiales. Sci Rep. 2014 ;4 :3610.

23. Ogórek R, Dyląg M, Kozak B. Dark stains on rock surfaces in Driny Cave (Little Carpathian Mountains, Slovakia). Extremophiles. 2016 ;20 :641–52.

24. Garg KL, Jain KK, Mishra AK. Role of fungi in the deterioration of wall paintings. Sci Tot Env. 1995 ;167 :255–71.

25. De Hoog G, Von Arx J. Revision of *Scolecobasidium* and *Pleurophragmium*. Kavaka. 1973 ;1 :55–60. 26. Lefèvre M. La ‘maladie verte’ de Lascaux. Stud Conserv. 1974 ;19 :126–56.

27. Dupont J, Jacquet C, Dennetière B, Lacoste S, Bousta F, Orial G, et al. Invasion of the French Paleolithic painted cave of Lascaux by members of the *Fusarium solani* species complex. Mycologia. 2007 ;99 :526–33.

28. Saiz-Jimenez C. Microbiological and environmental issues in show caves. World J Microbiol Biotechnol. 2012 ;28 :2453–64.

29. Martin-Sanchez PM, Nováková A, Bastian F, Alabouvette C, Saiz-Jimenez C. Two new species of the genus *Ochroconis*, *O. lascauxensis* and *O. anomala* isolated from black stains in Lascaux Cave, France. Fungal Biol. 2012 ;116 :574–89.

30. De la Rosa JM, Martin-Sanchez PM, Sanchez-Cortes S, Hermosin B, Knicker H, Saiz-Jimenez C. Structure of melanins from the fungi *Ochroconis lascauxensis* and *Ochroconis anomala* contaminating rock art in the Lascaux Cave. Sci Rep. 2017 ;7 :13441.

31. Alonso L, Creuzé-des-Châtelliers C, Trabac T, Dubost A, Moënne-Loccoz Y, Pommier T. Rock substrate rather than black stain alterations drives microbial community structure in

the passage of Lascaux Cave. Microbiome. 2018 ;6 :216.

32. Nicolaus RA. Melanins. Paris :Hermann ;1968.

33. Alabouvette C, Saiz-Jiménez C. Écologie microbienne de la Grotte de Lascaux. CSIC-Instituto de Recursos Naturales y Agrobiología de Sevilla (IRNAS) ; 2011.

34. Alonso L, Pommier T, Kaufmann B, Dubost A, Chapulliot D, Doré J, et al. Anthropization level of Lascaux Cave microbiome shown by regional-scale comparisons of pristine and anthropized caves. Mol Ecol. 2019 ;28 :3383–94.

35. Alonso L, Pommier T, Simon L, Maucourt F, Doré J, Dubost A, et al. Microbiome analysis in Lascaux Cave in relation to black stain alterations of rock surfaces and collembola. Environ Microbiol Rep.Submitted.

36. Laiz L, Piñar G, Lubitz W, Saiz-Jimenez C. Monitoring the colonization of monuments by bacteria : cultivation versus molecular methods. Environ Microbiol. 2003 ;5 :72–4.

37. Nehmé B, Gilbert Y, Létourneau V, Forster RJ, Veillette M, Villemur R, et al. Culture-independent characterization of Archaeal biodiversity in swine confinement building bioaerosols. Appl Environ Microbiol. 2009 ;75 :5445–50.

38. Zhu J, Zhao Y, Liu M, Gonzalez-Rivas D, Xu X, Cai W, et al. Developing a new qPCR-based system for screening mutation. Small. 2019 ;15 :e1805285.

39. Herlemann DP, Labrenz M, Jürgens K, Bertilsson S, Waniek JJ, Andersson AF. Transitions in bacterial communities along the 2000 km salinity gradient of the Baltic Sea. ISME J. 2011 ;5 :1571–9.

40. Herfort L, Kim J-H, Coolen MJL, Abbas B, Schouten S, Herndl GJ, et al. Diversity of Archaea and detection of crenarchaeotal *amoA* genes in the rivers Rhine and Têt. Aquat Microb Ecol. 2009 ;55 :189–201.

41. Dollive S, Peterfreund GL, Sherrill-Mix S, Bittinger K, Sinha R, Hoffmann C, et al. A tool kit for quantifying eukaryotic rRNA gene sequences from human microbiome samples. Genome Biol. 2012 ;13 :R60.

42. Magoč T, Salzberg SL. FLASH : fast length adjustment of short reads to improve genome assemblies. Bioinformatics. 2011 ;27 :2957–63.

43. Mahé F, Rognes T, Quince C, de Vargas C, Dunthorn M. Swarm : robust and fast clustering method for amplicon-based studies. PeerJ. 2014 ;4 :e593.

44. Rognes T, Flouri T, Nichols B, Quince C, Mahé F. VSEARCH : a versatile open source tool for metagenomics. PeerJ. 2016 ;4 :e2584.

45. Zhang J, Madden TL. PowerBLAST : a new network BLAST application for interactive or automated sequence analysis and annotation. Genome Res. 1997 ;7 :649–56.

46. Quast C, Pruesse E, Yilmaz P, Gerken J, Schweer T, Yarza P, et al. The SILVA ribosomal RNA gene database project : improved data processing and web-based tools. Nucleic Acids Res. 2013 ;41 :D590–6.

47. Escudié F, Auer L, Bernard M, Mariadassou M, Cauquil L, Vidal K, et al. FROGS : Find, Rapidly, OTUs with Galaxy Solution. Bioinformatics. 2018 ;34 :1287–94.

48. Bolger AM, Lohse M, Usadel B. Trimmomatic : a flexible trimmer for Illumina sequence data. Bioinformatics. 2014 ;30 :2114–20.

49. Li D, Liu C-M, Luo R, Sadakane K, Lam T-W. MEGAHIT : an ultra-fast single-node solution for large and complex metagenomics assembly. Bioinformatics. 2015 ;31 :1674–6.

50. Langmead B, Salzberg SL. Fast gapped-read alignment with Bowtie 2. Nat Methods. 2012 ;9 :357–9. 51. Schmieder R, Edwards R. Quality control and preprocessing of metagenomic datasets. Bioinformatics. 2011 ;27 :863–4.

52. Hyatt D, Chen G-L, LoCascio PF, Land ML, Larimer FW, Hauser LJ. Prodigal : prokaryotic gene recognition and translation initiation site identification. BMC Bioinformatics. 2010 ;11 :119.

53. Seemann T. Barrnap. 2022. Available from : *https : //github.com/tseemann/barrnap*

54. Wang Q, Garrity GM, Tiedje JM, Cole JR. Naive Bayesian classifier for rapid assignment of rRNA sequences into the new bacterial taxonomy. Appl Environ Microbiol. 2007 ;73 :5261–7.

55. Kanehisa M, Goto S. KEGG : Kyoto Encyclopedia of Genes and Genomes. Nucleic Acids Res. 2000 ;28 :27–30.

56. Karp PD, Riley M, Paley SM, Pellegrini-Toole A. The MetaCyc database. Nucleic Acids Res. 2002 ;30 :59–61.

57. Galperin MY, Wolf YI, Makarova KS, Vera Alvarez R, Landsman D, Koonin EV. COG database update : focus on microbial diversity, model organisms, and widespread pathogens. Nucleic Acids Res. 2021 ;49 :274–81.

58. Kang DD, Li F, Kirton E, Thomas A, Egan R, An H, et al. MetaBAT 2 : an adaptive binning algorithm for robust and efficient genome reconstruction from metagenome assemblies. PeerJ. 2019 ;7 :e7359.

59. Wu Y-W, Tang Y-H, Tringe SG, Simmons BA, Singer SW. MaxBin : an automated binning method to recover individual genomes from metagenomes using an expectation-maximization algorithm. Microbiome. 2014 ;2 :26.

60. Sieber CMK, Probst AJ, Sharrar A, Thomas BC, Hess M, Tringe SG, et al. Recovery of genomes from metagenomes via a dereplication, aggregation and scoring strategy. Nat Microbiol. 2018 ;3 :836–43.

61. Parks DH, Imelfort M, Skennerton CT, Hugenholtz P, Tyson GW. CheckM : assessing the quality of microbial genomes recovered from isolates, single cells, and metagenomes. Genome Res. 2015 ;25 :1043–55.

62. Simão FA, Waterhouse RM, Ioannidis P, Kriventseva EV, Zdobnov EM. BUSCO : assessing genome assembly and annotation completeness with single-copy orthologs. Bioinformatics. 2015 ;31 :3210–2.

63. Gu Z. Circlize : Circular visualization. 2022. Available from : $https : //CRAN.R - project.org/package = circlize$

64. Hammer Ø, Harper D., Ryan P. PAST : paleontological statis- tics software package for education and data analysis. Palaeontol Electron. 2001 ;4 :1-9.

65. Chao A. Estimating the population size for capture-recapture data with unequal catchability. Biometrics. 1987 ;43 :783–91.

66. Shannon CE. A mathematical theory of communication. Bell Syst Tech J. 1948 ;27 :623–56.

67. Oksanen J, Blanchet FG, Friendly M, Kindt R, Legendre P, McGlinn D, et al. vegan : community ecology package. 2020. Available from : $https : //CRAN.R - project.org/package = vegan$

68. R Core Team. R : A language and environment for statistical computing. Vienna, Austria : R Foundation for Statistical Computing ; 2020. Available from : $https : //www.R - project.org/$

69. Clarke KR. Non-parametric multivariate analyses of changes in community structure. Aust J Ecol. 1993 ;18 :117–43.

70. Sievert C. Interactive web-based data visualization with R, plotly, and shiny. 2022. Available from : $https : //plotly - r.com/$

71. Yu G, Hu E. enrichplot : Visualization of functional enrichment result. Bioconductor version : Release (3.15) ; 2022. Available from : $https : //bioconductor.org/packages/enrichplot/$

72. Dembele D. fcros : A method to search for differentially expressed genes and to detect recurrent chromosomal copy number aberrations. 2019. Available from : $https : //CRAN.R - project.org/package = fcros$

73. Ischia M, Wakamatsu K, Napolitano A, Briganti S, Garcia-Borron J-C, Kovacs D, et al. Melanins and melanogenesis : methods, standards, protocols. Pigment Cell Melanoma Res. 2013 ;26 :616–33.

74. Riley PA, Borovansky J. Melanins and melanosomes : Biosynthesis, structure, physiological and pathological functions. Hoboken, NJ : John Wiley and Sons, Inc ; 2011.

75. Buchert J, Selinheimo E, Kruus K, Mattinen M-L, Lantto R, Autio K. 6 - Using

crosslinking enzymes to improve textural and other properties of food. Woodhead Publishing ; 2007 :101–39.

76. Zaidi KU, Ali AS, Ali SA, Naaz I. Microbial tyrosinases : Promising enzymes for pharmaceutical, food bioprocessing, and environmental industry. Biochem Res Int. 2014 ;2014 :854687.

77. Solano F. Melanins : Skin pigments and much more—Types, structural models, biological functions, and formation routes. New J Sci. 2014 ;2014 :e498276.

78. Munoz-Munoz JL, García-Molina F, Varón R, Tudela J, García-Cánovas F, Rodríguez-López JN. Generation of hydrogen peroxide in the melanin biosynthesis pathway. Biochim Biophys Acta. 2009 ;1794 :1017–29.

79. Schnitzler N, Peltroche-Llacsahuanga H, Bestier N, Zündorf J, Lütticken R, Haase G. Effect of melanin and carotenoids of *Exophiala dermatitidis* on phagocytosis, oxidative burst, and killing by human neutrophils. Infect Immun. 1999 ;67 :94–101.

80. Rapoport A, Guzhova I, Bernetti L, Buzzini P, Kieliszek M, Kot AM. Carotenoids and some other pigments from fungi and yeasts. Metabolites. 2021 ;11 :92.

81. Neujahr HY, Kjellén KG. Phenol hydroxylase from yeast. Reaction with phenol derivatives. J Biol Chem. 1978 ;253 :8835–41.

82. Powlowski J, Shingler V. Genetics and biochemistry of phenol degradation by *Pseudomonas* sp. CF600. Biodegradation. 1994 ;5 :219–36.

83. Schuchmann MN, Bothe E, Sonntag J von, Sonntag C von. Reaction of OH radicals with benzoquinone in aqueous solutions. J Chem Soc. 1998 ;0 :791–6.

84. Mason HS. The chemistry of melanin ; mechanism of the oxidation of catechol by tyrosinase. J Biol Chem. 1949 ;181 :803–12.

85. Sakagami Y, Yokoyama H, Nishimura H, Ose Y, Tashima T. Mechanism of resistance to benzalkonium chloride by *Pseudomonas aeruginosa*. Appl Environ Microbiol. 1989 ;55 :2036–40.

86. Tezel U, Tandukar M, Martinez RJ, Sobecky PA, Pavlostathis SG. Aerobic biotransformation of n-Tetradecylbenzyldimethylammonium chloride by an enriched *Pseudomonas* spp. community. Environ Sci Technol. 2012 ;46 :8714–22.

87. Lyon DY, Vogel TM. 6.10 - Bioaugmentation as a strategy for the treatment of persistent pollutants. Oxford :Pergamon ; 2011 :119–31.

88. Chatterjee DK, Kellogg ST, Hamada S, Chakrabarty AM. Plasmid specifying total degradation of 3-chlorobenzoate by a modified ortho pathway. J Bacteriol. 1981 ;146 :639–46.

89. Pollmann K, Beil S, Pieper DH. Transformation of chlorinated benzenes and toluenes by *Ralstonia* sp. strain PS12 *tecA* (tetrachlorobenzene dioxygenase) and *tecB* (chlorobenzene dihydrodiol dehydrogenase) gene products. Appl Environ Microbiol. 2001 ;67 :4057–63.

90. Alonso L. Hétérogénéité spatio-temporelle du microbiote de la grotte de Lascaux. Université de Lyon ; 2018.

Supplementary data

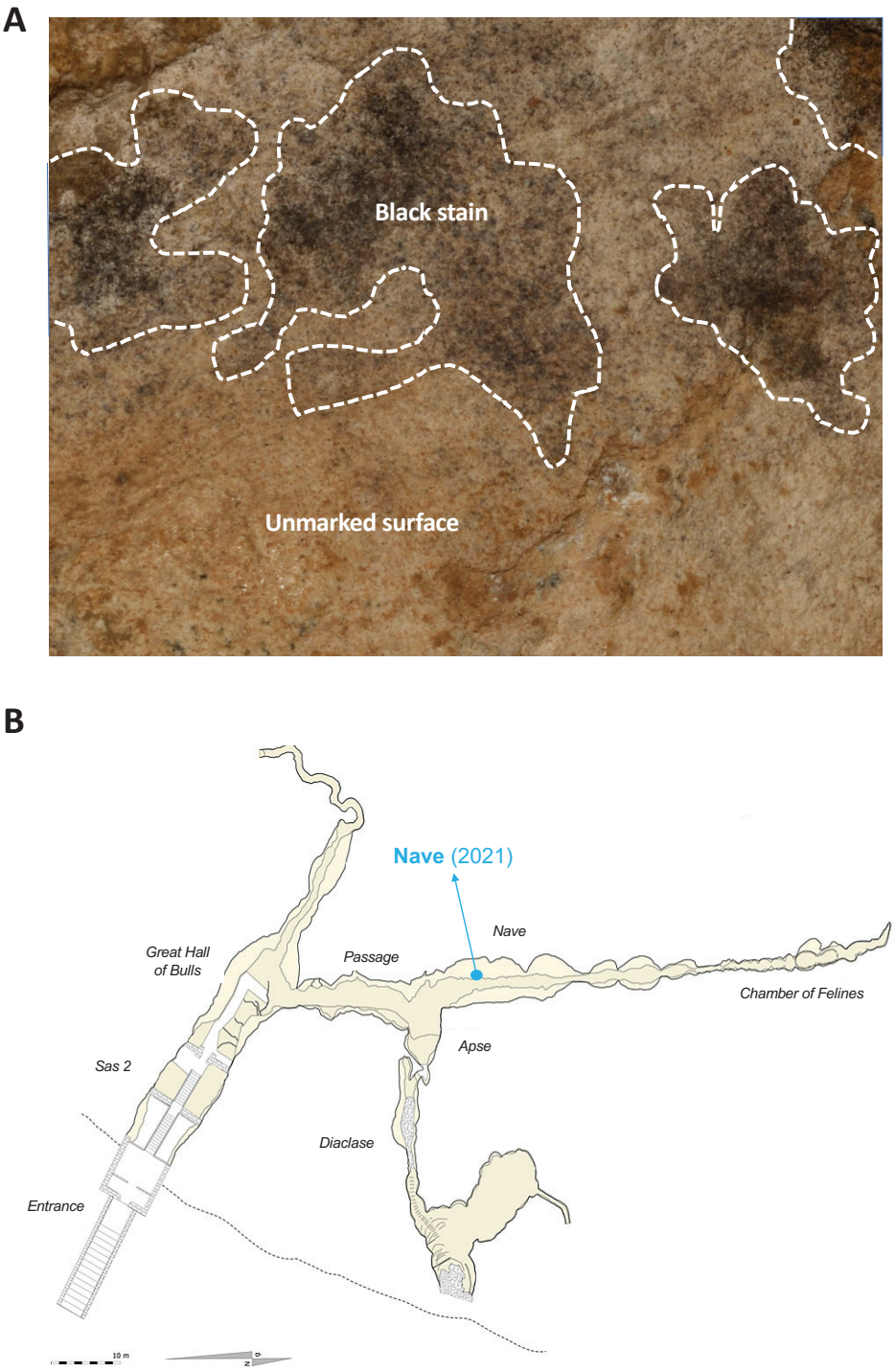

Supplementary fig S1. (A) Photograph of unmarked surfaces (UN) and black stains (BS) in the Nave (Source : S. Géraud, DRAC Nouvelle Aquitaine). (B) Map of Lascaux Cave presenting the locations studied (Source of the map : S. Konik, Centre National de la Préhistoire).

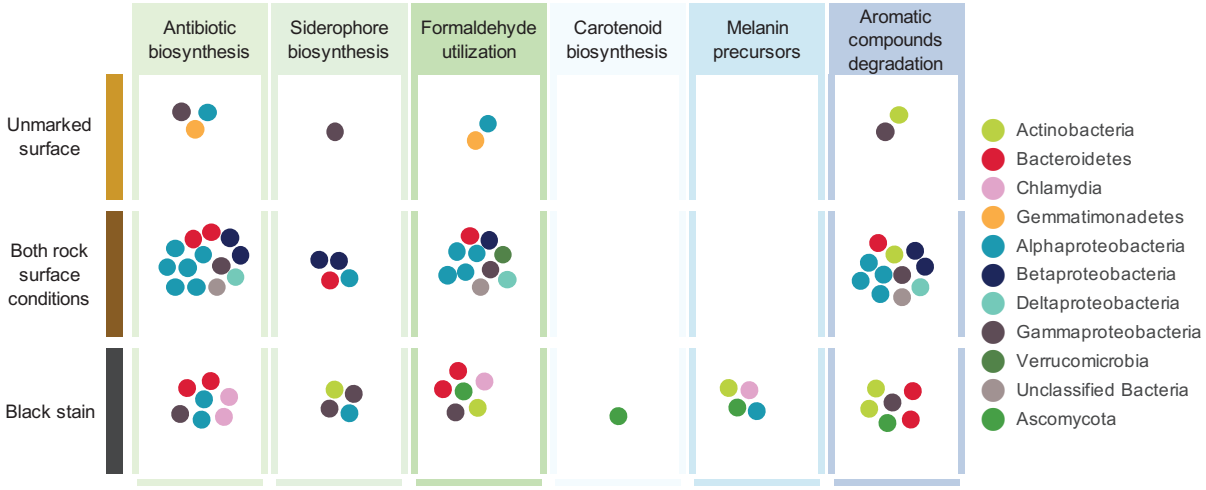

Supplementary fig S2. Genetic potential distribution in each rock surface condition identified in genomic bins. Each point represents a genomic bin in which the corresponding metabolic class (i.e. Antibiotic biosynthesis, Siderophore biosynthesis, Formaldehyde utilization, Carotenoid biosynthesis, or Melanin precursor and aromatic compounds degradation) has been identified. Details of genomic bins (ID, completeness, contamination, taxonomy and coverage) are presented in Supplementary Table S3.

Supplementary table S1. Details of the amplicon and shotgun metagenome sequencing procedures in the different samples from Lascaux Cave.

Sample ID	Sample type	Number of bacterial reads according to amplicon sequencing	Number of archaeal reads according to amplicon sequencing	Number of microeukaryotic reads according to amplicon sequencing	Number of shotgun metagenomic reads	Number of bacterial reads according to shotgun metagenomic sequencing	Number of archaeal reads according to shotgun metagenomic sequencing	Number of microeukaryotic reads according to shotgun metagenomic sequencing
UN1	Unmarked surface	161,176	17,388	268,819	156,652,616	133,193,460	94,952	181,008
UN2	Unmarked surface	148,085	55,002	261,395	153,939,324	128,194,664	328,322	111,592
UN3	Unmarked surface	196,171	127,029	297,227	166,428,240	127,717,260	91,074	2,230,124
BS1	Black stain	146,591	15,809	380,594	151,801,036	124,242,664	10,866	2,659,242
BS2	Black stain	127,994	11,353	275,903	167,415,128	138,018,498	19,806	701,898
BS3	Black stain	149,097	53,549	210,384	155,391,304	137,847,218	20,132	100,843
Normalization		127,994	11,353	210,384	151,801,036	NA	NA	NA

Supplementary table S2. Details of the quality of shotgun metagenome bioinformatic analysis.

Characteristics	Results
Number of contigs	61968
Total length	608767283
Longest contig	1924787
Shortest contig	2000
N50	29699
N90	3041
Contigs at superkingdom (k) rank	59141 (95.4%), in 4 superkingdoms
Contigs at phylum (p) rank	53967 (87.1%), in 29 phyla
Contigs at class (c) rank	44380 (71.6%), in 48 classes
Contigs at order (o) rank	36111 (58.3%), in 89 orders
Contigs at family (f) rank	29352 (47.4%), in 134 families
Contigs at genus (g) rank	23078 (37.2%), in 223 genera
Contigs at species (s) rank	2305 (3.7%), in 219 species
Congruent	57992 (93.6%)
Disparity > 0	3977 (6.4%)
Disparity ≥ 0.25	2030 (3.3%)

N50: is the minimum contig length to cover 50% of the genome.

N90: is the minimum contig length to cover 90% of the genome.

Congruent means that all genes in the contig belong to the same taxa.

Disparity is the percentage of paired comparisons between genes that belong to different taxa.

Supplementary table S3. Details of reconstructed bins (ID, completeness, contamination, taxonomy and coverage). UN : Unmarked surface ; BS : Black stain.

BIN ID	Completeness (contamination) %	Taxonomical identification				Coverage				
		Kingdom	Phylum	Class	Genus	UN1	UN2	UN3	BS1	BS2	BS3
BIN1	89.76 (5.38)	Bacteria	Proteobacteria	Gammaproteobacteria	*Pseudomonas*	19.41	7.01	34.11	0.00	0.01	0.00
BIN2	94.83 (0.05)	Bacteria	Gemmatimonadetes	Gemmatimonadetes	*Gemmatimonas*	12.36	4.81	17.78	0.00	0.00	0.00
BIN3	92.22 (6.86)	Bacteria	Proteobacteria	Alphaproteobacteria	*Phyllobacterium*	36.92	25.23	0.06	0.00	0.00	0.00
BIN4	86.27 (5.38)	Bacteria	Actinobacteria	Thermoleophilia	Not identified	3.73	55.03	10.55	0.00	0.01	0.00
BIN5	91.47 (3.42)	Archaea	Thaumarchaeota	Nitrososphaeria	*Candidatus Nitrosocosmicus*	0.24	6.11	59.62	0.00	0.00	0.02
BIN6	87.28 (2.37)	Bacteria	Proteobacteria	Alphaproteobacteria	*Sphingomonas*	2.683	1.649	1.029	38.144	19.310	3.243
BIN7	76.70 (3.31)	Bacteria	Bacteroidetes	Chitinophagia	*Chitinophaga*	2.149	2.522	5.084	37.807	31.576	21.424
BIN8	98.28 (7.03)	Bacteria	Not identified	Not identified	Not identified	75.598	54.086	7.411	36.549	27.361	11.710
BIN9	81.82 (0.95)	Bacteria	Proteobacteria	Gammaproteobacteria	*Xanthomonas*	56.519	28.749	1.198	37.811	39.516	22.820
BIN10	90.44 (1.53)	Bacteria	Bacteroidetes	Chitinophagia	*Chitinophaga*	315.375	68.709	0.589	37.818	20.959	16.865
BIN11	79.54 (2.16)	Bacteria	Proteobacteria	Betaproteobacteria	Not identified	77.236	32.132	4.553	20.779	16.357	6.817
BIN12	76.87 (7.30)	Bacteria	Proteobacteria	Alphaproteobacteria	*Brevundimonas*	623.814	965.290	984.695	166.449	704.012	3.598
BIN13	93.27 (2.62)	Bacteria	Verrucomicrobia	Verrucomicrobiae	*Akkermansia*	118.596	43.043	6.351	14.528	19.461	8.984
BIN14	85.47 (2.17)	Bacteria	Proteobacteria	Alphaproteobacteria	*Phyllobacterium*	29.748	26.040	4.111	37.820	0.736	2.635
BIN15	89.00 (1.98)	Bacteria	Proteobacteria	Alphaproteobacteria	*Mesorhizobium*	8.355	5.605	5.279	12.963	25.383	4.062
BIN16	88.76 (0.80)	Bacteria	Proteobacteria	Betaproteobacteria	*Advenella*	133.199	62.680	1.758	80.413	17.537	11.224
BIN17	92.30 (6.90)	Bacteria	Proteobacteria	Alphaproteobacteria	*Bradyrhizobium*	16.815	11.946	3.249	6.938	5.724	5.172
BIN18	77.51 (1.20)	Bacteria	Proteobacteria	Alphaproteobacteria	*Agrobacterium*	5.091	0.016	6.541	37.850	13.288	3.717
BIN19	86.02(1.45)	Bacteria	Actinobacteria	Actinomycetia	*Nocardioides*	10.901	0.269	0.700	37.816	88.161	77.476
BIN20	97.32 (3.19)	Bacteria	Proteobacteria	Deltaproteobacteria	*Polyangiaceae*	100.279	41.372	1.039	5.320	5.395	4.175
BIN21	78.99 (1.13)	Bacteria	Proteobacteria	Alphaproteobacteria	*Hyphomicrobium*	0.00	0.00	0.00	37.813	82.190	27.298
BIN22	85.71 (0.85)	Bacteria	Actinobacteria	Actinomycetia	Not identified	0.00	0.10	0.00	60.390	124.968	193.752
BIN23	76.93 (1.71)	Bacteria	Proteobacteria	Alphaproteobacteria	Not identified	0.01	0.00	0.04	37.817	7.517	9.471
BIN24	90.52 (4.25)	Bacteria	Chlamydiae	Chlamydiia	Not identified	0.00	0.02	0.00	14.811	12.635	3.392
BIN25	81.47 (5.50)	Bacteria	Bacteroidetes	Not identified	Not identified	0.03	0.00	0.00	14.907	31.413	54.207
BIN26	80.82 (2.59)	Bacteria	Proteobacteria	Gammaproteobacteria	*Legionella*	0.00	0.00	0.00	37.809	22.352	25.311
BIN27	78.56 (3.82)	Bacteria	Chlamydiae	Chlamydiia	Not identified	0.00	0.00	0.02	37.810	14.210	9.526
BIN28	85.59 (2.26)	Bacteria	Bacteroidetes	Chitinophagia	*Chitinophaga*	0.00	0.00	0.05	37.814	38.205	8.899
BIN29	82.41 (1.69)	Bacteria	Proteobacteria	Gammaproteobacteria	*Pseudomonas*	0.00	0.00	0.00	37.815	9.641	3.480
BIN30	78.57 (1.22)	Bacteria	Actinobacteria	Not identified	Not identified	0.311	0.00	0.00	120.804	156.949	41.184
BIN31	88.60 (1.35)	Eukaryota	Ascomycota	Eurotiomycetes	*Exophiala*	0.00	0.00	0.02	37.819	131.408	19.524

Coverage: average number of sample nucleotide bases aligned to a specific locus in a reconstructed genome.

Supplementary table S4. Details of metabolic pathways in *Pseudomonas* bins. B : Biosynthesis ; D : Degradation.

Number of pathways	Metabolic pathway name	Type of reaction	Pathway class
1	cis-dodecenoyl biosynthesis	B	Alcohol
2	(S,S)-butanediol biosynthesis	B	Alcohol
3	glycerol degradation I	D	Alcohol
4	glycerol degradation IV	D	Alcohol
5	oxidative ethanol degradation III (microsomal)	D	Alcohol
6	ethanol degradation II (cytosol)	D	Alcohol
7	(S,S)-butanediol degradation	D	Alcohol
8	putrescine biosynthesis III	B	Amines and polyamines
9	spermidine biosynthesis I	B	Amines and polyamines
10	ureide biosynthesis	B	Amines and polyamines
11	putrescine biosynthesis II	B	Amines and polyamines
12	heme biosynthesis from uroporphyrinogen-III II	B	Amines and polyamines
13	choline degradation I	B	Amines and polyamines
14	heme biosynthesis from uroporphyrinogen-III I	B	Amines and polyamines
15	UDP-*N*-acetyl-D-glucosamine biosynthesis I	B	Amines and polyamines
16	ethanolamine utilization	D	Amines and polyamines
17	putrescine degradation III	D	Amines and polyamines
18	urea degradation II	D	Amines and polyamines
19	urea degradation I	D	Amines and polyamines
20	choline-*O*-sulfate degradation	D	Amines and polyamines
21	beta-alanine biosynthesis III	B	Amino acids
22	alanine biosynthesis I	B	Amino acids
23	arginine biosynthesis I	B	Amino acids
24	arginine biosynthesis II (acetyl cycle)	B	Amino acids
25	aspartate biosynthesis	B	Amino acids
26	cysteine biosynthesis IV (fungi)	B	Amino acids
27	glutamate and glutamine biosynthesis	B	Amino acids
28	glutamate biosynthesis I	B	Amino acids
29	glutamate biosynthesis III	B	Amino acids
30	glutamate biosynthesis IV	B	Amino acids
31	glutamine biosynthesis III	B	Amino acids
32	glycine biosynthesis III	B	Amino acids
33	glycine biosynthesis IV	B	Amino acids
34	histidine biosynthesis	B	Amino acids
35	homocysteine and cysteine interconversion	B	Amino acids
36	homoserine biosynthesis	B	Amino acids
37	isoleucine biosynthesis I (from threonine)	B	Amino acids
38	isoleucine biosynthesis II	B	Amino acids
39	isoleucine biosynthesis III	B	Amino acids

40	isoleucine biosynthesis V	B	Amino acids
41	leucine biosynthesis	B	Amino acids
42	lysine biosynthesis I	B	Amino acids
43	methionine biosynthesis III	B	Amino acids
44	ornithine biosynthesis	B	Amino acids
45	superpathway of alanine biosynthesis	B	Amino acids
46	superpathway of leucine, valine, and isoleucine biosynthesis	B	Amino acids
47	superpathway of methionine biosynthesis (by sulfhydrylation)	B	Amino acids
48	superpathway of phenylalanine, tyrosine, and tryptophan biosynthesis	B	Amino acids
49	alanine biosynthesis II	B	Amino acids
50	tyrosine biosynthesis IV	B	Amino acids
51	cardiolipin biosynthesis II	B	Amino acids
52	cysteine biosynthesis/homocysteine degradation	B	Amino acids
53	glutamate biosynthesis V	B	Amino acids
54	superpathway of sulfur amino acid biosynthesis	B	Amino acids
55	asparagine biosynthesis I	B	Amino acids
56	glycine betaine biosynthesis I (Gram-negative bacteria)	B	Amino acids
57	phenylalanine biosynthesis I	B	Amino acids
58	glycine betaine biosynthesis II (Gram-positive bacteria)	B	Amino acids
59	cysteine biosynthesis I	B	Amino acids
60	serine biosynthesis	B	Amino acids
61	uridine-5'-phosphate biosynthesis	B	Amino acids
62	glycine cleavage complex	B	Amino acids
63	tryptophan biosynthesis	B	Amino acids
64	superpathway of serine and glycine biosynthesis I	B	Amino acids
65	glycine biosynthesis I	B	Amino acids
66	L-glutamine biosynthesis II (tRNA-dependent)	B	Amino acids
67	glutamine biosynthesis I	B	Amino acids
68	alanine biosynthesis III	B	Amino acids
69	S-adenosyl-L-methionine cycle II	B	Amino acids
70	tyrosine biosynthesis I	B	Amino acids
71	alanine degradation IV	D	Amino acids
72	arginine degradation II (AST pathway)	D	Amino acids
73	arginine degradation IX (arginine:pyruvate transaminase pathway)	D	Amino acids
74	arginine degradation VIII (arginine oxidase pathway)	D	Amino acids
75	asparagine degradation I	D	Amino acids
76	aspartate degradation I	D	Amino acids
77	aspartate degradation II	D	Amino acids
78	citrulline degradation	D	Amino acids
79	glutamine degradation I	D	Amino acids
80	glutamine degradation II	D	Amino acids
81	histidine degradation II	D	Amino acids

82	isoleucine degradation I	D	Amino acids
83	leucine degradation I	D	Amino acids
84	threonine degradation II	D	Amino acids
85	alanine degradation III	D	Amino acids
86	alanine degradation II (to D-lactate)	D	Amino acids
87	L-cysteine degradation II	D	Amino acids
88	methionine degradation II	D	Amino acids
89	arginine degradation IV	D	Amino acids
90	histidine degradation VI	D	Amino acids
91	glutamate degradation I	D	Amino acids
92	histidine degradation I	D	Amino acids
93	L-serine degradation	D	Amino acids
94	urate biosynthesis/inosine 5'-phosphate degradation	D	Amino acids
95	methionine degradation III	D	Amino acids
96	beta-alanine degradation I	D	Amino acids
97	beta-alanine degradation II	D	Amino acids
98	tryptophan degradation to 2-amino-3-carboxymuconate semialdehyde	D	Amino acids
99	tyrosine degradation I	D	Amino acids
100	arginine dependent acid resistance	D	Amino acids
101	*m*-xylene degradation to *m*-toluate	D	Aromatic Compounds
102	4-hydroxybenzoate biosynthesis II (bacteria and fungi)	B	Aromatic Compounds
103	4-hydroxybenzoate biosynthesis V	B	Aromatic Compounds
104	5-aminoimidazole ribonucleotide biosynthesis II	B	Aromatic Compounds
105	chorismate biosynthesis I	B	Aromatic Compounds
106	3-dehydroquinate biosynthesis I	B	Aromatic Compounds
107	3-amino-5-hydroxybenzoate biosynthesis	B	Aromatic Compounds
108	*p*-xylene degradation to *p*-toluate	D	Aromatic Compounds
109	2-nitrobenzoate degradation I	D	Aromatic Compounds
110	2,4-dinitrotoluene degradation	D	Aromatic Compounds
111	3-chloroacrylic acid degradation	D	Aromatic Compounds
112	4-aminobutyrate degradation I	D	Aromatic Compounds
113	4-aminobutyrate degradation III	D	Aromatic Compounds
114	benzoate degradation I (aerobic)	D	Aromatic Compounds
115	ferulate degradation	D	Aromatic Compounds
116	gentisate degradation	D	Aromatic Compounds
117	protocatechuate degradation II (ortho-cleavage pathway)	D	Aromatic Compounds
118	glycolysis III	B	Carbohydrates
119	pentose phosphate pathway	B	Carbohydrates
120	pentose phosphate pathway (oxidative branch)	B	Carbohydrates
121	superpathway of glutamate biosynthesis	B	Carbohydrates
122	superpathway of glycolysis and Entner-Doudoroff	B	Carbohydrates
123	bypass	B	Carbohydrates

124	trehalose biosynthesis IV	B	Carbohydrates
125	trehalose biosynthesis V	B	Carbohydrates
126	UDP-D-galacturonate biosynthesis I (from UDP-D-glucuronate)	B	Carbohydrates
127	GDP-mannose biosynthesis	B	Carbohydrates
128	pentose phosphate pathway (non-oxidative branch)	B	Carbohydrates
129	pentose phosphate pathway (partial)	B	Carbohydrates
130	dTDP-L-rhamnose biosynthesis I	B	Carbohydrates
131	dTDP-L-rhamnose biosynthesis II	B	Carbohydrates
132	Entner-Doudoroff pathway I	B	Carbohydrates
133	glycolate and glyoxylate degradation I	D	Carbohydrates
134	sucrose degradation I	D	Carbohydrates
135	sucrose degradation III	D	Carbohydrates
136	sucrose degradation IV	D	Carbohydrates
137	trehalose degradation I (low osmolarity)	D	Carbohydrates
138	sorbitol degradation I	D	Carbohydrates
139	D-glucarate degradation I	D	Carbohydrates
140	2-amino-3-carboxymuconate semialdehyde degradation to 2-oxopentenoate	D	Carbohydrates
141	2-amino-3-carboxymuconate semialdehyde degradation to glutaryl-CoA	D	Carbohydrates
142	acetate conversion to acetyl-CoA	D	Carbohydrates
143	acetate formation from acetyl-CoA I	D	Carbohydrates
144	D-galactarate degradation I	D	Carbohydrates
145	D-galactarate degradation II	D	Carbohydrates
146	D-galactonate degradation	D	Carbohydrates
147	D-glucarate degradation II	D	Carbohydrates
148	glycogen degradation II	D	Carbohydrates
149	D-gluconate degradation	D	Carbohydrates
150	D-mannose degradation	D	Carbohydrates
151	fructose degradation	D	Carbohydrates
152	GDP-glucose biosynthesis	D	Carbohydrates
153	glucose degradation (oxidative)	D	Carbohydrates
154	glutaryl-CoA degradation	D	Carbohydrates
155	peptidoglycan biosynthesis I (meso-diaminopimelate containing)	B	Cell Structure
156	peptidoglycan biosynthesis III (mycobacteria)	B	Cell Structure
157	UDP-*N*-acetylmuramoyl-pentapeptide biosynthesis III	B	Cell Structure
158	l,2-Dichloroethane degradation	D	Aromatic compounds
159	trans, trans-farnesyl diphosphate biosynthesis	B	Cofactors
160	6-hydroxymethyl-dihydropterin diphosphate biosynthesis	B	Cofactors
161	7-keto-8-aminopelargonate biosynthesis I	B	Cofactors
162	adenosylcobalamin biosynthesis II (late cobalt incorporation)	B	Cofactors
163	adenosylcobalamin salvage from cobinamide I	B	Cofactors
164	biotin biosynthesis from 7-keto-8-aminopelargonate	B	Cofactors
165	biotin biosynthesis I	B	Cofactors

166	biotin biosynthesis II	B	Cofactors
167	flavin biosynthesis I (bacteria and plants)	B	Cofactors
168	geranyl diphosphate biosynthesis	B	Cofactors
169	geranylgeranyldiphosphate biosynthesis	B	Cofactors
170	glutathione biosynthesis	B	Cofactors
171	heme biosynthesis I	B	Cofactors
172	heme biosynthesis II	B	Cofactors
173	heptaprenyl diphosphate biosynthesis	B	Cofactors
174	lipoate biosynthesis and incorporation I	B	Cofactors
175	lipoate biosynthesis and incorporation II	B	Cofactors
176	NAD biosynthesis II (from tryptophan)	B	Cofactors
177	polyisoprenoid biosynthesis	B	Cofactors
178	superpathway of geranylgeranyldiphosphate biosynthesis II (via MEP)	B	Cofactors
179	superpathway of pyridoxal 5'-phosphate biosynthesis and salvage	B	Cofactors
180	superpathway of tetrahydrofolate biosynthesis and salvage	B	Cofactors
181	tetrapyrrole biosynthesis I	B	Cofactors
182	tetrapyrrole biosynthesis II	B	Cofactors
183	siroheme biosynthesis	B	Cofactors
184	pantothenate and coenzyme A biosynthesis I	B	Cofactors
185	phosphopantothenate biosynthesis I	B	Cofactors
186	formylTHF biosynthesis I	B	Cofactors
187	adenosylcobalamin salvage from cobalamin	B	Cofactors
188	coenzyme A biosynthesis	B	Cofactors
189	factor 43 biosynthesis	B	Cofactors
190	S-adenosyl-L-methionine biosynthesis	B	Cofactors
191	menaquinol-6 biosynthesis	B	Cofactors
192	menaquinol-8 biosynthesis	B	Cofactors
193	menaquinol-9 biosynthesis	B	Cofactors
194	thioredoxin pathway	B	Cofactors
195	gamma-linolenate biosynthesis II	B	Fatty acid and Lipid
196	biotin-carboxyl carrier protein assembly	B	Fatty acid and Lipid
197	fatty acid elongation – saturated	B	Fatty acid and Lipid
198	palmitoleate biosynthesis I	B	Fatty acid and Lipid
199	fatty acid beta oxidation III (unsaturated, odd number)	B	Fatty acid and Lipid
200	phospholipid biosynthesis I	B	Fatty acid and Lipid
201	lipid IV A biosynthesis	B	Fatty acid and Lipid
202	CDP-diacylglycerol biosynthesis III	B	Fatty acid and Lipid
203	fatty acid beta-oxidation II (core pathway)	B	Fatty acid and Lipid
204	phosphatidylglycerol biosynthesis I (plastidic)	B	Fatty acid and Lipid
205	phosphatidylglycerol biosynthesis II (non-plastidic)	B	Fatty acid and Lipid
206	cyclopropane and cyclopropene fatty acid biosynthesis	B	Fatty acid and Lipid
207	cyclopropane fatty acid (CFA) biosynthesis	B	Fatty acid and Lipid

208	phosphatidylethanolamine biosynthesis I	B	Fatty acid and Lipid
209	CDP-diacylglycerol biosynthesis I	B	Fatty acid and Lipid
210	CDP-diacylglycerol biosynthesis II	B	Fatty acid and Lipid
211	fatty acid activation	B	Fatty acid and Lipid
212	fatty acid omega oxidation	B	Fatty acid and Lipid
213	fatty acid biosynthesis initiation I	B	Fatty acid and Lipid
214	(S)-acetoin biosynthesis	B	Fermentation
215	heterolactic fermentation	F	Fermentation
216	formaldehyde oxidation IV (thiol-independent)	O	Formaldehyde
217	formate oxidation to CO_2	O	Formaldehyde
218	PRPP biosynthesis II	B	Inorganic Nutrients
219	ammonia assimilation cycle II	D	Inorganic Nutrients
220	cyanate degradation	D	Inorganic Nutrients
221	phosphonoacetate degradation	D	Inorganic Nutrients
222	thiosulfate disproportionation III (rhodanese)	D	Inorganic Nutrients
224	purine nucleotides *de novo* biosynthesis II	B	Nucleotides
225	xanthine and xanthosine salvage	B	Nucleotides
226	superpathway of 5-aminoimidazole ribonucleotide biosynthesis	B	Nucleotides
227	inosine-5'-phosphate biosynthesis I	B	Nucleotides
228	pyrimidine ribonucleotides *de novo* biosynthesis	B	Nucleotides
229	inosine-5'-phosphate biosynthesis II	B	Nucleotides
230	beta-carboline biosynthesis	B	Secondary Metabolites
231	betaxanthin biosynthesis (via dopamine)	B	Secondary Metabolites
232	Biosynthesis of vancomycin group antibiotics	B	Secondary Metabolites
233	Inositol metabolism	B	Secondary Metabolites
234	isoprene biosynthesis	B	Secondary Metabolites
235	methylthiopropionate biosynthesis	B	Secondary Metabolites
236	tetracycline biosynthesis	B	Secondary Metabolites
237	valine biosynthesis	B	Secondary Metabolites
238	methylerythritol phosphate pathway	B	Secondary Metabolites
239	superpathway of acetyl-CoA biosynthesis	B	Secondary Metabolites
240	superpathway of rifamycin B biosynthesis	B	Secondary Metabolites
241	pyoverdine I biosynthesis	B	Siderophores

Article 7. Microbial diversity and secondary metabolism potential in relation to dark alterations in Paleolithic Lascaux Cave

ZELIA BONTEMPS[1], DANIS ABROUK[1], YVAN MOENNE-LOCCOZ[1] AND MYLENE HUGONI[1,2,3]

[1]Univ Lyon, Université Claude Bernard Lyon 1, CNRS, INRAE, VetAgro Sup, UMR Ecologie Microbienne, F-69622 Villeurbanne, France
[2]Univ Lyon, Université Claude Bernard Lyon 1, CNRS, INSA de Lyon, UMR Microbiologie Adaptation et Pathogénie, F-69622 Villeurbanne, France
[3]Institut Universitaire de France (IUF)

Corresponding author
Mylene HUGONI. Univ Lyon, INSA Lyon, CNRS, UMR 5240 Microbiologie Adaptation et Pathogénie, F-69621 Villeurbanne, France mylene.hugoni@univ-lyon1.fr

Abstract

Background : Tourism activities in Paleolithic show caves can cause an imbalance in cave microbiota and the formation of cave wall alterations, including dark zones under severe anthropization. However, dark zones formation and evolution are poorly understood. Here, a metagenomic approach (Illumina NovaSeq 6000) and reconstruction of Metagenome-Assembled Genomes (MAGs) were used in the Apse (in two different years) and Passage of Lascaux Cave to compare microbial diversity and metabolic potential of dark zones vs unmarked surfaces nearby.

Results : Metagenomic results were largely convergent with metabarcoding data, except that limited metagenomic sequences were identified for microeukaryotes. Metagenomes were similar in both years but differed between locations, yet the latter displayed similarities, as follows. Genes and pathways for aromatic compound degradation were well present in and outside dark zones, as expected from past usage of organic biocides. Dark zones coincided with a potential for biosynthesis of pigments (i.e. melanin in both rooms and also carotenoids in the Apse). Genes or pathways for production of antimicrobials were evidenced in unmarked surfaces, suggesting that antagonism might restrict development of pigmented microorganisms.

Conclusion : This work proposes a conceptual framework of dark zone formation in relation to microbial secondary metabolism, which may help to understand wall alterations under severe cave anthropization.

Key words

Metagenomics ; Metagenomes assembled genomes ; Paleolithic cave ; Melanin ; Aromatic compounds degradation

Introduction

Show caves are among the most important geotouristic sites world-wide, with more than 250 million people visiting them each year [1–3]. Show cave attract tourist attention for underground lakes e.g. in Cross cave (Slovenia), speleothems such as stalactites and stalagmites e.g. in Kartchner cave (Arizona, USA) and Aven d'Orgnac (France), or parietal artwork e.g. in Lascaux Cave (France) and Altamira Cave (Spain) [4–7]. However, caves are extremely fragile environments and can be affected by intense touristic activity, because of development work including cave floor excavation to facilitate access [8], installation of stairs, elevators, lighting system, masonry [9] and sometimes digging of a tunnel [10], as well as human frequentation that brings microorganisms in and changes climatic conditions [7]. This can be problematic for conservation of Paleolithic artwork, as it can cause alterations on the walls (biodeterioration, Lampenflora, calcite veil, gypsum efflorescences, dark ferromanganese deposits, microbial stains, etc.) in various subterranean environments [5,11–16]. In several caves, antibiotic and chemical treatments were applied to cave floors and walls in an attempt to mitigate microbial alterations, which sometimes exacerbated further the imbalance of the cave microbiota [9,12].

These conservation problems are well illustrated in Lascaux Cave, where tourism-related anthropization resulted in various cave wall alterations and led to cave closure in 1963 [12]. The alterations on walls corresponded to an abnormal proliferation of the algae *Brateococcus minor* in the 1960s (green biofilms) and later of microorganisms such as the fungi *Fusarium solani* in 2001 (white stains), as well as *Ochroconis lascauxensis* and other black melanized fungi since late 2001 (black stains) [17]. These proliferations were treated with chemical and antibiotic compounds applied directly on walls, such as formaldehyde, quicklime, streptomycin, polymixin and benzalkonium chloride (BAC). The last type of rock wall alteration corresponds to dark zones, which started in the Apse in 2008 and developed in different rooms in recent years (Alonso et al. submitted). They are zones of darker shade than on unmarked surfaces around, but without the black color of black stains documented in relation to black melanized fungi. Their chemical basis is not known, and perhaps they entail synthesis of pigments and/or chemical modifications of metals, as documented for other alterations [6,18]. Preliminary microbial analysis evidenced a particular microbial community in dark zones, with the counter-selection of the Gammaproteobacteria class (Alonso et al. submitted), as well as the selection of pigmented fungi (e.g. *Ochroconis*) and the Alphaproteobacteria class including the genus *Bosea* described as producer of carotenoids (yellow-orange pigments corresponding to isoprenoid polyenes) and other pigments [19].

Previous work on dark zones was carried out using metabarcoding (Alonso et al. submitted), which (i) might entail a PCR bias when considering microbial diversity and (ii) does not enable reliable prediction of microbial functions involved in these surface alterations. Thus, the objective of this work was to use high-throughput metagenomic sequencing (i.e. NovaSeq) to compare the microbial ecology of dark zones vs unmarked surfaces nearby, in terms of microbial diversity and metabolic potential relevant to understand dark zone formation in Lascaux Cave.

In dark zones of the Apse, pigmented fungi such as *Ochroconis lascauxensis* become selected, whereas *Pseudomonas* bacteria are counter-selected as indicated by metabarcoding (Alonso et al. submitted), and here we hypothesized that they would be confirmed with a PCR-free meta-

genomic approach. A second hypothesis is that these differences in taxonomic diversity would translate into key differences in metabolic potential. More specifically, two issues were targeted. One issue is the past application of chemical treatments such as BAC, as some bacteria and fungi from polluted soil or caves present the ability to degrade BAC into benzyldimetylamine, benzylamine and benzoic acid usable by fungi for their growth and metabolism e.g. pigment biosynthesis [20,21], and it can be expected that microbial communities would be enriched in (i) aromatic compound degradation pathways, in and outside dark zones, and (ii) pathways involved in biosynthesis of pigments e.g. carotenoids or chemical modifications of metals, specifically in dark zones. The other issue is the patchy distribution of dark zones, which raises the possibility that pigmented fungi may be controlled by antimicrobials produced by other microorganisms present on unmarked surfaces [22], thereby limiting the expansion of dark zones. For example, bacterial genera such as *Pseudomonas* or *Streptomyces*, widely present in caves [23,24], have the potential to secrete antimicrobial compounds, like the *Pseudomonas* metabolites 2,4-diacetylphloroglucinol [26,27], pyrrolnitrine [28] or hydrogen cyanide [29] and a wide range of *Streptomyces* antimicrobials [30]. In caves, metabarcoding data indicate that the diversity of the microbial community can differ significantly from one room to the other but fluctuations in time are typically minor, including in Lascaux [25]. Against this background, our third hypothesis was that metagenomic data may differ when comparing the two Lascaux locations studied, but without a significant effect of sampling time.

Materials and Methods

Samples collection and nucleic acid extraction

Lascaux Cave is located near Montignac in Périgord, South-West of France (N 45°03'13.087" and E 1°10'12.362"). The cave has been closed for tourist visits since 1963 due to cave wall alterations. Human presence in now restricted and restrained to scientists with special authorization (from DRAC Nouvelle-Aquitaine, Ministry of Culture). The area chosen in this work included art-free natural limestone surfaces in the Apse, where dark zones started to form (2008), and nearby an artificial calcareous substrate (masonry benches) located at the end of the Passage, with dark zones that started in 2016 (Supplementary Fig S1). In both cases, dark zones keep growing. Samplings were carried out in December 2020 (only in the Apse) and April 2021 (both in Apse and Passage), in the upper inclined plane at the right side of the Apse and in the vertical part of the left bench of the Passage. Samples (on areas < 1 cm^1 each) were collected in triplicate, in dark zone alterations and on unmarked surfaces nearby (about 10 cm away) using sterile swabs in the Apse (because scalpels were not authorized) and scalpels in the Passage. Samples were placed in liquid nitrogen before leaving the cave and kept at -80°C until DNA extraction.

DNA extraction was performed using the FastDNA SPIN Kit For Soil (MP Biomedicals, Illkirch, France), following the manufacturer's instructions and adapted to low amounts of sample (80 s at a speed setting of 6.0 m/s followed by 15 min centrifugation at 4°C). The elution step was achieved using two volumes of 50 μl elution buffer for each sample. The resulting DNA concentrations were quantified using the Qubit dsDNA HS Assay Kit (Invitrogen, Carlsbad, USA) following the manufacturer's instructions. The DNA extracts were stored at -20°C until library preparation.

Illumina NovaSeq 6000 metagenomic library preparation, sequencing and analysis

Eighteen metagenomic libraries were constructed for limestone and dark zone samples using a NEBNext Ultra DNA Library Prep Kit (fragment size 350 bp) (Illumina, San Diego, USA) according to the manufacturer's recommendations. Sequencing was performed by Genewiz company (Leipzig, Germany) using Illumina NovaSeq 6000 system 2 x 150 bp (at least 60 million reads per sample). Adapter sequences were removed and low quality reads were filtered using Trimmomatic with default settings [31]. All metagenomes were then pooled and co-assembled using MEGAHIT [32]. Reads were mapped against contigs using Bowtie to estimate coverage [33]. Assembly quality is presented in Supplementary Tables S1 and S2. Gene prediction was achieved using Prodigal [34] and rRNA detected using barrnap [35], before classification using RDP classifier [36]. The latest version of KEGG database was used (April 2022) for functional annotation [37]. To allow sample comparisons, metagenomes were normalized to the lowest number of sequences (60,997,870 reads ; see Supplementary Table S1 for details). Reconstruction of metagenome-assembled genomes (MAGs), also known as bins, was conducted using two different algorithms implemented in MetaBAT-2 [38] and Maxbin 2.0 [39] with contigs longer than 2000 bp. Both binning tools increased the number of bins during reconstruction. Redundant bins obtained from both binning algorithms were identified and removed using DAS Tool [40]. The completeness and contamination level of the genomic bins were then evaluated using CheckM (for prokaryotic bins) and Busco (for microeukaryotic bins) [41,42]. Only MAGs with a contamination level under 5 % and completeness above 75 % were analyzed. Genetic composition of MAGs was then explored using KEGG [37], MetaCyc [43] and COG [44] based on genes identified in the co-assembly. Metabolic pathways in which 75 % of the genes were present were considered and represented using 'circlize' and 'CircleHeatmap' packages in R software [45] (detailed information on selected functional genes were presented in Supplementary Table S3).

Raw sequences were deposited in the NCBI public database under Bioproject PRJNA878937 and MAGs files are available in FigShare ($10.6084/m9.figshare.20626938$).

Statistical analyses

Statistical analyses (Student t tests, variance analysis) were carried out using R software [46]. Community composition was first compared through Non-metric Multidimensional Scaling analysis (NMDS) computed at the taxa level, using vegan package in R 4.1.1 [47]. The procedure computes a stress value, which measures the difference between the ranks on the ordination configuration and the ranks in the original dissimilarity matrix for each replicate. Stress values below 0.1 are considered without risk of drawing false inferences, those under 0.2 are acceptable, but interpretation potential is limited with values > 0.2 [48]. Permutational analysis of variance (PERMANOVA) was conducted using the vegan and pairwiseAdonis packages in R [47,49] to test differences ($P < 0.05$) in overall community composition and to confirm NMDS results. Community structures were analysed through the phyloseq R package (McMurdie 2012), with Tukey-HSD posthoc tests. A Holm-Bonferroni correction was applied on P values to lower alpha risk.

Results

Microbial community structure

NMDS analysis of the whole metagenomic rRNA dataset showed that microbial community structure statistically depended on the room (i.e. Apse or Passage ; 37% of the variation) and rock surface condition (i.e. dark zone or unmarked samples ; 18% of the variation), but much less on the sampling time (i.e. 2020 or 2021 ; 6% of the variation) (Table 1). NMDS ordination was confirmed by pairwise adonis tests for the effect of room ($P = 0.004$ for Passage vs Apse, $P = 0.004$ for Passage vs Apse 2020, and $P = 0.005$ for Passage vs Apse 2021) and surface condition (dark zone vs unmarked surface ; $P = 0.007$ with all samples, $P = 0.001$ in Apse 2020, $P = 0.001$ in Apse 2021 and $P = 0.019$ in Passage 2021), and the lack of effect of time (P = 0.081) (Fig 1, Table 1). NMDS distinguished four groups of samples corresponding to (i) unmarked surfaces from the Apse (2020 and 2021), (ii) dark zones from the Apse (2020 and 2021), (iii) unmarked surfaces from the Passage (2021), and (iv) close to the latter the dark zones from the Passage (2021) (Fig 1).

Table 1. Effect of environmental factors, i.e. location (Apse and Passage), alteration (unmarked surfaces and dark zone) and time (2020 and 2021) on microbial community composition. (A) The differences between groups were tested using PERMANOVA and (B) groups were tested using pairwise adonis on Bray-Curtis dissimilarity matrices.

A

Factor	Df	F	*P*	R^2
Room	2	10.806	**0.001**	0.365
Alteration	1	10.554	**0.001**	0.178
Year	1	2.183	0.071	0.056
Room × Alteration	2	7.469	**0.001**	0.252
Room × Year	2	2.151	0.041	0.067
Year × Alteration	2	9.874	0.055	0.081
Room × Alteration × Year	1	6.433	**0.006**	0.014

B

pair1	pair2	Df	F	*P*	R^2
Apse 2020	Passage 2021	1	1.35	**0.004**	0.41
Apse 2020	Apse 2021	1	0.10	0.757	0.05
Passage 2021	Apse 2021	1	1.17	**0.005**	0.34

Microbial community composition

Microbial community composition was assessed after pooling Illumina NovaSeq ribosomal sequences from the three replicates (i.e. per room and rock surface condition. The 18 metagenome datasets consisted in 245,692 contigs (> 2,000 bp) on average, with 888,686 bp for the longest contig (Supplementary Table S2). After assembly process, metagenomes were affiliated at 84.6% (±4.5%) to Bacteria, 1.8% (±0.8%)to Eukaryota, and (±0.04%) to Archaea (Supplementary Table S1).

The unmarked surfaces from both the Apse and the Passage displayed 11 microbial phyla. As expected from community structure data, the Apse (2020 and 2021) and Passage (2021) samples from unmarked surfaces presented contrasted microbial compositions (Fig 2, Supplementary Fig S2). Indeed, some bacterial phyla were enriched in the Apse compared with the Passage, such

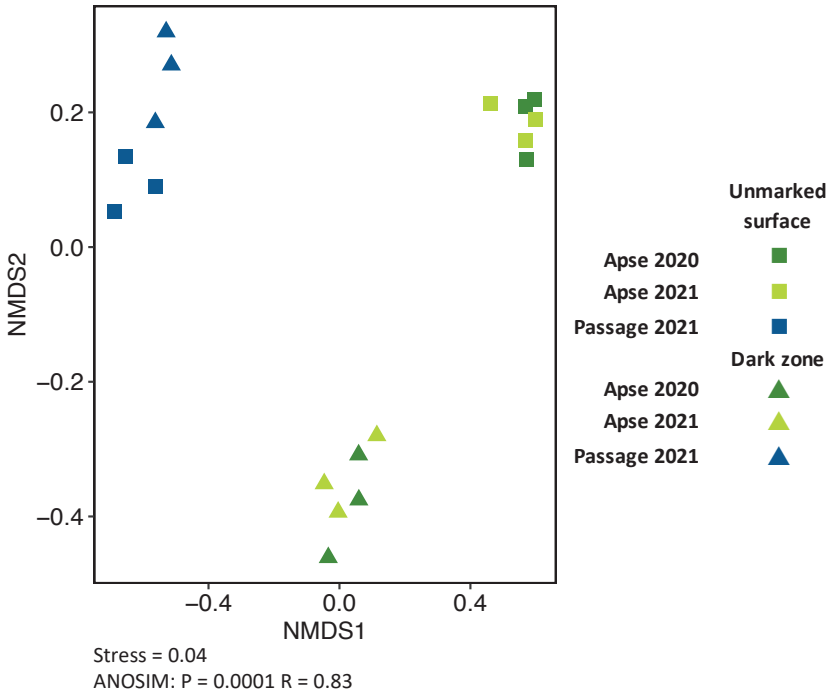

Fig 1. Non-metric multidimensional scaling (NMDS) analysis of microbial community structure in Lascaux's Apse and Passage according to rock surface condition and time. Green colors are used for the Apse and blue for the Passage. The squares represent the unmarked surfaces and triangles the dark zones.

as Acidobacteria (7.6% vs 0.9%) and Proteobacteria (65.4 vs 28.4%), whereas others were in lower proportion in the Apse, such as Bacteroidetes (0.1% vs 12.0%) and Actinobacteria (4.6% vs 49.5) (Fig 2A). Not surprisingly, this type of finding held still true when considering lower taxonomic levels, such as class and genus (Fig 2B, Supplementary Fig S2, Supplementary Fig S3). For instance, Gammaproteobacteria were more abundant in the Apse than in the Passage (45.1% vs 4.9%, Fig 2B), which was mainly due to the *Pseudomonas* genus abundant in the Apse (42.1%) but rare in the Passage (<0.1%) (Supplementary Fig S3). Conversely, the Apse displayed a lower proportion of Actinomycetia (4.0 vs 46.5%, Fig 2B), among which the Jiangella genus reached <0.1% in the Apse but 9.1% in the Passage (Supplementary Fig S3). In contrast, the Alphaproteobacteria class had a similar relative abundance in the Apse (16.6%) and the Passage (19.8%).

Dark zone alterations from the Apse and the Passage were characterized by the presence of 10 different phyla. They displayed similarities in community composition, e.g. the predominance of the Proteobacteria phylum (64.5% on average ; Fig 2A) and Alphaproteobacteria class (46.9% on average ; Fig 2B), but also a few differences. At the phylum level, dark zone samples presented a higher proportion of Acidobacteria (1.9% vs <0.1%), Bacteroidetes (11.9% vs 7.3%) and Actinobacteria (17.4% vs 4.5%) in the Apse compared with the Passage (Fig 2A). At the class level, Gammaproteobacteria (16.3% vs 4.7%), Actinomycetia (16.2% vs 4.2%) and Chitinophagia (8.3% vs 4.2%) were also more abundant in the Apse, whereas the Betaproteobacteria were less abundant (2.3% vs 5.6%, which paralleled the levels of the *Achromobacter* genus i.e. 0.3% vs 3.9%, respectively ; Supplementary Fig S3) (Fig 2B).

When comparing dark zones and unmarked surfaces, the relative abundance of the Acido-

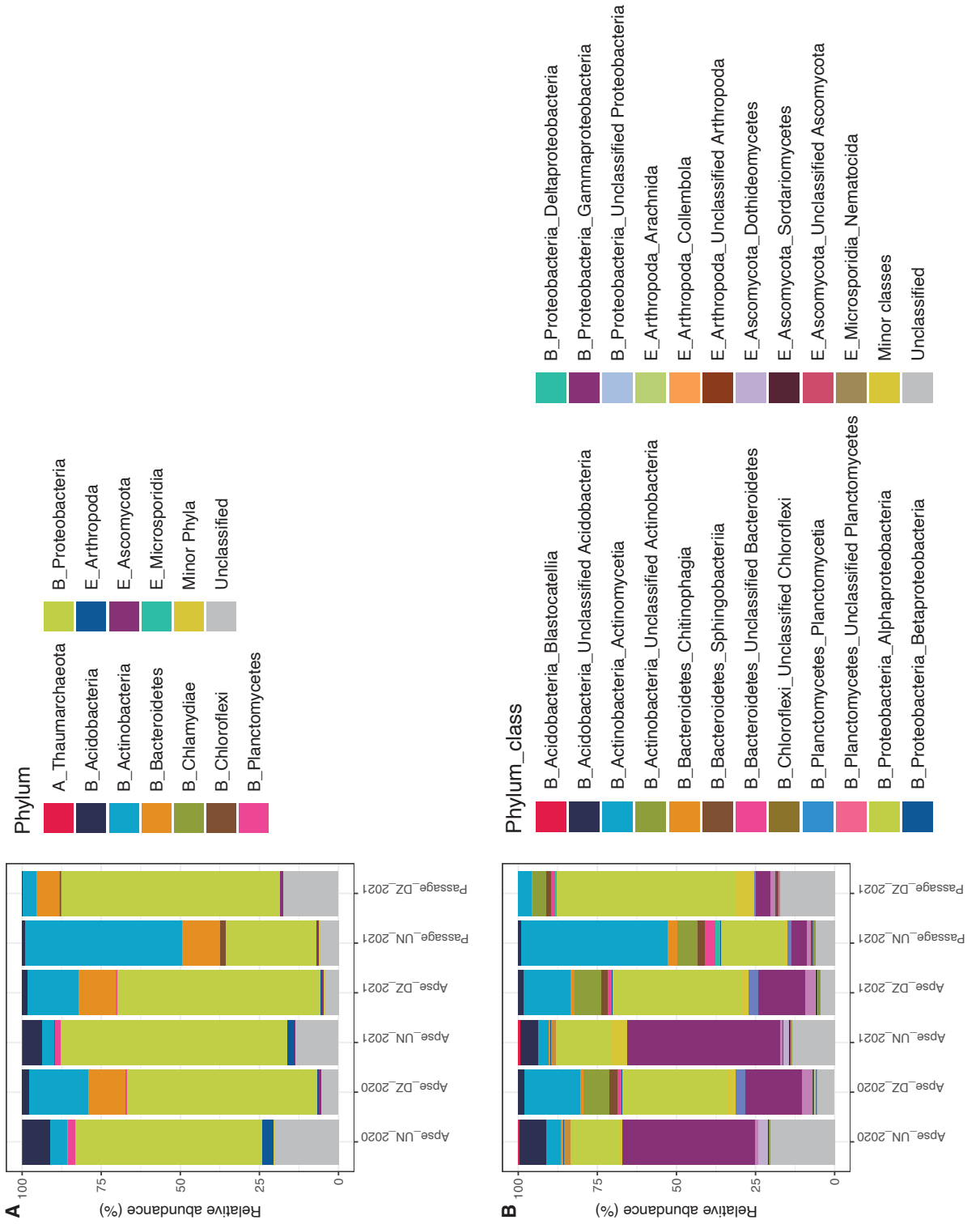

Fig 2. Composition of microbial communities at the (A) phylum and (B) class taxonomic levels, based on relative abundance (% of sequences). UN, unmarked surface ; DZ, dark zone. Phyla or classes presenting a relative abundance <0.05% were considered as minor phyla or minor classes, respectively.

bacteria phylum was lower in dark zones (0.8% vs 7.6% in the Apse and 4.5% vs 49.5% in the Passage). Conversely, the Proteobacteria were at similar levels in and outside dark zones in the Apse (65.4% vs 62.1%), but in the Passage they represented 69.2% in dark zones vs only 28.5%

in unmarked surfaces. In addition, the Bacteroidetes amounted to 9.6% in dark zones vs only 0.1% in unmarked surfaces of the Apse, but 7.3% in dark zones vs as much as 12.0% in unmarked surfaces of the Passage. At class level, dark zones (in comparison with unmarked surfaces) displayed a higher relative abundance of Alphaproteobacteria (37.0% vs 16.6% in the Apse and 56.8% vs 20.2% in the Passage), Deltaproteobacteria in the Apse (3.1% vs <0.1%) but not the Passage (0.5% vs 1.1%), and Actinomycetia in the Apse (16.2% vs 4.1%) but not the Passage (4.2% vs 46.6%). Conversely, the Betaproteobacteria were at similar levels in and outside dark zones in the Apse (2.3% vs 2.8%), but in the Passage they reached 5.6% in dark zones vs only 0.9% in unmarked surfaces. In addition, dark zones (in comparison with unmarked surfaces) exhibited a lower relative abundance of Gammaproteobacteria in the Apse (16.3% vs 45.1%) but not in the Passage (4.9% vs 4.7%). At the genus level, *Achromobacter* and *Mezorhizobium* were at lower levels in dark zones than on unmarked surfaces in the Apse (0.3% vs 2.4% and 1.9% vs 2.7%, respectively) and the Passage (3.2% vs 14.2% and 0.1% vs 6.4%, respectively), and so was *Pseudomonas* in the Apse (<0.1% vs 42.0%) but not in the Passage (3.8% vs 3.2%). Conversely, *Chitinophaga* amounted to 8.8% of sequences in dark zones vs only <0.1% in unmarked surfaces, but levels were similar in the Passage (5.1% vs. 3.6%).

The first hypothesis was that microbial diversity indicated by metabarcoding would be confirmed with a PCR-free metagenomic approach. This hypothesis proved correct in the Apse for Bacteria, with noticeably a counter-selection of the Gammaproteobacteria (e.g. *Pseudomonas*) as well as the selection of Alphaproteobacteria class in dark zones, both for metabarcoding and metagenomic datasets, but not for microeukaryotes due to a significant amount of unidentified contigs (Supplementary Fig S3 and S4). For the Passage the hypothesis was not valid for Bacteria and microeukaryotes, in both surface conditions. For instance, the counter-selection of Gammaproteobacteria (including *Pseudomonas*) and selection of Chitinophagia (Bacteroidota) observed by metabarcoding was not confirmed by metagenomic approach.

Microbial genetic potential

The shotgun metagenomes (n = 18) from each rock surface condition were used to explore the genetic potential of communities thriving in Lascaux cave. Based on contigs analysis, up to 1.95×10^6 genes with predicted functions were identified per sample (average : 9.04×10^5 genes). These genes were distributed into at least 13,824 different molecular-level functions according to KEGG orthology. First, the focus was put on pathways for aromatic compound degradation, expected to be operational in and outside dark zones, and indeed genes *brcD* and *brcC* (benzoyl-CoA reductase subunits D and C), *pcpD* (tetrachlorobenzoquinone reductase), *phtD* (4,5-dihydroxyphthalate decarboxylase) and *poxF* (phenol hydroxylase P5) were found in and outside dark zones, in the Apse and the Passage, and at similar levels in and outside dark zones (respectively $P = 0.07$, $P = 0.13$, $P = 0.32$, $P = 0.10$, $P = 0.10$ in the Apse and $P = 0.12$, $P = 0.30$, $P = 0.10$, $P = 0.15$, $P = 0.20$ in the Passage) (Fig 3). The genes for degradation of polycyclic aromatic hydrocarbons *padAb* and *padAd* (phthalate 3,4-dioxygenase subunits beta and alpha) and *phdK* (2-formylbenzoate dehydrogenase), and toluene *bbsA* and *bbsC* (both benzoylsuccinyl-CoA thiolases) and *poxF* were evidenced in and outside dark zone, at similar levels in the Apse (respectively $P = 0.42$, $P = 0.06$,$P = 0.21$ for the former and $P =$

0.10, $P = 0.23$, $P = 0.18$ for the latter), at higher levels for *bbsA* ($P = 0.02$), *bbsC* ($P = 0.02$) and lower levels for *padAb* ($P = 0.04$), *padAd* ($P = 6.3 \times 10^{-5}$), *phdK* ($P = 0.01$), *poxF* ($P = 7.8 \times 10^{-5}$) in dark zones in the Passage. In addition, dark zones (in comparison with unmarked surfaces) exhibited a lower relative number of genes *badH* (2-hydroxycyclohexanecarboxyl-CoA dehydrogenase) for benzoate degradation ($P = 1.2 \times 10^{-4}$) and *bbsF* (benzylsuccinate CoA-transferase) for toluene degradation ($P = 1.3 \times 10^{-4}$) in the Apse, but not in the Passage ($P = 0.19$ and $P = 0.08$, respectively). Therefore, genes for aromatic compound degradation were found both in and outside dark zones, as expected, and often occurred at similar levels.

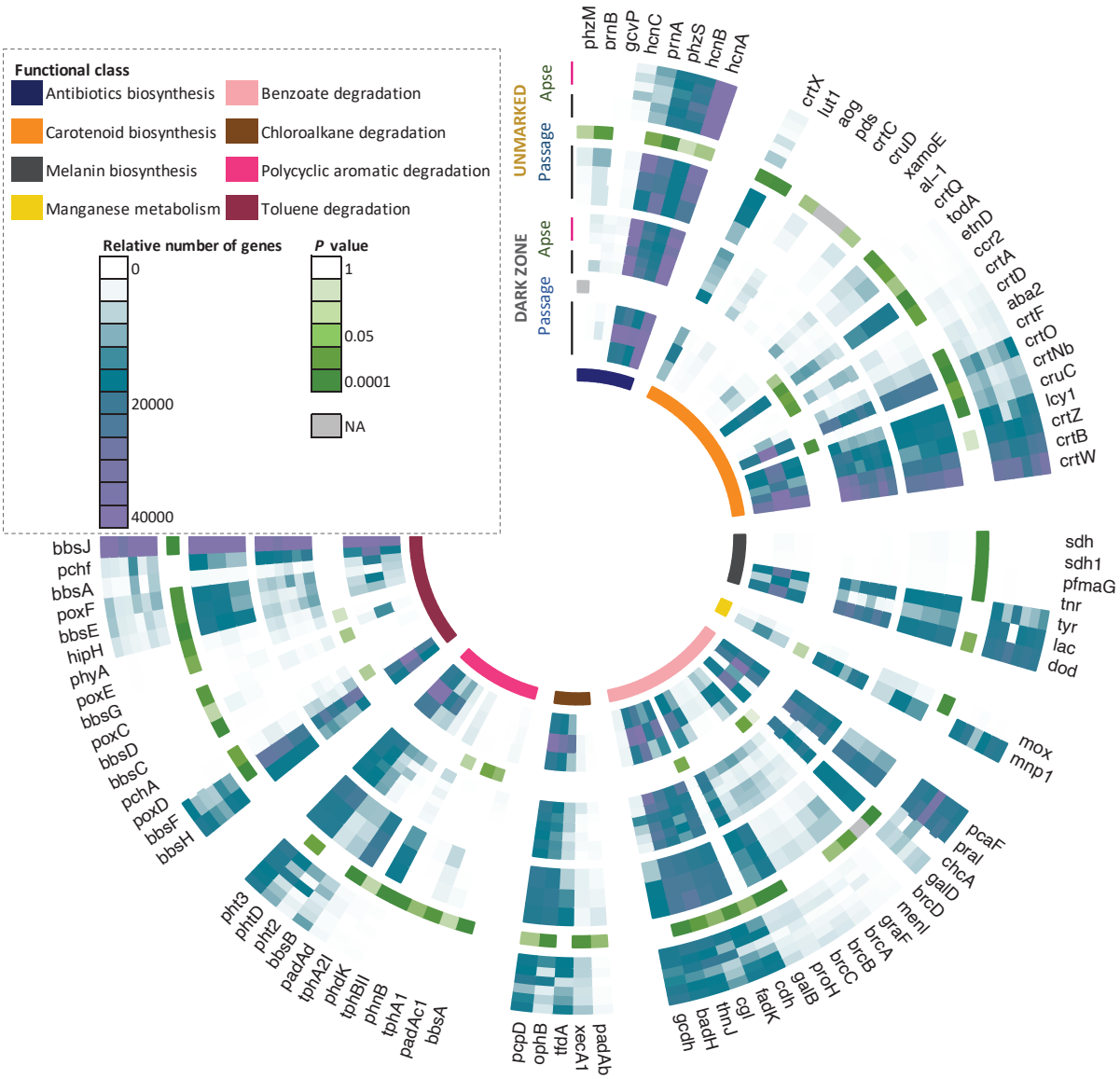

Fig 3. Relative abundance of metabolic genes identified in samples from unmarked surfaces and altered surfaces in the Apse and the Passage. The relative abundance of selected genes is represented using a gradient (0 to 40,000 sequences), with purple shades indicating higher abundances. The sampling year is indicated with a pink vertical line for 2020 and a black vertical line for 2021. The significance of Wilcoxon tests for comparison of unmarked surfaces and dark zones is represented by colorsplaced between unmarked-surface data and dark-zone data, using a gradient (P value of 1 to 0.0001), with green shades indicating significant P values. NA (Non-Applicable) : relative abundance of selected genes was 0. Metabolic functions associated to selected genes are detailed in Supplementary Table S3.

Second, since the darker shade associated with dark zones might entail microbial pigment production (hypothesis), we assessed the possibility that biosynthetic genes for organic compounds (pigments) would be more prevalent in dark zones than on unmarked surfaces. Consistent with this hypothesis, dark zones (in comparison with unmarked surfaces) displayed a higher relative number of carotenoid biosynthesis genes *crtA* (spheroidene monooxygenase, $P = 7.5 \times 10^{-4}$), *crtB* (15-cis-phytoene synthase, $P = 0.03$), *crtD* (1-hydroxycarotenoid 3,4-desaturase, $P = 9.4 \times 10^{-5}$), *crtQ* (4,4'-diaponeurosporenoate glycosyltransferase, $P = 1.1 \times 10^{-4}$), *crtX* (zeaxanthin glucosyltransferase, $P = 0.02$), *crtZ* (beta-carotene hydroxylase, $P = 2.4 \times 10^{-4}$) and melanin (dark pigments resulting from polymerization of phenolic and/or indolic compounds) biosynthesis genes *dod* (DOPA 4,5-dioxygenase, $P = 0.04$) and *tyr* (tyrosinase, $P = 2.9 \times 10^{-3}$) in the Apse, but not in the Passage (all $P > 0.05$) (Fig 4). Another possibility for darker shades would be the contribution of metal biotransformations, and here genes related to manganese oxidation i.e. *mox* (manganese peroxidase) and *mnp1* (manganese oxidase) were found, but at similar levels in and outside dark zones, both in the Apse ($P = 0.20$ for *mox*, $P = 0.08$ for *mnp1*) and the Passage ($P = 0.29$ for *mox*, $P = 0.10$ for *mnp1*) (Fig 4). Thus, the hypothesis that dark zones are enriched in pigment biosynthesis genes proved correct in the Apse (i.e. for carotenoids and melanins) but not in the Passage, whereas the metal metabolism hypothesis was not substantiated.

Third, dark zones occur as patches on wall surfaces, suggesting that pigmented fungi could be inhibited by other microorganisms present on unmarked surfaces. To assess this possibility, genes coding for antimicrobials were sought, but only four biosynthetic genes were identified. Biosynthetic genes were at similar relative numbers in and outside dark zones for pyrrolnitrin (*prnB*) in the Apse ($P = 0.13$) and Passage ($P = 0.07$), and for hydrogen cyanide (*hcnC* ; $P = 0.30$ and $P = 0.56$, respectively) (Fig 4). Conversely, the biosynthesis genes for hydrogen cyanide (*hcnB*) and pyocyanin (*phzS*) were in lower amounts in dark zone than in unmarked surfaces in the Apse ($P = 0.02$ and $P = 2.1 \times 10^{-4}$, respectively), but in similar amounts in the Passage ($P = 0.21$ and $P = 0.23$, respectively). Therefore, there was evidence for higher numbers of hydrogen cyanide and pyocyanin genes in unmarked surfaces but only in the Apse, but few genes coding for antimicrobials were evidenced.

Fourth, the last hypothesis was that metagenomic data would differ according to Lascaux location. All genes involved in the types of metabolic functions above were found both in the Apse and Passage, but only 35% of them there were at similar relative abundances ($P > 0.05$) in unmarked surfaces from both locations e.g. the melanin genes *tyr* (tyrosinase) and *lac* (laccase) and gene *bbsB* (acyltransferase) for degradation of polycyclic aromatics). On unmarked surfaces, the relative abundance of hydrogen cyanide gene *hcnB* ($P = 0.03$) was higher in the Apse compared with the Passage, and that of pyrrolnitrin genes *prnA* ($P = 0.01$), *prnB* ($P = 5.7 \times 10^{-4}$), benzoate degradation genes e.g. *thnJ* ($P = 6.5 \times 10^{-4}$), *badH* ($P = 2.3 \times 10^{-5}$), toluene degradation genes e.g. *bbsF* ($P = 7.6 \times 10^{-5}$), and genes for degradation of polycyclic aromatic hydrocarbon e.g. *padAd* ($P = 0.02$) and *phdK* ($P = 1.4 \times 10^{-4}$) was lower (Fig 3). In dark zones, more than 85% of the genes studied were at similar relative abundances ($P > 0.05$) in the Apse and Passage, e.g. genes *hcnB*, *hcnC* (hydrogen cyanide), *prnA*, *prnB* (pyrrolnitrin), *phzS* (pyocyanin), *lac*, *tyr*, *dod* (melanin), and *tfdA* (chloroalkane degradation). In dark zones, the relative abundance of carotenoid biosynthesis genes *ccr2* ($P = 4.2 \times 10^{-4}$) and *cruC* ($P =$

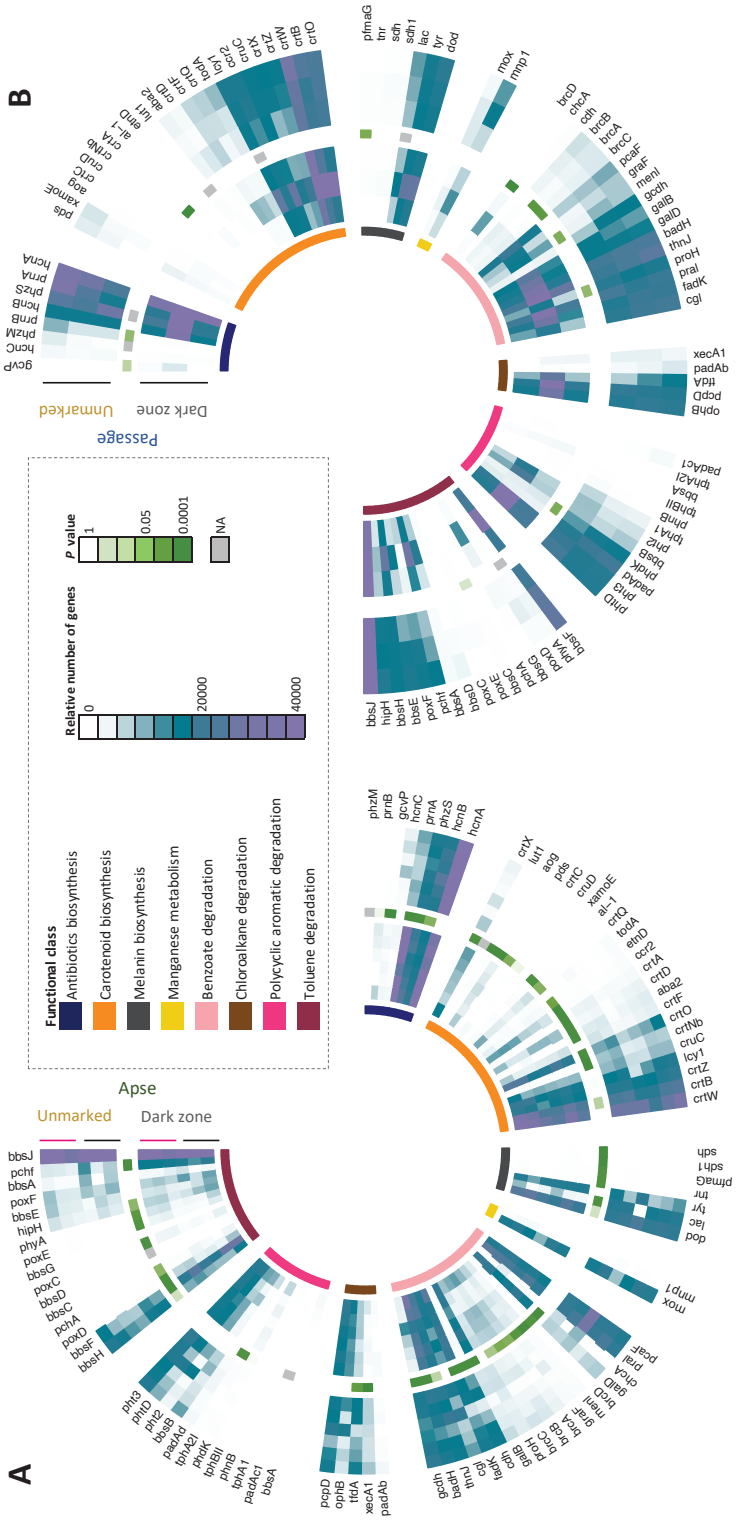

Fig 4. Relative abundance of metabolic genes identified in samples from (A) the Apse and (B) the Passage for unmarked surfaces and altered surfaces. The relative abundance of selected genes is represented using a gradient (0 to 40,000 sequences), with purple shades indicating higher abundances. The sampling year is indicated with a pink vertical line for 2020 and a black vertical line for 2021. The significance of Wilcoxon tests for comparison of unmarked surfaces and dark zones is represented by colorsplaced between unmarked-surface data and dark-zone data, using a gradient (P value of 1 to 0.0001), with green shades indicating significant P values. NA (Non-Applicable) : relative abundance of selected genes was 0. Metabolic functions associated to selected genes are detailed in Supplementary Table S3.

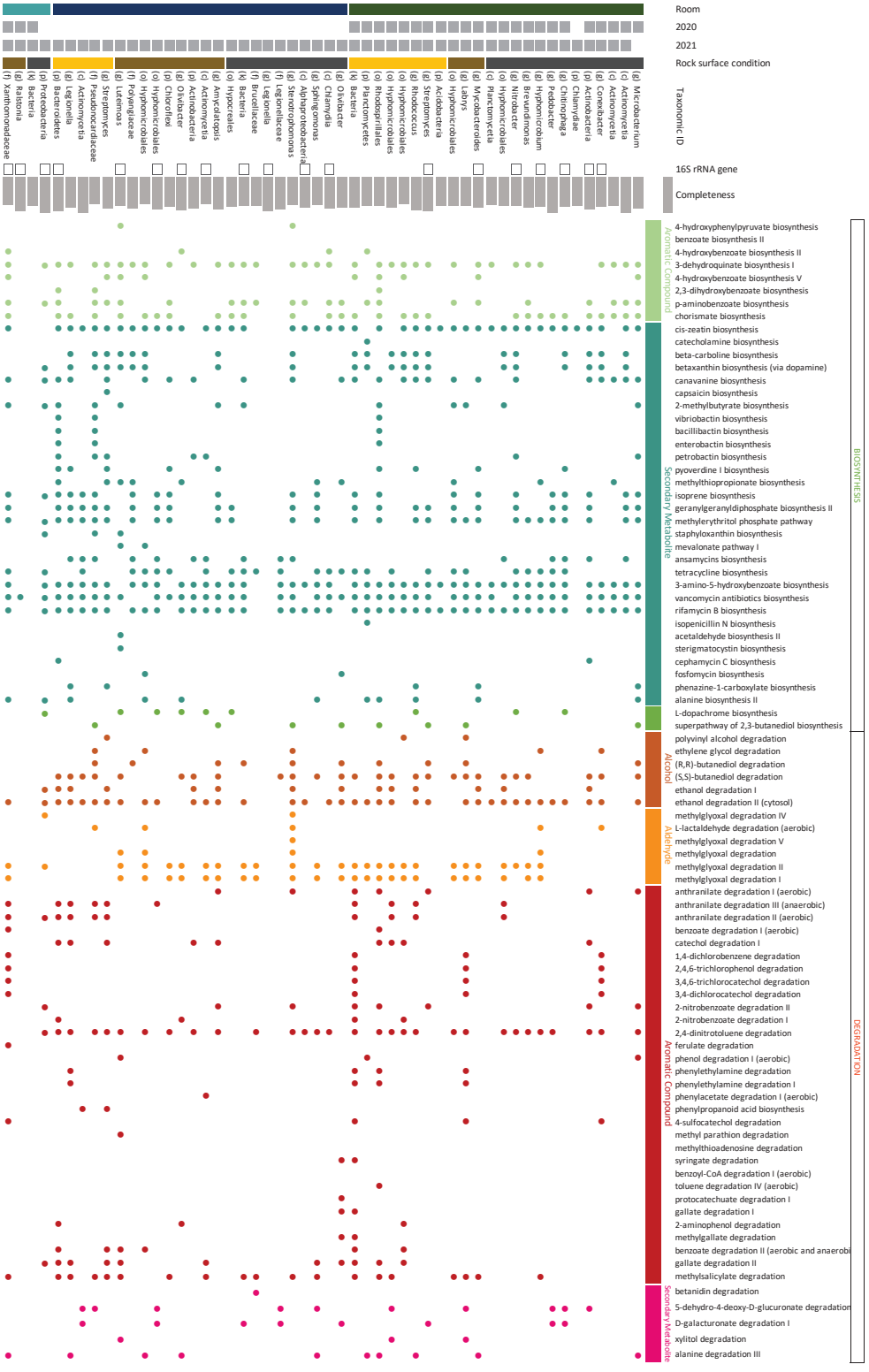

Fig 5. Metabolic pathways identified in reconstructed MAGs presenting >75% completeness and <5% of contamination. The taxonomic column indicates the taxonomic level assigned for the MAGs with (d) : domain, (p) : phylum, (c) : class, (o) : order, (g) : genus. Taxonomic affiliations are detailed in Supplementary Table S4. Identification of the pathways was carried out with MetaCyc and the KEGG pathway mapping tool. Green dots indicate biosynthesis pathways (aromatic compounds, secondary metabolites) and red dots degradation pathways (alcohols, aldehydes, aromatic compounds, and secondary metabolites).

2.4×10^{-4}, Fig 3) and toluene degradation genes *poxC* ($P = 0.02$), *poxD* ($P = 0.03$) and *poxE* ($P = 0.03$) was lower in the Apse compared with the Passage, and that of manganese metabolism gene *mox* ($P = 0.03$) and benzoyl-CoA reductase gene *brcD* ($P = 0.04$) was higher. Therefore, this hypothesis proved correct.

Genomes assembled from community metagenomes

MAGs (Metagenome-Assembled Genomes) were reconstructed to scale up from individual genes to metabolic pathways and identify potential actors involved in metabolic pathways of interest. MAGs corresponding to representative microbial lineages present in Lascaux Cave were assembled, and metabolic capabilities were inferred from the MAGs presenting $> 75\%$ completeness and contamination levels $< 5\%$ (Fig 5 and Supplementary Table S4).

First, we considered that genes for aromatic compound degradation were present in and out of dark zones, and here degradation pathways of benzoate, chlorobenzene and chlorophenol (and butanediol) were identified with MAGs reconstructed from both surface conditions, in the Apse (*Labrys*) or in both rooms (Xanthomonadaceae, *Labrys*, *Luteimonas* and *Ralstonia*) (Fig 5). The metabolic pathways involved in the degradation of nitroaromatic compounds such as 2-nitrobenzoate and 2,4-dinitrotoluene were identified in MAGs reconstructed from Apse unmarked surfaces (Alphaproteobacteria and *Streptomyces*, respectively) but also in MAGs reconstructed from Passage dark zones (all proteobacterial MAGs, excepted *Legionella*). Metabolic pathways for degradation of aromatic compounds such anthranilate and catechol were identified only in MAGs reconstructed from unmarked surfaces in the Apse (Actinobacteria, Hyphomicrobiales and Rhodospirillales) and Passsage (Actinobacteria, *Legionella*, *Streptomyces*). Therefore, metabolic pathways associated with the degradation of aromatic compounds were found both in and out of the dark zones, as expected, but these pathways were overall present in greater numbers (2.4 vs 9.7 pathways on average, $P = 0.004$) in MAGs reconstructed from the unmarked surfaces.

Second, since microbial pigment production or metal biotransformations might be associated with darker shades on walls (i.e. dark zone), we assessed the occurrence of relevant metabolic pathways in MAGs. Metabolic pathways for biosynthesis of terpenoids, derived from carotenoids, such as the betaxanthin, geranyl-diphosphate and methylerythritol phosphate biosynthetic pathways were identified in MAGs originating from unmarked surfaces in the Apse (Actinobacteria, Hyphomicrobiales, Rhodospirillales, etc.) or both Apse and Passage (Actinobacteria and *Legionella*) (Fig 5). Conversely, metabolic pathways associated with melanin biosynthesis, such as the L-dopachrome biosynthesis pathway, were identified in MAGs reconstructed from dark zone samples of the Apse only (*Nitrobacter*, *Chitinophaga*, Hypocreales) or of both rooms (Proteobacteria). Furthermore, no metabolic pathway involved in manganese metabolism was identified. Hence, the hypothesis that dark zones are enriched in pigment biosynthetic pathways was correct for melanin biosynthesis in both rooms, whereas the hypothesis of carotenoid and metal metabolism was not supported by MAG data.

Third, we considered metabolic pathways involved in the biosynthesis of antimicrobial compounds, in relation to the hypothesis that they might result into the inhibition of pigmented microorganisms on the unmarked surfaces. MAG analysis did not find pyrrolnitrin and HCN

pathways despite the occurrence of individual biosynthetic genes (see above), but evidenced biosynthesis pathways for tetracycline in unmarked surfaces of the Apse (*Streptomyces*), vancomycins in both rock surface conditions of both rooms (Hyphomicrobiales, *Microbacterium*, *Pedobacter*, etc.), and rifamycins in dark zones of the Apse (*Nitrobacter*, *Chitinophaga*, etc.) and both surface conditions of the Passage (Hypomicrobiales, *Sphingomonas*, *Streptomyces*, etc.) (Fig 5). Metabolic pathways for biosynthesis of siderophores (pyoverdine, petrobactin, enterobactin and bacillibactin) were identified in MAGs from unmarked surfaces, both for the Apse (Rhodospirillales, Bacteria) and the Passage (Pseudonocardiaceae, Bacteroidetes). Therefore, at the MAG level there is evidence for an enrichment in unmarked surfaces of metabolic pathways involved in the biosynthesis of tetracycline and siderophores, but not for other antimicrobial compounds.

Fourth, the final hypothesis was that the metagenomic data would differ with Lascaux location. Indeed, the reconstructed MAGs were generally specific to their sampling location and only four MAGs originated from both rooms (for Bacteria, Proteobacteria, Xanthomonadaceae and *Ralstonia*) (Fig 5).

Discussion

For the two types of rock surface conditions and locations, a large proportion of Bacteria was identified (>84%), whereas microeukaryotes were poorly represented in all datasets (1.8%), including Fungi which accounted for 0.7% of sequences. This pattern was also observed using reconstructed genomes (MAGs), with only 1 out of the 53 MAGs affiliated with microeukaryotes (Fungi). Two explanations are possible. . First, the low representation of microeukaryotes may be due to a limitation of bioinformatic methods for metagenomic analyses, which are not yet effective for eukaryotic sequences. Indeed, tools and databases devoted to metagenomic analyses are still highly biased toward prokaryote analyses [50,51]. Moreover, tools allowing the binning and quality estimation of MAGs are still limited, because (i) genome size is classically larger for eukaryotes than prokaryotes and (ii) eukaryotic marker genes present in large multiple copy numbers (between 14 and 1442 ITS copies for fungi compared with only 1-21 copies for bacterial 16S genes) are often considered as indicators of contamination during the quality estimation of MAGs, distorting the result and leading to the non-selection of MAGs [52,53], therefore reducing the relative amount of eukaryotic MAGs. This is a significant issue with metagenomics in all types of environments [50,54]. Second, it could also be that Bacteria outnumber the other types of microorganisms in caves [55,56]. Indeed, quantitative PCR levels were 1 or 2 log higher for 16S vs 18S rRNA genes in various Lascaux conditions [25].

In this work, the priority was put on dark zones of the Apse, where the first identification of a dark zone was made (based on June 2008' photographic archives). In the Apse, Acidobacteria and Proteobacteria (especially Gammaproteobacteria) predominated on unmarked surfaces, as previously reported in Lascaux Cave [12,56] and other karstic caves [24,57,58], based on cloning-sequencing and especially metabarcoding. Here, this was confirmed by metagenomic analysis of 16S rRNA markers (and in fact metabarcoding and metagenomics results for bacteria were convergent for all four conditions studied). Thus, we confirmed and expanded previous findings (Alonso et al., submitted) that dark zone formation on wall surfaces of the Apse coincides

with major shifts in microbial community composition. This includes the counter-selection of *Pseudomonas* and the selection of various Alphaproteobacteria and the Bacteroidota genus *Chitinophaga*, a pioneer genus as soon as dark zone formation starts (unpublished observation). However, metagenomics did not prove effective to document community changes for microeukaryotes, as discussed above. For instance, we did not manage to detect any sequence affiliated with the black fungus *Ochroconis*, one of the most abundant taxa evidenced by 18S rRNA gene and ITS2 metabarcoding [25])

In the Apse, metagenomics brought new insight into the process of dark zone formation. First, it showed that genes and metabolic pathways for aromatic compound degradation and catechol formation were well present in microorganisms, both for dark zones and unmarked surfaces. BAC applied to the walls of Lascaux Cave displays a benzene ring [59], and catabolism by several microorganisms including *Pseudomonas* [60][60] may lead to the formation of catechol and fuel microbial growth. Second, metagenomics evidenced in dark zones of the Apse an enrichment in pigment biosynthesis genes, both for carotenoids and melanins. It is of interest that catechol (see above) is a precursor of melanin in bacteria and fungi [61–63]. BAC degradation yields benzyldimethylamine, benzylamine and benzoic acid that might also be used for pigment biosynthesis [20,21]. In dark zones, some of the reconstructed MAGs affiliated to Proteobacteria, *Nitrobacter* (Alphaproteobacteria) and *Chitinophaga* (Bacteroidetes) presented L-dopachrome biosynthesis pathways, suggesting their ability to produce melanin. Indeed, L-dopachrome is involved in melanin biosynthesis [62,64], by being spontaneously decomposed into 5,6-dihydroxyindole and CO_2 [65] or enzymatically decomposed into 5,6-dihydroxyindole-2-carboxylate (L-dopachrome tautomerase)[66]. Third, the possibility that pigmented microorganisms may be controlled by antimicrobials produced by other microorganisms present on unmarked surfaces is in accordance with the occurrence of biosynthetic genes for hydrogen cyanide, pyrrolnitrin, pyocyanin and the enrichment in unmarked surfaces of metabolic pathways involved in the biosynthesis of tetracycline and siderophores. Bacterial genera such as *Pseudomonas* or *Streptomyces*, widely present in caves [23,56], have the potential to secrete these antimicrobial compounds [26,28,30].

In this work, we extended the analysis to include also dark zones with contrasted features, i.e. located elsewhere (in the Passage), on a distinct surface (an artificial limestone masonery bench), which received the same chemical treatments as in the Apse (formaldehyde, benzalkonium chloride, etc.) but also additional ones (benzalkonium chloride, myristalkonium chloride, 2-octyl-2H-isothiazol-3-one, Parmetol DF12 and 3% isothiazolinone ; [6,12]), and that formed much later (from 2016 on). Differences in substrate composition alone can impact microbial ecology in caves [67–71] and may be relevant here. Not surprisingly, the metagenomic dataset indicated a significant difference in community composition, overall, between the Apse and the Passage (adonis : $P = 0.001$, $R^2 = 0.36$). Since microbial community composition differed, it is not surprising that distinct dynamics were observed in relation to dark zone formation. In particular, the counter-selection of *Pseudomonas* in the Apse was not found here, as this genus represented only 0.3% in unmarked surfaces (and 3.5% in dark zones) of the Passage. In the Passage, the main features of dark zones were the selection of the classes Alphaproteobacteria and Betaproteobacteria (as in the Apse) and the counter-selection of Acidobacteria class and *Chitinophaga* genus (unlike in the Apse). Against this background, some of the functional parti-

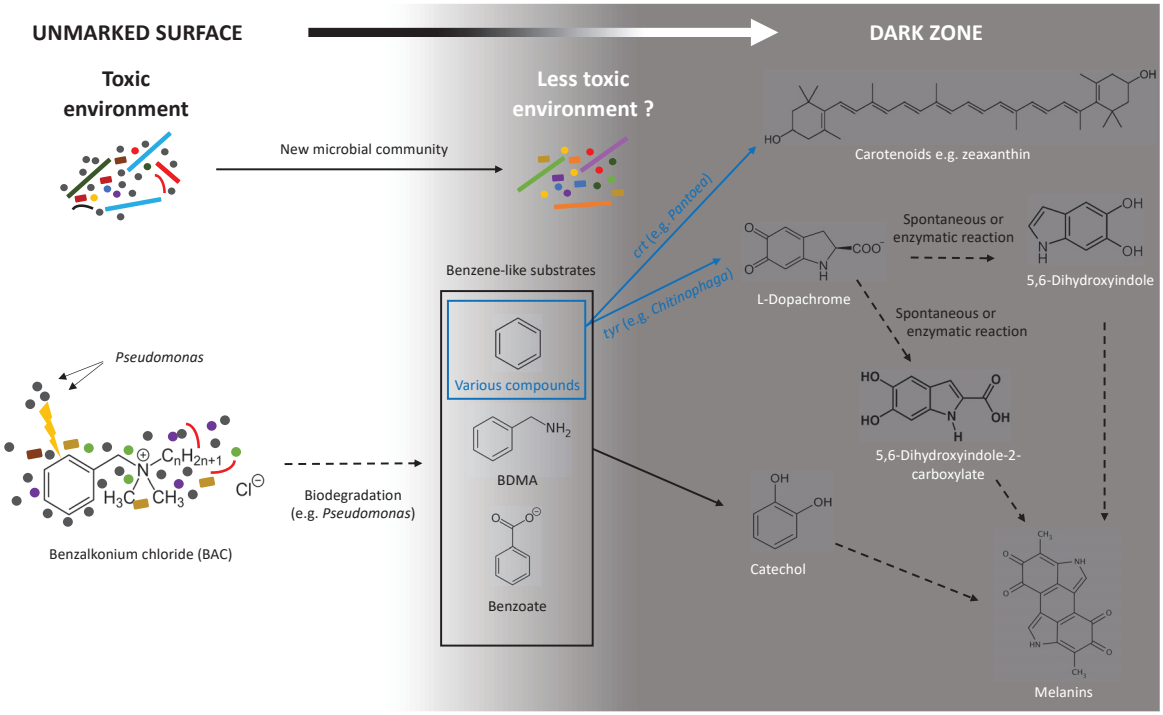

Fig 6. Conceptual model of dark zone formation integrating taxonomic and functional metagenomic information provided by the present work. The black arrows represent metabolic pathways identified in this study. The dotted arrows represent the metabolic pathways not identified in this study but expected to occur based on literature information. The blue arrows indicate the link between various benzene-like compounds that can derive from the degradation of BAC, which can then be transformed into carotenoids or L-dopachrome in dark zones. BAC : benzalkonium chloride ; BDMA : benzyldimethylamine.

cularities identified in the Apse were also applicable to the Passage, i.e. (i) aromatic compound degradation genes and pathways well present both in and outside dark zones, (ii) the enrichment of dark zones in melanin synthesis pathway, with in the Passage a MAG affiliated to Hypocreales (Ascomycota) presenting a L-dopachrome biosynthesis pathway, and (iii) a decreased in siderophore biosynthesis pathways in dark zones. However, others were not relevant in the Passage, such as the enrichment of dark zones in biosynthetic genes for (i) carotenoids and (ii) hydrogen cyanide and pyocyanin genes, which occurred only in the Apse.

Overall, the formation of dark zones in the two rooms presents similarities, and we speculate that the following conceptual framework can be proposed for dark zone formation in Lascaux Cave (Fig 6). First, BAC and other toxic chemicals applied on cave walls may be degraded by resistant microorganisms using aromatic compound degradation pathway(s), for instance via benzoyl-CoA and implicating *Pseudomonas*, *Streptomyces* or other bacteria. Second, BAC degradation products – including benzyldimethylamine, an intermediate almost 500 times less toxic than BAC [72,73] and catechol – sustain microbial growth. Third, these degradation products may also provide (i) melanin precursors, for instance via the synthesis of L-dopachrome, subsequently transformed into 5,6-dihydroxyindole or 5,6-dihydroxyindole-2-carboxylate, and (ii) metabolites for synthesis of carotenoids, which may be especially relevant in cave wall micro-environments where antagonistic microorganisms are less prevalent in the community. This proposition is compatible with previous hypotheses on other Lascaux alterations (black

stains) attributed to melanized fungi, as outlined by Martin-Sanchez *et al.* (2012), Bastian *et al.* (2009), Alabouvette and Saiz-Jimenez (2011).

Conclusion

Dark zone alterations are of great concern for cave conservation, but their microbial features need clarification. The present metagenomic work fills a gap by revealing common secondary metabolism traits in two contrasted Lascaux locations, including microbial potentials for degradation of BAC biocides (thereby providing growth substrates), synthesis of melanin or carotenoid (that may contribute to the dark shade of wall alterations), and production of antimicrobials that might regulate community composition. Understanding the taxonomic and functional processes involved in alteration formation is expected to better guide conservation strategies for this major Paleolithic site.

Acknowledgements

Funding was provided by DRAC Nouvelle Aquitaine (Bordeaux, France). We thank S. Géraud, J.C. Portais, M. Mauriac (DRAC Nouvelle Aquitaine) and D. Henry-Lormelle (restorer team) for information and help, and Lascaux Scientific Board for useful discussions.

Authorship contributions statement

ZB contributed to sampling, acquired data, interpreted results, wrote the manuscript and prepared figures and tables ; DA acquired data ; YML obtained funding, managed the project, designed the experiments, contributed to sampling, interpreted results and revised the manuscript ; MH interpreted results and revised the manuscript.

Declaration of competing interest

The authors declare that they have no known competing financial interest or personal relationships that could have influenced the work reported in this paper.

References

1. Biot V. Grottes et cavernes, un patrimoine à (re)valoriser. Espac Tour Loisirs. 2006 ;238 :15 –21.

2. Cigna A, Forti P, Moreira JC, Carvalho CN. Caves : the most important geotouristic feature in the world. Tour Karst Areas. 2013 ;6 :9–26.

3. Cigna A. Tourism and show caves. Geomorphology. 2016 ;60 :217–33.

4. Ikner LA, Toomey RS, Nolan G, Neilson JW, Pryor BM, Maier RM. Culturable microbial diversity and the impact of tourism in Kartchner Caverns, Arizona. Microb Ecol. 2007 ;53 :30–42.

5. Portillo MC, Gonzalez JM, Saiz-Jimenez C. Metabolically active microbial communities of yellow and grey colonizations on the walls of Altamira Cave, Spain. J Appl Microbiol. 2008 ;104 :681–91.

6. Martin-Sanchez PM, Miller AZ, Saiz-Jimenez C. 13. Lascaux Cave : An example of fragile ecological balance in subterranean environments. In : Engel A.S. (Eds.), Microbial life in cave systems. Berlin :De Gruyter ;2015.p279–301.

7. Bontemps Z, Alonso L, Pommier T, Hugoni M, Moënne-Loccoz Y. Microbial ecology of tourist Paleolithic caves. Sci Tot Environ. 2021 ;816 :151492.

8. Russell MJ, MacLean VL. Management issues in a Tasmanian tourist cave : potential microclimatic impacts of cave modifications. J Environ Manage. 2008 ;87 :474–83.

9. Dupont J, Jacquet C, Dennetière B, Lacoste S, Bousta F, Orial G, et al. Invasion of the French Paleolithic painted cave of Lascaux by members of the *Fusarium solani* species complex. Mycologia. 2007 ;99 :526–33.

10. Gauchon C, Jaillet S, Prud'homme F. Dynamique de la construction topographique et toponymique à l'aven d'Orgnac (Ardèche, France). Collect EDYTEM Cah Géographie. 2012 ;13 :157 –76.

11. Chalmin E, d'Orlyé F, Zinger L, Charlet L, Geremia RA, Orial G, et al. Biotic versus abiotic calcite formation on prehistoric cave paintings : the Arcy-sur-Cure 'Grande Grotte' (Yonne, France) case. Geol Soc Lond. 2007 ;279 :185–97.

12. Bastian F, Jurado V, Nováková A, Alabouvette C, Saiz-Jimenez C. The microbiology of Lascaux Cave. Microbiology. 2010 ;156 :644–52.

13. Papier S, Baele J-M, Gillan D, Barriquand L, Barriquand J. Manganese geomicrobiology of the black deposits from the Azé cave, Saône-et-loire, France. Quaternaire. 2011 ;4 :297–305.

14. Lepinay C, Mihajlovski A, Touron S, Seyer D, Bousta F, Di Martino P. Bacterial diversity associated with saline efflorescences damaging the walls of a French decorated prehistoric cave registered as a World Cultural Heritage Site. Int Biodeterior Biodegrad. 2018 ;130 :55–64.

15. Baquedano Estévez C, Moreno Merino L, De la Losa Román A, Duran Valsero J. The lampenflora in show caves and its treatment : an emerging ecological problem. Int J Speleol. 2019 ;48 :249-277.

16. He J, Zhang N, Muhammad A, Shen X, Sun C, Li Q, et al. From surviving to thriving, the assembly processes of microbial communities in stone biodeterioration : A case study of the West Lake UNESCO World Heritage area in China. Sci Tot Environ. 2022 ;805 :150395.

17. Lefèvre M. La 'Maladie Verte' de Lascaux. Stud Conserv. 1974 ;19 :126–56.

18. Saiz-Jimenez C. Microbiological and environmental issues in show caves. World J Microbiol Biotechnol. 2012 ;28 :2453–64.

19. Dieser M, Greenwood M, Foreman CM. Carotenoid pigmentation in antarctic heterotrophic bacteria as a strategy to withstand environmental stresses. Arct Antarct Alp Res. 2010 ;42 :396–405.

20. Patrauchan MA, Oriel PJ. Degradation of benzyldimethylalkylammonium chloride by *Aeromonas hydrophila* sp. K. J Appl Microbiol. 2003 ;94 :266–72.

21. Alabouvette C, Saiz-Jiménez C. Écologie microbienne de la grotte de Lascaux. CSIC-Instituto de Recursos Naturales y Agrobiología de Sevilla (IRNAS) 2011.

22. Frey-Klett P, Burlinson P, Deveau A, Barret M, Tarkka M, Sarniguet A. Bacterial-fungal interactions : hyphens between agricultural, clinical, environmental, and food microbiologists. Microbiol Mol Biol Rev. 2011 ;75 :583–609.

23. Maciejewska M, Adam D, Naômé A, Martinet L, Tenconi E, Całusińska M, et al. Assessment of the potential role of *Streptomyces* in Cave Moonmilk formation. Front Microbiol. 2017 ;8 :1181.

24. Alonso L, Pommier T, Kaufmann B, Dubost A, Chapulliot D, Doré J, et al. Anthropization level of Lascaux Cave microbiome shown by regional-scale comparisons of pristine and anthropized caves. Mol Ecol. 2019 ;28 :3383–94.

25. Alonso L, Creuzé-des-Châtelliers C, Trabac T, Dubost A, Moënne-Loccoz Y, Pommier T. Rock substrate rather than black stain alterations drives microbial community structure in the Passage of Lascaux Cave. Microbiome. 2018 ;6 :216.

26. Almario J, Bruto M, Vacheron J, Prigent-Combaret C, Moënne-Loccoz Y, Muller D. Distribution of 2,4-diacetylphloroglucinol biosynthetic genes among the *Pseudomonas* spp. reveals unexpected polyphyletism. Front Microbiol. 2017 ;8 :1218.

27. Kong D, Wang X, Nie J, Niu G. Regulation of antibiotic production by signaling molecules in *Streptomyces*. Front Microbiol. 2019 ;10 :2927.

28. Howell CR, Stipanovic RD. Control of *Rhizoctonia solani* on cotton seedlings with *Pseudomonas fluorescens* and with an antibiotic produced by the bacterium. Phytopathology. 1979 ;69 :480-82

29. Michelsen CF, Stougaard P. Hydrogen cyanide synthesis and antifungal activity of the biocontrol strain *Pseudomonas fluorescens* In5 from Greenland is highly dependent on growth medium. Can J Microbiol. 2012 ;58 :381–90.

30. Rangseekaew P, Pathom-aree W. Cave actinobacteria as producers of bioactive metabolites. Front Microbiol. 2019 ;10 :387

31. Bolger AM, Lohse M, Usadel B. Trimmomatic : a flexible trimmer for Illumina sequence data. Bioinformatics. 2014 ;30 :2114–20.

32. Li D, Liu C-M, Luo R, Sadakane K, Lam T-W. MEGAHIT : an ultra-fast single-node solution for large and complex metagenomics assembly. Bioinformatics. 2015 ;31 :1674–6.

33. Langmead B, Salzberg SL. Fast gapped-read alignment with Bowtie 2. Nat Methods. 2012 ;9 :357–9.

34. Hyatt D, Chen G-L, LoCascio PF, Land ML, Larimer FW, Hauser LJ. Prodigal : prokaryotic gene recognition and translation initiation site identification. BMC Bioinformatics. 2010 ;11 :119.

35. Seemann T. Barrnap. 2022. Available from : *https* : *//github.com/tseemann/barrnap*

36. Wang Q, Garrity GM, Tiedje JM, Cole JR. Naive Bayesian classifier for rapid assignment of rRNA sequences into the new bacterial taxonomy. Appl Environ Microbiol. 2007 ;73 :5261–7.

37. Kanehisa M, Goto S. KEGG : Kyoto Encyclopedia of Genes and Genomes. Nucleic Acids Res. 2000 ;28 :27–30.

38. Kang DD, Li F, Kirton E, Thomas A, Egan R, An H, et al. MetaBAT 2 : An adaptive binning algorithm for robust and efficient genome reconstruction from metagenome assemblies. PeerJ. 2019 ;7 :e7359.

39. Wu Y-W, Tang Y-H, Tringe SG, Simmons BA, Singer SW. MaxBin : An automated binning method to recover individual genomes from metagenomes using an expectation-maximization algorithm. Microbiome. 2014 ;2 :26.

40. Sieber CMK, Probst AJ, Sharrar A, Thomas BC, Hess M, Tringe SG, et al. Recovery of genomes from metagenomes via a dereplication, aggregation and scoring strategy. Nat Microbiol. 2018 ;3 :836–43.

41. Parks DH, Imelfort M, Skennerton CT, Hugenholtz P, Tyson GW. CheckM : assessing the quality of microbial genomes recovered from isolates, single cells, and metagenomes. Genome Res. 2015 ;25 :1043–55.

42. Simão FA, Waterhouse RM, Ioannidis P, Kriventseva EV, Zdobnov EM. BUSCO : assessing genome assembly and annotation completeness with single-copy orthologs. Bioinformatics. 2015 ;31 :3210–2.

43. Karp PD, Riley M, Paley SM, Pellegrini-Toole A. The MetaCyc database. Nucleic Acids Res. 2002 ;30 :59–61.

44. Galperin MY, Wolf YI, Makarova KS, Vera Alvarez R, Landsman D, Koonin EV. COG database update : Focus on microbial diversity, model organisms, and widespread pathogens. Nucleic Acids Res. 2021 ;49 :D274–81.

45. Gu Z. circlize : Circular visualization. 2022. Available from : *https* : *//CRAN.R − project.org/package = circlize*

46. R Core Team. R : A language and environment for statistical computing. R Foundation for Statistical Computing. 2020. Available from : *https* : *//www.R − project.org/*

47. Oksanen J, Blanchet FG, Friendly M, Kindt R, Legendre P, McGlinn D, et al. vegan : Community ecology package. 2020. Available from : *https* : *//CRAN.R−project.org/package = vegan*

48. Clarke KR. Non-parametric multivariate analyses of changes in community structure. Aust J Ecol. 1993 ;18 :117–43.

49. Arbizu PM. pairwiseAdonis. 2021. Available from : *https : //github.com/pmartinezarbizu /pairwiseAdonis*

50. Escobar-Zepeda A, Vera-Ponce de León A, Sanchez-Flores A. The road to metagenomics : From microbiology to DNA sequencing technologies and bioinformatics. Front Genet. 2015 ;6 :348

51. Marcelino VR, Clausen PTLC, Buchmann JP, Wille M, Iredell JR, Meyer W, et al. CCMetagen : comprehensive and accurate identification of eukaryotes and prokaryotes in metagenomic data. Genome Biol. 2020 ;21 :103.

52. Falentin H, Auer L, Mariadassou M, Pascal G, Rué O, Dugat-Bony E, et al. Guide pratique à destination des biologistes, bioinformaticiens et statisticiens qui souhaitent s'initier aux analyses métabarcoding. Cah Tech INRA. 2019 ;2019 :1–23.

53. Saary P, Mitchell AL, Finn RD. Estimating the quality of eukaryotic genomes recovered from metagenomic analysis with EukCC. Genome Biol. 2020 ;21 :244.

54. Gilbert JA, Dupont CL. Microbial metagenomics : beyond the genome. Annu Rev Mar Sci. 2011 ;3 :347–71.

55. Mendoza MLZ, Lundberg J, Ivarsson M, Campos P, Nylander JAA, Sallstedt T, et al. Metagenomic analysis from the interior of a speleothem in Tjuv-Ante's Cave, northern Sweden. pLoS One. 2016 ;11 :e0151577.

56. Wiseschart A, Mhuantong W, Tangphatsornruang S, Chantasingh D, Pootanakit K. Shotgun metagenomic sequencing from Manao-Pee cave, Thailand, reveals insight into the microbial community structure and its metabolic potential. BMC Microbiol. 2019 ;19 :144-156.

57. Dhami NK, Mukherjee A, Watkin ELJ. Microbial diversity and mineralogical-mechanical properties of calcitic cave speleothems in natural and in vitro biomineralization conditions. Front Microbiol. 2018 ;9 :10.

58. Kimble JC, Winter AS, Spilde MN, Sinsabaugh RL, Northup DE. A potential central role of Thaumarchaeota in N-Cycling in a semi-arid environment, Fort Stanton Cave, Snowy River passage, New Mexico, USA. FEMS Microbiol Ecol. 2018 ;94 :173.

59. Merchel Piovesan Pereira B, Tagkopoulos I. Benzalkonium chlorides : Uses, regulatory status, and microbial resistance. Appl Environ Microbiol. 2019 ;85 :e00377-19.

60. Ertekin E, Hatt JK, Konstantinidis KT, Tezel U. Similar microbial consortia and genes are involved in the biodegradation of benzalkonium chlorides in different environments. Environ Sci Technol. 2016 ;50 :4304–13.

61. Solano F. Melanins : Skin pigments and much more—Types, structural models, biological functions, and formation routes. New J Sci. 2014 ;14 :e498276.

62. De la Rosa JM, Martin-Sanchez PM, Sanchez-Cortes S, Hermosin B, Knicker H, Saiz-Jimenez C. Structure of melanins from the fungi *Ochroconis lascauxensis* and *Ochroconis anomala* contaminating rock art in the Lascaux Cave. Sci Rep. 2017 ;7 :13441.

63. Azman A-S, Mawang C-I, Abubakar S. Bacterial pigments : The bioactivities and as an alternative for therapeutic applications. Nat Prod Commun. 2018 ;13 :1934578X1801301240.

64. Nicolaus RA. Melanins. Paris :Hermann ;1968.

65. Munoz-Munoz JL, García-Molina F, Varón R, Tudela J, García-Cánovas F, Rodríguez-López JN. Generation of hydrogen peroxide in the melanin biosynthesis pathway. Biochim Biophys Acta. 2009 ;1794 :1017–29.

66. Pawelek JM. Dopachrome conversion factor functions as an isomerase. Biochem Biophys Res Commun. 1990 ;166 :1328–33.

67. Cañveras CS-J S Sanchez-Moral, V Sloer. Microorganisms and microbially induced fabrics in cave walls. Geomicrobiol J. 2001 ;18 :223–40.

68. Barton HA, Jurado V. What's up down there ? Microbial diversity in caves microorganisms in caves survive under nutrient-poor conditions and are metabolically versatile and unexpectedly diverse. Microbes. 2007 ;2 :132-138.

69. Barton HA, Northup DE. Geomicrobiology in cave environments : past, current and future perspectives. J Cave Karst Stud. 2007 ;69 :163–78.

70. Lavoie K, Ruhumbika T, Bawa A, Whitney A, De Ondarza J. High levels of antibiotic resistance but no antibiotic production detected along a gypsum gradient in Great Onyx Cave, KY, USA. Diversity. 2017 ;9 :42.

71. Espino del Castillo A, Beraldi-Campesi H, Amador-Lemus P, Beltrán HI, Borgne SL. Bacterial diversity associated with mineral substrates and hot springs from caves and tunnels of the Naica underground system (Chihuahua, Mexico). Int J Speleol. 2018 ;47 :213–27.

72. Tezel U, Tandukar M, Martinez RJ, Sobecky PA, Pavlostathis SG. Aerobic biotransformation of n-tetradecylbenzyldimethylammonium chloride by an enriched *Pseudomonas* spp. community. Environ Sci Technol. 2012 ;46 :8714–22.

73. Tandukar M, Oh S, Tezel U, Konstantinidis KT, Pavlostathis SG. Long-term exposure to benzalkonium chloride disinfectants results in change of microbial community structure and increased antimicrobial resistance. Environ Sci Technol. 2013 ;47 :9730–8.

Supplementary data

Supplementary table S1. Metagenome characteristics before and after bio-informatic treatment. UN : Unmarked surface ; DZ : Dark zone ; Nb : number ; ORF : Open Reading Frame ; rRNA : ribosomal RNA ; tRNA : transfer RNA ; tmRNA : transfer-messenger RNA.

Sample	Nb raw reads	Mean quality score	% Bases ≥ 30	Nb cleaned reads	Nb Bacteria reads	Nb Archaea reads	Nb Eukaryota reads	Number of ORFs	Number of rRNAs	Number of tRNAs/tmRNAs
Apse_DZ_20	85,673,155	35.86	93.64	78,510,880	5,386,148	6,633	837,177	830,735	514	5,977
Apse_DZ_20	81,226,290	35.82	93.44	96,894,768	53,422,381	19,491	951,802	881,323	506	6,426
Apse_DZ_20	88,841,391	35.87	93.67	74,273,320	45,700,743	108,331	2,496,531	918,169	518	5,929
Apse_UN_20	102,718,931	36.01	94.33	81,440,904	55,412,434	9,66	604,451	885,744	528	4,86
Apse_UN_20	98,531,687	35.96	94.08	90,727,978	45,528,099	83,763	1,774,902	853,627	524	4,697
Apse_UN_20	66,825,010	36.00	94.28	60,997,870	49,293,283	79,499	1,893,948	779,836	490	4,019
Apse_DZ_21	98,486,488	35.88	93.65	89,278,002	53,844,638	8,354	856,427	728,927	488	5,131
Apse_DZ_21	104,961,917	35.75	93.04	95,557,330	54,382,377	7,051	435,671	833,271	538	6,065
Apse_DZ_21	140,424,511	35.98	94.15	132,209,678	54,368,032	19,507	769,913	758,261	486	5,564
Apse_UN_21	105,941,549	36.02	94.37	95,739,378	55,577,808	33,936	475,881	887,385	477	6,279
Apse_UN_21	92,595,905	35.90	93.90	86,021,596	48,824,622	113,186	1,879,684	888,181	462	6,111
Apse_UN_21	91,971,486	35.96	94.06	83,749,236	46,137,316	82,127	2,963,412	744,163	417	5,326
Passage_DZ_21	106,030,598	36.06	94.43	100,124,694	44,258,631	41,925	587,684	895,017	564	6,453
Passage_DZ_21	174,354,227	36.07	94.53	162,688,142	52,981,579	14,388	1,067,357	861,287	536	6,152
Passage_DZ_21	76,943,124	35.84	93.43	71,118,530	51,782,492	53,151	203,302	871,98	573	6,923
Passage_UN_21	142,219,108	35.87	93.68	128,964,288	54,888,846	33,842	388,215	651,108	491	4,076
Passage_UN_21	139,190,902	35.93	93.89	127,902,520	54,408,935	37,11	599,080	850,836	517	4,495
Passage_UN_21	109,737,221	35.95	93.99	100,947,270	53,742,721	77,092	661,644	910,773	533	5,049

Supplementary table S2. Quality of shotgun metagenome assembly.

Characteristics	Results
Number of contigs	245692
Total length	2,000,301,993 bp
Longest contig	888686 bp
Shortest contig	2000 bp
N50	15821
N90	2842
Contigs at superkingdom (k) rank	196773 (80.1%), in 4 superkingdoms
Contigs at phylum (p) rank	179330 (73.0%), in 64 phyla
Contigs at class (c) rank	154005 (62.7%), in 96 classes
Contigs at order (o) rank	118396 (48.2%), in 217 orders
Contigs at family (f) rank	82624 (33.6%), in 345 families
Contigs at genus (g) rank	76655 (31.2%), in 644 genera
Contigs at species (s) rank	24710 (10.1%), in 747 species
Congruent	231460 (94.2%)
Disparity > 0	14233 (5.8%)
Disparity ≥ 0.25	7850 (3.2%)

N50: is the minimum contig length to cover 50% of the genome.
N90: is the minimum contig length to cover 90% of the genome.
Congruent means that all genes in the contig belong to the same taxa.
Disparity is the percentage of paired comparisons between genes that belong to different taxa.

Supplementary table S3. Detailed information on selected functional genes.

Gene	KEGG number	Function	Hierarchical classes (KEGG)		
prnA	K14266	tryptophan 7-halogenase [EC:1.14.19.9]	Metabolism	Biosynthesis of other secondary metabolites	Staurosporine biosynthesis
prnB	K19981	monodechloroaminopyrrolnitrin synthase	Metabolism	Biosynthesis of other secondary metabolites	Staurosporine biosynthesis
gcvP	K00281	glycine dehydrogenase [EC:1.4.4.2]	Metabolism	Carbohydrate metabolism	Glyoxylate and dicarboxylate metabolism
hcnA	K10814	hydrogen cyanide synthase HcnA [EC:1.4.99.5]	Metabolism	Metabolism of other amino acids	Cyanoamino acid metabolism
hcnB	K10815	hydrogen cyanide synthase HcnB [EC:1.4.99.5]	Metabolism	Metabolism of other amino acids	Cyanoamino acid metabolism
hcnC	K10816	hydrogen cyanide synthase HcnC [EC:1.4.99.5]	Metabolism	Metabolism of other amino acids	Cyanoamino acid metabolism
phzM	K21103	phenazine-1-carboxylate N-methyltransferase [EC:2.1.1.327]	Metabolism	Biosynthesis of other secondary metabolites	Phenazine biosynthesis
phzS	K20940	5-methylphenazine-1-carboxylate 1-monooxygenase [EC:1.14.13.218]	Metabolism	Biosynthesis of other secondary metabolites	Phenazine biosynthesis
tnr	K17739	tetrahydroxynaphthalene reductase [EC:1.1.1.252]	Not Included in Pathway or Brite	Unclassified: metabolism	Unclassified: metabolism
sdh	K17740	scytalone dehydratase [EC:4.2.1.94]	Not Included in Pathway or Brite	Unclassified: metabolism	Unclassified: metabolism
tyr	K00505	tyrosinase [EC:1.14.18.1]	Metabolism	Amino acid metabolism	Tyrosine metabolism
dod	K10253	DOPA 4,5-dioxygenase [EC:1.14.99.-]	Not Included in Pathway or Brite	Unclassified: metabolism	Unclassified: metabolism
dod	K15777	4,5-DOPA dioxygenase extradiol [EC:1.13.11.-]	Metabolism	Biosynthesis of other secondary metabolites	Betalain biosynthesis
pfmaG	K17739	tetrahydroxynaphthalene reductase [EC:1.1.1.252]	Not Included in Pathway or Brite	Unclassified: metabolism	Unclassified: metabolism
sdh1	K17740	scytalone dehydratase [EC:4.2.1.94]	Not Included in Pathway or Brite	Unclassified: metabolism	Unclassified: metabolism
lac	K05909	laccase [EC:1.10.3.2]	Not Included in Pathway or Brite	Unclassified: metabolism	Unclassified: metabolism
crtZ	K02294	beta-carotene hydroxylase [EC:1.14.13.-]	Metabolism	Metabolism of terpenoids and polyketides	Carotenoid biosynthesis
crtB	K17841	15-cis-phytoene synthase	Metabolism	Metabolism of terpenoids and polyketides	Carotenoid biosynthesis
todA	K17842	toluene dioxygenase [EC:1.13.11.59]	Metabolism	Metabolism of terpenoids and polyketides	Carotenoid biosynthesis
Z-Iso	K15744	zeta-carotene isomerase [EC:5.2.1.12]	Metabolism	Metabolism of terpenoids and polyketides	Carotenoid biosynthesis
al-1	K15745	phytoene desaturase (3,4-didehydrolycopene-forming) [EC:1.3.99.30]	Metabolism	Metabolism of terpenoids and polyketides	Carotenoid biosynthesis
aog	K14595	abscisate beta-glucosyltransferase [EC:2.4.1.263]	Metabolism	Metabolism of terpenoids and polyketides	Carotenoid biosynthesis
crtX	K14596	zeaxanthin glucosyltransferase [EC:2.4.1.276]	Metabolism	Metabolism of terpenoids and polyketides	Carotenoid biosynthesis
cruC	K14597	chlorobactene glucosyltransferase	Metabolism	Metabolism of terpenoids and polyketides	Carotenoid biosynthesis
cruD	K14598	chlorobactene lauroyltransferase	Metabolism	Metabolism of terpenoids and polyketides	Carotenoid biosynthesis
crtNb	K10210	diapolycopene oxygenase [EC:1.14.99.44]	Metabolism	Metabolism of terpenoids and polyketides	Carotenoid biosynthesis
crtQ	K10211	4,4'-diaponeurosporenoate glycosyltransferase [EC:2.4.1.-]	Metabolism	Metabolism of terpenoids and polyketides	Carotenoid biosynthesis
crtO	K10212	glycosyl-4,4'-diaponeurosporenoate acyltransferase [EC:2.3.1.-]	Metabolism	Metabolism of terpenoids and polyketides	Carotenoid biosynthesis
pds	K02293	15-cis-phytoene desaturase [EC:1.3.5.5]	Metabolism	Metabolism of terpenoids and polyketides	Carotenoid biosynthesis
ccr2	K09835	prolycopene isomerase [EC:5.2.1.13]	Metabolism	Metabolism of terpenoids and polyketides	Carotenoid biosynthesis
lut1	K09837	carotenoid epsilon hydroxylase [EC:1.14.14.158]	Metabolism	Metabolism of terpenoids and polyketides	Carotenoid biosynthesis
zep	K09838	zeaxanthin epoxidase [EC:1.14.15.21]	Metabolism	Metabolism of terpenoids and polyketides	Carotenoid biosynthesis
aba2	K09841	xanthoxin dehydrogenase [EC:1.1.1.288]	Metabolism	Metabolism of terpenoids and polyketides	Carotenoid biosynthesis
crtC	K09844	carotenoid 1,2-hydratase [EC:4.2.1.131]	Metabolism	Metabolism of terpenoids and polyketides	Carotenoid biosynthesis
crtD	K09845	1-hydroxycarotenoid 3,4-desaturase [EC:1.3.99.27]	Metabolism	Metabolism of terpenoids and polyketides	Carotenoid biosynthesis
crtF	K09846	demethylspheroidene O-methyltransferase [EC:2.1.1.210]	Metabolism	Metabolism of terpenoids and polyketides	Carotenoid biosynthesis
crtA	K09847	spheroidene monooxygenase [EC:1.14.15.9]	Metabolism	Metabolism of terpenoids and polyketides	Carotenoid biosynthesis
lcy1	K06443	lycopene beta-cyclase [EC:5.5.1.19]	Metabolism	Metabolism of terpenoids and polyketides	Carotenoid biosynthesis
crtB	K02291	15-cis-phytoene synthase [EC:2.5.1.32]	Metabolism	Metabolism of terpenoids and polyketides	Carotenoid biosynthesis
crtW	K02292	beta-carotene ketolase (CrtO type)	Metabolism	Metabolism of terpenoids and polyketides	Carotenoid biosynthesis
mnp1	K20205	manganese peroxidase [EC:1.11.1.13]	Not Included in Pathway or Brite	Unclassified: metabolism	Enzymes with EC numbers
mox	K22348	manganese oxidase [EC:1.16.3.3]	Not Included in Pathway or Brite	Unclassified: metabolism	Enzymes with EC numbers
pral	K00481	p-hydroxybenzoate 3-monooxygenase [EC:1.14.13.2]	Metabolism	Xenobiotics biodegradation and metabolism	Benzoate degradation
brcC	K04112	benzoyl-CoA reductase subunit C [EC:1.3.7.8]	Metabolism	Xenobiotics biodegradation and metabolism	Benzoate degradation
brcB	K04113	benzoyl-CoA reductase subunit B [EC:1.3.7.8]	Metabolism	Xenobiotics biodegradation and metabolism	Benzoate degradation
brcA	K04114	benzoyl-CoA reductase subunit A [EC:1.3.7.8]	Metabolism	Xenobiotics biodegradation and metabolism	Benzoate degradation
brcD	K04115	benzoyl-CoA reductase subunit D [EC:1.3.7.8]	Metabolism	Xenobiotics biodegradation and metabolism	Benzoate degradation
fadK	K04116	cyclohexanecarboxylate-CoA ligase [EC:6.2.1.-]	Metabolism	Xenobiotics biodegradation and metabolism	Benzoate degradation
thnJ	K04118	pimeloyl-CoA dehydrogenase [EC:1.3.1.62]	Metabolism	Xenobiotics biodegradation and metabolism	Benzoate degradation

badH	K07535	2-hydroxycyclohexanecarboxyl-CoA dehydrogenase [EC:1.1.1.-]	Metabolism	Xenobiotics biodegradation and metabolism	Benzoate degradation
menI	K07536	2-ketocyclohexanecarboxyl-CoA hydrolase [EC:3.1.2.-]	Metabolism	Xenobiotics biodegradation and metabolism	Benzoate degradation
cdh	K07537	cyclohexa-1,5-dienecarbonyl-CoA hydratase [EC:4.2.1.100]	Metabolism	Xenobiotics biodegradation and metabolism	Benzoate degradation
pcaF	K07823	3-oxoadipyl-CoA thiolase [EC:2.3.1.174]	Metabolism	Xenobiotics biodegradation and metabolism	Benzoate degradation
galB	K10220	4-oxalmesaconate hydratase [EC:4.2.1.83]	Metabolism	Xenobiotics biodegradation and metabolism	Benzoate degradation
gcdh	K16173	glutaryl-CoA dehydrogenase (non-decarboxylating) [EC:1.3.99.32]	Metabolism	Xenobiotics biodegradation and metabolism	Benzoate degradation
galD	K16514	4-oxalomesaconate tautomerase [EC:5.3.2.8]	Metabolism	Xenobiotics biodegradation and metabolism	Benzoate degradation
proH	K16515	4-oxalomesaconate hydratase [EC:4.2.1.83]	Metabolism	Xenobiotics biodegradation and metabolism	Benzoate degradation
chcA	K19067	cyclohexane-1-carbonyl-CoA dehydrogenase [EC:1.3.8.11]	Metabolism	Xenobiotics biodegradation and metabolism	Benzoate degradation
graF	K20941	gamma-resorcylate decarboxylase [EC:4.1.1.103]	Metabolism	Xenobiotics biodegradation and metabolism	Benzoate degradation
cgl	K22270	3-hydroxybenzoate 6-monooxygenase [EC:1.14.13.24]	Metabolism	Xenobiotics biodegradation and metabolism	Benzoate degradation
xamoE	K22354	alkene monooxygenase beta subunit [EC:1.14.13.69]	Metabolism	Xenobiotics biodegradation and metabolism	Chloroalkane and chloroalkene degradation
etnD	K22356	alkene monooxygenase reductase	Metabolism	Xenobiotics biodegradation and metabolism	Chloroalkane and chloroalkene degradation
xecA1	K22363	2-hydroxypropyl-CoM lyase [EC:4.4.1.23]	Metabolism	Xenobiotics biodegradation and metabolism	Chloroalkane and chloroalkene degradation
tfdA	K06912	alpha-ketoglutarate-dependent 2,4-dichlorophenoxyacetate dioxygenase [EC:1.14.11.-]	Metabolism	Xenobiotics biodegradation and metabolism	Chlorocyclohexane and chlorobenzene degradation
pcpD	K21607	tetrachlorobenzoquinone reductase [EC:1.1.1.404]	Metabolism	Xenobiotics biodegradation and metabolism	Chlorocyclohexane and chlorobenzene degradation
phtD	K04102	4,5-dihydroxyphthalate decarboxylase [EC:4.1.1.55]	Metabolism	Xenobiotics biodegradation and metabolism	Polycyclic aromatic hydrocarbon degradation
ophB	K18067	phthalate 4,5-cis-dihydrodiol dehydrogenase [EC:1.3.1.64]	Metabolism	Xenobiotics biodegradation and metabolism	Polycyclic aromatic hydrocarbon degradation
pht3	K18068	phthalate 4,5-dioxygenase [EC:1.14.12.7]	Metabolism	Xenobiotics biodegradation and metabolism	Polycyclic aromatic hydrocarbon degradation
pht2	K18069	phthalate 4,5-dioxygenase reductase component [EC:1.18.1.-]	Metabolism	Xenobiotics biodegradation and metabolism	Polycyclic aromatic hydrocarbon degradation
tphA2I	K18074	terephthalate 1,2-dioxygenase oxygenase component alpha subunit [EC:1.14.12.15]	Metabolism	Xenobiotics biodegradation and metabolism	Polycyclic aromatic hydrocarbon degradation
tphBII	K18076	1,2-dihydroxy-3,5-cyclohexadiene-1,4-dicarboxylate dehydrogenase [EC:1.3.1.53]	Metabolism	Xenobiotics biodegradation and metabolism	Polycyclic aromatic hydrocarbon degradation
tphA1	K18077	terephthalate 1,2-dioxygenase reductase component [EC:1.18.1.-]	Metabolism	Xenobiotics biodegradation and metabolism	Polycyclic aromatic hydrocarbon degradation
padAd	K18251	phthalate 3,4-dioxygenase subunit alpha [EC:1.14.12.-]	Metabolism	Xenobiotics biodegradation and metabolism	Polycyclic aromatic hydrocarbon degradation
padAb	K18252	phthalate 3,4-dioxygenase subunit beta [EC:1.14.12.-]	Metabolism	Xenobiotics biodegradation and metabolism	Polycyclic aromatic hydrocarbon degradation
padAc1	K18253	phthalate 3,4-dioxygenase ferredoxin component	Metabolism	Xenobiotics biodegradation and metabolism	Polycyclic aromatic hydrocarbon degradation
padAd	K18254	phthalate 3,4-dioxygenase ferredoxin reductase component [EC:1.18.1.3]	Metabolism	Xenobiotics biodegradation and metabolism	Polycyclic aromatic hydrocarbon degradation
phnB	K18257	cis-3,4-dihydrophenanthrene-3,4-diol dehydrogenase [EC:1.3.1.49]	Metabolism	Xenobiotics biodegradation and metabolism	Polycyclic aromatic hydrocarbon degradation
phdK	K18275	2-formylbenzoate dehydrogenase [EC:1.2.1.78]	Metabolism	Xenobiotics biodegradation and metabolism	Polycyclic aromatic hydrocarbon degradation
pchf	K05797	4-cresol dehydrogenase (hydroxylating) flavoprotein subunit [EC:1.17.9.1]	Metabolism	Xenobiotics biodegradation and metabolism	Toluene degradation
bbsE	K07543	benzylsuccinate CoA-transferase BbsE subunit [EC:2.8.3.15]	Metabolism	Xenobiotics biodegradation and metabolism	Toluene degradation
bbsF	K07544	benzylsuccinate CoA-transferase BbsF subunit [EC:2.8.3.15]	Metabolism	Xenobiotics biodegradation and metabolism	Toluene degradation
bbsG	K07545	(R)-benzylsuccinyl-CoA dehydrogenase [EC:1.3.8.3]	Metabolism	Xenobiotics biodegradation and metabolism	Toluene degradation
bbsH	K07546	E-phenylitaconyl-CoA hydratase [EC:4.2.1.-]	Metabolism	Xenobiotics biodegradation and metabolism	Toluene degradation
bbsC	K07547	2-[hydroxy(phenyl)methyl]-succinyl-CoA dehydrogenase BbsC subunit [EC:1.1.1.35]	Metabolism	Xenobiotics biodegradation and metabolism	Toluene degradation
bbsD	K07548	2-[hydroxy(phenyl)methyl]-succinyl-CoA dehydrogenase BbsD subunit [EC:1.1.1.35]	Metabolism	Xenobiotics biodegradation and metabolism	Toluene degradation
bbsA	K07549	benzoylsuccinyl-CoA thiolase BbsA subunit [EC:2.3.1.-]	Metabolism	Xenobiotics biodegradation and metabolism	Toluene degradation
bbsB	K07550	benzoylsuccinyl-CoA thiolase BbsB subunit [EC:2.3.1.-]	Metabolism	Xenobiotics biodegradation and metabolism	Toluene degradation
pchA	K20199	4-hydroxybenzaldehyde dehydrogenase (NADP+) [EC:1.2.1.96]	Metabolism	Xenobiotics biodegradation and metabolism	Toluene degradation
hipH	K20218	4-hydroxyisophthalate hydroxylase	Metabolism	Xenobiotics biodegradation and metabolism	Toluene degradation
poxD	K16242	phenol hydroxylase P3 protein [EC:1.14.13.-]	Metabolism	Xenobiotics biodegradation and metabolism	Toluene degradation
phyA	K16243	phenol hydroxylase P1 protein	Metabolism	Xenobiotics biodegradation and metabolism	Toluene degradation
poxC	K16244	phenol hydroxylase P2 protein	Metabolism	Xenobiotics biodegradation and metabolism	Toluene degradation
poxE	K16245	phenol hydroxylase P4 protein	Metabolism	Xenobiotics biodegradation and metabolism	Toluene degradation
poxF	K16246	phenol hydroxylase P5 protein	Metabolism	Xenobiotics biodegradation and metabolism	Toluene degradation

Supplementary table S4. MAG taxonomic information. (p) : Phylum ; (c) : Class ; (o) : Order ; (f) : Family ; (g) : Genus.

MAG number	Domain	Phylum	Class	Order	Family	Genus	Final taxonomy
MAG1	Bacteria	Actinobacteria	Actinomycetia	Micrococcales	Microbacteriaceae	*Microbacterium*	*(g) Microbacterium*
MAG2	Bacteria	Actinobacteria	Actinomycetia	Not identified	Not identified	Not identified	(c) Actinomycetia
MAG3	Bacteria	Actinobacteria	Actinomycetia	Not identified	Not identified	Not identified	(c) Actinomycetia
MAG4	Bacteria	Actinobacteria	Thermoleophilia	Solirubrobacterales	Conexibacteraceae	*Conexibacter*	*(g) Conexibacter*
MAG5	Bacteria	Actinobacteria	Not identified	Not identified	Not identified	Not identified	(p) Actinobacteria
MAG6	Bacteria	Chlamydiae	Not identified	Not identified	Not identified	Not identified	(p) Chlamydiae
MAG7	Bacteria	Bacteroidetes	Chitinophagia	Chitinophagales	Chitinophagaceae	*Chitinophaga*	*(g) Chitinophaga*
MAG8	Bacteria	Bacteroidetes	Sphingobacteriia	Sphingobacteriales	Sphingobacteriaceae	*Pedobacter*	*(g) Pedobacter*
MAG9	Bacteria	Proteobacteria	Alphaproteobacteria	Hyphomicrobiales	Hyphomicrobiaceae	*Hyphomicrobium*	*(g) Hyphomicrobium*
MAG10	Bacteria	Proteobacteria	Alphaproteobacteria	Caulobacterales	Caulobacteraceae	*Brevundimonas*	*(g) Brevundimonas*
MAG11	Bacteria	Proteobacteria	Alphaproteobacteria	Hyphomicrobiales	Bradyrhizobiaceae	*Nitrobacter*	*(g) Nitrobacter*
MAG12	Bacteria	Proteobacteria	Alphaproteobacteria	Hyphomicrobiales	Not identified	Not identified	(o) Hyphomicrobiales
MAG13	Bacteria	Planctomycetes	Planctomycetia	Not identified	Not identified	Not identified	(c) Planctomycetia
MAG14	Bacteria	Actinobacteria	Actinomycetia	Corynebacteriales	Mycobacteriaceae	*Mycobacteroides*	*(g) Mycobacteroides*
MAG15	Bacteria	Proteobacteria	Alphaproteobacteria	Hyphomicrobiales	Xanthobacteraceae	*Labrys*	*(g) Labrys*
MAG16	Bacteria	Proteobacteria	Alphaproteobacteria	Hyphomicrobiales	Not identified	Not identified	(o) Hyphomicrobiales
MAG17	Bacteria	Acidobacteria	Not identified	Not identified	Not identified	Not identified	(p) Acidobacteria
MAG18	Bacteria	Actinobacteria	Actinomycetia	Streptomycetales	Streptomycetaceae	*Streptomyces*	*(g) Streptomyces*
MAG19	Bacteria	Actinobacteria	Actinomycetia	Corynebacteriales	Nocardiaceae	*Rhodococcus*	*(g) Rhodococcus*
MAG20	Bacteria	Proteobacteria	Alphaproteobacteria	Hyphomicrobiales	Not identified	Not identified	(o) Hyphomicrobiales
MAG21	Bacteria	Proteobacteria	Alphaproteobacteria	Hyphomicrobiales	Not identified	Not identified	(o) Hyphomicrobiales
MAG22	Bacteria	Proteobacteria	Alphaproteobacteria	Rhodospirillales	Not identified	Not identified	(o) Rhodospirillales
MAG23	Bacteria	Planctomycetes	Not identified	Not identified	Not identified	Not identified	(p) Planctomycetes
MAG24	Bacteria	Not identified	Not identified	Not identified	Not identified	Not identified	(k) Bacteria
MAG25	Bacteria	Bacteroidetes	Sphingobacteriia	Sphingobacteriales	Sphingobacteriaceae	*Olivibacter*	*(g) Olivibacter*
MAG26	Bacteria	Chlamydiae	Chlamydiia	Not identified	Not identified	Not identified	(c) Chlamydiia
MAG27	Bacteria	Proteobacteria	Alphaproteobacteria	Sphingomonadacea	Sphingomonadaceae	*Sphingomonas*	*(g) Sphingomonas*
MAG28	Bacteria	Proteobacteria	Alphaproteobacteria	Not identified	Not identified	Not identified	(c) Alphaproteobacteria
MAG29	Bacteria	Proteobacteria	Gammaproteobacteria	Xanthomonadales	Xanthomonadaceae	*Stenotrophomonas*	*(g) Stenotrophomonas*
MAG30	Bacteria	Proteobacteria	Gammaproteobacteria	Legionellales	Legionellaceae	Not identified	(f) Legionellaceae
MAG31	Bacteria	Proteobacteria	Gammaproteobacteria	Legionellales	Legionellaceae	*Legionella*	*(g) Legionella*
MAG32	Bacteria	Not identified	Not identified	Not identified	Not identified	Not identified	(f) Brucellaceae
MAG33	Bacteria	Not identified	Not identified	Not identified	Not identified	Not identified	(k) Bacteria
MAG34	Fungi	Ascomycota	Sordariomycota	Hypocreales	Not identified	Not identified	(o) Hypocreales
MAG35	Bacteria	Actinobacteria	Actinomycetia	Pseudonocardiales	Pseudonocardiaceae	*Amycolatopsis*	*(g) Amycolatopsis*
MAG36	Bacteria	Actinobacteria	Actinomycetia	Not identified	Not identified	Not identified	(c) Actinomycetia
MAG37	Bacteria	Actinobacteria	Not identified	Not identified	Not identified	Not identified	(p) Actinobacteria
MAG38	Bacteria	Bacteroidetes	Sphingobacteriia	Sphingobacteriales	Sphingobacteriaceae	*Olivibacter*	*(g) Olivibacter*
MAG39	Bacteria	Chloroflexi	Not identified	Not identified	Not identified	Not identified	(p) Chloroflexi
MAG40	Bacteria	Proteobacteria	Alphaproteobacteria	Hyphomicrobiales	Not identified	Not identified	(o) Hyphomicrobiales
MAG41	Bacteria	Proteobacteria	Alphaproteobacteria	Hyphomicrobiales	Not identified	Not identified	(o) Hyphomicrobiales
MAG42	Bacteria	Proteobacteria	Deltaproteobacteria	Myxococcale	Polyangiaceae	Not identified	(f) Polyangiaceae
MAG43	Bacteria	Proteobacteria	Gammaproteobacteria	Xanthomonadales	Xanthomonadaceae	*Luteimoas*	*(g) Luteimoas*
MAG44	Bacteria	Actinobacteria	Actinomycetia	Streptomycetales	Streptomycetaceae	*Streptomyces*	*(g) Streptomyces*
MAG45	Bacteria	Actinobacteria	Actinomycetia	Pseudonocardiales	Pseudonocardiaceae	Not identified	(f) Pseudonocardiaceae
MAG46	Bacteria	Actinobacteria	Actinomycetia	Not identified	Not identified	Not identified	(c) Actinomycetia
MAG47	Bacteria	Proteobacteria	Gammaproteobacteria	Legionellales	Legionellaceae	*Legionella*	*(g) Legionella*
MAG48	Bacteria	Bacteroidetes	Not identified	Not identified	Not identified	Not identified	(p) Bacteroidetes
MAG49	Bacteria	Proteobacteria	Not identified	Not identified	Not identified	Not identified	(p) Proteobacteria
MAG50	Bacteria	Not identified	Not identified	Not identified	Not identified	Not identified	(k) Bacteria
MAG51	Bacteria	Proteobacteria	Betaproteobacteria	Burkholderiales	Burkholderiaceae	*Ralstonia*	*(g) Ralstonia*
MAG52	Bacteria	Proteobacteria	Gammaproteobacteria	Xanthomonadales	Xanthomonadaceae	Not identified	(f) Xanthomonadaceae

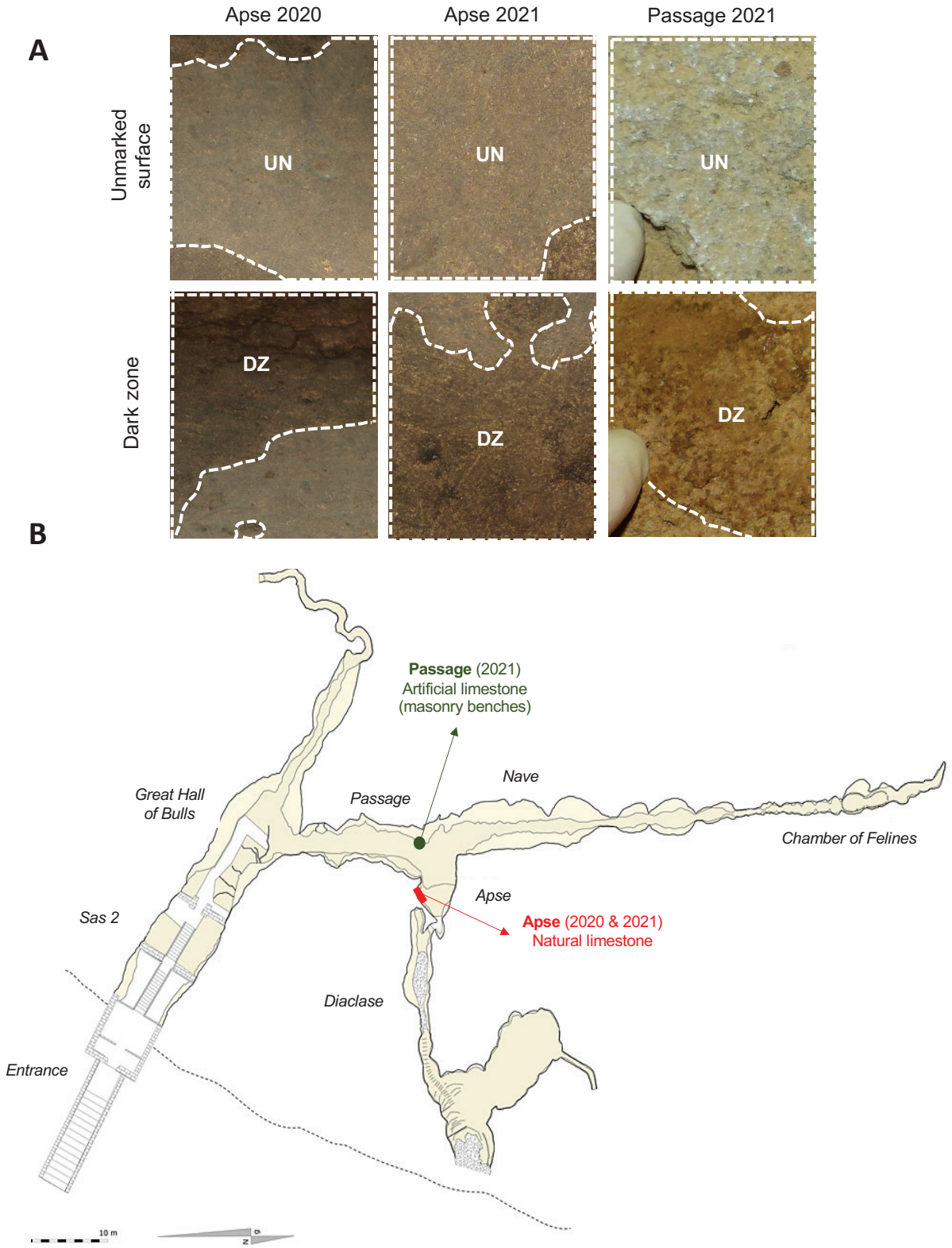

Supplementary fig S1. (A) Photograph of unmarked surfaces (UN) and dark zones (DZ) in the Apse (2020 and 2021) and Passage (2021) (Source : S. Géraud, DRAC Nouvelle Aquitaine). (B) Map of Lascaux Cave presenting the locations studied. The natural limestone is indicated in red and artificial limestone in green (Source of the map : S. Konik, Centre National de la Préhistoire)

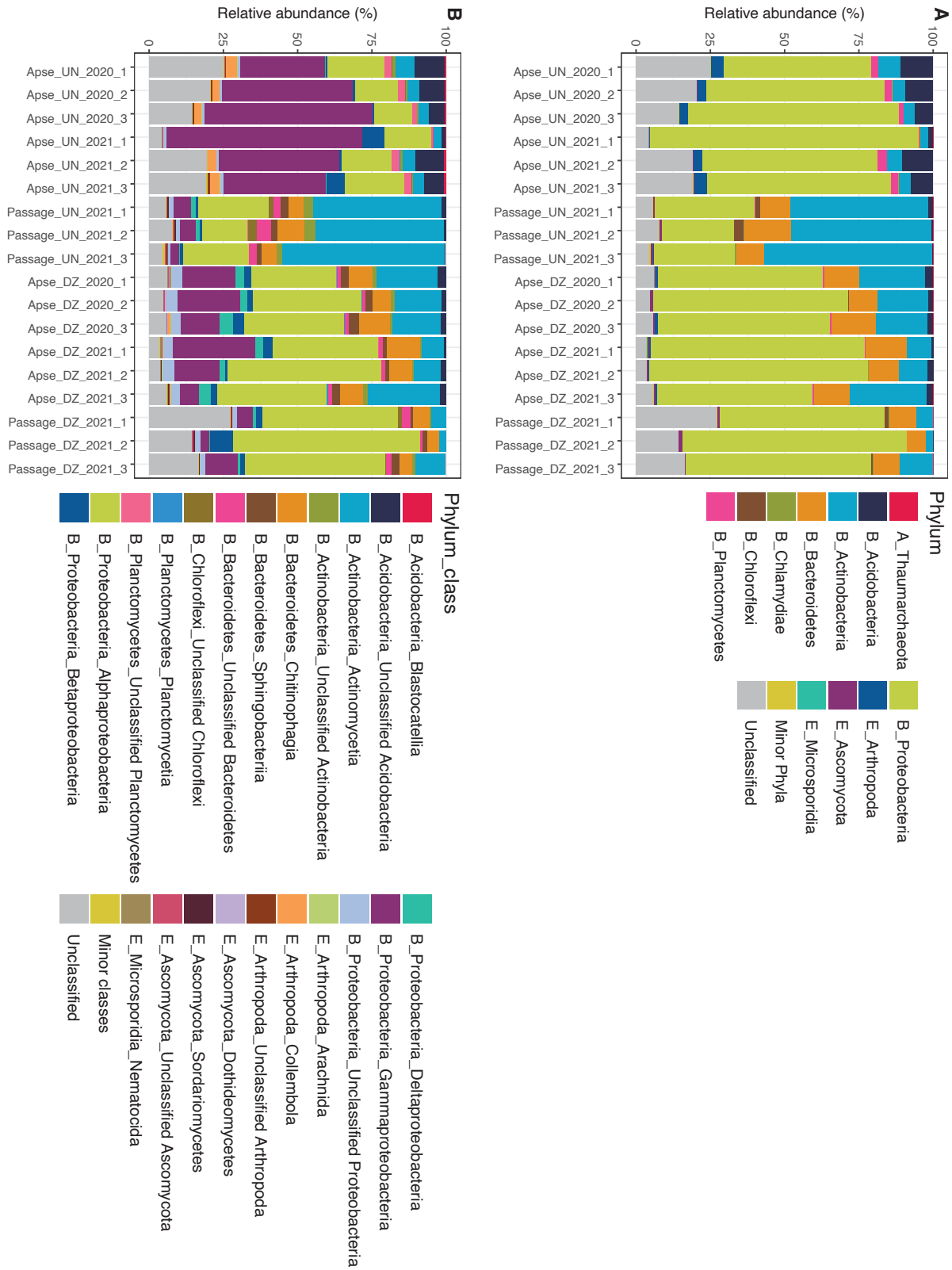

Supplementary fig S2. Relative abundance (% of sequences) of community taxa for each replicate at the (A) phylum and (B) class taxonomic levels. UN, unmarked surface ; DZ, dark zone. Phyla or classes with a relative abundance <0.05% were considered as minor phyla or minor classes, respectively.

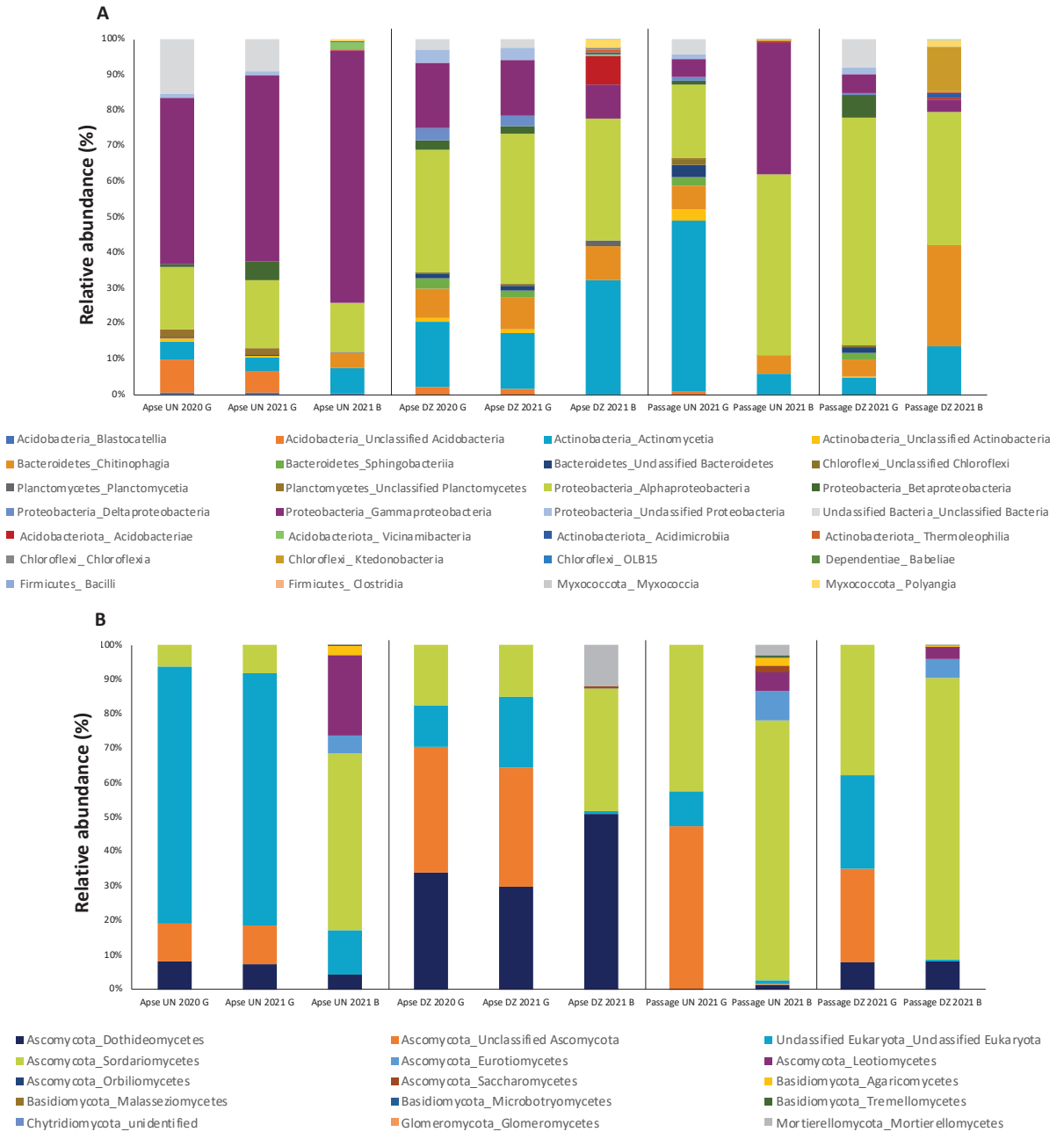

Supplementary fig S3. Distribution of the most abundant microbial classes according to sequencing method, rock surface condition, room and time. The heatmap was coupled to a hierarchical clustering analysis of the samples. Genera with a relative abundance <0.05% were considered as minor genera. UN, unmarked surface ; DZ, dark zone. B, metabarcoding approach ; G, metagenomic approach.

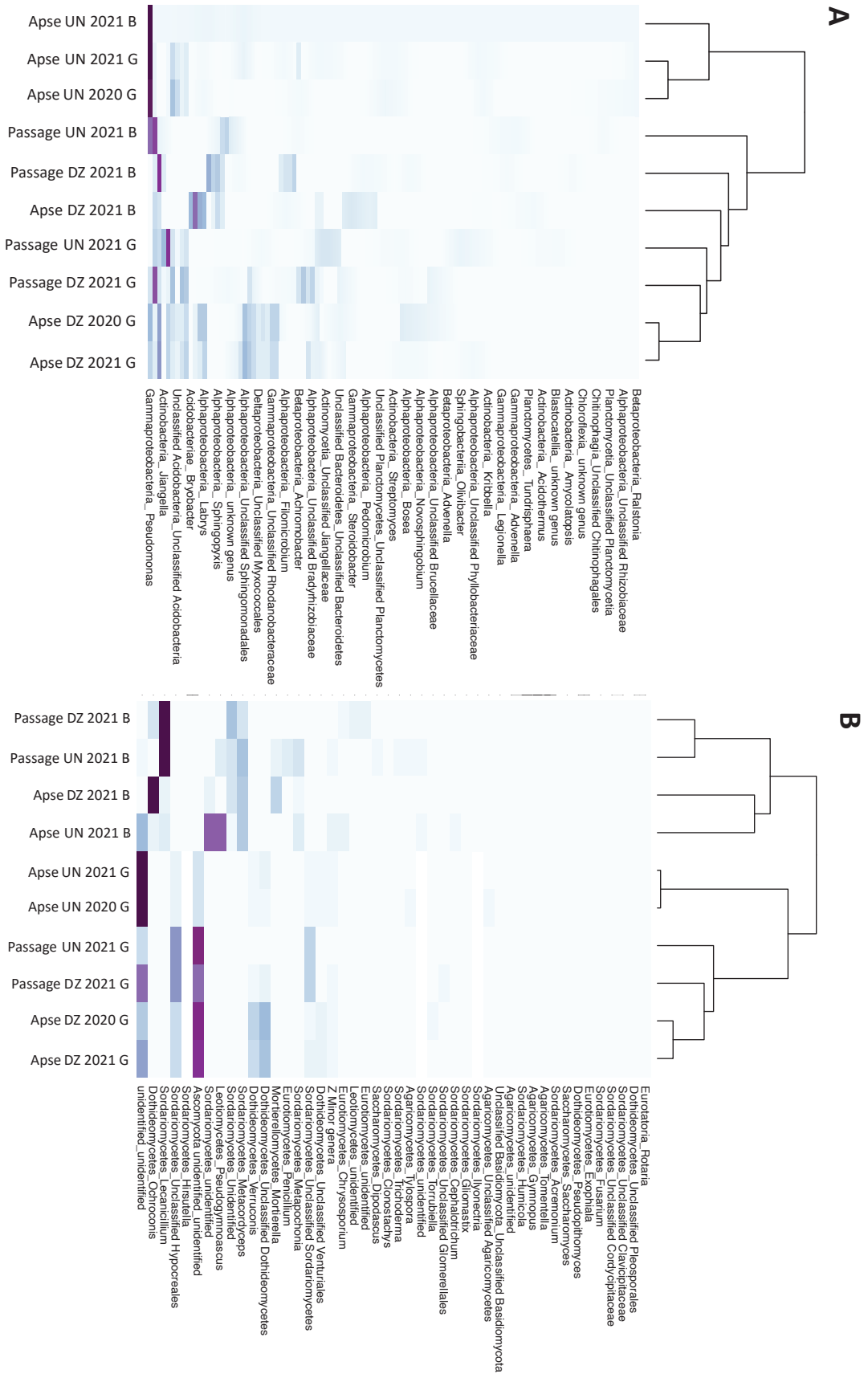

Supplementary fig S4. Distribution of the most abundant microbial genera according to sequencing method, rock surface condition, room and time. The heatmap was coupled to a hierarchical clustering analysis of the samples. Classes with a relative abundance <0.05% were considered as minor classes. UN, unmarked surface ; DZ, dark zone. B, metabarcoding approach ; G, metagenomic approach.

CHAPITRE 5

Discussion générale et perspectives

Les écosystèmes karstiques attirent chaque année l'attention de millions de visiteurs de par la présence de lacs souterrains, de concrétions et/ou d'art pariétal, faisant d'eux le centre de l'activité géo-touristique mondiale [Biot, 2006, Cigna *et al.*, 2013, Cigna, 2016]. L'exploitation touristique des grottes implique une anthropisation de l'écosystème (modification des cavités souterraines par l'homme) avec par exemple la mise en place d'un système d'éclairage artificiel, la fréquentation touristique, le décaissage du sol de la grotte, des travaux de maçonnerie, l'installation d'escaliers, ascenseurs, etc. [Russell et MacLean, 2008, Gauchon *et al.*, 2012, Dupont *et al.*, 2007]. Cependant, le développement d'une activité touristique dans les grottes peut fortement affecter leur équilibre environnemental, qu'il soit biotique ou abiotique [Alonso, 2018] entrainant dans la majorité des cas des problématiques pour la conservation de l'art pariétal [Bontemps *et al.*, 2021]. Même si les cavités naturelles représentent des milieux pauvres dits oligotrophes (<2mg TOC/L), ces écosystèmes hébergent une biomasse microbienne abondante et diversifiée. Ainsi, l'anthropisation du milieu peut entraîner dans certains cas un déséquilibre du microbiote des grottes se traduisant par la biodétérioration des parois [Alonso *et al.*, 2018, Bontemps *et al.*, 2021]. C'est le cas des grottes emblématiques telles que la grotte d'Altamira (Espagne), la grotte de Lascaux (France), la grotte de Moidons (France) ou encore la grotte d'Arcy-Sur-Cure (France), où l'anthropisation des sites a conduit à la formation d'altérations sur les parois [Borderie *et al.*, 2016, Chalmin *et al.*, 2007, Bastian *et al.*, 2010]. Ces altérations ont entraîné des problèmes de conservation du patrimoine culturel et ont conduit à la réduction drastique de la fréquentation touristique ou même dans certains cas, à la fermeture définitive des cavités au public [Martin-Sanchez *et al.*, 2015, Bastian *et al.*, 2010, Chalmin *et al.*, 2007].

Dès 1948, la grotte de Lascaux a été le théâtre de nombreux aménagements afin de permettre le développement des activités touristiques (100 000 visiteurs par an) [Martin-Sanchez *et al.*, 2015]. Ces activités ont entrainé un déséquilibre de l'écosystème ayant engendré la prolifération anormale de microorganismes sur les parois à trois reprises : (i) un biofilm d'algues vertes (*Brateoccocus minor*) formé sur les parois en 1960, des traitements composés d'antibiotiques et de formaldéhyde ont été appliqués sur les parois permettant l'élimination de ces algues [Lefèvre, 1974], (ii) un mycélium blanc du champignon *Fusarium solani* était présent sous forme de duvet sur une grande partie des parois de la grotte et il a été traité au chlorure de benzalkonium [Martin-Sanchez *et al.*, 2015], (iii) des altérations noires ont été identifiées sur les parois de la grotte fin 2001 (appelées communément taches noires) et (iv) en 2008 des altérations de teinte foncée/grisâtre ont été identifiées dans l'Abside (appelées communément zones sombres) [Alonso *et al.*, 2018]. Des études précédentes portant sur ces altérations ont mis en évidence une forte prédominance des bactéries affiliées au genre *Pseudomonas* sur les parois saines et à l'inverse une prédominance des champignons pigmentés sur les parois altérées [Bastian *et al.*, 2009a, Alonso *et al.*, 2018]. Ces modifications étaient considérées comme limitées à l'Abside (pour les zones sombres). Cependant, une surveillance étroite dans plusieurs autres salles de la grotte a révélée des changements visuels ressemblant à ceux des zones sombres sur plusieurs parois rocheuses (parois naturelles ainsi que sur des parois artificielles en calcaire construites pour permettre les activités touristiques), malgré l'hétérogénéité spatiale du microbiote de Lascaux [Alonso *et al.*, 2018]. A ce jour, les taches noires et zones sombres évoluent toujours dans la grotte et sont donc des enjeux d'actualité au cœur des politiques de conservation.

Ainsi, au cours de son histoire, la grotte de Lascaux a subi une perturbation d'origine anthropique due aux différents aménagements, visites touristiques et traitements chimiques et/ou antibiotiques. Cela à entrainé plusieurs états (visuels et microbiologiques) de réponse à cette perturbation : (i) un état dit résistant, correspondant au calcaire dépourvu d'altérations (taches noires et/ou zones sombres), (ii) un état dit impacté, correspondant au calcaire altéré (taches noires et zones sombres) et (iii) un état dit résilient, correspondant à une atténuation des altérations comme observé pour certaines taches noires du Cabinet des Félins.

Au cours de ces travaux de thèse nous nous sommes intéressés à l'étude des dynamiques de la diversité microbienne dans la grotte de Lascaux avec une approche globale en utilisant le séquençage à haut débit des acides nucléiques. Nous discuterons au travers de différentes parties les résultats majeurs obtenus. La première partie sera centrée sur l'impact de la perturbation sur la diversité microbienne des trois domaines du vivant, prenant en compte l'hétérogénéité de la grotte de Lascaux (effet du substrat minéral, du temps d'échantillonnage, du niveau d'anthropisation, etc.). La deuxième partie sera axée, à l'inverse, sur l'effet de la diversité dans la modulation de la réponse à la perturbation. La troisième partie s'intéressera aux rétroactions entre la perturbation et la diversité microbienne. Enfin, une dernière partie sera consacrée aux limites de ces travaux de thèse ainsi qu'aux perspectives de recherche qui en découlent.

La perturbation affecte la diversité microbienne

L'historique des interventions humaines recensées dans la grotte qui est réalisé depuis plusieurs décennies par le personnel de la grotte de Lascaux, permet de relier les différentes étapes d'anthropisation (e.g. salles les plus visitées ou traitées) de la grotte et la composition des communautés microbiennes résistantes, ou pas à la perturbation tout en prenant en compte l'hétérogénéité de l'écosystème.

Indépendamment de la méthode utilisée nos travaux ont permis de confirmer une hétérogénéité des communautés microbiennes de la grotte de Lascaux au niveau de la structure, la composition taxonomique et fonctionnelle des communautés [Alonso *et al.*, 2019] (Figure 1). Par exemple, les classes bactériennes Chloroflexia et Planctomycetes sont plus abondantes dans la salle des Taureaux par rapport aux autres salles, tandis que les classes Chitinophagia et Actimycetia étaient relativement plus abondantes dans les communautés résistantes du Passage. La classe dominante des Gammaprotéobactéries présente une abondance relative plus élevée dans l'Abside par rapport au Passage. Les résultats de métagénomique indiquent également une hétérogénéité du potentiel fonctionnel des communautés résistantes à la perturbation. Cette hétérogénéité taxonomique et fonctionnelle peut être liée à plusieurs facteurs, comme le substrat minéral. Plusieurs types de substrats sont recensés dans la grotte : calcaire naturel, calcaire artificiel (maçonné) et des blocs de calcaire Santonien (couche stratigraphique du crétacé supérieur) composant le mur séparant le SAS-2 et la salle des Taureaux. Par exemple la sélection de *Pseudomonas* retrouvée dans l'Abside mais pas dans le Passage peut suggérer une colonisation préférentielle de ce genre sur le calcaire naturel (Figure 1). Il a été reconnu que les substrats minéraux étaient un facteur important de structuration des communautés microbiennes [Brewer et Fierer, 2018, Dhami *et al.*, 2018, Alonso *et al.*, 2018]. En effet, les surfaces minérales, de par leur teneur en nutriments, leurs taux de dissolution variables et leur micro-porosité, peuvent

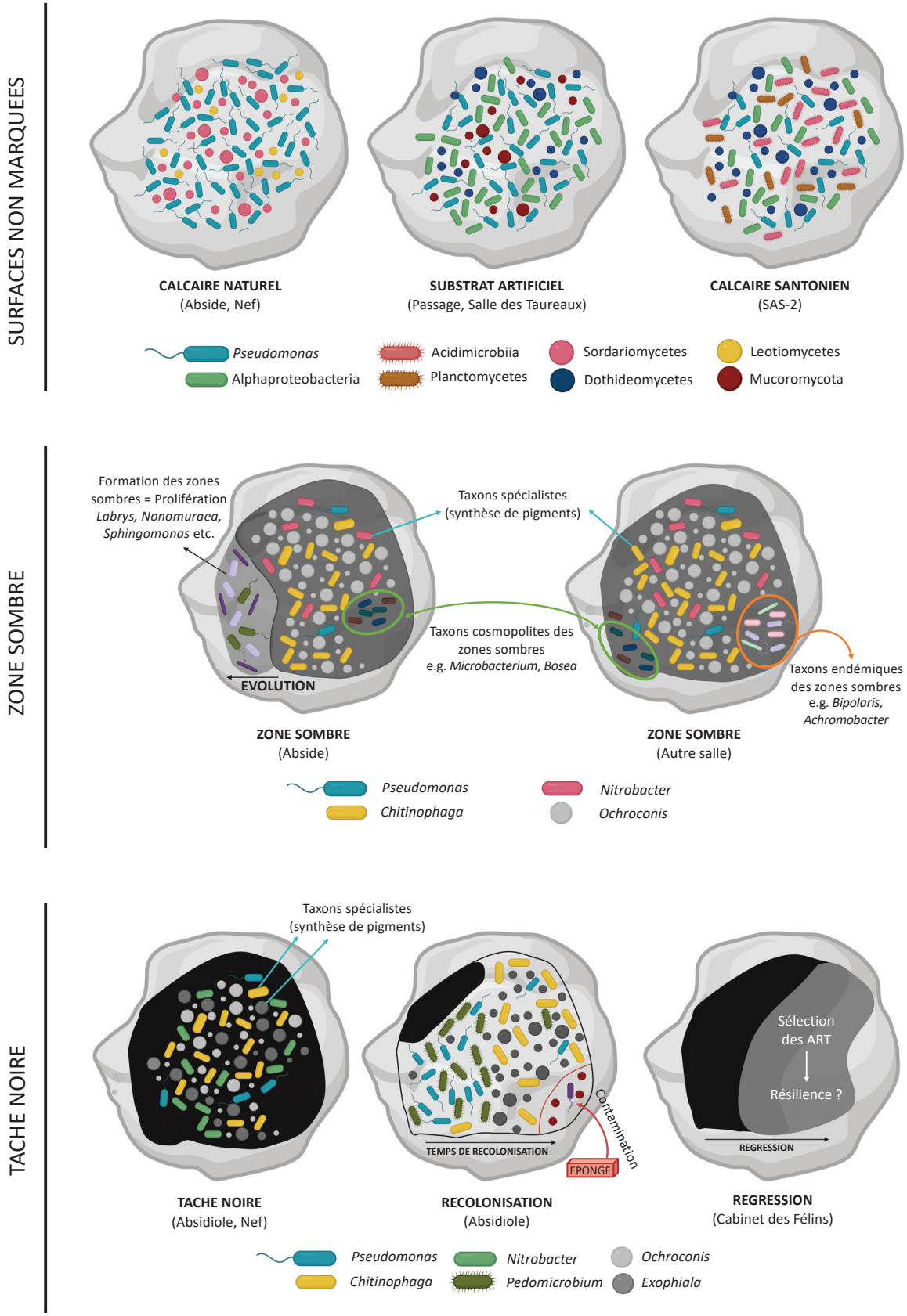

Figure 1. Représentation schématique des communautés microbiennes dans les différentes conditions de surfaces observées dans la grotte de Lascaux. ART : Always Rare Taxa

être considérées comme des interfaces réactives servant de supports physiques à la fixation des microorganismes et de réserves de nutriments [Uroz *et al.*, 2015,Finley *et al.*, 2022]. La présence de fissures, de cavités et de pores peut favoriser le développement de certains micro-organismes et assurer une protection microbienne contre les facteurs extrinsèques [Uroz *et al.*, 2015], comme par exemple dans notre cas l'application de biocides sur les parois. Cela pourrait en partie expliquer les différences de composition des communautés résistantes entre ces différents substrats. De plus, l'application de traitements chimiques et antibiotiques est différente selon les salles, ce qui peut en accentuer l'hétérogénéité taxonomique et fonctionnelle des communautés résistantes de la grotte [Martin-Sanchez *et al.*, 2015]. Les salles du Passage, de l'Abside et de la Nef ont été très fortement anthropisées avec l'application d'un traitement supplémentaire en janvier 2008 comprenant du Vitalub Q50 (majoritairement composé de chlorure de benzalkonium), du sulfate de streptomycine et du sulfate de polymyxine [Martin-Sanchez *et al.*, 2015] (Figure 2).

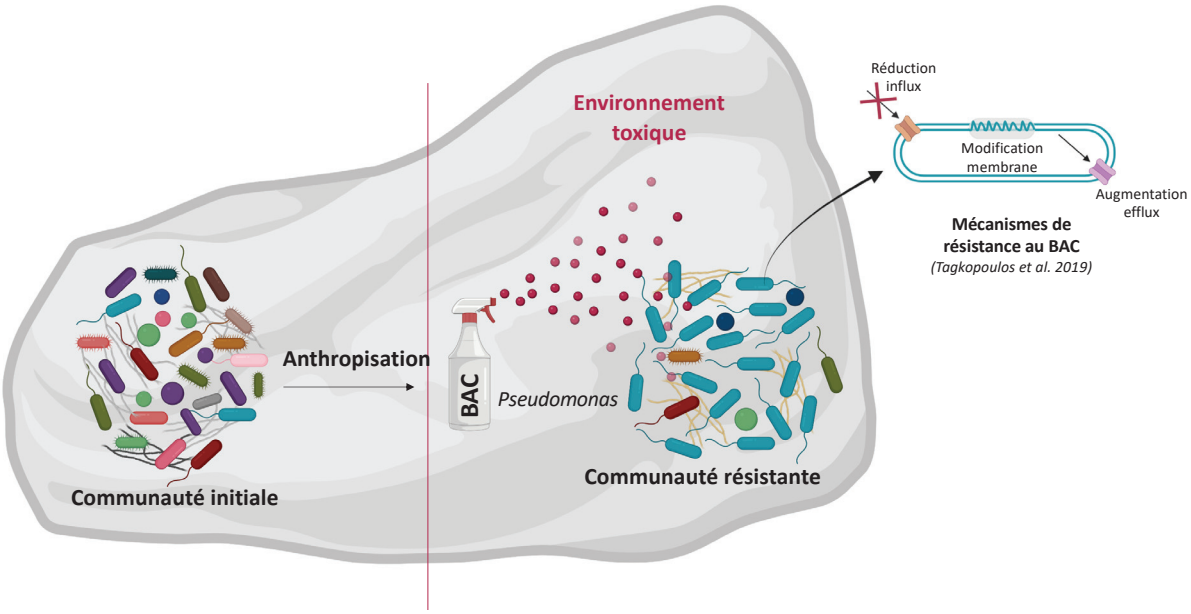

Figure 2. Schéma de la communauté microbienne résistante (i.e. surfaces non altérées) de la grotte de Lascaux regroupant les données taxonomiques et fonctionnelles de ces travaux de thèse

Cela correspond avec l'observation d'une abondance élevée de Gammaproteobacteria (dominées par le genre *Pseudomonas* >50% des séquences) dans les surfaces non marquées de ces salles. La sélection importante de *Pseudomonas* dans les communautés résistantes est observée dans les précédentes études microbiologiques de la grotte de Lascaux [Alonso, 2018,Alonso *et al.*, 2018] par métabarcoding mais également ici par les techniques de métagénomique et PCRq. Les Protéobactéries sont un phylum très abondant dans les grottes en général [Bontemps *et al.*, 2021], mais une telle proportion de *Pseudomonas* n'a jamais été observée auparavant dans ces environnements. La grotte de Lascaux est une des seules grottes anthropisées étudiées à avoir subi une forte anthropisation (traitements chimiques) [Alonso *et al.*, 2019], indiquant que cette perturbation anthropique a un impact prépondérant sur la diversité microbienne des communautés résistantes. Ce résultat est en accord avec la littérature qui démontre que l'exposition à long terme au chlorure de benzalkonium (BAC), engendre une réduction de la diversité des communautés entrainant l'enrichissement – la sélection - d'espèces résistantes au BAC, princi-

palement des espèces affiliées au genre *Pseudomonas* (classe Gammaproteobacteria). En effet, le chlorure de benzalkonium, composé majoritaire des traitements chimiques appliqués sur les parois est connu dans la littérature pour impacter la bicouche lipidique des membranes [Tagkopoulos *et al.*, 2019]. Il a été démontré que certains microorganismes mettent en place des mécanismes de résistance au BAC : (i) une modification de la composition membranaire avec la présence de phospholipides et d'acides gras, (ii) l'absorption du BAC se faisant par les porines, une diminution de l'influx réduisant la sensibilité au biocide, et (iii) à l'inverse, une régulation plus élevée des pompes à efflux réduit la concentration de biocide à l'intérieur de la cellule, permettant aux bactéries de survivre malgré des concentrations environnementales plus élevées en BAC (Figure 2). Ces mécanismes ont été identifiés chez les bactéries affiliées au genre *Pseudomonas*. En plus d'être résistant au BAC, le genre *Pseudomonas* est capable de le dégrader. Les produits de dégradation du BAC (benzyldiméthylamine, benzylméthylamine, benzylamine, benzaldéhyde, etc.) peuvent être utilisés comme source de carbone et d'azote par les *Pseudomonas* [Ertekin *et al.*, 2016]. Un génome affilié à l'espèce *Pseudomonas spelaei* a pu être reconstruit à partir des échantillons de calcaire naturel. Cette espèce a été isolée à partir de calcite dans une grotte en Inde [Nimaichand *et al.*, 2015, Sungthong et Nakaew, 2015], suggérant une spécificité de certaines espèces de *Pseudomonas* à l'environnement karstique. L'annotation fonctionnelle réalisée sur ce génome reconstruit indique (i) un potentiel fonctionnel réduit, certainement dû à la vie dans des environnements karstiques où les processus biologiques sont plus lents [Engel, 2010, Barton et Jurado, 2007] ainsi qu'à la toxicité de l'environnement imposé par la présence du BAC [Tandukar *et al.*, 2013], (ii) la présence de voies métaboliques impliquées dans la dégradation de composés chloroaromatiques (BAC), et (iii) la capacité à synthétiser des composés antimicrobiens. La forte sélection de *Pseudomonas* dont le potentiel génétique est réduit est l'une des conséquences majeures de la perturbation sur les communautés microbiennes de la grotte.

L'hétérogénéité du microbiote des parois non altérées de la grotte semble être lié à la localisation, le type de substrat (i.e. porosité, composition, etc.) en lien avec l'application différentielle de biocides sur les parois. Cependant, malgré une hétérogénéité du microbiote, l'impact de la perturbation sur la diversité taxonomique et fonctionnelle des communautés microbiennes de la grotte de Lascaux semble impliquer la sélection de microorganismes spécialistes (e.g. *Pseudomonas*) dans les communautés résistantes, possédant la capacité de résister aux biocides appliqués et de participer à leur dégradation.

La diversité module les effets de la perturbation

Dans notre travail, des changements communautaires ont été mis en évidence, correspondant à la formation d'altérations sur les parois de la cavité (taches noires et zones sombres). Ici, la modulation de la diversité a probablement permis la mise en place d'un autre type de réponse à la perturbation (altération sur les parois) et la communauté microbienne de ces altérations est donc qualifiée de « communauté impactée ». Dans chaque partie de ces travaux de thèse, l'étude des altérations au sein de plusieurs salles de la grotte de Lascaux par métabarcoding, métagénomique et PCRq, révèle une diversité microbienne différente par rapport aux surfaces non altérées (i.e. communautés résistantes) pour les trois domaines du vivant. Les changements communautaires associés à la formation de taches noires et de zones sombres peuvent être perçus

au niveau taxonomique du phylum pour les bactéries, et des classes pour les microeucaryotes. Une contre sélection du phylum Proteobacteria et à l'inverse une sélection des Bacteroidota dans les communautés impactées sont observées pour les bactéries. Les Bacteroidota sont préférentiellement retrouvés dans les grottes anthropisées, ainsi ils pourraient être considérés comme bioindicateurs d'anthropisation et plus précisément impliqués dans les processus conduisant à une prolifération anormale de microorganismes sur les parois [Pfendler *et al.*, 2018, Tomczyk-Żak et Zielenkiewicz, 2016, Zhou et Ning, 2017, Alonso *et al.*, 2019].

Actuellement, peu de données sont disponibles concernant les altérations des grottes et aucune étude ne traite des processus microbiens impliqués dans leur formation et leur évolution. Notre travail a permis de mieux caractériser l'évolution, la formation et la dissémination des zones sombres dans la grotte ainsi que la caractérisation et la reformation de taches noires après nettoyage mécanique. Lors d'un échantillonnage microspatialisé suivant l'évolution d'une zone sombre, nous avons pu déterminer que la zone correspondant à la 'nouvelle zone sombre' (i.e bordure de la zone sombre qui est nouvellement apparue) est la zone ou les changements communautaires s'établissent pour les bactéries, microeucaryotes et champignons. Le début de la formation de la zone sombre coïncide avec le développement de genres bactériens comme *Labrys* (Alphaprotéobactéries connues pour leur capacité à dégrader des composés halogénés et la méthylotrophie facultative) [Miller *et al.*, 2005, Wong et Huyop, 2020], *Nonomuraea* et *Sphingomonas*, qui est concomitant avec la prolifération du champignon noir *Ochroconis* et la contre-sélection de *Pseudomonas* (Figure 1). Le changement brutal de la communauté est très bien illustré avec *Ochroconis*, genre fongique emblématique des zones sombres car il est établi dès que la nouvelle zone sombre apparaît. Ce constat est également fait lors de la reformation des taches noires, où le champignon noir mélanisé *Exophiala* semble participer activement à la recolonisation des taches noires après nettoyage. Ces champignons noirs ont été identifiés sur des altérations de type taches noires dans d'autres écosystèmes karstiques [Martin-Sanchez *et al.*, 2012]. La formation des zones sombres se fait par des changements communautaires rapides, ne nécessitant pas l'établissement préalable d'une communauté microbienne comprenant des taxons auxiliaires, contrairement à ce qui est connu dans le cadre de la formation de biofilms [Berne *et al.*, 2015, Crouzet *et al.*, 2014, Donlan, 2002, Zheng *et al.*, 2021]. A l'inverse, la recolonisation des taches noires après nettoyage mécanique au scalpel est un processus plus lent. Nous avons mis en évidence divers taxons impliqués dans la recolonisation initiale des taches nettoyées, à savoir les bactéries *Pseudomonas*, *Pedomicrobium* et les champignons *Ochroconis* à mélanisation noire, puis des taxons impliqués plus tardivement dans la recolonisation (à partir de 4 mois) comme les bactéries du genre *Luteimonas*, *Chitinophaga* et le genre fongique *Exophiala*, etc (Figure 1). Les surfaces 19 mois après le nettoyage étaient différentes des surfaces non tachées et des surfaces tachées non nettoyées, soit parce que la succession microbienne différait de la succession originale pendant la formation des taches ou alors parce que le temps de recolonisation des taches noires nettoyées dans l'Absidiole est supérieur à 1 an et demi.

Nos travaux ont mis en évidence par métabarcoding et métagénomique que le type de substrat géologique a un impact sur la composition microbienne des communautés résistantes (i.e. surfaces non altérées). En effet les zones sombres échantillonnées dans différentes salles présentaient des similitudes dans leur composition microbienne, cela suggère donc que ces altérations

rassemblent un mélange de taxons cosmopolites (probablement déterminants dans la formation de l'altération) et de taxons endémiques à chaque emplacement de la grotte de Lascaux. Certains changements dans la composition microbienne des communautés impactées sont caractéristiques et communs aux deux types d'altérations, et peuvent être dus à certains taxons considérés comme endémiques des altérations. Une contre sélection de bactéries *Pseudomonas* (genre) et de champignons *Pseudogymnoascus* (genre) est observée, ainsi qu'à l'inverse une sélection de champignons Hypocreales (classe), *Ochroconis* (genre) et de bactéries Alphaproteobacteria (classe), *Chitinophaga* (genre) et *Nitrobacter* (genre). La dégradation du chlorure de benzalkonium (ammonium quaternaire) fournit probablement des composés azotées à *Nitrobacter* lui donnant ainsi le substrat nécessaire pour effectuer la seconde étape de nitrification (transformation de nitrite en nitrate). On peut donc faire l'hypothèse que la dégradation du BAC couplée à la présence de bactéries du genre *Nitrobacter* influence le fonctionnement initial du cycle de l'azote et/ou la disponibilité de certaines formes azote dans la communauté microbienne des surfaces altérées. L'azote étant nécessaire à la synthèse de mélanines (excepté les mélanines de type allomélanine et pyomélanine) [Cao *et al.*, 2021], cela pourrait favoriser l'apparition des altérations sur les parois de la grotte. Nos résultats mettent également en évidence une différence de composition des microorganismes pigmentés en fonction des types d'altérations étudiés notamment pour les champignons noirs (e.g. *Ochroconis*, *Exophiala*, etc.). Le genre *Ochroconis* est retrouvé abondamment dans les deux types d'altérations, tandis que le genre *Exophiala* est identifié uniquement dans les taches noires (Figure 2).

Les analyses de métagénomique sur les deux types d'altérations ont permis la reconstruction de génomes affiliés à la plupart de ces microorganismes. Plusieurs clusters de gènes impliqués dans la synthèse de pigments (mélanines et caroténoïdes) ont été identifiés (Figure 3). Les gènes *tyr*, identifiés principalement dans les MAGs affiliés à *Chitinophaga*, *Nitrobacter* et *Exophiala*, codent pour des enzymes de type tyrosinases qui jouent un rôle central dans la synthèse de mélanine [Hearing *et al.*, 1982] (Figure 3). En effet par réaction catalytique, la L-tyrosine est convertie en L-dopa puis en dopa-quinone qui par réaction spontanée se transforme en L-dopachrome, précurseur de mélanine [Munoz-Munoz *et al.*, 2009, Solano, 2014]. Les clusters de gènes *xyl*, *cat* et *tod*, ont été identifiés dans les génomes reconstruits d'*Hyphomicrobium* et *Exophiala* impliqués dans la dégradation du catéchol, précurseur de mélanine [Park *et al.*, 2003, Romero-Arroyo *et al.*, 1995, Zylstra *et al.*, 1988]. Également, l'analyse du potentiel génétique des communautés impactées a permis de suggérer que la coloration des altérations est dûe à un assemblage de plusieurs pigments. Ces altérations sont en effet composées d'un ensemble de mélanines (catéchol mélanine, DHN-mélanine et DOPA-mélanine) et de caroténoïdes produits à la fois par des bactéries et par des champignons (ex. *Chitinophaga*, *Exophiala*).

Un autre type de réponse à la perturbation correspondant à des taches atténuées est observé uniquement dans le Cabinet des Félins, probablement parce que cette salle se situe en partie terminale de la grotte, non accessible aux visiteurs et avec une seule application de biocide dans les années 2000. Ces taches atténuées peuvent être considérées comme un état résilient. L'analyse des processus d'assemblage des communautés a mis en évidence de fortes signatures stochastiques pour les taxons rares (abondance relative $<0.001\%$) dans les communautés microbiennes résistantes et impactées (i.e. surface non tachée et tache noire, respectivement), probablement

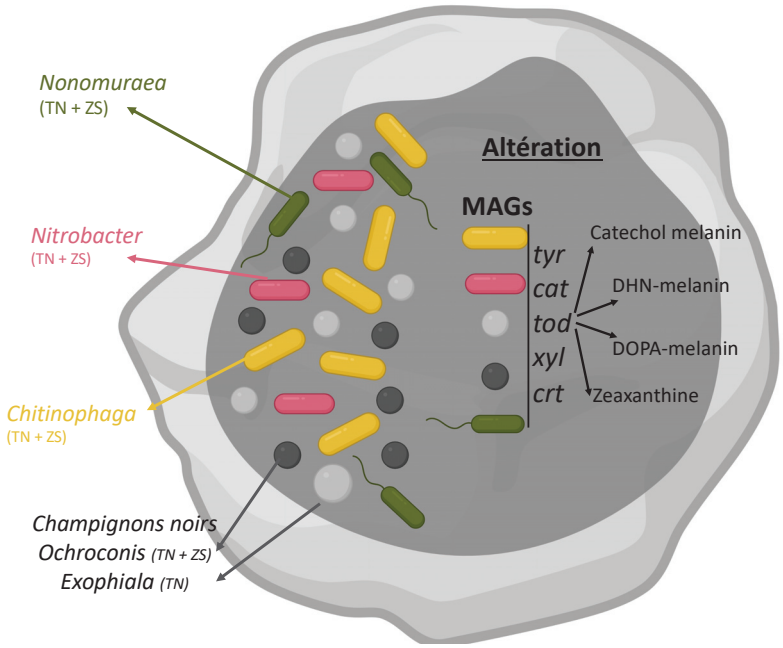

Figure 3. Schéma de la communauté microbienne impactée (taches noires et zones sombres) des paroi de la grotte de Lascaux regroupant les données taxonomiques et fonctionnelles de ces travaux de thèse. TN : Tache noire ; ZS : Zone sombre

parce que la perturbation était soit mineure pour tous les taxons, soit forte pour les taxons dominants, atténuant ainsi la compétition envers les taxons rares. A l'inverse, les processus de sélection sont importants dans les communautés résilientes (i.e. taches atténuées), peut-être parce que les taxons dominants deviennent mieux adaptés et imposent des pressions de sélection, ou parce que les microorganismes de la biosphère rare présentent une écologie spécifique et parfois unique qui peut différer considérablement de celles des représentants plus abondants [Lynch et Neufeld, 2015]. Ces taxons peuvent être sélectionnés pour des opportunités trophiques ou écologiques (i.e. *Mycobacterium*, *Sphingobium*, *Phyllobacterium* et *Vicinamibacter*, capable de dégrader les composés aromatiques) [Teng *et al.*, 2017, Vieira *et al.*, 2017, Dudhagara et Dave, 2018]. Également, nous avons constaté que la sélection des taxons toujours rares dans la communauté résiliente était valable pour les trois domaines de la vie, ce qui suggère des comportements écologiques communs ainsi que des relations de coopération peut-être impliquées dans la réponse aux perturbations. Ces résultats suggèrent donc que les taxons rares sont d'une importance majeure pour le fonctionnement de l'écosystème car ils représentent la majorité de la diversité microbienne et fournissent un large réservoir de fonctions écologiques et un moyen de résilience plus efficace [Galand *et al.*, 2009]. Cependant, l'étude de la biosphère rare est complexe, car elle est sujette aux artefacts expérimentaux ('bruit' de séquençage) et aux artefacts biologiques (dormance et gradients taphonomiques) [Lynch et Neufeld, 2015].

La relation entre la perturbation et la diversité est-elle régulée par la rétroaction ?

Nos travaux permettent une meilleure compréhension de l'interaction perturbation-diversité dans la grotte de Lascaux. En effet, cette thèse dans sa globalité, suggère que malgré l'hétérogénéité de l'écosystème, la formation d'altérations sur les parois est due à la perturbation anthropique de

l'écosystème en lien avec la modulation de la diversité. Les mécanismes sous-jacents à l'apparition de taches noires ou de zones sombres peuvent être conceptuellement divisés en plusieurs étapes dont certaines restent encore inconnues à ce jour (Figure 4).

Première étape : La perturbation anthropique de la grotte de Lascaux a engendré la sélection de microorganismes capables de survivre dans ces conditions (cf : 'La perturbation affecte la diversité microbienne ?' - page 313). L'application de traitements chimiques notamment de BAC sur les parois a rendu l'environnement toxique pour de nombreux microorganismes [Ertekin *et al.*, 2016, Tandukar *et al.*, 2013, Tagkopoulos *et al.*, 2019]. Les microorganismes capables de résister à ces conditions vont constituer la communauté résistante de la grotte, c'est-à-dire sur les surfaces non marquées. C'est le cas des bactéries affiliées au genre *Pseudomonas* qui représentent plus de >60% des séquences en moyenne sur le substrat naturel (Abside, Nef), >30% sur le substrat articiel (Passage, Salle des Taureaux) et >15% sur les blocs de calcaire du Santonien (SAS-2). Les différences observées pour l'abondance relative des *Pseudomonas* sont dues aux différentes propriétés des surfaces minérales (différence peut-être dans l'adsorption de biocides).

Deuxième étape : Cette communauté résistante peut donc soit (i) rester intacte pendant de nombreuses années, ne provoquant pas l'apparition d'altérations sur les parois, soit (ii) un processus (encore non identifié) peut initier la dégradation du BAC par des taxons spécialistes de la communautés résistantes. Des souches appartenant aux genres bactériens *Pseudomonas*, *Mycobacterium*, *Bacillus* et *Listeria* sont capables de dégrader le BAC [Tagkopoulos *et al.*, 2019]. La dégradation par désalkylation convertit le BAC en produits chimiques moins toxiques, permettant à certains microorganismes de les utiliser comme substrats et source d'énergie [Tandukar *et al.*, 2013, Zhang *et al.*, 2011]. Cela suggère que l'environnement moins toxique engendre une augmentation de l'activité de certains microorganismes de la communauté résistante et/ou permet le développement d'autres microorganismes. En effet, le potentiel métabolique des génomes reconstruits à partir d'échantillons de calcaire, semble être plus faible par rapport à celui des génomes reconstruits pour les communautés impactées (*Pseudomonas*, *Streptomyces*, etc.). La réactivation du métabolisme de certains microorganismes, avec notamment une forte abondance des gènes appartenant à la classe métabolique 'Signaling molecules and interaction' et un niveau d'interaction plus élevé dans le calcaire proche de l'altération (réseaux de co-occurrence) laisse à penser que la dégradation du BAC par la communauté résistante, implique une diminution de la toxicité de l'environnement, initiant des changements communautaires majeurs.

Troisième étape : Ces changements communautaires aboutissent à l'apparition d'altérations sur les parois (Cf. 'La diversité module les effets de la perturbation ?'). Plusieurs changements communautaires sont caractéristiques des altérations : (i) la contre-sélection des genres *Pseudomonas* (bactérie) et *Pseudogymnoascus* (champignon), (ii) la sélection de champignons noirs (*Ochroconis*, *Exophiala*, *Acremonium*), de certaines alphaproteobactéries et de certains genres bactériens (*Chitinophaga, Nonomurae, Labrys,* etc.). Une relation entre ces changements communautaires peut-être établie dans certains cas. La très faible abondance (<0.1%) du champignon noir *Ochroconis* dans la communauté résistante peut-être due à la présence de composés antimicrobiens synthétisés par les *Pseudomonas*, tels que les phénazines, le 2-diacétylphloroglucinol (DAPG), la pyocyanine, la pyrolnitrine etc. [Almario *et al.*, 2017, Bruto *et al.*, 2014, Michelsen et Stougaard, 2012]. Cela est confirmé par l'observation à la fois de *Pseudomonas* et *Ochroconis*

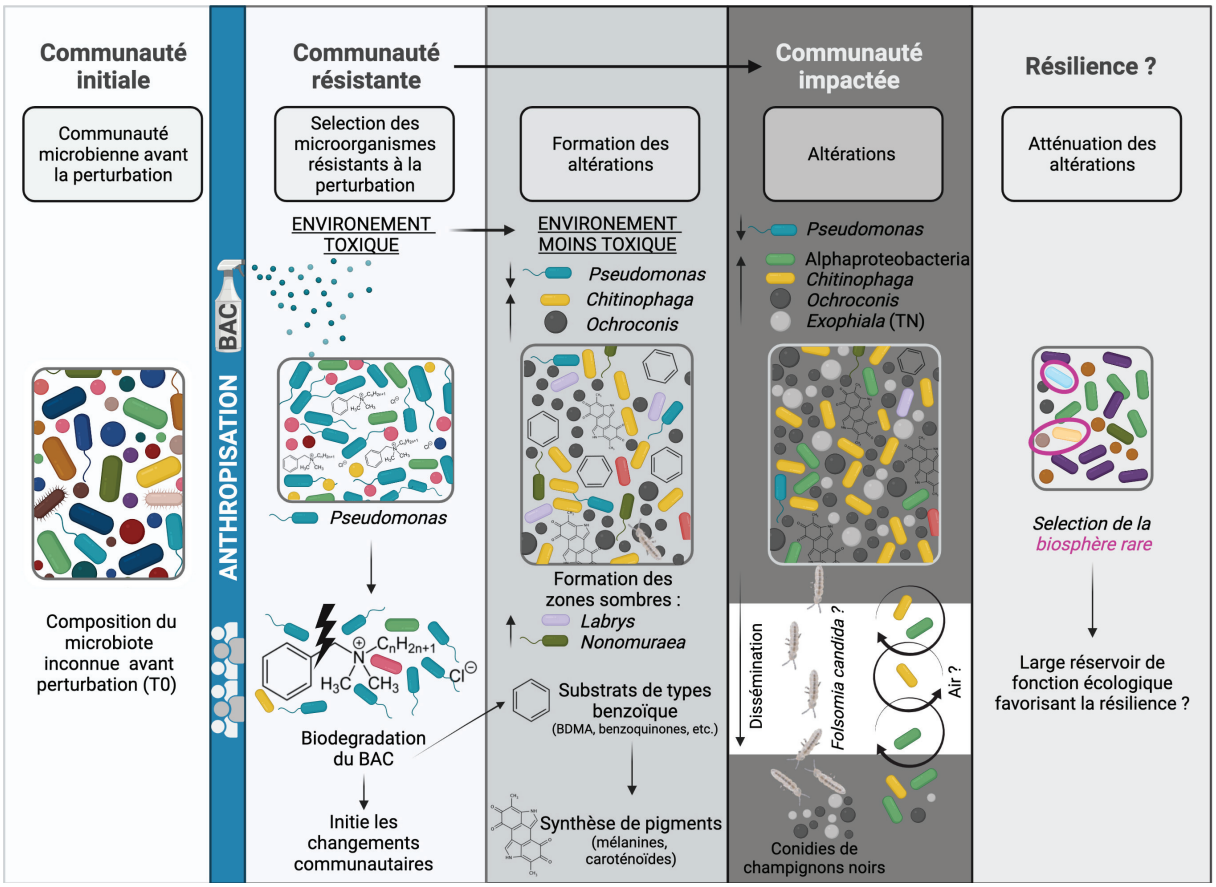

Figure 4. Modèle conceptuel des processus impliqués dans la formation, l'évolution et la dissémination des altérations des parois de la grotte de Lascaux. TN : Tache noire ; ZS : Zone sombre, BAC : Chlorure de benzalkonium.

dans plusieurs modules avec des interactions négatives (i.e. suggérant des interactions de type antagonisme entre ces deux microorganismes). A l'inverse, la contre-sélection du genre *Pseudomonas* dans les altérations est peut-être liée à la présence du genre bactérien *Nonomuraea*, genre déjà isolé dans les grottes, pouvant synthétiser des composés anti-*Pseudomonas* [Nimaichand *et al.*, 2015]. Nos travaux ont mis en évidence une absence de taxons fongiques spécifiques aux zones sombres, suggérant que les bactéries pourraient jouer un rôle particulier dans la formation de zones sombres. Il est également possible que la formation de zone sombre implique également des contributions d'autres microorganismes spécifiques aux zones sombres de chaque salle de la grotte, comme par exemple la présence de bactéries telles que *Achromobacter* et *Nectria* dans la Nef. Des taxons peuvent donc être caractérisés comme spécifiques (endémiques) des altérations. Cela suggère que l'apparition de nouvelles altérations est en lien avec l'aire de répartition de ces taxons. Plusieurs hypothèses peuvent être évoquées pour expliquer la répartition hétérogène des altérations sur les parois : (i) les flux d'air vont permettre de manière aléatoire le contact entre ces taxons et une paroi, (ii) le changement progressif des conditions climatiques résultant peut-être du rechauffement climatique et/ou de la suppression progressive du système de gestion de l'air dans la grotte, (iii) la présence d'arthropodes vecteurs de ces microorganismes, ou (iv) une combinaison de ces facteurs. Les études réalisées dans la grotte de Lascaux ont montré la présence de collemboles et notamment l'espèce *Folsomia candida* sur les parois de l'Abside [Alabouvette et Sáiz-Jiménez, 2011](Alonso et al. en préparation). Ces col-

lemboles consomment des microorganismes et notamment des champignons noirs qu'ils peuvent disséminer (in vitro) [Scheu et Simmerling, 2004, Bastian *et al.*, 2009b] rendant leur système digestif et déjections foncés. Une partie du carbone organique contenu dans ces microorganismes s'intègre dans la biomasse des collemboles mais certains composants sont relargués sur les parois via leurs fèces, tels que des conidies de champignons noirs fonctionnelles [Alonso, 2018]. Cela suggère la mise en place d'interactions entre les microorganismes endémiques des altérations et les collemboles, facilitant probablement la dissémination des taxons spécifiques aux altérations sur les parois saines.

Quatrième étape : Étant donné que la plupart des changements microbiens a eu lieu depuis le début de l'altération visuelle (i.e. nouvelle zone sombre et stades primaires de recolonisation de tache noire), cela suggère que les processus microbiens (c'est-à-dire les patrons d'expression génique) conduisant à l'apparition des altérations sont opérationnels dès que les populations microbiennes correspondantes s'établissent (*Ochroconis*). Grâce aux analyses du potentiel fonctionnel des communautés microbiennes des trois domaines du vivant, nos travaux ont mis en évidence plusieurs mécanismes conduisant à la synthèse de pigments (mélanines et caroténoïdes). Premièrement la communauté résistante lors de la dégradation des composés chloroaromatiques produit des benzoquinones (via la synthèse et la dégradation de composés intermédiaires). Ces benzoquinones vont pouvoir être utilisés par les communautés résistantes (*Hyphomicrobium*, *Chitinophaga*, etc.), pour permettre la formation de catéchol-mélanine. Une réaction de dismutation entre le catéchol et une benzoquinone peut générer des radicaux semi-quinones ou réagir avec H_2O pour générer du 1,2,4-trihydroxybenzène. Des réactions spontanées (encore inconnues) génèrent des dimères biphénoliques aromatiques ou du diphénylène-dioxyde-2,3-quinone résultant en un polymère catéchol-mélanine indéfini [Mason, 1949, Nicolaus *et al.*, 1964]. D'autres polymères de mélanine peuvent être synthétisés par des microorganismes de communautés microbiennes résistantes (*Chitinophaga*, Actinomycetia, Bacteroidetes et *Exophiala*), tels que l'eumélanine. La coloration des altérations implique un ou plusieurs microorganismes spécialistes de la biosynthèse de pigments et endémiques des altérations.

Cinquième étape : Une fois les altérations établies sur les parois, des évènements encore inconnus à ce jour peuvent induire l'atténuation des taches noires, impliquant la mise en place d'une communauté microbienne dite résiliente. Cependant les évènements nécessaires à l'atténuation des taches semblent être portés par des taxons rares. Les processus favorisant le développement de la biosphère rare sont très peu décrits [Galand *et al.*, 2009, Lynch et Neufeld, 2015] et le développement d'outils moléculaires permettant la reconstruction génomique et donc l'annotation fonctionnelle de ces taxons permettrait une meilleure compréhension de la relation de cause à effet entre l'impact d'une perturbation et la diversité des communautés microbiennes.

La formation et la répartition hétérogène des altérations sur les parois de la grotte de Lascaux serait liée à une conjonction de différentes conditions nécessaires pour la formation d'une altération, qui probablement survient d'évènements aléatoires. Cette proposition est compatible avec les hypothèses précedentes émises par Martin-Sanchez et al. (2012), Alabouvette and Saiz-Jimenez (2011).

Actuellement la stratégie de conservation de la grotte repose sur la faible fréquentation humaine (limité à la présence de scientifiques) et sur le nettoyage mécanique de certaines alté-

rations. Le nettoyage mécanique se fait grâce à l'utilisation de scalpel stérile et d'éponge (AION D3, Japon). Ces travaux de thèse ont permis de mettre en évidence que l'utilisation d'une éponge pour le nettoyage mécanique, peut avoir un impact significatif sur les communautés microbiennes et contribuer à la contamination des surfaces des grottes par des microorganismes ayant un potentiel de bioaltération. En effet nous avons identifié l'apport de taxons allochtones (*Filomicrobium*, *Isaria*, *Cephalotrichum*) par le nettoyage des parois à l'éponge. Ces taxons sont connus pour être des acteurs de la biodégradation des peintures dans les milieux souterrains [Nováková, 2009, Miller *et al.*, 2020, Diaz-Herraiz *et al.*, 2014]. De plus, le nettoyage mécanique à l'aide d'une éponge peut modifier les propriétés de surface des roches, sélectionnant certaines espèces ayant des propriétés d'adhésion particulières et capables de prospérer [Barton *et al.*, 2007, Uroz *et al.*, 2015]. Ainsi, notre travail a permis de mettre en évidence un problème dans les procédures actuelles de traitement des altérations dans les grottes.

Limites et perspectives de ces travaux de thèse

Certains processus impliqués dans la réponse des communautés microbiennes de la grotte de Lascaux face à la perturbation anthropique restent encore inconnus. La limite majeure de cette thèse est une absence de connaissances sur la composition du microbiote de la grotte avant perturbation (T0), ne permettant pas de déduire l'impact réel de la perturbation chimique sur les communautés microbiennes de la grotte de Lascaux. Également, des contraintes liées à l'échantillonnage notamment à cause de la fragilité de la grotte ont engendré des difficultés pour certaines analyses. La faible quantité de matière pour de nombreux échantillons a été l'une des difficultés de ma thèse, ne permettant pas l'obtention d'une quantité de matière suffisante pour le séquençage de métagénomes. Ainsi, certaines analyses comportent moins de répétitions que ce qui était prévu (métagénomique sur les taches noires de la Nef). De plus, les possibilités et la durée d'échantillonnage dans la grotte étant limitées, ceci implique un nombre limité d'échantillons par condition ou encore un manque de réplicats de certaines conditions dans le temps (un deuxième échantillonnage dans le Cabinet des Félins n'a pas pu être effectué avant l'été 2022).

Historiquement, les études en écologie microbienne utilisent des approches basées sur la mise en culture ainsi que le séquençage des amplicons et la métagénomique pour caractériser la diversité microbienne des écosystèmes [Overmann *et al.*, 2017]. Toutes nos analyses sont essentiellement fondées sur le séquençage à haut débit des acides nucléiques (métabarcoding et métagénomique). Quelle que soit la méthodologie, des biais techniques et analytiques ont été identifiés. De l'ADN de microorganismes morts peut être inclus dans l'analyse, pouvant affecter l'estimation de la diversité microbienne et réduire également la capacité à assembler les séquences en métagénomique. En métabarcoding, l'amplification de l'ADN induit plusieurs problèmes concernant notamment la formation de chimères, des mutations ponctuelles et des aspécificités potentielles dues au choix des amorces [Eloe-Fadrosh *et al.*, 2016]. De plus, le nombre de copies de gènes par génome peut varier considérablement d'un taxon à l'autre, faussant ainsi les estimations quantitatives de la diversité [Louca *et al.*, 2018]. La taille des amplicons reste un problème crucial pour une meilleure affiliation taxonomique, car des amplicons plus longs fourniront une affiliation taxonomique plus fiable, ce problème est en partie compensé grâce au séquençage shotgun métagénomique générant après assemblage des plus longs fragments (pro-

cédure d'assemblage induisant elle-même des biais) mais ces affiliations taxonomiques reposent sur les bases de données, qui sont incomplètes. Cependant, l'affiliation taxonomique des fragments d'ADN ne permet pas d'aller jusqu'à l'espèce, excepté pour le MAGs de *Pseudomonas spelaei* reconstruit à partir de calcaire non marqué de la Nef. Un séquençage du génome entier pourrait permettre de mieux caractériser ces microorganismes, de plus des analyses de génomique comparative pourraient-être réalisées entre *Pseudomonas* issus du calcaire non marquée ou des altérations de la grotte de Lascaux. Cela pourrait nous permettre par exemple, d'observer la présence de gènes permettant la synthèse de pyomélanine (pigment noir) dans les *Pseudomonas* provenant des altérations ou apporter des informations importantes sur la capacité de prolifération, la résistance aux biocides et à la régulation de la synthèse des mélanines.

Le séquençage métagénomique dans des environnements divers et complexes ne peut identifier que les représentants les plus abondants (tels que *Pseudomonas* dans notre cas) et donc néglige l'assemblage des séquences de la biosphère rare, bien qu'elle semble jouer un rôle important dans les écosystèmes [Pascoal *et al.*, 2021, Lynch et Neufeld, 2015]. Pour permettre une meilleure analyse métagénomique de la biosphère rare, la complexité de la communauté doit être réduite. L'exemple le plus extrême concerne l'application du tri cellulaire (FACS) pour réaliser de la génomique unicellulaire fournissant des informations génomiques avec une résolution au niveau de la souche [Blainey, 2013, Woyke *et al.*, 2017]. Les assemblages de SAG (Single Amplified Genome), contrairement au MAGs, permettent d'obtenir des génomes qui ne résultent pas de consensus provenant d'une multitude de cellules mais les SAGs obtenus sont le plus souvent fragmentés et incomplets et le processus global est fortement sujet à la contamination [Stepanauskas, 2012, Alteio *et al.*, 2020]. Afin de contourner les biais associés à la métagénomique et à la génomique unicellulaire l'utilisation de la technique de mini-métagénome, couplant une approche de tri cellulaire et de séquençage métagénomique peut-être une solution [Alteio *et al.*, 2020, Yu *et al.*, 2017]. La combinaison des techniques de mini-métagénomes et de métagénomes permettrait de saisir une diversité microbienne holistique. Grâce à l'utilisation de ces deux techniques, une étude des sols forestiers a découvert une diversité bactérienne et archéenne du sol qui n'était pas accessible en utilisant uniquement la métagénomique [Alteio *et al.*, 2020]. La réalisation de mini-métagénomes dans les écosystèmes karstiques pourrait diminuer les biais d'assemblage dus aux taxons dominants et permettre la reconstruction de génomes d'organismes rares de la biosphère. Dans notre cas, la reconstruction de génomes d'organismes rares pourrait nous permettre d'obtenir des informations taxonomiques et fonctionnelles cruciales pour comprendre le rôle potentiel de ces microorganismes dans l'atténuation des taches noires (résilience) mais aussi dans l'évolution et le développement des deux types d'altérations des parois de la grotte de Lascaux.

De plus, la combinaison de plusieurs techniques de séquençage à haut-débit pourrait permettre d'obtenir des génomes mieux reconstruits. Le séquençage à lecture longue s'est démocratisé (Oxford Nanopore Technology, PacBio, etc.) et permet la récupération de génomes microbiens hautement contigus, mais un polissage à lecture courte (technologie Illumina) pour corriger les insertions et les suppressions dérivées de régions homopolymères permet de générer des génomes microbiens presque finis [Sereika *et al.*, 2022].

Cependant, l'amélioration de la qualité de l'assemblage ne suffit pas à pallier les problèmes dus aux outils et bases de données consacrés aux analyses métagénomiques. En effet, ces outils

sont fortement biaisés vers les analyses procaryotes restant donc encore inadaptés pour l'analyse des microeucaryotes. Ce constat est également fait sur les outils permettant le binning et l'estimation de la qualité des MAGs, qui sont encore limités car (i) la taille des génomes eucaryotes est classiquement plus grande par rapport aux procaryotes et (ii) les gènes marqueurs présents en multiples copies sont souvent considérés comme des indicateurs de contamination lors de l'estimation de la qualité des MAGs, faussant le résultat et conduisant à la non-sélection des MAGs [Saary *et al.*, 2020, West *et al.*, 2018]. La difficulté à identifier et à reconstruire des génomes de champignons dans nos métagénomes représente une des limites de ces travaux de thèse (avec un unique génome de champignon reconstruit dans les taches noires de la Nef appartenant au genre *Exophiala*). En effet la teinte noire/sombre des altérations présentes dans la grotte semble être liée à la production de pigments organiques (mélanines) par des champignons noirs. Obtenir des informations sur le potentiel fonctionnel de ces microorganismes serait un atout majeur pour la compréhension des processus de formation/évolution des altérations.

En plus des approches moléculaires nouvelles, l'utilisation d'une approche intégrative à travers l'interdisciplinarité semble nécessaire pour une meilleure compréhension de nos résultats. Les études des environnements karstiques nécessitent une approche interdisciplinaire holistique qui considère simultanément les composants physiques, chimiques et biologiques des systèmes environnementaux. Ici, la mise en perspective de nos résultats avec les propriétés physico-chimiques de la grotte n'a pas pu être établie et serait un atout majeur à notre étude, permettant de mieux comprendre par exemple l'impact réel de la minéralogie sur la composition et la structure des communautés microbiennes. Un autre objectif de l'interdisciplinarité est la construction d'une base de données compilant les altérations des parois des grottes, leur caractérisation, les méthodes de diagnostic, le mécanisme de leur formation, les paramètres gouvernant leur évolution pour mieux guider et prévenir les stratégies de conservation des grottes ornées.

Conclusion

L'ensemble de ces travaux contribue à mieux comprendre les dynamiques de la diversité microbienne lors de la formation, l'évolution et la dissémination des altérations (taches noires et zones sombres) déclenchées par l'ensemble des perturbation anthropiques survenues dans la grotte de Lascaux. Les résultats obtenus par séquençage haut-débit nous ont permis d'identifier les successions microbiennes impliquées dans l'évolution des altérations à plusieurs échelles spatio-temporelles et à identifier les interactions et processus microbiens sous-jacents. Nous avons démontré dans un premier temps à travers un échantillonnage micro-spatialisé que le début de la formation des zones sombres coïncide avec le développement des genres bactériens *Labrys*, *Nonomuraea* et *Sphingomonas*, ce qui est concomitant avec la prolifération de genre fongique *Ochroconis* et la contre-sélection des *Pseudomonas*. Ces résultats mettent en évidence un changement brutal des communautés lors de la formation de zone sombre nous permettant de valider la première hypothèse ('la formation et l'évolution des zones sombres seraient liées à des successions microbiennes rapides car les zones altérées et zones saines sont visuellement très différentes, sans zones de transition apparente'). Dans un deuxième temps le développement des zones sombres dans plusieurs salles de la grotte de Lascaux a été étudié. Nous avons confirmé une hétérogénéité du microbiote des surfaces non marquées et observé des change-

ments microbiens en lien avec l'emplacement des zones sombres dans la grotte. En détail, les zones sombres abritent des taxons bactériens et fongiques cosmopolites à l'échelle de Lascaux, ainsi que des taxons spécifiques aux zones sombres (uniquement des bactéries). Ces observations nous permettent de valider la deuxième hypothèse ('Au moins une partie des changements de la communauté microbienne liés à la formation de zone sombre implique des taxons cosmopolites et endémiques'). Dans un troisième temps, nous avons étudié des dynamiques microbiennes de régression et de repousse de certaines taches noires, mettant en évidence (i) un nouveau scenario écologique basé sur les processus d'assemblage de la biosphère rare des trois domaines du vivant, suggèrant un rôle important de ces taxons dans la résilience, (ii) que le nettoyage mécanique des taches noires permettait de générer artificiellement une succession microbienne dont les premiers acteurs sont affiliés aux genres *Pseudomonas*, *Pedomicrobium* et *Ochroconis*, et (iii) que l'utilisation d'une éponge pour le nettoyage mécanique contribue à la contamination des surfaces par des microorganismes exogènes ayant un potentiel de bioaltération. Toutefois, notre hypothèse selon laquelle les dynamiques de régression de certaines taches noires dans le Cabinet des Félins et de repousse des taches noires dans l'Absidiole seraient liées à des successions microbiennes particulières voire même opposées, n'a pas été vérifiée. Nous avons démontré dans un quatrième temps que la couleur noire des taches était due à la présence de voies métaboliques impliquées dans la biosynthèse de différents pigments organiques tels que des caroténoïdes et des mélanines (catéchol-mélanine, DHN mélanine et DOPA mélanine) produits par des champignons (e.g. champignon noir *Exophiala*) et des bactéries (e.g. *Chitinophaga*) dans les deux types d'altérations. De plus, le potentiel génétique des communautés microbiennes montre un lien possible entre la synthèse de mélanine et la dégradation des produits chimiques précédemment appliqués sur les parois de la grotte, suggérant que les micro-organismes producteurs de pigments sont favorisés par l'application de biocides. Ces résultats indiquent que les gènes contribuant à la synthèse de pigments sont davantage présents dans la communauté microbienne des zones altérées, nous permettant de valider la quatrième hypothèse ('les taches noires étant attribuées à l'activité des champignons pigmentés et ces champignons colonisant les deux types d'altérations, nous pouvons penser que les mêmes types de fonctions fongiques de pigmentation seraient impliquées dans les deux cas et qu'elles concerneraient des taxons spécialistes.').

L'ensemble de ces résultats nous montre que les perturbations, en lien avec l'hétérogénéité de l'écosystème, aboutissent à des modifications de l'assemblage communautaire, impactant notamment la répartition des taxons (endémiques vs cosmopolites) et leurs abondances (dominants vs rares) dans la communauté microbienne, validant l'hypothèse générale de ce manuscrit.

Cette thèse a permis de caractériser la diversité, la structure, la composition, les interactions et potentiel fonctionnel des communautés microbiennes des trois domaines du vivant de la grotte de Lascaux. Ces informations permettent de mieux comprendre les processus microbiens impliqués dans les processus de formation et d'évolution des altérations dans la grotte et d'alimenter la réflexion sur les stratégies de conservation de ce patrimoine culturel.

Bibliographie

Abdelfattah, A., Malacrino, A., Wisniewski, M., Cacciola, S. O. et Schena, L. (2018). Metabarcoding : A powerful tool to investigate microbial communities and shape future plant protection strategies. *Biological Control*, 120:1–10.

Abreu, C. I., Friedman, J., Andersen Woltz, V. L. et Gore, J. (2019). Mortality causes universal changes in microbial community composition. *Nature Communications*, 10(1):1–9.

Al-Mufti, M., Sydes, C., Furness, S., Grime, J. et Band, S. (1977). A quantitative analysis of shoot phenology and dominance in herbaceous vegetation. *The Journal of Ecology*, 65(3):759–791.

Alabouvette, C. et Sáiz-Jiménez, C. (2011). *Écologie microbienne de la Grotte de Lascaux*. CSIC-Instituto de Recursos Naturales y Agrobiología de Sevilla (IRNAS).

Allemand, L. et Bahn, P. G. (2005). Best way to protect rock art is to leave it alone. *Nature*, 433(7028):800–800.

Allison, G. (2004). The influence of species diversity and stress intensity on community resistance and resilience. *Ecological Monographs*, 74(1):117–134.

Allison, S. D. et Martiny, J. B. (2008). Resistance, resilience, and redundancy in microbial communities. *Proceedings of the National Academy of Sciences USA*, 105:11512–11519.

Almario, J., Bruto, M., Vacheron, J., Prigent-Combaret, C., Moënne-Loccoz, Y. et Muller, D. (2017). Distribution of 2,4-diacetylphloroglucinol biosynthetic genes among the *Pseudomonas* spp. reveals unexpected polyphyletism. *Frontiers in Microbiology*, 8:1218.

Alonso, L. (2018). *Hétérogénéité spatio-temporelle du microbiote de la grotte de Lascaux*. Thèse de doctorat, Université de Lyon.

Alonso, L., Creuzé-des Châtelliers, C., Trabac, T., Dubost, A., Moënne-Loccoz, Y. et Pommier, T. (2018). Rock substrate rather than black stain alterations drives microbial community structure in the passage of Lascaux Cave. *Microbiome*, 6(1):1–15.

Alonso, L., Pommier, T., Kaufmann, B., Dubost, A., Chapulliot, D., Doré, J., Douady, C. J. et Moënne-Loccoz, Y. (2019). Anthropization level of Lascaux Cave microbiome shown by regional-scale comparisons of pristine and anthropized caves. *Molecular Ecology*, 28(14):3383–3394.

Alteio, L., Schulz, F., Seshadri, R., Varghese, N., Rodriguez-Reillo, W., Ryan, E., Goudeau, D., Eichorst, S., Malmstrom, R., Bowers, R. *et al.* (2020). Complementary metagenomic approaches improve reconstruction of microbial diversity in a forest soil. *mSystems*, 5(2):e00768–19.

Avery, S. V. (2006). Microbial cell individuality and the underlying sources of heterogeneity. *Nature Reviews Microbiology*, 4(8):577–587.

Banerjee, S. et Joshi, S. (2013). Insights into cave architecture and the role of bacterial biofilm. *Proceedings of the National Academy of Sciences USA*, 83(3):277–290.

Baquedano Estevez, C., Moreno Merino, L., de la Losa Román, A. et Duran Valsero, J. J. (2019). The lampenflora in show caves and its treatment : an emerging ecological problem. *International Journal of Speleology*, 48(3):4.

Barbault, R. (1997). *Biodiversité : introduction à la biologie de la conservation*. Hachette Paris.

Barton, H. A. et Jurado, V. (2007). What's up down there ? Microbial diversity in caves. *Microbes*, 2:132–138.

Barton, H. A., Northup, D. E. *et al.* (2007). Geomicrobiology in cave environments : past, current and future perspectives. *Journal of Cave and Karst Studies*, 69(1):163–178.

Bastian, F. et Alabouvette, C. (2009). Lights and shadows on the conservation of a rock art cave : the case of Lascaux Cave. *International Journal of Speleology*, 38(1):6.

Bastian, F., Alabouvette, C., Jurado, V. et Saiz-Jimenez, C. (2009a). Impact of biocide treatments on the bacterial communities of the Lascaux Cave. *Naturwissenschaften*, 96(7): 863–868.

Bastian, F., Alabouvette, C. et Saiz-Jimenez, C. (2009b). The impact of arthropods on fungal community structure in Lascaux Cave. *Journal of Applied Microbiology*, 106(5):1456–1462.

Bastian, F., Jurado, V., Nováková, A., Alabouvette, C. et Sáiz-Jiménez, C. (2010). The microbiology of Lascaux Cave. *Microbiology*, 156(3):644–652.

Beisner, B. E., Haydon, D. T. et Cuddington, K. (2003). Alternative stable states in ecology. *Frontiers in Ecology and the Environment*, 1(7):376–382.

Bell, E. A., Boehnke, P., Harrison, T. M. et Mao, W. L. (2015). Potentially biogenic carbon preserved in a 4.1 billion-year-old zircon. *Proceedings of the National Academy of Sciences USA*, 112(47):14518–14521.

Bennett, A. F. et Lenski, R. E. (1993). Evolutionary adaptation to temperature. Thermal niches of experimental lines of *Escherichia coli*. *Evolution*, 47(1):1–12.

Berne, C., Ducret, A., Hardy, G. G. et Brun, Y. V. (2015). Adhesins involved in attachment to abiotic surfaces by gram-negative bacteria. *Microbial biofilms*, 4:163–199.

Biot, V. (2006). *Le tourisme souterrain en France*, volume 15. Karstologia Mémoires.

Blainey, P. C. (2013). The future is now : single-cell genomics of bacteria and archaea. *FEMS Microbiology Reviews*, 37(3):407–427.

Bontemps, Z., Alonso, L., Pommier, T., Hugoni, M. et Moënne-Loccoz, Y. (2021). Microbial ecology of tourist paleolithic caves. *Science of the Total Environment*, 816:151492.

Borderie, F., Denis, M., Barani, A., Alaoui-Sossé, B. et Aleya, L. (2016). Microbial composition and ecological features of phototrophic biofilms proliferating in the moidons caves (France) : investigation at the single-cell level. *Environmental Science and Pollution Research*, 23(12):12039–12049.

Botton, S., Van Heusden, M., Parsons, J., Smidt, H. et Van Straalen, N. (2006). Resilience of microbial systems towards disturbances. *Critical Reviews in Microbiology*, 32(2):101–112.

Brewer, T. E. et Fierer, N. (2018). Tales from the tomb : the microbial ecology of exposed rock surfaces. *Environmental Microbiology*, 20(3):958–970.

Bruno, J. F., Stachowicz, J. J. et Bertness, M. D. (2003). Inclusion of facilitation into ecological theory. *Trends in Ecology & Evolution*, 18(3):119–125.

Bruto, M., Prigent-Combaret, C., Muller, D. et Moënne-Loccoz, Y. (2014). Analysis of genes contributing to plant-beneficial functions in plant growth-promoting rhizobacteria and related proteobacteria. *Scientific Reports*, 4(1):1–10.

Canaveras, C., Sanchez-Moral, S., Sloer, V. et Saiz-Jimenez, C. (2001). Microorganisms and microbially induced fabrics in cave walls. *Geomicrobiology Journal*, 18(3):223–240.

Cao, W., Zhou, X., McCallum, N. C., Hu, Z., Ni, Q. Z., Kapoor, U., Heil, C. M., Cay, K. S., Zand, T., Mantanona, A. J. *et al.* (2021). Unraveling the structure and function of melanin through synthesis. *Journal of the American Chemical Society*, 143(7):2622–2637.

Chalmin, E., d'Orlyé, F., Zinger, L., Charlet, L., Geremia, R., Orial, G., Menu, M., Baffier, D. et Reiche, I. (2007). Biotic versus abiotic calcite formation on prehistoric cave paintings : the Arcy-sur-Cure 'Grande Grotte'(Yonne, France) case. *Geological Society*, 279(1):185–197.

Cigna, A. A. (2016). Tourism and show caves. *Zeitschrift für Geomorphologie*, 60(2):217–233.

Cigna, A. A., Forti, P. *et al.* (2013). Caves : the most important geotouristic feature in the world. *Tourism and Karst Areas*, 6(1):9–26.

Compson, Z. G., McClenaghan, B., Singer, G. A., Fahner, N. A. et Hajibabaei, M. (2020). Metabarcoding from microbes to mammals : comprehensive bioassessment on a global scale. *Frontiers in Ecology and Evolution*, 8:581835.

Connell, J. H. (1997). Disturbance and recovery of coral assemblages. *Coral Reefs*, 16(1):S101–S113.

Cox, F., Newsham, K. K. et Robinson, C. H. (2019). Endemic and cosmopolitan fungal taxa exhibit differential abundances in total and active communities of antarctic soils. *Environmental Microbiology*, 21(5):1586–1596.

Cramer, M. J. et Willig, M. R. (2002). Habitat heterogeneity, habitat associations, and rodent species diversity in a sand–shinnery-oak landscape. *Journal of Mammalogy*, 83(3):743–753.

Crouzet, M., Le Senechal, C., Brözel, V. S., Costaglioli, P., Barthe, C., Bonneu, M., Garbay, B. et Vilain, S. (2014). Exploring early steps in biofilm formation : set-up of an experimental system for molecular studies. *BMC Microbiology*, 14(1):1–12.

Cuezva, S., Sanchez-Moral, S., Saiz-Jimenez, C. et Cañaveras, J. C. (2009). Microbial communities and associated mineral fabrics in Altamira Cave, Spain. *International Journal of Speleology*, 38(1):9.

De Leo, F., Iero, A., Zammit, G. et Urzì, C. E. (2012). Chemoorganotrophic bacteria isolated from biodeteriorated surfaces in cave and catacombs. *International Journal of Speleology*, 41:125–136.

Devictor, V., Julliard, R. et Jiguet, F. (2008). Distribution of specialist and generalist species along spatial gradients of habitat disturbance and fragmentation. *Oikos*, 117(4):507–514.

Dhami, N. K., Mukherjee, A. et Watkin, E. L. (2018). Microbial diversity and mineralogical-mechanical properties of calcitic cave speleothems in natural and in vitro biomineralization conditions. *Frontiers in Microbiology*, 9:40.

Diaz-Herraiz, M., Jurado, V., Cuezva, S., Laiz, L., Pallecchi, P., Tiano, P., Sanchez-Moral, S. et Saiz-Jimenez, C. (2014). Deterioration of an Etruscan tomb by bacteria from the order Rhizobiales. *Scientific Reports*, 4(1):1–7.

Donlan, R. M. (2002). Biofilms : microbial life on surfaces. *Emerging Infectious Diseases*, 8(9):881.

Dudhagara, D. R. et Dave, B. P. (2018). *Mycobacterium as polycyclic aromatic hydrocarbons (PAHs) degrader*. BoD-Books.

Dupont, J., Jacquet, C., Dennetiere, B., Lacoste, S., Bousta, F., Orial, G., Cruaud, C., Couloux, A. et Roquebert, M.-F. (2007). Invasion of the French paleolithic painted cave of Lascaux by members of the *Fusarium solani* species complex. *Mycologia*, 99(4):526–533.

Eloe-Fadrosh, E. A., Ivanova, N. N., Woyke, T. et Kyrpides, N. C. (2016). Metagenomics uncovers gaps in amplicon-based detection of microbial diversity. *Nature Microbiology*, 1(4):1–4.

Engel, A. S. (2010). Microbial diversity of cave ecosystems. *In Geomicrobiology : molecular and environmental perspective*, pages 219–238. Springer.

Ertekin, E., Hatt, J. K., Konstantinidis, K. T. et Tezel, U. (2016). Similar microbial consortia and genes are involved in the biodegradation of benzalkonium chlorides in different environments. *Environmental Science & Technology*, 50(8):4304–4313.

Faust, K. et Raes, J. (2012). Microbial interactions : from networks to models. *Nature Reviews Microbiology*, 10(8):538–550.

Finley, B. K., Mau, R. L., Hayer, M., Stone, B. W., Morrissey, E. M., Koch, B. J., Rasmussen, C., Dijkstra, P., Schwartz, E. et Hungate, B. A. (2022). Soil minerals affect taxon-specific bacterial growth. *The ISME Journal*, 16(5):1318–1326.

Galand, P. E., Casamayor, E. O., Kirchman, D. L. et Lovejoy, C. (2009). Ecology of the rare microbial biosphere of the Arctic Ocean. *Proceedings of the National Academy of Sciences USA*, 106(52):22427–22432.

Gauchon, C., Jaillet, S. et Prud'Homme, F. (2012). Dynamique de la construction topographique et toponymique à l'aven d'Orgnac. Ardèche, France.

Glasby, T. M. et Underwood, A. (1996). Sampling to differentiate between pulse and press perturbations. *Environmental Monitoring and Assessment*, 42(3):241–252.

Grime, J. P. (1977). Evidence for the existence of three primary strategies in plants and its relevance to ecological and evolutionary theory. *The American Naturalist*, 111(982):1169–1194.

Hall, L. S., Krausman, P. R. et Morrison, M. L. (1997). The habitat concept and a plea for standard terminology. *Wildlife Society Bulletin*, 25(1):173–182.

He, J., Zhang, N., Muhammad, A., Shen, X., Sun, C., Li, Q., Hu, Y. et Shao, Y. (2022). From surviving to thriving, the assembly processes of microbial communities in stone biodeterioration : A case study of the west lake unesco world heritage area in china. *Science of The Total Environment*, 805:150395.

Hearing, V. J., Korner, A. M. et Pawelek, J. M. (1982). New regulators of melanogenesis are associated with purified tyrosinase isozymes. *Journal of Investigative Dermatology*, 79(1):16–18.

Huston, M. A. (2014). Disturbance, productivity, and species diversity : empiricism vs. logic in ecological theory. *Ecology*, 95(9):2382–2396.

Jentsch, A., Kreyling, J., Elmer, M., Gellesch, E., Glaser, B., Grant, K., Hein, R., Lara, M., Mirzae, H., Nadler, S. E. *et al.* (2011). Climate extremes initiate ecosystem-regulating functions while maintaining productivity. *Journal of Ecology*, 99(3):689–702.

Jiao, S. et Lu, Y. (2020). Soil pH and temperature regulate assembly processes of abundant and rare bacterial communities in agricultural ecosystems. *Environmental Microbiology*, 22(3):1052–1065.

Kilroy, C. (2007). *Diatom communities in New Zealand subalpine mire pools : distribution, ecology and taxonomy of endemic and cosmopolitan taxa.* Thèse de doctorat, University of Canterbury.

Kilroy, C., Biggs, B. J. et Vyverman, W. (2007). Rules for macroorganisms applied to microorganisms : patterns of endemism in benthic freshwater diatoms. *Oikos*, 116(4):550–564.

Konopka, A. (2009). What is microbial community ecology ? *The ISME Journal*, 3(11):1223–1230.

Lefèvre, M. (1974). La 'maladie verte'de Lascaux. *Studies in Conservation*, 19(3):126–156.

Little, A., Robinson, C. J., Peterson, S. B. et Raffa, K. F. (2012). Rules of engagement : Interspecies interactions that regulate microbial communities. *In The Social Biology of Microbial Communities : Workshop Summary*, volume 62, pages 375–401. National Academies Press.

Loreau, M. et De Mazancourt, C. (2013). Biodiversity and ecosystem stability : a synthesis of underlying mechanisms. *Ecology Letters*, 16:106–115.

Louca, S., Doebeli, M. et Parfrey, L. W. (2018). Correcting for 16S rRNA gene copy numbers in microbiome surveys remains an unsolved problem. *Microbiome*, 6(1):1–12.

Lynch, M. D. et Neufeld, J. D. (2015). Ecology and exploration of the rare biosphere. *Nature Reviews Microbiology*, 13(4):217–229.

Lyons, K. G., Brigham, C., Traut, B. et Schwartz, M. W. (2005). Rare species and ecosystem functioning. *Conservation Biology*, 19(4):1019–1024.

MacArthur, R. H. et MacArthur, J. W. (1961). On bird species diversity. *Ecology*, 42(3):594–598.

MacDougall, A. S. et Turkington, R. (2005). Are invasive species the drivers or passengers of change in degraded ecosystems ? *Ecology*, 86(1):42–55.

Madsen, E. L. (2011). Microorganisms and their roles in fundamental biogeochemical cycles. *Current Opinion in Biotechnology*, 22(3):456–464.

Martin-Sanchez, P. M., Miller, A. Z. et Saiz-Jimenez, C. (2015). Lascaux Cave : An example of fragile ecological balance in subterranean environments. *Microbial Life of Cave Systems*, pages 279–302.

Martin-Sanchez, P. M., Nováková, A., Bastian, F., Alabouvette, C. et Saiz-Jimenez, C. (2012). Two new species of the genus *Ochroconis*, *O. lascauxensis* and *O. anomala* isolated from black stains in Lascaux Cave, France. *Fungal Biology*, 116(5):574–589.

Mason, H. S. (1949). The chemistry of melanin : Mechanism of the oxidation of catechol by tyrosinase. *Journal of Biological Chemistry*, 181(2):803–812.

Maurice, C. F., Haiser, H. J. et Turnbaugh, P. J. (2013). Xenobiotics shape the physiology and gene expression of the active human gut microbiome. *Cell*, 152(1-2):39–50.

McKinney, M. L. et Lockwood, J. L. (1999). Biotic homogenization : a few winners replacing many losers in the next mass extinction. *Trends in Ecology & Evolution*, 14(11):450–453.

Michelsen, C. F. et Stougaard, P. (2012). Hydrogen cyanide synthesis and antifungal activity of the biocontrol strain *Pseudomonas fluorescens* In5 from Greenland is highly dependent on growth medium. *Canadian Journal of Microbiology*, 58(4):381–390.

Miller, A. Z., García-Sánchez, A. M., L. Coutinho, M., Costa Pereira, M. F., Gázquez, F., Calaforra, J. M., Forti, P., Martínez-Frías, J., Toulkeridis, T., Caldeira, A. T. *et al.* (2020). Colored microbial coatings in show caves from the Galapagos Islands (Ecuador) : first microbiological approach. *Coatings*, 10(11):1134.

Miller, J. A., Kalyuzhnaya, M. G., Noyes, E., Lara, J. C., Lidstrom, M. E. et Chistoserdova, L. (2005). *Labrys methylaminiphilus* sp. nov., a novel facultatively methylotrophic bacterium from a freshwater lake sediment. *International Journal of Systematic and Evolutionary Microbiology*, 55(3):1247–1253.

Munoz-Munoz, J. L., García-Molina, F., Varón, R., Tudela, J., García-Cánovas, F. et Rodríguez-López, J. N. (2009). Generation of hydrogen peroxide in the melanin biosynthesis pathway. *Biochimica Proteins and Proteomics*, 1794(7):1017–1029.

Nicolaus, R., Piattelli, M. et Fattorusso, E. (1964). The structure of melanins and melanogenesis—iv : On some natural melanins. *Tetrahedron*, 20(5):1163–1172.

Nimaichand, S., Devi, A. M., Tamreihao, K., Ningthoujam, D. S. et Li, W.-J. (2015). Actinobacterial diversity in limestone deposit sites in Hundung, Manipur (India) and their antimicrobial activities. *Frontiers in Microbiology*, 6:413.

Nováková, A. (2009). Microscopic fungi isolated from the Domica cave system (slovak karst national park, Slovakia). a review. *International Journal of Speleology*, 38(1):8.

Overmann, J., Abt, B. et Sikorski, J. (2017). Present and future of culturing bacteria. *Annual Review of Microbiology*, 71:711–730.

Paine, R. T., Tegner, M. J. et Johnson, E. A. (1998). Compounded perturbations yield ecological surprises. *Ecosystems*, 1(6):535–545.

Park, D.-W., Lee, J.-H., Lee, D.-H., Lee, K. et Kim, C.-K. (2003). Sequence characteristics of *xylJQK* genes responsible for catechol degradation in benzoate-catabolizing *Pseudomonas* sp. s-47. *Journal of Microbiology and Biotechnology*, 13(5):700–705.

Pascoal, F., Costa, R. et Magalhães, C. (2021). The microbial rare biosphere : current concepts, methods and ecological principles. *FEMS Microbiology Ecology*, 97(1):fiaa227.

Pašić, L., Kovče, B., Sket, B. et Herzog-Velikonja, B. (2009). Diversity of microbial communities colonizing the walls of a Karstic cave in Slovenia. *FEMS Microbiology Ecology*, 71(1):50–60.

Pfendler, S., Karimi, B., Maron, P.-A., Ciadamidaro, L., Valot, B., Bousta, F., Alaoui-Sosse, L., Alaoui-Sosse, B. et Aleya, L. (2018). Biofilm biodiversity in French and swiss show caves using the metabarcoding approach : First data. *Science of the Total Environment*, 615:1207–1217.

Philippot, L., Griffiths, B. S. et Langenheder, S. (2021). Microbial community resilience across ecosystems and multiple disturbances. *Microbiology and Molecular Biology Reviews*, 85(2):e00026–20.

Pimm, S. L. (1984). The complexity and stability of ecosystems. *Nature*, 307(5949):321–326.

Plante, C. J. (2017). Defining disturbance for microbial ecology. *Microbial Ecology*, 74(2):259–263.

Portillo, M. C. et Gonzalez, J. M. (2009). Comparing bacterial community fingerprints from white colonizations in altamira cave (spain). *World Journal of Microbiology and Biotechnology*, 25(8):1347–1352.

Portillo, M. d. C., Gonzalez, J. et Saiz-Jimenez, C. (2008). Metabolically active microbial communities of yellow and grey colonizations on the walls of altamira cave, spain. *Journal of Applied Microbiology*, 104(3):681–691.

Prescott, L. M., Willey, J. M., Sherwood, L. M. et Woolverton, C. J. (2018). *Microbiologie*. De Boeck Supérieur.

Prieur, C. (2015). Reconstruction de signaux avec peu d'échantillons. *Université Grenoble*.

Romero-Arroyo, C. E., Schell, M. A., Gaines 3rd, G. et Neidle, E. L. (1995). *catM* encodes a lysr-type transcriptional activator regulating catechol degradation in *Acinetobacter calcoaceticus*. *Journal of Bacteriology*, 177(20):5891–5898.

Russell, M. J. et MacLean, V. L. (2008). Management issues in a tasmanian tourist cave : Potential microclimatic impacts of cave modifications. *Journal of Environmental Management*, 87(3):474–483.

Rykiel J, E. J. (1985). Towards a definition of ecological disturbance. *Australian Journal of Ecology*, 10(3):361–365.

Saary, P., Mitchell, A. L. et Finn, R. D. (2020). Estimating the quality of eukaryotic genomes recovered from metagenomic analysis with eukcc. *Genome Biology*, 21(1):1–21.

Sáiz-Jiménez, C. (1995). Deposition of anthropogenic compounds on monuments and their effect on airborne microorganisms. *Aerobiologia*, 11(3):161–175.

Santillan, E., Constancias, F. et Wuertz, S. (2020). Press disturbance alters community structure and assembly mechanisms of bacterial taxa and functional genes in mesocosm-scale bioreactors. *mSystems*, 5(4):e00471–20.

Scheu, S. et Simmerling, F. (2004). Growth and reproduction of fungal feeding collembola as affected by fungal species, melanin and mixed diets. *Oecologia*, 139(3):347–353.

Sereika, M., Kirkegaard, R. H., Karst, S. M., Michaelsen, T. Y., Sørensen, E. A., Wollenberg, R. D. et Albertsen, M. (2022). Oxford nanopore r10.4 long-read sequencing enables the generation of near-finished bacterial genomes from pure cultures and metagenomes without short-read or reference polishing. *Nature Methods*, 19:1–4.

Shade, A., Peter, H., Allison, S. D., Baho, D. L., Berga, M., Bürgmann, H., Huber, D. H., Langenheder, S., Lennon, J. T., Martiny, J. B. *et al.* (2012). Fundamentals of microbial community resistance and resilience. *Frontiers in Microbiology*, 3:417.

Sogin, M. L., Morrison, H. G., Huber, J. A., Welch, D. M., Huse, S. M., Neal, P. R., Arrieta, J. M. et Herndl, G. J. (2006). Microbial diversity in the deep sea and the underexplored "rare biosphere". *Proceedings of the National Academy of Sciences USA*, 103(32):12115–12120.

Solano, F. (2014). Melanins : skin pigments and much more—types, structural models, biological functions, and formation routes. *New Journal of Science*, 2014:1–28.

Sousa, W. P. (1984). The role of disturbance in natural communities. *Annual Review of Ecology and Systematics*, 15:353–391.

Stepanauskas, R. (2012). Single cell genomics : an individual look at microbes. *Current Opinion in Microbiology*, 15(5):613–620.

Stevenson, B. S. et Schmidt, T. M. (2004). Life history implications of rRNA gene copy number in *Escherichia coli*. *Applied and Environmental Microbiology*, 70(11):6670–6677.

Sungthong, R. et Nakaew, N. (2015). The genus *Nonomuraea* : a review of a rare actinomycete taxon for novel metabolites. *Journal of Basic Microbiology*, 55(5):554–565.

Tagkopoulos, I. *et al.* (2019). Benzalkonium chlorides : Uses, regulatory status, and microbial resistance. *Applied and Environmental Microbiology*, 85(13):e00377–19.

Tandukar, M., Oh, S., Tezel, U., Konstantinidis, K. T. et Pavlostathis, S. G. (2013). Long-term exposure to benzalkonium chloride disinfectants results in change of microbial community structure and increased antimicrobial resistance. *Environmental Science & Technology*, 47(17):9730–9738.

Teng, Y., Feng, S., Ren, W., Zhu, L., Ma, W., Christie, P. et Luo, Y. (2017). Phytoremediation of diphenylarsinic-acid-contaminated soil by *Pteris vittata* associated with *Phyllobacterium myrsinacearum* RC6b. *International Journal of Phytoremediation*, 19(5):463–469.

Tocino, S. (2007). La gestion des réseaux d'orgnac-issirac : un exemple original de valorisation de réseaux souterrains fragiles et à haute valeur patrimoniale. *Collection EDYTEM. Cahiers de géographie*, 5(1):36–37.

Tomczyk-Żak, K. et Zielenkiewicz, U. (2016). Microbial diversity in caves. *Geomicrobiology Journal*, 33(1):20–38.

Uroz, S., Kelly, L. C., Turpault, M.-P., Lepleux, C. et Frey-Klett, P. (2015). The mineralosphere concept : mineralogical control of the distribution and function of mineral-associated bacterial communities. *Trends in Microbiology*, 23(12):751–762.

Urzì, C., De Leo, F., Bruno, L. et Albertano, P. (2010). Microbial diversity in paleolithic caves : a study case on the phototrophic biofilms of the cave of bats (zuheros, spain). *Microbial ecology*, 60(1):116–129.

Vieira, S., Luckner, M., Wanner, G. et Overmann, J. (2017). *Luteitalea pratensis* gen. nov., sp. nov. a new member of subdivision 6 Acidobacteria isolated from temperate grassland soil. *International Journal of Systematic and Evolutionary Microbiology*, 67(5):1408–1414.

Warren, M., Hill, J., Thomas, J., Asher, J., Fox, R., Huntley, B., Roy, D., Telfer, M., Jeffcoate, S., Harding, P. *et al.* (2001). Rapid responses of british butterflies to opposing forces of climate and habitat change. *Nature*, 414(6859):65–69.

West, P. T., Probst, A. J., Grigoriev, I. V., Thomas, B. C. et Banfield, J. F. (2018). Genome-reconstruction for eukaryotes from complex natural microbial communities. *Genome Research*, 28(4):569–580.

White, D. P., Schneider, B. K., Santen, R. J., McDermott, M., Pickett, C. K., Zwillich, C. W. et Weil, J. V. (1985). Influence of testosterone on ventilation and chemosensitivity in male subjects. *Journal of Applied Physiology*, 59(5):1452–1457.

Wilson, M. V. et Shmida, A. (1984). Measuring beta diversity with presence-absence data. *The Journal of Ecology*, 63(3):1055–1064.

Wong, W.-Y. et Huyop, F. (2020). Isolation and characterization of bacteria from melaka rubber estate agricultural soil to utilize 2,2-DCP as only carbon source. *Applied and Environmental Microbiology*, (1):1–7.

Woyke, T., Doud, D. F. et Schulz, F. (2017). The trajectory of microbial single-cell sequencing. *Nature Methods*, 14(11):1045–1054.

Yachi, S. et Loreau, M. (1999). Biodiversity and ecosystem productivity in a fluctuating environment : the insurance hypothesis. *Proceedings of the National Academy of Sciences USA*, 96(4):1463–1468.

Yu, F. B., Blainey, P. C., Schulz, F., Woyke, T., Horowitz, M. A. et Quake, S. R. (2017). Microfluidic-based mini-metagenomics enables discovery of novel microbial lineages from complex environmental samples. *eLife*, 6:e26580.

Zaneveld, J. R., McMinds, R. et Vega Thurber, R. (2017). Stress and stability : applying the anna karenina principle to animal microbiomes. *Nature Microbiology*, 2(9):1–8.

Zhang, C., Tezel, U., Li, K., Liu, D., Ren, R., Du, J. et Pavlostathis, S. G. (2011). Evaluation and modeling of benzalkonium chloride inhibition and biodegradation in activated sludge. *Water Research*, 45(3):1238–1246.

Zheng, S., Bawazir, M., Dhall, A., Kim, H.-E., He, L., Heo, J. et Hwang, G. (2021). Implication of surface properties, bacterial motility, and hydrodynamic conditions on bacterial surface sensing and their initial adhesion. *Frontiers in Bioengineering and Biotechnology*, 9:643722.

Zhou, J. et Ning, D. (2017). Stochastic community assembly : does it matter in microbial ecology ? *Microbiology and Molecular Biology Reviews*, 81(4):e00002–17.

Zylstra, G. J., McCombie, W. R., Gibson, D. et Finette, B. (1988). Toluene degradation by *Pseudomonas putida* F1 : genetic organization of the *tod* operon. *Applied and Environmental Microbiology*, 54(6):1498–1503.

Annexes

Avant-propos

En parallèle de mon projet de thèse, j'ai eu la possibilité de travailler sur un autre environnement souterrain anthropisé (l'Aven d'Orgnac) dans le cadre du projet CavesLife (coord. Thierry Heulin)**(Article 8)**. L'Aven d'Orgnac est une grotte située en Ardèche, dans le Sud-Est de la France (N 44° 19' 12" et E 4° 24' 43"). Découverte en 1935, elle est fréquentée par plus de 140 000 personnes par an [Biot, 2006]. L'ouverture d'Orgnac I, section de 1km de long, aux touristes en 1939 a nécessité des aménagements et a conduit à une anthropisation du milieu [Gauchon *et al.*, 2012] qui n'a cessé de croître par la suite avec la découverte dès 1965 de tronçons supplémentaires, nommés Orgnac II, Orgnac III où des visites accompagnées, qualifiées de "randonnées ou trek", sont organisées et Orgnac IV où il n'y a pas de visites sauf autorisation spéciale pour les spéléologues [Tocino, 2007]. Aujourd'hui, l'Aven d'Orgnac présente donc un gradient d'anthropisation, de la zone la plus touristique (Orgnac I ou II) à la zone moins fréquentée (Orgnac III) en passant par une zone très peu fréquentée (Orgnac IV). D'autres gradients d'anthropisation peuvent également être définis au sein même de chacune des zones qui comprend des chemins centraux où les touristes et les spéléologues marchent et s'arrêtent, ainsi que des positions latérales de part et d'autre, non piétinées. L'objectif de ce travail était de caractériser la structure et la composition des communautés microbiennes le long d'un double gradient d'anthropisation au sein d'une même grotte (Aven d'Orgnac). Ainsi, nous avons comparé trois zones à travers un gradient d'anthropisation longitudinal (zones touristiques, de randonnes ou trek et de spéléologie) et un gradient d'anthropisation transversal (positions centrale et latérale d'une même zone), en tenant compte de la diversité des substrats minéraux de la grotte (principalement des dépôts d'argile, de précipité de calcite et socle calcaire). La diversité des communautés procaryotiques et microeucaryotiques présentes sur les parois des grottes a été évaluée par séquençage Illumina MiSeq.

Ces travaux ont été réalisés en collaboration avec le laboratoire EDYTEM de Chambéry (J-J Delannoy, Y. Perrette), le génoscope d'Evry (K. Labadie), le CEA de Cadarache (T. Heulin, W. Achouak) et l'UMR Écologie Microbienne (J. Doré, Y. Moënne-Loccoz) qui ont participé avec à l'échantillonnage en 2018 et 2019. L'UMR Écologie Microbienne a ensuite réalisé les extractions de l'ADN environnemental, le Genoscope d'Evry a effectué l'amplification des gènes ciblant l'ARNr 16S (procaryotes) et l'ARNr 18S (microeucaryotes) et le séquençage Illumina MiSeq 2×300 bp.

Mon rôle dans ce travail a été le suivant : J'ai traité les données de séquençage brutes, j'ai ensuite analysé ces données permettant d'observer le profil taxonomique des communautés microbiennes des trois domaines du vivant à l'aide notamment de statistiques multivariées.

Lors ma deuxième année de thèse, ma co-directrice de thèse M. Hugoni a eu l'opportunité de préparer un chapitre d'ouvrage détaillant la méthodologie pour étudier les trois domaines du vivant par métabarcoding dans Methods in molecular biology, travail auquel j'ai contribué **(Article 9)**. Les microorganismes sont des acteurs clés de nombreux cycles biogéochimiques sur Terre. En effet, les microeucaryotes, les archées et les bactéries sont responsables de nombreux processus dans les écosystèmes terrestres ou aquatiques [Madsen, 2011]. Dans les écosystèmes naturels où la majorité des microorganismes est encore non-cultivée, le décryptage des interac-

tions microbiennes est difficile et le séquençage simultané de la diversité des trois domaines du vivant est indispensable pour reconstituer d'éventuelles interactions qui pourraient aider à mieux comprendre les processus écologiques complexes, et ainsi orienter les procédures expérimentales pour évaluer les interactions microbiennes se produisant in situ [Faust et Raes, 2012].. Cependant, la plupart des études portant sur l'étude de la diversité microbienne dans les écosystèmes naturels traite encore de la description d'un seul domaine de la vie, essayant d'évaluer le fonctionnement de l'écosystème en déchiffrant uniquement la diversité des bactéries, archées ou bien des microeucaryotes (avec une focalisation importante sur les champignons). Les approches de métabarcoding, reposant sur le séquençage d'un fragment cible d'ADN, sont reconnues comme des outils puissants permettant la caractérisation exhaustive de la diversité microbienne dans des contextes écologiques contrastés [Abdelfattah *et al.*, 2018,Compson *et al.*, 2020] et dans plusieurs échantillons simultanément pour un coût réduit. Les écosystèmes aquatiques salins et/ou hypersalins représentent un réservoir de diversité où des gradients physico-chimiques comme les concentrations de sel, vont imposer des contraintes sur la préparation des échantillons et donc l'efficacité de séquençage et la restitution correcte de la diversité microbienne présente dans les échantillons.

Ce travail a été réalisé en collaboration avec l'UMR Microbiologie Adaptation Pathogénie (Lyon), l'UMR Mycoplasmoses Animales (Lyon) et l'entreprise Microsynth (Suisse). Ici nous présentons un ensemble complet de protocoles dédié au métabarcoding des trois domaines de la vie appliqué à des échantillons aquatiques salés, détaillant toutes les étapes nécessaires, de la collecte d'échantillons jusqu'à l'analyse des séquences pour étudier la diversité microbienne présente dans les écosystèmes naturels.

Mon rôle dans ce travail a été le suivant : j'ai participé à la réalisation des figures de la revue, relu et corrigé le manuscrit. J'ai également réalisé une veille bibliographique et fait part de mon expérience personnelle dans la préparation des échantillons, protocoles de biologique moléculaire et de traitement des données.

L'ensemble de ces travaux a permis la rédaction de deux publications 'Metabarcoding assessment of anthropisation gradients in Aven d'Orgnac cave' (soumission prévue en 2023) et la publication d'un chapitre d'ouvrage en 2022 'Metabarcoding of the three domains of life in aquatic saline ecosystems' dans le livre 'Microbial Environmental Genomics', section Methods in molecular biology, Springer Series.

Article 8. Metabarcoding assessment of anthropisation gradients in Aven d'Orgnac cave

ZELIA BONTEMPS[1], JEANNE DORE[1], KARINE LABADIE[2], MYLENE HUGONI[1,3,4], WAFA ACHOUAK[5], YVES PERRETTE[6], JEAN-JACQUES DELANNOY[6], THIERRY HEULIN[5] AND YVAN MOENNE-LOCCOZ[1]

[1]Univ Lyon, Université Claude Bernard Lyon 1, CNRS, INRAE, VetAgro Sup, UMR Ecologie Microbienne, F-69622 Villeurbanne, France
[2]Génoscope, CEA Evry, 2 rue Gaston Crémieux, 91006 Evry cedex, France
[3]Univ Lyon, Université Claude Bernard Lyon 1, CNRS, INSA de Lyon, UMR Microbiologie Adaptation et Pathogénie, F-69622 Villeurbanne, France
[4]Institut Universitaire de France (IUF)
[5]CEA, DSV, DEVM, Laboratoire d'Ecologie Microbiennede la Rhizosphère et des Environnements extrêmes(LEMiRE), UMR 6191 CNRS, CEA, Aix Marseille-Univ,IFR-E 112, Saint-Paul-Lez-Durance F-13108, France
[6]EDYTEM, Université de Savoie, CNRS, Pôle Montagne, 73376 Le Bourget du Lac, France

Current address for Mylène Hugoni : Univ Lyon, INSA Lyon, CNRS, UMR 5240 Microbiologie Adaptation et Pathogénie, F-69621 Villeurbanne, France

Corresponding author
Yvan MOENNE-LOCCOZ
Univ Lyon, Université Claude Bernard Lyon 1, CNRS, INRAE, VetAgro Sup, UMR5557 Ecologie Microbienne, 43 bd du 11 novembre 1918, F-69622 Villeurbanne, France
yvan.moenne-loccoz@univ-lyon1.fr

Abstract

Rédaction en cours.

Keywords

Anthropization ; Metabarcoding ; Substrate ; Microbial ecology.

Introduction

Limestone areas are prone to the development of karstic underground systems following dissolution by percolating water (Cuezva et al. 2012). Caves represent particular, stable environments for life (Northup and Lavoie 2001, Engel 2010, Bastian et al. 2010, Cuezva et al. 2009). Despite nutrient limitation (oligotrophy, total organic carbon < 2 mg per liter or even lower ; Tomczyk-Żak and Zielenkiewicz 2016), caves are largely colonized by microorganisms with an average of 106 cells/g of rock (Barton and Jurado 2007, Tomczyk-Żak and Zielenkiewicz 2016), and these microorganisms play a significant part in biogeochemical cycling and dissolution/precipitation processes (e.g. speleothem formation) (Northup and Lavoie 2001).

Natural caves have been visited for over 400 years (Pfendler et al. 2018) notably for concretions (stalactites and stalagmites), underground lakes and/or parietal artwork (Cigna 2016, Bontemps et al. 2021). More than 800 caves worldwide are open to the public, representing $>$ 250 million tourist visits each year. However, touristic activities can change environmental balance in caves, as a consequence of facilities to accommodate visitors (artificial light systems, stairs, concrete pathways, masonry, etc.) (Baffier and Girard 1997, Dupont et al. 2007, Russell and MacLean 2008, Cigna et al. 2013). The visitors themselves can cause strong modification in cave balance, with an increase in temperature (e.g. +1.5°C in Lascaux Cave ; Dupont et al. 2007), water vapor levels and CO_2 concentration (which can affect the chemical equilibrium of calcite), the consumption of oxygen, the release of body heat and possibly the introduction of allochthonous microorganisms (Cañveras 2001, Russell and MacLean 2008, Diaz-Herraiz et al. 2014, Alonso et al. 2019). Consequently, tourism-related anthropization might modify environmental conditions and the structure and composition of microbial communities (Alonso et al. 2019). Indeed, anthropization is expected to cause a decrease in diversity and a modification of the structure of communities, particularly in prokaryotes, with possibly a higher proportion of Bacteroidetes and the absence of Euryarchaeota (Zhou et al. 2007, Duan et al. 2017, Pfendler et al. 2018, Alonso et al. 2019). However, most of the studies involved the comparison of non-anthropized versus anthropized caves, an approach limited by confounding factors as cavities typically displayed contrasted geological and physico-chemical properties. Findings need to be strengthened by the assessment of various anthropization conditions in a same geological context, i.e. in caves exhibiting a variety of anthropization levels, which is available in Aven d'Orgnac.

The Aven d'Orgnac is located in Ardèche in South-East France (N 44° 19' 12" and E 4° 24' 43"). Discovered in 1935, it is visited by more than 140,000 persons per year (Biot et al. 2007, Delannoy and Jaillet 2009). It is composed of a series of very large rooms totaling more than 5 km in length. The opening of Orgnac I (1 km long) to tourists in 1939 necessitated the digging of a 120 m tunnel, the establishment of a lighting system etc. Elevators were installed in 1965 and 2003 (Gauchon et al. 2012). In 1965, 4 km of additional underground networks were discovered and classified as sections Orgnac II (), Orgnac III (where accompanied visits, qualified as 'treks', are organized) and Orgnac IV (under integral protection, i.e. no visits except for approved speleologists) (Tocino 2007). Therefore, the Aven d'Orgnac displays a gradient of anthropization, from the tourist zone (Orgnac I or II) to the trek zone (Orgnac III) to the speleologist zone (Orgnac IV). Other anthropization gradients can also be considered, as each

of the three zones include central areas/paths where tourists, trackers and speleologists walk or pause, as well as lateral positions on either sides where they do not. Since 1996, underground conditions (temperature, relative humidity, radon-alpha radioactivity and CO_2 concentrations) are monitored (Bourges et al. 2006).

The objective of this work was to characterize the structure and composition of microbial communities along a double anthropization gradient within a single cave (Aven d'Orgnac). Thus, we compared three zones across a longitudinal anthropization gradient (tourist, trek and speleologist zones) and a transversal anthropization gradient (central and lateral positions), taking into consideration the diversity of mineral substrates in the cave (mainly clay deposits, calcite precipitate and limestone bedrock). The microbial community of cave walls was assessed by MiSeq Illumina sequencing of DNA extracts targeting bacteria and microeukaryotes (including fungi, protozoa, etc.).

Material and Methods

Sample collection

Orgnac Cave, located near Orgnac-l'Aven (Ardèche county, in South-East France ; GPS coordinates 44.321502, 4.411738) was sampled in November 2018 and April 2019. An anthropisation transect was identified for sampling, including the tourist spot Belvédère (where regular visitors stop for a sound and light show ; Tourist zone), an intermediate area (along a path used for small-group guided tours ; Trek zone), and the Red Room located further (only a few speleologists might reach this area each year ; Speleologist zone). Samples were taken in central position (i.e. at the level of the path used for treks and speleologist explorations) and a lateral position (i.e. at least 10 m from the speleologist path) in relation to the transect, giving 3 x 2 = 6 treatment combinations. In addition, three mineral substrates (clay deposits, limestone bedrock, calcite precipitate on stalagmites or stalactictes), were sampled (where available) for each of the 6 treatment combinations. Six samples were collected in each case for each of the two sampling campaign, giving 6 treatment combinations x 3 mineral substrates x 2 campaigns x 6 replicates = 216 samples, but only some of the samples yielded sufficient amounts of DNA for effective sequencing, and the investigation was pursued using treatment combinations and mineral substrates for which sequencing for at least 4 replicates was available over the two samplings, i.e. with 112 samples (Table S1).

Sampling, DNA extraction and metabarcoding sequencing

Cave wall samples (in the order of 100-300 mg each) were obtained using sterile scalpels, placed in cryotubes and put directly in liquid nitrogen. DNA extraction from cave wall samples was performed using the FastDNA SPIN Kit for Soil (MP Biomedicals, Illkirch, France), following the manufacturer's instructions. Because of low DNA yields, this was done twice for each sample, giving two 50μl DNA extracts subsequently pooled. DNA concentrations were measured using a NanoPhotometer (Implen, Munich, Germany). For microbial community characterization, sequencing of metabarcoding markers (16S rRNA genes for procaryotes and 18S rRNA genes for eukaryotes) was carried out at the Genoscope.

Table 1. List of the 112 samples used in the investigation, based on successful metabarcoding sequencing of DNA extracts.

Treatment combination			Sampling time		
Transect zone	**Central vs lateral position**	**Mineral substrate**	**November 2018**	**April 2019**	**Total**
Tourist zone	Lateral	Clay deposits	6	5	11
	Central	Clay deposits	6	0	6
	Central	Calcite precipitate	6	6	12
Trek zone	Lateral	Limestone bedrock	1	5	6
	Lateral	Calcite precipitate	0	4	4
	Lateral	Clay deposits	6	4	10
	Central	Clay deposits	5	0	5
Speleologist zone	Lateral	Limestone bedrock	0	6	6
	Lateral	Clay deposits	6	0	6
	Central	Clay deposits	6	6	12
			52	60	112

Analysis of metabarcoding data

For each of the two data sets, the paired-end reads were demultiplexed and in adaptors. The reads were merged based on maximum 10% mismatches in the overlap region, using Fast Length Adjustment of Short reads (FLASh)(Magoč and Salzberg 2011). Denoising was performed by removing reads that did not match expected length (200-500 bp) or contained ambiguous bases (N). Following sequence dereplication, clusterization was done using SWARM (Mahé et al. 2014), based on a local clustering threshold rather (instead of a global clustering threshold) and 3 as aggregation distance, resulting in the identification of operational taxonomic units (OTUs). Chimeric OTUs identified with VSEARCH (Rognes et al. 2016) were discarded and low-abundance sequences were filtered out, using a threshold of 0.005% of all sequences (Bokulich et al. 2013). OTUs were affiliated using both RDP Classifier and BLASTn (Zhang and Madden 1997) against the 138.1 SILVA database (Quast et al. 2013) for the 16S and 18S rRNA genes, a procedure automated with FROGS (Escudié et al. 2018). Contaminant OTUs were identified using negative control samples and removed. For sample comparisons, normalization was performed by randomly resampling to 7,181 (16S rRNA sequences) and 15,505 sequences (18S rRNA sequences).

Several α-diversity indices were computed using the Paleontological Statistics (PAST) software version 4.04 (Hammer et al. 2001), i.e. Chao1 (estimation of richness) (Chao 1987), Shannon's H' (which considers the numbers of both individuals and OTUs) (Shannon 1948), Simpson 1-D (corresponding to the probability that two individuals in a sample belong to different taxa) (Simpson 1949), Shannon's evenness E' (which takes into account abundance of species relative to other species in a given community) (Heip and Engel 1974) and the number of taxa (i.e. number of OTUs). Diversity index data were analyzed using ANOVA and Tukey-HSD tests using 'vegan' package in R version 4.0.3 (R Core Team 2020). Non-metric MultiDimensional Scaling (NMDS) comparisons were carried out using 'phyloseq' package in R (McMurdie and Holmes 2013), and stress values were computed (stress values < 0.1 are considered without risk

and those < 0.2 are acceptable (Clarke 1993)). Non-parametric tests of analysis of similarities (ANOSIM) and pairwise multilevel Adonis comparisons were done using the R packages 'vegan' and 'pairwiseAdonis' (Oksanen et al. 2020, Arbizu 2021), respectively, to assess differences in microbial community composition ($P < 0.05$). All analyses used similarity matrices obtained with the Bray-Curtis similarity index.

When considering all samples, the effect of sampling time on diversity was not significant based on Chao-1 richness (ANOVA ; $P = 0.561$ for bacteria and $P = 0.621$ for microeukaryotes), Simpson 1-D index ($P = 0.958$ and $P = 0.646$), Shannon H' index ($P = 0.824$ and $P = 0.547$), Evenness index ($P = 0.662$ and $P = 0.617$) and number of taxa ($P = 0.694$ and $P = 0.748$). It was also the case when assessing clay deposits only (balanced design), with Chao-1 richness (ANOVA ; $P = 0.741$ for bacteria and $P = 0.428$ for microeukaryotes), Simpson 1-D index ($P = 0.784$ and $P = 0.846$), Shannon H' index ($P = 0.736$ and $P = 0.810$), E' Evenness index ($P = 0.589$ and $P = 0.601$) and number of taxa ($P = 0.698$ and $P = 0.514$). The effect of sampling time was not significant either on the structure of microbial communities, based on NMDS and ANOSIM/Adonis for bacteria ($P = 0.068$) and microeukaryotes ($P = 0.184$). Therefore, data from the two sampling times were pooled.

Results

Variations in diversity indices

Diversity indices were always higher for bacteria than for microeukaryotes (Figure 1). They also varied according to the cave zone and the central/lateral location, as follows. First, the number of taxa (i.e. of OTUs) was significantly lower in the tourist zone than the trek and speleologist zones when considering bacterial (ANOVA ; $P = 1.9 \times 10^{-6}$ for all samples and $P = 1.1 \times 10^{-6}$ for clay deposits) and microeukaryotic communities ($P < 2.0 \times 10/up-6$ for all samples and for clay deposits) (Figure 1). Differences between central and lateral positions were not significant.

Second, the Simpson's index of diversity for bacteria was statistically lower in the tourist zone than the trek/speleologist zones ($P = 5.84 \times 10^{-9}$ for all samples and $P = 2.15 \times 10^{-10}$ for clay deposits) (Figure 1). For microeukaryotes, it was also lower in the tourist zone than the trek zone ($P = 0.062$ for all samples and $P = 0.078$ for clay deposits), whereas the speleologist zone was in intermediate position. Differences between central and lateral positions were not significant. When considering mineral substrates, differences were not significant for bacteria ($P = 0.62$), whereas Simpson's index was higher on clay deposits than on calcite precipitate and limestone bedrock (P = 2.52 10-4) for microeukaryotes.

Third, Shannon H' indices for bacteria ($P = 3.11 \times 10^{-12}$ for all samples and $P = 1.68 \times 10^{-12}$ for clay deposits) and microeukaryotes ($P = 5.3 \times 10^{-9}$ for all samples and $P = 4.91 \times 10^{-11}$ for clay deposits) were lower in the tourist zone than the trek/speleologist zones (Figure 1). Differences between central and lateral positions were not significant. In the three zones, the Shannon diversity index was statistically higher on clay deposits than on calcite precipitate and limestone bedrock (without any difference between the latter two) for bacterial ($P = 5.68 \times 10^{-4}$) and microeukaryotic communities ($P = 3.45 \times 10^{-14}$).

Fourth, the evenness index for bacteria was higher in the speleologist zone than the trek zone, whereas the lowest value was found in the tourist zone (respectively $P = 2.93 \times 10^{-11}$, P

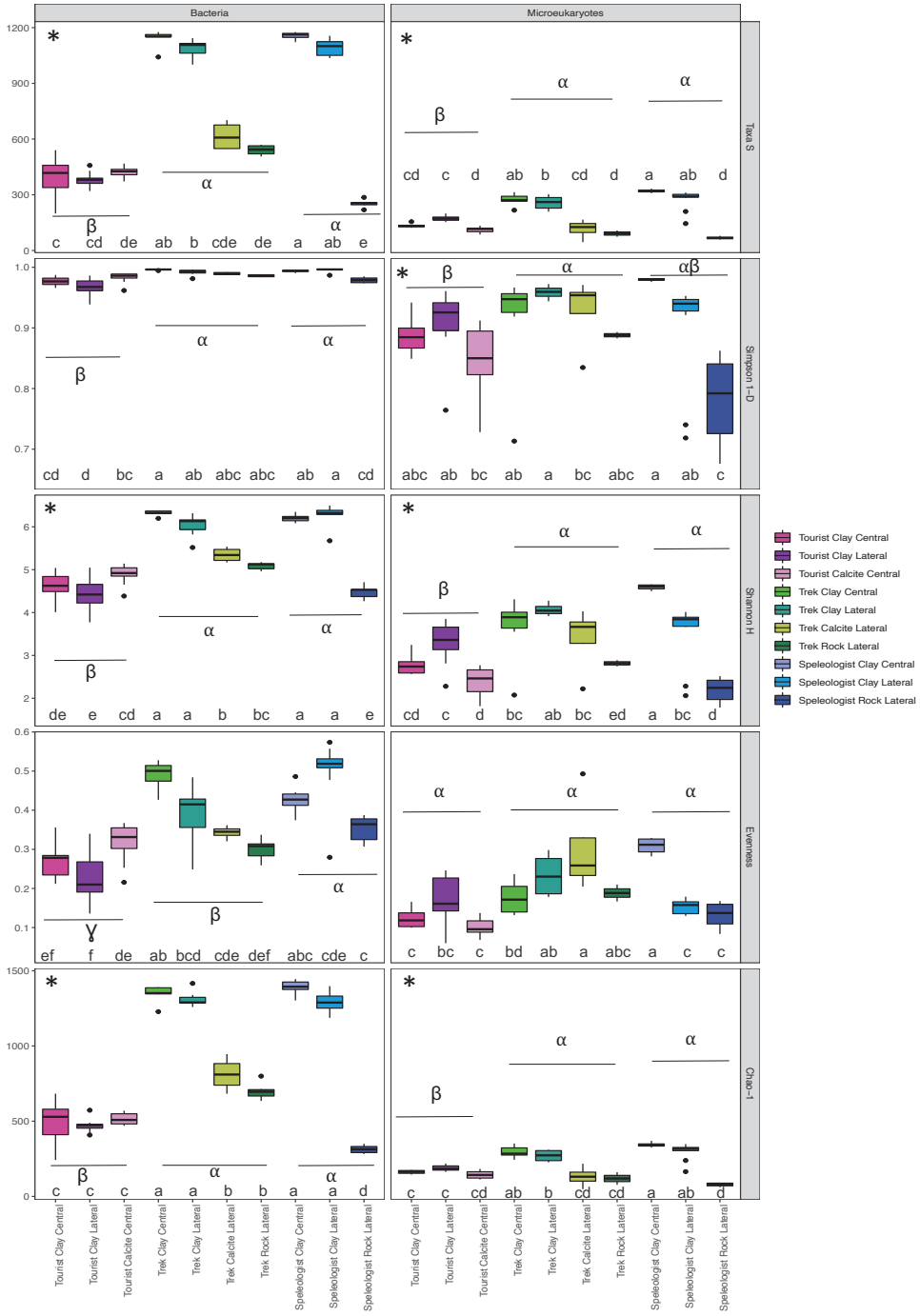

Figure 1. Diversity indices (Number of taxa, Simpson 1-D, Shannon H', Evenness and Chao-1) for the bacterial (A) and micro-eukaryotic (B) communities, according to sampling zone (tourist zone, trek zone and speleologist zone), location (central and lateral) and mineral surface (clay deposits, calcite precipitate, limestone bedrock). Differences between tourist, trek, and speleologist zones are shown using α, β and γ. Differences between clay deposits and the other mineral substrates are indicated using *.

$= 1.41 \times 10^{-9}$ and $P = 3.21 \times 10^{-8}$ for all samples; $P = 3.86 \times 10^{-12}$, $P = 1.01 \times 10^{-9}$ and $P = 1.77 \times 10^{-11}$ for clay deposits) Differences were not significant for the microeukaryotic community ($P = 0.30$ for all samples and $P = 0.42$ for clay deposits) (Figure 1). Differences between central and lateral positions were not significant. This is the only diversity index for which there was

no difference between the three mineral substrates (P = 0.07 for bacteria and P = 0.19 for microeukaryotes).

Fifth, the Chao-1 index was statistically lower in the tourist zone than the trek and speleologist zones, for bacteria ($P = 3.97 \times 10^{-12}$ for all samples and $P = 8.92 \times 10^{-13}$ for clay deposits) and microeukaryotes ($P = 1.85 \times 10^{-10}$ for all samples and $P = 2.32 \times 10^{-11}$ for clay deposits) (Figure 1). Differences between central and lateral positions were not significant. In the three zones, the index was statistically higher on clay deposits than on calcite precipitate and limestone bedrock for bacterial ($P = 1.51 \times 10^{-6}$) and microeukaryotic communities ($P = 2.23 \times 10^{-4}$). For bacteria in the trek zone, there was no difference between calcite precipitate and limestone bedrock. For bacteria and microeukaryotes in the speleologist zone, limestone bedrock (on lateral position) differed from clay deposits.

In summary, the five metrics showed that microbial biodiversity was lower in the tourist zone, both for bacteria and microeukaryotes. For each taxonomic marker and diversity index, the difference between central and lateral positions was not significant.

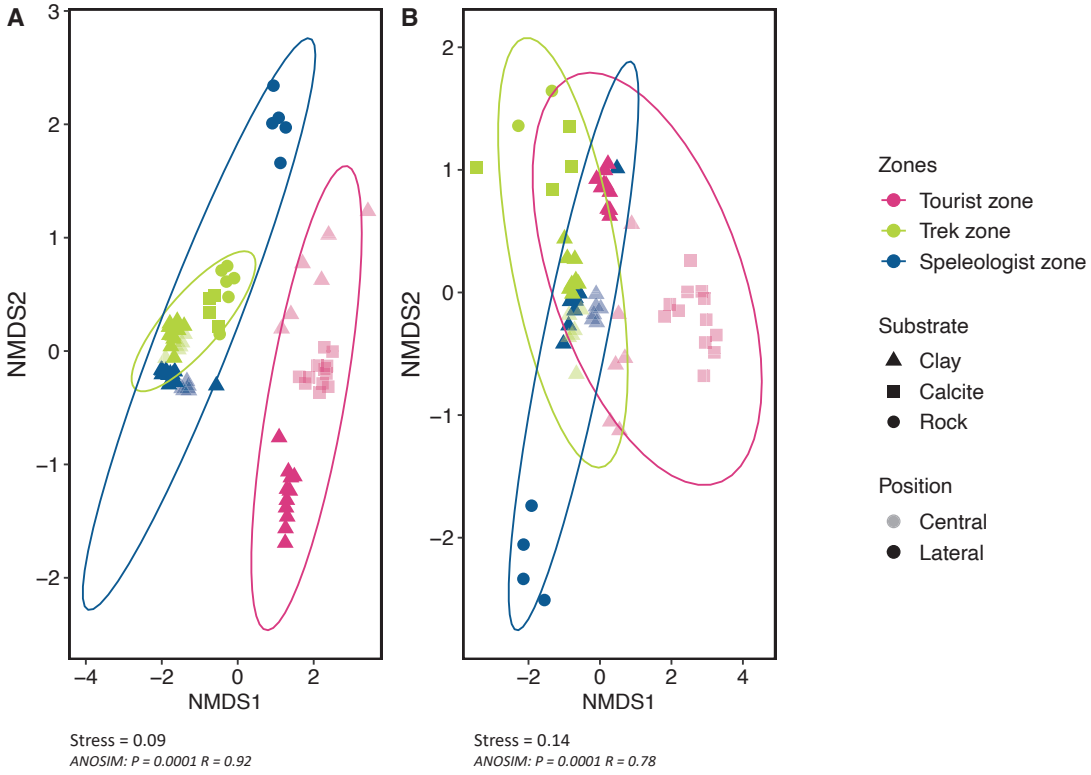

Figure 2. Non-metric multidimensional scaling (NMDS) analysis of microbial community structure for bacteria (A) and micro-eukaryotes (B), according to sampling zone (tourist zone, trek zone and speleologist zone), location (central and lateral) and mineral surface (clay deposits, calcite precipitate, limestone bedrock). Ellipses (95% confidence intervals) are used to indicate the different sampling zones.

Differences in microbial community structure

For bacteria, the zone anthropization gradient accounted for 29.7% of the variation in community structure data and the central vs lateral position only 4.3%, whereas 24.0% of the variation was linked to the mineral substrate (Table S1). NMDS and Adonis indicated that the tourist

zone was clearly distinct from the trek and speleologist zones, regardless of whether only clay deposits samples or all samples were considered (Figure 2A). The trek and speleologist zones also differed but less, based on analysis of clay deposit samples, limestone bedrock samples (lateral position), or all samples. The difference between central and lateral locations, for clay deposits, was significant in the tourist zone ($P = 0.001$) but not in the trek zone ($P = 0.16$) or speleologist zone ($P = 0.054$).

For microeukaryotes, the sampling zone explained 19.4% of community variation and the central vs lateral position only 6.8%, whereas the mineral substrate accounted to 23.2% of the variation (Table S1). NMDS and Adonis showed that the tourist zone differed from the trek and speleologist zones, based on clay deposit samples only or on all samples (Figure 2B). The trek and speleologist zones were very different when assessing limestone bedrock samples (lateral position), but differed less when considering only clay deposit samples, or all samples together. Clay deposits in central vs lateral locations differed in each of the three zones. In summary, microbial community structure was statistically different in the most anthropized (tourist) zone. The difference between central and lateral locations was also significant but accounted for a small amount of data variation.

Variation in taxonomic composition of the bacterial community

The normalized bacterial dataset consisted of 2415 OTUs. Proteobacteria (33.6% of all bacterial sequences), Actinobacteriota (18.6%) and Acidobacteriota (7.4%) predominated in the community (Figure 3A).

When comparing the three zones sampled, the Proteobacteria phylum amounted to 46.3% of sequences in the tourist zone, but only 28.4% in the trek zone and 27.7% in the speleologist zone. For Bacteroidota, the levels were 6.6%, 1.3% and 2.1%, respectively (Figure 3A). Conversely, Myxococcota, Dadabacteria and Acidobacteriota accounted to 0.8%, 0.2% and 4.0% in the tourist zone, versus as much as 4.9%, 1.2% and 8.8% in the trek zone and 2.5%, 1.5% and 8.9% in the speleologist zone, respectively. Contrasted results were also observed at class level, for Alphaproteobacteria (30.4% in the tourist zone, 17.0% in the trek zone and 10.0% in the speleologist zone) and Bacteroidia (6.6%, 0.8% and 2.8%), as well as for Acidobacteria (0.2% in the tourist zone, 3.8% in the trek zone and 3.4% in the speleologist zone), Acidimicrobiia (2.0%, 13.4% and 0.2%) and Thermoleophilia (0.4%, 5.4% and 3.7%) (Figure 3C).

The comparison between central and lateral positions explains little of the variation in communities (Figure 2) but is of interest at phylum and class levels for clay deposits. In the tourist zone, the Actinobacteriota phylum amounted to 33.2% and Nitrospirota 2.2% in central position, compared with respectively 5.8% and 11.4% in lateral position (Figure 3A). At class level, Alphaproteobacteria, Gammaproteobacteria, Nitrospiria and Actinobacteria accounted for 42.6%, 6.6%, 2.2% and 28.6% in central position, versus 29.4%, 27.1%, 11.4% and 5.4% in lateral position, respectively (Figure 3C). In the trek zone, the Actinobacteriota and Chloroflexi phyla represent 16.0% and 9.3% of sequences in central position, compared with 20.6% and 7.4% in lateral position, respectively. The Alphaproteobacteria, Planctomycetes, bacteriap25 and Methylomirabilia classes accounted for 6.6%, 5.5%, 1.8% and 9.3% in central position, vs 19.1%, 12.6%, 9.8% and 1.2% in lateral position, respectively. In the speleologist zone, Actinobacteriota

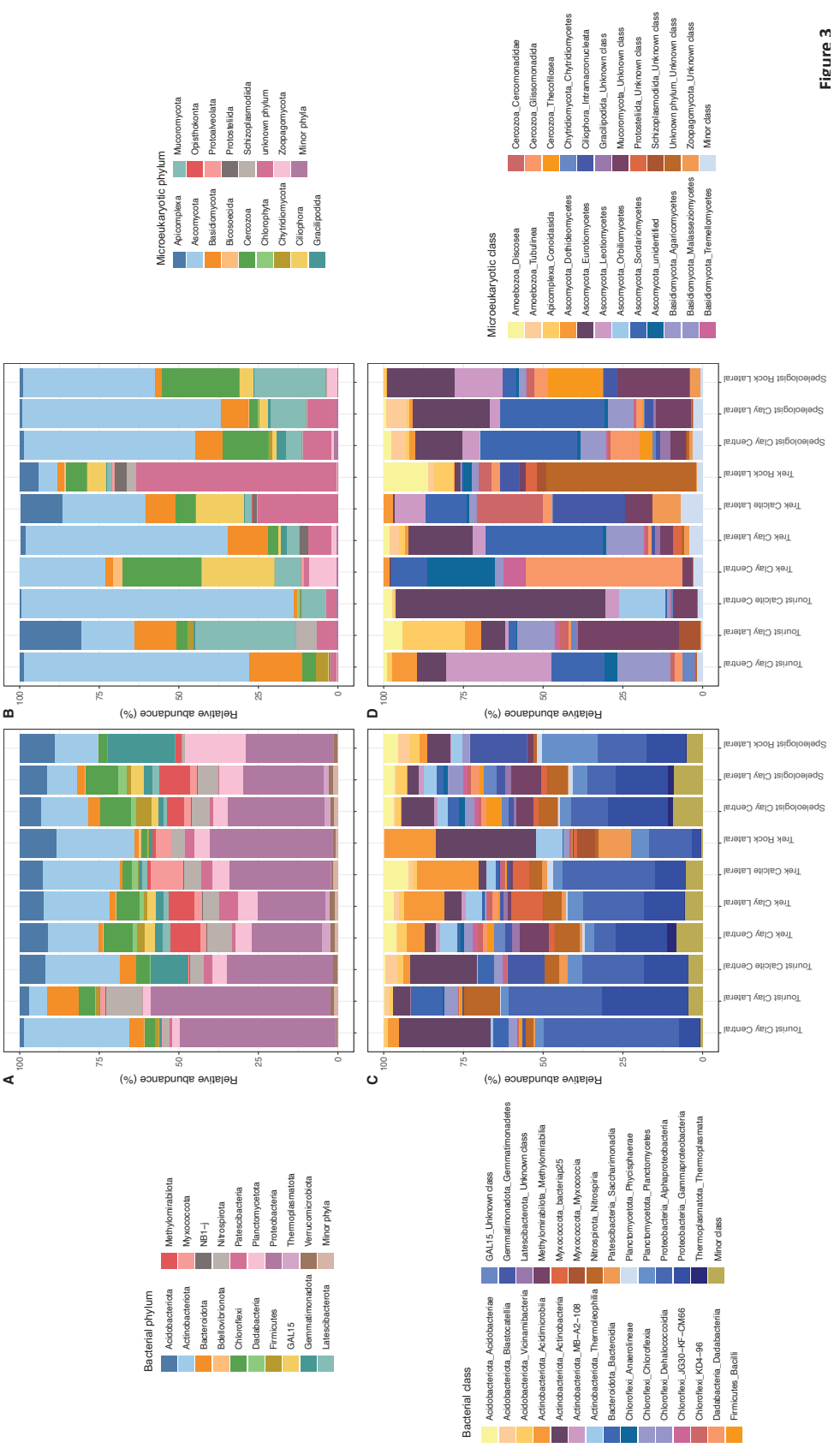

Figure 3. Relative abundance (% of sequences) of bacterial phyla (A) and classes (C), and microeukaryotic phyla (B) and classes (D). Phyla or classes of relative abundance $< 0.1\%$ were considered as minor phyla or minor class, respectively.

and Methylomirabilota amounted to 14.7% and 5.4% in central position, and 9.3% and 9.8% in lateral position. At class level, Actinobacteria represented 11.4% in central position compared with 3.7% in lateral position.

When comparing mineral substrates, Bacteroidota amounted to 4.0%, Chloroflexi 7.5%, Firmicutes 1.9% and Methylomirabilota 5.4% on clay deposits, whereas levels were only 2.9%, 3.5%, 0.3% and 0.7% on calcite precipitate and 0.7%, 2.3%, 0.3% and 1.4% on limestone bedrock, respectively (Figure 3A). The relative abundance of Myxococcota was 5.3% on calcite precipitate versus 1.8% on clay deposits and 2.6% on limestone bedrock. Gemmatimonadota and Planctomycetota amounted to 11.0% and 12.1% on limestone bedrock, but only 1.7% and 4.7% on clay deposits and 6.3% and 5.2% on calcite precipitate, respectively. At the class taxonomic level, Gammaproteobacteria, Methylomirabilia, Bacilli and Dehalococcoidia amounted to 16.3%, 4.2%, 1.9% and 1.7% on clay deposits, compared with 11.9%, 0.5%, 0.2% and <0.1% on calcite precipitate and 7.6%, 1.1%, 0.2% and <0.1% on limestone bedrock, respectively (Figure 3C). The bacteriap25 class (in the Myxococcota phylum) represented 2.5% of sequences on calcite precipitate, vs only 1.6% on clay deposits and 0.6% on limestone bedrock. Planctomycetes, Gemmatimonadetes and Thermophilia classes accounted for 11.5%, 9.0% and 5.9% on limestone bedrock, but only 3.4%, 1.4% and 3.2% on clay deposits and 3.7%, 5.2% and 1.6% on calcite precipitate, respectively.

OTU distribution was investigated for clay deposits, as the latter were successfully sampled in all six treatment (i.e. zone × position) combinations. This concerned 2271 of 2415 OTUs (Figure 4A). As many as 563 of them (24.8%) were retrieved in all three zones (tourist, trek and speleologist), but another 980 OTUs (43.1%) were evidenced in both the trek and speleologist zones. In addition, 346 OTUs (15.2%) were found exclusively in the tourist zone, 91 OTUs (4.1%) in the trek zone and 36 OTUs (1.6%) in the speleologist zone.

Variation in taxonomic composition of the microeukaryotic community

The normalized microeukaryotic dataset consisted of 763 OTUs. Most 18S rRNA sequences (65.8%) corresponded to fungi especially Ascomycota, which represented 45.3% of all sequences.

When comparing the three zones sampled, the Ascomycota and Basidiomycota phyla accounted for respectively 57.4% and 10.4% of sequences in the tourist zone, 30.5% and 6.7% in the trek zone, and 52.7% and 6.6% in the speleologist zone (Figure 3B). Cercozoa, Ciliophora and the sum of all unidentified phyla amounted to 2.7%, <0.1% and 3.7% in the tourist zone, but as much as 10.2%, 11.3% and 24.2% in the trek zone and 13.9%, 2.8% and 6.0% in the speleologist zone, respectively. At class taxonomic level, the Eurotiomycetes, Leotiomycetes, Agaricomycetes and Cercomonadidae represented respectively 27.4%, 12.9%, 9.8% and 1.4% of sequences in the tourist zone, compared with 5.8%, 3.5%, 3.4% and 6.3% in the trek zone and 20.0%, 7.9%, 6.0% and 1.3% in the speleologist zone, respectively (Figure 3D). The Sordariomycetes class reached a relative abundance of 22.5% in the speleologist zone but only 6.5% in the tourist zone (6.5%) and 15.5% in the trek zone.

When comparing central and lateral positions (possible only on clay deposits), in the tourist zone the Ascomycota, Apicomplexa and Mucoromycota phyla amounted to 70.7%, 1.4% and 0.2% in central position, compared with 16.5%, 19.5% and 31.8% in lateral position (Figure

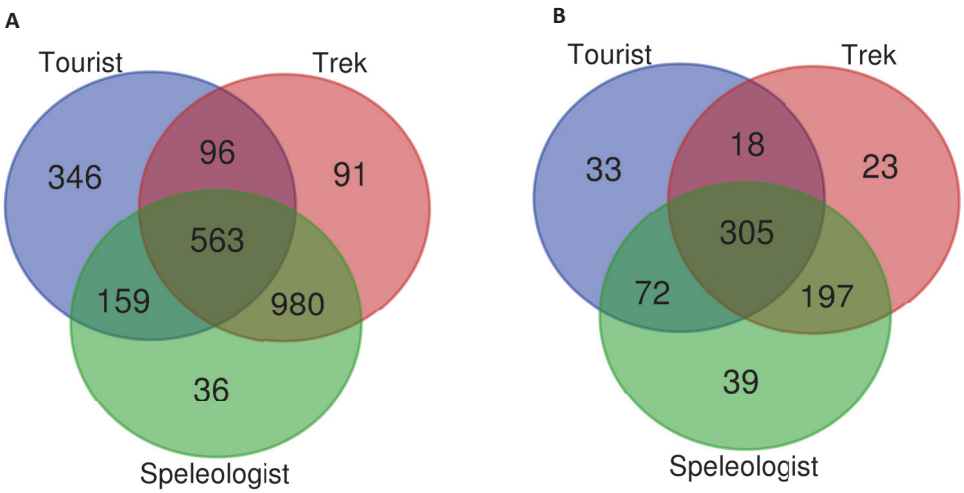

Figure 4. Venn diagrams showing the distribution of 16S rRNA OTUs (A) and 18S rRNA OTUs (B) for samples of clay deposits.

3B). The Conoidasida, Leotiomycetes and Sordariomycetes classes accounted for respectively 1.4%, 33.4% and 16.6% of sequences in central position, versus 19.5%, 1.1% and 2.3% in lateral position (Figure 3D). In the trek zone, the Ascomycota, Cercozoa and Ciliophora phyla represented 26.9%, 24.6% and 22.8% in central position, compared with 63.4%, 3.2% and 0.9% in lateral position. The Leotiomycextes, Sordariomycetes and Glissomonadida classes accounted for respectively <0.1%, 11.4% and 49.4% of sequences in central position, versus 3.9%, 36.8% and 1.2% in lateral position. In the speleologist zone, the Ascomycota, Mucoromycota and Cercozoa amounted to respectively 53.9%, 4.9% and 14.4% in central position, and 62.5%, 11.3% and 2.9% in lateral position. At class level, the Eurotiomycetes, an unknown Mucoromycota class and the Glissomonadida represented respectively 14.8%, 4.9% and 9.1% in central position compared with 24.3%, 11.2% and 2.0% in lateral position.

When comparing mineral substrates, the Basidiomycota phylum amounted to 10.4% on clay deposits, versus only 5.2% on calcite precipitate and 2.2% on limestone bedrock (Figure 3B). The relative abundance of Apicomplexa was 7.0% on calcite precipitate, compared with 4.1% on clay deposits and 3.5% on limestone bedrock. Cercozoa, Mucoromycota and all unknown phyla together accounted for respectively 15.5%, 12.2% and 31.6% on limestone bedrock, versus only 8.8%, 10.1% and 5.7% on clay deposits and 3.2%, 4.9% and 14.2% on calcite precipitate, respectively. At the class level, Conoidasida, Sordariomycetes and Agaricomycetes amounted to respectively 5.7%, 16.8% and 10.0% on clay deposits, but only 0.3%, 6.5% and 1.1% on calcite precipitate and 3.5%, 2.6% and 1.2% on limestone bedrock, respectively (Figure 3D). Eurotiomycetes, Cercomonadidae and Intramacronucleata classes had a relative abundance of respectively 33.0%, 10.4% and 11.4% on calcite precipitate, versus only 9.3%, 1.7% and 0.2% on clay deposits and 11.4%, 3.2% and 5.3% on limestone bedrock. An unknown Mucoromycota class and another microeukaryotic class accounted for respectively 12.2% and 23.5% of sequences on limestone bedrock, but 9.8% and 0.3% on clay deposits and 8.0% and <0.1% on calcite precipitate, respectively.

Clay deposits, which were successfully assessed in all six zone × position combinations, yielded 687 of 715 microeukaryotic OTUs, almost half of them (305 OTUs, 44.4%) found in

all three sampling zones whereas 197 other OTUs (28.7%) were retrieved both in the trek and speleologist zones. Also, 33 OTUs (4.8%) were documented only in the tourist zone, 23 OTUs (3.3%) in the trek zone and 39 OTUs (5.7%) in the speleologist zone. (Figure 4B).

Discussion

Rédaction en cours.

Conclusion

Rédaction en cours.

References

Alonso, L., T. Pommier, B. Kaufmann, A. Dubost, D. Chapulliot, J. Doré, C. J. Douady, and Y. Moënne-Loccoz. 2019. Anthropization level of Lascaux Cave microbiome shown by regional-scale comparisons of pristine and anthropized caves. Molecular Ecology 28 :3383–3394.

Arbizu, P. M. 2021. pairwiseAdonis. R.

Baffier, D., and M. Girard. 1997. The karst of Arcy-sur-Cure (Yonne) and its palaeolithic human occupations. Quaternaire 8 :245–255.

Banerjee, S., and S. R. Joshi. 2013. Insights into Cave Architecture and the Role of Bacterial Biofilm. Proceedings of the National Academy of Sciences, India Section B : Biological Sciences 83 :277–290.

Barton, H. A., and V. Jurado. 2007. What's Up Down There ? Microbial Diversity in Caves Microorganisms in caves survive under nutrient-poor conditions and are metabolically versatile and unexpectedly diverse.

Barton, H. A., and D. E. Northup. 2007. Geomicrobiology in cave environments : past, current and future perspectives. Journal of cave and karst studies 69 :163–178.

Bastian, F., V. Jurado, A. Nováková, C. Alabouvette, and C. Saiz-Jimenez. 2010. The microbiology of Lascaux Cave. Microbiology (Reading, England) 156 :644–652.

Biot, V., M. Duval, and C. Gauchon. 2007. L'aven d'Orgnac : identification d'un haut lieu du tourisme souterrain. Collection EDYTEM. Cahiers de géographie 5 :12–35.

Bokulich, N. A., S. Subramanian, J. J. Faith, D. Gevers, J. I. Gordon, R. Knight, D. A. Mills, and J. G. Caporaso. 2013. Quality-filtering vastly improves diversity estimates from Illumina amplicon sequencing. Nature methods 10 :57–59.

Bontemps, Z., L. Alonso, T. Pommier, M. Hugoni, and Y. Moënne-Loccoz. 2021. Microbial ecology of tourist Paleolithic caves. Science of The Total Environment :151492.

Bourges, F., P. Genthon, A. Mangin, and D. D'Hulst. 2006. Microclimates of l'Aven d'Orgnac and other French limestone caves (Chauvet, Esparros, Marsoulas). International Journal of Climatology 26 :1651–1670.

Cañveras, C. S.-J., S. Sanchez-Moral, V. Sloer. 2001. Microorganisms and Microbially Induced Fabrics in Cave Walls. Geomicrobiology Journal 18 :223–240.

Chao, A. 1987. Estimating the Population Size for Capture-Recapture Data with Unequal Catchability. Biometrics 43 :783–791.

Cigna, A. 2016. Tourism and show caves. Geomorphology, Supplementary Issues 60 :217–233.

Cigna, A., P. Forti, J. C. Moreira, and C. N. de Carvalho. 2013. Caves : the most important geotouristic feature in the world. Tourism and Karst Areas 6 :9–26.

Clarke, K. R. 1993. Non-parametric multivariate analyses of changes in community structure. Australian Journal of Ecology 18 :117–143.

Cuezva, S., A. Fernandez-Cortes, E. Porca, L. Pašić, V. Jurado, M. Hernandez-Marine, P. Serrano-Ortiz, B. Hermosin, J. C. Cañaveras, and S. Sanchez-Moral. 2012. The biogeochemical role of actinobacteria in Altamira cave, Spain. FEMS microbiology ecology 81 :281–290.

Cuezva, S., S. Sanchez-Moral, C. Saiz-Jimenez, and J. Cañaveras. 2009. Microbial Communities and Associated Mineral Fabrics in Altamira Cave, Spain. International Journal of Speleology 38.

De Leo, F. de, A. Iero, G. Zammit, and C. E. Urzi. 2012. Chemoorganotrophic bacteria isolated from biodeteriorated surfaces in cave and catacombs. International Journal of Speleology 41 :125–136.

Delannoy, jean-jacques, and S. Jaillet. 2009, February. Aven d' Orgnac - Géomorphologie, Sédimentologie, Archives Naturelles et Modélisation 3D.

Di Russo, C., G. Carchini, M. Rampini, M. Lucarelli, and V. Sbordoni. 1997. Long term stability of a terrestrial cave community. International Journal of Speleology 26.

Diaz-Herraiz, M., V. Jurado, S. Cuezva, L. Laiz, P. Pallecchi, P. Tiano, S. Sanchez-Moral, and C. Saiz-Jimenez. 2014. Deterioration of an Etruscan tomb by bacteria from the order Rhizobiales. Scientific Reports 4 :3610.

Duan, Y., F. Wu, W. Wang, D. He, J.-D. Gu, H. Feng, T. Chen, G. Liu, and L. An. 2017. The microbial community characteristics of ancient painted sculptures in Maijishan Grottoes, China. PloS One 12 :e0179718.

Dupont, J., C. Jacquet, B. Dennetière, S. Lacoste, F. Bousta, G. Orial, C. Cruaud, A. Couloux, and M.-F. Roquebert. 2007. Invasion of the French Paleolithic painted cave of Lascaux by members of the *Fusarium solani* species complex. Mycologia 99 :526–533.

Engel, A. S. 2010. Microbial Diversity of Cave Ecosystems. Pages 219–238 in L. L. Barton, M. Mandl, and A. Loy, editors. Geomicrobiology : Molecular and Environmental Perspective. Springer Netherlands, Dordrecht.

Engel, and Northup. 2008. Caves and karst as model systems for advancing the microbial sciences. In Frontiers of Karst Research : Proceedings and recommendations of the workshop held May 3 :37–48.

Escudié, F., L. Auer, M. Bernard, M. Mariadassou, L. Cauquil, K. Vidal, S. Maman, G. Hernandez-Raquet, S. Combes, and G. Pascal. 2018. FROGS : Find, Rapidly, OTUs with Galaxy Solution. Bioinformatics (Oxford, England) 34 :1287–1294.

Gauchon, C., S. Jaillet, and F. Prud'homme. 2012. Dynamique de la construction topographique et toponymique à l'aven d'Orgnac (Ardèche, France). Collection EDYTEM. Cahiers de géographie 13 :157–176.

Hammer, Ø., D. . Harper, and P. Ryan. 2001. PAST : paleontological statis- tics software package for education and data analysis. Palaeontologia Electronica 4.

Magoč, T., and S. L. Salzberg. 2011. FLASH : fast length adjustment of short reads to improve genome assemblies. Bioinformatics (Oxford, England) 27 :2957–2963.

Mahé, F., T. Rognes, C. Quince, C. de Vargas, and M. Dunthorn. 2014. Swarm : robust and fast clustering method for amplicon-based studies. PeerJ 2.

McMurdie, P. J., and S. Holmes. 2013. phyloseq : An R Package for Reproducible Interactive Analysis and Graphics of Microbiome Census Data. PLOS ONE 8 :e61217.

Mohen, J., and Y. Taborin. 2019. Les sociétés de la préhistoire. Hachette éducation. Hachette.

Northup, D., and K. Lavoie. 2001. Geomicrobiology of Caves : A Review. Geomicrobiology Journal 18 :199–222.

Oksanen, J., F. G. Blanchet, M. Friendly, R. Kindt, P. Legendre, D. McGlinn, P. R. Minchin, R. B. O'Hara, G. L. Simpson, P. Solymos, M. H. H. Stevens, E. Szoecs, and H. Wagner. 2020. vegan : Community Ecology Package.

Pasić, L., B. Kovce, B. Sket, and B. Herzog-Velikonja. 2010. Diversity of microbial communities colonizing the walls of a Karstic cave in Slovenia. FEMS microbiology ecology 71 :50–60.

Pfendler, S., B. Karimi, P.-A. Maron, L. Ciadamidaro, B. Valot, F. Bousta, L. Alaoui-Sosse,

B. Alaoui-Sosse, and L. Aleya. 2018. Biofilm biodiversity in French and Swiss show caves using the metabarcoding approach : First data. Science of The Total Environment 615 :1207–1217.

Quast, C., E. Pruesse, P. Yilmaz, J. Gerken, T. Schweer, P. Yarza, J. Peplies, and F. O. Glöckner. 2013. The SILVA ribosomal RNA gene database project : improved data processing and web-based tools. Nucleic Acids Research 41 :D590–D596.

R Core Team. 2020. R : A language and environment for statistical computing. R Foundation for Statistical Computing, Vienna, Austria.

Rognes, T., T. Flouri, B. Nichols, C. Quince, and F. Mahé. 2016. VSEARCH : a versatile open source tool for metagenomics. PeerJ 4 :e2584.

Russell, M. J., and V. L. MacLean. 2008. Management issues in a Tasmanian tourist cave : potential microclimatic impacts of cave modifications. Journal of Environmental Management 87 :474–483.

Shannon, C. E. 1948. A Mathematical Theory of Communication. Bell System Technical Journal 27 :623–656.

Simpson, E. H. 1949. Measurement of Diversity. Nature 163 :688–688.

Tocino, S. 2007. La gestion des réseaux d'Orgnac-Issirac : un exemple original de valorisation de réseaux souterrains fragiles et à haute valeur patrimoniale. Collection EDYTEM. Cahiers de géographie 5 :36–37.

Tomczyk-Żak, K., and U. Zielenkiewicz. 2016. Microbial Diversity in Caves. Geomicrobiology Journal 33 :20–38.

Zhang, J., and T. L. Madden. 1997. PowerBLAST : a new network BLAST application for interactive or automated sequence analysis and annotation. Genome Research 7 :649–656.

Zhou, J., Y. Gu, C. Zou, and M. Mo. 2007. Phylogenetic diversity of bacteria in an earth-cave in Guizhou province, southwest of China. Journal of Microbiology (Seoul, Korea) 45 :105–112.

Supplementary data

Table S1. Effect of environmental factors i.e. sampling zone (tourist zone, trek zone and speleologist zone), location (central and lateral locations) and mineral substrate (clay deposits, calcite precipitate, limestone bedrock) on microbial community composition. The differences between groups were tested using PERMANOVA on Bray-Curtis dissimilarity matrices for bacterial and microeukaryotic datasets.

	Bacteria (16S rRNA gene)				Microeukaryotes (18S rRNA gene)			
Factor	**Df**	**F**	***P***	**R^2**	**Df**	**F**	***P***	**R^2**
Zone	2	41.530	0.001	0.297	2	18.731	0.001	0.194
Mineral substrate	2	33.600	0.001	0.240	2	22.369	0.001	0.232
Position	1	12.073	0.031	0.043	1	13.140	0.027	0.068
Zone × Mineral substrate	3	15.515	0.001	0.111	3	10.741	0.001	0.111
Zone × Position	2	9.364	0.001	0.067	2	7.790	0.009	0.080
Mineral substrate × Position	2	10.807	0.001	0.071	2	9.637	0.001	0.094
Zone × Mineral substrate × Position	1	7.533	0.001	0.024	1	4.681	0.001	0.023

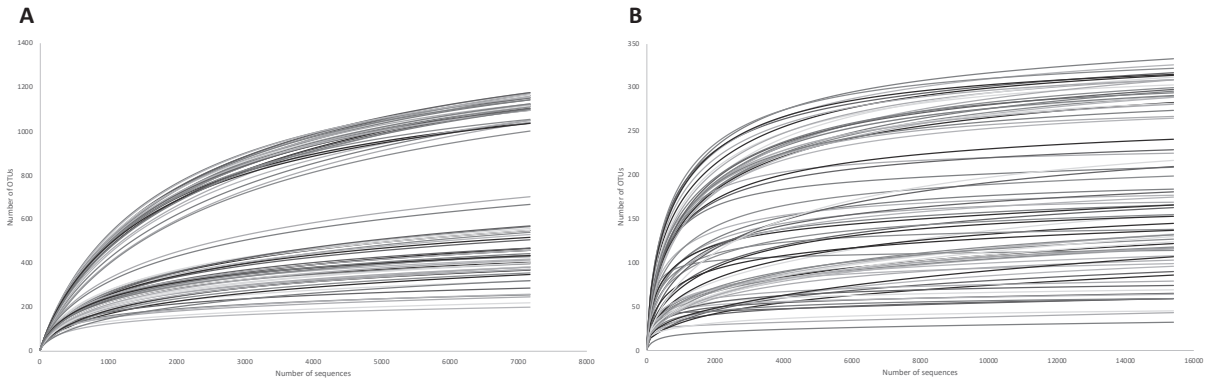

Figure S1. Rarefaction curves at OTU level for all 112 samples in the case of bacteria (16S rRNA gene dataset) (A) and microeukaryotes (18S rRNA gene dataset) (B) based on observed data.

Article 9. Metabarcoding of the three domains of life in aquatic saline ecosystems

DELPHINE MELAYAH[1], ZELIA BONTEMPS[2], MAXIME BRUTO[3], AGNES NGUYEN[4], PHILIPPE OGER[1] AND MYLENE HUGONI[1,5,*]

[1]Université de Lyon, INSA Lyon, CNRS, UMR5240 Microbiologie Adaptation et Pathogénie, F-69621 Villeurbanne, France
[2]Université de Lyon, Université Claude Bernard Lyon 1, CNRS, INRAE, VetAgro Sup, UMR Ecologie Microbienne, F-69622 Villeurbanne, France
[3]Université de Lyon, VetAgro Sup, Anses, UMR Mycoplasmoses Animales, F-69280 Marcy l'Etoile, France
[4]Microsynth France, 170 avenue Gabriel Péri 69120 Vaulx-en-Velin, France
[5]Institut Universitaire de France (IUF)

Corresponding author
Mylène HUGONI
Univ Lyon, INSA Lyon, CNRS, UMR5240 Microbiologie Adaptation et Pathogénie, F-69621 Villeurbanne, France – Phone : +33 (0)472436006.
Email : mylene.hugoni@univ-lyon1.fr

Running head : Exhaustive microbial diversity in saline ecosystems

Accepted 16 June 2022
Editor : Francis Martin and Stephane Uroz

Abstract

High-throughput amplicon sequencing, known as metabarcoding, is a powerful technique to decipher about exhaustive microbial diversity considering specific gene markers. While most of the studies investigating ecosystem functioning through microbial diversity targeted only one domain of life, either Bacteria, or Archaea or microeukaryotes, the remaining challenge in microbial ecology is to uncover the integrate view of microbial diversity occurring in ecosystems. Indeed, interactions occurring between the different microbial counterparts are known recognized having a great impact on stability and resilience of ecosystems. Here, we summarize protocols describing sampling, molecular and simultaneous metabarcoding of Bacteria, Archaea and microeukaryotes, as well as bioinformatic pipeline allowing the study of exhaustive microbial diversity in natural aquatic saline samples.

Key words

Bacteria, Archaea, Microeukaryotes, Biodiversity, Targeted high-throughput sequencing

1. Introduction

Microorganisms are key players of many bio-geochemical cycles on Earth. Altogether, Eukaryota, Archaea, and Bacteria, are responsible for many processes either in terrestrial or aquatic ecosystems (1). Microbial interactions contribute to ecosystem functioning and stability, thus maintaining ecosystem health (2, 3). While sequencing advances have revealed the tremendous microbial diversity recovered in all ecosystems on Earth and now allow a fine description of microbial community structures in contrasted ecological niches, the remaining challenge is to integrate an exhaustive view of microbial diversity thriving in complex ecosystems. Indeed, in natural ecosystems where the majority of microorganisms are still uncultured, deciphering microbial interactions is rather difficult and the simultaneous sequencing of the diversity of the three domains of life is essential to reconstruct possible relationships (i.e. co-occurrence networks) that could help gaining insights into complex ecological processes (4) and thus orient experimental procedures to assess microbial interactions occurring *in situ*.

However, most studies investigating microbial diversity in natural ecosystems still deal with the description of only one domain of life, trying to assess ecosystem functioning by deciphering only the bacterial (5, 6), the archaeal (7–9), or the microeukaryotic diversity (10, 11). Nevertheless, the prerequisite to apprehend potential microbial interactions occurring in complex natural ecosystems is first to establish a molecular inventory of all archaeal, bacterial and microeukaryotic diversities. Metabarcoding approaches, relying on the sequencing of one short DNA fragment, are recognized as powerful tools allowing the exhaustive characterization of microbial diversity in contrasted ecological contexts (12–14) and in several samples simultaneously for a reasonable cost depending on the sequencing depth expected and technology, thanks to multiplexing which enables to process 96 or 384 samples at the same time (15). By amplifying specific marker genes (i.e. typically bacterial and/or archaeal 16S rRNA genes, eukaryotic 18S rRNA genes (15–17), metabarcoding approaches have allowed the description of hidden microbial worlds (18–20), highlighting for example the presence of an unsuspected huge rare biosphere among the three domains of life (16, 21, 22). Metabarcoding (also termed monogenic metagenomics) is not to be confounded with shotgun metagenomics. While metabarcoding is based on the in-depth analysis of a single marker obtained by PCR, shotgun metagenomics is based on the direct sequencing of environmental genomic DNA and thus integrate multiple markers from organisms of the different domains of life. Consequently, for a similar depth of taxonomic information, the cost for metagenomics is several orders of magnitude higher than for metabarcoding.

Aquatic saline and/or hypersaline ecosystems represent a large diversity reservoir. Their analysis might be affected by physico-chemical factors such as salt concentrations, which impose constraints on sample preparation by affecting for example the efficiency of cell lysis and/or nucleic acid extraction and purification. In the present chapter, we present a complete set of protocols for the metabarcoding of the 3 domains of life in aquatic samples, highlighting all necessary steps from sample collection all the way to sequence analysis to decipher the exhaustive microbial diversity in natural ecosystems.

2. Materials

1. Thermo Scientific™ Nalgene™ Heavy-Duty PPCO Vacuum Bottles with Closure : Lab Pack

2. Mini Diaphragm Vacuum Pump LABOPORT® (reference N811 KT.18, Avantar)

3. Thermo Scientific™ Nalgene™ Reusable Filter Units 500mL

4. Neoprene vacuum tubing (reference 181-0282, Avantar)

5. Isopore membrane filter, pore size 0.22 µm, diameter 47 mm Merck Millipore

6. Isopore membrane filter, 3.0 µm pore size, hydrophilic polycarbonate membrane, 47 mm diameter

7. 20µm mesh

8. Stainless steel clamp for membrane with rounded ends

9. DNA/RNA Shield

10. Niskin bottle

11. ZymoBIOMICS DNA Mini Kit which contains the ZR BashingBead Lysis Tubes

12. 0.2 ml 8-Strip 'Non-Flex' Natural PCR Tubes, Ind-Attached Flat Caps (Xtra-Clear)

13. Eppendorf® Safe-Lock microcentrifuge tubes, Forensic DNA Grade, volume 1.5 mL, pack of 500 tubes (10 bags x 50 pcs.)

14. Eppendorf® Safe-Lock microcentrifuge tubes, Forensic DNA Grade, volume 0.5 mL, pack of 500 tubes (10 bags x 50 pcs.)

15. Eppendorf® Safe-Lock microcentrifuge tubes, Forensic DNA Grade, volume 2.0 mL, pack of 500 tubes (10 bags x 50 pcs.)

16. L-100XP Optima Ultracentrifuge with a near vertical rotor such as the NVT 100 rotor (Beckman Coulter Diagnostics, Brea, CA)

17. MP Biomedicals™ Instrument FastPrep-24™ 5G

18. NanoPhotometer® NP80

19. Invitrogen Qubit 4 Fluorometer

20. Invitrogen™ Quant-iT™ 1X dsDNA BR (broad range) Assay Kit

21. Thermo Scientific™ SpeedVac™ SRF110 Refrigerated Centrifugal Vacuum Concentrator and Rotors

22. Molecular grade nuclease-free water

23.PCR step-up under laminar flow hood with UV

24. T100 Thermal Cycler

25. Invitrogen™ Taq DNA Polymerase, native (5U/µL)

26. BSA, Molecular Biology Grade

27. MP Biomedicals™ dNTPs Mix (5mm each)

28. Primers (see Note 1) :

357F (5'-TCGTCGGCAGCGTCAGATGTGTATAAGAGACAGCCTACGGGAGGCAGCAG-3')

926R (5'GTCTCGTGGGCTCGGAGATGTGTATAAGAGACAGCCGTCAATTCMTTTRAGT-3')

519F (5'-TCGTCGGCAGCGTCAGATGTGTATAAGAGACAGCAGCMGCCGCGGTAA-3')

915R (5'-GTCTCGTGGGCTCGGAGATGTGTATAAGAGACAGGTGCTCCCCCGCCAATTCCT-3')

515F (5'-TCGTCGGCAGCGTCAGATGTGTATAAGAGACAGGTGYCAGCMGCCGCGGTA-3')

951R (5'-GTCTCGTGGGCTCGGAGATGTGTATAAGAGACAGTTGGYRAATGCTTTCGC-3')

29. AMPure XP PCR Purification kit

30. Ethanol 96% molecular grade

31. TE Buffer 50X solution molecular biology grade

32. Magnet plate

33. QIAxcel DNA Screening Kit on QIAxcel Advanced System with QX Alignment Marker 15 bp/5 kb

34. HOT FIREPol® Blend Master Mix Ready to Load 2,5 $MgCl_2$ mM final concentration

35. 10x GC-rich Enhancer

36. 1 pmol forward i5 indexed primer i5 (5'- AAT GAT ACG GCG ACC ACC GAG ATC TAC AC (i5) TCG TCG GCA GCG TC 3', Microsynth AG) and 1 pmol reverse i7 indexed primer i7 (5'-CAA GCA GAA GAC GGC ATA CGA GAT (i7) GTC TCG TGG GCT CGG 3', Microsynth AG). Each i5 and i7 primers has different 8-bp index sequence to identify each sample after sequencing. These index sequences are listed in Table 1.

37. NaOH, molecular biology grade

38. HT1 (Hybridization Buffer)

39. PhiX Control v3

40. MiSeq Reagent Kit v3 (600-cycle)

41. MiSeq System (reference SY-410-1003, Illumina Inc.)

42. A computer with an access to internet

43. Create an account on the Genotoul platform (http ://bioinfo.genotoul.fr/index.php/ask-for/create-an-account-2/)

44. Software : FROGS pipeline on the Genotoul platform

3. Methods

3.1 Sampling

1. Depending on the aquatic ecosystem and the trophic status considered, collected sample volumes may vary greatly (see Note 2). Water sampling is conducted using an individual Niskin bottle when considering small volumes or a combination of several ones when considering bigger volumes. Water samples are collected in pre-cleaned containers. We encourage performing biological replicates of the sampling for a better integration of the microbial diversity present, at least three per sampling points.

2. Sampling can be carried out at a punctual depth or in an integrative way between two different depths, depending on the ecological question addressed.

3.2. Sample processing and preservation of water samples

1. Water samples should be processed rapidly preferentially on field, or alternatively in the lab.

2. If working on aquatic ecosystems in which the target microorganisms live together with larger organisms such as zooplankton, we advise an initial filtration on a 20um mesh filter to reduce the representation of non-microbial biomass on the final collection filters. Then, sequentially filter the water samples through 5um or 3um (depending on the microbial size targeted),

Table 1. Indexed primers for the indexing second-step PCR on 96 samples. Oligonucleotide sequences.

Primer Name	Sequence (5'-3')	Index Sequence (i5 or i7)
i5_S502	AATGATACGGCGACCACCGAGATCTACAC**CTCTCTAT**TCGTCGGCAGCGTC	CTCTCTAT
i5_S503	AATGATACGGCGACCACCGAGATCTACAC**TATCCTCT**TCGTCGGCAGCGTC	TATCCTCT
i5_S505	AATGATACGGCGACCACCGAGATCTACAC**GTAAGGAG**TCGTCGGCAGCGTC	GTAAGGAG
i5_S506	AATGATACGGCGACCACCGAGATCTACAC**ACTGCATA**TCGTCGGCAGCGTC	ACTGCATA
i5_S507	AATGATACGGCGACCACCGAGATCTACAC**AAGGAGTA**TCGTCGGCAGCGTC	AAGGAGTA
i5_S508	AATGATACGGCGACCACCGAGATCTACAC**CTAAGCCT**TCGTCGGCAGCGTC	CTAAGCCT
i5_S510	AATGATACGGCGACCACCGAGATCTACAC**CGTCTAAT**TCGTCGGCAGCGTC	CGTCTAAT
i5_S511	AATGATACGGCGACCACCGAGATCTACAC**TCTCTCCG**TCGTCGGCAGCGTC	TCTCTCCG
i7_N701	CAAGCAGAAGACGGCATACGAGAT**TCGCCTTA**GTCTCGTGGGCTCGG	TCGCCTTA
i7_N702	CAAGCAGAAGACGGCATACGAGAT**CTAGTACG**GTCTCGTGGGCTCGG	CTAGTACG
i7_N703	CAAGCAGAAGACGGCATACGAGAT**TTCTGCCT**GTCTCGTGGGCTCGG	TTCTGCCT
i7_N704	CAAGCAGAAGACGGCATACGAGAT**GCTCAGGA**GTCTCGTGGGCTCGG	GCTCAGGA
i7_N705	CAAGCAGAAGACGGCATACGAGAT**AGGAGTCC**GTCTCGTGGGCTCGG	AGGAGTCC
i7_N706	CAAGCAGAAGACGGCATACGAGAT**CATGCCTA**GTCTCGTGGGCTCGG	CATGCCTA
i7_N707	CAAGCAGAAGACGGCATACGAGAT**GTAGAGAG**GTCTCGTGGGCTCGG	GTAGAGAG
i7_N710	CAAGCAGAAGACGGCATACGAGAT**CAGCCTCG**GTCTCGTGGGCTCGG	CAGCCTCG
i7_N711	CAAGCAGAAGACGGCATACGAGAT**TGCCTCTT**GTCTCGTGGGCTCGG	TGCCTCTT
i7_N712	CAAGCAGAAGACGGCATACGAGAT**TCCTCTAC**GTCTCGTGGGCTCGG	TCCTCTAC
i7_N714	CAAGCAGAAGACGGCATACGAGAT**TCATGAGC**GTCTCGTGGGCTCGG	TCATGAGC
i7_N715	CAAGCAGAAGACGGCATACGAGAT**CCTGAGAT**GTCTCGTGGGCTCGG	CCTGAGAT

and 0.22um pore-size filters using filter holders and pumping system (peristaltic systems or classical vacuum pumps considering a pressure < 10 kPa). Filter until the filters clog. We encourage to perform at least three technical replicates of the filters to avoid biases that could occur at this stage. Filters should be placed individually in ZR BashingBeadTM Lysis Tubes (0.1 and 0.5 mm beads included) provided with the ZymoBIOMICS DNA Mini kit, using sterile stainless-steel clamps. Add 750uL of DNA/RNA Shield (samples requires to be submerged) to allow for the preservation of nucleic acids preservation while being compatible with further molecular analyses. Store at -20°C until nucleic acids extraction.

3.3. Nucleic acid extraction and purification

The following protocols aim to extract high yields of DNA from recalcitrant samples that could present high salinity and/or important quantities of humic substances that could interfere with extraction procedures and further molecular analyses. It is based on the use of the ZymoBIOMICS DNA Mini kit, which in our hands has given the best and most reproducible results. To work properly, avoiding any contamination with other experiment conducted in the lab, dedicate a separate laboratory area, pipettors and materials. Use only filtered tips, sterile tubes and reagents. Wear gloves at all times. Pipet at a 45-degree angle with open tubes facing away from

you and use a PCR hood. To ensure the absence of aerosolized contaminants include extraction blanks. The possibility of DNA contaminations of the samples at the extraction step is then assayed by PCR amplification of the 16S rRNA gene from extraction blanks after 35 cycles of PCR. The protocol assumes that the biomass from the water samples has been collected as described above on 5um and/or 3um and/or 0.2um polycarbonate filters, diameter 47mm (Millipore). The ZymoBIOMICS DNA Mini kit will be used to extract DNA directly from the filters following the manufacturer's instructions to the exception that the first three steps have been adapted as follows for better extraction rates and quality of nucleic acids : 1. Thaw the samples, which contains beads, filter and DNA/RNA Shield, gently on ice for at least 30min.

2. Add 600 uL of a cooled, homemade mix of phenol :chloroform :isoamyl alcohol (25 :24 :1 ; pH 8.0). Cap tightly the tubes to secure.

3. Place the tubes into the FastPrep-24TM. Process your tubes at 6 meters/sec for 45 sec. Remove the tubes from the machine and let cool on ice for 10 minutes. Place the tubes back in the FastPrep-24 for a second run at 6 meters/sec for 45 sec.

4. Centrifuge at 10,000 x g for 10 minutes at 4°C.

5. Transfer the upper aqueous phase carefully to the Zymo-Spin III-F Filter placed in a collection tube (both provided in the ZymoBIOMICS DNA Mini kit). Make sure that all the aqueous phase was collected to maximize DNA extraction yields but make sure to not transfer any of the organic phase.

6. For the next steps of the extraction proceed as mentioned in the manufacturer's guideline (see below).

7. Centrifuge at 8,000 x g for 1 minute to clean the aqueous phase and collect it in the collection tube. Discard the Zymo-Spin III-F Filter.

8. Add 1.2 mL of ZymoBIOMICS DNA Binding Buffer to the filtrate. Mix gently by pipetting twice.

9. Transfer 800 uL of the mixture from the previous step to the Zymo-Spin IIC-Z Column placed in a collection tube and centrifuge at 10,000 x g for 1 minute.

10. Discard the flow through from the collection tube and repeat step 9 until the remaining volume of the mixture has been treated.

11. Add 400 uL ZymoBIOMICS DNA Wash Buffer 1 to the Zymo-Spin IIC-Z Column placed in a new collection tube and centrifuge at 10,000 x g for 1 minute. Discard the flow-through.

12. Add 700 uL ZymoBIOMICS DNA Wash Buffer 2 to the Zymo-Spin IIC-Z Column placed in a collection tube and centrifuge at 10,000 x g for 1 minute. Discard the flow-through.

13. Repeat the washing by adding 200 uL ZymoBIOMICS DNA Wash Buffer 2 to the Zymo-Spin IIC-Z Column and centrifuge at 10,000 x g for 1 minute. Discard the flow-through.

14. Transfer the Zymo-Spin IIC-Z Column to a clean 1.5 mL microcentrifuge tube and add a minimal volume 50 uL of ZymoBIOMICS DNase/RNase Free Water directly to the column matrix and incubate for 1 minute at room temperature. Centrifuge at 10,000 x g for 1 minute to elute the DNA.

15. To ensure maximal elution rates, add the 50uL of the eluate that were just collected back on the column matrix. Incubate a further 1 min and centrifuge at 10,000 x g for 1 minute to finally elute DNA.

16. A final purification step is performed with the Zymo-Spin III-HCR Filter. Place the filter in a clean collection tube and add 600 uL ZymoBIOMICS HRC Prep Solution. Centrifuge at 8,000 x g for 3 minutes. Place the Zymo-Spin III-HCR Filter in a clean 1.5 mL microcentrifuge safe-lock tube.

17. Transfer the eluted DNA onto the Zymo-Spin III-HCR Filter and centrifuge at exactly 16,000 x g for 3 minutes. DNA is then suitable for molecular analysis and amplicons libraries preparation.

18. Check DNA quality using either an agarose gel electrophoresis and a spectrophotometer such as NanoPhotometer® NP80. Determine the precise concentration of extracted and purified DNA using the Qubit Fluorometer and dsDNA BR Assay kit according to the manufacturer's instructions. The minimal amount for subsequent analyses is 20 ng/uL. If needed use a SpeedVac SRF110 to concentrate the eluted DNA to reach a final concentration higher than 20 ng/uL and quantify again with the Qubit kit.

3.4. PCR amplification and sequencing of the taxonomic gene markers

3.4.1 Amplicon libraires construction by two-step PCR

1. First step PCR, gene-specific amplification : ideally, for each sample, a total of 20 ng (1uL, concentration 20ng/uL) of purified environmental genomic DNA is used as DNA template. PCR reactions are conducted in triplicates. Each independent 30 uL reaction was performed using 0.75U of Invitrogen™ Taq DNA Polymerase, native (stock concentration 5U/uL), 1X PCR Buffer (stock concentration 10X), 2mM of $MgCl_2$ (stock concentration 50mM), 0.4uM of each primer (stock concentration 10mM), 0.1mM of each dNTP (stock concentration 5mM), 7ug of BSA (stock concentration 20mg/mL) and 1 uL of template DNA at concentration 20 ng/uL (see Note 3). Include a negative control (using 1uL of sterile water as template) to check for PCR contamination. See Table 2 for volumes to add.

Table 2. First step PCR reaction, reagent, volume and concentration.

Reagent	Stock concentration	Final concentration in 30 µL reaction mix	Pipetted volume (µL) in 30 µL reaction mix
Invitrogen™ *Taq* DNA Polymerase	5U.µL	$0.025U.\mu L^{-1}$	0.15
PCR Buffer	10X	1X	3
$MgCl_2$	50mM	2mM	1.2
Primer forward	10mM	0.4mM	1.2
Primer reverse	10mM	0.4mM	1.2
dNTP	5mM	0.1mM	0.6
BSA	$20mg.mL^{-1}$	$0.23mg.mL^{-1}$	0.35
H_2O			22.3

2. Run the PCR with the following cycling parameters, depending on the gene marker :

- bacterial 16S rRNA gene marker : 95°C for 3 min ; 35 cycles of 95°C for 45 s, 50°C for 45 s, 72°C for 1 min 30 s, followed by 72°C for 10 min

- archaeal 16S rRNA gene marker : 94°C for 10 min ; 35 cycles of 94°C for 1 min, 58°C for 1 min, 72°C for 1 min 30 s, followed by 72°C for 10 min

- eukaryotic 18S rRNA gene marker : 95°C for 10 min ; 35 cycles of 94°C for 1 min, 55°C for 1 min, 72°C for 1 min 30 s, followed by 72°C for 10 min.

3. Check the size of the amplified PCR product (i.e., amplicons) by electrophoresis in a 1% agarose gel (w/v).

4. The triplicates for each sample can be sequenced individually or as a pool (if so the amplicons replicates need to be poolled for each sample). Quantify the amplicons using the Qubit Fluorometer and the dsDNA BR Assay kit according to manufacturer's instructions. Adjust the concentration to 20 ng/uL which is ideal for metabarcoding sequencing.

5. Amplicons are purified using Agencourt AMPure XP PCR Purification kit (Beckman Coulter Diagnostics) according to the manufacturer's instructions using a ratio of 0.8 :1 of magnetic beads. A volume of 25 uL of molecular grade TE 1X buffer is used to elute the DNA product.

6. The concentration is quantified for each amplicon using QuantiFluor® dsDNA System kit (Promega) on a Qubit 2.0 Fluorometer.

7. Each amplicon is diluted to 5 ng/uL using molecular grade TE 1X buffer.

8. Second step PCR (also called indexing amplification). Each amplicon is amplified again using Illumina overhanging adapter sequences (referred as α and β in the 3.4.1. section) as primer templates, to add P5 and P7 sequences that bind to the sequencing flow cell and the dual 8 bp index sequences. In each reaction, 4 uL of first step PCR product at 5 ng/uL is used as DNA template (if your sample's DNA concentration is below 5 ng/uL you still have to use 4 uL of undiluted first step PCR product). Each 25 ul PCR reaction is performed using 1X of Solis BioDyne HOT FIREPol Blend Master Mix Ready to Load (stock concentration 5X. it already contains PCR buffer, BSA and dNTPs), 1X of Solis BioDyne GC-rich Enhancer (stock concentration 10X), 0.1 uM of one combination of i5 and i7 indexed primers per sample (stock concentration 2.5 uM) and 4 uL of the DNA template. Be careful to use one combination of i5 and i7 indexed primers per sample, so each sample should be indexed with different primers, to be identified and demultiplexed after sequencing. Include a negative control using 4 uL of molecular grade nuclease-free water to check for eventual PCR contamination. See Table 3 for volumes to add.

Table 3. Second step PCR reaction, reagent, volume and concentration.

Reagent	Stock concentration	Volume	Final concentration
Solis BioDyne HOT FIREPol® Blend Master Mix Ready to Load	5X	5 µL	1X
Solis BioDyne GC-rich Enhancer	10X	2,5 µL	1X
i5 indexed primer	2,5 µM	1 µL	0,1 µM
i7 indexed primer	2,5 µM	1 µL	0,1 µM
DNA template		4 µL	
Nuclease-free water		11,5 µL	
Final volume		25 µL	

9. Run the PCR with the following cycling parameters : 95°C for 12 min ; 12 cycles of (95°C for 20 s, 54°C for 30 s, 72°C for 1 min), followed by 72°C for 10 min, on a T100 thermal cycler

(Bio-Rad).

10. Indexed amplicons are purified using the Agencourt AMPure XP PCR Purification kit (Beckman Coulter Diagnostics) according to the manufacturer's instructions with a ratio of 0,8 :1 of magnetic beads. 25 uL of molecular grade TE 1X buffer (Fisher Scientific) are used to elute the DNA product. The construction of the amplicon library for sequencing is finished.

11. The concentration is quantified for each amplicon using the QuantiFluor® dsDNA System kit on a Qubit 2.0 Fluorometer.

12. 10 ng of indexed-amplicons are ran on QIAxcel DNA Screening Kit cartridge on QIAxcel system according to Qiagen manufacturer's instructions, using AL320 method, to check product size.

13. Proceed to the dilution and pooling of the amplicon libraries. The final amplicon libraries concentrations are converted from ng/ul to nM using the following formula :

$$Concentration(nM) = \frac{concentration(ng/uL)}{(660(g/mol))*(librarysize(bp))} * 10^6$$

where the library size is : insert size + 136 bp (Illumina adapter length with the dual indexes).

14. Prepare a library pool with 4 nM of each individual amplicon library (based on dsDNA concentration) in molecular grade TE 1X buffer (Fisher scientific) into a 1.5 mL tube.

3.4.2 Amplicon library sequencing

The next step is the denaturation and sequencing of the pooled libraries according to Illumina manufacturer's instructions.

1. MiSeq reagent cartridge v3 600-cycle and HT1 buffer are thawed 1 hour at room temperature in a water bath and stored at 4°C until used.

2. Prepare a fresh dilution of 1 mL 0.2 N NaOH in molecular grade nuclease-free water.

3. 5 uL of 4 nM pooled library is combined with 5 uL of the fresh dilution 0.2 N NaOH into a 1.5 mL tube. Vortex briefly and then centrifuge at 280 x g for 1 minute. The mix is incubated at room temperature for 5 minutes.

4. After incubation, add 990 uL of HT1 buffer (Illumina) to the tube containing the denatured library and place the tube on ice. The result is 1 mL of a 20 pM denatured pooled library. From this step on, all manipulations should be performed on ice.

5. Dilute the 20 pM denatured pooled library to the desired concentration (between 4 pM and 20 pM depending on the PCR product, size, %GC, etc.) to have a 1 mL final diluted denatured pooled library.

6. In parallel, first dilute the 10 nM Illumina phiX control to 4 nM by combining 2 uL of phiX control and 3 uL of 10 mM Tris-Cl, pH 8.5 with 0.1% Tween 20. Denature as described above and bring to the same final concentration as for the pooled libraries.

7. The final step is to spike the diluted denatured pooled library with 10% of the diluted denatured phiX control : 60 uL of diluted phiX with 540 uL of diluted pooled library.

8. Load 600 ul of the mix phiX / samples into the MiSeq reagent cartridge v3 600-cycle in the reservoir "Load Samples".

9. Start the paired-end 2*300 bp sequencing run on the MiSeq system according to Illumina manufacturer's instructions.

10. The demultiplexing step of the fastq sequences is done by the MiSeq system according to the input sample sheet, with dual indexes sequences and the corresponding sample name.

All the above steps, starting from the indexing amplification to the sequencing of the pooled-libraries can be performed by a few sequencing companies, such as Microsynth France (Vaux-en-Velin, France).

3.5. Bioinformatic analyses

The data you will obtain from the sequencing service provider will always be *fastq* files (Figure 1). The *fastq* format is as follows : for each sequence, you get the :

- first line being the sequence name, always starting with an @
- second line being your nucleotide sequence
- third line being a +
- fourth line being the per base quality Phred score, encoded in an ASCII format, from a minimal quality score of 0 to a maximal quality score of 41

Several methods and pipelines are devoted to metabarcoding data analyses consisting all in the same analysis strategy (Figure 1) :

- Uploading the raw data on a dedicated server for further processing,
- Quality checking of the reads to evaluate the accuracy of sequencing service provided, in other word, are you satisfied, and will you be able to process your data correctly or do they need to be re-sequenced ?
- Merging the pairs in the case of paired-end sequencing and removing reads containing ambiguous bases (N) from the dataset. During this step only unique sequences will be kept facilitating the calculation time and preserve bioinformatic resources, named dereplication step. In FROGS, this step is referred as Pre-process.
- Clustering the reads into Operational Taxonomic Units (OTUs),
- Eliminating the chimeric OTUs that resulted from PCR step biases,
- Eliminating low abundant sequences, such as singletons that could be sequencing errors inducing an overestimated richness,
- Affiliating the taxonomy of OTUs,
- Removing contaminant OTUs (this step implies the identification of non-desired OTUs from negative controls or from the aspecificity or primers used and their removing prior to any analysis)
- Extracting a file to work on (process normalization, phylogenetic analyses, statistical multivariate analyses, etc.)

Here, we will present a user-friendly pipeline named FROGS, that can be used hosted in a Galaxy environment ($https://sigenae-workbench.toulouse.inra.fr/galaxy/$) or can be installed locally with the conda toolshed (23) ($http://frogs.toulouse.inra.fr$) from the Toulouse server (Figure 2). In the following example, we will present a possible metabarcoding analysis flowchart using FROGS 3.2 in the Galaxy environment, as it does not need any installation on the user side (Figure 2). Before using this platform, one needs to register ($http://bioinfo.genotoul.fr/index.php/ask-for/create-an-account-2/$) and then log in here : $https://vm-galaxy-prod.toulouse.inrae.fr/galaxy_main/$. The principle is to work in a

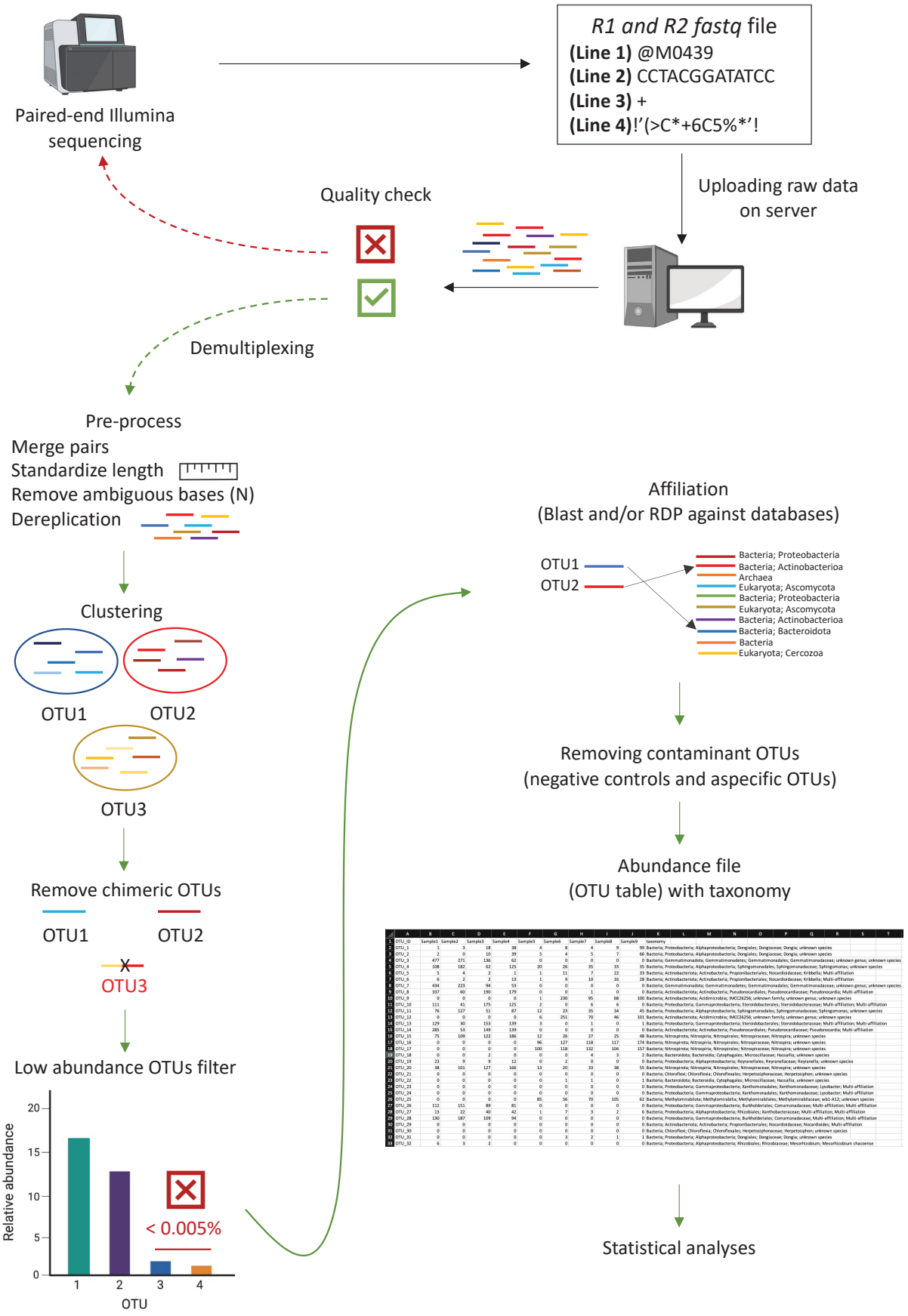

Figure 1. Schematic view of metabarcoding sequences processing.

History that is created and where you upload your data and process them, you can recover all the steps you performed at any time, even if the Galaxy session is shut down for a moment. We advise working with one History per taxonomic marker, thus the procedure below is declined for one marker and have to be repeated for other markers in independent Histories.

Figure 2. Galaxy environment description. Screen capture come from the Galaxy Toulouse server hosted here : $https : //vm - galaxy - prod.toulouse.inrae.fr/galaxy_main/$.

1. The first step is to Upload the fastq files to Galaxy. Usually, the service provider gives two fastq files per sample, named $SAMPLER1.fastq$ and $SAMPLER2.fastq$ corresponding to the forward and reverse reads, which indicates that the demultiplexing step has been done but that the paired-ends have not been merged and that you should merge your reads yourself. The latter case is the most usual and is the one for which the analysis will be further described.

Uploading is performed using the Upload File tool under the Get Data section of Galaxy. Once the data is added to a New History (named at your convenience), you will be able to work with it. 2. The second step will be to check the quality of the reads using the FastQC Read Quality reports tool. This will allow controlling that quality is satisfying along the reads. Each $SAMPLER1.fastq$ and $SAMPLER2.fastq$ files will be processed separately. Once the quality is validated, the FROGS process could start.

3. Then FROGS pipeline could be set up (see Note 4).

a. Pre-process of the data. Launch the FROGS Pre-process tool that will merge, denoise and dereplicate your reads. In this section you have to specify which type of sequencer was used (usually Illumina), precise that your input consisted in Files by samples and that the files are not merged (i.e. the FROGS pipeline named it “contiged”). Then, for all your samples, specify their Name avoiding special characters and spaces, select the R1 fastq file and R2 fast file available in the History corresponded to the samples.

Considering the above protocol, other options need to be filled, such as Reads 1 and Reads 2 size : specify 301 (when sequencing with the Illumina 2*300 bp paired-end, the reads are 301 bp), Mismatch rate : 0.1 (meaning that paired-end reads were merged with a maximum of 10%

mismatches in the overlapping region, Merge software : Vsearch (24). Final options consisted in setting Minimum and Maximum amplicon size depending on the library you consider (i.e. those parameters have been defined as optimal ones working on an hypersaline lake for which we determine following thresholds, bacterial 16S rRNA genes amplified with 357F/926R : Min 450 bp – Max 580 bp, archaeal 16S rRNA genes amplified with 519F/915R : Min 370 bp – Max 580 bp, eukaryotic 18S rRNA genes amplified with 515F/951R : Min 250 bp – Max 420 bp) and to choose Sequencing protocol as Custom protocol such as PCR primers are sequencing primers. Then Execute.

b. Clustering reads in OTUs. FROGS Clustering swarm step consists in clustering reads in OTUs using SWARM (25) that works with a local clustering threshold instead of a global one. Include the Efficient denoising and Aggregation distance clustering set up to 3. Then Execute.
c. Removing chimeric OTUs. Chimeric OTUs are removed using the FROGS Remove chimera tool, using VSEARCH (24). Then Execute.

d. Removing low abundant OTUs. OTUs representing less than 0.005% of the total number of sequences (26) along with singletons are removed using the FROGS OTU Filters tool, except if the analysis focusses on particular taxa. To calibrate this tool, choose the option Minimum OTU abundancy : as proportion and Minimum proportion of sequences abundancy to keep OTU : 0.00005. Then Execute.

e. OTUs Affiliation. FROGS Affiliation OTU allowed taxonomic affiliation with both Blast (27) and RDP Assignation (28) (say Yes). Reference databases depend on which taxonomic marker you work with. Select silva138.1 16S (or latest release) for both bacterial and archaeal 16S rRNA genes markers and silva138.1 18S for eukaryotic 16S rRNA genes markers. Then Execute.

f. Removing contaminant OTUs. The affiliation.biom file resulting from the previous step could be converted in a tsv file for a manual identification of all OTUs to remove because for example of aspecificity of primers (for example in the eukaryotic dataset, remove metazoan OTUs as primers are designed to study microbial compartment and conserve only microbial eukaryotes OTUs, in the archaeal and bacterial datasets, identify non archaeal and bacterial OTUs, respectively) or OTUs arising from control samples. To get a stringent procedure and cleaner datasets, we suggest removing all OTUs retrieved in controls before any biological analysis. List according a fasta sequence file format all OTUs to remove and use the FROGS OTU Filters tool using the Search for contaminant OTU option to remove contaminant OTUs.

g. Generate a Standard biom file, widely used in metabarcoding analyses softwares. FROGS BIOM to std BIOM will allow you to Convert a FROGS BIOM in fully compatible BIOM that you need to download to process further analysis steps. This standard biom file could be loaded in the R environment to process further analyses using dedicated packages such as phyloseq or other.

4. Notes

Note 1. To investigate simultaneously the diversity of the three domains of life, amplicon libraries are prepared targeting the bacterial 16S rRNA gene, the archaeal 16S rRNA gene and the eukaryotic 18SrRNA gene. These markers are recognized universal taxonomic mar-

kers for use in microbial study. The V3-V5 region from the bacterial 16S rRNA gene was targeted using the universal primers 357F (5'-α-CCTACGGGAGGCAGCAG-3') and 926R (5'-β-CCGTCAATTCMTTTRAGT-3') (29). The V4-V5 region of the archaeal 16S rRNA gene was targeted using the primer pair 519F (5'-α-CAGCMGCCGCGGTAA-3') and 915R (5'-β-GTGCTCCCCCGCCAATTCCT-3') (29). For the eukaryotic communities, the V4 region of the 18S rRNA marker was targeted using the primer pair 515F (5'-α-GTGYCAGCMGCCGCGGTA-3') and 951R (5'-β-TTGGYRAATGCTTTCGC-3') (30). Note that α and β in all primer sequences correspond to the Illumina overhanging adapter sequences (5' TCG TCG GCA GCG TCA GAT GTG TAT AAG AGA CAG 3' and 5' GTC TCG TGG GCT CGG AGA TGT GTA TAA GAG ACA G 3', for α and β respectively), which allow the construction of amplicon libraries in a two-step PCR.

The expected lengths of amplicons are 550, 400 and 400 bp for bacterial, archaeal, and eukaryotic markers, respectively.

Note 2. The volume sampled has to be adjusted according to the Chlorophyll a concentration. We advice to sample a volume from 30mL (i.e. in ecosystems where Chlorophyll a is about 600-700 ug/L) to 300mL or more (i.e. in ecosystems where Chlorophyll a is about 5-10 ug/L). In oligotrophic ecosystems, such as open marine zones, sampling could range from 20 to 300 L.

Note 3. If your DNA concentration is below 20ng/uL you have to use 1uL anyway.

Note 4. Note that for each step, several resulting files will be available in your History. Indeed, declined for each step, fasta files (including all unique sequences in fasta format), count.tsv files (containing the initial count of all unique sequences in each sample), abundance.biom files (containing the abundance of each OTUs in each sample, biom referred as Biological Observation Matrix), report.html files (including a report of remaining sequences and/or OTUs at each step) and tsv files (corresponding to a text file indicating the read composition of each OTUs) could be retrieved. Also note that for each step, the output file consisted in the input file for the further step.

5. References

1. Madsen EL (2011) Microorganisms and their roles in fundamental biogeochemical cycles. Curr Opin Biotechnol 22 :456–464. https ://doi.org/10.1016/j.copbio.2011.01.008

2. Braga RM, Dourado MN, Araújo WL (2016) Microbial interactions : ecology in a molecular perspective. Braz J Microbiol 47 :86–98. https ://doi.org/10.1016/j.bjm.2016.10.005

3. López-García P, Moreira D (2021) Physical connections : prokaryotes parasitizing their kin. Environ Microbiol Rep 13 :54–61. https ://doi.org/10.1111/1758-2229.12910

4. Faust K, Raes J (2012) Microbial interactions : from networks to models. Nat Rev Microbiol 10 :538–550. https ://doi.org/10.1038/nrmicro2832

5. Tamaki H, Sekiguchi Y, Hanada S, et al (2005) Comparative analysis of bacterial diversity in freshwater sediment of a shallow eutrophic lake by molecular and improved cultivation-based techniques. Appl Environ Microbiol 71 :2162–2169. https ://doi.org/10.1128/AEM.71.4.2162-2169.2005

6. Wang X, Wang Z, Jiang P, et al (2018) Bacterial diversity and community structure in the rhizosphere of four Ferula species. Sci Rep 8 :5345. https ://doi.org/10.1038/s41598-018-22802-y

7. Hugoni M, Domaizon I, Taib N, et al (2015) Temporal dynamics of active Archaea in oxygen-depleted zones of two deep lakes. Environ Microbiol Rep 7 :321–329. https ://doi.org/10.1111/1758-2229.12251

8. Dutta A, Sar P, Sarkar J, et al (2019) Archaeal Communities in Deep Terrestrial Subsurface Underneath the Deccan Traps, India. Front Microbiol 10 :1362. https ://doi.org/10.3389/fmicb.2019.01362

9. Zhang M, Chai L, Huang M, et al (2020) Deciphering the archaeal communities in tree rhizosphere of the Qinghai-Tibetan plateau. BMC Microbiol 20 :235. https ://doi.org/10.1186/s12866-020-01913-5

10. Debroas D, Hugoni M, Domaizon I (2015) Evidence for an active rare biosphere within freshwater protists community. Mol Ecol 24 :1236–1247. https ://doi.org/10.1111/mec.13116

11. Wu P-F, Li D-X, Kong L-F, et al (2020) The diversity and biogeography of microeukaryotes in the euphotic zone of the northwestern Pacific Ocean. Sci Total Environ 698 :134289. https ://doi.org/10.1016/j .scitotenv.2019.134289

12. Abdelfattah A, Malacrinò A, Wisniewski M, et al (2018) Metabarcoding : A powerful tool to investigate microbial communities and shape future plant protection strategies. Biol Control 120 :1–10. https ://doi.org/10.1016/j.biocontrol.2017.07.009

13. Hernández-Andrade A, Moo-Millan J, Cigarroa-Toledo N, et al (2020) Metabarcoding : A Powerful Yet Still Underestimated Approach for the Comprehensive Study of Vector-Borne Pathogen Transmission Cycles and Their Dynamics. In : Claborn D, Bhattacharya S, Roy S (eds) Vector-Borne Diseases - Recent Developments in Epidemiology and Control. IntechOpen

14. Compson ZG, McClenaghan B, Singer GAC, et al (2020) Metabarcoding From Microbes to Mammals : Comprehensive Bioassessment on a Global Scale. Front Ecol Evol 8 :581835. https ://doi.org/10.3389 /fevo.2020.581835

15. Taberlet P, Coissac E, Pompanon F, et al (2012) Towards next-generation biodiversity assessment using DNA metabarcoding : NEXT-GENERATION DNA METABARCODING. Mol Ecol 21 :2045–2050. https ://doi.org/10.1111/j.1365-294X.2012.05470.x

16. Hugoni M, Taib N, Debroas D, et al (2013) Structure of the rare archaeal biosphere and seasonal dynamics of active ecotypes in surface coastal waters. Proc Natl Acad Sci U S A 110 :6004–6009. https ://doi.org/10.1073/pnas.1216863110

17. Lepère C, Domaizon I, Taïb N, et al (2013) Geographic distance and ecosystem size determine the distribution of smallest protists in lacustrine ecosystems. FEMS Microbiol Ecol 85 :85–94. https ://doi.org/10.1111/1574-6941.12100

18. Caporaso JG, Lauber CL, Walters WA, et al (2011) Global patterns of 16S rRNA diversity at a depth of millions of sequences per sample. Proc Natl Acad Sci U S A 108 :4516–4522. https ://doi.org/10.107 3/pnas.1000080107

19. Bálint M, Bahram M, Eren AM, et al (2016) Millions of reads, thousands of taxa : microbial community structure and associations analyzed via marker genes. FEMS Microbiol Rev 40 :686–700. https ://doi.org/10.1093/femsre/fuw017

20. Burki F, Sandin MM, Jamy M (2021) Diversity and ecology of protists revealed by metabarcoding. Curr Biol 31 :R1267–R1280. https ://doi.org/10.1016/j.cub.2021.07.066

21. Caron DA, Countway PD (2009) Hypotheses on the role of the protistan rare biosphere in a changing world. Aquat Microb Ecol 57 :227–238

22. Campbell BJ, Yu L, Heidelberg JF, Kirchman DL (2011) Activity of abundant and rare bacteria in a coastal ocean. Proc Natl Acad Sci U S A 108 :12776–12781. https ://doi.org/10.1073 /pnas.1101405108

23. Escudié F, Auer L, Bernard M, et al (2017) FROGS : Find, Rapidly, OTUs with Galaxy Solution. Bioinformatics 34 :1287–1294. https ://doi.org/10.1093/bioinformatics/btx791

24. Rognes T, Flouri T, Nichols B, et al (2016) VSEARCH : a versatile open source tool for metagenomics. PeerJ 4 :e2584. https ://doi.org/10.7717/peerj.2584

25. Mahé F, Rognes T, Quince C, et al (2014) Swarm : robust and fast clustering method for amplicon-based studies. PeerJ 2 :e593

26. Bokulich NA, Subramanian S, Faith JJ, et al (2013) Quality-filtering vastly improves diversity estimates from Illumina amplicon sequencing. Nat Methods 10 :57–59. https ://doi.org/10

.1038/nmeth.2276

27. Camacho C, Coulouris G, Avagyan V, et al (2009) BLAST+ : architecture and applications. BMC Bioinformatics 10 :421. https ://doi.org/10.1186/1471-2105-10-421

28. Wang Q, Garrity GM, Tiedje JM, Cole JR (2007) Naive Bayesian classifier for rapid assignment of rRNA sequences into the new bacterial taxonomy. Appl Environ Microbiol 73 :5261–5267. https ://doi.org/10.1128/AEM.00062-07

29. Hugoni M, Escalas A, Bernard C, et al (2018) Spatiotemporal variations in microbial diversity across the three domains of life in a tropical thalassohaline lake (Dziani Dzaha, Mayotte Island). Mol Ecol 27 :4775–4786

30. Lepère C, Domaizon I, Hugoni M, et al (2016) Diversity and Dynamics of Active Small Microbial Eukaryotes in the Anoxic Zone of a Freshwater Meromictic Lake (Pavin, France). Front Microbiol 7 :130. https ://doi.org/10.3389/fmicb.2016.00130

Dynamique de la diversité microbienne dans la grotte de Lascaux

Résumé : Les grottes paléolithiques attirent un million de touristes par an, faisant d'elles des milieux fortement anthropisés. L'anthropisation de la grotte de Lascaux, célèbre pour son art pariétale, à entrainé un déséquilibre du microbiote de la grotte et une prolifération anormale de certains microorganismes. Aujourd'hui deux types d'altérations microbiennes (taches noires et zones sombres) sur les parois de la grotte sont des menaces pour sa conservation.

L'objectif général de cette thèse était de mieux comprendre les dynamiques des communautés microbiennes des trois domaines du vivant, au niveau des altérations (taches noires et zones sombres) présentes sur les parois de la grotte de Lascaux. Il s'agissait notamment d'identifier les communautés microbiennes de la grotte à différentes échelles spatio-temporelles et de comprendre les dynamiques de la diversité microbienne lors de la formation, l'évolution et la dissémination des altérations en utilisant le séquençage à haut débit d'acides nucléiques par des approches ciblées (métabarcoding MiSeq) et non ciblées (métagénomique shotgun). Ces recherches visaient à tester quatre hypothèses : (i) la formation et l'évolution des zones sombres seraient liées à des successions microbiennes rapides car les zones altérées et zones saines sont visuellement très différentes, sans zone de transition apparente, (ii) au moins une partie des changements de la communauté microbienne liés à la formation de zone sombre implique des taxons cosmopolites à l'échelle de la grotte, mais aussi des taxons endémiques conformément aux spécificités du microbiote des différentes pièces ou surfaces, (iii) les dynamiques de régression et de repousse de certaines taches noires seraient liées à des successions microbiennes particulières, et (iv) les taches noires étant attribuées à l'activité des champignons pigmentés, la synthèse de pigments concernerait des taxons spécialistes des conditions environnementales particulières correspondant aux altèrations.

Nos recherches ont montré, premièrement, que la formation des zones sombres implique un changement brutal de la communauté microbienne impliquant une seule zone de transition en bordure de zone altérée. Deuxièmement, les zones sombres présentent un mélange de taxons cosmopolites des altérations et de taxons endémiques à chaque endroit de Lascaux, suggérant que la propagation de ces altérations pourrait se poursuivre en fonction de la zone de distribution des taxons cosmopolites. Troisièmement, le nettoyage mécanique des taches noires a mis en évidence des taxons spécifiques liés à la recolonisation des zones altérées sur les parois, tandis que l'atténuation des taches noires (uniquement dans le Cabinet des Félins) est probablement liée à la sélection déterministe de taxons de la biosphère rare. Quatrièmement, le potentiel génétique analysé pour les deux types d'altérations a mis en évidence (i) un lien possible entre la dégradation du chlorure de benzalkonium (biocide utilisé à Lascaux) et la biosynthèse de pigments, et (ii) la présence de voies métaboliques de synthèse de mélanines et de caroténoïdes dans les communautés des deux types d'altérations, chez les bactéries et les microeucaryotes.

Ce projet a caractérisé l'impact de la perturbation anthropique sur la diversité, la structure, la composition et le potentiel génétique des communautés microbiennes de la grotte de Lascaux. Il a permis de mieux comprendre les dynamiques microbiennes associées à la formation, l'évolution et la dissémination des altérations apportant de nouvelles connaissances pour mieux guider les stratégies de conservation de ce site paléolithique emblématique.

Mots-clés : Grotte de Lascaux, Perturbation, Altérations des parois, Successions microbiennes, Potentiel fonctionnel, Mélanines, MAGs